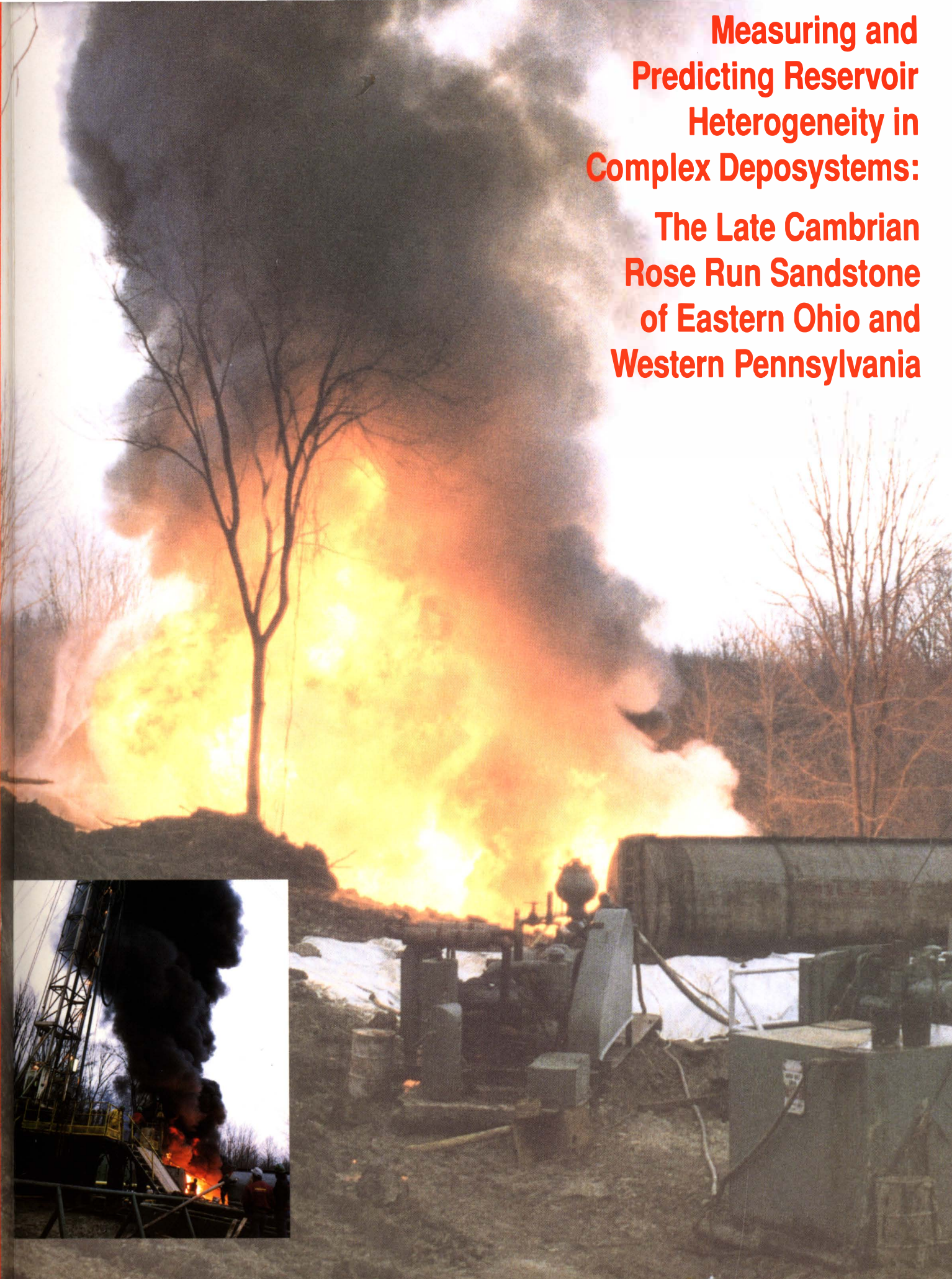


**Measuring and
Predicting Reservoir
Heterogeneity in
Complex Deposystems:**

**The Late Cambrian
Rose Run Sandstone
of Eastern Ohio and
Western Pennsylvania**

Measuring and Predicting Heterogeneity in Complex Deposystems

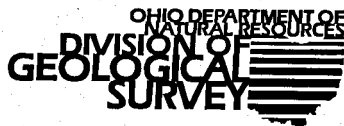


Front cover:

Cover photo: Daylight photo of natural oil and gas production flare, Cambrian Rose Run sandstone from the Bakerwell Incorporated, 1-63D Boal Unit in Lot 22, Washington Township, Coshocton County, Ohio: API Number 3403126450. Inset photo: The well was drilled in on air to the base of the Ordovician Beekmantown dolomite; switched over to 9.5 pounds of treated brine on fluid where 1,900 barrels of brine were lost in the Rose Run; 100 feet of Beekmantown and all five Rose Run sandstone beds are present; tubing pressure is 900 pounds, gauge casing pressure is 1,450 pounds; production natural, is choked back at 60+ barrels of oil and 50,000 cubic feet of gas per day; oil is deep green Pennsylvania grade, gravity 42°.

Photos by William M. Rike

STATE OF OHIO
George V. Voinovich, Governor
DEPARTMENT OF NATURAL RESOURCES
Frances S. Buchholzer, Director
DIVISION OF GEOLOGICAL SURVEY
Thomas M. Berg, Chief



Measuring and Predicting Reservoir Heterogeneity
in Complex Deposystems:

**The Late Cambrian Rose Run Sandstone
of Eastern Ohio and Western Pennsylvania**

By:

Ronald A. Riley
John A. Harper
Mark T. Baranoski
Christopher D. Laughrey
Richard W. Carlton

Prepared for:

U.S. Department of Energy
Assistant Secretary for Fossil Energy
Work Performed Under Contract No. DE-AC22-90BC14657

1993



Appalachian Oil and Natural Gas Research Consortium
National Research Center for Coal and Energy
West Virginia University
P.O. Box 6064
Evansdale Drive
Morgantown, WV 26506-6064

Table of Contents

	Page		Page
Preface	iv	Case Studies	49
List of Figures	v	Introduction	49
List of Tables	viii	Southeastern Holmes County, Ohio	49
Abstract	ix	South-Central Ashtabula County, Ohio	66
Executive Summary	xi	Southwestern Portage and North-Central Stark Counties, Ohio	67
Introduction	1	Eastern Coshocton and Western Tuscarawas Counties, Ohio	77
Previous Studies	2	Northwestern Crawford County, Pennsylvania	100
Current Methods of Study	3	Microscopic (Thin Section-Scale) Heterogeneity	102
Acknowledgements	3	Introduction	102
Summary of Historical Production	5	Petrography, Petrology, and Petrophysics	103
Heterogeneity of the Rose Run Sandstone	7	Beekmantown/Mines and Copper Ridge/ Ore Hill Dolostones	103
Megascopic (Global- to Regional-Scale) Heterogeneity	7	Rose Run Sandstone	104
Introduction	7	Kerbel/Lower Sandy	121
Global Perspective	7	Summary of Research Results	127
Paleogeography, Provenance, and Plate Tectonics	7	References	129
Paleoceanography and Paleoclimatology	10	Appendices	135
Depositional Setting	12	I— Summary of Current Methodology	137
Stratigraphy	13	II— Availability of Products	145
Introduction	13	III— Stratigraphic Relationship of Ohio Cores to Geophysical Logs	149
Problems of Nomenclature	13	IV— Porosity and Permeability Data	163
Regional Cross Sections	14	V— Graphical Descriptions of Ohio Cores	175
Regional Maps	14	VI— Production Data from Ohio Wells	197
Knox Unconformity and Adjacent Strata	16	VII— One-Dimensional Seismic Models	209
Structural Geology	19	VIII— Dolomite Types Found in Thin Sections of Cores from Ohio	215
Introduction	19	IX— Petrographic Data for the Rose Run Sandstone of Ohio	221
Influential Structural Features	20	X— Modal Analyses of Cores	229
Regional Maps and Seismic Sections	30	XI— Relative Percent Porosity Types Found in Thin Sections	241
Mesoscopic (Field- to Well-Scale) Heterogeneity	32	XII— Catalogue of Upper Cambrian and Lower Ordovician Cores	247
Introduction	32	XIII— Survey of Industry's Use of Seismic Data for the Location of Exploration and Development Wells Drilled in Ohio	251
Heterogeneity Types	33	XIV— Glossary of Geophysical Terms Used in this Study (from Sheriff, 1982)	255
Lithofacies	35		
Cross-Bedded and Flaser-Bedded Sandstone	35		
Interbedded Sandstone and Dolostone	35		
Bioturbated Dolostone	36		
Laminated Dolostone	36		
Sandstone, Dolostone, and Mixed Lithofacies	36		
Depositional Framework	46		

Preface

State geological surveys have a common mission to provide public information on the location, quantity, and quality of fossil fuel and mineral resources within each state so as to allow for responsible development and use of identified resources. In this period of ever-increasing concern about the availability of energy resources, state surveys have the responsibility of providing basic data and interpretations about their state's oil and gas resources. To that end, the Ohio and Pennsylvania Geological Surveys have participated with the Appalachian Oil and Natural Gas Research Consortium at West Virginia University to gather subsurface information about the Rose Run sandstone reservoir, presently the most active exploratory play in the Appalachian Basin. In order to conduct successful exploration, drilling, and production of hydrocarbons from the Rose Run sandstone, it is crucial to thoroughly understand the degree of geological heterogeneity in this stratigraphic unit. Vertical, lateral, and internal heterogeneities of all scales and complexities control the movement and trapping of hydrocarbons in the Rose Run. To predict the spatial distribution of these heterogeneities requires an up-to-date understanding of depositional environments and tectonic controls on sedimentary patterns. The Ohio and Pennsylvania Geological Surveys are pleased to apply this understanding for the benefit of the oil and gas producers of both states.

Thomas M. Berg
State Geologist and Chief
Division of Geological Survey
Ohio Department of Natural Resources

Donald M. Hoskins
Director and State Geologist
Pennsylvania Geological Survey
Department of Environmental Resources

The Appalachian Oil and Natural Gas Research Consortium is a partnership among two departments and one center at West Virginia University and four state geological surveys in the Appalachian basin. Partners include the departments of Geology and Geography and Petroleum and Natural Gas Engineering at WVU, and the geological surveys in West Virginia, Ohio, Pennsylvania, and Kentucky. The Consortium is managed through the National Research Center for Coal and Energy at WVU. Organized in 1989, the Consortium's prime objective is to increase the utilization of the petroleum resources in the Appalachian basin in an environmentally acceptable manner. To accomplish this, the Consortium has attempted to increase research in energy-related areas by creating strong research teams with a broad regional base to compete for research dollars, while soliciting the support of industry as well. This publication is one of the products of our initial DOE-funded research project designed to measure and predict reservoir heterogeneity in complex deposystems. A research team consisting of survey geologists in Ohio and Pennsylvania, actively assisted by geologists in industry, performed all of the research on the Rose Run phase of the project. I believe this publication will be a valuable resource for those operators involved in the Rose Run play in eastern Ohio, and eventually in western Pennsylvania.

Douglas G. Patchen
Consortium Director

List of Figures and Tables

- Figure 1. Location of the Rose Run study area.
2. Summary of Rose Run drilling activity in Ohio, 1981 to 1991.
3. Generalized correlation diagram for Cambrian and Ordovician rocks.
4. Changes in Cambrian and Ordovician stratigraphic nomenclature used in Ohio.
5. Locations of cores used in this study.
6. Locations of seismic data, sonic logs, and synthetic seismograms used in this study.
7. Map of producing fields and pools.
8. Generalized paleogeography and depositional setting of the Laurentian plate during the Late Cambrian.
9. Global Late Cambrian plate tectonic reconstruction.
10. Diagrammatic model of the plate tectonic history of the study area from Late Precambrian to Middle Ordovician.
11. Paleotectonics and sandstone provenance in North America.
12. QFL (quartz, feldspar, lithics) diagram with provenance types.
13. Paleooceanography and paleoclimatology of the earth during the Late Cambrian.
14. Late Cambrian depositional and stratigraphic relationships on the continental shelf of eastern North America illustrating the concept of the rimmed shelf with platform morphology.
15. Type section of the Rose Run sandstone.
16. Location of regional cross sections constructed for this study.
17. Log suite for the Rose Run sandstone and adjacent units.
18. Regional cross section A–A’.
19. Regional isopach map of the Rose Run sandstone.
20. Generalized cross sections of the Appalachian basin.
21. Photographs of cores from wells in Coshocton County, Ohio showing the Knox unconformity.
- Figure 22. Map of the study area showing major tectonic features that affected Late Cambrian deposition and subsequent structural development in Ohio and Pennsylvania.
23. Two concepts of the Rome trough in the central Appalachian basin.
24. Interpreted seismic section display, Carter County, Kentucky.
25. Interpreted seismic section display, Portage County, Ohio.
26. Uninterpreted and interpreted seismic section displays, Fayette County, Ohio.
27. Interpreted seismic section display, Pickaway County, Ohio.
28. Uninterpreted and interpreted seismic section displays in eastern Ohio.
29. Interpreted seismic section display, Coshocton County, Ohio.
30. Regional structure map on the Knox unconformity.
31. Regional structure map on top of the Rose Run sandstone.
32. Classification of reservoir heterogeneity types.
33. Cross-bedded and flaser-bedded sandstone lithofacies from core 2898, Jackson County, Ohio.
34. Cross-bedded and flaser-bedded sandstone lithofacies in cores from Columbiana and Morgan Counties, Ohio.
35. Interbedded sandstone and dolostone lithofacies in cores from Coshocton and Columbiana Counties, Ohio.
36. Bioturbated dolostone lithofacies in cores from Coshocton and Morgan Counties, Ohio.
37. Laminated dolostone lithofacies from core 2850, Columbiana County, Ohio.
38. Geophysical log signature through the Gatesburg Formation in the #2 Hammermill well, Erie County, Pennsylvania.
39. Graphical descriptions of cores 1 and 2 from the #2 Hammermill well, Erie County, Pennsylvania.

- Figure 40. Herringbone cross stratification in outcrop.
41. The Rose Run dolostone lithofacies in outcrop photograph of storm-deposited flat-pebble conglomerate subfacies.
 42. Photographs of thrombolitic algal mounds.
 43. Photographs of ooid-peloid shoal and “ribbon rock” subfacies.
 44. Photographs of prism-cracked wavy laminites.
 45. Graphical plot of core analysis data from the Gatesburg Formation core recovered from the #1 Shade Mountain well, Juniata County, Pennsylvania.
 46. Graphical core description of the Gatesburg Formation in the #1 Shade Mountain well, Juniata County, Pennsylvania.
 47. Inferred depositional environment of Mississippian Frobisher Evaporite in southeastern Saskatchewan.
 48. Photomicrographs of ooid dolograins.
 49. Isopach map of Copper Ridge/Ore Hill sandstone in Tuscarawas, Holmes, and Coshocton Counties, Ohio.
 50. Isopach map of a Copper Ridge/Ore Hill sandstone in southeastern Holmes County, Ohio.
 51. Wells penetrating the Knox unconformity or deeper in Holmes County, Ohio.
 52. Structure map on top of the Knox unconformity, Holmes County, Ohio.
 53. Isopach map of the Middle Ordovician Wells Creek/Shadow Lake interval in Holmes County, Ohio.
 54. Isopach map of the Wells Creek/Shadow Lake-through-Trenton interval in Holmes County, Ohio.
 55. Structure map on top of the Upper Ordovician Trenton Limestone in Holmes County, Ohio.
 56. Structure map on the base of the Lower Silurian “Packer Shell” in Holmes County, Ohio.
 57. Structure map on top of the Mississippian Berea Sandstone in Holmes County, Ohio.
 58. Cross section A-A’ in Holmes County, Ohio.
 59. Interpreted seismic section display, Holmes County, Ohio.
 60. Uninterpreted and interpreted seismic section displays, Holmes County, Ohio.
 61. Color attribute correlation panels.

- Figure 62. Interpreted seismic section attribute displays, Holmes County, Ohio.
63. Interpreted seismic section attribute displays, Holmes County, Ohio.
 64. One-dimensional model and synthetic seismogram of a non-remnant geological scenario with 50 feet of Wells Creek Formation and zero feet of Beekmantown/Mines dolomite.
 65. Geologic models of a Rose Run erosional remnant.
 66. Wells penetrating the Knox unconformity or deeper in Ashtabula County, Ohio.
 67. Cross section B-B’ in Ashtabula County, Ohio.
 68. Isopach map of the Rose Run sandstone in Ashtabula County, Ohio.
 69. Structure map on top of the Knox unconformity in Ashtabula County, Ohio.
 70. Isopach map of the Middle Ordovician Wells Creek Formation in Ashtabula County, Ohio.
 71. Structure map on top of the Upper Ordovician Trenton Formation in Ashtabula County, Ohio.
 72. Structure map on the base of the Lower Silurian “Packer Shell” in Ashtabula County, Ohio.
 73. Wells penetrating the Knox unconformity or deeper in Portage and Stark Counties, Ohio.
 74. Interpreted seismic section display, Portage County, Ohio.
 75. Seismic section display, Portage County, Ohio.
 76. Structural cross section C-C’ across portions of Portage and Stark Counties, Ohio.
 77. Structure map on top of the Knox unconformity in Portage and Stark Counties, Ohio.
 78. Isopach map of the Rose Run sandstone beneath the Beekmantown/Mines dolomite in Portage and Stark Counties, Ohio.
 79. Isopach map of the Middle Ordovician Wells Creek Formation in Portage and Stark Counties, Ohio.
 80. Structure map on top of the Trenton Limestone in Portage and Stark Counties, Ohio.
 81. Structure map on top of the Mississippian Berea Sandstone in Portage and Stark Counties, Ohio.
 82. Well locations penetrating the Knox unconformity in eastern Coshocton and western Tuscarawas Counties, Ohio.

- Figure 83. Structure map on top of the Knox unconformity in eastern Coshocton and western Tuscarawas Counties, Ohio.
84. Isopach map of the Rose Run sandstone in eastern Coshocton and western Tuscarawas Counties, Ohio.
85. Isopach map of the Beekmantown/Mines dolomite in eastern Coshocton and western Tuscarawas Counties, Ohio.
86. Stratigraphic cross section D–D' in eastern Coshocton and western Tuscarawas Counties, Ohio.
87. FMS image of vuggy porosity in the Beekmantown/Mines dolomite from the #3-A Reiss well, Coshocton County, Ohio.
88. Isopach map of the Wells Creek Formation in eastern Coshocton and western Tuscarawas Counties, Ohio.
89. Structure map on top of the Trenton Limestone in eastern Coshocton and western Tuscarawas Counties, Ohio.
90. Isopach map of the Wells Creek-Trenton interval in eastern Coshocton and western Tuscarawas Counties, Ohio.
91. Structure map on the base of the "Packer Shell" in eastern Coshocton and western Tuscarawas Counties, Ohio.
92. Structure map on top of the Onondaga Limestone in eastern Coshocton and western Tuscarawas Counties, Ohio.
93. Interpreted seismic section display, Coshocton County, Ohio.
94. Plot of elan lithology, delta-T compressional, delta-T shear, bulk density, gamma ray, acoustic impedance, reflection coefficients, zero phase synthetic seismogram stack, zero phase vertical seismic profile corridor stack, and dipmeter in the #3-A Reiss well.
95. Interpreted offset vertical seismic profile with correlation and depth migration from the #3-A Reiss well.
96. Amplitude envelope of synthetic profile incorporating models 1 to 10 at zero phase.
97. Seismic section display, Coshocton County, Ohio.
98. Seismic section display, Coshocton County, Ohio.
99. Interpreted seismic section displays, Coshocton County, Ohio.
- Figure 100. Geologic models of a Beekmantown/Mines remnant adjacent to a channel-fill sandstone in the Rose Run.
101. Interpreted seismic section attribute displays, Coshocton County, Ohio.
102. Interpreted seismic section attribute displays, Coshocton County, Ohio.
103. Map showing the location of Rose Run producing area in western Crawford and Erie Counties, Pennsylvania.
104. Structure contour map on top of the Knox unconformity in western Crawford and Erie Counties, Pennsylvania.
105. Isopach map of the Shadow Lake Formation in western Crawford and Erie Counties, Pennsylvania.
106. Structure contour map on top of the Trenton Limestone, in the vicinity of the #1 Scull well, western Crawford County, Pennsylvania.
107. Paleostructural cross section E–E' in western Crawford and Erie Counties, Pennsylvania.
108. Mean grain size versus sorting in Rose Run sandstones from cores 1 and 2 from the #2 Hammermill well in Erie County, Pennsylvania.
109. Intergranular volume-cement diagram with all Rose Run samples from the #2 Hammermill well in Erie County, Pennsylvania plotted.
110. Intergranular volume-cement diagram with only Rose Run samples that lack dolomite cement plotted.
111. Intergranular volume-cement diagram with only dolomite-cemented samples plotted.
112. Intergranular volume-cement diagram with all data shown.
113. Compactional porosity loss plotted against cementational porosity loss in the Rose Run sandstone samples from the #2 Hammermill well in Erie County, Pennsylvania.
114. Enlarged intergranular porosity in Rose Run sandstone samples from Ohio.
115. Porosity developed in Rose Run sandstone samples from Ohio.
116. Ratio of secondary porosity to reduced primary and intercrystalline porosity versus total porosity for Rose Run sandstones from the #2 Hammermill well in Erie County, Pennsylvania.

Figure 117. Frequency polygon for porosity in the Rose Run sandstones from the #2 Hammermill well in Erie County, Pennsylvania.

118. Type 4 and type 2 dolomites from Ohio.
119. Type 1 and type 7 dolomites from Ohio.
120. Relative timing of major diagenetic events for the Rose Run sandstone.
121. Triangular plot of porosity types in the Rose Run sandstones from the #2 Hammermill well in Erie County, Pennsylvania.
122. Vuggy porosity in a Beekmantown/Mines dolostone from the #2 Hammermill well in Erie County, Pennsylvania.
123. Capillary pressure curves of three Rose Run samples from the #2 Hammermill well in Erie County, Pennsylvania.
124. Graphical description of core 3 from the #2 Hammermill well in Erie County, Pennsylvania.
125. X-ray diffraction scan of a Lower Sandy member arkosic arenite from from core 3 in the #2 Hammermill well, Erie County, Pennsylvania.

- Table 1. Petrographic data for sandstones from the #2 Hammermill well, Erie County, Pennsylvania.
2. Average percent dolomite, clay, quartz overgrowths (OG), feldspar overgrowths (OG), and porosity for each Ohio county studied.
 3. Summary of sandstone data sets for plot shown in Figure 110. Data are for the #2 Hammermill well in Erie County, Pennsylvania.
 4. Variations in porosity for sandstone facies in the #2 Hammermill well in Erie County, Pennsylvania.
 5. Examples of Rose Run sandstones from Ohio that display the various combinations of porosity and permeability.
 6. Typical seismic reflection processing parameters.

Abstract

The Upper Cambrian Rose Run sandstone of eastern Ohio and western Pennsylvania is currently the most active exploratory play in the Appalachian basin. Oil and gas production results from an interplay of reservoir heterogeneities at three scales: 1) megascopic, or global to regional scale; 2) mesoscopic, or field to well scale; and 3) microscopic, or thin-section scale.

Deposition of the Rose Run sandstone occurred as a result of a combination of global and regional variations in climate, geography, sea level, and tectonic movements. The arrangement of crustal plates during the Late Cambrian had a profound effect on global oceanographic and atmospheric circulation patterns. These in turn affected climate and sea level fluctuations around the world. Regionally, Rose Run heterogeneities consist of depositional, stratigraphic, and structural variations. Upper Cambrian rocks in eastern North America represent deposition on, or adjacent to, a broad rimmed platform of low relief that was subject to periodic sea level changes. This resulted in a series of complex mixed carbonate-siliciclastic sequences, dominated by carbonates, that are difficult to predict from well to well or outcrop to outcrop. Much of the heterogeneity observed in the Rose Run is related to the large variety of depositional processes whose sedimentary products were vertically stacked as interbedded carbonate and siliciclastic facies sequences as a result of sea-level variations across the shallow platform.

Structural complexities resulting from reactivated basement faults affected both deposition of the Rose Run and related strata and later development of Upper Cambrian reservoirs and traps. Extensional features, such as the Rome trough, wrench fault assemblages (cross-strike structural discontinuities), and tectonic inversion of basement faults can be recognized in seismic data and by traditional mapping efforts. The eventual effect of these structures was to offset strata, create fractures, and provide channels for fluid migration through the Lower Ordovician and Upper Cambrian rocks. However, the single most important prominent regional feature associated with Rose Run heterogeneity is the Knox unconformity, a major erosional surface that truncated the Upper Cambrian and Lower Ordovician rocks of eastern North America.

This feature played a major role in the entrapment of hydrocarbons within Cambrian strata of the region by: 1) juxtaposing Rose Run sandstone reservoirs with impermeable dolostones and shales of the overlying Middle Ordovician Wells Creek/Shadow Lake interval;

and 2) creating paleotopographic highs, or paleoremnants, on the Beekmantown/Mines dolostone that was subjected to karstic processes such as dissolution and creation of vugs and other cavities that became potential reservoirs.

At the field to well scale, mixtures of carbonate and siliciclastic rocks are the result of both spatial and temporal variability, creating acute and complex reservoir heterogeneities. Eight types of reservoir heterogeneity (modified from Weber, 1986), occur within the Rose Run and Beekmantown/Mines intervals, including: 1) faults; 2) discrete genetic units; 3) permeability zonation within genetic units; 4) baffles within genetic units; 5) laminations and cross-bedding; 6) microscopic textural and mineralogic variations; 7) fractures, and 8) erosional truncation and paleotopography.

Each is important locally, on a field-by-field or well-by-well basis. In addition, the Upper Cambrian rocks of the study area consist of several lithofacies consisting of various sandstone, dolostone, and mixed dolostone-sandstone associations. Reservoir heterogeneity types are restricted to specific lithofacies, and hydrocarbon production within Rose Run and Beekmantown/Mines oil and gas fields results from a complex interplay of many of the heterogeneity types and their associated lithofacies. Cross-bedded and flaser-bedded sandstones, the dominant siliciclastic lithofacies in the Rose Run sandstone, has the highest reservoir quality observed. Interbedded sandstone and dolostone lithofacies exhibit good reservoir quality. Bioturbated dolostone and laminated dolostone lithofacies generally exhibit poor reservoir quality.

Five case studies of productive fields in Ohio and Pennsylvania indicate that production from Upper Cambrian and Lower Ordovician rocks is also associated with six possible trapping mechanisms, including: 1) erosional remnants; 2) fault-related traps; 3) combination fault-related and erosional remnants; 4) erosional truncations at an angular unconformity; 5) anticlines and plunging noses; and 6) updip or lateral pinchouts of facies. The major controls of lateral continuity or heterogeneity of Beekmantown/Mines dolostone and Rose Run sandstone are erosional truncation and paleotopography on the Knox unconformity. In general, seismic exploration can play an integral role in the understanding of heterogeneity. Use of advanced seismic techniques, such as instantaneous phase and frequency-attribute processing of seismic reflection data, and vertical seismic profiling (VSP), appears to be effective in defining the presence of hydrocarbons,

evaluating zones of vuggy porosity, and diagnosing stratigraphic changes and fracturing within a reservoir. However, the use of seismic data as a predictive tool is limited in certain fields, such as areas of limited drilling.

On a microscopic scale, heterogeneity in the Rose Run sandstone and adjacent units is reflected primarily by diagenetic changes and by variations in microstructures and textural features which affect the oil and gas producing potential of the reservoir rocks. Understanding the composition and texture of a sandstone is useful for measuring and predicting reservoir heterogeneity because rocks with contrasting compositions respond differently to diagenesis. Rose Run sandstones are predominantly quartz arenites and subarkoses. The four major cementing agents include dolomite, clay minerals, quartz overgrowths, and feldspar overgrowths; because dolomitization was pervasive, dolomite is the dominant cement. Six pore textures occur in the rocks, including intergranular, oversized, moldic, intraconstituent, fracture, and intercrystalline;

secondary intergranular porosity is the most abundant type. Local dissolution of dolomite and, to a lesser degree, feldspars and clays, created good to excellent porosity in many of the Rose Run sandstone beds. Hydrocarbon potential is affected by porosity and permeability variations, clay and dolomite variability, and microfacies variability. Sandstones that have significant quantities of dolomite cement tend to have high porosities but low permeabilities. Sandstones with rare to absent dolomite tend to have high porosities and permeabilities, whereas sandstones that are poorly sorted, dolomite-rich, and interlaminated or interbedded with fine-grained silty sandstones have low porosities and permeabilities. The rock underwent a long and very complicated burial history. Diagenetic and compactional attributes acquired by the sandstones during burial dictates the distribution of fluids and the amount of recoverable hydrocarbons in the rocks.

Executive Summary

The Ohio Division of Geological Survey (ODGS) and Pennsylvania Bureau of Topographic and Geologic Survey (PTGS) conducted a cooperative two-year multidisciplinary research program designed to measure and predict reservoir heterogeneity in the Upper Cambrian Rose Run sandstone in those two states. During the initial year of research, the team focused on regional-scale approaches to defining and describing heterogeneity in this and adjacent units. The second year studies concentrated primarily on heterogeneities observable and predictable in fields, outcrops, well cores, and thin sections.

The Upper Cambrian Rose Run sandstone, a unit composed of interbedded dolostones and sandstones, has produced both oil and natural gas in Ohio and Pennsylvania since the mid-1960's. Since 1961 more than 2,000 wells have been drilled in the two states in the search for exploitable hydrocarbons in the Lower Ordovician and Upper Cambrian Knox Dolomite, of which the Rose Run is a part. Today, drilling of the Rose Run sandstone and overlying Beekmantown/Mines interval of eastern Ohio is the most active exploratory play in the Appalachian basin.

Many geologic factors affect the occurrence and producibility of oil and natural gas in the Rose Run sandstone. Among the more important factors are: 1) depositional setting; 2) stratigraphy; 3) regional and local structural variations; 4) development of a major erosional surface on the rocks during the Early and Middle Ordovician, the Knox unconformity; 5) lithofacies variations within the rocks; 6) and the diagenetic history of the formation, including development of cements and modification of porosity during a 500 million-year history of burial, uplift, and fluid migration. The proximity of folded and faulted rocks to the Knox unconformity surface has produced a paleotopography on the underlying rocks that helps control reservoir potential.

Fifteen cores, hundreds of geophysical logs, and data from numerous seismic surveys were evaluated in the two states during this study. A network of interlocking stratigraphic cross sections was constructed that illustrates the regional stratigraphic and structural relationships of Precambrian rocks to the top of the Upper Ordovician Trenton Limestone. These cross sections aided in evaluating basin architecture during the Late Cambrian to Middle Ordovician, and its relationship to deposition, erosion, and tectonic deformation of the Rose Run sandstone. An isopach map of the Rose Run sandstone, and structure maps on the Knox unconformity and Rose Run sandstone, reveal the

complex interplay of tectonics and basin development on a regional scale.

Examination of the 15 cores, and three outcrops in central Pennsylvania, revealed that the Rose Run interval comprises a complex sequence of interbedded dolostones and sandstones. Some beds are cross-bedded or flaser-bedded quartz arenites or subarkoses, and some are dolostones composed of ooids, thrombolitic algal mounds and laminae, and rip-up clasts. Others are mixtures of these major lithofacies. Eight different types of reservoir heterogeneity, previously defined and adapted to this study, appear to be restricted to specific lithofacies.

Reprocessing of available seismic data revealed that attribute processing steps not commonly used by Rose Run investigators made dramatic improvements in the quality and interpretation of the data. Phase rotation of seismic data for attribute analyses resulted in a higher degree of correlation of synthetic seismograms generated from geophysical logs. Color area plots of certain data forms is advantageous in locating stratigraphic anomalies, fracturing, and possible hydrocarbon presence in the reservoir rocks. Modeling of vertical seismic profiling (VSP) data indicates that zones of vuggy porosity can be recognized on seismic data as an increase in amplitude on the reflector of the Beekmantown/Mines dolostone, which lies on the Rose Run sandstone and commonly forms paleoemnants beneath the Knox unconformity. Modeling of VSP data also shows that the presence of gas in the Rose Run sandstone might cause a four percent decrease in seismic velocity within the unit. This in turn results in a ten percent reduction of acoustic impedance, indicating that this variation might be a good diagnostic tool in predicting hydrocarbons in the reservoir.

A study of 199 thin sections from the 15 cores and three outcrops revealed that the Rose Run sandstone consists of individual quartz and feldspar grains cemented by dolomite, clay minerals, and overgrowths of quartz and feldspar. Dolomitization was pervasive in the unit, and it has obliterated nearly all of the original carbonate textures. Dolomite is the most important cementing mineral in the Rose Run sandstone, and it plays an important role in porosity and permeability variations. Local dissolution of dolomite and feldspars created good to excellent porosity in many of the Rose Run sandstone beds and laminae. However, thin interbedded dolostones, dolomitic sandstones, and thin shale beds created barriers between the more porous zones, thereby inhibiting vertical permeability.

Introduction

This report summarizes the work accomplished during a two-year cooperative study between the Ohio Division of Geologic Survey (ODGS) and the Pennsylvania Bureau of Topographic and Geologic Survey (PTGS) on the identification and description of the reservoir heterogeneity of the Late Cambrian Rose Run sandstone in Ohio and Pennsylvania (Figure 1). This report also includes discussions of the reservoir potential of the Beekmantown dolomite of Ohio (Mines Member of the Gatesburg Formation in Pennsylvania) because of their similar trapping mechanisms and the importance of the stratigraphic relationship between these two units. Together, the Rose Run and Beekmantown have produced over 33 billion cubic feet (bcf) of gas and 750,000 barrels of oil (bbl) in Ohio since the first production from the Rose Run in 1965. Most of the drilling activity has occurred since 1986 (Figure 2).

This is currently the most active exploratory play in the Appalachian basin. Drilling statistics collected by the Ohio Division of Oil and Gas indicate a rapid increase in drilling for Rose Run hydrocarbons since 1986 (Figure 2). Projections for 1992 point to approximately 125 Rose Run penetrations. Exploratory activity has also increased significantly away from the main producing areas in Coshocton, Holmes, and Tuscarawas Counties into Muskingum County and most counties along the subcrop beneath the Knox unconformity in Ohio. New discoveries yielding production from deeper units in the Knox Group and Rome Formation also have kept interest high in the Rose Run in these areas. Significant amounts of commercial hydrocarbons from wells in both states make it a viable target for continued exploitation throughout the region. To date, 99 percent of the Rose Run drilling activity has taken place in Ohio, and with the exception of two wells in northwestern Pennsylvania, all of the productive wells occur in Ohio. One well in south-central Kentucky had a significant show of gas in the Rose Run but was never put on line for production.

The typical Rose Run sandstone in the subsurface of eastern Ohio and western Pennsylvania consists of a heterogeneous series of quartz or feldspathic arenites of variable porosity and permeability, interbedded with mostly impermeable dolostones.

The interval of the Rose Run occurs within the Knox Dolomite of Ohio and Kentucky, and within the upper portion of the Gatesburg Formation of Pennsylvania (Figure 3). The Knox Dolomite in eastern Ohio is a Lower Ordovician and Upper Cambrian unit that is laterally equivalent with, from top to bottom, the lower portion of the Beekmantown Group (Lower Ordovician) and the Mines, upper sandy, and Ore Hill members of the Gatesburg (Upper Cambrian). Because the Knox and Gatesburg are not completely correlative, extensive use of these terms can cause considerable confusion. To eliminate confusion the term Rose Run is used throughout the report.

The Knox Group and Gatesburg Formation consist primarily of dolostones but include important beds and facies of sandstone, limestone, and evaporites that occur in mappable areas of the basin. Throughout much of the Appalachian basin a regional erosional surface called the Knox unconformity truncates the tops of these formations, and their correlatives in other states. The paleotopographic surface of the unconformity includes remnants of relatively higher relief (paleoremnants) that are primarily

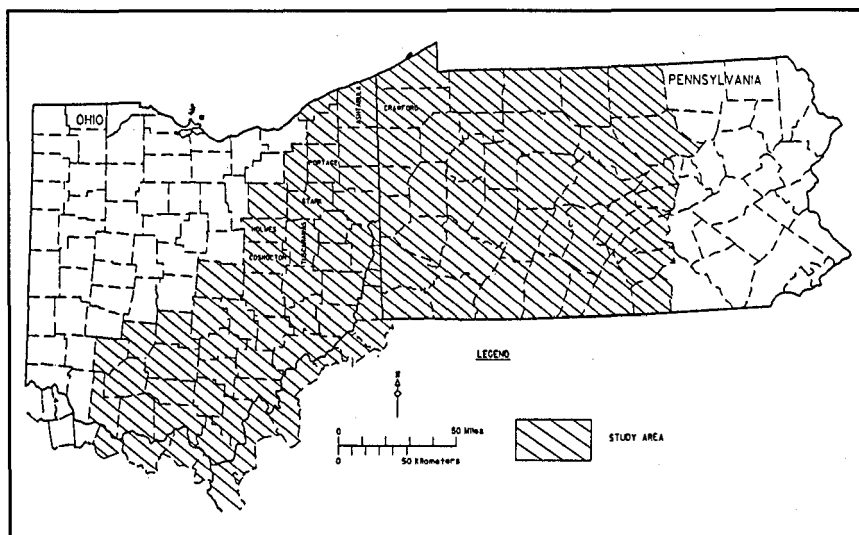


Figure 1. Location of the Rose Run study area.

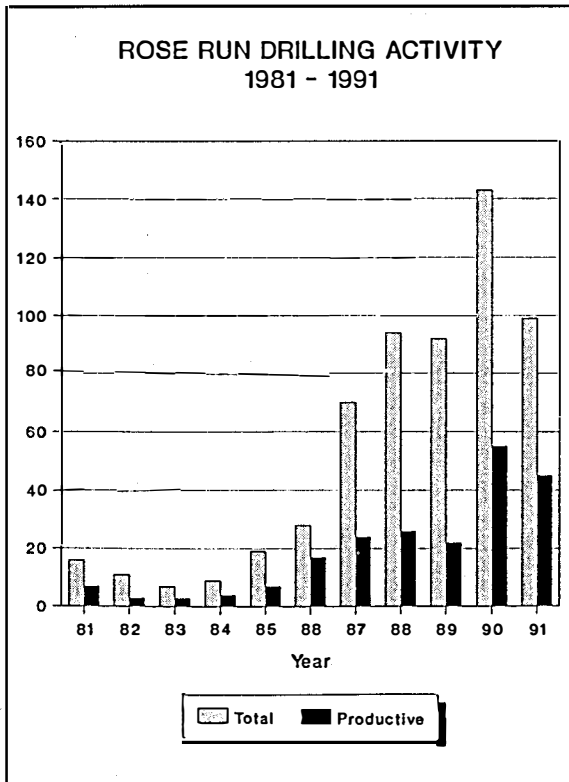


Figure 2. Summary of Rose Run drilling activity in Ohio, 1981 to 1991, (from McCormac, 1992).

responsible for creation of the Rose Run reservoirs. The juxtaposition of folded and faulted sandstone and dolomite beds, and classic angular truncation of beds beneath this unconformity, plays a subsidiary role regionally, but is very important locally.

Previous Studies

The Cambrian and Ordovician rocks of the Appalachian Basin have been studied and described in outcrop for over

150 years, beginning with the first geological surveys of New York, Pennsylvania, and Virginia. However, these rocks have remained virtual enigmas until only recently. Stratigraphic studies dominated earlier works, but they tended to confuse, rather than enlighten because nomenclature was drawn from many different areas, some as far away as the Mississippi Valley area (for example, Fettke, 1948). Summaries of older work can be found in Calvert (1962) and Janssens (1973) for Ohio, Wagner (1966b, 1966c, 1976) for Pennsylvania, McGuire and Howell (1963) for Kentucky, Flagler (1966) and Rickard (1973) for New York, and Markello and Read (1981, 1982), Mussman and Read (1986), Pfeil and Read (1980), and Read (1980, 1989) in Virginia.

Freeman (1949) first used the name Rose Run sandstone, placing the unit in the Elvins Group of the Ozarks and correlating it with the Davis Member of the Elvins. McGuire and Howell (1963) considered the Rose Run to be the oldest submember of the Chepultepec Dolomite Member (lowermost dolomite of the Beekmantown Formation), and used it to subdivide the Knox Dolomite Group into a lower Copper Ridge Formation and an upper Beekmantown Formation.

Calvert (1962) correlated the Sauk sequence (Mt. Simon Sandstone to Knox Dolomite interval) where it crops out in the Rose Hill district in Virginia and eastern Kentucky

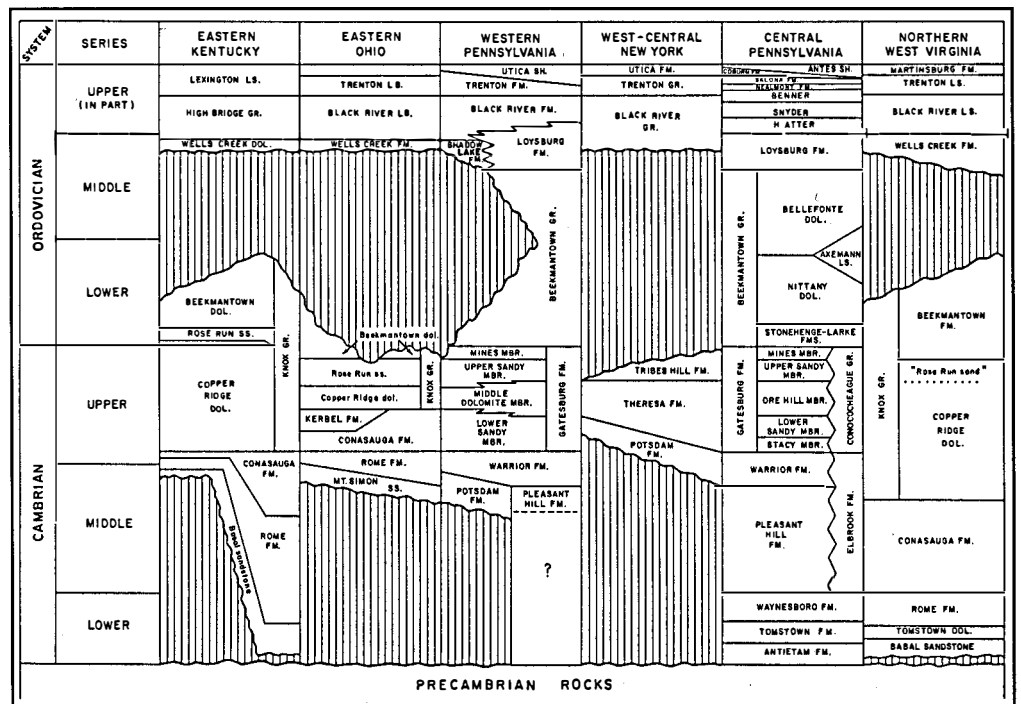


Figure 3. Generalized correlation diagram for Cambrian and Ordovician rocks in Ohio, Pennsylvania, and adjacent states.

to a well drilled to the Precambrian in Fayette County, Ohio. Based upon these correlations, he adopted the stratigraphic nomenclature used in Tennessee, Kentucky, and Virginia (Figure 4).

Wagner (1961) attempted to establish a workable nomenclature for Cambrian and Ordovician sequences in northwestern Pennsylvania where different nomenclatures used in Ohio, New York, and central Pennsylvania seemed to converge. He eventually (Wagner, 1966a-c, 1976) adopted the central Pennsylvania nomenclature of Kay (1944), Wilson (1952), and others for the majority of rocks in western Pennsylvania.

Janssens (1973), in a detailed stratigraphic study of the Cambrian and Lower Ordovician rocks in Ohio, recognized the Rose Run as a mappable unit in the subsurface in eastern Ohio, but did not attempt to name it formally (Figure 4). He recognized the Beekmantown, Rose Run, and Copper Ridge as informal units within the Knox Dolomite.

More recently Shearrow (1987) conducted a study of the Cambrian and Lower Ordovician focused in northwestern Ohio. He correlated his work into Michigan and agreed with Fettke (1948) in the use of Upper Mississippi Valley terminology for the Cambrian and Lower Ordovician section (Figure 4).

Ohio nomenclature used in this report (Figure 4) is a combination of Janssens (1973) and drillers' terms. Additional drilling to the Knox since Janssens (1973) shows that the Beekmantown, Rose Run, and Copper Ridge of drillers are correlatable units in the subsurface and should be recognized as formal units.

Petrography and petrology

of cores from Ohio comprised the major contributions of Baker (1974), Heald and Baker (1977), NuCorp Energy Company (1977), Atha (1981), Enterline (1991), and Reservoirs, Inc. (1992). In addition, Smith (1969) reported on the petrography and porosity relationships in the Gatesburg Formation of central Pennsylvania.

Current Methods of Study

Methods and techniques applied to aid in predicting the heterogeneity of the Cambrian Rose Run sandstone reservoir include: 1) well-log correlation and interpretation; 2) descriptions of numerous cores (Figure 5) and drill cuttings; 3) cross section generation; 4) construction of structure, isopach, lithostratigraphic, and paleotopographic maps; 5) petrographic analysis; 6) X-ray diffraction studies; 7) scanning electron microscopy; 8) porosity and permeability analyses; 9) mechanical well logging; and 10) reprocessing, modelling, and analysis of seismic data obtained in Ohio (Figure 6). See Appendix I for a complete description of the methods employed in this study.

Acknowledgements

Numerous individuals assisted us in this research effort, including: J. McDonald generated the computer

FETTKE (1948) UPPER MISSISSIPPI VALLEY		OBLVIERE (1964)		JANSSENS (1973)	DRILLERS	SHEARROW (1987)	THIS STUDY OHIO/PENNSYLVANIA
SUPER GROUP	GROUP	FORMATION	SUPER GROUP	GROUP	FORMATION AND MEMBER	FORMATION	FORMATION AND MEMBER
TRENTON	GALENA	OLBRIE STEWARTVILLE DOL. PRESSA L.S.	OTTAWA L.S.	TRENTON L.S.	TRENTON L.S.	TRENTON	TRENTON
	DEONIA SH. PLATEVILLE L.S.	BLACK RIVER		BLACK RIVER L.S.	BLACK RIVER	BLACK RIVER	BLACK RIVER
KNOX	ST. PETER SS.	CHAZY L.S.	BEEKMANTOWN	CHAZY L.S.	CHAZY L.S.	CHAZY L.S.	CHAZY L.S.
	SHAKOPEE DOL.	UPPER MIDDLE		UPPER MIDDLE	UPPER MIDDLE	UPPER MIDDLE	UPPER MIDDLE
	NEW RICHMOND SS.	LOWER		LOWER	LOWER	LOWER	LOWER
	ONEIDA DOL.	BECKMANTOWN		BECKMANTOWN	BECKMANTOWN	BECKMANTOWN	BECKMANTOWN
SAUK	TREMPEALEAU	CHEPIA TEPEC DOL.	KNOX DOL.	CHEPIA TEPEC DOL.	CHEPIA TEPEC DOL.	CHEPIA TEPEC DOL.	CHEPIA TEPEC DOL.
	FRANCISIA DRESBACH	LEE VALLEY		LEE VALLEY	LEE VALLEY	LEE VALLEY	LEE VALLEY
	EAU CLAIRE	COPPER RIDGE DOL.		COPPER RIDGE DOL.	COPPER RIDGE DOL.	COPPER RIDGE DOL.	COPPER RIDGE DOL.
MONTVALLO	MT. SIMON SS.	MAYNARDVILLE DOL.	KNOX DOL.	MAYNARDVILLE DOL.	MAYNARDVILLE DOL.	MAYNARDVILLE DOL.	MAYNARDVILLE DOL.
	PRECAMBRIAN	CONASAUBO SH. ROME FM. SHADE DOL.		CONASAUBO SH. ROME FM. SHADE DOL.	CONASAUBO SH. ROME FM. SHADE DOL.	CONASAUBO SH. ROME FM. SHADE DOL.	CONASAUBO SH. ROME FM. SHADE DOL.
PRECAMBRIAN	PRECAMBRIAN	MT. SIMON SSE	KNOX DOL.	MT. SIMON SS.	MT. SIMON SS.	MT. SIMON SS.	MT. SIMON SS.
	PRECAMBRIAN	PRECAMBRIAN		PRECAMBRIAN	PRECAMBRIAN	PRECAMBRIAN	PRECAMBRIAN

Figure 4. Changes in Cambrian and Ordovician stratigraphic nomenclature used in Ohio.

maps; A. Bailey and P. Nicklaus entered well completion data into the database; M. Lester, B. Stewart, and L. Balogh drafted the figures; G. Yates and R. Rea slabbled Rose Run and Beekmantown cores; W. Rike performed a petrologic study of well cuttings; L. Chubb ran X-ray diffraction scans of Rose Run core samples; B. Randall

correlated the Silurian "Packer Shell" marker to be used in mapping shallow structure; A. Janssens collected production data; B. Ullom provided extensive support in the write up and interpretations of seismic reflection data; B. Roth modeled well and seismic data; D. Gardner assisted with the interpretations of seismic data and monitored repro-

cessed seismic data.

S. Berkheiser, D. Hoskins, D. Patchen, R. Shumaker, and J. Wicks reviewed the manuscript.

We acknowledge the following companies and individuals without whose cooperation this project could not have been completed: NGO Development, Inc. and Consolidated Resources of America for allowing the Ohio Division of Geologic Survey to participate in evaluating a Rose Run well for this project; M. Garber and M. Puckett of Schlumberger Well Services for well logging and vertical seismic profile (VSP) interpretation and processing; Reservoir Inc. for porosity and permeability analyses and scanning electron microscopy (SEM) work on the Rose Run test well; Tom Atha, Bakerwell Services Incorporated, Excalibur Exploration Incorporated, Kenoil Incorporated, NGO Development Corporation, Stocker and Sitler Incorporated, and West Bay Exploration Company for donating seismic data used in this study; and Ed Blott, Frontier Processing Company, Hosking Geophysical Company, and Lauren Geophysical Processing Services for reprocessing seismic data for the study.

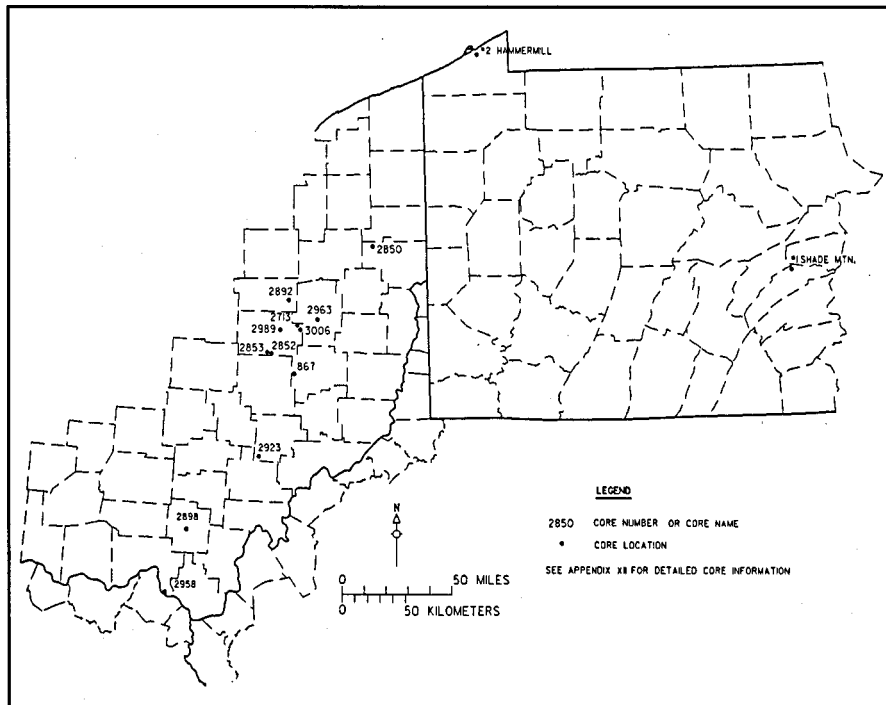


Figure 5. Locations of cores examined in this study. See Appendix XII for detailed information.

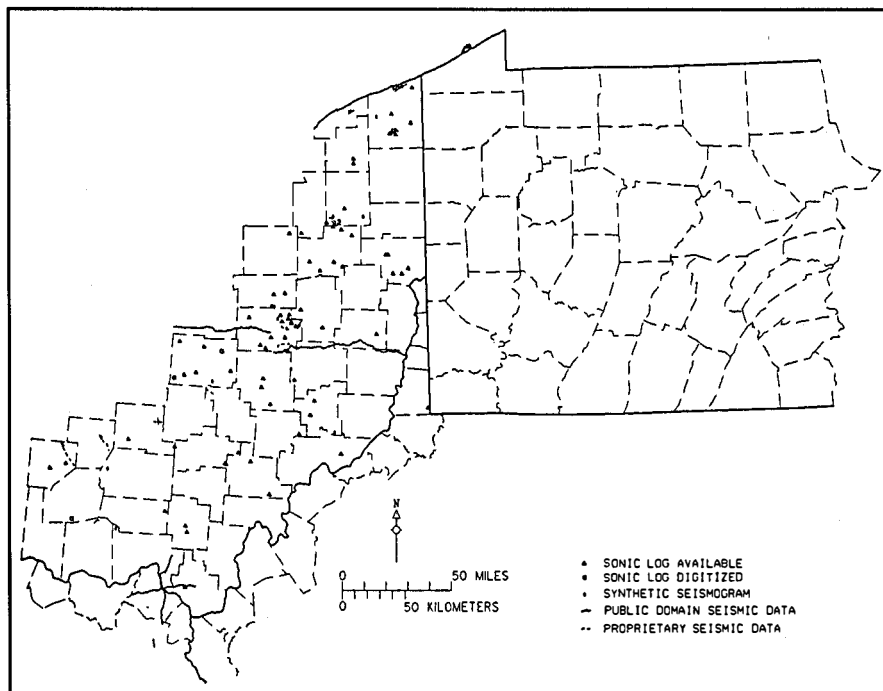


Figure 6. Locations of seismic data, sonic logs, and synthetic seismograms used in this study.

Summary of Historical Production

Although oil had been found in Cambrian rocks of Ohio in limited quantities prior to 1900, the discovery of oil near Tiffin, Pleasant Township, Seneca County in 1909 initiated a small flurry of activity throughout much of the central part of the state (Dolly and Busch, 1972). Between 1909 and 1938 Cambrian oil production was characteristically small, with initial potentials (IP's) of 25 to 100 barrels of oil per day (bopd), accompanied by produced brines. By 1940 the Cambrian section had virtually fallen into disfavor with the Ohio oil and gas industry.

A resurgence of interest in the potential reservoirs in the Cambrian section occurred in the early 1960's due to significant discoveries in Ontario and Ohio. Discovery of the Gobles oil field in Cambrian sandstones of Oxford County, Ontario restimulated interest in this portion of the geologic section in 1960. A year later United Producing Co. completed the #1 Orrie Myers well in Canaan Township, Morrow County, Ohio. According to Dolly and Busch (1972, p. 2336), this well was completed in a 123-foot section of vuggy dolostone with an open flow of 200 barrels of 39° API gravity oil between 2,908 and 3,031 feet. Ultimate recoverable reserves were estimated as high as 800,000 barrels of oil (bo). This discovery set off such an understandable flurry of interest in the Cambrian rocks of Morrow County and adjacent areas that between 1961 and 1964 a total of 1,610 wells were drilled in search of exploitable reserves; 1,340 wells were drilled in 1964 alone. So many wells were drilled, many at such close spacing and with so little regard for conservation, that the Ohio Division of Mines (regulatory predecessor of the Ohio Division of Oil and Gas) had to adopt new oil and gas regulations.

The discovery well for the Rose Run sandstone in Ohio, the Kin-Ark #1 Reuben Erb well, was drilled in 1965 in Clark Township, Holmes County. It penetrated 110 feet of the Rose Run and was completed with

an initial daily production rate of 2.1 million cubic feet of gas per day (MMcfd) and 10 barrels of oil (bbl). After the first six years of production, this well had produced approximately 831 MMcf (Janssens, 1973); it produced about 3,432 bo and 1.9 billion cubic feet of gas (Bcf) between 1975 and 1992.

During this period, the excitement of the Ohio Cambrian play spread to neighboring states. In northwestern Pennsylvania the Cambrian had been tested as early as 1941, but without success. Sporadic drilling between 1941 and 1963 resulted in thirteen wells in western and central Pennsylvania, but none of these had more than small shows of oil and/or natural gas. With the excitement over Cambrian production in Ohio as a spur, Pennsylvania's oil and gas industry, particularly Transcontinental Petroleum Corp. and James Drilling Co., initiated drilling programs that eventually resulted in 22 wells drilled between 1963 and 1966. Of these, two wells produced hydrocarbons and several others had "significant shows" of hydrocarbons.

The first successful well, the Transamerican Petroleum #1 Scull, drilled in Spring Township, Crawford County in 1964, had an untreated open flow of 2.59 MMcfd and

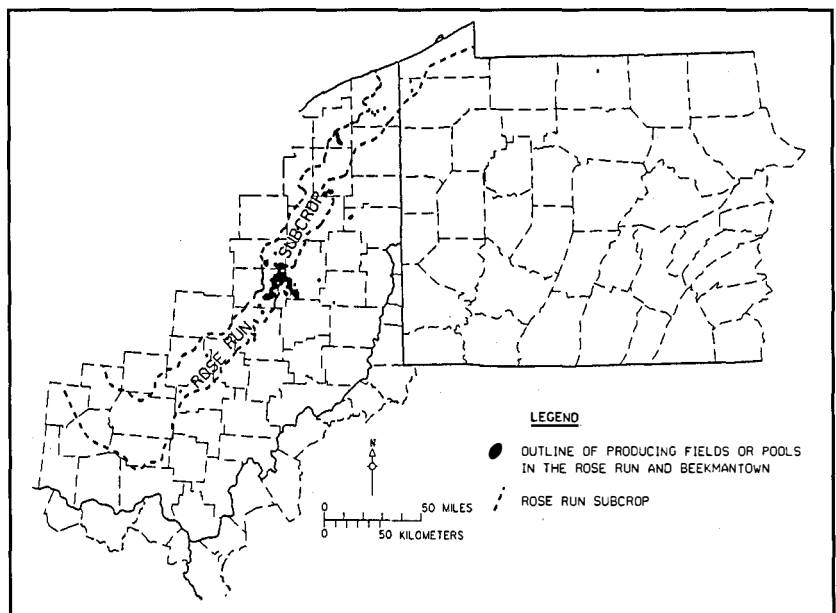


Figure 7. Map of producing fields and pools in the Rose Run sandstone and Beekmantown/Mines dolomite.

6 barrels of condensate per million cubic feet of gas from the interval 6,308 to 6,311 feet. The well was produced with high back pressure for 18 months. The well was then shut in for two months, and when it was reopened the flow of hydrocarbons had been replaced by water. The total production from the well was 190 MMcfg and 1,100 barrels of condensate (Harper and others, in press).

Since 1966, only 18 additional Cambrian tests have been drilled in Pennsylvania with only two successes, one produced from the Beekmantown/Mines interval and the other from the Ordovician Beekmantown Group (see Figure 3 for the distinction between these units). Several wells were drilled in central and eastern Pennsylvania as unsuccessful tests of the Eastern Overthrust Belt.

Interest in Cambrian production occurred once again in the late 1970's and 1980's as a result of higher prices for both oil and natural gas, and the discovery of some very high-reserve wells. This interest continues today as Ohio drillers put down record numbers of holes. From 1981 until 1991 the increase in drilling for Cambrian prospects has been three fold (Figure 2). Of 387 wells drilled to the Rose Run in Ohio during the period 1987-1990, 107 (28 percent) were considered productive. Unproduc-

tive Cambrian wells are commonly plugged back and treated in either the Lower Silurian Clinton/Medina sandstones or the Mississippian Berea Sandstone. During that same period, only five Cambrian tests were drilled in northwestern Pennsylvania, and all wells were plugged back and completed in the Medina Group. Cambrian (and Lower Ordovician) fields and pools discovered so far in the study area are shown in Figure 7.

Difficulties in exploration and production of the Rose Run is primarily to reservoir heterogeneity caused by erosional truncation and paleotopography on the Knox unconformity. Exploration techniques vary among operators. Many drillers simply lease enough land to drill a well, knowing that if the Cambrian proves unsuccessful the well can be plugged back and completed in the Lower Silurian Clinton/Medina section. The more serious investigators use subsurface mapping, seismic surveys, gravity, and magnetics to explore for subtle reservoirs and traps containing Rose Run hydrocarbons. These techniques have worked successfully in Ohio during the past decade, and some operators are beginning to apply the same techniques in Pennsylvania.

Heterogeneity of the Rose Run Sandstone

The interval of the Rose Run sandstone exhibits heterogeneity primarily at three scales: 1) megascopic, that is, it varies lithologically and structurally over a wide geographic extent because of regional-scale influences in depositional setting and tectonic deformation; 2) mesoscopic, in the sense that within a field, outcrop, or single well there is considerable lithologic variability both laterally and vertically within the section, and these are strongly modified by structural and paleotopographic anomalies; and 3) microscopic due to local- to regional-scale variations in composition and diagenesis.

Most of the work done on this project during the first year (FY 1991) consisted of examination of the megascopic heterogeneities of the Rose Run sandstone. This work concentrated on global (paleogeographic and plate tectonics), continental (Laurentian paleogeography and depositional setting), and regional (Ohio and Pennsylvania) perspectives. Second year (FY 1992) studies concentrated primarily on heterogeneities observable and predictable in fields, outcrops, wells, and thin sections.

Megascopic (Regional-Scale) Heterogeneity

Introduction

Reservoir heterogeneity of the Rose Run sandstone results from a complex set of factors which include: 1) global tectonic patterns and their effect on oceanic and atmospheric circulation patterns; 2) variable depositional settings and their associated lithofacies; 3) development of the Knox unconformity and Rose Run subcrop during the Early and/or Middle Ordovician; and 4) regional tectonic influences and associated structural controls. The Rose Run sandstone can be seen as a mixed carbonate-siliciclastic depositional sequence within a very thick carbonate-dominated unit. Discussions of megascopic heterogeneity for the Rose Run sandstone can not be adequately described without examining the entire Knox Dolomite in Ohio and Gatesburg Formation in Pennsylvania, and placing them within the perspectives of their regional depositional setting and tectonic deformation. Therefore, discussions of the Rose Run sandstone necessarily include discussions of the underlying and overlying rock units.

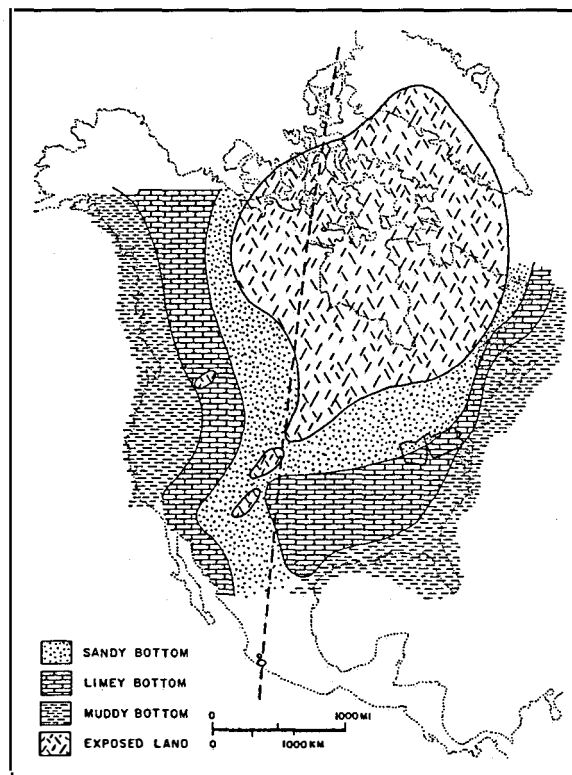


Figure 8. Generalized paleogeography and depositional setting of the Laurentian plate during the Late Cambrian (modified from Dott and Batten, 1976). The present landmass configuration, shown by dotted lines, and the outlines of Ohio and Pennsylvania are shown for orientation.

Global Perspective

Paleogeography, Provenance, and Plate Tectonics

During the Late Precambrian and Early Paleozoic, Ohio and Pennsylvania were part of a large crustal plate, called Laurentia, that occupied a position straddling the equator. Laurentia as illustrated in Figure 8 includes the continental shelf and parts of the continental slope and rise. The major land mass of Laurentia included what is now called the Canadian Shield and, according to some reconstructions, the Transcontinental Arch. In Figure 8 the Transcontinental Arch is shown as a peninsula and a series of islands.

The probable configuration of the Late Cambrian-Early Ordovician crustal plates is shown in Figure 9. The Iapetus Ocean seems to have originated in the Late Precambrian, between 650 and 570 Ma, when the northwestern margin

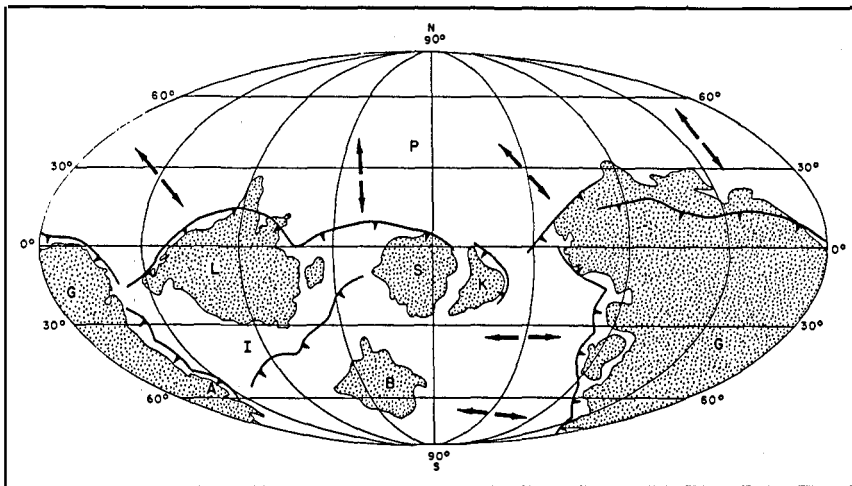


Figure 9. Global Late Cambrian plate tectonic reconstruction (modified from Scotese and McKerrow, 1991). Continents include Baltica (B), Gondwana (G), Kazakhstan (K), Laurentia (L), and Siberia (S). Seas include the Iapetus (I) and Paleotethys (P) Oceans.

of the Baltic plate rifted away from the southern margin of Laurentia (in terms of modern cardinal directions, the southern margin of Baltica and the eastern margin of Laurentia-Scotese and McKerrow, 1991; Figures 10A, 10B). At that time the southern margin of Laurentia, including the continental shelf area that would eventually become Ohio and Pennsylvania, became a passive continental margin.

During the Early and Middle Cambrian the Grenville rocks in much of what is now the study area of eastern Ohio and western Pennsylvania remained exposed to erosion. Sedimentary and metasedimentary rocks lithified from Early Cambrian clastic sediments occur only in central and eastern Pennsylvania, and most of the Middle Cambrian rocks lie in the eastern three-fourths of Pennsylvania. Deposition of basal orogenic sands on the Precambrian unconformity in Ohio and western Pennsylvania began late in the Middle Cambrian as sea level rose and/or the southern margin of Laurentia subsided in response to the weight of increasing amounts of sediment.

During the Early or Middle Cambrian an aulacogen, the Rome trough, formed along the southern margin of the exposed land mass of Laurentia. Harris (1978) described the Rome trough as the failed arm of a triple junction, extending from the Mississippi embayment through Kentucky to Pennsylvania, and into New York. The aulacogen probably originated on incipient Precambrian crustal-block faults derived from stresses during opening of the Iapetus Ocean.

Recycled orogenic sands continued to be deposited throughout much of the Late Cambrian, but by that time they were mixed with the shelf carbonates that eventually dominated sedimentation on the shelf. Sandstone suites from the central and eastern United States are mostly quartzose, reflecting their origin from tectonically stable portions of the craton (Dickinson and others, 1983; Figure 11).

Clastic petrofacies are distinctive detrital suites that

reflect the tectonic setting of their source area (Miall, 1984). Understanding the provenance of a sandstone's framework is useful for measuring and predicting reservoir heterogeneity because rocks with contrasting detrital compositions, "... respond differently to

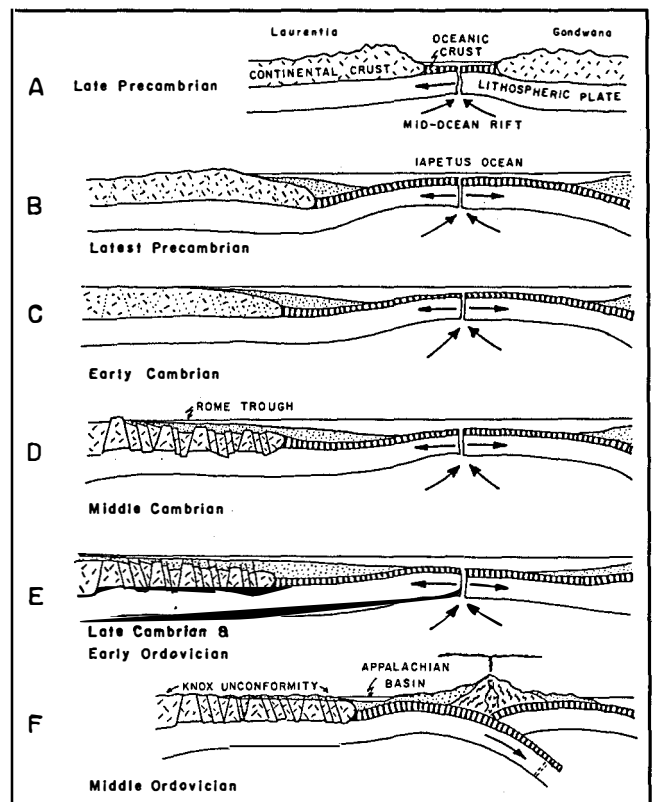


Figure 10. Diagrammatic model of the plate tectonic history of the study area from Late Precambrian to Middle Ordovician. The model is based in part on Dietz, 1972.

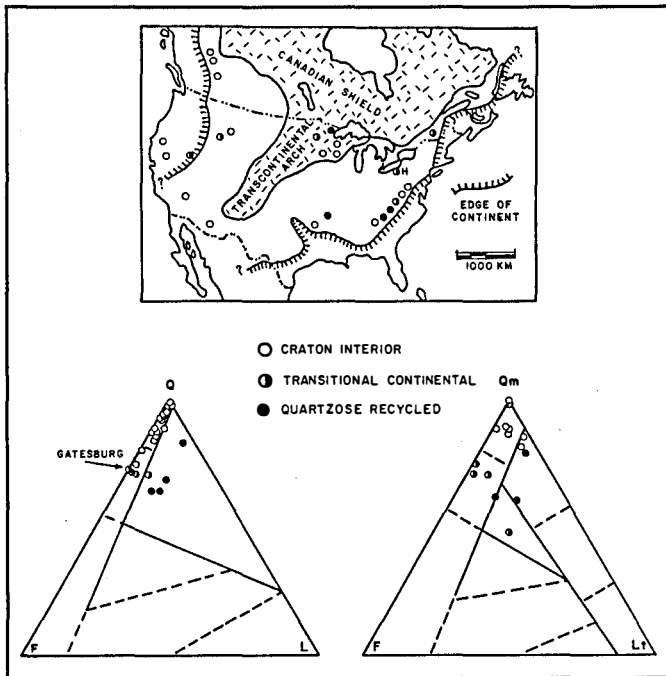


Figure 11. Paleotectonics and sandstone provenance in North America (modified from Dickinson and others, 1983). A. Paleotectonic map showing locations of sandstone suites for Late Precambrian to Middle Ordovician time. H (on Lake Erie)—Hammermill Paper Co. #2 Fee well, Erie County, PA. B. Ternary sandstone composition diagrams. QFL (left) and QmFLt (right) indicate most North American sandstone suites contain quartzose frameworks indicating their derivation from the stable craton. Some suites in different area have more feldspathic frameworks indicating a continental block provenance transitional between basement uplift and cratonic sediment sources. Rose Run and Conasauga/Gatesburg Lower Sandy sandstones fall into this latter category.

diagenesis, and thus display different trends of porosity reduction with depth of burial” (Dickinson and Suczek, 1979, p. 2164).

Dickinson and Suczek (1979) found that the modal quantities determined from thin-section point-count data were useful for diagnosing the tectonic setting of sandstone source areas. They recognized three general groups of provenances and their derivative sandstone suites: 1) continental block; 2) magmatic arc; and 3) recycled orogen. Detrital sources on continental blocks are shields and platforms, or faulted basement blocks. Island arcs or active continental margins provide the magmatic arc sandstone suites. Sources of sediment in recycled orogens are deformed and uplifted strata in subduction zones, along collision orogens, or within

foreland fold-thrust belts. In North America, most Cambrian to mid-Ordovician sandstone suites reflect provenances within the continental block.

Based on thin-section point-count data acquired during this study, the quartz arenites and subarkoses in the Rose Run sandstone all reflect a continental block provenance, specifically a source in the craton interior (Figures 11 and 12). The sandstones are compositionally mature and reflect their origin from crystalline Precambrian shield complexes and overlying platform rocks (Miall, 1984). The presence of feldspathic sandstones suggest that some basement uplift, with greater relief than land areas of the craton, supplied sediments to the passive margin of southern Laurentia. Potassium feldspar is abundant and widespread in the uppermost portions of the two principal Precambrian basement terranes of Ohio (Lidiak and Ceci, 1991), Potassium feldspars are substantially more abundant in older Cambrian sandstone (Pettijohn and others, 1973; Janssens, 1973). Sandstones in the Lower Sandy member in the Hammermill well are subarkoses and arkoses of a transitional continental block provenance (Figure 12).

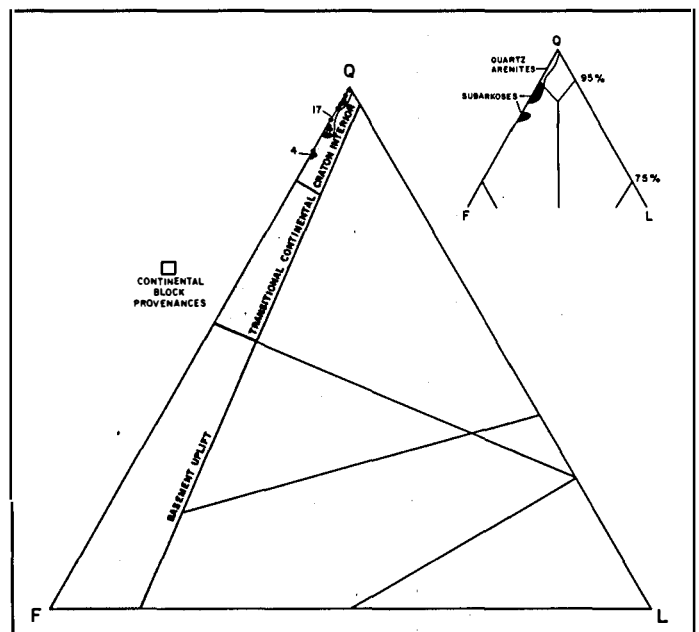


Figure 12. QFL (quartz, feldspar, lithics) diagram with provenance types. The upper portion of the compositional diagram for classifying sandstones (from Pettijohn and others, 1973) is to the upper right. Rose Run sandstones from the #2 Hammermill well are quartz arenites and subarkoses derived from the interior craton. Kerbel/Lower Sandy sandstones fall, in part, into the transitional continental field of the continental block provenance.

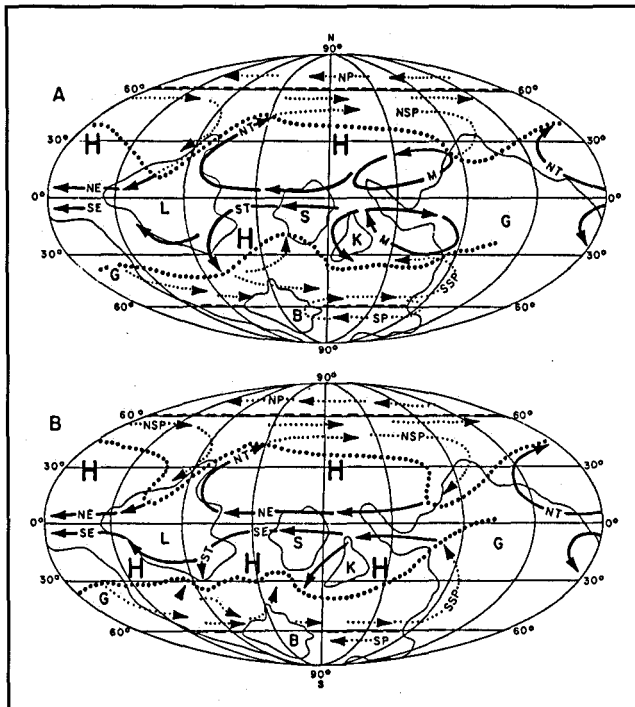


Figure 13. Paleogeography of earth during the Late Cambrian (modified from Wilde, 1991). A—Southern hemisphere summer and northern hemisphere winter. B—Northern hemisphere summer and southern hemisphere winter. Continents and seas are the same as those in Figure 9. Surface currents include north and south polar (NP and SP), north and south subpolar (NSP and SSP), north and south tropical (NT and ST), north and south equatorial (NE and SE), and monsoonal counter (M) currents. Oceanic and atmospheric high pressure cells are designated H.

Much of the sand apparently accumulated around the land mass, whereas most of the carbonates accumulated in the shallow waters of the shelf (Figure 9). Mixing of these sediments occurred during cyclical sea level changes. Movement within the Rome trough continued, thereby continuing to affect deposition (see Rose Run Structure below). By the end of the Cambrian, deposition of quartz sands had almost ceased, whereas the deposition of carbonates continued unabated.

The Iapetus Ocean continued to widen by mid-ocean rifting until sometime during the Early or Middle Ordovician (Figures 10C–E). According to Scotese and McKerrow (1991, p. 273), a former transform boundary in the ocean converted to a subduction zone and the Iapetus began to narrow. Previous workers (for example, Dewey and Bird, 1970) indicated that subduction was to the southwest, with Laurentia overriding the oceanic crust of Gondwana. More recent investigations, however, suggest that subduction actually occurred when the oceanic crust at the northeastern margin of the Avalonian belt, itself a fragment of the Gondwana plate, broke off and began to

override the southern margin of Laurentia (Figure 9), forming an island arc (Rodgers, 1987; Scotese and McKerrow, 1991).

The continental shelf of Laurentia buckled during the initial period of plate collision (Figure 10F). It was block faulted, folded, and regionally uplifted (Mussman and Read, 1986), initiating a period of erosion that beveled progressively older rocks and sediments from south to north (present east to west). This regional erosional surface, called the Knox unconformity, is characterized by erosional relief (subtle to modest paleotopography, with some monadnocks), and localized structural relief as well in the form of anticlinal flexures and block faulting. This surface was subsequently drowned during a higher stand of sea level in the Middle Ordovician. Deposition of post-Knox sediments include basal clastics and carbonates deposited on the margin of the foreland basin, toward the continental interior (Mussman and Read, 1986).

During the later Middle and early Late Ordovician the continental shelf returned to relatively stable conditions, accumulating shelf carbonates in large quantities. These carbonates mixed with clastic muds and occasional bentonites from recurrent tectonic disturbances originating from the convergence of Laurentia with the island arc, especially during the very early part of the Late Ordovician. These disturbances culminated in the Late Ordovician Taconian orogeny when Laurentia collided with the island arc, forming the first Appalachian mountains.

Paleogeography and Paleoclimatology

The global configuration of the planet during the Cambrian is speculative because of the absence of a global standard for Cambrian biostratigraphy, lack of reliable paleomagnetic data, and uncertainty about the absolute age of the Precambrian/Cambrian boundary (Scotese and McKerrow, 1991). The global configurations shown in Figures 9 and 13 are for latest Cambrian and are based on earliest Ordovician configurations. The following discussion on paleogeography is derived from an excellent paper by Wilde (1991), and readers interested in a more complete presentation of the subject are urged to consult this reference. The discussion on paleoclimatology is based on interpretation of Figure 9 using standard meteorological and climatological concepts. Both of these subjects are considered important in order to understand the physical conditions of ocean and atmosphere that led to the deposition of Upper Cambrian and Lower Ordovician sediments.

The oceanic circulation patterns are largely influenced by atmospheric circulation patterns to the point where the two systems commonly coincide. This is because surface oceanic currents are driven by wind. Oceanic circulation patterns during the Late Cambrian, as shown in Figure 13, are based on the planetary configuration of Scotese and McKerraw (1991). The oceanic currents that affected the southern seas of Laurentia resulted from several factors. First, the exposed land masses on the equator (Laurentia, Siberia, and portions of Gondwana) probably fragmented the global oceanic low pressure systems, with the major systems south of the high pressure centers that occupied the embayments in the northern ocean. Within these systems water currents flowed east to west, roughly parallel with the equator. Second, the other equatorial continents of Siberia and Kazakhstan broke up the circulation pattern of the relatively small southern ocean into high pressure centers. Third, a seaway on the southwest side of Laurentia connecting the northern and southern oceans would have produced a high pressure center in the southern hemisphere. All of these factors combined to move warm water along the southwestern margin of Laurentia.

Climatic and meteorological patterns are influenced by the distribution of land masses and oceans. During summer months temperatures tend to be higher and pressures lower on land; the opposite is true in winter. Heated air rises over land and cooler air flows in from the ocean to replace it, bringing moisture and wet monsoons to subtropical and warm temperate areas. In temperate areas northern and southern air masses come into contact and, at great altitude, create jet streams that may affect the weather patterns for an entire season.

The distribution of landmasses and oceans suggested for the Late Cambrian (Figures 9 and 13) would have affected global seasonal weather patterns essentially the same as we experience today, but with the northern and southern hemispheres switched. During summer large landmasses develop centers of low pressure into which considerable amounts of moist air flows (monsoons).

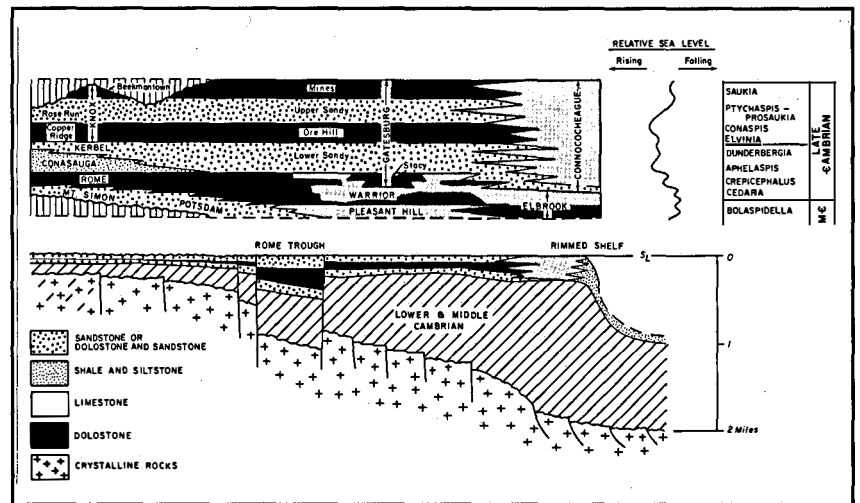


Figure 14. Late Cambrian depositional and stratigraphic relationships (modified from Read, 1989, Figs. 8 and 12). Top—Generalized chronostratigraphic relationships of the Late Cambrian rocks of Ohio and Pennsylvania. Names on the right are trilobite index genera. Bottom—Generalized cross section of the Late Cambrian continental shelf of eastern North America illustrating the concept of the rimmed shelf with platform morphology.

Because land was concentrated in the southern hemisphere during the Late Cambrian, monsoons would have been almost restricted to southern hemisphere summers. Anti-trade monsoon winds would have been generated along the coast of Gondwana, driving warm water eastward and poleward through the seaway between Gondwana and Kazakhstan (Wilde, 1991). The effect of this would have been to counter the flow of cool water from northern midlatitude high pressure systems. In northern hemisphere summer months the lack of large landmasses probably negated the development of monsoon winds there.

Because the southwest-facing coast of Laurentia, where the Rose Run and adjacent rocks were formed, lay between 0° and 30° south latitude (Figure 13) the dominant wind pattern would have been trade winds similar to Recent winds, with some variation due to the configuration of landmasses and oceans. These southeasterly winds must have carried warm maritime air from the moist western side of the high pressure center in the Iapetus Ocean (Figure 13). Along the east coast of Laurentia this air movement would then have provided abundant rainfall in a narrow zone between 15° and 30° south latitude. Although at least part of the east coast of Laurentia must have been abundantly wet during the summer, the position of the continent most likely would have created completely opposite conditions along the southwest coast. Continental west coasts in latitudes 15° to 30° (north or south) are extremely dry, generally with less than 10 inches of rainfall annually. Oceanic subtropical high-pressure cells

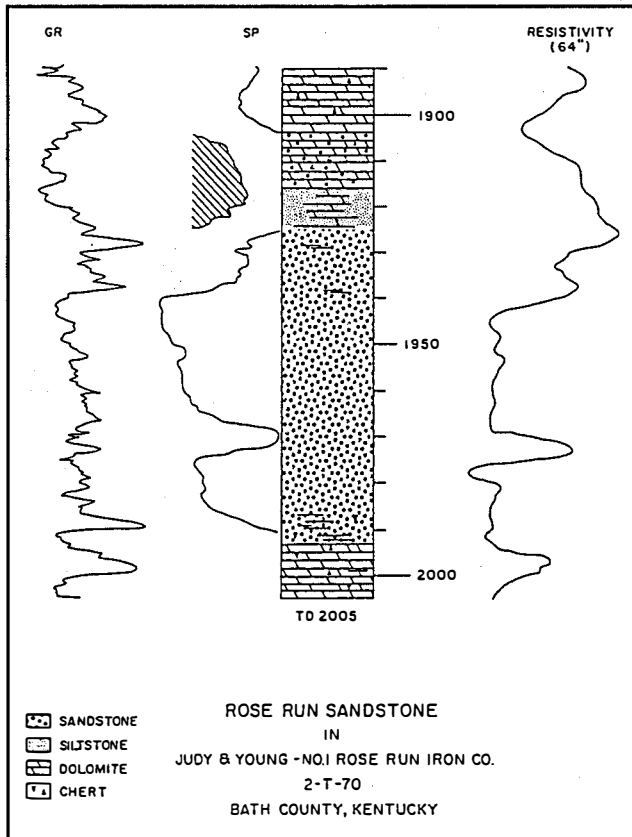


Figure 15. Type section of the Rose Run sandstone in the Judy and Young #1 Rose Run Iron Co. well in Bath County, Kentucky (modified from McGuire and Howell, 1963, Fig. 2-15). GR—gamma ray log; SP—spontaneous potential log.

are inherently dry on the east side because as the air moves downward and equatorward it warms to the point where it reduces relative humidity. On the west side of these cells, the air cools by moving upward and poleward, thereby taking on moisture. Thus, in the trade wind zone the continental coast west of a subtropical high pressure cell tends to receive heavy rainfall, whereas the coast east of that cell tends to be dry. Such conditions are termed West Coast Desert Climates. The principal difference between west coast and continental interior deserts is that the former tend to be relatively cool, with a mean annual temperature of 65°F due to oceanic upwelling along the coast, whereas temperatures average 10°F higher inland. Upwelling along the southwestern coast of Laurentia (Wilde, 1991), coupled with a high pressure system in the Iapetus to the west or southwest, suggests that this region experienced climatic conditions similar to those of Morocco, Baja California, and Western Australia, to name a few representative examples from the Recent.

Depositional Setting

Upper Cambrian rocks in eastern North America represent deposition on or adjacent to a rimmed shelf (Figure 14), a broad, continental shelf of low relief that was subject to periodic eustatic sea level changes. Although most documented sea level changes resulted from glacio-eustasy forced by Milankovitch astronomical cycles, Osleger and Read (1991) found no evidence to suggest that glaciation occurred during the Late Cambrian. At present, there is no documentable reason for the eustatic fluctuations, but the evidence for such fluctuations in the rock record is indisputable. This record consists of complex mixed carbonate-siliciclastic sequences, typically dominated by carbonates. Because of the low relief of the rimmed shelf, periodically raising and lowering sea level a few tens of feet was probably sufficient to drown or expose this surface nearly completely at various times. As a result, deposition during the Late Cambrian was cyclical, with fine-grained quartz sands or lime muds and sands alternating with carbonates exhibiting cryptalgal laminae and hemispheroids, ooids, and other features.

Late Cambrian depositional sequences commonly are cyclical at several scales, from the 300- to 2,000-foot thick “grand cycles” of Aitken (1966), to bed-scale cycles described by Pelto (1942), Krynine (1946), Wilson (1952), and Root (1964), among others.

Grand cycles frequently constitute large portions of formations to entire groups of formations characterized by fine-grained terrigenous mudstones, carbonates, and sandstones that grade upward into sequences consisting predominantly of carbonates. The Rose Run sandstone represents a portion of a grand cycle that correlates with Read’s Late Cambrian cyclic carbonate sequence 4 (Read, 1989, p. 152–153). This sequence includes the Conococheague Formation of Virginia, Gatesburg Formation of Pennsylvania and lower Knox Dolomite of Ohio (Figure 3). Peritidal carbonates dominate this sequence, but subtidal carbonates and peritidal sandstones also occur.

Smaller scale cycles tend to be only a 2.5 to ten feet thick, and mimic the grand cycles in composition. Within the Rose Run sandstone and adjacent units, cyclical peritidal and subtidal carbonate and sandstone sequences dominate the lithofacies, but sandstones interpreted as fluvial and

eolian occur in cores from Erie County, Pennsylvania. This suggests that continental facies may be more common than suspected, and just have not been recognized. Small-scale cycles are mostly asymmetrical and are genetically linked by shared lithofacies (Osleger and Read, 1991).

Stratigraphy

Introduction

The Rose Run sandstone was first described by Freeman (1949) from the Judy and Young #1 Rose Run Iron Co. well in Bath County, northeastern Kentucky. In that well the unit consists of about 70 feet of poorly sorted sandstone approximately 330 feet below the Knox unconformity (Figure 15). McGuire and Howell (1963) considered the Rose Run to be an informal member of the Chepultepec Dolomite, the upper unit of the Knox Dolomite and a correlative of the lower Beekmantown of Pennsylvania and New York. They used it to define the boundary between the Chepultepec and the subjacent Copper Ridge Dolomite (equivalent to the Ore Hill Member of the Gatesburg Formation of Pennsylvania). The name Rose Run was later applied by operators to similar rocks in Ohio and Pennsylvania during the drilling spree of the mid-1960's (see pg. 5, Summary of Historical Production).

The regional stratigraphy of the Upper Cambrian in the study area was established early in the course of this project by a series of cross sections in Ohio and Pennsylvania, and a regional Rose Run isopach map, constructed by Riley and Baranoski (1991) and Harper (1991). The cross section used both geophysical logs (mostly gamma-ray) and sample descriptions, where they existed, for the purpose of tying lithology to log formats. Discussion of the results of these studies is presented below.

Problems of Nomenclature

As in any regional study that crosses state boundaries, there are problems with nomenclature that must be dealt with and agreed upon by all parties involved. This study is no exception. Most of the stratigraphic names from the Middle Ordovician¹ to the Precambrian do not conform between Ohio and Pennsylvania (see Figure 3). For example, in Ohio the dolostones and sandstones of the

Lower Ordovician and Upper Cambrian are called Knox Dolomite, a name derived from Knox County, Tennessee. In Pennsylvania the Ordovician portion of the correlative sequence is called Beekmantown Group (or Formation) and the Cambrian portion is called Gatesburg Formation (in part), names derived from eastern New York and central Pennsylvania, respectively. The type Knox comprises, from bottom to top, blue, oolitic, often fossiliferous dolostone, dark-gray, granular dolostone, and light-gray, cherty dolostone (Safford, 1869). The type Beekmantown comprises interbedded limestones, magnesian limestones, dolostones, and sandstones (Clarke and Schuchert, 1899). The type Gatesburg consists of thick-bedded, steely-blue, coarsely crystalline dolostone with many interbedded layers of quartzose arenite, oolitic chert, and some limestone (Butts, 1918). It is obvious that the only lithologic similarities among these three formations is the use of the term dolostone.

Some of the names currently applied in Ohio come from as far away as Georgia (Conasauga Formation) and Wisconsin (Mt. Simon Sandstone), whereas all of the names applied in northwestern Pennsylvania originated either in central Pennsylvania or in an adjacent state or Canadian province. There has not been a concerted effort in Ohio to establish the validity of much of the stratigraphic nomenclature that has accumulated over the last 100 years. Many of the names were brought in by geologists and drillers from outside the region without regard for accuracy or consistency (drillers, especially, are notorious for using names that refer to rock color, type, or locality rather than formation). Similarly, some of the Cambrian and Ordovician formation names used in the subsurface of western Pennsylvania were applied by correlation of gamma ray signatures and well cuttings over distances of 100 miles or more with little regard to lithologic differences between that area and the type sections (see Wagner, 1966c).

Under the pre-1960 rules of stratigraphy, it was common practice to name and correlate formations on the basis of fossil content. Since 1960, however, the Code of Stratigraphic Nomenclature requires a formation (a lithostratigraphic unit) to be described and correlated only through lithologic criteria. Geologic age and biostratigraphy cannot be used as descriptive factors. Therefore, if Lower Ordovician rocks in Pennsylvania are called Beekmantown it should be because, lithologically, they are similar or identical to Beekmantown rocks in New York, not because they share the same chronostratigraphic or chronologic position.

¹Chronostratigraphic (particularly series) designations are based on global usage, rather than standard North American usage, as recommended by Palmer, 1983.

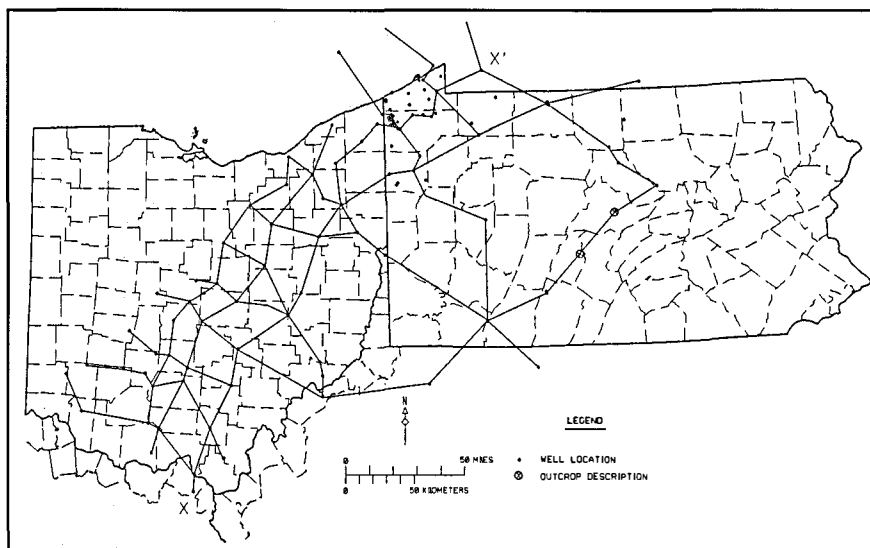


Figure 16. Location of regional cross sections constructed for this study. Cross section X-X' is shown in Figure 18.

It is unfortunate that in a work of this scope issues such as this can only be stated in generalizations. The problem is larger than the study can address; therefore, the problem must be set aside until some future work can resolve the problem. For this study, *in lieu* of addressing the situation further, two steps are taken to simplify matters. First, the name Rose Run sandstone is used for the dominant unit of interest (the middle arenaceous dolostones of the Knox Dolomite and the Upper Sandy Member of the Gatesburg Formation). Second, in this report, those stratigraphic units whose names do not agree across state boundaries are designated by the two disparate names, separated by a slash (e.g. Mt. Simon/Potsdam). The Ohio name is always used first. This method might seem cumbersome to the reader, but it is necessary because neither state is willing at this time to revise its exclusive stratigraphic nomenclature without further detailed study.

Regional Cross Sections

Figure 16 shows the locations of the regional cross sections completed during the study. Wells from both Ohio and Pennsylvania were tied together in a cross section whenever possible. Figure 17, a representative log suite from a Rose Run well in Ohio, has been included as an example of the type of information used in constructing these cross sections, and Figure 18 is an example of

cross section X-X' which is indicated on Figure 16. The entire interval from the top of the Upper Ordovician Trenton Limestone to the Precambrian basement was included in all sections. However, because of the time and space constraints, only the interval from the lower portion of the Late Ordovician Black River limestone to the Precambrian has been included in Figure 18. The cross sections proved very useful for establishing consistency during determination of formation tops and interval thicknesses. Some

of these cross sections currently are available as open-file reports (see Appendix II).

Regional Maps

Regional stratigraphic maps constructed for this study include subcrop and isopach maps of the Rose Run sandstone.

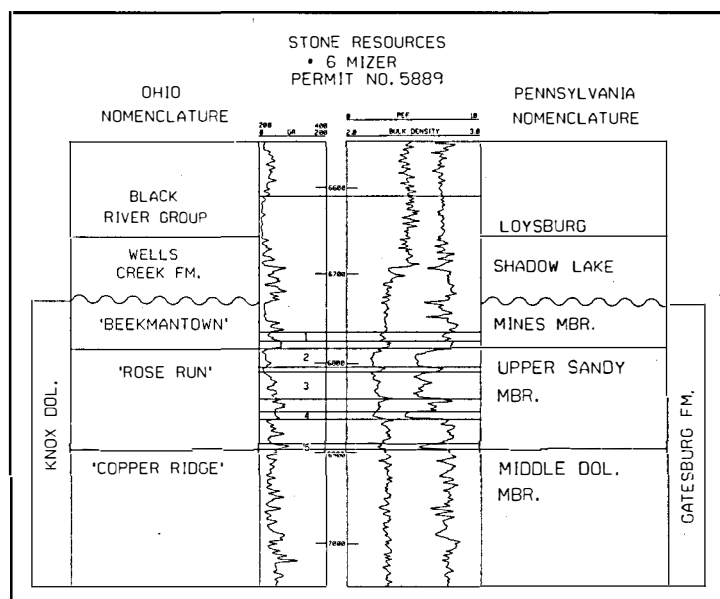


Figure 17. Log suite for the Rose Run sandstone and adjacent units for a typical well in the study area. Individual sandstone intervals are labeled 1 to 5.

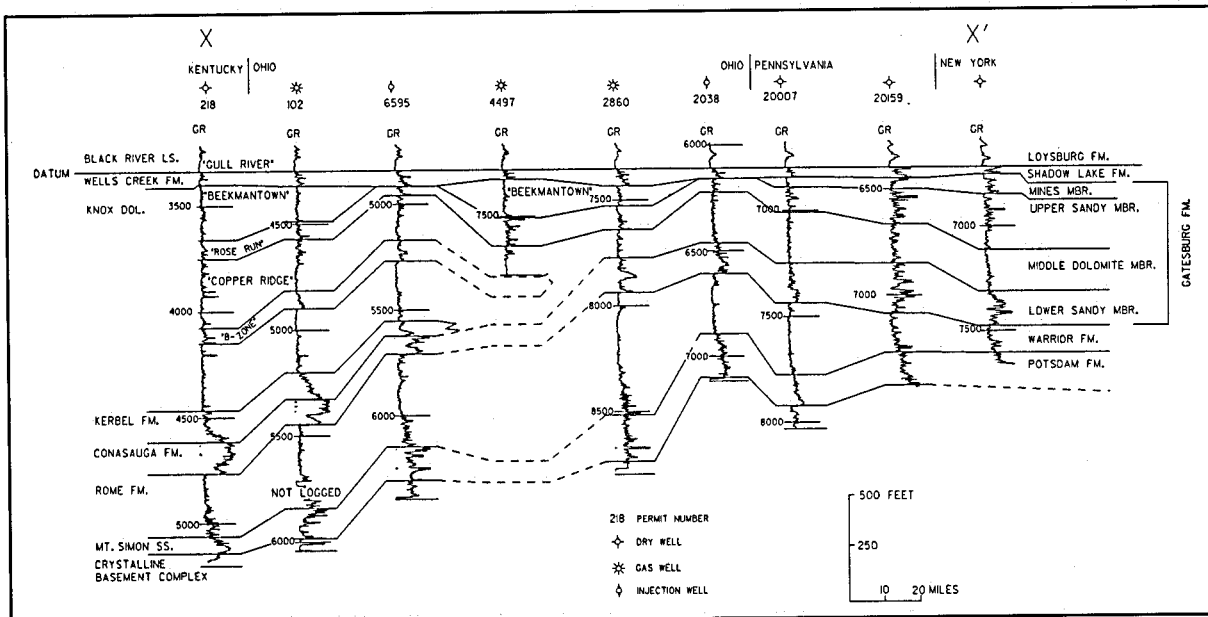


Figure 18. Regional stratigraphic cross section X-X'. See Figure 16 for location.

The regional subcrop map of the Rose Run (Figure 7) is based on the Ohio and Pennsylvania databases of wells that penetrate the Cambrian and Ordovician carbonates in the study area. The Ohio database includes 1,056 wells, of which approximately 30 are from Kentucky, Pennsylvania, and West Virginia. Sixty-six wells constitute the database in Pennsylvania, including nine from New York, Ohio, Ontario, and West Virginia. Because the two Surveys worked independently on this part of the project, there was some overlap between the two databases.

The Middle Ordovician Wells Creek/Shadow Lake clastics lie directly on the Rose Run sandstone in a narrow belt in eastern Ohio and northwestern Pennsylvania (Figure 7). West of the western edge of this belt the Knox unconformity has truncated strata down to the Copper Ridge/Ore Hill level. In contrast, to the east of the eastern limit of the subcrop belt the Wells Creek/Shadow Lake lies upon progressively younger rocks until the formation disappears by facies change somewhere over the Rome trough in western Pennsylvania. The exact position of this change is uncertain because of the dearth of well information southeast of the western edge of the Rome trough. It also is uncertain whether or not seismic surveying could delineate this change.

The sinuous nature of the subcrop belt is interesting. This is probably a reflection of local, as well as regional structural controls on the formations above and below the unconformity, as suggested by Dolly and Busch (1972). The depositional pattern of the Rose Run in south-central Ohio and northern Kentucky suggests control by the

Waverly Arch, a north-south trending feature that was first identified and named by Woodward (1961). Isopach maps of the Knox Dolomite by Janssens (1973), and of the Prairie du Chien Group by Shearrow (1987), indicate thinning over this feature. This thinning is coincident with the westward limit of the Rose Run. McGuire and Howell (1963) also recognized the influence of the Waverly Arch on Rose Run depositional patterns in northern Kentucky. Control of Rose Run deposition also may have been influenced by the West Hickman Creek-Bryan Station Fault, a basement fault that crosses and offsets the Rome trough in Kentucky. Offsets in the western edge of the subcrop belt in southeastern and south-central Ohio may reflect offset of structural controls along reactivated basement wrench faults. For more discussion of these basement structural features and their relationship to the Paleozoic cover, see Structural Geology below.

The well databases used to construct the isopach map of the Rose Run sandstone (Figure 19) are the same used to construct the subcrop map. The Rose Run interval thickens gradually from 0 feet at the western limit of the subcrop to about 200 feet throughout the area of eastern Ohio and northwestern Pennsylvania (Figure 19). Work done in Ohio indicates that the sand-to-carbonate ratio within the Rose Run interval decreases to the east and southeast, and west of the Waverly arch, suggesting a source to the north and northwest. East of this broad zone the contours are considerably narrower. Part of the reason for this steepening is that the regional Cambrian and Ordovician surface had been buckled during initial plate

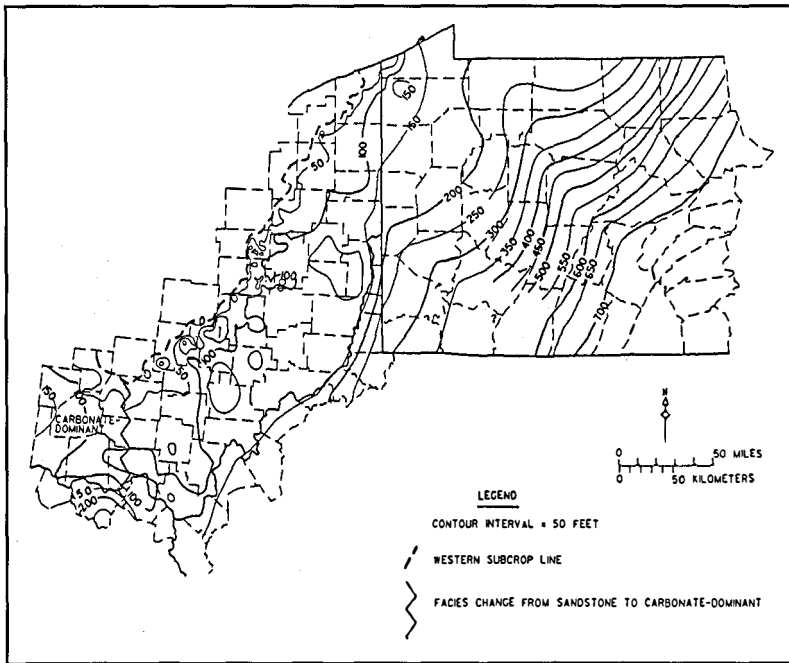


Figure 19. Regional isopach map of the Rose Run sandstone in Ohio and western Pennsylvania.

convergence in the Early Ordovician, with the western edge of the Rome trough acting as a hinge between the subsiding eastern basin and the more stable western craton. Thus, when the area was uplifted and exposed, erosion proceeded to expose older strata on the craton than in the basin. The broad zone of 0 to 200 feet-thick Rose Run mostly contains an incomplete section of the unit. Another reason for the rapidity of thickening (about 5 feet of thickening per mile) may be depositional. According to structural studies (see pg. 20, Influential Structural Features), the Rome trough was an actively subsiding graben complex during Rose Run deposition. This fault movement resulted in formation of a basin within the continental shelf that allowed large amounts of clastic sediment to build up. Deposition during the Late Cambrian, as evidenced by the Amoco Production Co. #1 Svetz well in Somerset County, Pennsylvania, for example, resulted in more than 700 feet of Rose Run sandstone in the deepest part of the trough in Pennsylvania. The well penetrated about 700 feet of Rose Run before drilling was stopped at 21,460 feet.

The irregular nature of the isopach map in the area between the western limit and the 200-foot contour is due to erosion. Various paleotopographic features, including erosional remnants (monadnocks), are present along the subcrop trend as a result of paleodrainage. Monadnocks represent small outliers along the subcrop trend where ancient streams carved channels around the more resistant sections, leaving small isolated bodies of preserved

Beekmantown and Rose Run strata. These monadnocks, which have been determined by detailed mapping to occupy 80 acres or less, are primary targets for exploration along the subcrop trend. Erosional remnants are characterized by thinning of the Wells Creek/Shadow Lake interval, and possible draping of strata in the Black River Limestone.

The detailed paleotopography developed on the Rose Run in this area is inconspicuous in Figure 19, yet some larger-scale features can be discerned. For example, some of the V-shaped contours in eastern Ohio suggest major river systems draining the higher lands over the Waverly arch to the west. The isolated closures in various parts of the map suggest large monadnocks.

Knox Unconformity and Adjacent Strata

At sometime during the Early Ordovician, a transform boundary in the Iapetus Ocean became a subduction zone, and the passive southeastern margin of the Laurentian plate began sliding down under the adjacent edge of the Gondwanan plate (the Avalonian margin-Scotese and McKerrrow, 1991). This change from a passive to a convergent margin initiated several major changes in sea level and in tectonic and depositional controls (Jacobi, 1981; Mussman and Read, 1986; Read, 1989). By the early Middle Ordovician (Whitrockian Stage) much of the southern continental shelf of Laurentia was emergent. An erosional surface developed across the shelf, called the Knox unconformity, is regional in nature; it can be recognized throughout most of the present Appalachians and, perhaps, most of North America (see Mussman and Read, 1986, Fig. 17).

Tectonic deformation due to plate collision was modest (no known mountain ranges resulted from it), but unmistakable. Read (1989) suggested that older rift faults from the opening of Iapetus were reactivated in reverse direction, causing initial uplift of the shelf margin. As convergence continued, folding and faulting also occurred in various areas of the shelf.

The Knox erosional surface exposed older and older rocks on both the east and west sides of the Waverly arch (present cardinal directions). Based on conodont work in Virginia by Harris and Repetski (1982) it appears that the Knox unconformity occurs within the Beekmantown. In central Pennsylvania the unconformity, if it exists at all (see below) probably would occur within the lower portion of the Bellefonte Formation, the upper unit in the Beekmantown (Figure 3). About 1,450 feet of pre-Bellefonte Beekmantown strata have been measured in Blair County (Butts, 1918, 1945), and more than 2,200 feet in Centre County (Butts and Moore, 1936; Krynine, 1946). West of the western margin of the Rome trough the unconformity truncates lower Beekmantown strata (based on the Manufacturers Light and Heat #1 Jesse Hockenberry well in northwestern Butler County). In northwestern Pennsylvania and northeastern Ohio, the sub-Knox strata grow increasingly older toward the west, from Beekmantown/Mines dolostone to Rose Run sandstone. In Ontario the subcrop consists of rocks equivalent to either the Rome/Warrior or Kerbel/Lower Sandy. In northern Kentucky and southern Ohio the Rose Run sandstone does not appear to lie directly beneath the Knox unconformity (McGuire and Howell, 1963; Janssens, 1973; this study). However, correlations in Ohio indicate that the Rose Run changes facies from quartz sandstone to a more dominant dolostone in this area, and implies a Beekmantown equivalent in western Ohio. These correlations may also indicate a more regional extent of Woodward's (1961) Waverly arch.

Ryder and others (1992) report the occurrence of Chazyan (late Middle Ordovician) conodonts within at least the upper 1,500 feet of Beekmantown strata in the Amoco Production Co. #1 Leonard Svetz well in Somerset County. They tentatively placed the Early-Middle Ordovician boundary at 19,000 feet in this well, indicating that about 1,800 feet of Beekmantown represented Early Ordovician strata and about 3,000 feet represented Middle Ordovician. Because of a seeming lack of evidence for truncation of the Early Ordovician strata, Ryder and others (1992) concluded that the Knox unconformity probably does not exist within the Rome trough. This has not been confirmed.

The existence of the unconformity in central Pennsylvania has not been confirmed, either. Chavetz (1969), who considered the Knox unconformity to occur between strata equivalent to the Bellefonte and Loysburg formations (Figure 3), described the transition of strata between these two units as gradual. Mussman and Read (1986; also Read, 1989) interpreted information such as this, as well as the

more regional work of Colton (1970), to conclude that the unconformity passed laterally into a conformable sequence in Pennsylvania. In this scenario, central Pennsylvania was the site of a depocenter that influenced Cambrian and Ordovician sediment thickness and facies distributions on the shelf (Read, 1980, p. 1579, Fig. 2). However, the conclusion that the unconformity does not exist in central Pennsylvania is based on the assumption that "Knox" uplift and erosion would have occurred at the end of Beekmantown time. Harris and Repetski (1982), in proposing that this event actually occurred during Beekmantown time, assigned 700 feet of upper Beekmantown (Bellefonte) in Blair County (an area studied by Chavetz) to the Middle Ordovician. They did not specifically state that an unconformity existed in this area, however.

The suggestion that the central Pennsylvania area continued to be a center of deposition at the same time most of the remainder of Laurentia was undergoing erosion is difficult to accept, given the extent of the Knox unconformity and the fact that central Pennsylvania is situated on what was still the continental shelf. Without further study, however, it may never be firmly established one way or the other. There may be information hidden in studies that could be used to demonstrate or negate the existence of the unconformity. For example, Knowles (1966) and Lees (1967) documented a thick cherty zone near the base of the Bellefonte Formation in Centre and Bedford Counties, respectively. This chert zone occurs within the Beekmantown Formation where it crops out in Centre County west of the Rose Run outcrop sampled and photographed during this study. Ryder and others (1992) suggested that the top of this zone may coincide with the Knox unconformity in central Pennsylvania; however, this evidence is circumstantial at this time.

In terms of Rose Run heterogeneity and reservoir performance, the Knox unconformity is the single most important regional feature associated with the formation. The unconformity played a major role in the migration and entrapment of hydrocarbons within Cambrian strata in eastern North America. In addition to hydrocarbon production from the Rose Run and Beekmantown, rare historical production and shows also occurs in south-central Ohio from reworked sandstones deposited on top of the Knox unconformity. This sandstone traditionally has been referred to by drillers in Ohio as the "St. Peter." This unit probably is not equivalent stratigraphically to the St. Peter Sandstone of the Michigan Basin.

If all of the rocks above the unconformity could be stripped away, it would be possible to map a belt of

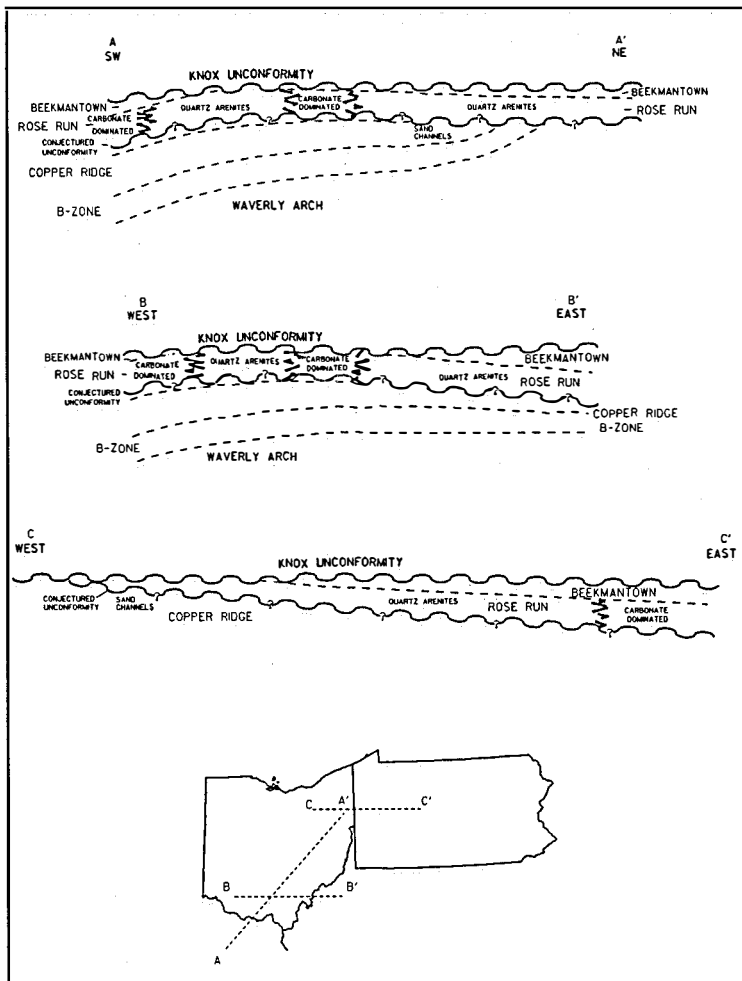


Figure 20. Generalized cross sections of the Appalachian basin.

sandstone and sandy dolostone extending approximately 400 miles from northeastern Kentucky to New York (Figure 7). The subcrop trends subparallel to oblique to the current structural configuration of the Appalachian basin. In southern Ohio the strike becomes northwest-southeast where the quartz-dominated Rose Run sandstone changes to a carbonate-dominated sandstone on the west flank of the Waverly arch (Figure 20). A similar facies change to carbonate-dominated sandstones occurs in the Rose Run in a narrow belt on the east flank of the Waverly arch and in western Pennsylvania (Figure 20). The quartz-dominated sandstones of the Rose Run extend southwestward beneath the Beekmantown dolomite along the western facies change into Kentucky, and eastward beneath the uppermost Gatesburg and Beekmantown subcrops into Kentucky, Pennsylvania, and West Virginia.

Facies variations beneath the Rose Run and above the "B-zone" in southern Ohio indicate a relatively higher radioactive carbonate facies that disappears to the east and northeast. Regional mapping of this Knox carbonate interval beneath the Rose Run indicates that the interval

increases in thickness to the southwest and decreases in thickness to the northeast where the "B-zone" appears to be absent because of a facies change, or forms a northwest-trending subcrop at another presumed major unconformity or disconformity (Figure 20). An alternative interpretation for change in the "B-zone" is a possible merging of "B-zone," Kerbel, and Conasauga facies in northeastern Ohio. More work needs to be done to resolve this problem. Correlations of the "B-zone" in western Ohio show that the unit disappears at the position of the Bellfountain outlier, further suggesting a possibility of a major regional unconformity or disconformity.

In western Morrow County, Ohio, paleotopographic relief on the Knox "resembles karst towers, karst cones, isolated hills, and intervening karst plains of present day mature karst terrains in tropical and humid climates" (Ryder, in press). Features such as vugs, fractures, and shale-filled cavities also indicate a paleokarst topography (Ryder, in press). In a regional study of the Knox unconformity in the southern portion of the Appalachian basin, Mussman and others (1988) interpreted a paleokarst topography

on the Knox unconformity that included filled sinkholes, caves, and intraformational breccias. Based on detailed subsurface mapping, it appears that similar features occur in east-central Ohio along the Rose Run subcrop. However, a mature paleokarst topography cannot be inferred in this area from the absence of paleocaliche and large-scale collapse zones. Vuggy porosity within the Beekmantown below the Knox unconformity probably results from the leaching of unstable grains by diffuse flow of meteoric waters whose recharge area was the exposed shelf. Different stands in the water table may have resulted in the formation of distinct lateral and vertical zonation of vuggy porosity in the Beekmantown that can be recognized on geophysical logs and correlated across township-wide areas. These zones, which are very important reservoirs, controlled the emplacement of hydrocarbons in these carbonates.

The erosional contact between the Beekmantown/Mines and the Wells Creek/Shadow Lake is present in cores from 4 wells in Ohio (cores 867, 2923, 2713, and 3006 in Figure 5). In these cores, the erosional surface separates

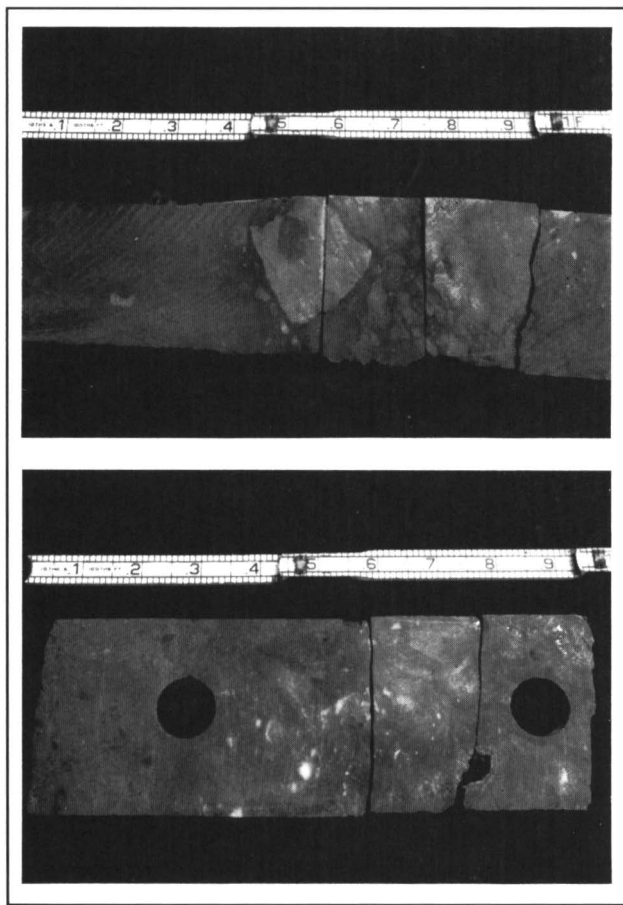


Figure 21. Photographs of cores from wells in Coshocton County, Ohio showing the Knox unconformity. Top—core 2713. Bottom—core 3006.

the silty dolostones and green to black shales of the Wells Creek/Shadow Lake from the grey to medium-brown, fine-crystalline dolostones of the Beekmantown/Mines. A thin veneer of green shale containing concentrations of pyrite often covers the Knox surface. Angular rip-up clasts of dolostone up to 3 inches across occur above the erosional surface in cores from Coshocton County (Figure 21). Numerous fine to coarse quartz grains, which decrease upward, float in a dolostone matrix above the Knox unconformity.

The Knox unconformity separates Rose Run sandstone from the Wells Creek/Shadow Lake interval in cores from Coshocton and Holmes counties, Ohio. In core 2853 from Coshocton County (Appendix III), a four-feet thick, grey, fine-grained, glauconitic, reworked sandstone with a basal wispy green shale containing concentrations of pyrite lies directly on a white, fine- to medium-grained sandstone exhibiting well-developed intergranular porosity. Dolomite rip-up clasts float in the sandstone matrix above the unconformity. This basal Wells Creek sandstone, the “St. Peter” of drillers, grades upward into a sandy, grey to

brown, microcrystalline dolostone. In core 2892 from Holmes County (Appendix III), a 3.5-foot thick bed of white to light-green, fine- to coarse-grained, very friable sandstone exhibiting very well-developed intergranular porosity lies on a light-grey to light-brown, microcrystalline, mottled dolostone in the lower Rose Run. Porosity logs were not run on this well but the resistivity log indicates that the basal Wells Creek sandstone probably is saturated with water. This sandstone exhibits very good reservoir quality and might have good hydrocarbon potential with the proper structural or stratigraphic trapping mechanism developed.

The sandstone above the unconformity also occurs in core 2923 from Morgan County, Ohio (Appendix III). In this core a four-foot thick bed of white to light-grey, very fine- to medium-grain, sandstone lies on a light- to medium-grey, fine-crystalline dolostone of the Beekmantown. Numerous rip-up clasts of dolostone and chert up to 1/4 inch across are present above the erosional surface. This sandstone has moderately- to well-developed intergranular porosity based upon mesoscopic examination of the core. It grades upward into a medium- to dark-grey, low-porosity siltstone.

Structural Geology

Introduction

Harding and Lowell (1979) described two major modes of structural styles, basement involved and detached, that Harper (1989) documented or speculated on in the subsurface of western Pennsylvania. Although these structural styles also exist in Ohio (Figure 22), detached structures are limited to extreme eastern Ohio. Basement involved structural styles, often called “thick-skinned tectonics,” include extensional fault blocks, compressive fault blocks and high-angle basement thrusts, wrench fault assemblages, and basement warps. Detached structural styles, commonly called “thin-skinned tectonics,” include decollement thrust-fold assemblages, detached normal-fault assemblages (growth faults), salt structures, and shale structures. Wrench fault assemblages separating adjacent detached zones should be added to this list. Recurrent movement along basement structures has had a direct affect on many detached structures, as well as on the distribution of sedimentary facies, hydrocarbon development, source and reservoir rocks, and traps (Harper, 1989).

Extensional basement faulting includes down-to-the-east normal faulting initiated during the opening of the Iapetus Ocean in the Late Precambrian, and development of the Rome trough during the Cambrian. Compressive block

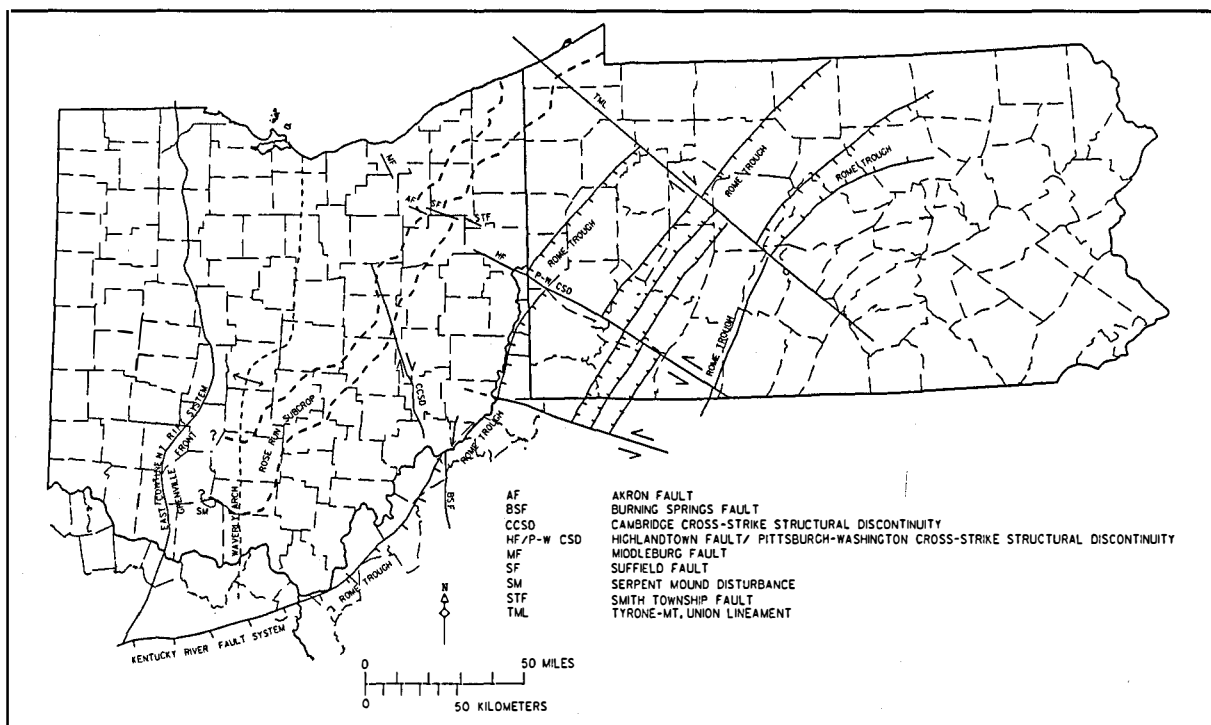


Figure 22. Map of the study area showing major tectonic features that affected Late Cambrian deposition and subsequent structural development in Ohio and Pennsylvania.

faulting cannot be documented with any degree of reliability, but probably occurred during the Cambrian (and the development of the Waverly arch) as evidenced by the amount of feldspathic sandstones in the Mt. Simon/Potsdam, Rome/Warrior, Conasauga/Gatesburg Lower Sandy, and Rose Run intervals. The presence of feldspathic sandstones implies close proximity to basement uplift areas. Also, plate margin convergence during the Early Ordovician may have initiated a reversal of movement on old rift faults (Read, 1989), which would have created compressive fault blocks near the margin. Wrench faults probably originated as transform faults during Precambrian rifting (Thomas, 1977), and later became zones of crustal instability between adjacent crustal blocks (Lavin and others, 1982). In the study area the Tyrone-Mt. Union lineament, the Pittsburgh-Washington lineament (and correlative Highlandtown fault zone of Ohio), and the Cambridge cross-strike structural discontinuity (Cambridge arch of Orton, 1890) are the best examples of basement wrench faults. Basement warping might have replaced block faulting in the Rome trough after the deep-seated faults along crustal blocks locked up, probably in Early or Middle Ordovician.

Detachment structures are not as recognizable in the Cambrian and Ordovician section of the study area as they are in younger strata. The only detached structures that

have been documented are growth faults, wrench faults, some of which may have substituted vertical movement for the original strike-slip movement sometime during the Late Cambrian or Early Ordovician, and thrust faults that developed during the Alleghanian orogeny in the Late Permian (see Harper, 1989). These detached structures commonly developed in imitation of their basement counterparts. For example, the Cambrian growth faults described by Wagner (1976) occur over basement normal faults of the Rome trough. Also, several of the basement wrench fault assemblages, most notably the Tyrone-Mt. Union lineament, have influenced structure and deposition in western Pennsylvania throughout geologic time (Rodgers and Anderson, 1984), and still may be seismically active (Canich and Gold, 1985). The Cambridge cross-strike structural discontinuity in eastern Ohio (Figure 22) has been interpreted by Baranoski (1989) as a similar basement wrench fault. Many of these structures might be recognizable in the subsurface with the aid of seismic surveying. Others, such as unconformities, can be interpreted from a combination of seismic surveying, geophysical log interpretation, and well data (Figure 21).

Influential Structural Features

Based on geophysical logs and seismic data numerous basement or deep-seated structures influenced the

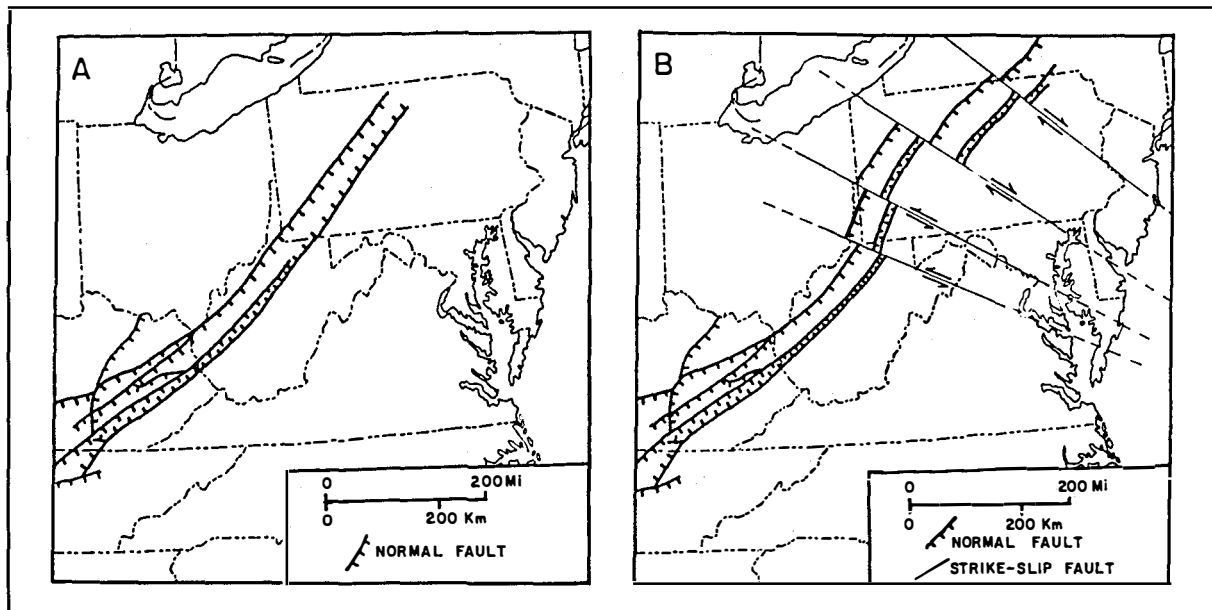


Figure 23. A. Commonly accepted configuration of the Rome Trough in the central Appalachian Basin (modified from Rankin, 1976). B. Reinterpretation of Figure 23A based on probable segmentation and offset along major basement wrench fault assemblages (from Harper and Laughrey, 1987—see text for explanation).

deposition and later diagenetic alteration of the Rose Run sandstone and adjacent rocks. These include the rift zones, wrench faults, growth faults, and basement faults and flexures shown in Figure 22. Beardsley (1992) suggested that many of these structures resulted from tectonic inversion along zones of weakness defined by Grenville thrust sheets during regional episodes of compression and extension in the Paleozoic.

The Rome trough is a series of graben structures recognized in Kentucky, West Virginia, and Pennsylvania. It is part of the Eastern Interior Aulacogen (Harris, 1978), a failed rift extending from the Mississippi Embayment to New York (Harris, 1978; Harper, 1989). In northwestern West Virginia the edge of the Rome trough has been delineated by a series of northeastern-trending gravity and magnetic anomalies (Kulander and Dean, 1978). In Ohio, mapping by Baranoski and Riley (1988; in press) indicates that the Rome trough steps up to the northwest into extreme southeastern Ohio from West Virginia and Kentucky. Ryder and others (1992) interpreted a group of basement faults in eastern Ohio and adjacent West Virginia as a structural hinge, called the Ohio-West Virginia hinge zone.

The Rome trough exhibits certain characteristics that are typical of aulacogens (Hoffman and others, 1974), including development in the interior of a foreland platform and long life. The Rome trough has been susceptible to reactivation during the entire post-Precambrian geologic record (as shown in Pennsylvania by Harper, 1989; 1992).

The developmental stages of such a structure were described by Harris (1978, p. 57) as: 1) a graben stage in which subsidence is confined to the graben and displacement occurs penecontemporaneously with sedimentation along block faults; 2) the transitional stage in which the boundary faults begin to lock up or have only minor recurrent movement; and 3) the downwarping stage in which the entire area subsides, thus forming a regional downwarp. From this information, it can be stated that the Rome trough reached stage 1 during the Early or Middle Cambrian (Read, 1989), stage 2 during the Late Cambrian or Early Ordovician, and stage 3 before the Late Ordovician.

Most illustrations of the Rome trough (e.g. Figure 23A) show the trough as a relatively simple, curved graben running from Kentucky to Pennsylvania. Laughrey and Harper (1986; also Harper, 1989) determined, however, that the trough was offset, at least in Pennsylvania, by a series of basement wrench faults (Figure 23B). This “best fit” interpretation was determined by studies of the Paleozoic rock cover. For example, offset of the trough along the Tyrone-Mt. Union lineament had been suggested by Lavin and others (1982) based on aeromagnetic and gravity anomalies. Segmentation of the trough by the Pittsburgh-Washington lineament is suggested by numerous data, including the work of Thomas (1977) indicating similar offsets throughout the Appalachians and Ouachitas along Late Precambrian-Early Paleozoic transform faults.

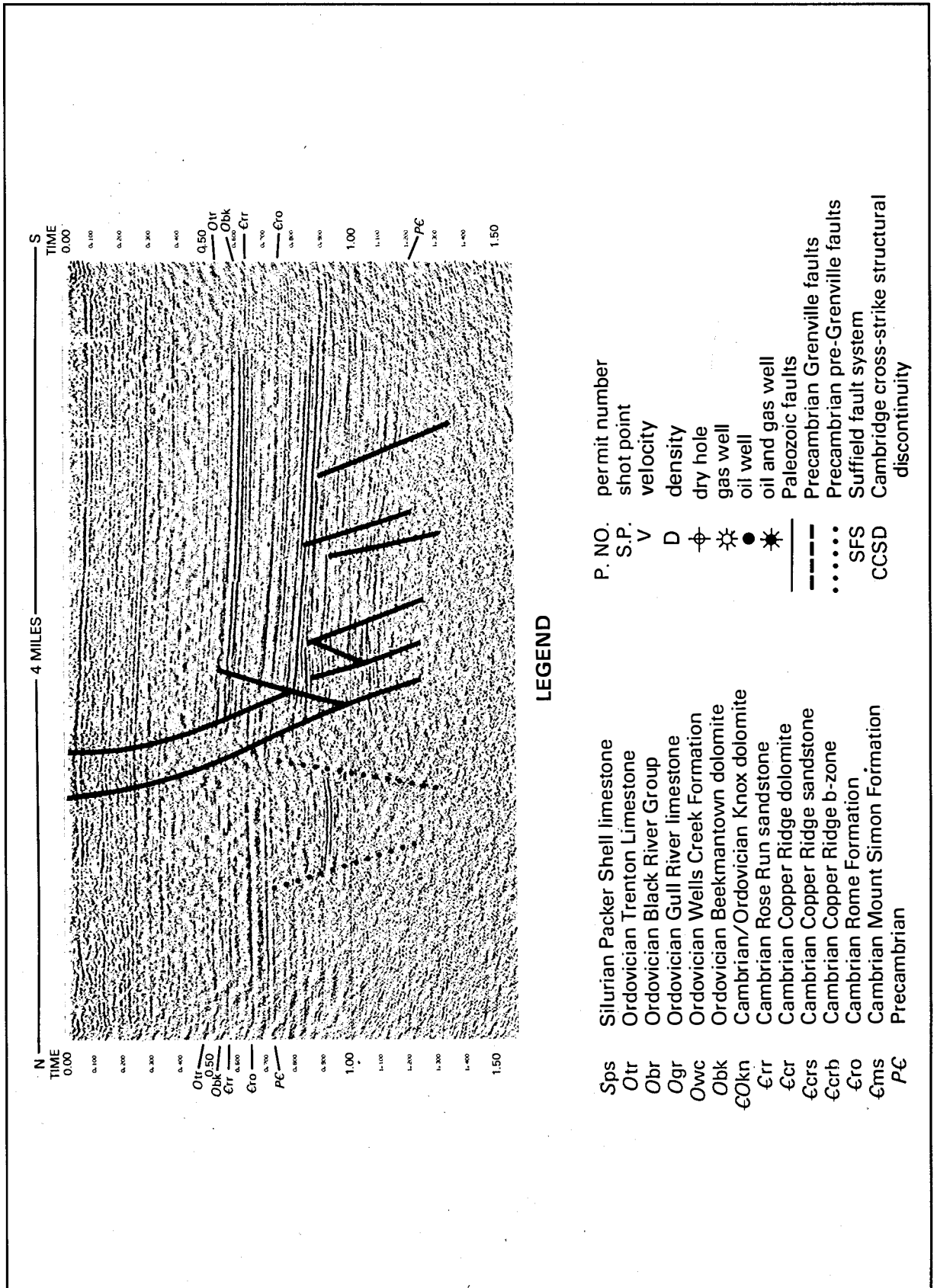


Figure 24. Interpreted seismic section display, Carter County, Kentucky: 1. second travel time, vibrators, 30-fold, migrated, normal polarity

Wagner (1976) speculated that the Rome trough affected deposition during the Late Cambrian and Early Ordovician by creating an actively subsiding depositional basin (his Olin basin). He mapped Upper Cambrian rocks thickening from 800 feet in northwestern Pennsylvania to over 1,200 feet within the trough, and Beekmantown rocks thicken from 400 feet to greater than 2,500 feet according to Wagner (1976, Figs. 8 and 10). Supplementary work by Ryder and others (1992) and Harper (1991), including two of the regional cross sections prepared for this study (Appendix II), provide additional evidence that the Rome trough affected deposition during the Late Cambrian and Early to Middle Ordovician. Harper's (1991) lines C-D and G-I cross the trough in north-central and southwestern Pennsylvania, respectively, showing offset along suspected basement and/or growth faults with thicker Rose Run through upper Beekmantown strata on the southeast side of the faults. In the Amoco Production Co. #1 Leonard Svetz well in Somerset County, the Beekmantown includes approximately 3,800 feet of dolostone and sandstone, a much thicker accumulation than in wells farther east and southeast.

Based on gamma-ray log correlations and well-sample control, Wagner (1976) reported a thick sandstone within the Rome trough that he called the Olin Sandstone Member of the Gatesburg Formation. Wagner felt that this sandstone occurred stratigraphically below the level of the Lower Sandy Member of the Gatesburg of northwestern Pennsylvania, but could be correlated with a portion of the Lower Sandy in central Pennsylvania and northeastern West Virginia. He suggested that a complete re-evaluation of the Cambrian stratigraphy of northwestern Pennsylvania was in order because of this discrepancy. During this investigation it was determined that the Olin Sandstone as originally defined does not exist. This same conclusion has been reached independently by Ryder (1989; also Ryder and others, 1992). The Olin Sandstone is actually the Rose Run sandstone which is considerably thicker within the Rome trough. In several of the wells in Harper's (1991) cross sections that penetrate the Rome trough in Pennsylvania and New York, the Rose Run reaches thicknesses in excess of 500 feet. This is especially evident in the Amoco Production Co. #1 Leonard Svetz well in Somerset Co. where the Rose Run is estimated at greater than 700 feet thick.

Reprocessed seismic reflection from COCORP OH-2 of eastern Ohio shows down-to-southeast faulting and tectonic thickening of Upper (and Middle?) Cambrian rocks where the Rome trough faulting diminishes as it steps up into Ohio. Seismic reflection data over the

northwestern portion of the Rome trough in adjacent portions of Kentucky (Figure 24) indicates significant faulting and tectonic thickening in these rocks.

Several authors have shown evidence for the existence of major basement wrench faults, including the Tyrone-Mt. Union lineament (Canich and Gold, 1977 and 1985; Rodgers and Anderson, 1984), the Highlandtown fault/Pittsburgh-Washington lineament (Parrish and Lavin, 1982; Lavin and others, 1982; Harper and Laughrey, 1987), the Suffield fault (Root, 1986), and the Cambridge cross-strike structural discontinuity (Baranoski, 1989) (Figure 22). These and other wrench fault assemblages cross the structural grain of the Appalachians and thus are termed cross-strike structural discontinuities, or CSD's (Wheeler, 1980). Some of these wrench faults probably had a vertical component as well as a horizontal component of movement. For example, the Highlandtown fault/Pittsburgh-Washington lineament, especially well-defined by aeromagnetic anomalies (Zietz and others, 1980), is represented by a magnetic gradient that may be interpreted as differences in basement elevation, difference in basement composition, or both (Harper, 1989). Normal and reverse faulting and anomalous isopach variations have been observed in the Silurian and Devonian on geophysical logs in southeastern Ohio by Baranoski (1989), which strongly suggest strike-slip movement along pre-existing basement faults. Proprietary seismic data in this area indicates structural offset in the basement. Rodgers and Anderson (1984) found no evidence of a strike-slip component in the shallower (i.e. Lower Devonian through Pennsylvanian) rocks associated with the Tyrone-Mt. Union lineament. They suggested instead that, after the Early Ordovician, the rocks northeast of the lineament were uplifted relative to those southwest.

Reactivation and movement along the Suffield fault system, a possible extension of the Highlandtown fault/Pittsburgh-Washington lineament in northeastern Ohio (Figure 22), has caused repeated faulting and associated fracturing throughout the Paleozoic. The interval of the Knox/Gatesburg decreases in thickness to the northeast in an area southwest of this trend, where the "B-zone" has been interpreted as absent by facies change or forms its own subcrop edge (Figure 20A). The latter interpretation suggests a major regional unconformity below the Rose Run sandstone. Seismic data across a portion of the Suffield fault system in Portage County show that the Beekmantown/Mines is present on the upper fault block and absent on the lower fault block (Figure 25). This line crosses a portion of the fault that is more subdued at the basement; thus, offset is subtle. Normal down-to-northeast

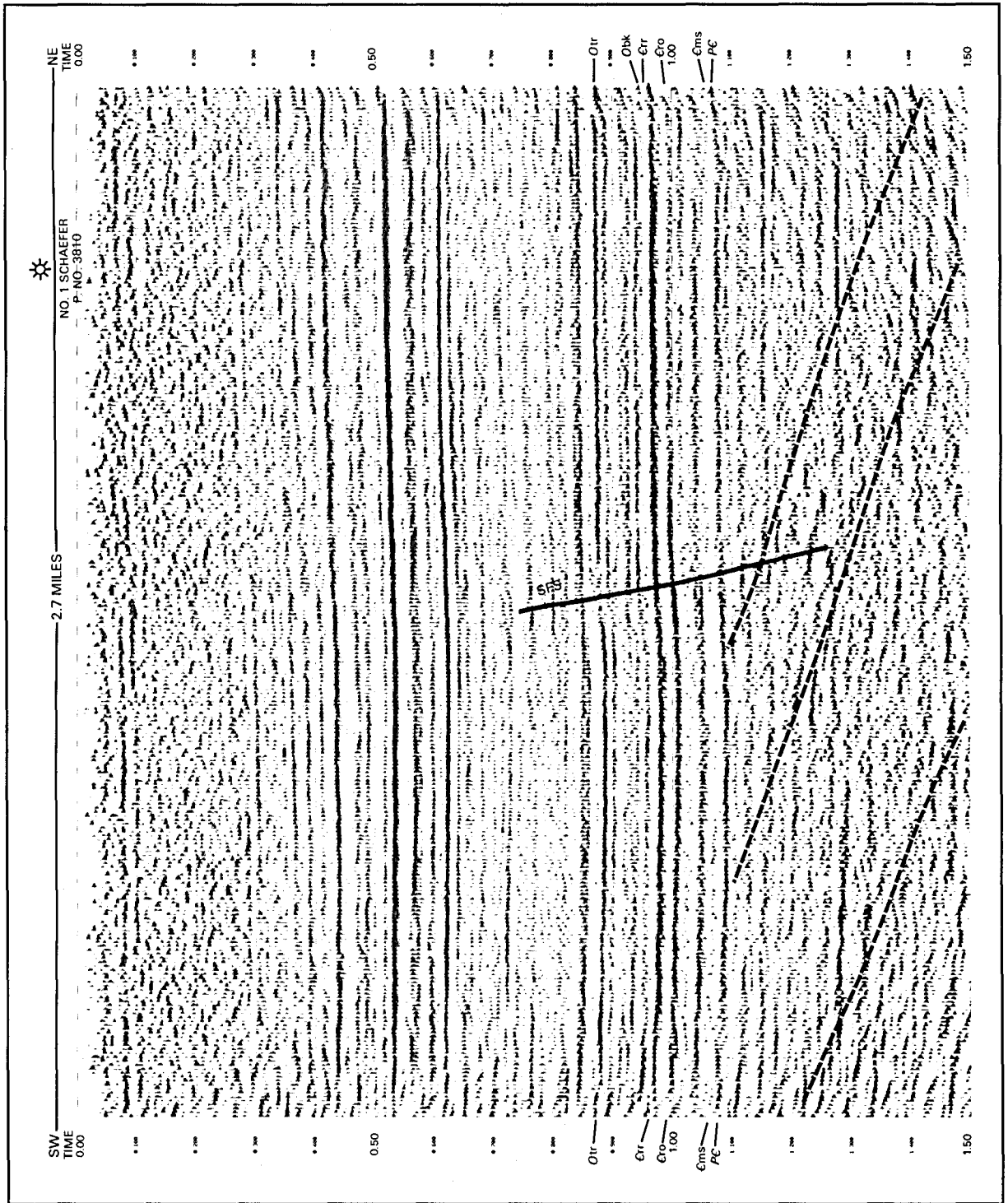


Figure 25. Interpreted seismic section display, Portage County, Ohio: 1992 processing, 1.5 seconds travel time, dynamite, 60-fold, whitened migrated, normal polarity. See Figure 24 for legend.

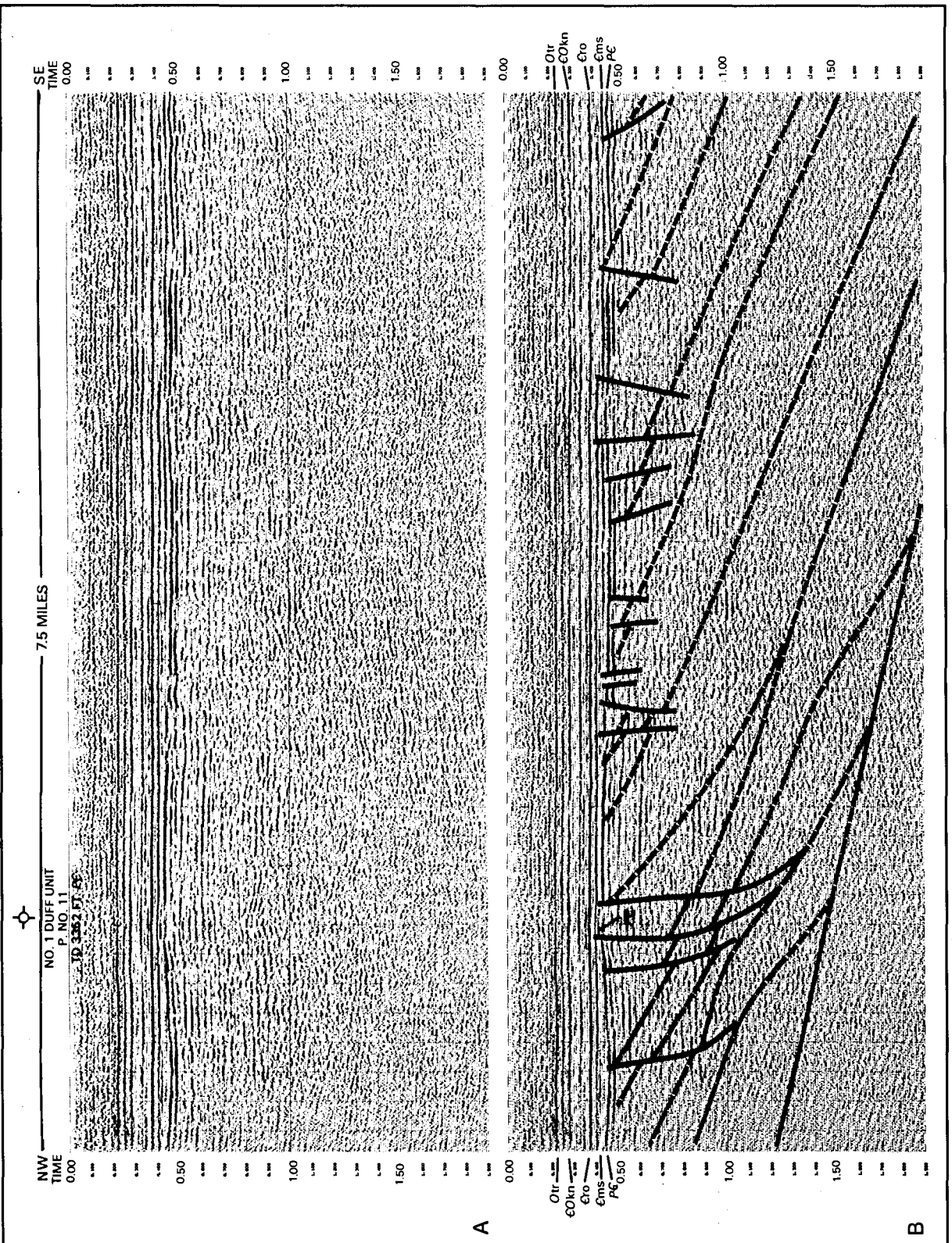


Figure 26. Uninterpreted (A) and interpreted (B) seismic section displays, Fayette County, Ohio: 1992 processing, 1.9 seconds travel time, dynamite, 12-fold, migrated, normal polarity. See Figure 24 for legend.

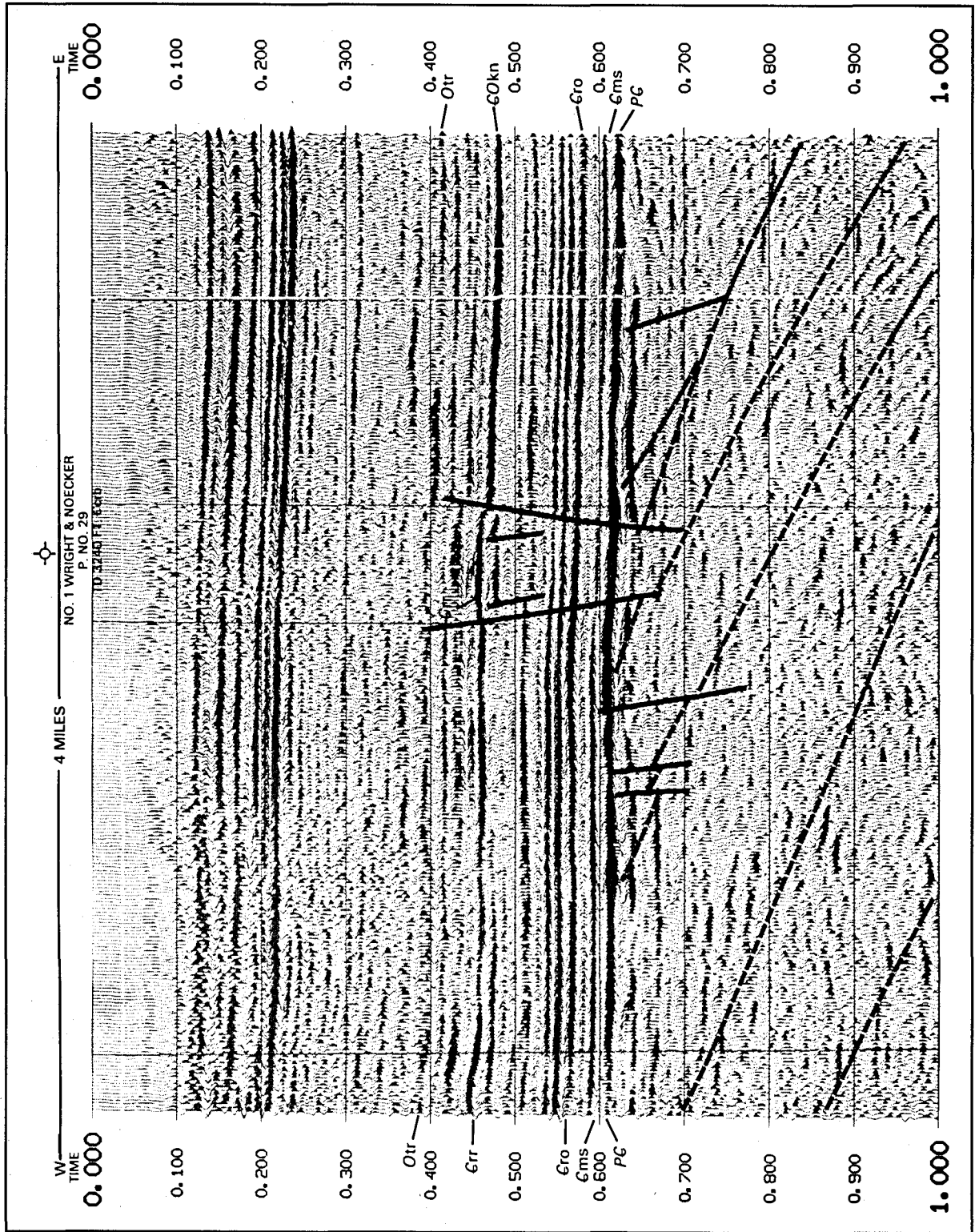


Figure 27. Interpreted seismic section display, Pickaway County, Ohio: 1.0 second travel time, vibrators, 30-fold, unmigrated, normal polarity. See Figure 24 for legend.

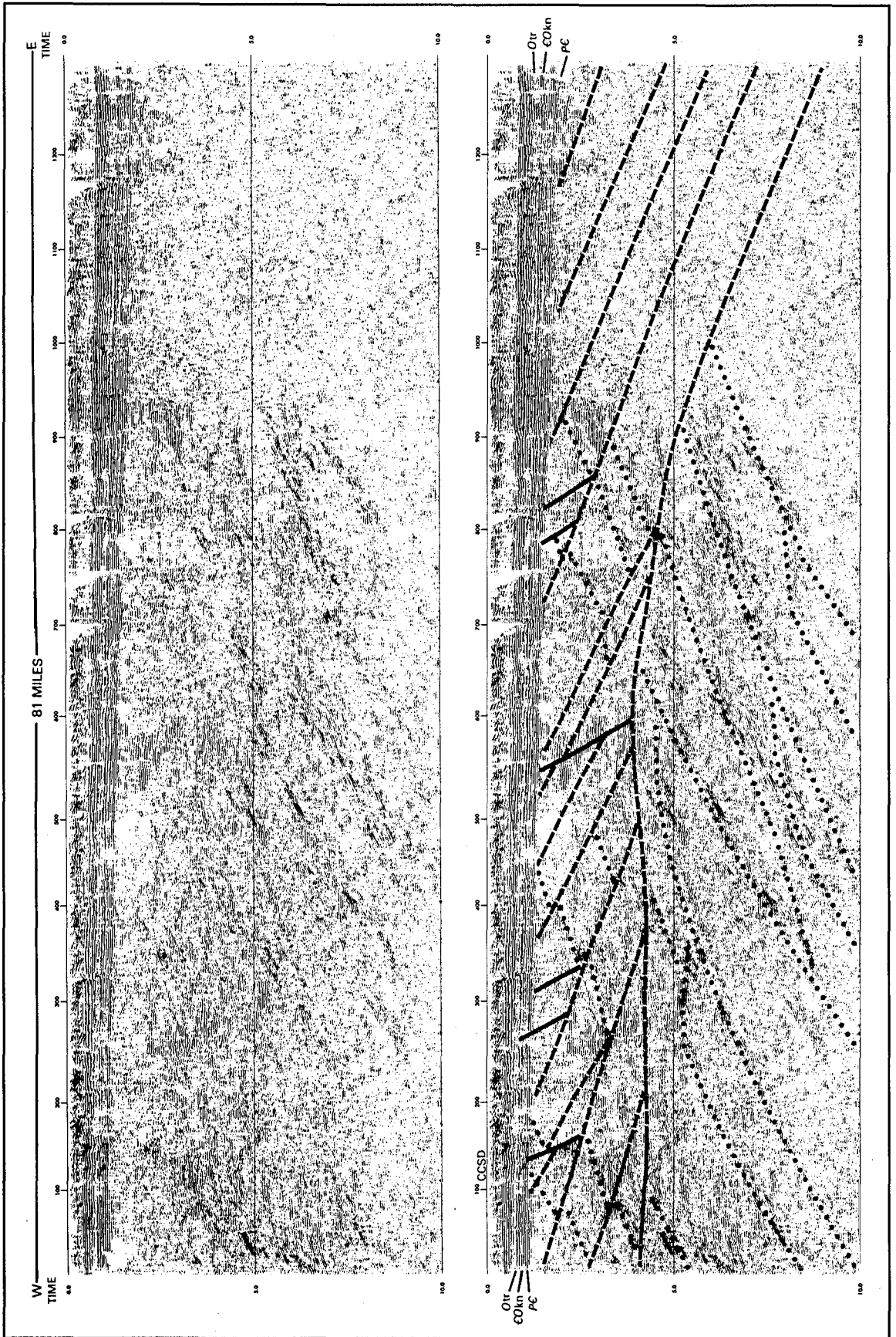


Figure 28. Uninterpreted (A) and interpreted (B) seismic section displays in eastern Ohio: 10.0 second travel time, vibrators, 60-fold, no wiggle variable area. See Figure 24 for legend.

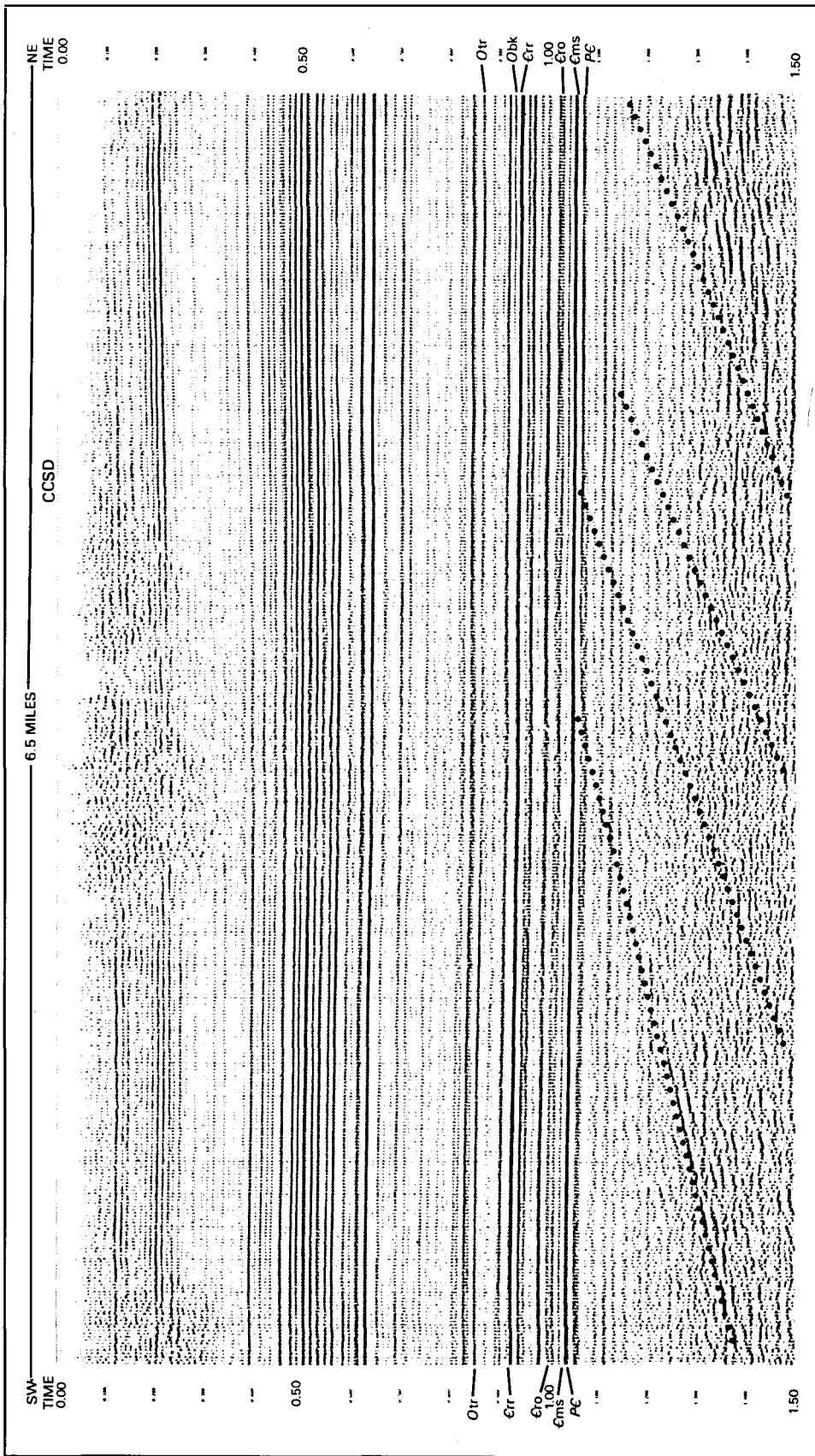


Figure 29. Interpreted seismic section display, Coshocton County, Ohio: 1.5 second travel time, vibrators, 60-fold, migrated, normal polarity. See Figure 24 for legend.

faulting during development of the Knox unconformity may have preserved the Beekmantown observed north of the fault. Left-lateral strike-slip movement has been interpreted along the fault during the Late Paleozoic. This is an example of tectonic inversion along zones of weakness defined by Grenville thrust sheets and basement highs.

Woodward (1961) mapped the thickness and distribution of Beekmantown dolomite where the Knox unconformity truncates it. He used the mapped pattern at the unconformity to describe a "broad low concealed arch extending from north-central Ohio southward into Kentucky," which he called the Waverly arch (Woodward, 1961, p. 1645) (Figure 22). McGuire and Howell (1963) also recognized the influence of the Waverly arch on Rose Run depositional patterns in northern Kentucky. Current work on the basement tectonics of western Ohio indicates that the Waverly arch might be controlled by deep basement faulting at the plate boundary between the Precambrian Grenville province on the east and the Precambrian east continent rift of Drahovzal and others (1992) to the west (Figure 22). Culotta and others (1990) interpreted a rift zone in western Ohio on the OH-1 COCORP deep seismic line.

A number of other geophysical studies have used regional gravity and magnetics to substantiate this finding. Regional mapping and cross sections constructed during this study suggest that the rift was actively subsiding during the Cambrian and Early Ordovician, causing increased accumulation of sediments, thus defining the west flank of the Waverly arch. Tectonic inversion at the Knox unconformity emphasized the feature. Current work suggests that the Waverly arch, in fact, may be an early subtle precursor to the Cincinnati arch, resulting from the migration of regional tectonic stresses deep in the crust.

Later subsidence of the Appalachian basin masked the presence of the Waverly arch in Ohio. Green (1957) recognized the absence of the Cincinnati arch during the Cambrian and Ordovician. Following Green's interpretation most workers today agree that the Cincinnati arch is not a product of uplift, but results from relatively rapid subsidence of the Appalachian, Illinois, and Michigan basins. Woodward (1961) also noted the absence of the Cincinnati arch during Cambrian sedimentation in western Ohio. It is curious, however, that in his report Woodward does not discuss the potential presence of the Rose Run sandstone beneath the Beekmantown/Mines.

Seismic reflection data from Fayette and Pickaway counties, Ohio show tectonic inversion and formation of a

small tectonic block on the Waverly arch. The interpreted Fayette County line (Figure 26) shows east-dipping Grenville thrust sheets below .5 seconds. Reactivation of thrust sheets and the formation of new high-angle faults during the Paleozoic formed a series of horsts and grabens. Note the thin Cambrian reflectors over the basement high at the Duff well (Figure 26), and thick Cambrian adjacent to the highs. Similar smaller relief features are located to the east on the line.

The interpreted Pickaway County seismic line also shows reactivated basement faults on the Waverly arch (Figure 27). In this example basement highs occur at the leading edge of Grenville thrust sheets, which have had Paleozoic normal faulting. A graben containing thicker Cambrian sediments, located at the edge of one of the thrust sheets, was structurally inverted during development of the Knox unconformity, resulting in a paleoremnant bounded by faults. Later down-to-east movement of the basement during the formation of the Appalachian basin resulted in a monocline at the position of this remnant, and a subtle anticline in the shallow Paleozoic reflectors over the basement faults. The #1 Wright and Noecker well drilled into this remnant reveals a well developed, very porous Rose Run sandstone and dolomitized lower Black River limestone. The dolomitized Black River indicates close proximity to faulting. Dolomitization near faults has been observed in rare instances throughout the study area. Small offsets typically cannot be detected by seismic reflection. Dolly and Busch (1972) and Wickstrom and Gray (1988) also recognized the presence of dolomitized carbonates near faults.

The subcrop of the Beekmantown/Mines and Rose Run at the Knox unconformity also was affected by the Cambridge CSD and the Akron and Suffield faults where the Rose Run subcrop pattern changes strike along a southwest-northeast trend. Locally the western Beekmantown and Rose Run subcrop edge varies at the Cambridge CSD in eastern Coshocton and Holmes counties (Figures 28 and 29). In these areas the subcrops change trend from northeast-southwest to the north-northwest and the subcrop broadens to the east. Faulting along the Cambridge CSD has been interpreted as a right-lateral strike-slip system. Although offsets are not seen at the top of Precambrian basement on the seismic line, it is hypothesized that bedding-plane strike-slip and basement structural inversion has taken place along a hinge-line, where Silurian and Devonian sediments increase in thickness eastward. Note the presence of west-dipping Precambrian reflectors on the seismic section in Figures 28 and 29. A number of wells with dolomitized Black River occur in

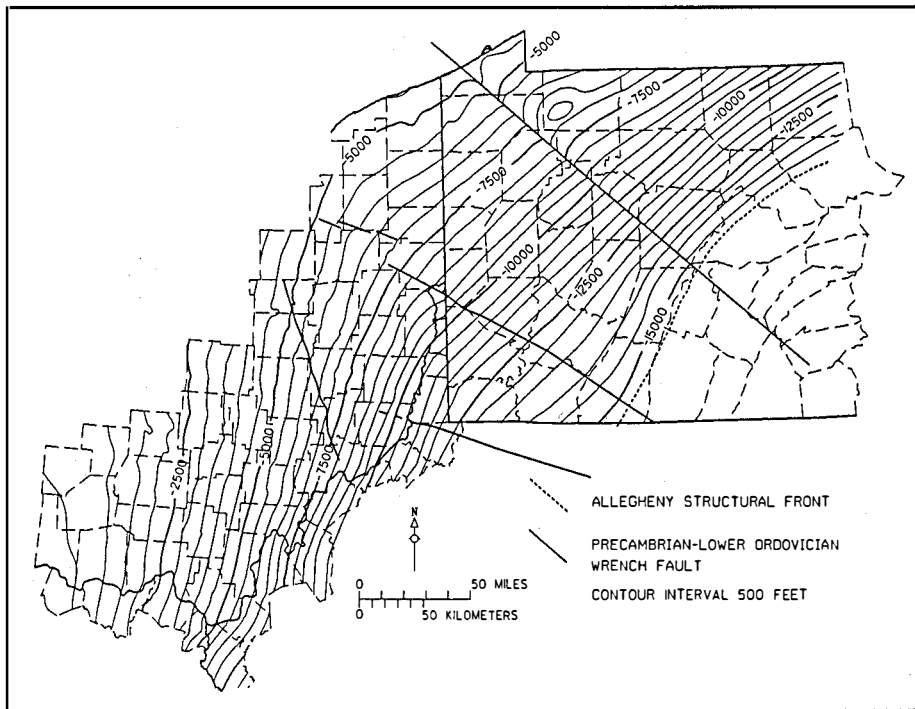


Figure 30. Regional structure map on the Knox unconformity in Ohio and western Pennsylvania.

the area, and as mentioned above are very suggestive of faulting.

Regional Maps and Seismic Sections

The well databases used to construct structure maps on the top of the Knox unconformity and Rose Run sandstone (Figures 30 and 31) are the same used to construct the subcrop and isopach maps (Figures 7 and 19). Because of the map scale used in this report, the Ohio Division of Geological Survey prepared open-file maps for readers interested in the locations and identifications of control wells used to construct the maps (see Appendix II).

Regional structure in the Appalachian Basin tends to follow a standard pattern from the Precambrian basement to the Middle Devonian; that is, subsea elevations decrease from northwest to southeast, with a certain amount of curvature due to flexures along the established Appalachian Basin salients and recesses (Colton, 1970 and others). From Middle Devonian through Pennsylvania and Permian the patterns differ somewhat, mostly because of vertical flexures and faulting as a result of detachment on one or more strata. Most of the structural similarities from horizon to horizon result from commonality of both depositional setting in a broad foreland basin and deformation during the Alleghanian orogeny at about 250 ma. On the local level structures may change rapidly within the space of one mile. Where a regional structure map

shows an almost unvarying plane surface gradually dipping eastward into the basin, a local map may show folding and faulting at a magnitude unmappable on the regional level. By and large, this appears to be the case with both the Knox unconformity (Figure 30) and Rose Run sandstone (Figure 31). Throughout eastern Ohio and much of western Pennsylvania the structure contours on the tops of the Rose Run sandstone and the unconformity indicate a gradual decrease in subsea elevation to the east and southeast.

Some of the roughness in the otherwise smooth contours are undoubtedly due to the paleotopography developed on the top of the Rose Run in Ohio and northwestern Pennsylvania.

The subsea configuration of the Knox unconformity is the simplest and easiest to describe. As Figure 30 illustrates the Knox unconformity currently dips gently to the east and southeast in Ohio and Pennsylvania. Dips range from approximately 50 feet per mile in northeastern Ohio and northwestern Pennsylvania to approximately 100 feet per mile in southeastern Ohio and western West Virginia. Other than a few local anomalies in the contours, probably due to paleotopography, the major disturbances occur in northwestern Pennsylvania. Here, the continuity of the contours has been upset by the Tyrone-Mt. Union lineament, described above as a major basement wrench fault separating crustal blocks (Lavin and others, 1982). The map could have been drawn without acknowledging the lineament, but throughout western Pennsylvania this would have created an enormous departure from the otherwise relatively smooth nature of the contours. Under the circumstances, it appears that the lineament, illustrated as a left lateral strike-slip fault, defines a "best fit" interpretation on the regional level. Faulting in the Knox also is interpreted along the Akron-Suffield-Smith fault system and Highlandtown fault in northeastern Ohio. This is supported by interpretation of seismic data.

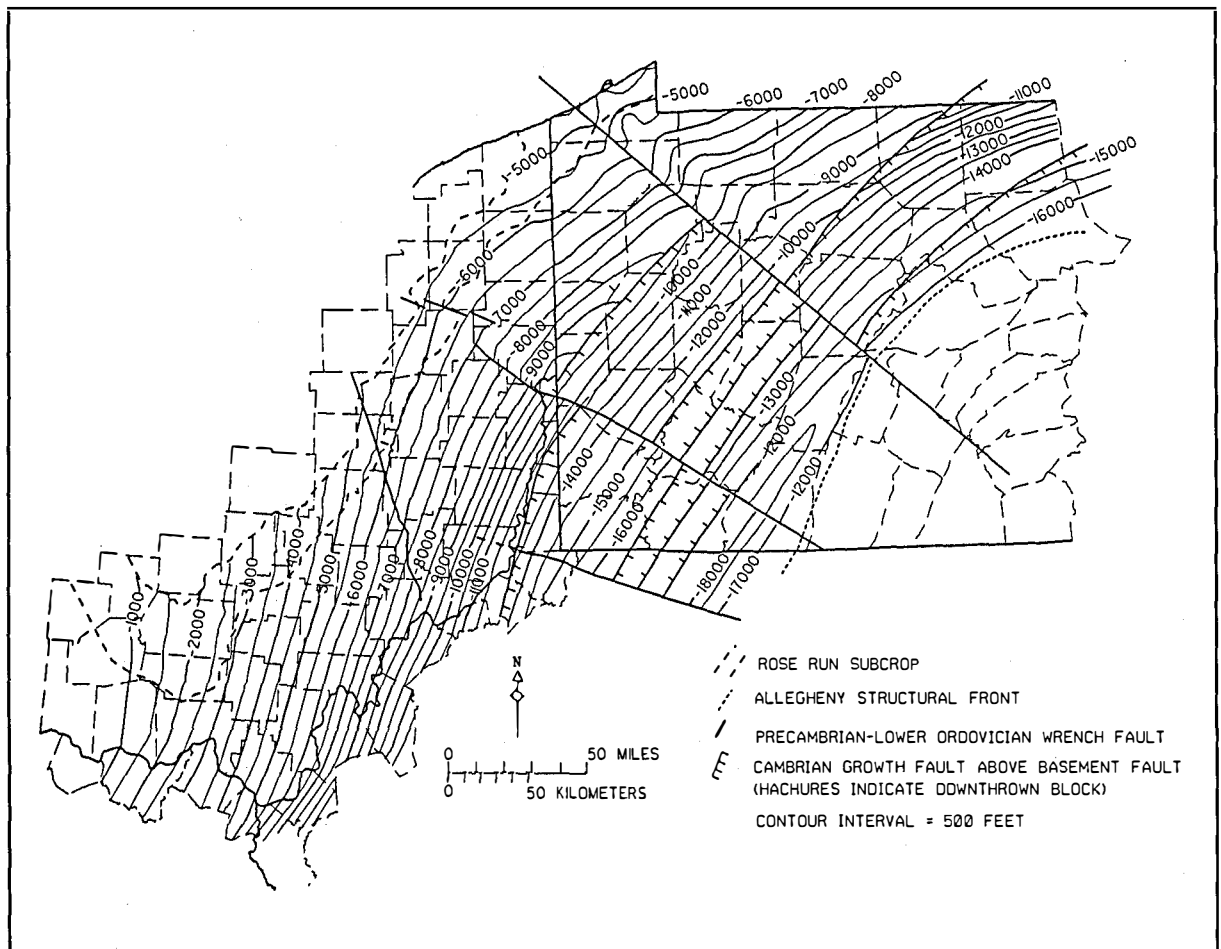


Figure 31. Regional structure map on top of the Rose Run sandstone in Ohio and western Pennsylvania.

An additional disturbance in the structure contours on the Knox unconformity occurs just to the northeast of the Tyrone-Mt. Union lineament in southwestern Warren County, Pennsylvania. This disturbance is defined by closure on the -7,000 feet contour and bending of shallower contours around it to the northwest. The exact nature of this disturbance is unknown, but it appears from the map to be a localized downward flexure of the unconformity surface. It should be kept in mind, however, that there is very little well control in this area, so the feature could be a plunging synclinal structure as well as a closed depression. In addition, no available seismic reflection data exist for the area; therefore, discussion of the anomaly currently is speculative. It is probable that such information exists and may be made available for future study. Meridian Exploration Corp. drilled a successful Beekmantown test (the #1 Hammermill Paper Co. well) on this anomaly in 1985, and it is likely that the prospect was based as much, or more, on seismic studies as on standard geological mapping.

Based on mapping, structure on the Rose Run sandstone (Figure 31) is relatively more complex than structure on the unconformity. Besides the Tyrone-Mt. Union lineament, the Highlandtown fault/Pittsburgh-Washington lineament and the Cambridge CSD apparently also had active parts in the structural configuration of the surface throughout its length in southwestern Pennsylvania and eastern Ohio. In addition, numerous growth faults above basement rift faults also occur. These have been offset by movement along the major wrench faults (lineaments and CSD's).

By correlating gamma ray log signatures and well cuttings, Wagner (1976) proposed the existence of Cambrian and Lower Ordovician growth faults in the subsurface of western Pennsylvania. Since that time much discussion has taken place concerning the numbers and positions, and indeed the existence, of these deep structures. Figure 31 has been constructed to reflect the concept of Wagner's growth faults. Proprietary seismic reflection data have

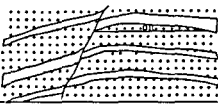

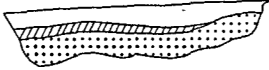

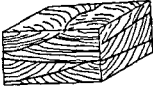

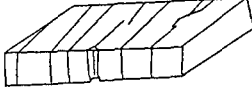
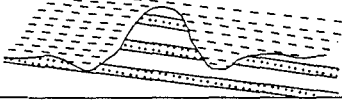
RESERVOIR HETEROGENEITY TYPE	
1 SEALING FAULT SEMI-SEALING FAULT NON-SEALING FAULT	
2 BOUNDARIES BETWEEN GENETIC UNITS	
3 PERMEABILITY ZONATION WITHIN GENETIC UNITS	
4 BAFFLES WITHIN GENETIC UNITS	
5 LAMINATION, CROSS-BEDDING	
6 MICROSCOPIC HETEROGENEITY TEXTURAL TYPES, MINERALOGY	
7 FRACTURING -TIGHT -OPEN	
8 EROSIONAL TRUNCATION AND PALEOTOPOGRAPHY	

Figure 32. Classification of reservoir heterogeneity types (modified from Weber, 1986).

established the presence of rift faults within fractured basement. However, the existence of the growth faults in the sedimentary cover is, as yet, strictly speculative. Such structures must have existed because the "best fit" for both the regional cross sections and regional mapping, which have been supplemented by geophysical studies (Davis, 1980; Chaffin, 1981), demand their existence.

The Rose Run sandstone increases in thickness to the southeast in Pennsylvania (see Figure 19), which should provide additional potential targets for hydrocarbon exploration, but it also increases in depth to the point where it is unlikely at this time to be drilled by the traditionally small independent Appalachian operator. With subsea elevations exceeding -15,000 feet in southwestern and south-central Pennsylvania, the Rose Run sandstone may be a likely target only for companies with large capital bases, such as the major oil companies.

Mesoscopic (Field- to Well-Scale) Heterogeneity

Introduction

The Cambrian and Ordovician reservoirs and targets discussed in this report occur within a thick sequence of predominantly shallow-water carbonates that comprise a part of what Ginsburg (1982) calls the "Great American Bank". The "Great American Bank" extended more than 1,875 miles along the length of the southern seaboard of Laurentia from Early Cambrian through Middle Ordovician (Hardie, 1986). This bank contained a complex mosaic of interdependent subenvironments in which depositional processes imprinted distinctive physical, diagenetic, and biogenic features on the sediments. Read (1989), Hardie (1989), and Osleger and Read (1991) interpreted the vertical stacking of various peritidal carbonate facies in this sequence to be the result of cyclical sea-level fluctuations; these cycles were shelf-wide features (Borer and Harris, 1991). Subtidal carbonate facies in the section occur within shallowing-upward sequences deposited in a shelf lagoon environment. These facies might be cyclical or non-cyclical (Demico, 1985; Read, 1989), and therefore might be either shelf-wide phenomenon or localized sedimentary accumulations. Finally, lowstand deposits of siliciclastic sediments, related to both third-order sea-level falls and short-term sea-level falls were transported onto the peritidal platform and mixed with subtidal facies as well. These clastics were transported across the shelf during sea-level lowstands and reworked during subsequent sea-level rises (Read, 1989). Mixtures of siliciclastic and carbonate lithologies encountered at the producing field to well scale are the result of both spatial and temporal variability. Reservoir heterogeneity is acute and complex, thus related in part to the depositional processes.

Classification schemes for defining heterogeneity types (Figure 32) from the field-scale level down to the well level are necessary to account for the heterogeneities during field development. Recognition of the types of reservoir heterogeneity in the Rose Run sandstone is based on core and log analyses. In many cases, heterogeneity types are restricted to specific lithofacies, as described

below. Detailed field-scale studies illustrate the influence each type of heterogeneity has on hydrocarbon production. Hydrocarbon production within Rose Run and Beekmantown oil and gas fields results from a complex interplay of many of these heterogeneity types.

Heterogeneity Types

Eight types of reservoir heterogeneity, modified from Weber (1986), occur within the Rose Run interval, as well as in associated and equivalent rocks. Lateral facies mixing in carbonate-siliciclastic depositional environments imparts considerable spatial variability to the geometry of reservoirs in these rocks. Temporal variability, due to eustasy, variations in sediment supply, and tectonic events (Reeckmann and Friedman, 1982; Lomando and Harris, 1991), further complicate the geometry of mixed carbonate-siliciclastic reservoirs. A wide range of energies in various depositional mediums in mixed carbonate-siliciclastic systems yield various baffles to fluid flow within the rocks (e.g. mudrock layers, carbonate laminites, etc.); baffles also form as diastems or unconformities as a result of cyclic sedimentation and/or non-cyclic deposition of multistory sandstone bodies. Lithofacies in mixed carbonate-siliciclastic sequences define specific flow units within the reservoirs, each with its own prevalent range of porosity and permeability values. Stratification within reservoir bodies controls the degree of anisotropy of fluid flow at the scale of individual sedimentary structures; the great variety of small-scale and large-scale structures in mixed carbonate-siliciclastic rocks constrain the continuity of fluid flow by controlling directional permeabilities. Finally, post-depositional deformation in the form of faults and fractures greatly enhances or retards fluid flow depending on the presence and effectiveness of seals.

A good example of reservoir heterogeneity as a result of faulting and subsequent fracturing (Figure 32, type 1) occurs along the Suffield fault system in southwestern Portage County, Ohio, and along an unnamed fault in the Conneaut field in northwestern Crawford County, Pennsylvania. Subsurface mapping and seismic data verify the existence of northwest-southeast trending faults that control, in part, the entrapment of hydrocarbons in the Rose Run.

Heterogeneity as a result of boundaries between genetic units (Figure 32, type 2) is evident in stray sandstones in the Copper Ridge/Ore Hill unit. Some of these sandstones have been mapped using subsurface well control. They are channel sandstones, as evidenced by their narrow, sinuous

shapes, and are encased in less permeable, nonporous Copper Ridge/Ore Hill dolostones.

Porosity and permeability zonation (Figure 32, type 3) occurs in both the Rose Run sandstone and the Beekmantown dolomite, but it is most dramatic in the bioturbated dolostone lithofacies of the Beekmantown where vuggy porosity has been developed in zones up to seven feet thick. The dolostone typically is relatively impermeable; only in the vuggy zones is the permeability enhanced by creation of wide pore throats due to carbonate dissolution. These vuggy zones probably developed through selective dissolution by meteoric water (Longman, 1980) or mesogenetic brines (Mazzullo and Harris, 1992), and can be correlated over township-wide areas. Based on geophysical log and core analyses, porosity in this lithofacies is normally less than four percent, and accompanied by very low permeabilities. In Coshocton and Tuscarawas counties, Ohio, well-developed pinpoint and massive vuggy porosity occur locally near the Knox unconformity. Porosity and permeability data from the #1-A Oakleaf and #1-A Lower cores from Coshocton County, Ohio indicate these vuggy zones in the Beekmantown that create permeability zonation (Appendix IV). Vuggy porosity also occurs in this lithofacies approximately 30 miles downdip from the Rose Run subcrop in Scioto County, Ohio. Permeability measurements from a vuggy zone in the Beekmantown/Mines in core 2958 from the Aristech well in Scioto County showed a maximum permeability (K_{max}) of 231 millidarcies (md) (Appendix IV).

Two types of heterogeneity evident within the cross-bedded and flaser-bedded, argillaceous sandstone lithofacies include permeability baffles within a genetic unit and cross-bedding that acts as a series of baffles (Figure 32, types 4 and 5). Vertical permeability variations result, in part, from thin argillaceous shale laminae that are prevalent in this lithofacies. Discontinuous to continuous shale laminae serve as baffles to vertical fluid flow; low vertical permeabilities associated with very high horizontal permeabilities illustrate this effect in core 2898 from Jackson County, Ohio (Appendix IV). The fact that these laminae are discontinuous and can not be correlated from well to well is the major drawback in attempting to predict or quantify this type of heterogeneity. Cross-bedding probably has less of an influence on fluid flow in this lithofacies. High horizontal permeabilities indicate low permeability contrasts in adjacent cross-bed sets. Limited data precludes quantitative analyses at this time.

Textural, mineralogical, and diagenetic changes in the rocks result in heterogeneities at the microscopic level

(Figure 32, type 6). This topic is discussed under Microscopic (Thin Section-Scale) Heterogeneity.

Secondary vuggy porosity associated with fracturing (Figure 32, type 7) occurs in the Beekmantown/Mines dolomite, and has produced hydrocarbons in Columbiana County, Ohio, near the Highlandtown fault system. Fractured dolostone within the Beekmantown/Mines is present in cores 2713, 867, and 2923 from Coshocton, Guernsey, and Morgan counties, Ohio, respectively (Appendix III). However, secondary mineralization commonly heals fractures and associated vugs; vugs up to 1 inch across are commonly filled with white dolomite. In southwest Morgan County, Ohio, intense fracturing resulted in brecciated zones composed of green shale and angular clasts of dolomite up to 2 inches across. Secondary mineralization by white dolomite healed the fractures near this brecciated zone, thereby partially reducing or totally eliminating the secondary porosity.

Naturally occurring and drilling-induced fractures were observed throughout the Rose Run and Beekmantown in the cooperative #3-A Reiss well venture based on the Formation Microscanner (FMS) images. Most of these fractures appear to have been induced by drilling. Azimuths of drilling-induced fractures aid in determining minimum *in situ* stress. Azimuths calculated from the FMS showed two dominant trends, a predominant northeast-southwest trend and a secondary northwest-southeast trend. Fracturing in the overlying Middle Silurian Lockport Dolomite also indicated a predominant trend of N60°E. FMS images also revealed the presence of both open and partially-healed naturally occurring fractures.

Two different generations of fractures have been described in a silicified oolitic dolostone in the Rose Run from the core of the Aristech monitor test/well in Scioto County, Ohio (A. T. Kearney, Inc. 1991). Much of the fracture porosity was reduced by secondary mineralization of carbonates. The first generation of fracturing formed prior to silicification and is partially filled by silicified calcite and ankerite. The second generation set is partially open and forms an orthogonal pattern across the brecciated clasts. One fractured core sample from the Aristech well (Appendix IV) had a porosity of 9.1 percent, and horizontal (K-90) and vertical permeabilities of 3.3 md and .07 md, respectively. The maximum permeability (Kmax) measured for this sample was 6.0 md.

Reservoir heterogeneity as a result of erosional truncation and paleotopography (Figure 32, type 8) occurs at the

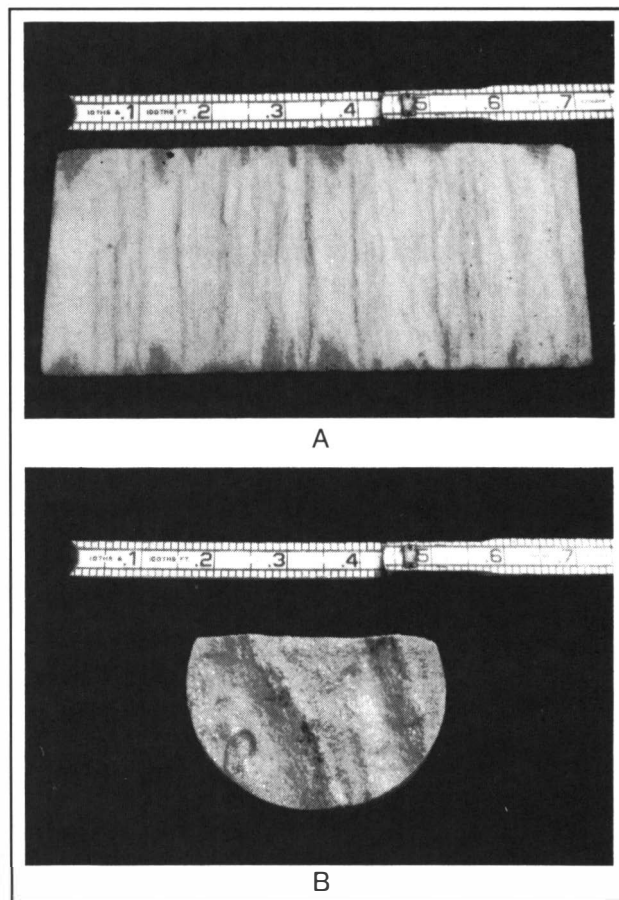


Figure 33. Photographs of the cross-bedded and flaser-bedded sandstone lithofacies from core 2898, Jackson County, Ohio. A—Side view showing the flasers. B—End view showing asymmetric ripples.

Knox unconformity. This is the most significant aspect of reservoir heterogeneity affecting hydrocarbon production in the Rose Run sandstone play. Based on cores and geophysical log correlations, up to five Rose Run sandstone units, separated by non-porous dolostones, may be present across county-wide areas; however, they are not regionally persistent across the entire study area. The dolostones act as baffles to fluid flow and create fluid-flow compartments within the Rose Run. In Holmes and Coshocton counties, Ohio, operators traditionally number these sandstones 1 through 5 based upon gamma ray- and density-log curve characteristics (Figure 17). Hydrocarbons have been produced from all five of these sandstones in stratigraphic pinchouts and erosional remnant traps along the subcrop trend from Fairfield County, Ohio to Crawford County, Pennsylvania. Field-scale studies of some typical erosional remnant plays in Holmes and Ashtabula counties, Ohio are discussed in detail.

Lithofacies

Four lithofacies occur within the Knox/Gatesburg interval in Ohio based upon examination of cores, subsurface mapping, and petrophysical analyses. They consist of the following: (1) cross-bedded and flaser-bedded, argillaceous sandstone, (2) interbedded, glauconitic sandstone and dolostone, (3) bioturbated dolostone and (4) laminated dolostone. These specific lithofacies have not been recognized in well cores from Pennsylvania; instead, the Rose Run has been divided into sandstone, dolostone, and mixed facies.

Cross-Bedded and Flaser-Bedded Sandstone

Cross-bedded and flaser-bedded sandstone constitutes the dominant lithofacies observed in cored intervals of the Rose Run sandstone in Ohio (Appendix V). This is the major Rose Run reservoir facies, represented by a sequence of stacked siliciclastic deposits separated by thin beds of dolostone.

Lithologically, the sandstone consists of white, fine- to medium-grained, sub- to well-rounded, moderately sorted, quartz arenites to subarkoses. Alternating layers of very fine and coarse grains are common. These rocks exhibit good intergranular porosity, giving it the highest reservoir quality of all lithofacies observed in cores. Average porosities measured from geophysical logs range from 8 to 12 percent with values as high as 14 percent. Porosities measured from cores analyses (Appendix IV) are in close agreement with those derived from geophysical logs. High porosities and permeabilities are not restricted to wells along the subcrop trend as indicated by cores in Jackson and Scioto County, Ohio. The Jackson County core (Appendix IV, core 2898) contains 26 samples having permeabilities greater than 1.0 md, seven of which are greater than 100 md. Only one sample was available from this lithofacies in the Scioto County well (Appendix IV, Aristech core), and it had a permeability of 80 md. Reservoir quality based on these porosities and permeabilities indicates there is good hydrocarbon trapping potential away from the highly explored areas along the subcrop trend (an Aristech monitor well drilled in Scioto County had a show of gas in the Rose Run). Structures and/or fault closure probably would be necessary for hydrocarbon entrapment.

Continuous to discontinuous wavy green shale partings and flaser-bedding are distributed throughout this lithofacies (Figure 33A). Intercalated mud in the form of flasers results from the accumulation of mud in ripple troughs. In

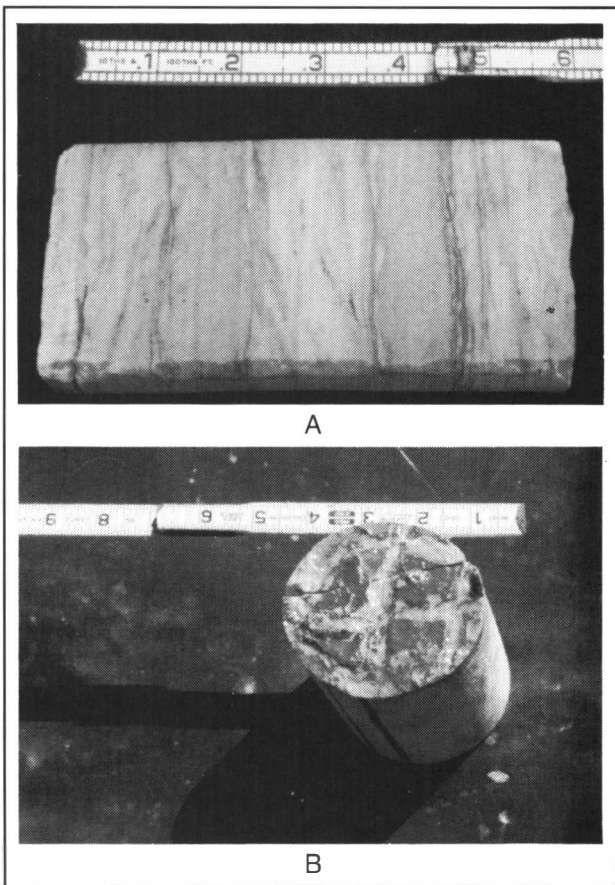


Figure 34. Photographs of the cross-bedded and flaser-bedded sandstone lithofacies. A—Side view of core 2850, Columbiana County, Ohio showing cross beds. B—Side view of core 2923, Morgan County, Ohio, showing polygonal mudcracks in cross-bedded sandstone.

a flaser-bedded unit asymmetric ripples with a wavelength of approximately 1.5 inches occur on the end of a core in Jackson County (Figure 33B). Low-angle cross-bedding is the most common sedimentary structure within this lithofacies (Figure 34A). Cross-bedding also is evident in sandstone bodies in the #3-A Reiss well using the FMS tool. Cross-beds at a depth of 7,000 feet dip to the southwest; the angle of dip increases upward from 7 to 12 degrees. Polygonal mudcracks also occur in several of the cores, indicating subaerial exposure of the sandstones during low stands in sea level (Figure 34B).

Interbedded Sandstone and Dolostone

Thin horizontal beds of interbedded sandstone and dolostone, commonly less than one inch thick, are present within two of the Rose Run whole diameter cores from Ohio. Sandstone beds in core 2853 from Coshocton County (Appendix III) contain large amounts of glauconite and alternate with thin beds of arenaceous dolostone

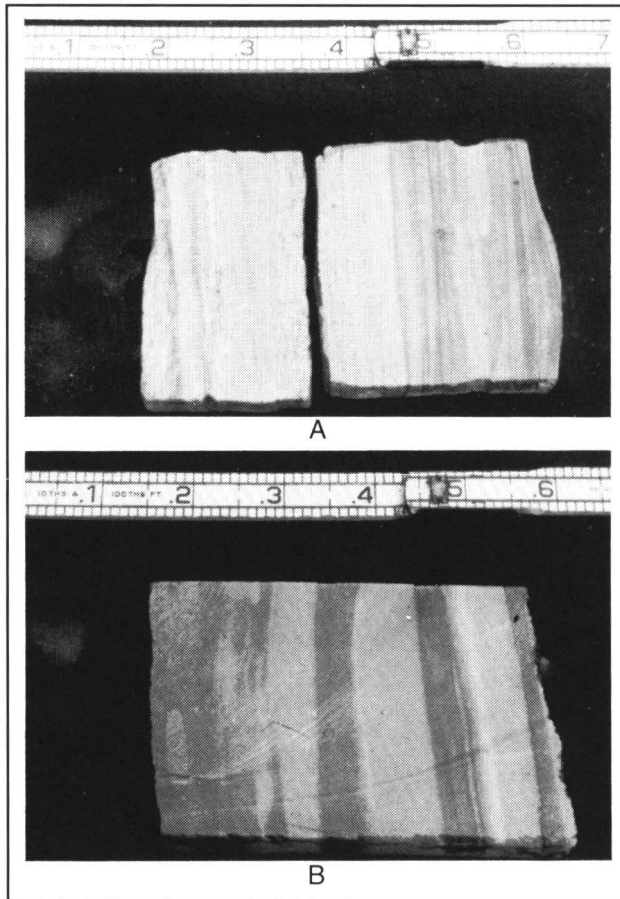


Figure 35. Photographs of the interbedded sandstone and dolostone lithofacies. A—Interbedded glauconitic sandstone and dolostone from core 2853, Coshocton County, Ohio. B—Interbedded sandstone and dolostone from core 2850, Columbiana County, Ohio.

(Figure 35A). In the Coshocton County core this lithofacies occurs within the Rose Run approximately six feet below the Knox unconformity. Geophysical logs were not run on this well so the stratigraphic position of this lithofacies within the Rose Run cannot be determined. In core 2850 from Columbiana County (Appendix III) interbedded sandstones and dolostones are located at the top of the Rose Run unit, directly underlying the Beekmantown/Mines (Figure 35B). Glauconitic sandstones exhibit very good intergranular porosity and have good reservoir quality. Arenaceous dolostones are more dense and have low porosities and permeabilities that serve as baffles to prevent fluid flow.

Bioturbated Dolostone

Although the bioturbated dolostone lithofacies generally has low reservoir quality, locally it may have well-interconnected vuggy porosity in the Beekmantown/Mines near the Knox unconformity. These localized zones of massive vuggy porosity have yielded some of the highest

gas production of any reservoir within Cambrian strata along the Rose Run subcrop play. Bioturbated dolostone is prevalent throughout the carbonates within the Beekmantown/Mines, Rose Run, and Copper Ridge/Ore Hill units in Ohio (Appendix III).

This lithofacies consists of grey to brown, fine- to medium-crystalline, mottled dolostone (Figure 36). It may be locally stylolitic and contain traces of glauconite. Local erosional contacts are present that are coated with thin lenses of dark-green shale, and often contain dolomite rip-up clasts up to one inch across. Chert nodules up to one inch across also occur within this lithofacies. As the dolostone grades into sandstone in the Rose Run, fine- to coarse-grained quartz grains appear to float in the dolostone matrix near the lithofacies boundaries. Desiccation features present in several of the cores indicate subaerial exposure.

Laminated Dolostone

The laminated dolostone lithofacies is present in core 2850 from Columbiana County, Ohio (Appendix III). This lithofacies exhibits poor reservoir quality and has not produced hydrocarbons in Ohio. Based on correlation to geophysical logs, this lithofacies in the Columbiana County core is situated near the base of the Beekmantown/Mines approximately six feet above the top of the Rose Run contact.

This lithofacies consists of light- to medium-brown, microcrystalline, laminated dolostone (Figure 37A).

Digitate algal stromatolites are present with individual laminae approximately 1 centimeter thick (Figure 37B). A silicified dolostone breccia overlies the stromatolite unit. Silicified clasts up to three inches across contain numerous silicified ooids. Ooids are radial and the concentric banding has been preserved through replacement of original carbonate texture by silica. The ooids range in size from medium to coarse grained. Based on the mesoscopic examination of cores, there is no visible porosity evident in the laminated dolostone lithofacies. Neutron and density logs also indicate that porosities are less than two percent. This nonporous lithofacies might act as a seal for trapping hydrocarbons in the Rose Run. Permeability data are not available for this lithofacies.

Sandstone, Dolostone, and Mixed Lithofacies

Rose Run sandstones in western Pennsylvania are generally interpreted as paralic to shallow marine in origin (Wagner, 1966c; Lytle and others, 1971); however, there are very few detailed environmental interpretations in the literature. The repeated cycles of algal dolomite, oolitic

dolostones, and quartzose to dolomitic sandstones testify to a close association of shifting peritidal and adjacent shallow subtidal deposits. Read (1989) included the Rose Run interval within one of his stratigraphic sequences of the Cambro-Ordovician passive margin succession in the Appalachians, his *sequence 4* (Figure 14). He recognized cyclic peritidal carbonates, non-cyclic subtidal carbonates, and marine-reworked siliciclastics. Smith (1969) suggested that an eolian, as well as coastal, siliciclastic component mixed with the inner and outer shelf carbonates of the Rose Run sequence. Enterline (1991) recognized four descriptive to genetic lithofacies—cross bedded sandstone, oncolite dolomite, bioturbated dolomite, and algal laminated/stromatolite dolomite—that he interpreted as peritidal deposits.

A facies is a body of rock with specified characteristics; sedimentary facies are defined on the basis of color, bedding, composition, texture, fossils, and sedimentary structures (Reading, 1978; Walker, 1979). The term facies may be used in a genetic sense (e.g. “turbidite facies,” “algal laminated dolomite facies”) or an environmental sense (e.g. “fluvial facies”). In Pennsylvania, however, the term facies is used in a strictly observational sense (e.g. “sandstone facies”), and they are discussed in terms of observed processes and interpretations of the environments in which they might have formed. The sedimentology of the subsurface intervals is so poorly understood because the data are very sparse, and because the facies designations are applied directly to geophysical well logs. In the discussion of carbonates in the Shell Oil #1 Shade Mountain well core in Juniata County, however, a genetic facies approach is used because specific microfacies (Wilson, 1975) can be distinguished (see pg. 35, Lithofacies).

We divided the Rose Run interval in Pennsylvania into sandstone or dolostone lithofacies and mixed sandstone and dolostone associations. Johnson (1978) defined mixed associations of shallow marine siliciclastic lithofacies and interpreted them as part of a continuum of physical energy condition. The single and mixed lithofacies associations used here, however, represent both lateral facies mixing and vertical variations in lithologic sequences induced by cyclic sea level changes and/or changes in sediment supply. These facies associations represent both spatial variability and temporal variability in a carbonate-siliciclastic mixed sequence (Lomando and Harris, 1991).

Three principal facies occur in the cores and outcrops examined during this study: 1) a sandstone facies (S); 2) mixed sandstone and dolostone associates (M); and

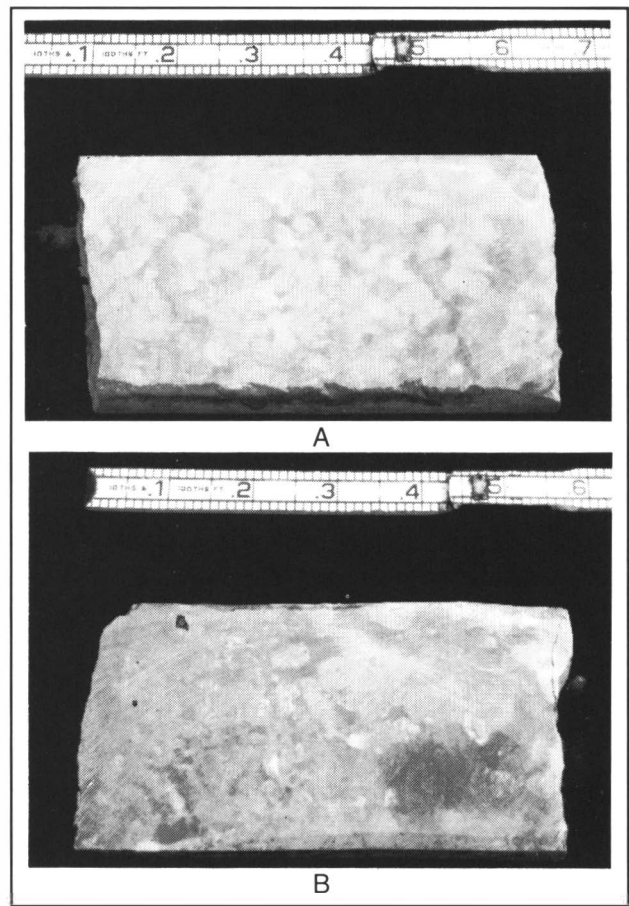


Figure 36. Photographs of the bioturbated dolostone lithofacies. A—Core 2989, Coshocton County, Ohio. B—Core 2923, Morgan County, Ohio.

3) a dolostone facies (D). The mixed facies (M) is subdivided into sandstone-dominated (*Ms*), equally mixed sandstone-dolostone (*Me*), and dolostone-dominated (*Md*) associations. The equally mixed sandstone-dolostone association (*Me*) can be further subdivided into medium-bedded (*Mem*) and thick-bedded (*Met*) categories.

Sandstone Facies (S)—Sandstone facies (S) occurs in both cores 1 and 2 in the #2 Hammermill well (Figures 38 and 39). It also occurs in a highway outcrop section along Route 453 southeast of Tyrone in Huntingdon County, Pennsylvania.

In the #2 Hammermill well core 1, the sandstone facies consists of very light-gray, fine-grained, well-sorted quartz arenite. Silica is the dominant cement. Authigenic illite comprises four to five percent of the binder. The sandstones are thick to very thick bedded, a characteristic that defines this facies. The rocks lack apparent sedimentary structures. Porosity and permeability are very low (Table 1, pg. 123).

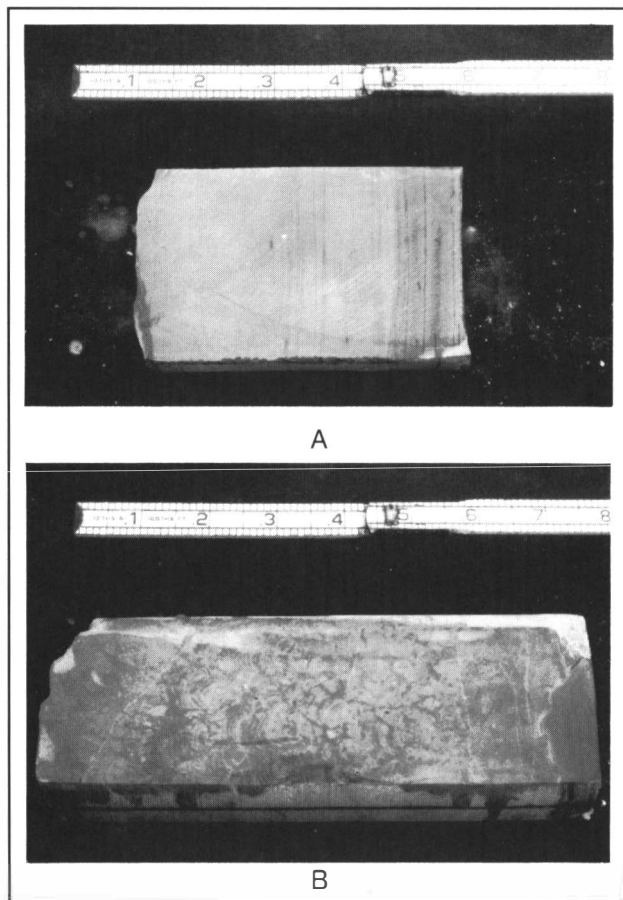


Figure 37. Photographs of the laminated dolostone lithofacies from core 2850, Columbiana County, Ohio. A—Laminated dolostone. B—Digitate algal stromatolite.

In the #2 Hammermill well core 2, the sandstone facies consists of white to very light-gray, fine- to medium-grained, moderately-sorted to well-sorted subarkose. The sandstones contain highly variable amounts of quartz and dolomite cements, with lesser amounts of feldspar and illite cements. The sandstones are thick to very thick bedded, cross-bedded, and contain basal lags of dolostone and shaly dolostone clasts. Porosity and permeability vary, but are generally good (Appendix IV).

In outcrop, the sandstone facies are thick to very thick bedded. Some cross-bedding occurs, including excellently displayed herringbone cross-stratification. The sandstone is light-gray, fine-grained, well-sorted quartz arenite. The principal cement is silica. Porosity and permeability are low. Thin sections reveal little visible porosity, and borehole logs indicate only 2 to 4 percent porosity throughout the section.

Mixed Sandstone and Dolostone Facies (M)—Mixed sandstone and dolostone facies occur in core 1 from the

#2 Hammermill well and are ubiquitous in outcrops. All three subdivisions of this facies occur in core 1 (Figure 39) and in the outcrops examined.

Facies Ms comprises mixed sandstone-dolostone lithologies, but is dominated by sandstone. The sandstones consist of fine- to medium-grained, moderately well-sorted quartz arenites. The principal cement is dolomite. Dolomite cements are polymodal, with planar- to planar-s textures, and contain ghosts of former peloids and ooids when viewed under the microscope in diffused plane-polarized light. Many of the ooid ghosts have detrital quartz nuclei. The sandstones are medium bedded and porous (Table 1, pg.123).

Dolostones in facies *Ms* are medium bedded rocks with unimodal, planar-s textures. They contain up to 40 percent detrital quartz and feldspar. The dolostones contain some visible ooid and peloid ghosts.

Rocks within facies *Me* contain approximately equal amounts of sandstone and dolostone. The distinction between *Mem* and *Met* is one of bed thickness (Figure 39).

Mem consists of thinly interstratified, medium-thick (~ 15 cm) beds of fine-grained, well-sorted quartz arenite and dolostone. Dolostones in this facies consist

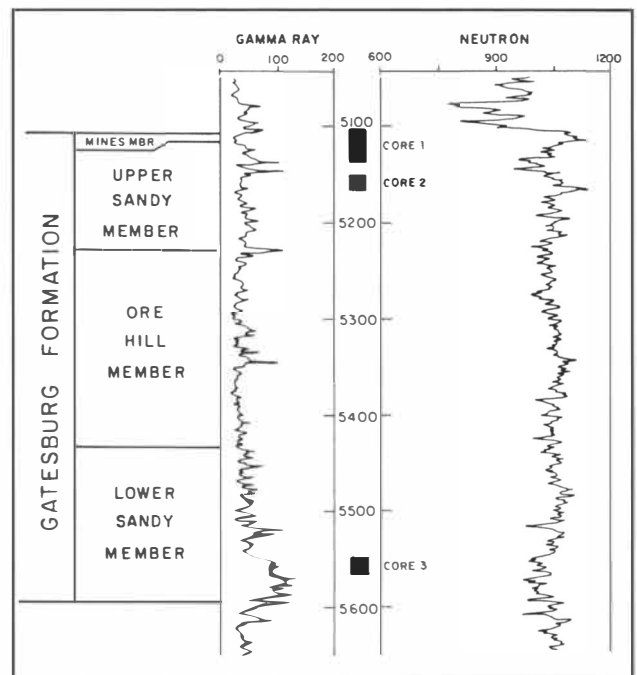


Figure 38. Geophysical log signature through the Knox/Gatesburg interval in the #2 Hammermill well, Erie County, Pennsylvania. Black boxes indicate recovered whole-diameter core intervals. Gamma ray is measured in API units. Neutron is measured in Birdwell neutron log units. Depth is in feet.

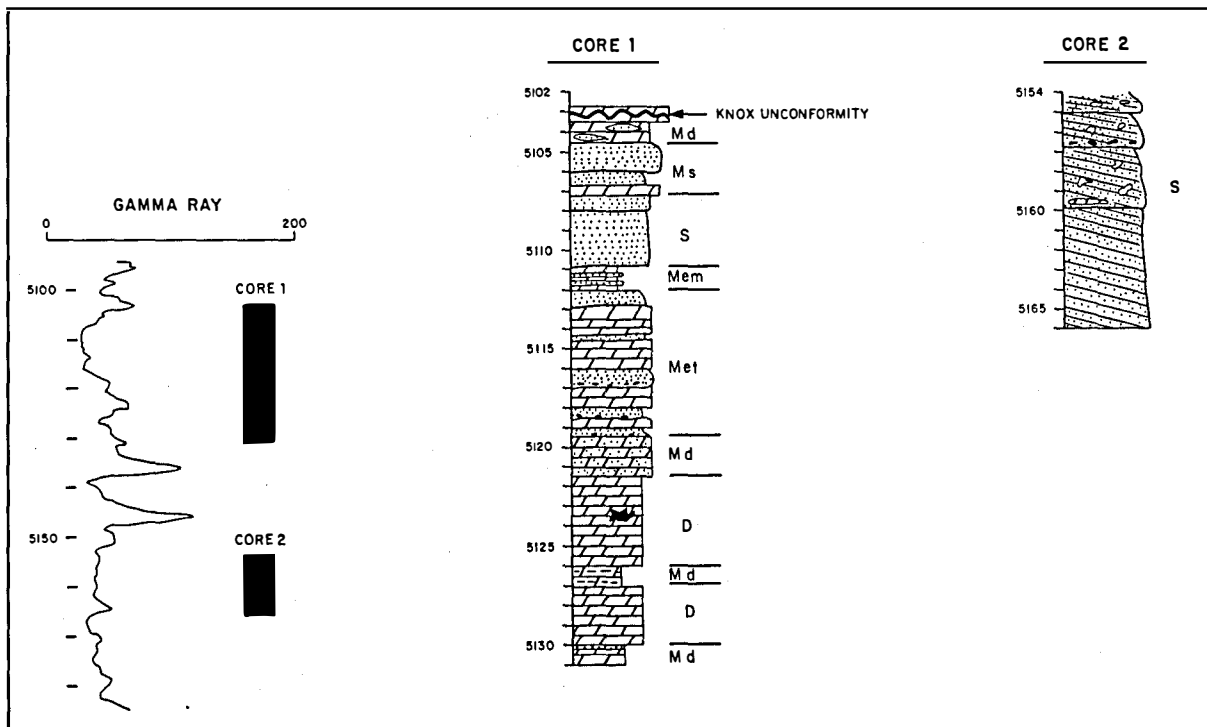


Figure 39. Graphical descriptions of cores 1 and 2 from the #2 Hammernill well, Erie County, Pennsylvania (from Laughrey, in press). Gamma ray log (measured in API units) and cored intervals (dark boxes) on left. Symbols for core lithologies are standard.

of medium-gray, unimodal, planar-s dolomite, with both medium-to fine-grained quartz and occasional feldspar floating in the carbonate groundmass. Dolomite crystals are decimicron-sized. Mudcracks do occur, but these are indistinct in most samples. Some dolostone beds consist of medium dark-gray, polymodal, nonplanar dolostone. Dolomite laminae grade upward, with crystal size decreasing from decimicron-size to smaller decimicron-size and micron-size dolomite. Dolomite laminae contain silt-size quartz, muscovite, feldspar, and pyrite. The dolostones contain wavy and flaser cross laminations. Porosity in both sandstones and dolostones from facies *Mem* is very low.

Facies Met consists of thick (> 30 cm) beds of sandstone interstratified with thick beds of dolostone. The sandstones are moderately well- to very well-sorted, fine- to medium-grained quartz arenites. Sandstone porosity varies from poor to good. Pervasive dolomite cementation obliterated porosity in some samples, but most sandstones have porosities between six and twelve percent. Some outcrop samples exhibit true herringbone cross-stratification with sharp set boundaries (Figure 40), i.e. opposite-dipping sets of avalanche cross-stratification (see Klein, 1977, p. 20–21). Mudcracks are preserved at the tops of some herringbone cross-stratified cosets (Figure 40).

Dolostones in facies *Met* are medium dark-gray, unimodal, planar-s dolomites with nonmimically replaced allochems. The latter consist of ooids, probable peloids, and possible shell fragments—all visible in diffused plane polarized light. Some of the dolostone matrix supports very fine- to coarse-grained quartz and feldspar detritus. The rocks display nodular bedding, mudcracks, and bioturbation.

Dolostones dominate facies *Md*. The dolostone is polymodal, planar-s to nonplanar, which contains nonmimically replaced ooids, peloids, and void-filling dolomite. Crystals are decimicron to centimicron-sized. Original matrix, if ever present, cannot be distinguished from void-filling dolomite. Some ooid nuclei consist of detrital sand- and silt-sized quartz and feldspar. The dolostones are bioturbated and mottled; burrows contain large amounts of detrital siliciclastic silt. Porosity appears to be low. Polymodal nonplanar dolomites are wavy, flaser, and lenticular cross-laminated, with minor lenses of quartz silt detritus. Micron- and decimicron-size crystals occur within discrete laminae.

Sandstones in facies *Md* occur as lenses and laminations of fine-grained, well-sorted quartz arenite. Lenses occur within dolostone. Laminated sandstones are interlaminated with dolomitic siltstone and dolostone. Porosity is extremely variable, three to ten percent, but generally low.

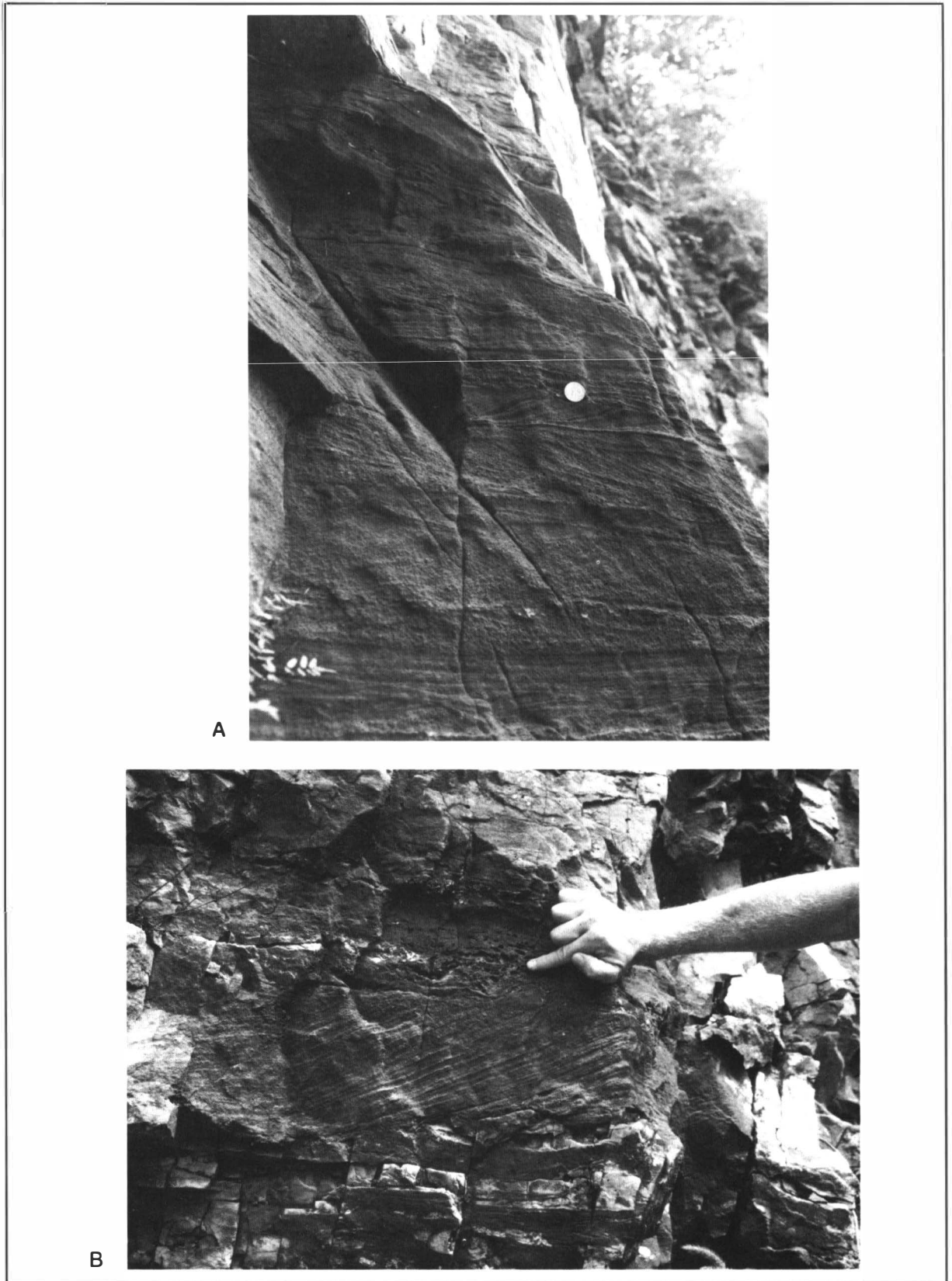
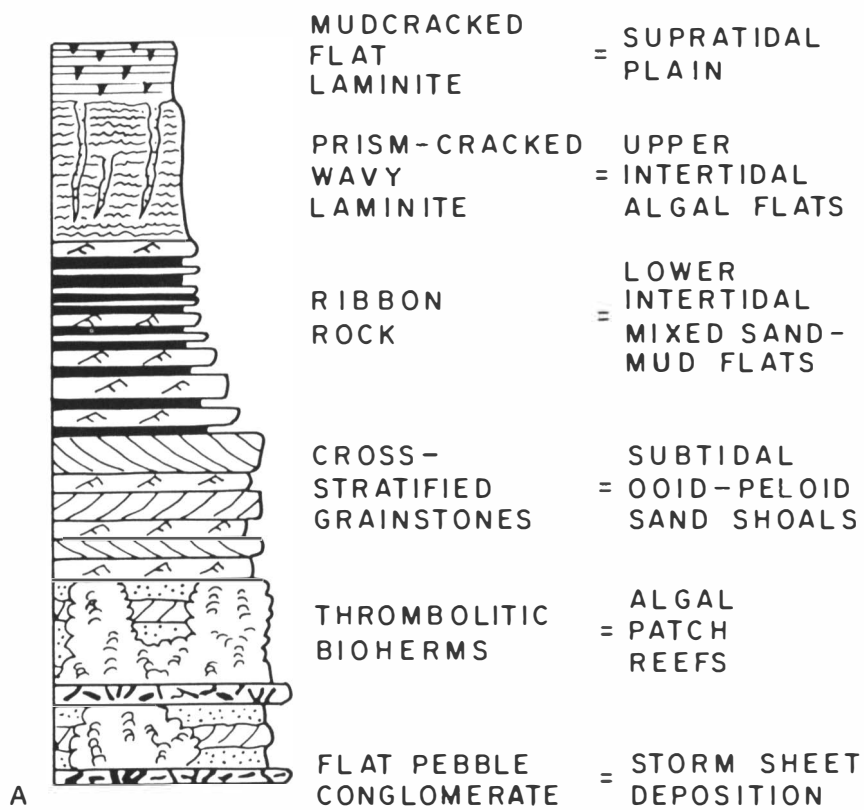


Figure 40. Herringbone cross-stratification in the Rose Run sandstone outcrop, Huntingdon County, Pennsylvania. A—Herringbone cross-strata within a thick sandstone sequence. The quarter rests on the top of a tidal cycle. B—Asymmetric herringbone strata sequence within peritidal dolostones. Finger points to rip-up clasts.



A



B

Figure 41. The Rose Run dolostone lithofacies in outcrop in Huntingdon County, Pennsylvania. A—Subfacies of the dolostone lithofacies (D), from Hardie (1986). The subfacies comprise a shallowing-upward tidal-flat sequence. B—Flat-pebble conglomerate, deposited by storm sheet deposition.

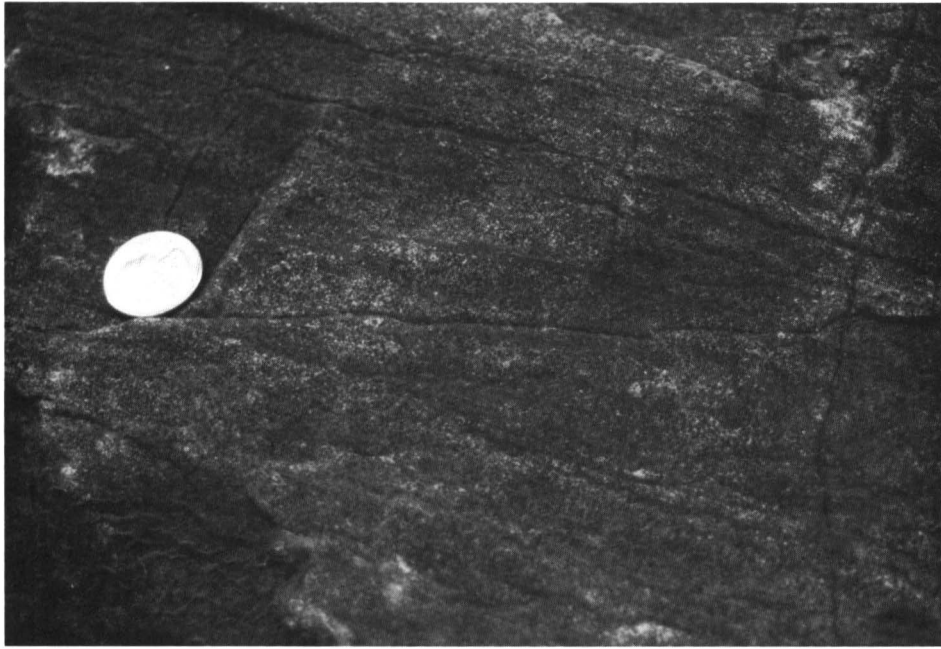


A

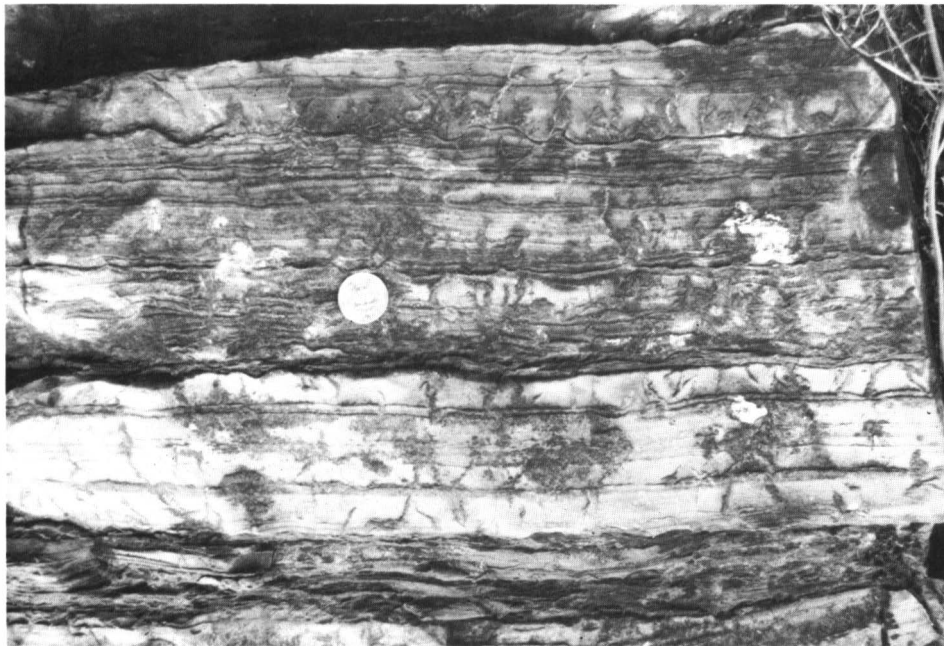


B

Figure 42. Photographs of the Rose Run dolostone lithofacies in outcrop in Huntingdon County, Pennsylvania. A—Large thrombolitic mound deposited as an algal patch reef. See Davies (1970) for modern examples from Shark Bay, western Australia. B—Close-up of a thrombolitic mound showing how such meter-scale features are actually composed of clusters of small digitate stromatolites.

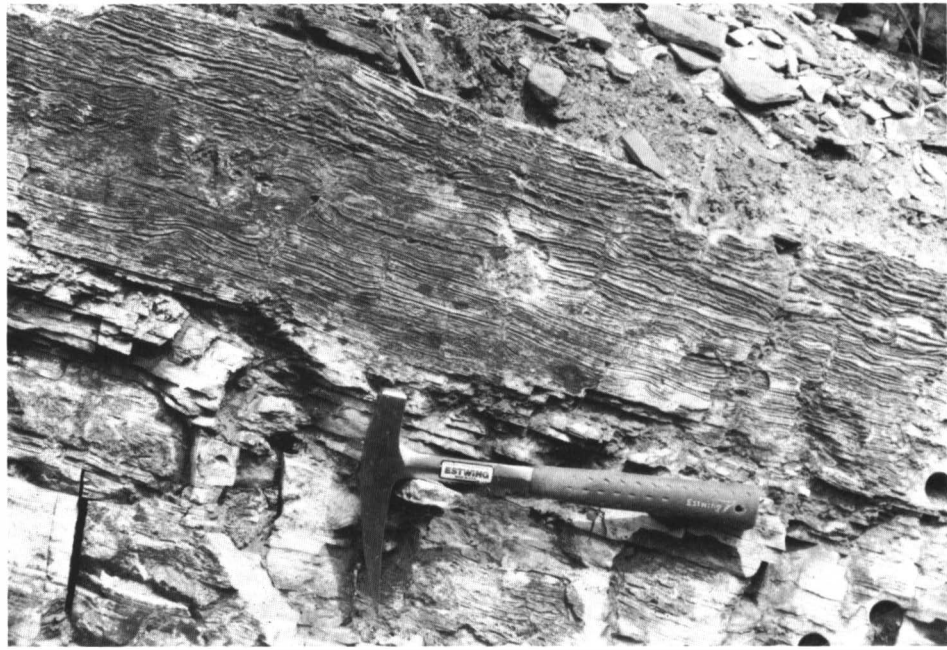


A

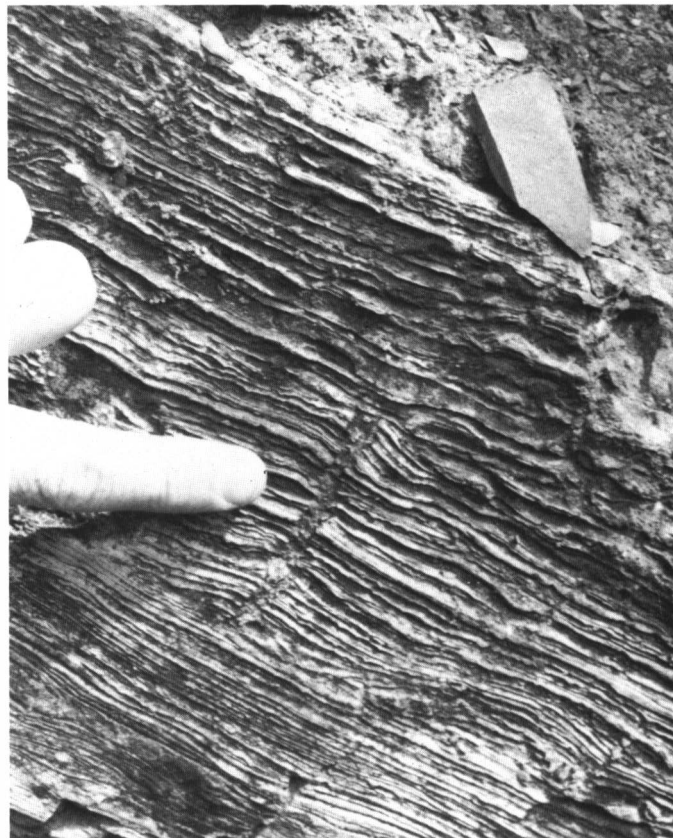


B

Figure 43. Photographs of the Rose Run dolostone lithofacies in outcrop in Huntingdon County, Pennsylvania. A—Ooid-peloid shoal subfacies. B—“Ribbon rocks”, i.e. thin-bedded, wave-rippled and burrowed dolostones that originated in a mixed sand and mud intertidal zone.



A



B

Figure 44. Photographs of the Rose Run dolostone lithofacies in outcrop in Huntingdon County, Pennsylvania. A—Prism-cracked wavy laminite interpreted as upper intertidal algal flats. B—Close-up of prism-cracked wavy laminite subfacies. Note how the edges of the prism crack appears to be ragged and is draped by small pieces of peloidal laminae that, “defy gravity” (Hardie, 1986). The sediment is interpreted to have stuck on the sides of cracks in the algal mats.

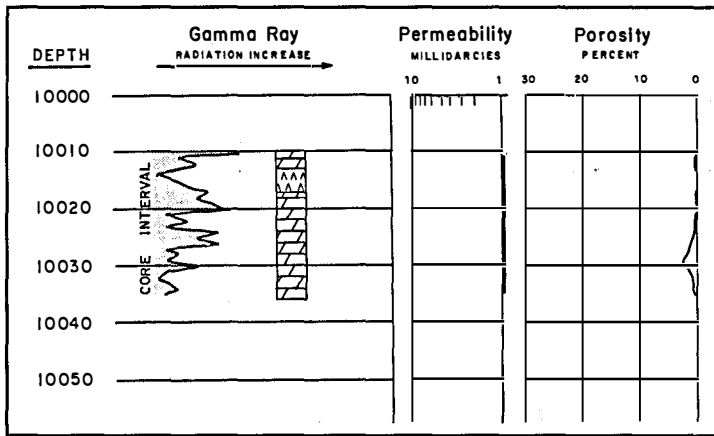


Figure 45. Graphical plot of core analysis data from the Gatesburg Formation core recovered from the #1 Shade Mountain well, Juniata County, Pennsylvania. The gamma ray signature was obtained by scintillometer from the core.

Dolostone Facies (D)—Rocks of the dolostone facies (D) mostly consist of unimodal to polymodal planar-s dolomite. In core 1 from the #2 Hammermill well, these rocks are light-gray to light olive-gray and display nodular bedding and some very strong bioturbation. Quartz and feldspar silt lines and partially fills some burrows. Many samples show nonmimic replacement of ooids, peloids, and intraclasts. Dolomite crystal sizes range from micron-size to centimicron-size; smaller crystal sizes define some nonmimically replaced allochems. Some samples contain calcite nodules. Some are pyritic. Some intervals in this facies are highly porous.

Ooid dolograins dominate this facies in outcrops. The rocks are light olive-gray to greenish-gray. The dolostones consist of polymodal, planar-s dolomite with replaced ooid allochems, partial to complete ooid molds, and void-filling dolomite. Most allochems are mimically replaced by dolomite, but some nonmimic replacement also took place. Ooid allochems in the dolostones from central Pennsylvania outcrops exhibit uniform isopachous fringes of mimically replaced marine cement that originally had a radial-fibrous fabric. Centimicron-sized planar-s dolomite fills intergranular voids; although this dolomite texture resembles equant, pore-filling

sparite of meteoric or deep connate origin, it is difficult to tell if this is a mimic of earlier cements now replaced by dolomite or strictly a dolomite cement texture.

Outcropping rocks of the dolostone facies in central Pennsylvania also contain “ribbon rocks” (thin-bedded, wave-rippled and burrowed dolostone), wavy dololaminite, flat pebble conglomerates, and thrombotic algal mounds (Figures 41 to 44).

Shell Oil Co. tested the Gatesburg Formation in central Pennsylvania in 1964 when they drilled the #1 Shade Mountain Unit well in Juniata County. This well was drilled on the Shade Mountain anticline where it penetrated duplex thrust sheets. The well encountered

only a show of gas, but the company recovered a small core of the Gatesburg Formation from between 10,010 and 10,035 feet (Figure 45). The recovered rocks consist of dolostone and anhydrite. Measured porosities in these rocks are very low and permeabilities are less than 0.1 md (Figure 45).

The core contains stacked shallowing-upward carbonate sequences (Figure 46). One complete sequence consists of subtidal shelf-lagoon sediments overlain by intertidal and supratidal sediments respectively. Evaporites cap the sequence and these are of special significance. The individual dolostone subfacies recognized in this core are described.

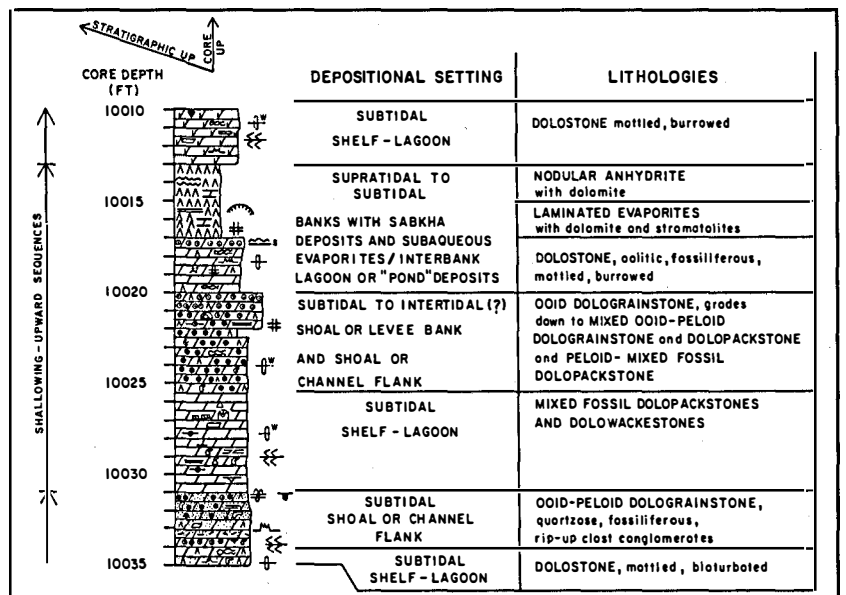


Figure 46. Graphical core description of the Gatesburg Formation in the #1 Shade Mountain well, Juniata County, Pennsylvania. Symbols are taken from the AAPG Sample Examination Manual (Swanson, 1981).

Subtidal shelf-lagoon subfacies.—

These rocks consist of mixed-fossil dolopackstones and dolowackestones. Fossils include algal remains and shell material, including brachiopods. Horizontal laminations and cross-lamination occur sporadically in the core. Some of the bedding is nodular. Some birds-eye structures, tepee structures, and pull-apart structures are present also. Trace amounts of feldspar are scattered throughout the rock. The dolostones are mottled and well-burrowed. This subfacies contains minor anhydrite and chert.

Subtidal shoal or channel flank subfacies.—

This subfacies consists of mixed ooid-peloid dolograins and dolopackstones and peloid-mixed fossil dolopackstones. The fossils are undifferentiated shell material. The rocks contain scattered quartz and feldspar, and minor amounts of anhydrite. Rip up clasts occur in some of the rocks. Horizontal laminations and nodular bedding are present and the rocks are bioturbated.

Shoal or levee bank subfacies.—This subfacies consists of ooid dolograins that grade downward into the mixed ooid-peloid dolograins of the shoal flank or channel flank subfacies.

Sabkha and subaqueous evaporite subfacies.—This subfacies contains nodular and laminated anhydrite, along with rippled and lenticular dolostone and stromatolites. This subfacies also contains an *interbank lagoon* or “*pond*” subfacies comprised of oolitic, mottled and burrowed, fossiliferous dolostones. We interpret the evaporites as having formed along the high portion of carbonate banks as normal subkha successions (nodular anhydrite) or in the interbank ponds and lagoons as subaqueous evaporites (laminated anhydrite and stromatolites) as suggested in Figure 47.

Hardie (1986, p. 41) suggested that the climate during Gatesburg time was, “. . . dry enough to produce some growth of evaporite minerals within the supratidal sediments but not arid enough to accumulate a cap of sabkha evaporite deposits,” which agrees with the discussion of paleoclimate given above. Read (1989) suggested a semiarid climate, with an overall evaporative depositional setting. The recognition of evaporite minerals in the Gatesburg Formation and its equivalents has, to

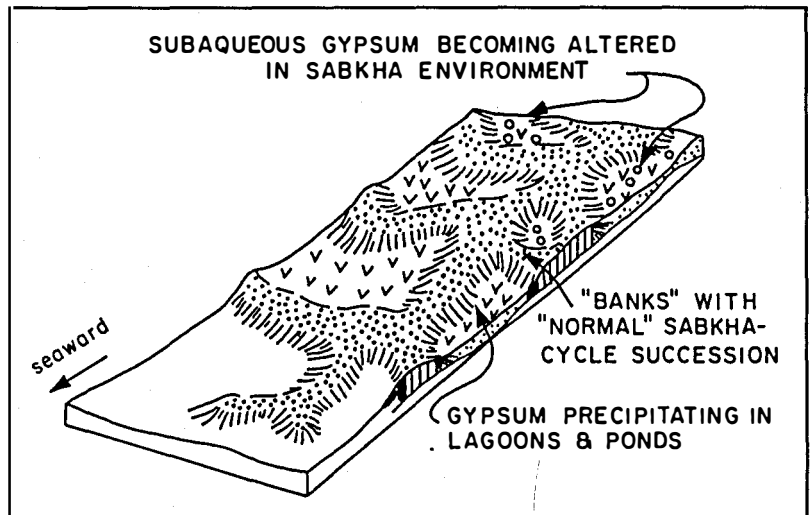


Figure 47. Inferred depositional environment of Mississippian Frobisher Evaporite in southeastern Saskatchewan provides a valid model for Late Cambrian Knox/Gatesburg deposition in central Pennsylvania (from Kendall, 1984). Numerous shallow maritime lakes, ponds, or lagoon are isolated by carbonate shoals and banks on top of which strips of supratidal sabkha rest.

date, been indirect. Hardie (1986) discussed displacive calcite nodules that originally might have been supratidal gypsum. Folk and Pittman (1971) suggested that length-slow chalcedony in the Gatesburg was evidence for vanished evaporites. The Gatesburg Formation rocks recovered from the Shell Oil Co. #1 Shade Mountain Unit well provides unequivocal evidence of evaporite deposition in central Pennsylvania during Late Cambrian time.

Depositional Framework

Much of the heterogeneity observed in the Rose Run reservoirs is related to the depositional environment that provided the vertical stacking of interbedded siliciclastic and carbonate facies during cyclical fluctuations of sea level. Both regional and field-scale heterogeneity occurred as the result of sea-level variations across a shallow carbonate-siliciclastic shelf, as described by Read (1989) (Figure 14).

Rose Run strata record, in part, deposition in peritidal to shallow subtidal marine environments. Many authors, including Mussman and Read (1986), Anderson (1991), Enterline (1991), and Ryder (in press), have interpreted the depositional environment of the Knox/Gatesburg and equivalent strata as tidal-flat. Although much of the Knox/Gatesburg represents tidal-flat deposition, such a singular designation clearly is not appropriate for the entire interval. A number of sedimentary features in the lithofacies described above support a broader interpretation of peritidal deposition. These include: 1) wavy, flaser,

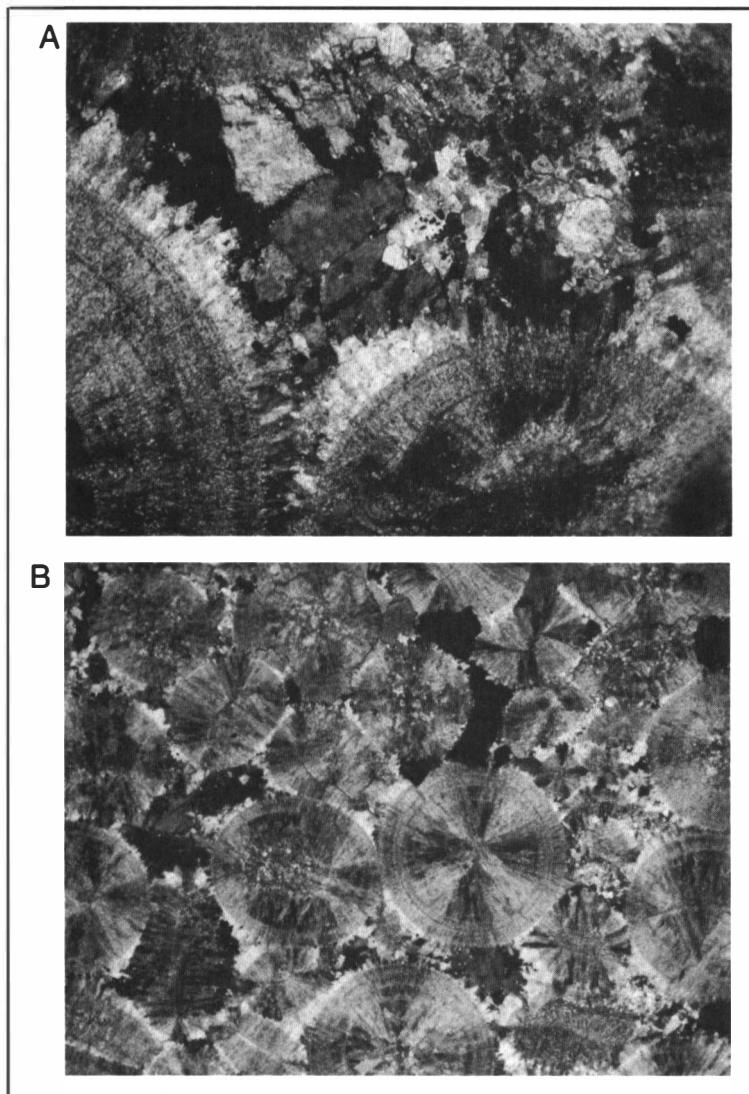


Figure 48. Ooid dolograins in the Dolostone Facies, Huntingdon County, Pennsylvania. A—Typical fabric of the ooids. Note the presence of both concentric and radial fabrics. B—Isopachous fringe and pore-filling cement textures.

and lenticular cross-lamination indicative of the alternation of bedload and suspension deposition during variable phases of high to low, or non-existent, subaqueous current flow (Klein, 1977). Reinech and Wunderlich (1968) attribute flaser-bedding to an intertidal environment where incomplete mud laminae are trapped in ripple troughs during periods of slack water; 2) mudcracks indicate exposure of the sediments to the atmosphere in the supratidal environment or, during extreme hot and arid conditions, in the intertidal environment; 3) herringbone cross-stratification represents sandwave migration in response to reversing current flow. For example, the rocks in Figure 40 exhibit herringbone cross-stratification and mudcracks that reveal a flood-to-ebb tide sequence followed by exposure to the atmosphere) 4) ooids and

peloids indicate proximity to the littoral and shallow marine realm, whereas burrows and bioturbation suggest organic activity, although fossils are rare in the rocks. Mottling as a result of bioturbation is common within the intertidal zone (Shinn, 1983; Wilson, 1983); 5) nodular chert, possibly a secondary replacement feature after nodular evaporites, might signify the presence of an arid supratidal environment (Shinn, 1983; Hardie, 1986); 6) basal lags of dolostone and shaly dolostone in the sandstones indicate scour, possibly due to erosion along tidal channel thalwegs; and 7) algal laminae and hemi-spheroids indicate deposition in the upper intertidal to lower supratidal zone. According to Shinn (1983), horizontal laminations and absence of mottling in tidal flat deposits are limited to the upper intertidal to supratidal zone (see also detailed discussions by Logan and others, 1964, and Bathurst, 1971).

The ooid grainstones, on the other hand, represent subtidal, shallow marine deposition. Although dolomitization has destroyed the depositional fabric of the original carbonate facies, careful examination in thin sections reveals the former presence of ooids and peloids (see Petrography, Petrology, and Petrophysics). The dolostone facies in several cores from Ohio, and in outcrop in central Pennsylvania, contain abundant ooids and peloids.

Ooids form in agitated marine waters in carbonate sand shoals and in tidal deltas associated with tidal inlets (Ball, 1967; Hine, 1977). Ooids also form on tidal flats and beaches, in lagoons, and in some non-marine and hypersaline environments (Tucker, 1981). However, these are not nearly so common as subtidal sand shoals. The ooid grainstones of the Knox/Gatesburg interval are interpreted as subtidal, shallow marine deposits because of their thickness and extent, and because they reveal a vestige of former submarine carbonate cementation, i.e. mimically replaced isopachous fibrous cement on ooids (Figure 48). In outcrop in central Pennsylvania, these dolostones are associated with thrombolitic bioherms (Figure 42) that Hardie (1986) interpreted as algal patch reefs.

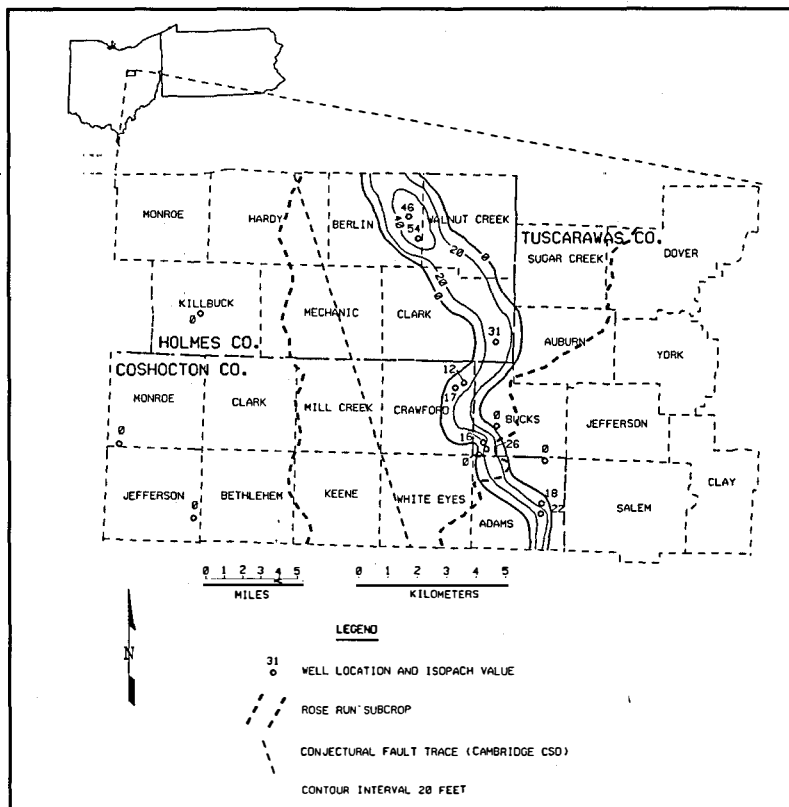


Figure 49. Isopach map of Copper Ridge/Ore Hill sandstone in Tuscarawas, Holmes, and Coshocton counties, Ohio. The Rose Run subcrop occurs between the dashed lines.

Based on detailed log correlations and isopach maps, sandstone strata in the Rose Run consists of coalesced lenticular bodies of wide areal extent covering tens of miles. Sandstones such as these are thought to have been deposited by waning storm-generated currents and later reworked by wave activity (Goldring and Bridges, 1973; Johnson, 1978). In contrast, sandstones within the Copper Ridge/Ore Hill dolomite sequence occur as narrow, sinuous, meandering tidal channels. Based on examination of cores and geophysical logs, reservoir quality is good in both of these sandstone types. Prolific hydrocarbon production occurs within these Rose Run sandstones where they pinch out beneath the Knox unconformity, or where they are preserved within erosional remnants.

The well-developed porous sandstone encountered in the Copper Ridge/Ore Hill of the #3-A Reiss in Coshocton County, Ohio provides an example of one of these narrow-bodied, channel sandstone deposits. Subsurface mapping based on all available wells penetrating this horizon shows it to be a meandering, sinuous, sandstone body trending northwest-southwest from Berlin Township, Holmes County to Adams Township, Coshocton County (Figure 49). The channel trends parallel to subparallel to

the Cambridge CSD, suggesting possible tectonic control of the deposition of this sand body. This sandstone unit reaches a maximum thickness of 54 feet in Holmes County (permit number 1279). Additional deep well control is necessary to determine the lateral extent of this tidal-channel sand. It is not known if this unit has been eroded or pinches out to the northwest. Although there has not been any known hydrocarbon production from this sandstone body to date, the potential exists if the sandstone can be found associated with a structural feature or at lateral pinchouts. A stratigraphically younger sandstone in the Copper Ridge/Ore Hill has been mapped in Mechanic Township, Holmes County, Ohio. This channel sandstone trends northwest-southeast (Figure 50) parallel or subparallel to the Cambridge CSD.

Sandstone lithofacies described from northwestern Pennsylvania (facies S) are more difficult to interpret, but suggest a possible fluvial origin based on descriptions of Core 2 from the #2 Hammermill well (Figure 39). The sandstones are feldspathic; the feldspar species resemble those present in the Grenville terrane that would have supplied river-derived detritus (Lidiak and Ceci, 1991) (see Petrography, Petrology, and Petrophysics). The sandstones consist of multiple, stacked, fining-upwards sequences, having erosional lags at the bases of upward-fining sets. The sandstones exhibit unidirectional cross-bedding. These sandstones might represent deposition by ephemeral streams entering the paralic environment. Partial analogues include the Gascoyne and Wooramel rivers of western Australia, which drain into Shark Bay (Davies, 1970), or ephemeral fluvial sediments recognized in the Mississippian St. Louis Limestone of southeastern Kansas by Handford and Francka (1991, fig. 15) and by Tucker and Chalcraft (1991) in the Permian Queen Formation of the West Texas Permian basin region.

The facies S sandstones in core 1 from the Hammermill well reveal very little. These sandstones consist of remarkably pure quartz arenites that coarsen upwards. They lack apparent sedimentary structures, grain size trends, or

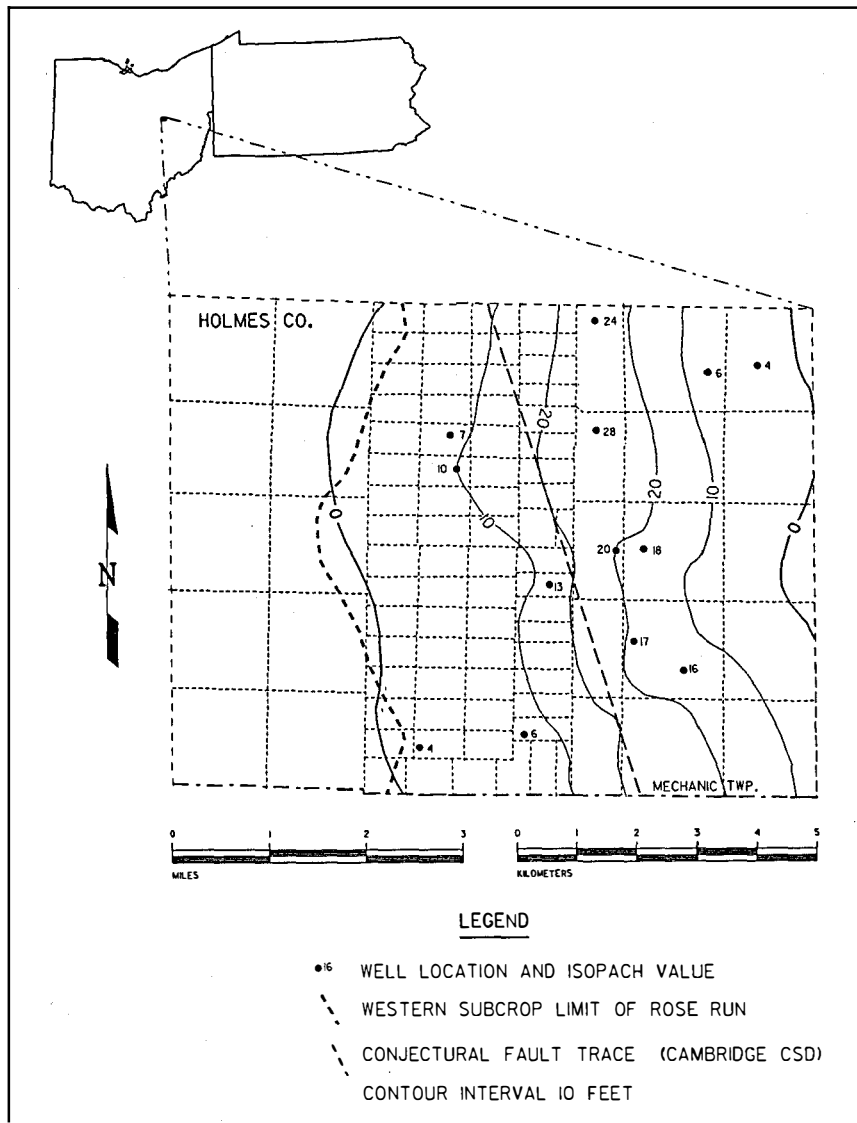


Figure 50. Isopach map of a Copper Ridge/Ore Hill sandstone in southeastern Holmes County, Ohio.

fossils. Although sandstones of the heterolithic facies are clearly tidal, the thickness of the S sandstone in core 1, its lack of erosional clasts and scour features, and the coarsening-upwards grain size trends preclude a tidal channel origin as proposed by Enterline (1991). These sandstones might be eolian coastal dunes, marine-reworked subtidal sands, or some combination of both (Shinn, 1980).

Facies S sandstones in outcrop are equally enigmatic. Although some herringbone cross-bedding and cross-lamination occurs in quantity in some beds, these rocks generally consist of nearly featureless quartz arenites. Herringbone cross-stratification, where it occurs, is evidence for some aspect of tidal deposition. Smith (1969)

proposed an eolian-beach depositional origin for these sandstones.

Case Studies

Introduction

Within the study area six possible trapping mechanisms occur in the Upper Cambrian reservoirs in Ohio and Pennsylvania: 1) erosional remnants; 2) fault-related traps; 3) combination fault-related and erosional remnant traps; 4) erosional truncation at an angular unconformity (quartz sandstone and vuggy dolomite); 5) anticlines and plunging noses; and 6) updip or lateral pinchout of facies (interfingering of porous quartz blanket sandstone with tight dolostone, and abrupt change of porous quartz channel sandstone against tight dolostone). Of these six types, the first four were documented in this report as affecting hydrocarbon production from the Rose Run. Detailed case studies in five productive areas along the subcrop are presented below.

Geophysical log correlations, core descriptions, and seismic interpretation show that the major controls of lateral continuity or heterogeneity of Rose Run sandstones and Beekmantown/Mines dolomite are erosional truncation and paleotopography on the Knox unconformity. At the field scale the interpretation of seismic data plays a fundamental role in measuring and predicting changes in heterogeneity that define a reservoir. Therefore, an emphasis has been placed on seismic modeling, processing of seismic data, the use of synthetic seismograms, and the importance of all three in field-scale studies of heterogeneity.

Southeastern Holmes County, Ohio

Holmes County has been one of the more intensely explored areas of east-central Ohio for hydrocarbon

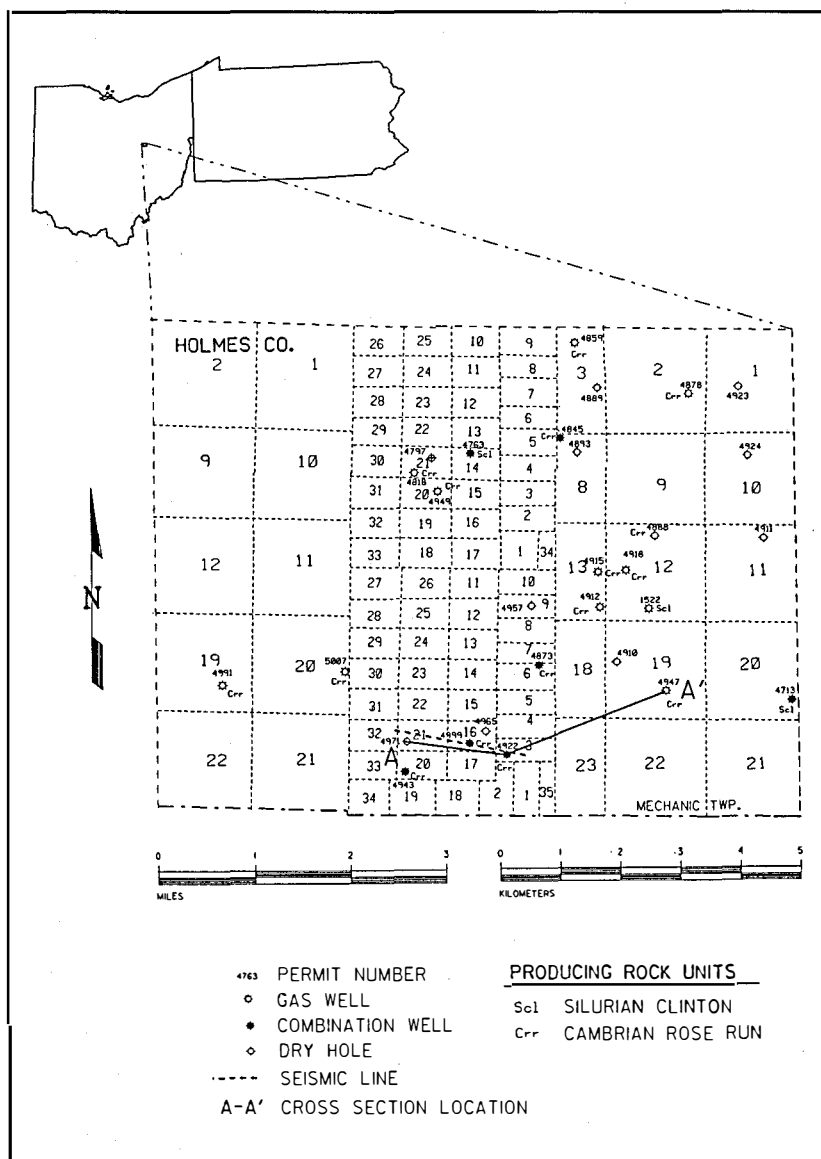


Figure 51. Base map showing wells penetrating the Knox unconformity or deeper in Holmes County, Ohio.

production from Rose Run sandstone (Figure 51). Historically, the Rose Run produced primarily natural gas in this area; however, recent drilling in Clark and Mechanic Townships discovered significant associated oil and condensate production, as well as minor production from sandstones in the Copper Ridge/Ore Hill dolomite, approximately 100 feet below the Rose Run. This portion of the study concentrates on Mechanic Township where available seismic data can be tied to wells producing oil and gas from the Rose Run sandstone.

Holmes County is situated within a relatively broad section of the Rose Run subcrop. We speculate that reactivated basement faulting along the Cambridge CSD resulted in uplift on the east side of the lineament. Erosion

at the Knox unconformity probably exposed a greater surface area of the Rose Run sandstone, broadening the subcrop to the east. Remnants developed from the erosion of arenaceous and carbonate rocks at the Knox unconformity appear on maps and seismic data as apparent structural closures. This is the dominant form of Rose Run heterogeneity in this area. We recognize four types of trapping mechanisms in Cambrian rocks of Holmes County: 1) porous sandstone remnants encased in impermeable carbonates; 2) faulted remnants; 3) truncation of sandstone at an angular unconformity; and 4) lateral pinchout of porous sandstone into impermeable dolostones. Localized faulting and structural closure may enhance the above trapping mechanisms in Holmes County.

Heterogeneity within the Rose Run sandstone and underlying Copper Ridge/Ore Hill sandstone of Holmes County has been defined using well control and seismic data. Based upon Weber's (1986) classification, fault-controlled heterogeneity (type 1) and erosional truncation and paleotopography (type 8) appear to be the most common reservoir

heterogeneity types controlling hydrocarbon distribution in this area. Interpretation of seismic data and subsurface data suggests a combination of these types. However, this is interpretive and any faults are conjectural in this example. Because of the minimal throws on most of the faults, faulting with visible offset is difficult to image with seismic reflection data in Ohio. Type 8 heterogeneity is the easiest to document, and appears to be the dominant heterogeneity type associated with a trapping mechanism. Examples of type 8 heterogeneity, and presence of Copper Ridge/Ore Hill sandstone adjacent to nonporous dolostones, exist in Holmes County. The Copper Ridge/Ore Hill sandstones, which have been interpreted as incised channel deposits, occur parallel to subparallel with the CSD.

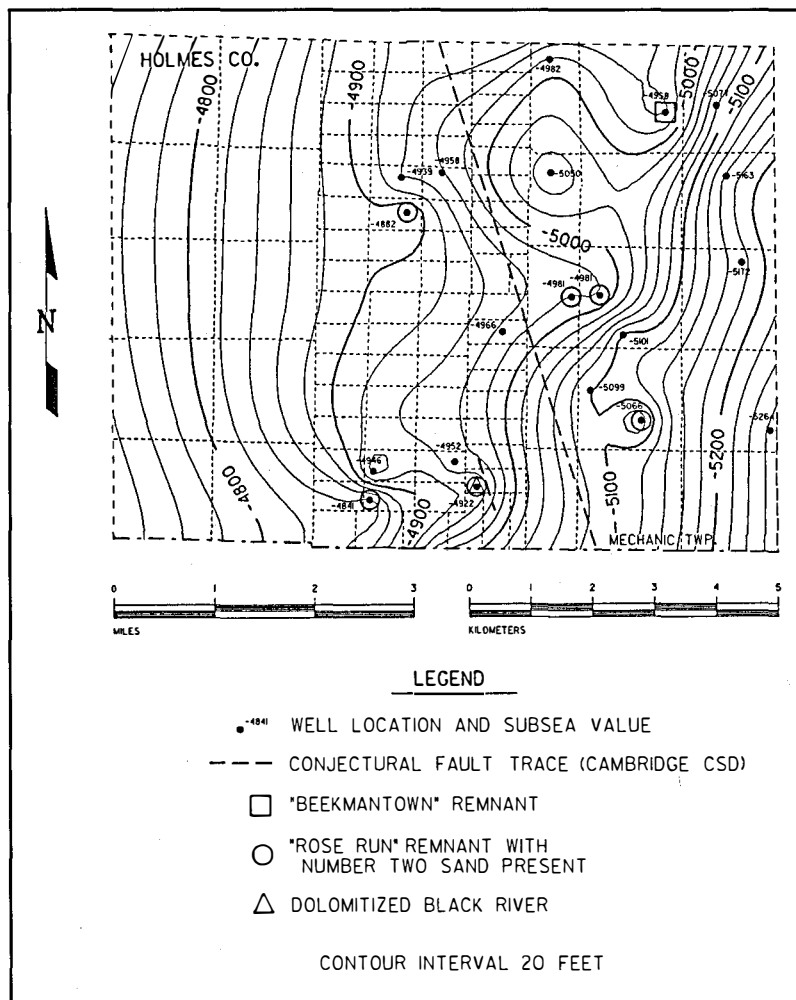


Figure 52. Structure map on top of the Knox unconformity, Holmes County, Ohio.

Type 8 heterogeneity (paleoremnants in this study represents the primary trapping mechanism for Rose Run hydrocarbons in Holmes County. Remnants in Mechanic Township can be easily identified using well control and seismic data (discussed below). The structure map on the Knox unconformity of Mechanic Township (Figure 52) shows regional dip to the east with a number of structural highs and lows plunging dominantly eastward. Subsea structure on the top of the Knox ranges from -4,740 to -5,260 feet across the township. These apparent structural highs on the Knox unconformity are overlain by thin Wells Creek/Shadow Lake (Figure 53). The thickness of the Wells Creek/Shadow Lake interval ranges from zero to 72 feet across the township. The unconformity exposes the number two Rose Run sandstone or Beekmantown/ Mines in the major producing remnants. Slight thinning of the lower portion of the Upper Ordovician Black River limestone due to compaction of sediments may have occurred over some of these remnants, but compaction of

rocks above the Black River has not been observed. The isopach map of the Wells Creek/Shadow Lake-through-Trenton interval (Figure 54) ranges from 650 to 710 feet across the township. Thickness differences are attributed to slight compaction of the lower Black River and Wells Creek/Shadow Lake. However, local reactivation of basement structures has affected the thickness of sediments above some remnants.

Heterogeneity of the producing remnant in Holmes County also has been enhanced by later structural movement that may have altered the trapping mechanism of the remnant. Structural movement after deposition of the Wells Creek/Shadow Lake interval either removed or enhanced the apparent structure of some of these remnants, as illustrated by comparison of Figures 55 to 57. Structural reactivation occurred at different times at the position of some of the remnants. For example, minor structural uplift, accompanied by faulting and fracturing, occurred after deposition of the Upper Ordovician Trenton Limestone, Lower Silurian "Packer Shell," and

Mississippian Berea Sandstone. All structure maps, with the exception of the Berea (Figure 57), show the predominant eastward dip of the Appalachian basin. Structure maps on the base of the "Packer Shell" and, especially, the top of the Berea show the trend of the Cambridge CSD. Significant structural reversal along this CSD occurs on the Berea structure. The trend of the CSD does not show on the Knox unconformity or Trenton structure maps, possibly due to the lower density of wells penetrating the Knox Dolomite. Structure across the township varies as follows: Trenton, -4,020 to -4,480 feet; "Packer Shell," -2,600 to -2,900; and Berea 80 to 160 feet. Reactivation of basement faults might have controlled the paleotopography at the Knox unconformity, and the structural positions and deposition of overlying units.

An east-west structural cross section in Mechanic Township (Figure 58) illustrates wells penetrating faulted Rose Run remnants with thin Wells Creek/Shadow Lake

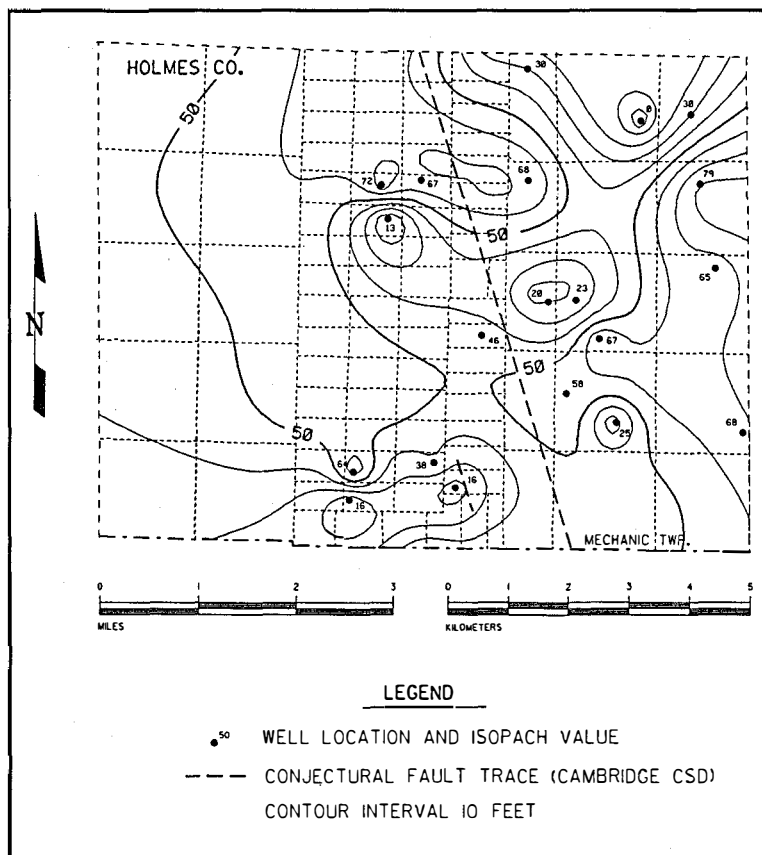


Figure 53. Isopach map of the Middle Ordovician Wells Creek/Shadow Lake interval in Holmes County, Ohio.

interval. The #22184 Hershberger (permit number 4922) and #1 Stutzman (permit number 4947) wells produce from Rose Run remnants overlain by thin Wells Creek/Shadow Lake interval. The #22184 Hershberger well produced 13 thousand barrels of oil (Mbo) and 50 MMcf_g during the first year of production from the Rose Run and Copper Ridge/Ore Hill; production data are not available for the #1 Stutzman well. At the west end of this cross section the #1 L. Yoder (permit number 4971) had a complete Wells Creek section and was a dry hole. The lithology of the Ordovician Black River, "Gull River"/Loysburg, and Wells Creek/Shadow Lake in the #22184 Hershberger well are not typical, based on the Litho-density log run in the hole. The photo-electric factor (PE) curve on the right track of the log indicates the presence of dolomite in the Black River and "Gull River"/Loysburg. This anomaly is interpreted as dolomitization by upwardly migrating fluids proximal to a reactivated fault (conjectural) sometime after deposition of the Trenton Limestone. Although the dolomitization of the units above the Knox unconformity can be mistaken for Beekmantown/Mines dolomite, this is not common. The structure maps on the Trenton, "Packer Shell," and Berea (Figures 55 to 57)

indicate that minor upward structural movement occurred at the #22184 Hershberger and #1 Stutzman after deposition of the Berea. The isopach maps of the Wells Creek/Shadow Lake and Wells Creek/Shadow Lake-through-Trenton interval (Figures 53 and 54) indicate similar thicknesses at the locations of the two wells.

In 1991, Bakerwell, Inc., acquired a 1.5 mile line of 30-fold dynamite seismic reflection data over a portion of Mechanic Township. The line ties with two producing wells, the #22184 Hershberger and #1 M. Yoder, and a nonproducing well, the #1 L. Yoder (permit number 4971) (Figure 51). The #1 L. Yoder is actually 400 feet south of the line.

The seismic reflection data were reprocessed by standard practices, and included refraction statics and multiple spectral enhancement passes of the data. It should be noted that noise attenuation was not performed after the post-migration spectral enhancement pass;

hence, the data may have a little more high frequency noise than they should. The processor stated that because migration is, in essence, a filtering technique that removes high frequencies, it is necessary to restore the higher frequency content after migration. This is not an industry-standard practice. Interpretation was performed on a normal polarity display of enhanced migrated data (Figure 59).

The east end of the line near the #22184 Hershberger well exhibits breakup at the Trenton time horizon, possibly due to faulting and fracturing, porosity development, or a combination of both. This well occurs in an area adjacent to a possible fault that might have splayed off the Cambridge CSD to the east of the seismic survey line. As discussed above, the Black River section in this well is dolomitized, which is consistent with the concept that faulting and fracturing could provide conduits for mineralized fluids to cause dolomitization. The data quality on the end of the line is good, but it is not full fold (the fold is about 10). The lack of redundancy in the data poses the problem of lower confidence limits in interpretation near the end of the line.

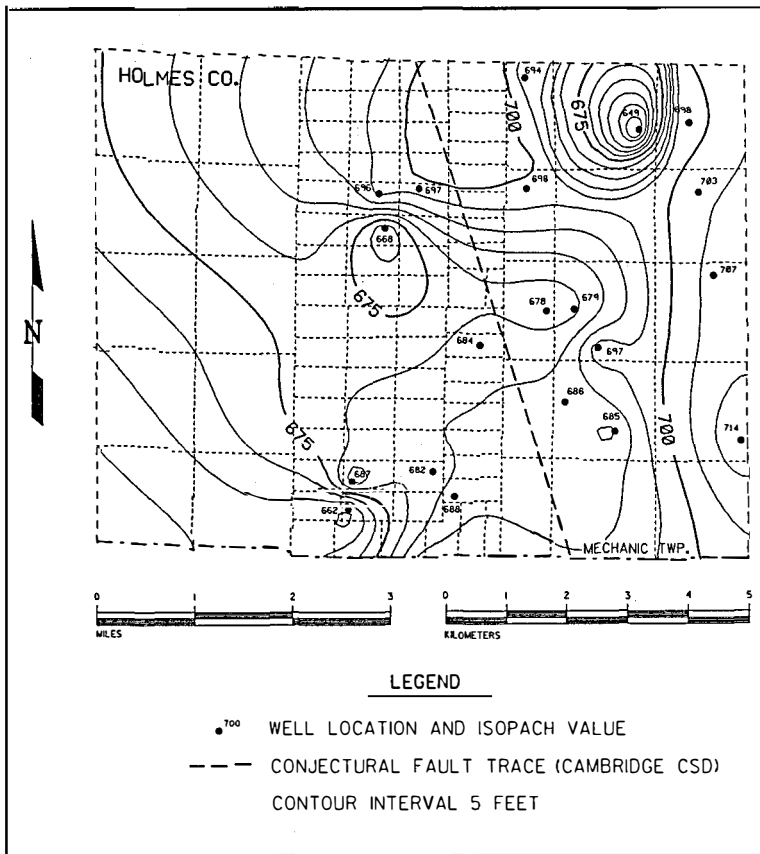


Figure 54. Isopach map of the Wells Creek/Shadow Lake-through-Trenton interval in Holmes County, Ohio.

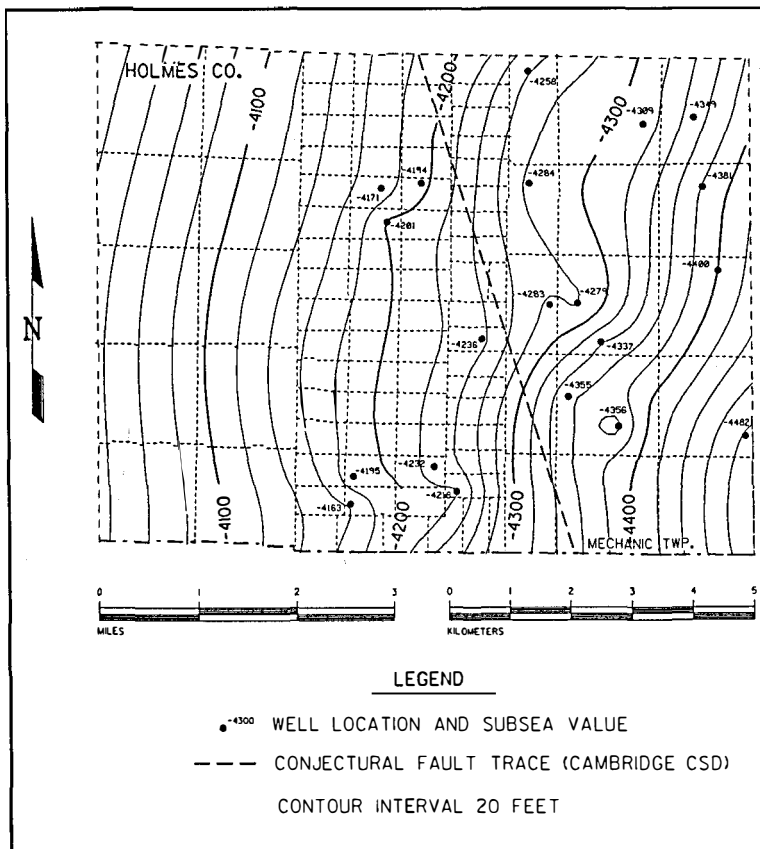


Figure 55. Structure map on top of the Upper Ordovician Trenton Limestone in Holmes County, Ohio.

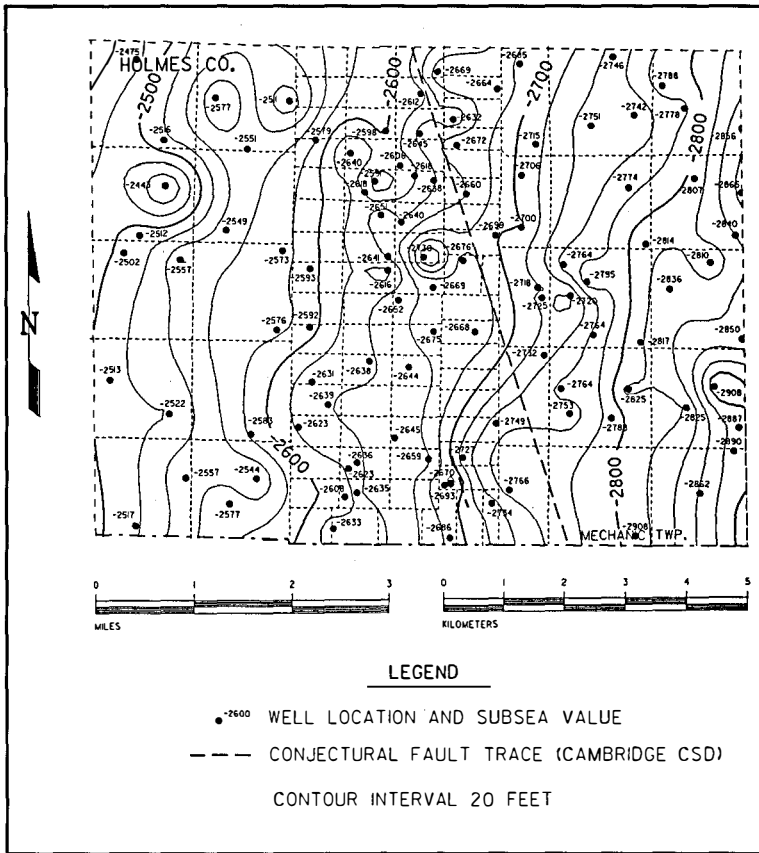


Figure 56. Structure map on the base of the Lower Silurian "Packer Shell" in Holmes County, Ohio.

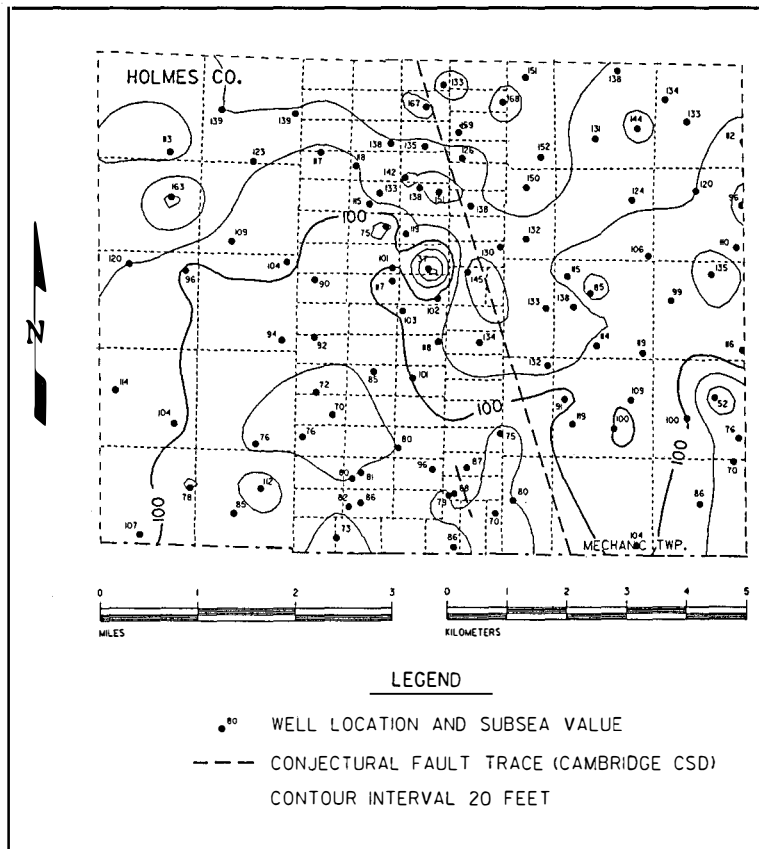


Figure 57. Structure map on top of the Mississippian Berea Sandstone in Holmes County, Ohio.

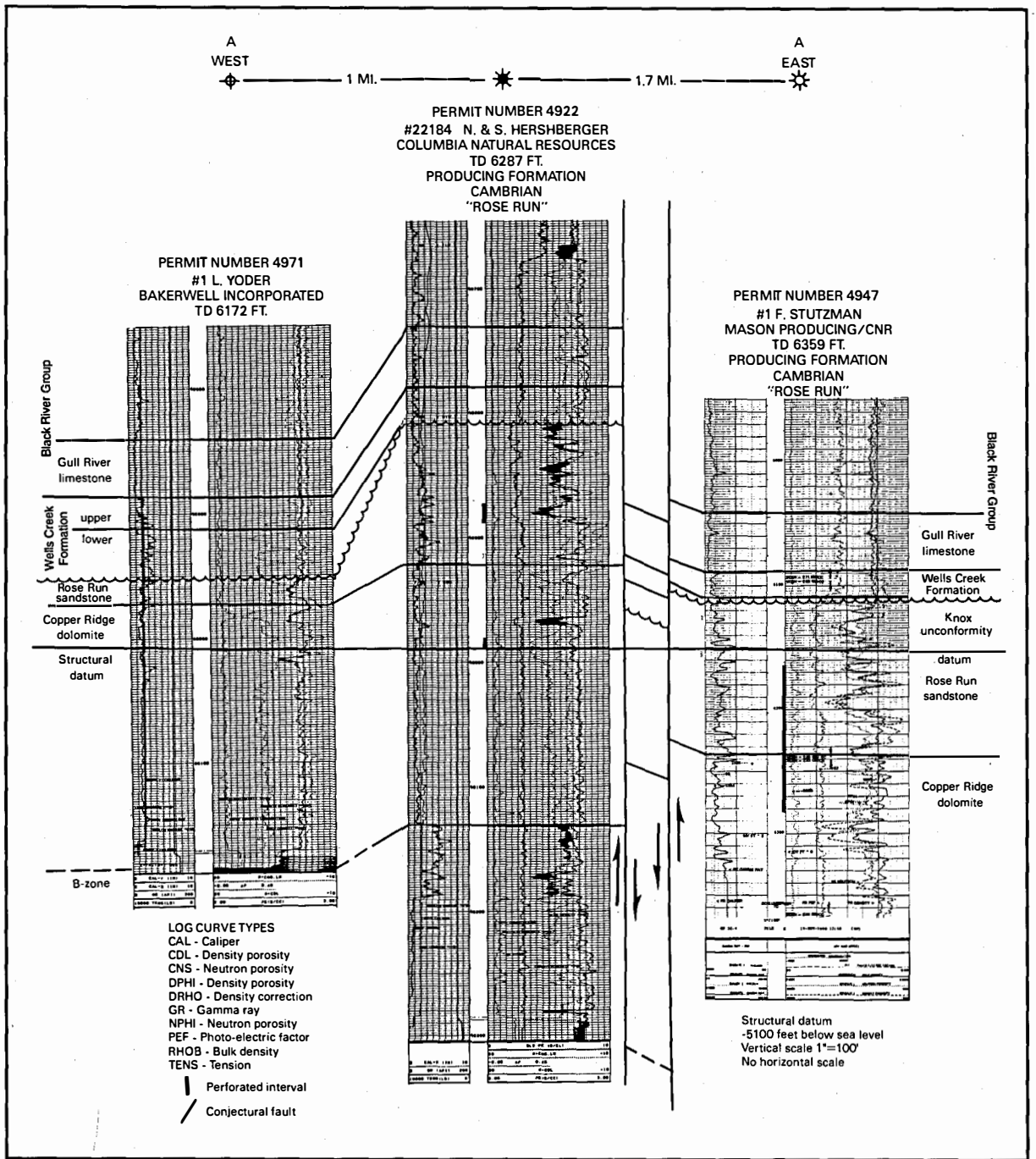


Figure 58. Cross section A—A' in Holmes County, Ohio. See Figure 51 for locations of the wells.

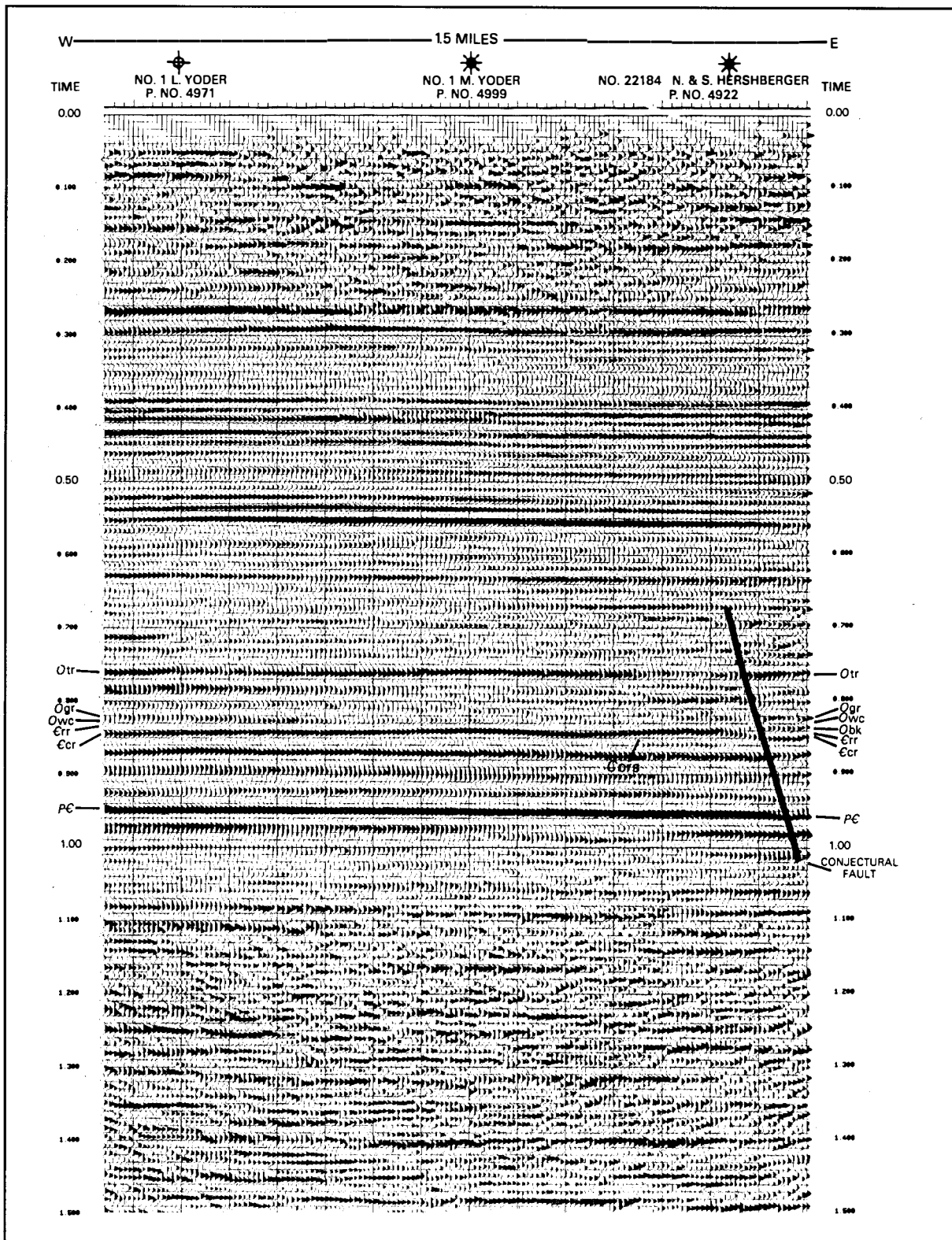


Figure 59. Interpreted seismic section display, Holmes County, Ohio: 1992 reprocessing, 0.6 to 1.0 second travel time, 30-fold, enhanced migration, 120° phase rotation, normal polarity. See Figure 24 for legend.

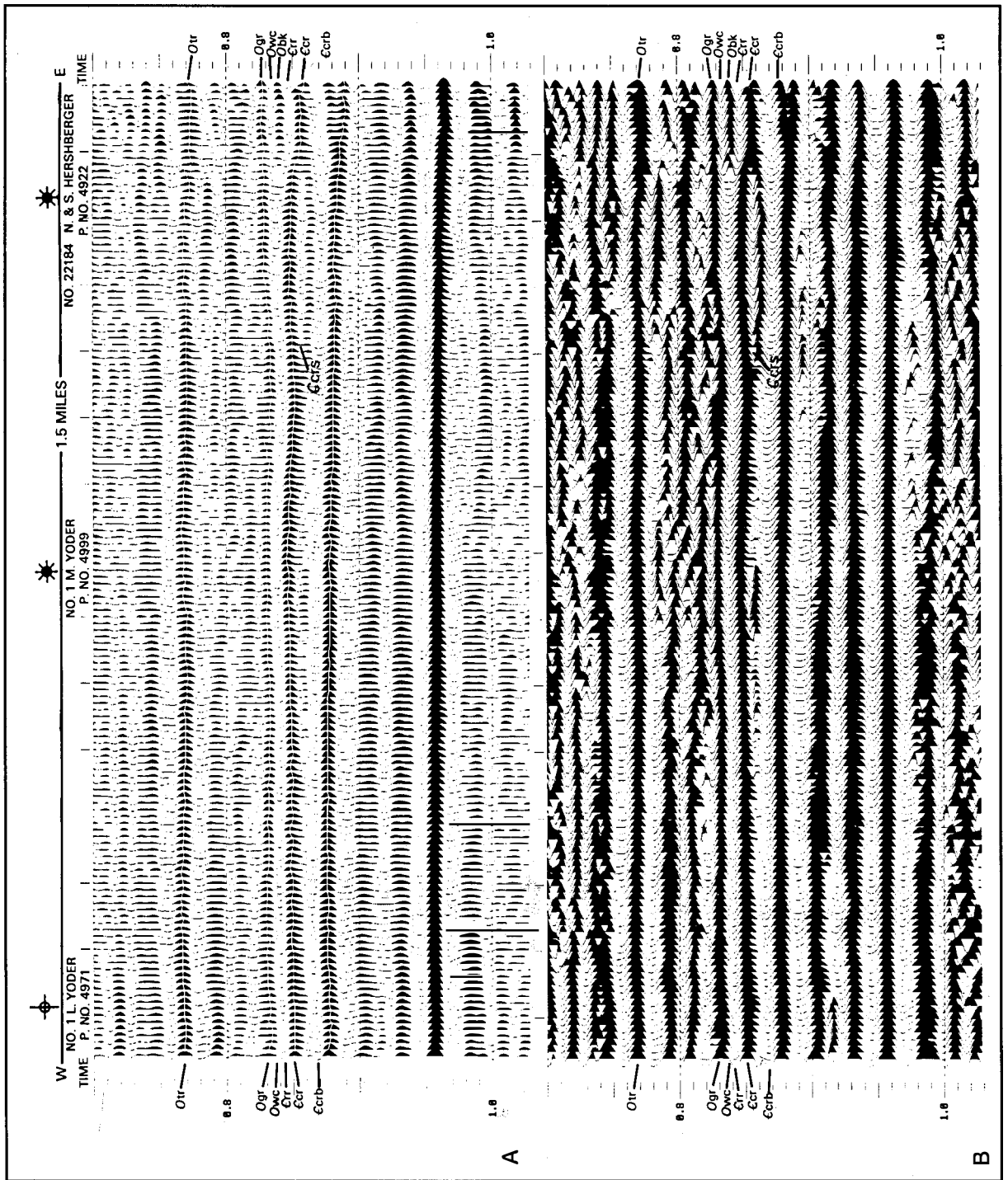


Figure 60. Uninterpreted (A) and interpreted (B) seismic section display, Holmes County, Ohio: 1992 reprocessing, 0.7 to 1.0 second travel time, dynamite, 30-fold, enhanced migration, 120° phase rotation. A—normal polarity, B—trace cosine. See Figure 24 for legend.

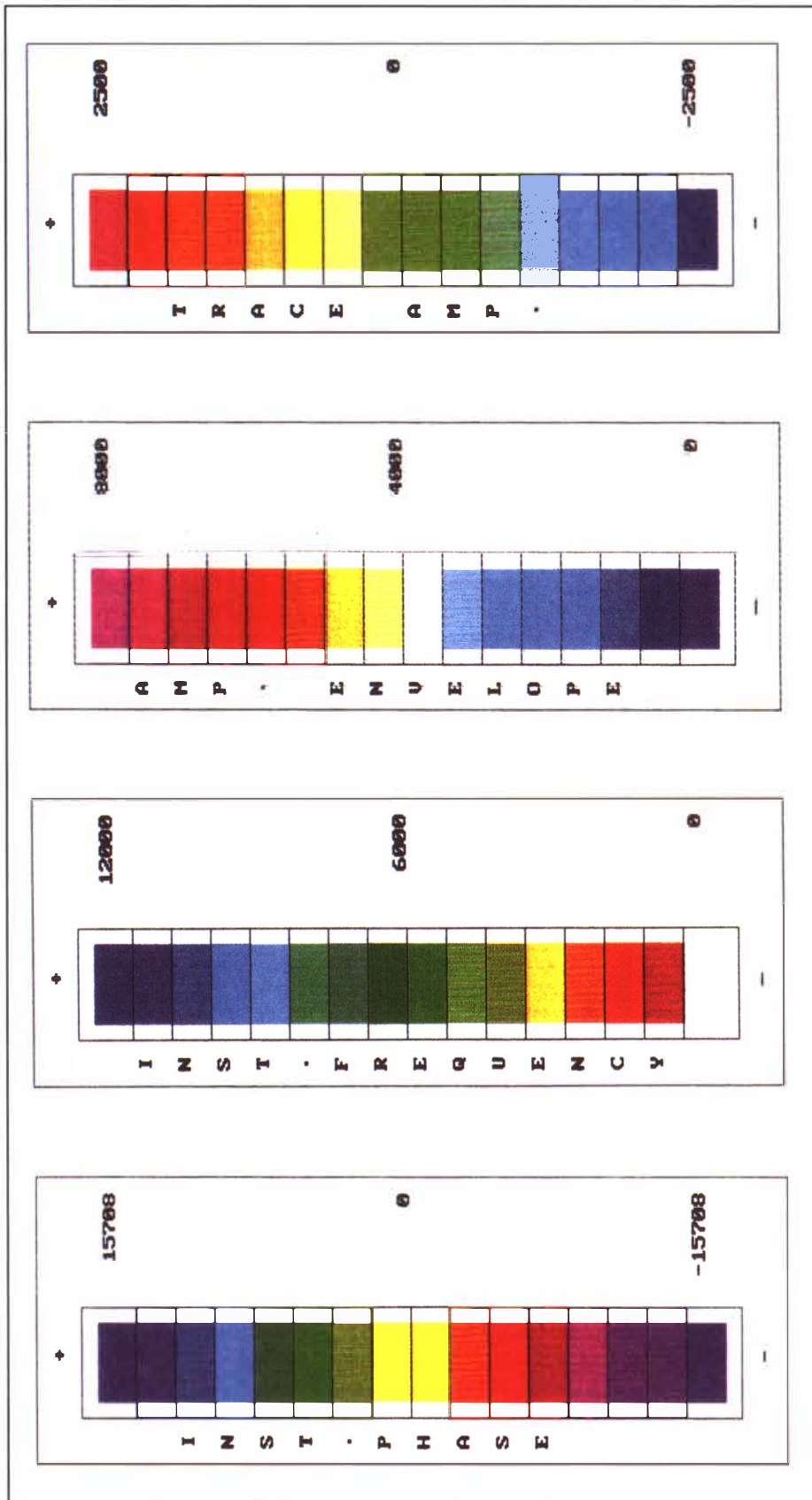


Figure 61. Color attribute correlation panels for Figures 62, 63, 101, and 102.

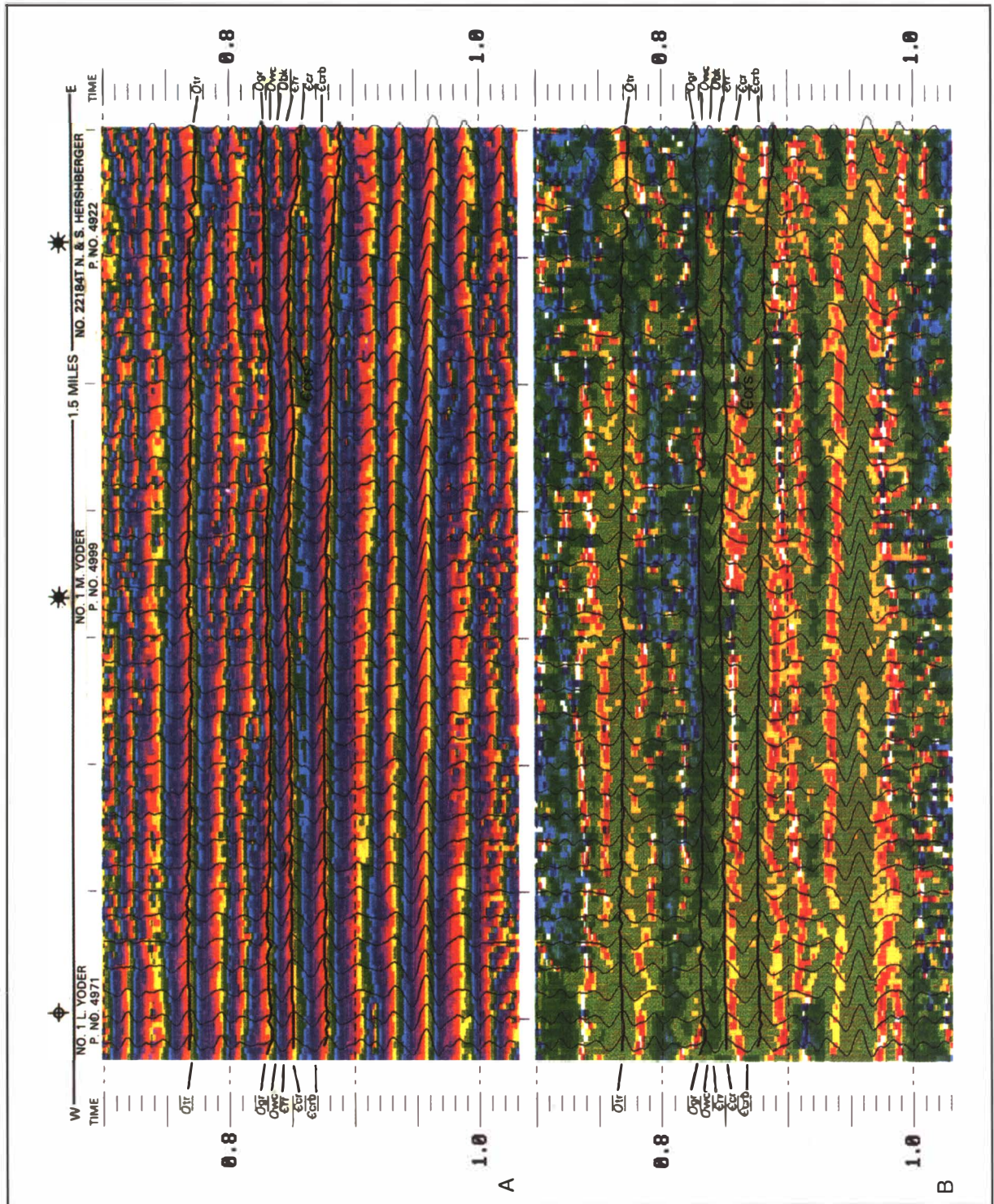


Figure 62. Interpreted seismic section attribute displays, Holmes County, Ohio: 1992 reprocessing, 0.7 to 1.0 second travel time, dynamite 30-fold, enhanced migration, 120° phase rotation. A—instantaneous phase, B—instantaneous frequency. See Figure 24 for legend.

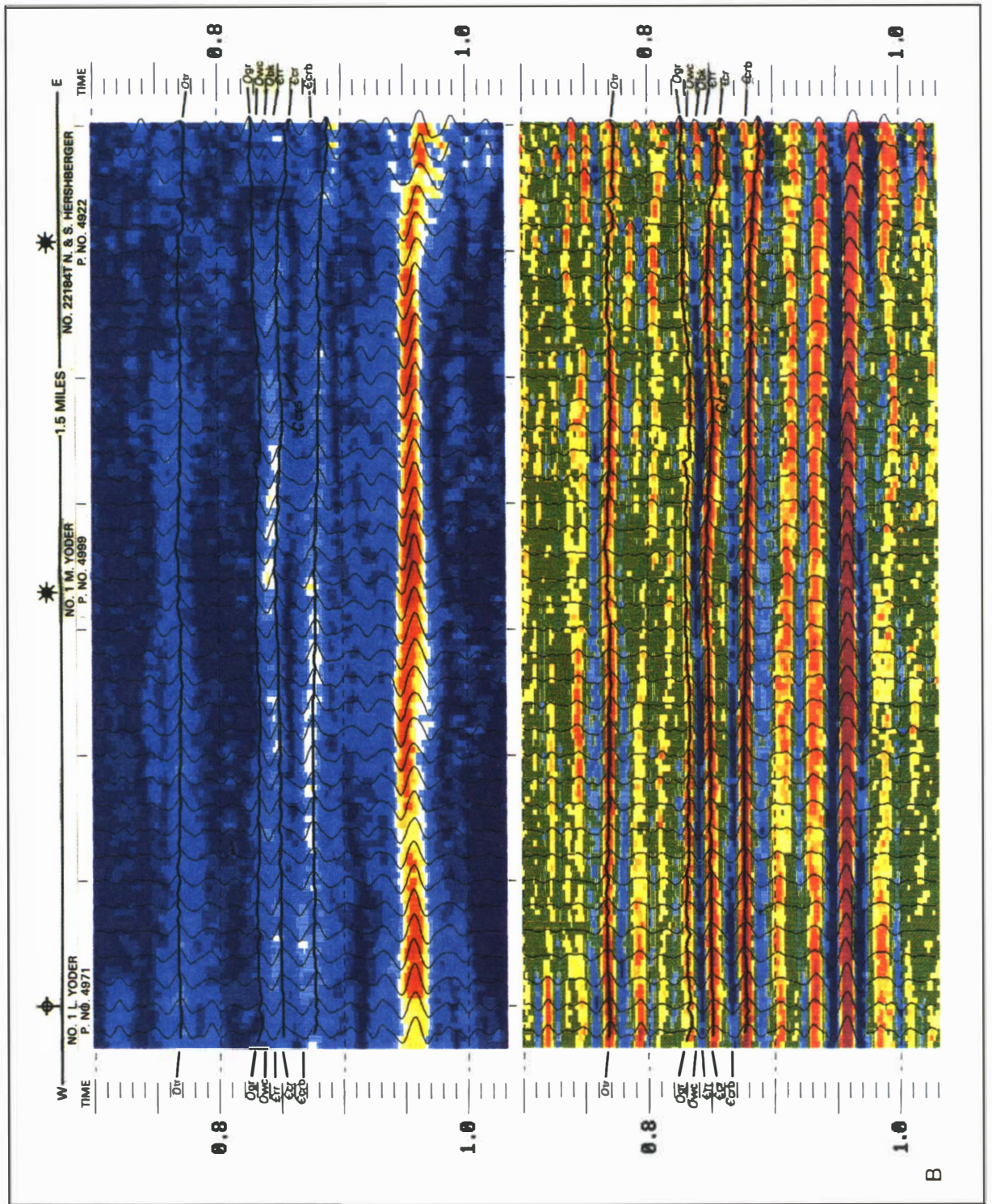


Figure 63. Interpreted seismic section attribute displays, Holmes County, Ohio: 1992 reprocessing, 0.7 to 1.0 second travel time, dynamite 30-fold, enhanced migration, 120° phase rotation. A—amplitude envelope, B—trace amplitude. See Figure 24 for legend.

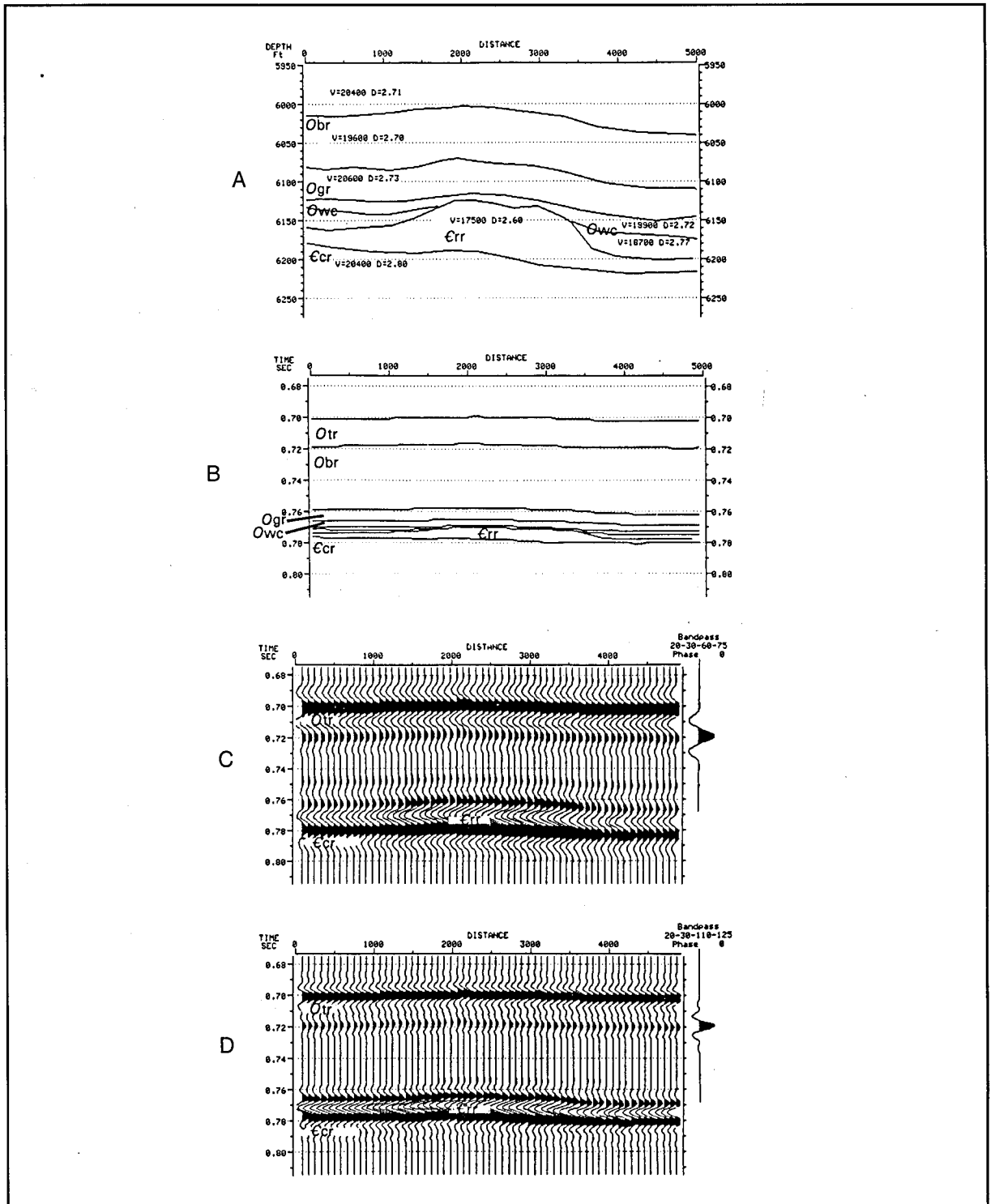


Figure 65. A—Geologic model of a Rose Run erosional remnant. B—Time section of a Rose Run erosional remnant. C—Low frequency 2-D seismic model of a Rose Run remnant. Notice the amplitude anomaly above the Rose Run trough. D—High frequency 2-D seismic model of a Rose Run remnant. All figures from Roth (1992).

The Beekmantown/Mines reflector is absent across most of this seismic section, and this is corroborated by lack of Beekmantown/Mines in the wells drilled on the line. The Wells Creek/Shadow Lake interval is very thin in the #22184 Hershberger well. Across the inferred fault zone on the east end of the line, the Wells Creek/Shadow Lake and Beekmantown/Mines reflectors reappear (Figure 59). This may indicate a Beekmantown/Mines remnant on the east side of the inferred fault. An alternative interpretation is that the top of the Beekmantown/Mines is porous, and that the Wells Creek is thin over the remnant. Without corroborating log data, either interpretation is equally viable.

A peak below the Copper Ridge/Ore Hill sandstone reflector may represent Copper Ridge/Ore Hill dolomite (Figure 59). The #22184 Hershberger produces from the number 4 Rose Run sandstone and from a dolostone facies thought to be time equivalent to the Copper Ridge/Ore Hill sandstone channels that occur sporadically in this area. There is an amplitude damping in the overlying Rose Run that may be due to the presence of hydrocarbons, but this type of phenomenon has also been shown to occur as a result of the sandstone in the Copper Ridge/Ore Hill (see the discussion of detailed seismic data for Coshocton County below).

Amplitude, frequency, and phase attribute-analysis processing was performed on the seismic line to determine if any of the procedures could be diagnostic in the characterization of reservoir heterogeneity in the Rose Run sandstone. During attribute processing, only the time horizons representing the stratigraphic sequence of interest ("Gull River"/Loysburg through Copper Ridge/Ore Hill) were enhanced and phase rotated. A phase rotation of 120 degrees of migrated, spectrally enhanced data yielded the best fit of the surface-acquired seismic-reflection data with synthetic seismograms (Figure 59). For all further discussion, the migrated enhanced data has been phase rotated 120 degrees.

An automatic event-picking program was used to follow horizons of interest (Figure 60A). A plot of the trace cosine of migrated enhanced data is the wiggle trace representation of the instantaneous phase processing (Figure 60B). Anomalous signatures occur at 0.86 seconds near both the #22184 Hershberger and the #1 M. Yoder wells, corresponding to the time location of the reflector of the Copper Ridge/Ore Hill sandstone and the underlying dolomite. There appears to be no anomalous signature near the #1 L. Yoder well. However, this well, located 400 feet south of the seismic survey line, did not encounter a remnant. This well has no Rose Run production;

therefore, any assumption that the distance from the seismic reflection line may have compromised the imaging of anomalous signatures under the S.P. location for the well can be ruled out. The color area plot of instantaneous phase of enhanced migrated data shows phase anomalies coincident with the trace cosine anomalies (Figures 61 and 62A). The phase anomalies indicate coherent reflectors; they appear to define pod-like sandstone occurrences in the area of the wells. The plot of instantaneous frequency shows instantaneous frequency anomalies coincident with the trace cosine and phase anomalies (Figure 62B). The plot of the amplitude shows low amplitude anomalies well below the time of the phase and frequency anomalies (Figure 63). An erratic pattern in the amplitude envelope and trace amplitude occurs above the horizons of interest in both the #22184 Hershberger and the #1 M. Yoder wells. It appears that amplitude processing cannot be used to define reservoir heterogeneity in this case. Results of inversion processing of the synthetic seismogram from the #22184 Hershberger well agreed with the results of the attribute processing on the seismic reflection-record section.

In summary, attribute analyses are excellent diagnostic tools in addition to conventional processing techniques in the detection and prediction of hydrocarbons trapped in remnants, faults, and stratigraphic changes in the Copper Ridge/Ore Hill found in Holmes County. Instantaneous phase and frequency and amplitude processing revealed anomalies at the #1 M. Yoder and #22184 Hershberger wells located on the seismic line. These changes have been interpreted to be the result of the presence of oil and gas. However, changes in frequency and amplitude causing these unique seismic signatures may have been compromised by the possible occurrence of the Copper Ridge/Ore Hill sandstone below the location of the producing wells. The significant velocity contrast between sandstone and dolostone within the Copper Ridge/Ore Hill may have caused the anomalies. The anomalies observed in the Copper Ridge/Ore Hill also may be the result of constructive interference due to the presence of hydrocarbons in the Rose Run. In any event more drilling and seismic acquisition needs to be performed to map the presence of the Copper Ridge/Ore Hill sandstone and its affect on seismic signatures.

One-dimensional forward modeling of the Knox/Gatesburg by Roth (1992) is similar, but does not explicitly examine the scenarios present in the #22184 Hershberger well. In 1D modeling, if there is a thick enough Wells Creek/Shadow Lake section (Figure 64A), a shouldered trough characterizes a stratigraphic section in

which the Beekmantown/Mines is missing using high frequency bandpass filter (20/30 . . 110/125); a large amplitude trough characterizes the appearance of the Rose Run sandstone immediately below the "Gull River"/Loysburg if the Wells Creek/Shadow Lake section is thin or absent. In the #22184 Hershberger well the extremely thin Wells Creek/Shadow Lake section is probably below the resolving power of both 1D and 2D modeling techniques. The synthetic seismogram for this well demonstrates a large amplitude trough at the Rose Run (Figure 64B). The well produces oil and gas from the Rose Run sandstone and Copper Ridge/Ore Hill dolomite, but no models were constructed for this scenario.

The #1 M. Yoder well appears to produce from a characteristic Rose Run erosional remnant, a scenario for which Roth (1992) performed both 1D and 2D modeling (Figure 65). The 2D model (Figure 65C and D) shows a high-amplitude Rose Run trough, implying that the Wells Creek/Shadow Lake is absent or very thin. The 2D model of a Rose Run erosional remnant (Figures 65C and D) demonstrates a seismic signature similar to that seen on the line near the #1 M. Yoder well (Figure 59). In this scenario, the lower dominant frequency model (Figure 65C) revealed an amplitude anomaly or higher amplitude event in the Rose Run remnant. The amplitude change was not observable in the higher dominant frequency model (Figure 65D). This suggests that in some circumstances the lower frequency data may be more important when targeting Rose Run remnants (Roth, 1992).

One- and two-dimensional modeling exists both for Beekmantown/Mines erosional remnants and for faulting that decreases the thickness of Knox/Gatesburg strati-

graphic horizons. However, no published models exist for a down-to-the-east-faulted Beekmantown/Mines remnants that might be present on the east end of this seismic line. Roth's (1992) fault model might be applicable to a geological scenario. One-dimensional modeling of a Beekmantown/Mines remnant shows a doublet peak where the Beekmantown/Mines is 80 feet thick and has vuggy porosity at the top of the section (Puckett, 1992). However, this doublet might also be produced by a thicker Wells Creek/Shadow Lake section overlying the Beekmantown/Mines (Roth, 1992). Two-dimensional modeling of a Beekmantown/Mines remnant also shows that the doublet peak occurs where the Wells Creek/Shadow Lake is thin and there is no porosity at the top of the Beekmantown/Mines (Roth, 1992).

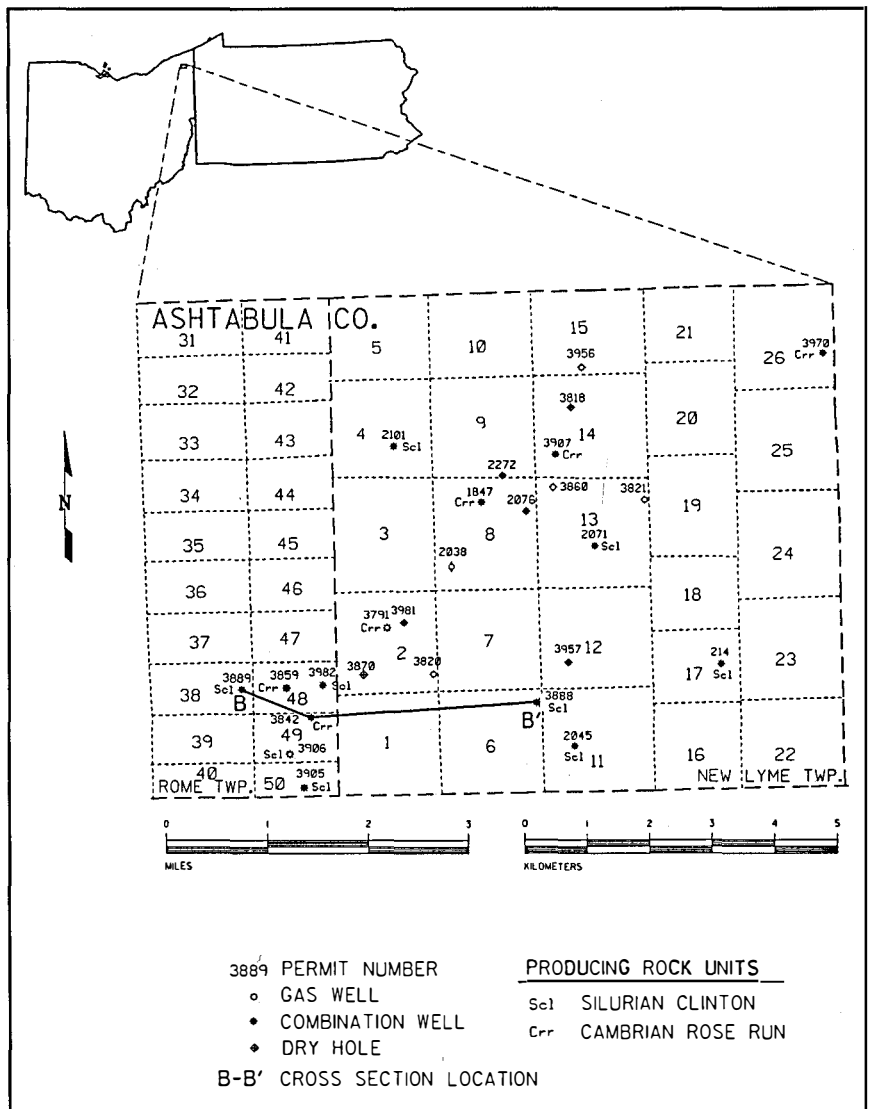


Figure 66. Base map showing wells penetrating the Knox unconformity or deeper in Ashtabula County, Ohio.

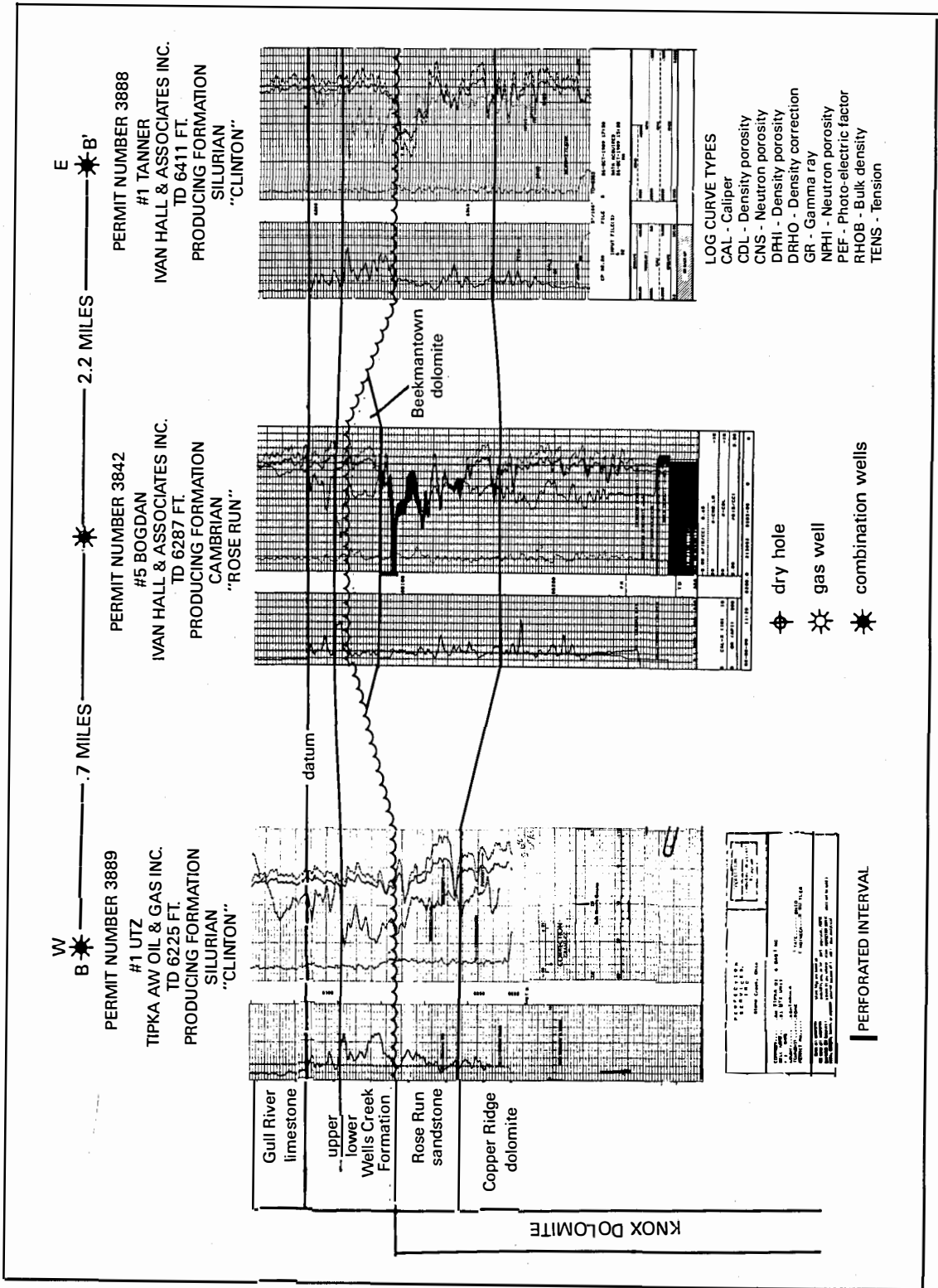


Figure 67. Cross section B-B' in Ashtabula County, Ohio. See Figure 66 for locations of the wells.

One- and two-dimensional modeling of various structural and stratigraphic scenarios were not explicitly done for the seismic signatures that are present below the S.P. locations of the #22184 Hershberger and #1 M. Yoder wells. The signals can be explained best by a combination of several models. The appearance of a doublet peak at the Beekmantown/Mines horizon on the east end of the seismic data suggests a faulted Beekmantown/Mines erosional remnant. Even though the seismic signature occurs at the end of a data line, we consider this interpretation to be valid because the data, which appear to be appropriately migrated, were acquired parallel to the direction of regional dip.

South-Central Ashtabula County, Ohio

Although it has not been as extensively explored as in east-central Ohio, the northern portion of the subcrop trend in northeastern Ohio, particularly in Ashtabula County (Figure 66), also has hydrocarbon production from the Rose Run sandstone. The Rose Run primarily produces gas in this area; however, recent drilling indicates the presence of significant associated oil production. The #1 Wilkins well (permit number 3970) in section 26 of New Lyme Township, Ashtabula County had an initial potential of 20 Mcfgpd and 40 Bo from the Rose Run after mechanical fracturing. Sandstones in the Lower Silurian Clinton/Medina interval provide good secondary objectives for hydrocarbon exploration in the Rose Run play. As in much of eastern Ohio, this region historically has been a Clinton/Medina production area.

Weber's (1986) type 8 heterogeneity, resulting from erosional truncation and paleotopography on the Knox/Gatesburg interval, controls hydrocarbon distribution for the Rose Run in this area. A stratigraphic cross section, using the base of the "Gull River"/Loysburg carbonates as a datum (Figure 67), shows a Beekmantown/Mines remnant similar to those described in Holmes County. This east-west trending cross section shows a dramatic thickening of the Rose Run section to 88 feet and presence of 21 feet of Beekmantown/Mines in the #5 Bogdan well (permit number 3842) in section 49 of Rome Township.

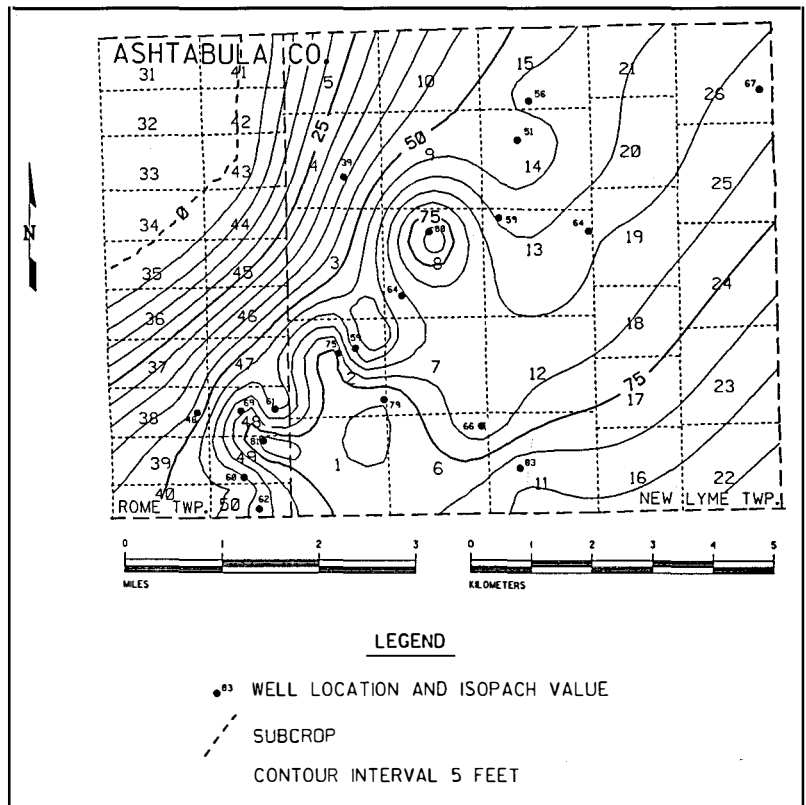


Figure 68. Isopach map of the Rose Run sandstone in Ashtabula County, Ohio.

This well was completed as an oil and gas well in the upper nine feet of the Rose Run. Neither of the adjacent wells in the cross section produced from the Rose Run. The Beekmantown/Mines is absent and only the lower 48 feet of Rose Run is present in the #1 Utz (permit number 3889), located approximately 0.7 mile to the west of the #5 Bogdan in section 38 of Rome Township. Approximately 2.2 miles to the east in section 6 of New Lyme Township, the #1 Tanner well (permit number 3888) encountered no Beekmantown/Mines and 67 feet of Rose Run.

The Rose Run ranges in thickness from zero feet at the subcrop edge in the northwest to a maximum of 90 feet in the southeast (Figure 68). Rapid thickening from 0 to approximately 50 feet takes place across a 2-mile wide area along the western edge of this subcrop. Erosion at the Knox unconformity produced an irregular topographic surface with localized areas of thin and thick Rose Run sandstone along this subcrop trend.

Enterline (1991) performed detailed petrologic work on Rose Run sandstone cores from the #2 Parobek (permit number 2038) and #TA-1 Beckwith (permit number 2071) wells in sections 8 and 13 of New Lyme Township, respectively. He recognized four lithofacies in the Rose

Run, including a sandstone facies, oncolite facies, bioturbated dolomite facies, and algal laminated/stromatolite facies. Low-angle cross-bedded quartz arenites and subarkoses characterized the sandstone facies.

The structure map on top of the Knox unconformity (Figure 69) shows regional dip to the south-southeast with subsea values ranging from -5,100 feet in the northwest to -5,340 feet in the southeast. In the southwest, a Knox paleotopographic high trends northwest-southeast at two wells producing from the Rose Run, the #1 Bogdan (permit number 3842) and #6 Bogdan (permit number 3859) in lots 49 and 48 of Rome Township. The operators produced approximately 400 MMcfg and 8 Mbo from these two wells during the first two years of production. A subtle Knox high trending northwest-southeast also occurs in the central part of the mapped area at the #3 Rhoa well (permit number 1847) in section 8 of New Lyme Township. This well produced approximately 800 MMcfg and 1 Mbo from the Rose Run after the first 10 years of production. Logs are not available for the #R-1 Reeve well (permit number 3907) in section 14 of New Lyme Township but it appears to be situated within a south-plunging structural high on the Knox. There are no available production data for the the #1 Wilkins well (permit number 3970) in New Lyme Township, another Rose Run producer. Lack of surrounding well control may be the reason for lack of discernible structure evident in this well.

Figure 70 shows depositional thinning of the Wells Creek/Shadow Lake interval over these Knox unconformity structural highs. In the southwest the interval thins to approximately 25 feet over the #1 Bogdan well, and to approximately 39 feet in the #3 Rhoa well. The regional thickness of the Wells Creek/Shadow Lake interval in this area typically is 50 feet.

Structural mapping on the top of the Trenton Limestone compares favorably with the Knox paleotopography (Figures 69 and 71). Figure 71 shows regional structural dip on the Trenton to the southeast with subsea depths ranging from -4,460 in the northwest to -4,720 in the southeast. A structural high trending northwest-southeast occurs in lots 48 and 49 of Rome Township at two

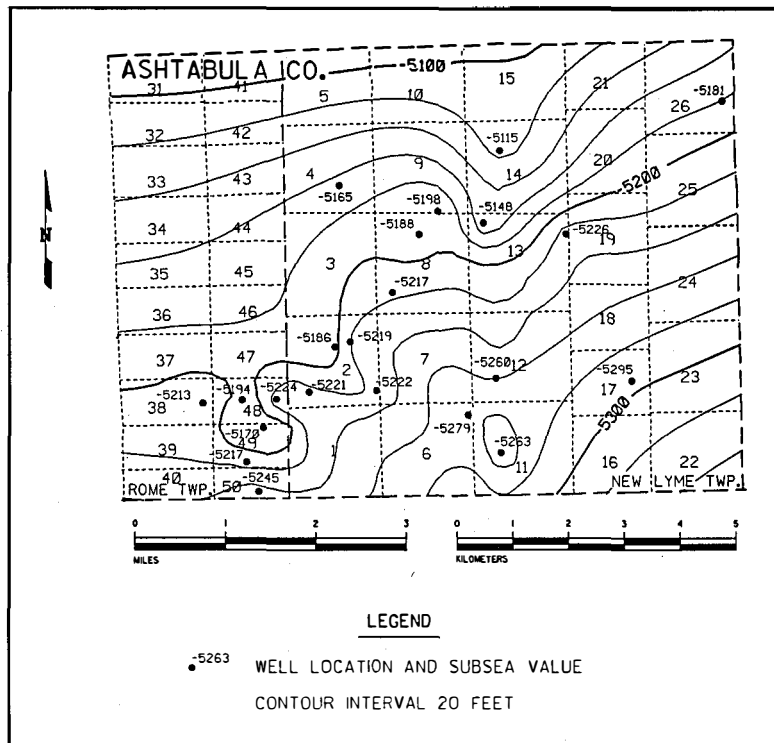


Figure 69. Structure map on top of the Knox unconformity in Ashtabula County Ohio.

producing Rose Run wells (permit numbers 3842 and 3859). Similarly, a south-plunging anticline occurs at a Rose Run producing well in section 14 in New Lyme Township (permit number 3907).

Structure mapped on the base of the "Packer Shell" reflects the deeper Knox paleotopography to a lesser degree (Figure 72). This map shows regional dip to the southeast with subsea depths ranging from -2,460 feet in the northwest to -2,660 feet in the southeast. A well-developed south-plunging structural nose in sections 13 and 14 of New Lyme Township reflects the deeper Knox structure. Also a subtle northwest-southeast trending structural nose occurs at the #3 Rhoa well (permit number 1847) in section 8 of New Lyme Township. Mapping structures on some shallow horizons, such as the "Packer Shell," may aid in developing areas of potential hydrocarbon exploration in the Rose Run.

Southwestern Portage and North-Central Stark Counties, Ohio

Southern Portage County, Ohio has been the site of hydrocarbon production from the Rose Run sandstone since completion of the Belden & Blake #1 Connor Comm. well (permit number 3841) in 1990 (Figure 73). This well produced 1,700 barrels of condensate and more than 87 MMcfg during the first 1.5 years of production (Janssens, 1992). Two other Rose Run combination oil

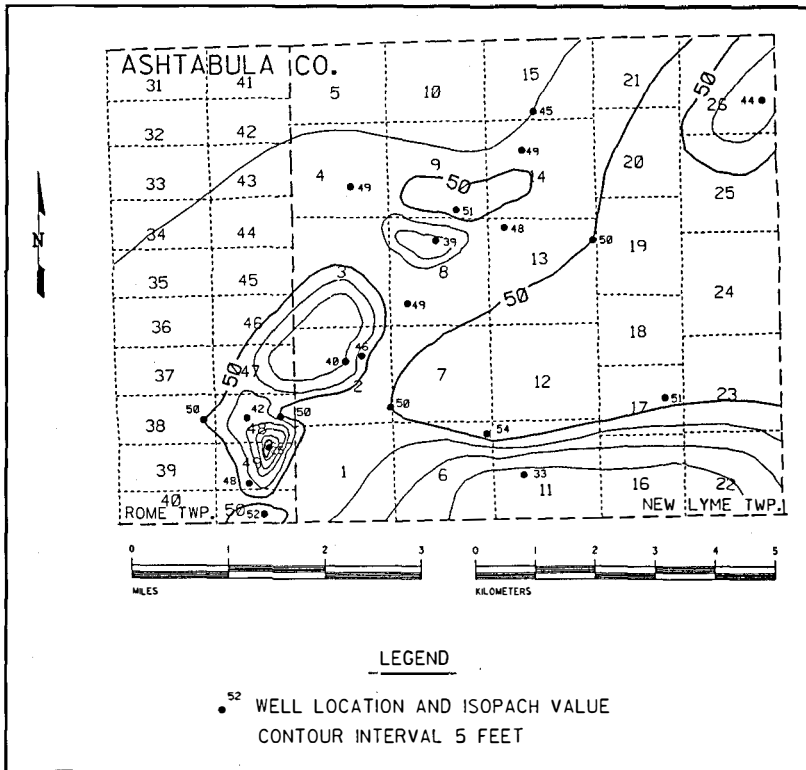


Figure 70. Isopach map of the Middle Ordovician Wells Creek/Shadow Lake interval in Ashtabula County, Ohio.

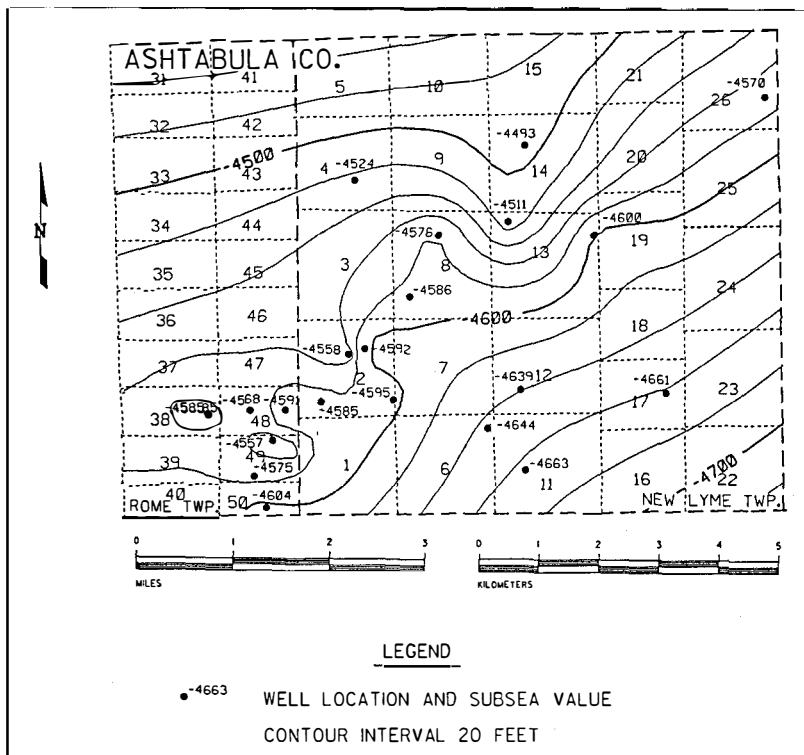


Figure 71. Structure map on top of the Upper Ordovician Trenton Limestone in Ashtabula County, Ohio.

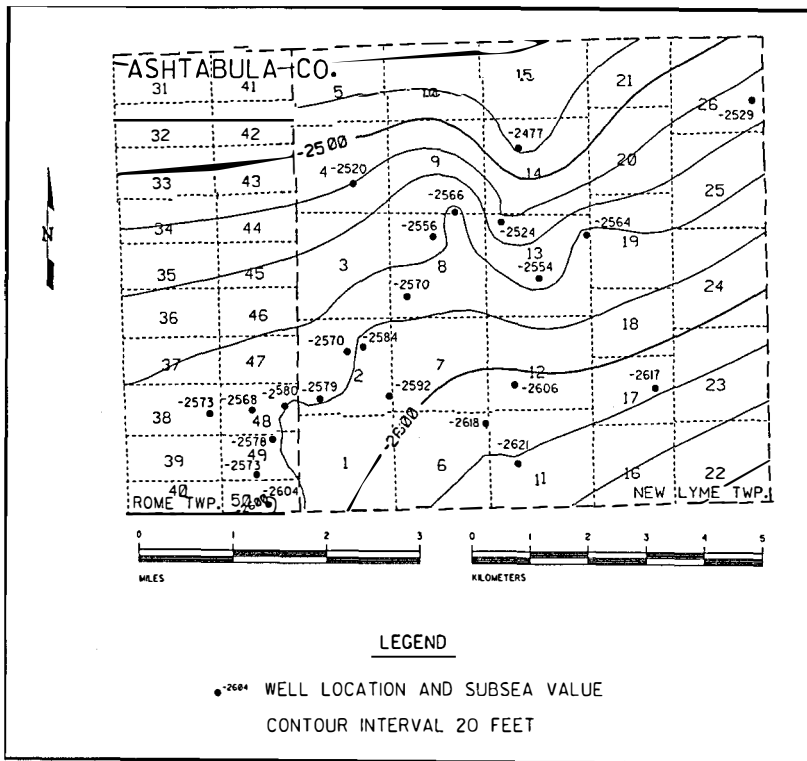


Figure 72. Structure map on the base of the Lower Silurian "Packer Shell" in Ashtabula County, Ohio.

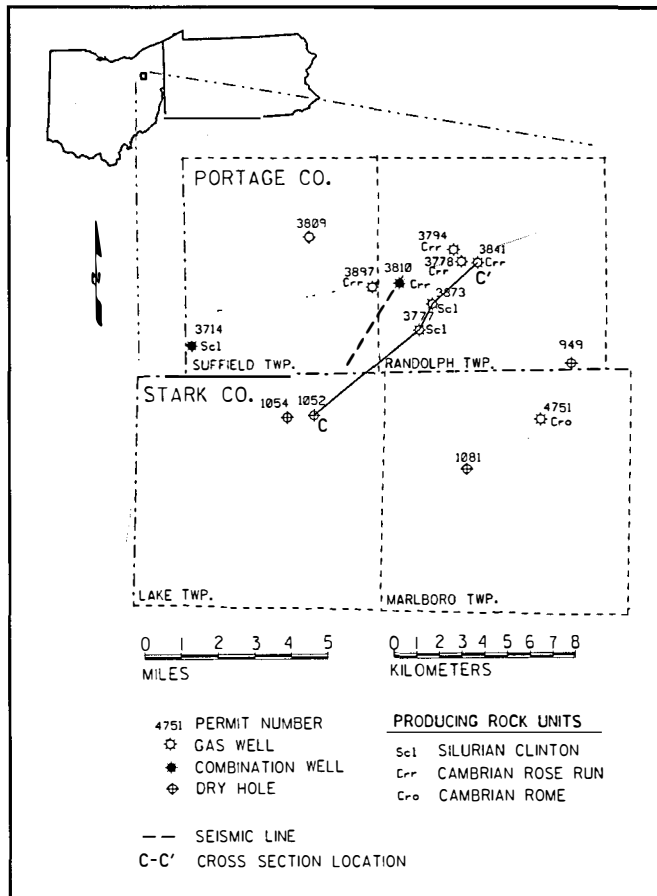


Figure 73. Base map showing wells penetrating the Knox unconformity or deeper in Portage and Stark counties, Ohio.

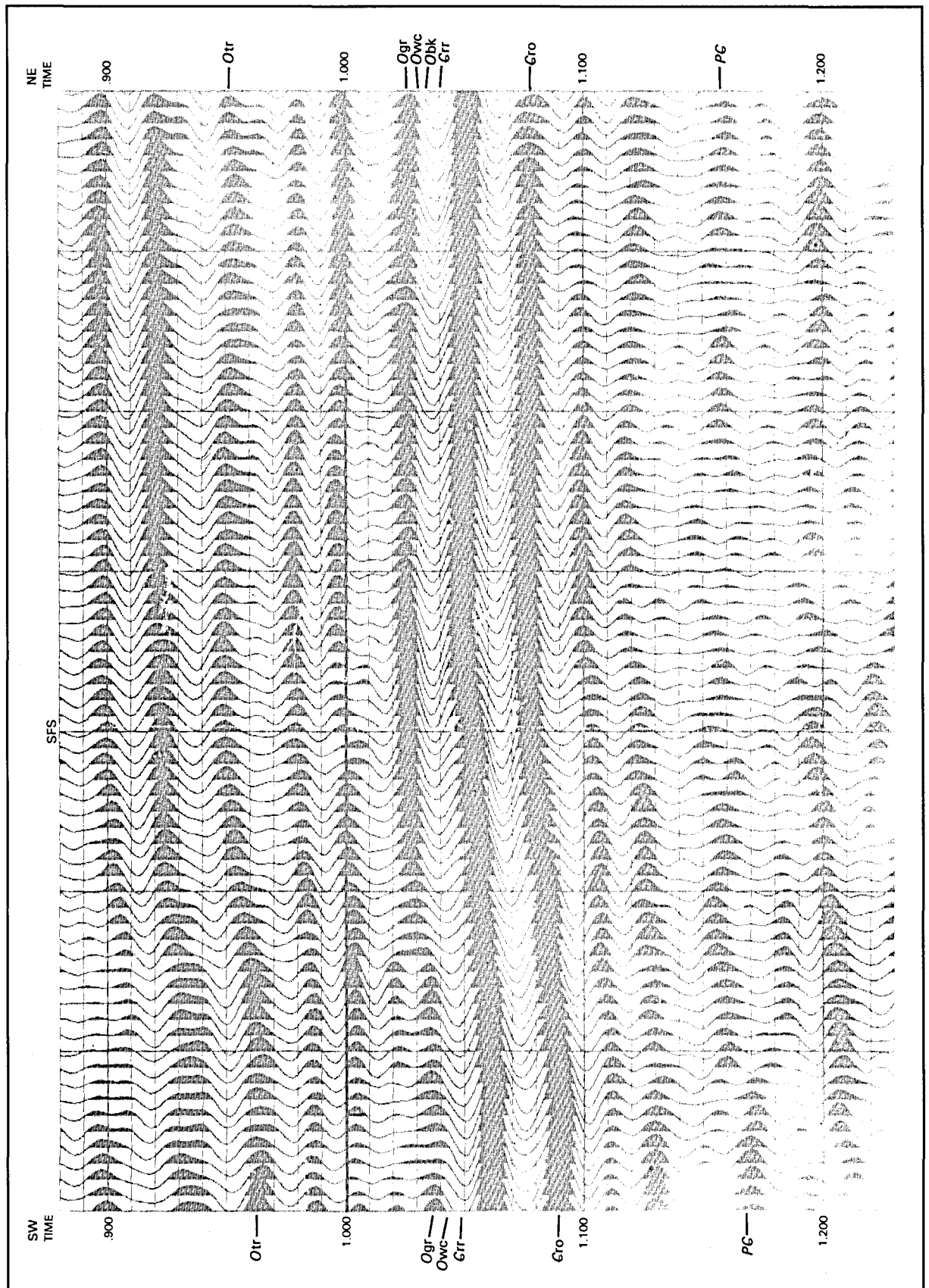


Figure 74. Interpreted seismic section display, Portage County, Ohio: 1989 processing without refraction statics, 0.9 to 1.2 seconds travel time, dynamite, 60-fold, 65 Hertz high cut filter, migration. See Figure 24 for legend.

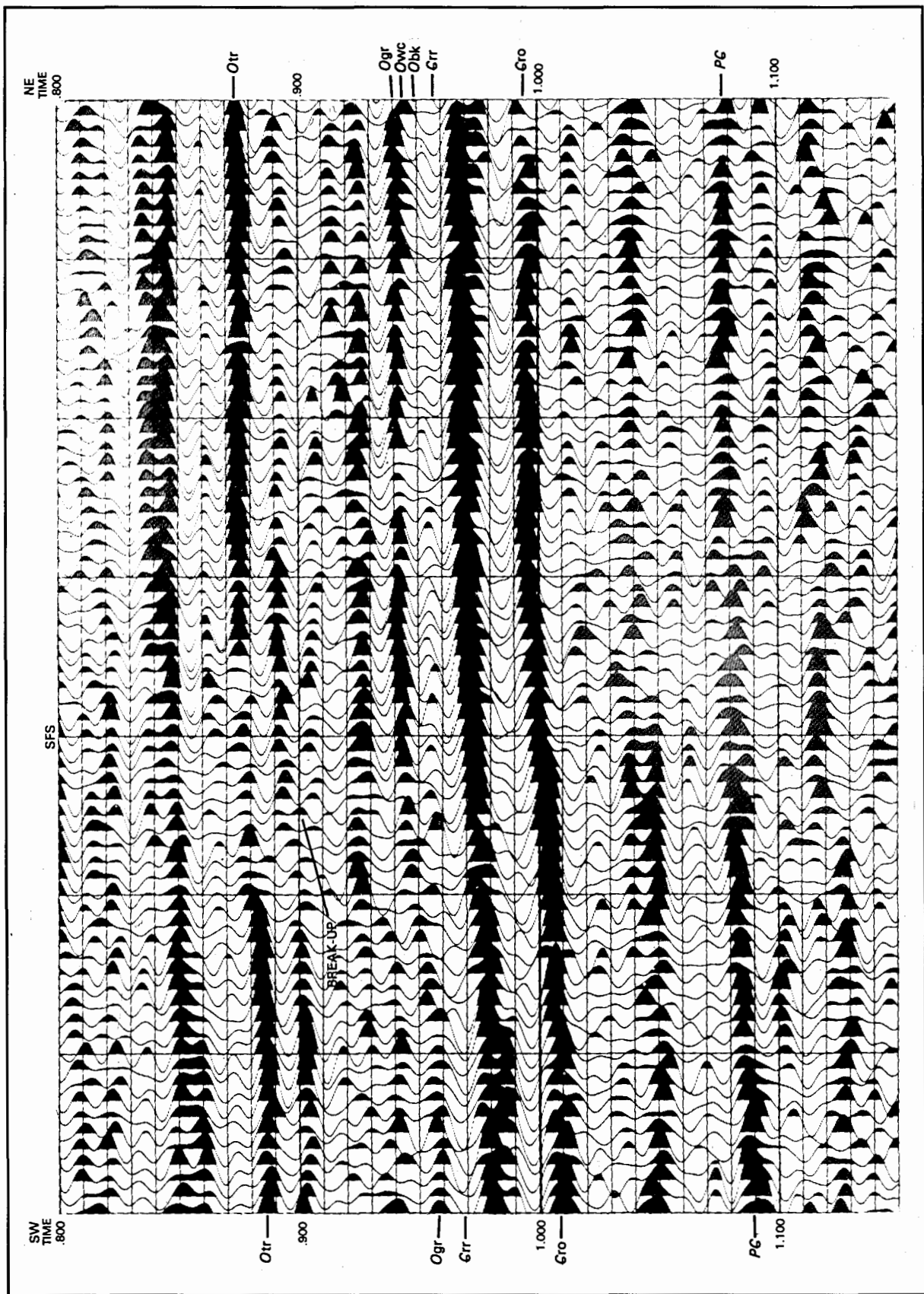


Figure 75. Seismic section display, Portage County, Ohio: 1992 processing, 0.8 to 1.1 seconds travel time, dynamite, 60-fold, enhanced migration, normal polarity. See Figure 24 for legend.

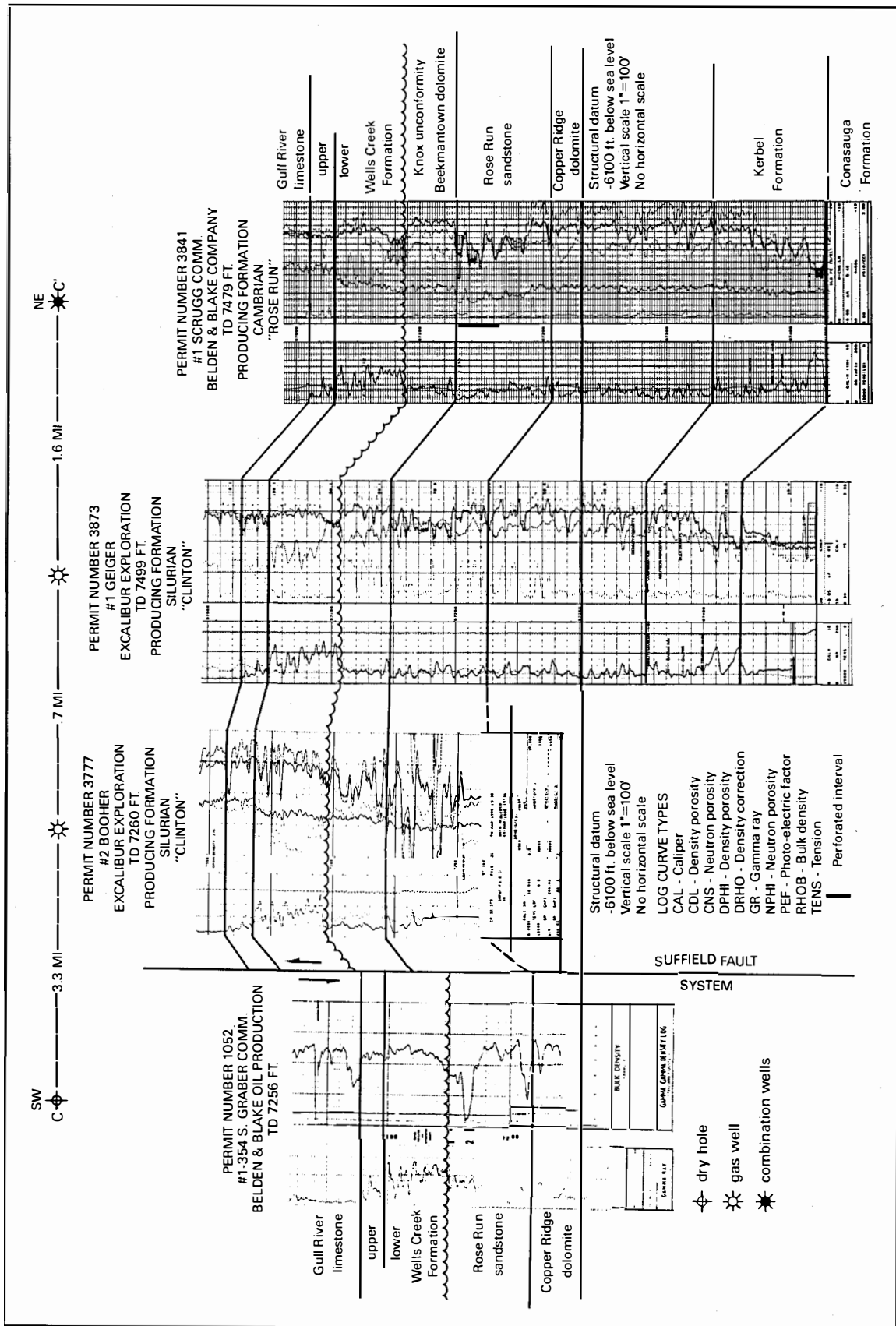


Figure 76. Structural cross section C-C' across portions of Portage and Stark counties, Ohio. See Figure 73 for location.

and gas wells, the Belden & Blake #1 Scruggs and the Excalibur Exploration #1 Schaefer, subsequently were drilled in the area. The Belden & Blake #1 Artim Comm. and Excalibur Exploration #1 Boyer, also in this area, produce mostly natural gas from the Rose Run. The primary types of heterogeneity in this area include faulting (type 1), fracturing (type 7), and, to a lesser degree, permeability zonation (type 3).

In 1989 Excalibur Exploration Inc. acquired a 2.7-mile line of seismic reflection data across part of Randolph Township in Portage County, Ohio (Figure 25), using four five-foot holes with 0.25 pounds of dynamite as a source, and 28 Hertz geophones. It was recorded in the 18-128 Hertz frequency bandwidth. The data were initially processed in 1989 using standard techniques, including pre-stack migration and normal attenuation of high frequencies with depth (Figures 74). Poor to nonexistent resolution of seismic signals of the "Gull River"/Loysburg-to-Beekmantown/Mines reflectors results from this processing format.

Excalibur Exploration chose the location for the #1 Schaefer well (permit number 3810) based on the subtle breakup at the Trenton and Knox unconformity reflectors. Correlation of this line with the nearest available synthetic seismogram, generated from the #1 Geiger well (permit number 3873), suggests that the lack of resolution of the "Gull River"/Loysburg-to-Beekmantown/Mines signals on the line can be accounted for by the lack of preserved high frequencies in the 1989 processing.

The data from the two lines were reprocessed with steps added to the processing flow, including refraction statics and multiple spectral whitening steps. The data were not pre-stack migrated. The difference in appearance of the Knox/Gatesburg sequence signature between the 1989 processing (Figure 74) and 1992 reprocessing where higher frequencies were preserved (Figure 75) is dramatic. The Beekmantown/Mines reflector appears as a weakly developed peak above the Rose Run northeast of a fault in the Precambrian basement. The "Gull River"/Loysburg-to-Beekmantown/Mines signal appears as a strong peak-trough-peak signal at the location of the #1 Schaefer well, as it should in an area with 40 to 60 feet of Beekmantown/Mines. The trough reflectors for the Wells Creek/Shadow Lake interval show relatively consistent time thicknesses across the line. A breakup of the Trenton reflectors occurs above the fault on both seismic sections. Aside from the Beekmantown/Mines, other reflectors continue on either side of the interpreted fault.

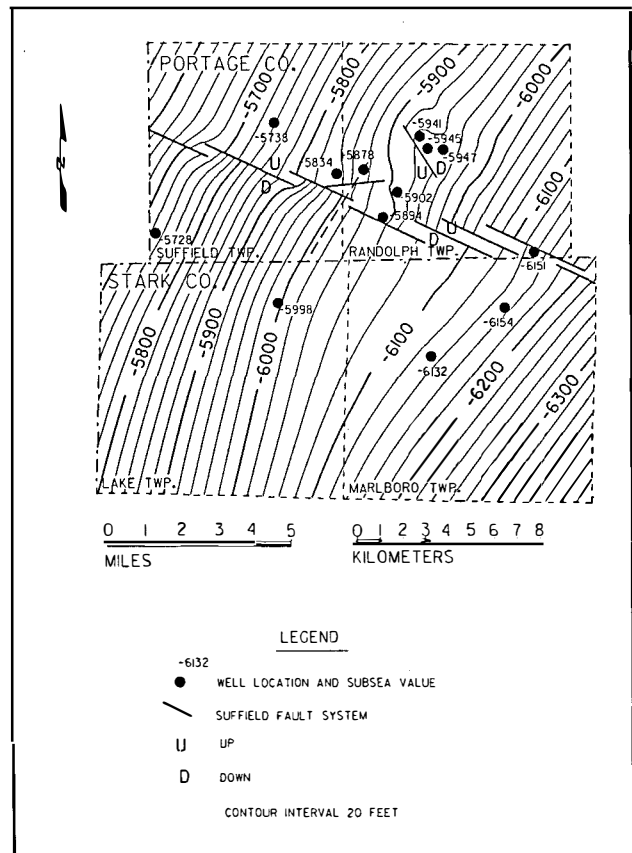


Figure 77. Structure map on top of the Knox unconformity in Portage and Stark counties, Ohio.

An examination of geophysical logs from the wells in the area indicates that subtle stratigraphic changes (lateral porosity decreases) may affect the reservoir heterogeneity of the Rose Run sandstone. Log-derived porosity values in the producing zones range from four to ten percent. Although productive zones may be slightly compartmentalized by local lateral changes in porosity, the primary control of reservoir heterogeneity appears to be due to fracturing and small offset faulting resulting from recurrent movement along basement faults (Figure 76). Analyses of the sonic and density logs from permit number 3777 indicates that the Beekmantown/Mines is highly fractured. This well is very close to the fault and was not completed in the Rose Run or Beekmantown/Mines due to the production of large volumes of brine. Paleoremnants have not been observed on seismic survey lines in this area, nor have such features been drilled.

Geologic and seismic mapping of this area indicates a major basement fault trending northwest-southeast beneath the producing area, the Suffield fault system (Akron-Suffield fault of Gray and others, 1982). Root (1986) interpreted this fault system as a portion of a

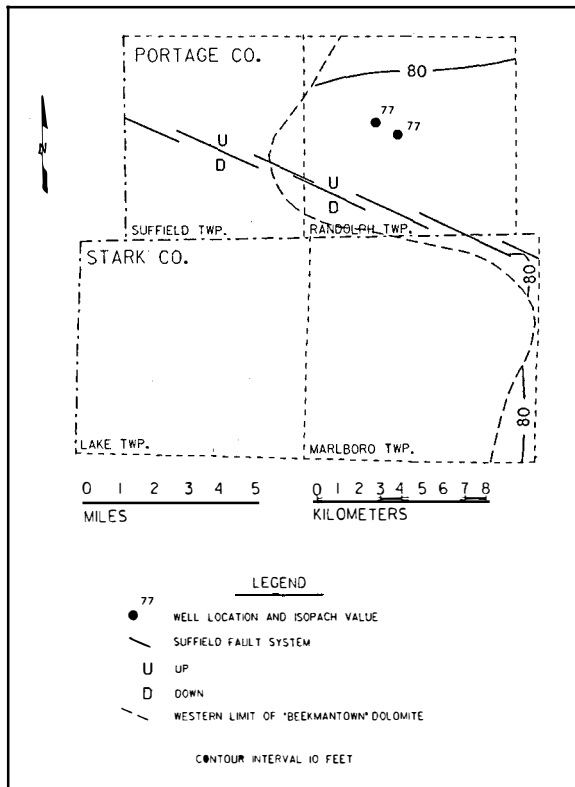


Figure 78. Isopach map of the Rose Run sandstone beneath the Beekmantown/Mines dolomite in Portage and Stark counties, Ohio.

regional strike-slip basement fault that extends southeastward from this area through Pennsylvania and Maryland. Structure on the Knox unconformity (Figure 77) dips southeast into the Appalachian Basin. A break in the contours occurs in southern Portage and northern Stark Counties at the Suffield fault system, where offset ranges from 60 to more than 80 feet on the northeast block. Rose Run thicknesses (Figure 78) are relatively consistent on the north side of the fault where the Beekmantown/Mines is present. We did not use thickness values for the Rose Run south of the fault because erosion beveled the surface. The paucity of Rose Run isopach data in areas where the Beekmantown/Mines occurs is due to wells not completely penetrating the Rose Run. The Wells Creek/Shadow Lake isopach map (Figure 79) also shows a consistent thickness across the area. Structure on the Trenton Limestone (Figure 80) appears to be similar to structure on the Knox unconformity (Figure 77). The breakup of the Trenton seismic reflectors above the fault may indicate fracturing associated with the upward propagation of faults after Trenton deposition. Structure on the Berea Sandstone (Figure 81) indicates a south dip across the fault with offsets of 60 to 100 feet, up to the northeast. The orientation of Berea structures, which is significantly different from that of the Knox and Trenton, results from

thicker Silurian and Devonian units on the north side of the fault and variations in lateral movement of these younger units during faulting.

Well control and seismic data indicate a very complex history along the Suffield fault system. Reactivation and movement along this system occurred repeatedly throughout the Paleozoic, causing faulting and associated fracturing in overlying sedimentary rocks. Both well and seismic data indicate that a major lithologic break takes place at the Knox unconformity, where the Beekmantown/Mines dolomite is present only on the higher northeastern block in the areas of producing Rose Run sandstone wells. The Wells Creek/Shadow Lake interval, which does not vary in thickness across the fault system, appears to conform to this offset of geologic units beneath the unconformity. This indicates that downward movement had ceased along the northeastern side of the Suffield fault system prior to deposition of the Wells Creek/Shadow Lake. Uniform time thickness reflectors on seismic sections above the Trenton imply relative quiescence on the fault until after the latest Devonian. Geologic mapping on the Berea Sandstone verifies an episode of upward movement on the fault after Berea deposition (Figure 81).

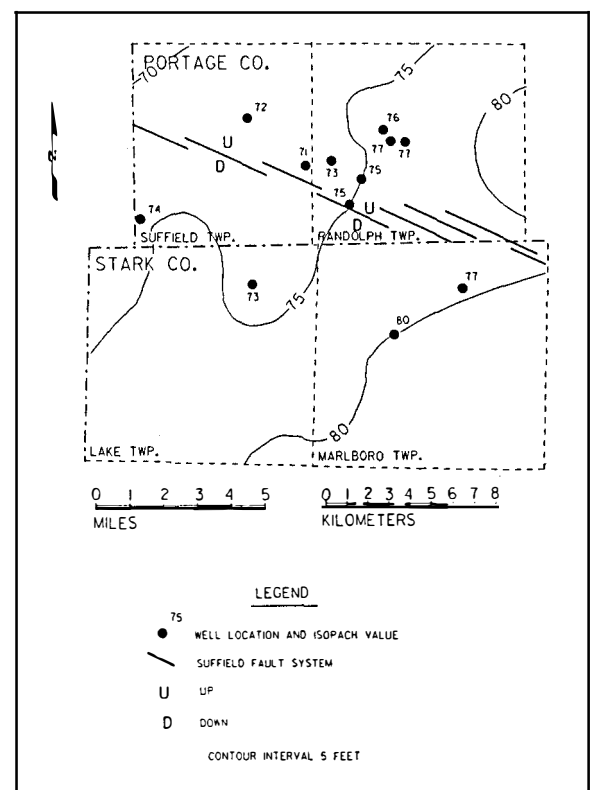


Figure 79. Isopach map of the Middle Ordovician Wells Creek/Shadow Lake interval in Portage and Stark counties, Ohio.

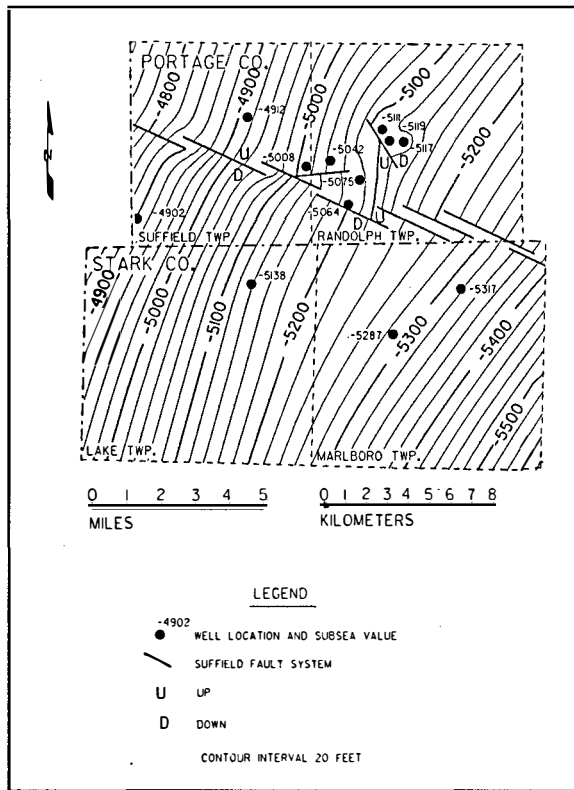


Figure 80. Structure map on top of the Trenton Limestone in Portage and Stark counties, Ohio.

Faulting and fracturing occurred during and after the Knox unconformity in any of three scenarios. In the first case, the northeastern fault block was lower than the southwestern fault block at the time of formation of the Knox unconformity, thus allowing for erosion to remove all strata down to, and including a portion of, the Rose Run sandstone on the southwestern block. During subsequent reactivation, movement along the fault reversed, uplifting the formerly lower northeastern block higher than the southwestern block. In the second case, the northeastern fault block was transported several miles northwestward along left-lateral strike-slip faults, thus bringing preserved Beekmantown/Mines into juxtaposition with eroded Rose Run sandstone. The third case involves a combination of the first two. Harper (1989, p. 228) suggested similar possibilities for differences in aeromagnetic anomalies across the Pittsburgh-Washington lineament (the southeastern extension of the Suffield Fault system) in Pennsylvania.

In contrast to Holmes County, Ohio, the use of well and seismic data is limited as a predictive tool to define Rose Run heterogeneity in the Portage County area. As a predictive tool seismic data have provided indirect evidence of fracturing in the Rose Run. The results of these data show that reservoir heterogeneity in the producing Rose

Run wells occurs in a gross fashion on the upper fault block of the Suffield fault system. A monoclinial flexure that occurs on Figures 25 and 74 at the position of the interpreted fault probably resulted in fractures propagating upward from the Precambrian into the Paleozoic. The "breakup" of seismic signal in the Ordovician Trenton/Black River interval (Figure 75) is also indirect evidence of fracturing. Thus, predicting heterogeneity on a well-by-well basis involves a high degree of interpretation. Evaluation of geologic and seismic data presented here indicates that fracturing and small-scale faulting, due to reactivation of the Suffield fault system, controlled reservoir heterogeneity in the producing Rose Run wells. Impermeable Beekmantown/Mines dolomite probably serves as a caprock for the reservoir, except near the fault where the Beekmantown/Mines is highly fractured. Rose Run production does not occur on the lower, southwestern block; however, fractures may provide traps where porous Rose Run sandstone is in fault contact with impermeable Copper Ridge/Ore Hill dolomite, assuming the overlying fractures are healed or terminate upward into impermeable rock. Paleoremnants, which to date had not been found, may also provide hydrocarbon reservoirs for both the Beekmantown/Mines and Rose Run. Silurian Clinton/

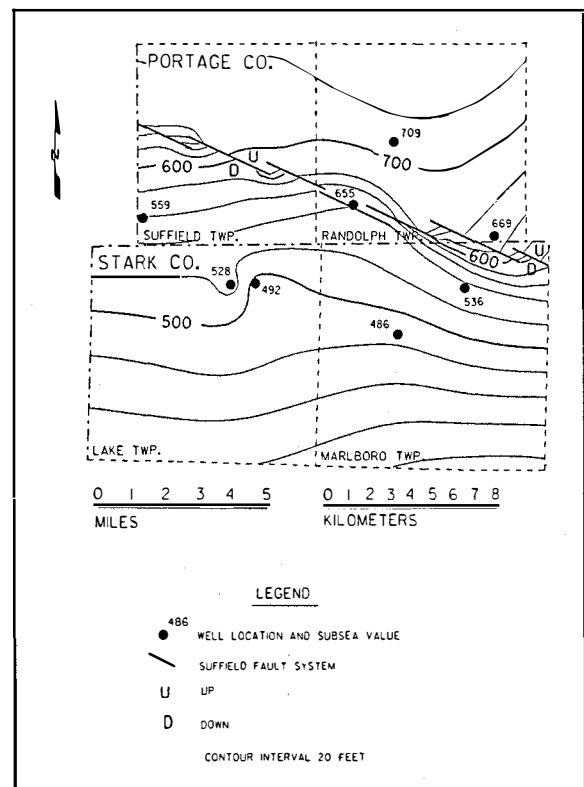


Figure 81. Structure map on top of the Mississippian Berea Sandstone in Portage and Stark counties, Ohio.

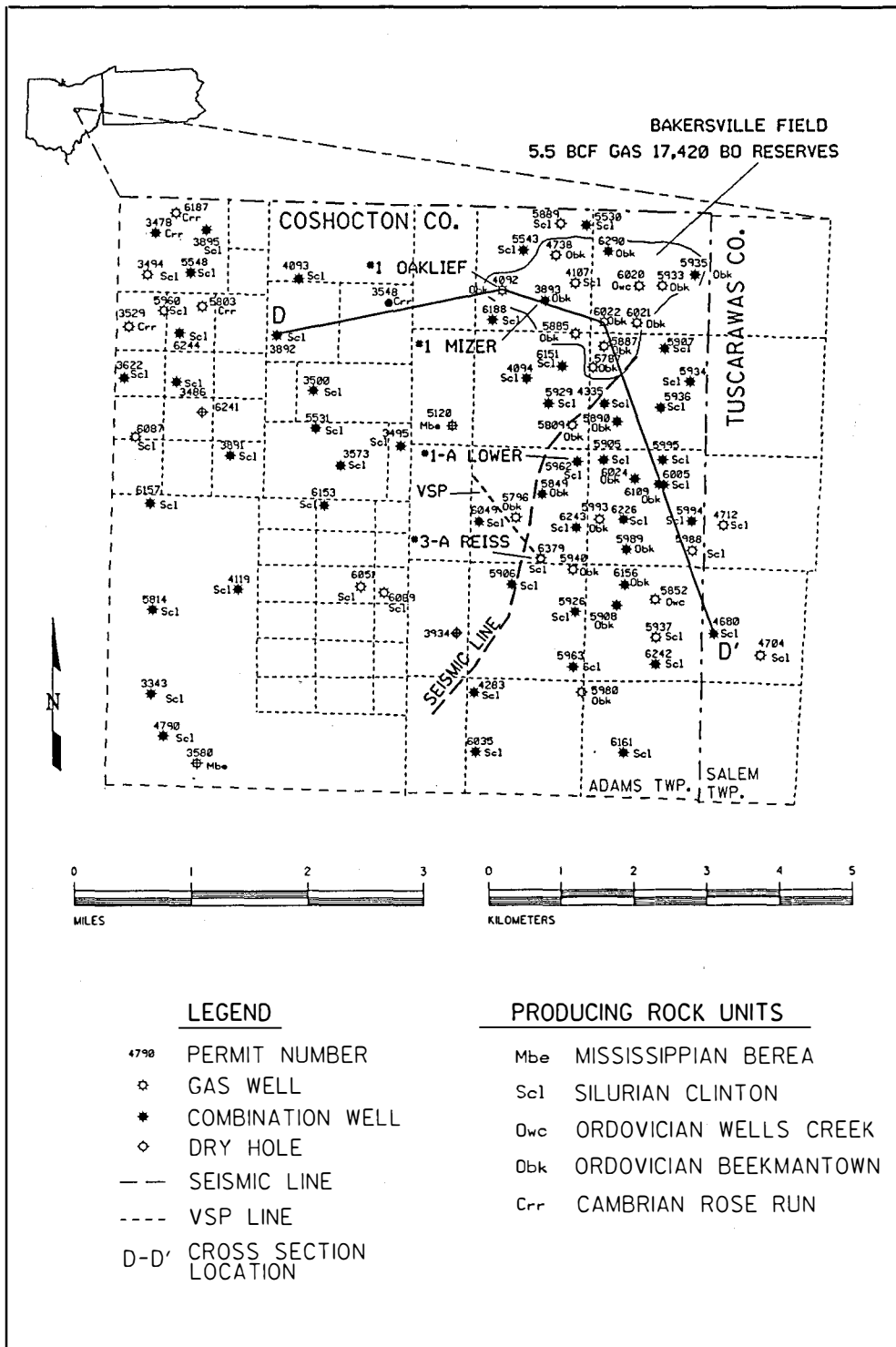


Figure 82. Base map showing well locations penetrating the Knox unconformity in eastern Coshocton and western Tuscarawas counties, Ohio.

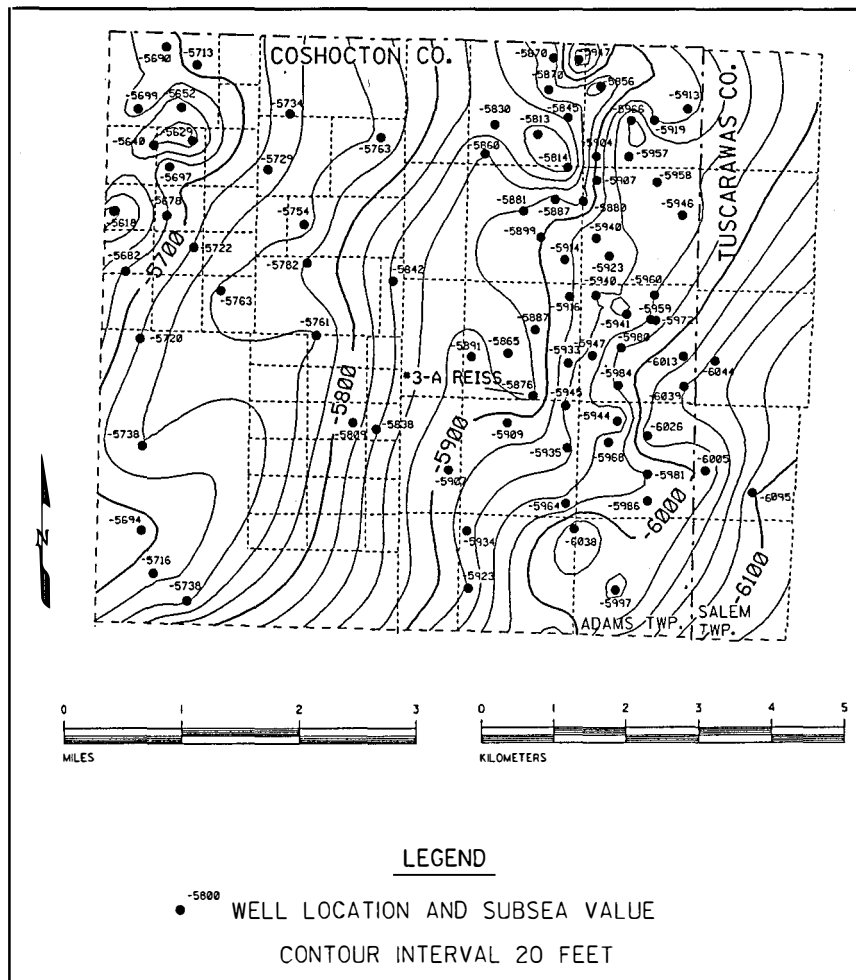


Figure 83. Structure map on top of the Knox unconformity in eastern Coshocton and western Tuscarawas counties, Ohio.

Medina sandstone and Mississippian Berea Sandstone reservoirs produce hydrocarbons from fractured reservoirs and small anticlines on the upper fault block. This shallower production supports the concept of basement-controlled faulting, associated fracturing, and development of folds.

Reservoir heterogeneity cannot be predicted with a high degree of reliability in this area because of the sparse deep well control and lack of significant typical seismic anomalies away from the Suffield fault system. The use of shallow well control to explore for deeper Knox structures is recommended; leads from shallow mapping may be evaluated by the acquisition of high-resolution seismic data, seismic modeling, and attribute analyses. Subtle lateral changes in porosity within the Rose Run sandstone may also affect the heterogeneity of this unit. However, as with most immature plays, more wells need to be drilled and cored, and more engineering data needs to be acquired, to fully evaluate this hypothesis. A few operators seeking

Rose Run production in other areas use these techniques in a limited fashion.

Eastern Coshocton and Western Tuscarawas Counties, Ohio

The primary exploratory objectives in Adams Township, Coshocton County and western Salem Township, Tuscarawas County include the Rose Run sandstone and Beekmantown/Mines dolomite. Secondary objectives for hydrocarbon production in this area include the Wells Creek/Shadow Lake interval, Clinton/Medina reservoirs, and Berea Sandstone. Zones of solution-enlarged vuggy porosity in the Beekmantown/Mines, associated with paleotopographic highs, constitute the primary heterogeneity (type 3) in this area. The following discussion focuses on the trapping mechanisms and heterogeneity associated with production from the

Beekmantown/Mines dolomite based upon subsurface mapping, seismic interpretation, and core analyses.

This is a subtle stratigraphic play that has yielded significant quantities of hydrocarbons from the Beekmantown/Mines in Coshocton County, and may be present in other localized regions along the subcrop trend. Production data available from nine of the wells in the Bakersville field (Figure 82) show that by the end of 1991, it has produced approximately 5.5 Bcfg and 17 Mbo from this reservoir. By itself, the #1 Mizer well (permit number 3893) yielded approximately 2.6 Bcfg and 9 Mbo (Appendix VI).

This area represents the heart of the Rose Run subcrop play in east-central Ohio. The structure map on the top of the Knox unconformity (Figure 83) illustrates the irregular erosional surface that dips regionally to the southeast. Subsea elevations range from -5,620 feet in the northwest to -6,120 feet in the southeast. The Bakersville field in northeastern Adams Township is situated on a structural

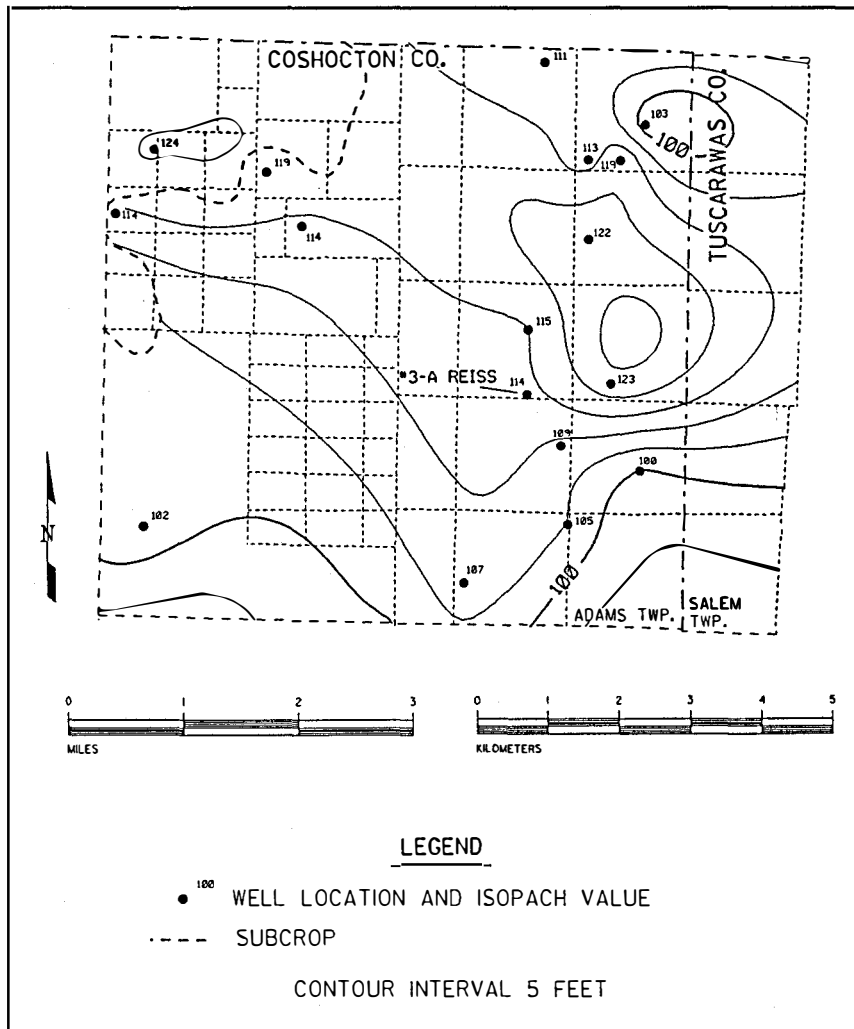


Figure 84. Isopach map of the Rose Run sandstone in eastern Coshocton and western Tuscarawas counties, Ohio.

high trending northwest-southeast. The #3-A Reiss well (permit 6379) (Figure 82), chosen as a stratigraphic test for this project, occurs along strike approximately two miles south of the Bakersville field on a northwest-southeast trending structural nose. The #1 Hachenbracht well (permit number 5908), approximately 0.7 miles to the southeast of the #3-A Reiss well, produced approximately 61 Mbo from the Beekmantown/Mines during the first 5 years of production.

The isopach map of the Rose Run sandstone (Figure 84) shows the thickness to be relatively consistent throughout this area, ranging from 100 to 120 feet. To the west of this area, however, the Rose Run becomes thinner across the subcrop beneath the Knox unconformity. Additional sandstone lenses which are not laterally continuous occur within the dolomite beneath the Rose Run. In Holmes County, Ohio these Copper Ridge/Ore Hill sandstones

are currently being explored for and have produced significant quantities of oil and gas in 1992.

Examination of sidewall cores from the #3-A Reiss well reveals that the Rose Run consists of a white to light-grey, fine- to coarse-grained quartz arenite to subarkose that contains some glauconite and interbedded dolostone. Sidewall cores show no major lithologic differences in the various sandstone lenses within the Rose Run interval other than a slight increase in feldspar content with depth. Based on examination of sidewall cores and Formation Microscanner (FMS) images, the Rose Run interval is featureless with the exception of cross-bedding and rip-up clasts near dolostone boundaries. A domed algal stromatolite can be interpreted from FMS images in one dolostone bed. Average porosities in the sandstones range from eight to ten percent, with values as high as 13 percent. Perme-

abilities to gas, based on core analyses (Appendix IV) range from .005 to 42.8 md. Eleven of the samples had permeabilities to gas greater than 1.0 md. The m exponent (pore geometry factor), from the Elemental Analysis log (ELAN), based on measurements from the EPT and MSFL logs, ranged from 1.8 to 2.3. Determination of correct m exponents is critical in well log analysis. The m exponent used to calculate resistivities can have a profound affect on calculated water saturations, causing "wet" zones to appear hydrocarbon saturated.

The Beekmantown/Mines dolomite ranges in thickness from 0 feet in the northwest to a maximum thickness of 178 feet in the Bakersville field (Figure 85). The Beekmantown/Mines reaches a thickness of 84 feet in an erosional remnant immediately east of the subcrop in northwestern Adams Township, Coshocton County. A northwest-southeast trending Beekmantown/Mines ridge

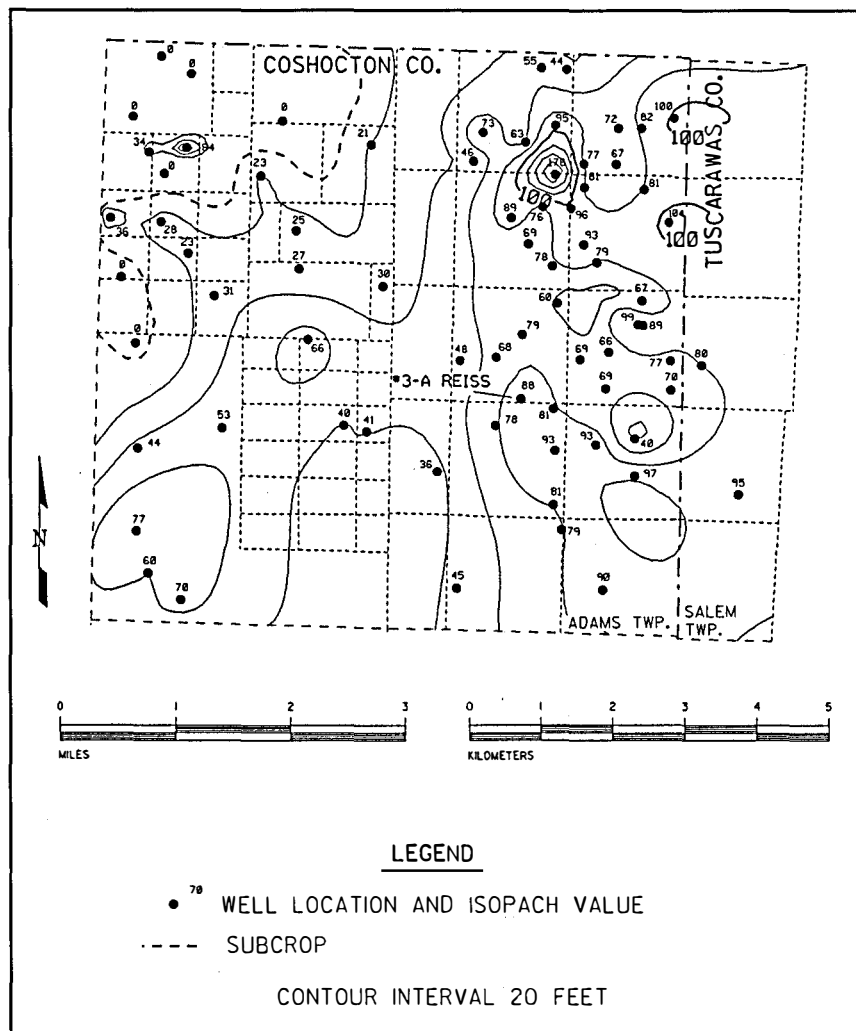


Figure 85. Isopach map of the Beekmantown/Mines dolomite in eastern Coshocton and western Tuscarawas counties, Ohio.

also occurs at the #3-A Reiss well. In the Bakersfield field, density logs used in conjunction with cores indicate secondary porosity from solution-enlarged vugs within the Beekmantown/Mines approximately 4 to 6 feet below the Knox unconformity (Figure 86, second well from the right). Zones up to seven feet thick and having porosities up to 20 percent can be seen on density logs. The Knox paleotopographic high associated with this solution-enlarged vuggy porosity created the stratigraphic trap responsible for hydrocarbon entrapment in this field.

Field-scale heterogeneity can be recognized within this reservoir by comparing the cores from the #1 Oaklief (permit number 4092), the #1-A Lower (permit number 5962), and the #3-A Reiss (permit number 6379) wells. Secondary mineralization of dolomite affected lateral variations in vuggy porosity. Permeabilities in the Beekmantown/Mines generally are less than .1 md,

except in localized areas where the vugs interconnect.

Core analyses in the #1 Oaklief well (Appendix IV) indicate porosities up to 8.4 percent and permeabilities up to 240 md in the Beekmantown/Mines interval between 6,880 to 6,892 feet. The neutron and density logs indicate a slightly porous zone throughout this interval, bounded by carbonates exhibiting higher densities. Examination of the core reveals this interval to be a brecciated zone with associated secondary vuggy porosity. However, most of the vugs do not interconnect and have been filled with white dolomite. The operator perforated the interval in the #1 Oaklief well from 6,876 to 6,887 feet, resulting in an IP of 40 Mcfgpd and a trace of oil. Cumulative production after 11 years was only 47,910 Mcfg. Lack of significant production in this well as compared to that found in the #1 Mizer well (permit number 3893) appears to be related to

reduction of solution-enlarged porosity by secondary mineralization.

Secondary mineralization of vuggy porosity also occurs in the core of the #1-A Lower well (permit number 5962). Porosities measured from core analyses in the Beekmantown/Mines generally are less than three percent, with the exception of two samples measured at approximately eight percent. Permeabilities also are low, except in the interval 6,780 to 6,786.9 feet where values are as high as 17 md (Appendix IV). Mesoscopic examination of the core shows this zone contains poor pinpoint vuggy porosity and small, unconnected, dolomite-filled vugs up to 0.25 inches. Anhydrite also fills some small vugs near this interval. The #1-A Lower well did not produce in either the Rose Run or the Beekmantown/Mines, and was plugged back to the Clinton/Medina.

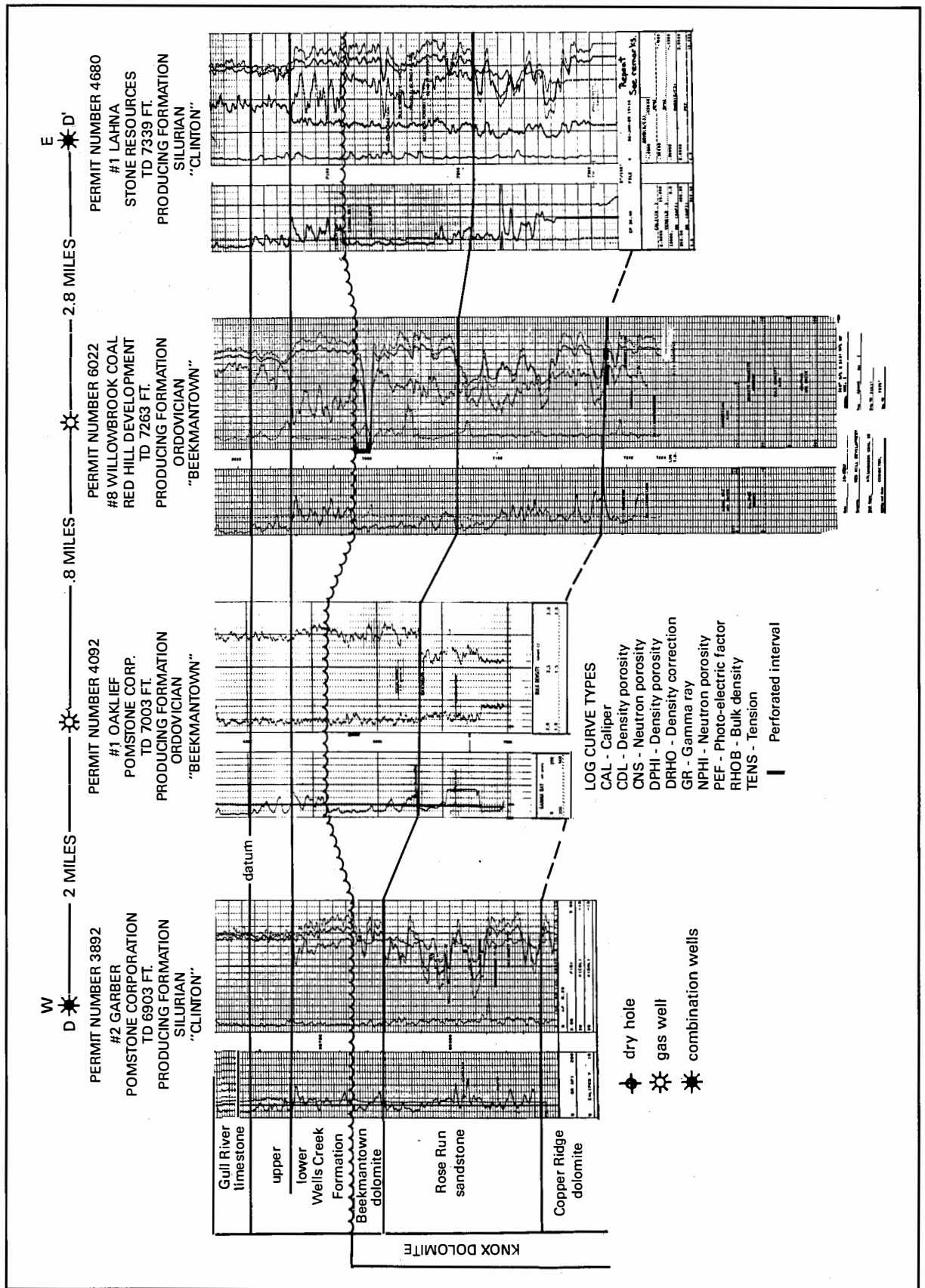


Figure 86. Stratigraphic cross section D-D' in eastern Coshocton and western Tuscarawas counties, Ohio. See Figure 82 for location.

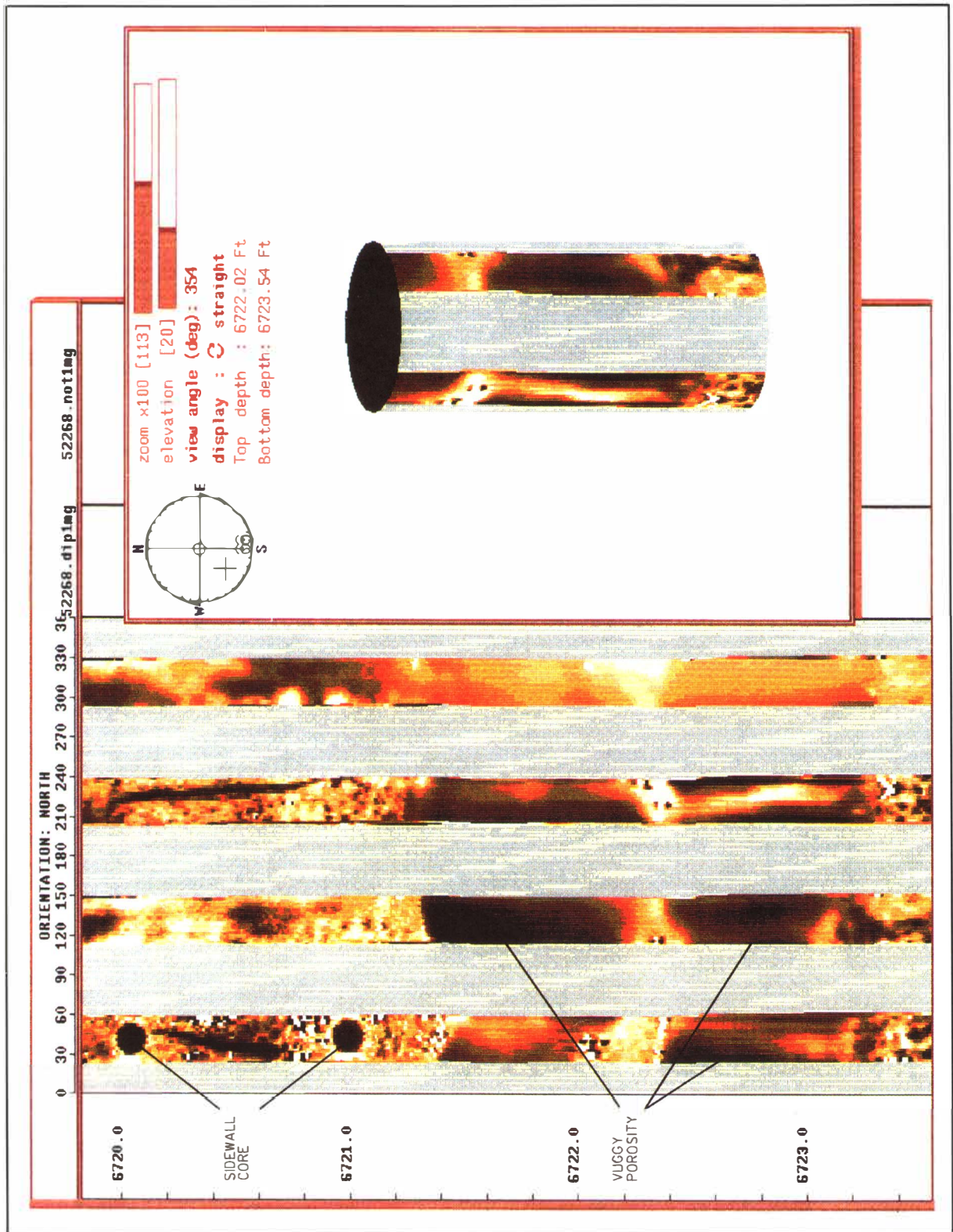


Figure 87. Formation MicroScanner image of vuggy porosity in the Beekmantown/Mines dolomite from the #3 Reiss well, permit number 6379, Coshocton County, Ohio.

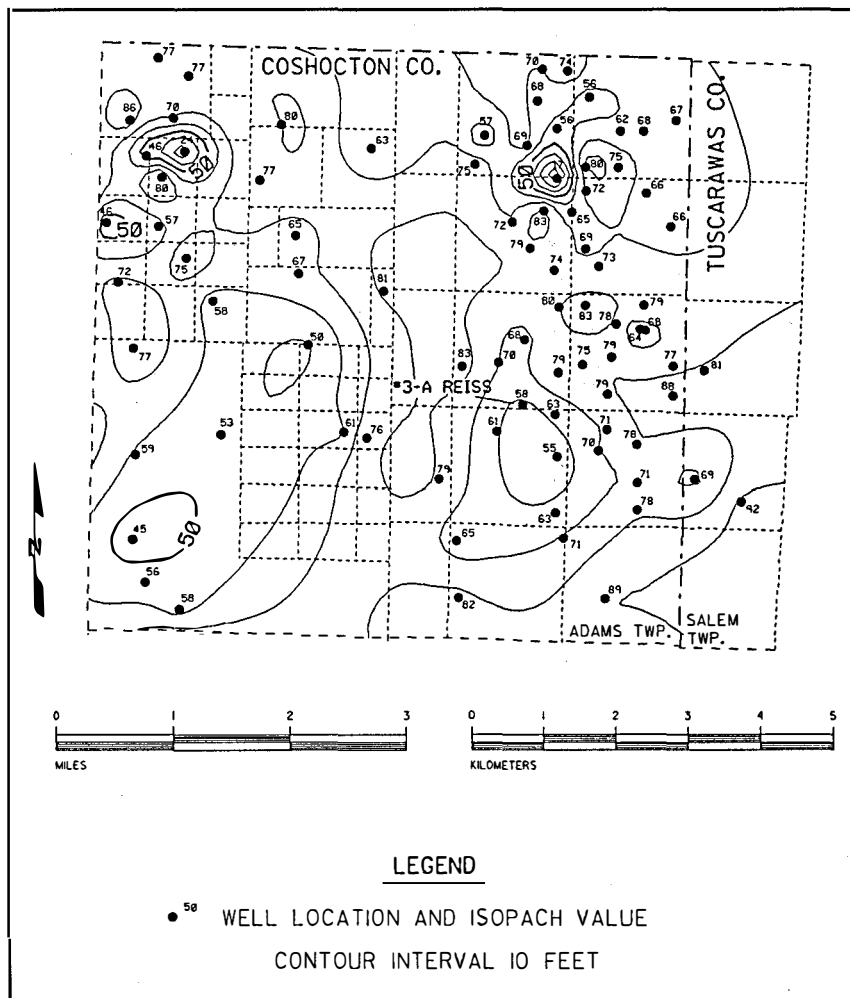


Figure 88. Isopach map of the Wells Creek/Shadow Lake interval in eastern Coshocton and western Tuscarawas counties, Ohio.

In the #3-A Reiss well, approximately 88 feet of Beekmantown/Mines dolomite overlies the Rose Run sandstone. Based on examination of sidewall cores from this well, the Beekmantown/Mines consists of a light-brown to grey, microcrystalline, mottled dolostone. At the contact between the Knox unconformity and the overlying Wells Creek/Shadow Lake interval, a 300-unit gas increase occurred that gradually increased to 400-units at total depth of 7,167 feet. The high-resolution log indicates three feet of vuggy porosity near the top of the Beekmantown/Mines, seven to 16 feet below the unconformity. Neutron and density logs indicate porosities exceeding 20 percent within these zones. The FMS reveals vugs up to one foot across throughout this interval (Figure 87). Smaller vugs occur adjacent to this zone of massive vuggy porosity. Permeabilities measured in sidewall cores from the dolostone adjacent to this zone range from .001 to .046 md (Appendix IV). There was no recovery from a sidewall core attempted within one of these massive vugs.

the southeast. A prominent northwest-southeast trending structural nose occurs at the Bakersville field. An east-west trending structural high is present over the erosional remnant in the northwest part of the map, and a slight northwest-southeast trending structural nose can be seen over the #3-A Reiss well. Similarly, the Trenton surface reflects the Knox low in the southwest portion of the mapped area. The map of the Wells Creek/Shadow Lake-through-Trenton interval thickness (Figure 90) correlates with the Knox structure map (Figure 83). Abrupt thinning of the Wells Creek/Shadow Lake occurs over the Knox high in northwestern Adams township. Subtle thinning of these units also occurs over the Bakersville field and the #3-A Reiss well. In the southeast, a thick Wells Creek/Shadow Lake-through-Trenton interval is present over a Knox low.

Operators commonly map structures and thicknesses of shallower horizons, such as the "Packer Shell," as a

The isopach map of the Wells Creek/Shadow Lake interval (Figure 88) indicates depositional thinning over Knox paleoremnants. Abrupt thinning occurs in the Bakersville field where the Wells Creek/Shadow Lake interval decreases to 17 feet. Thinning of the Wells Creek/Shadow Lake above Beekmantown/Mines remnants also occurs in the northwest portion of Figure 88, and at the #3-A Reiss well. The #3-A Reiss well contains approximately 58 feet of Wells Creek/Shadow Lake, which is slightly thinner than in any of the adjacent wells. This may be a result of draping of younger sediments, structural reactivation, or both.

The structure contour map on top of the Trenton Limestone (Figure 89) reflects the deeper Knox unconformity structure map. The Trenton Limestone dips to the southeast with sub-sea values ranging from -4,880 in the northwest to -5,280 in

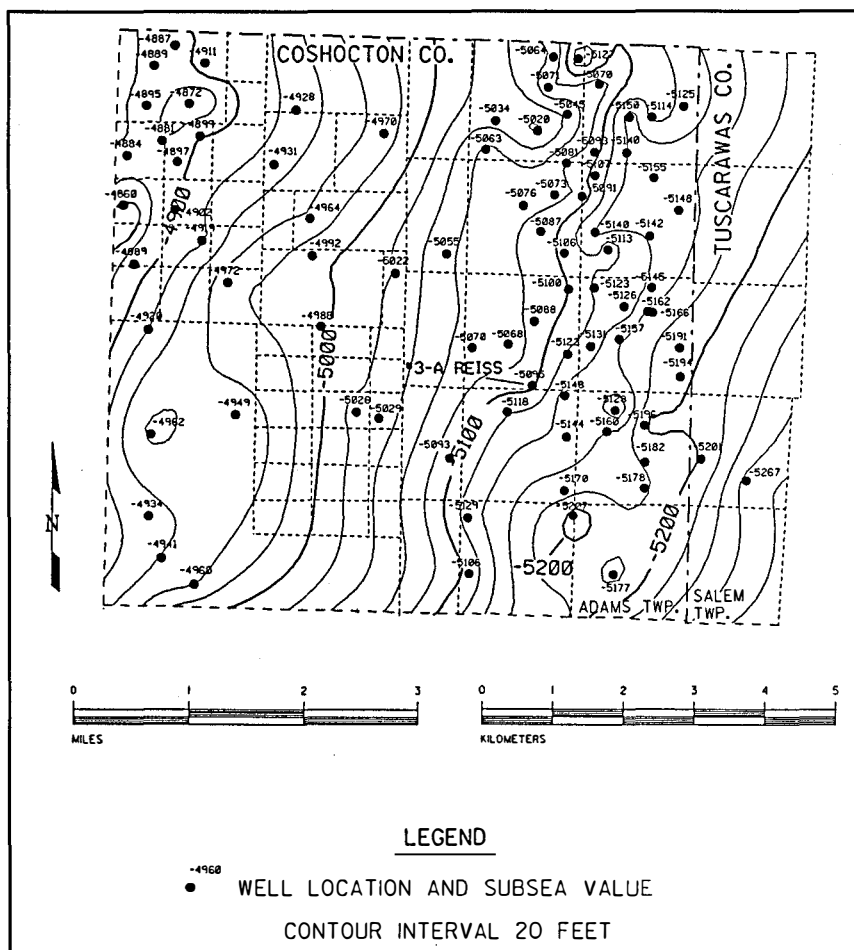


Figure 89. Structure map on top of the Upper Ordovician Trenton Limestone in eastern Coshocton and western Tuscarawas counties, Ohio.

method of developing leads and exploring for Rose Run and Beekmantown/Mines reservoirs along the subcrop trend. Structure contours on the base of the "Packer Shell" (Figure 91) reflect the deeper Knox unconformity structure map. This map shows regional dip to the southeast with subsea elevations ranging from -3,260 in the northwest to -3,620 in the southeast. A well-developed northwest-southeast trending structural nose occurs at the Bakersville field, mirroring the underlying Knox structure. A more subtle northwest-southeast trending structural nose also is present at the #3-A Reiss well. Structure contours on the Middle Devonian Onondaga Limestone (Figure 92) does not reveal the Knox unconformity structure map as well as the "Packer Shell" map. The Onondaga dips regionally to the southeast, having subsea values ranging from -1,880 in the northwest to -2,160 in the southeast. A subtle structural nose on the Onondaga map trending east-west is apparent over the Bakersville field.

In 1984, Stone Resources acquired a line of 30-fold vibrator data over an area of Adams Township, Coshocton County, Ohio (Figure 82). The input signal was a seven-second sweep from 30 to 120 Hertz. Original processing parameters included spiking deconvolution and pre-stack spectral whitening. The final bandpass filter was 14-18-105-115 Hertz. The data as presented in the original processing format are stacked and non-migrated data. Refraction statics were not performed in the original processing format because they were not commonly used at that time. As a result of this, and the fact that the data are non-migrated, the reflectors from 0.45 to 1.0 seconds appear to mimic surface topography. An apparent Knox high on this seismic section makes the area appear prospective for hydrocarbons (Figure 93). Note the northeast-dipping reflectors in the basement. Various authors have noted that many shallow tectonic features in the Appalachian basin occur along zones of weakness in the basement defined by Grenville thrust sheets (Beardsley and Cable, 1983; Ryder, 1992;

Seismic exploration plays an integral role in this area in the understanding of heterogeneity in general, and the results of this study show that seismic stratigraphic analysis can be used in measuring and predicting heterogenous changes in the Rose Run sandstone and Beekmantown/Mines dolomite in eastern Coshocton and western Tuscarawas counties. Seismic reprocessing and forward modeling of the vertical seismic profile (VSP) revealed the following:

- 1) amplitude variations in seismic data can be used to predict hydrocarbons in the Rose Run;
- 2) variations in the thickness of the Beekmantown/Mines can be predicted in a general sense using seismic data;
- 3) zones with vuggy porosity can be predicted using seismic data;
- 4) Copper Ridge/Ore Hill sandstones can be recognized using seismic data.

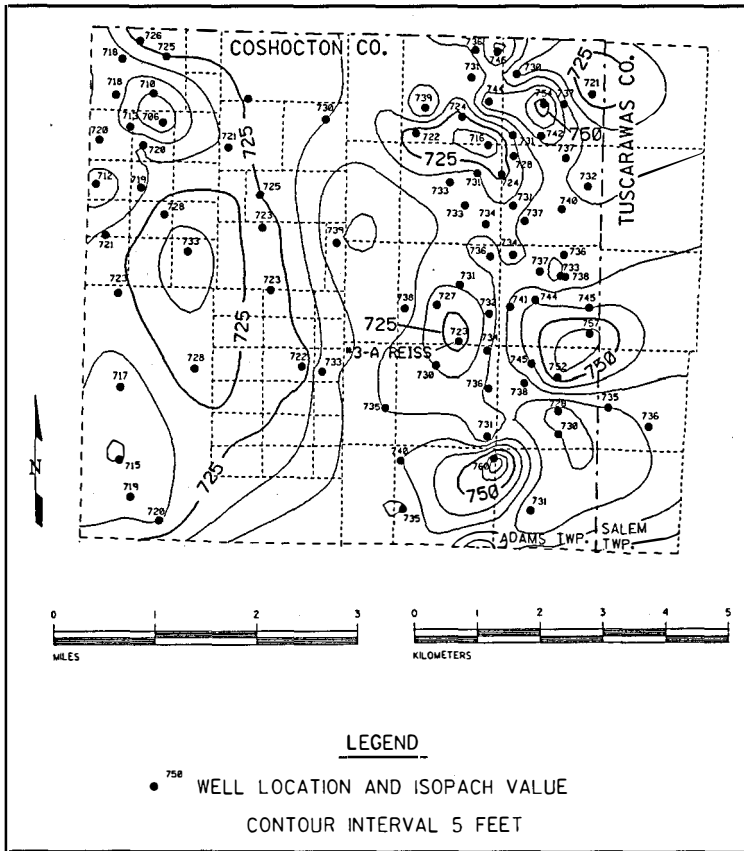


Figure 90. Isopach map of the Wells Creek/Shadow Lake-through-Trenton interval in eastern Coshocton and western Tuscarawas counties, Ohio.

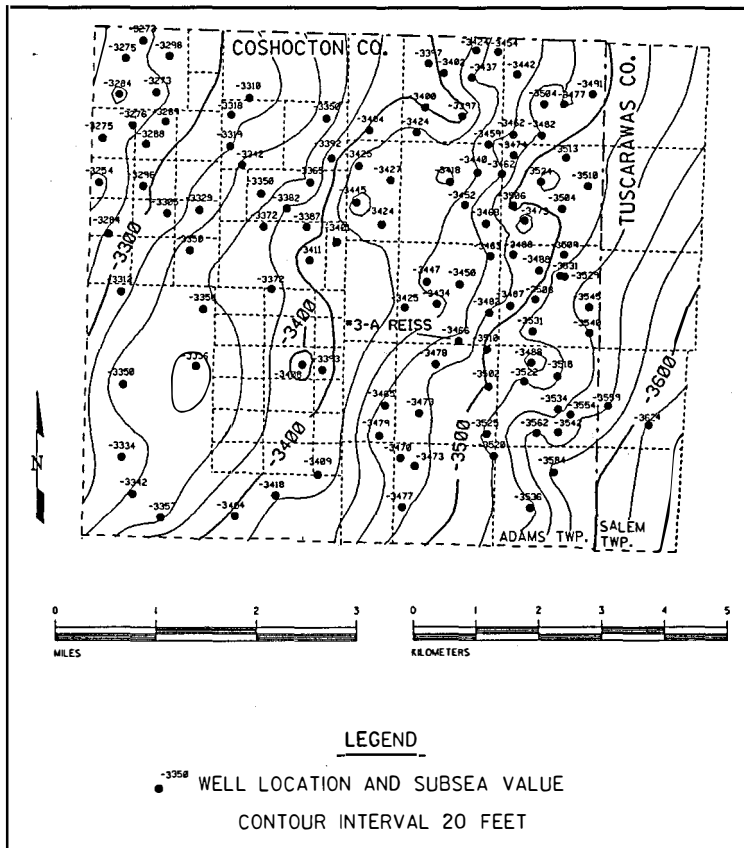


Figure 91. Structure map on the base of the Lower Silurian "Packer Shell" in eastern Coshocton and western Tuscarawas counties, Ohio.

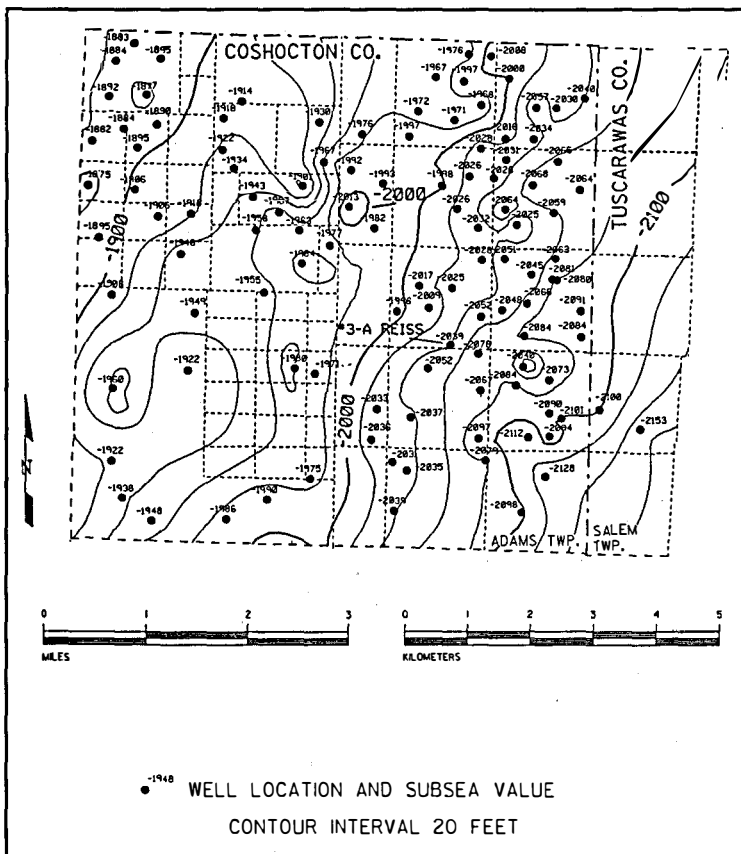


Figure 92. Structure map on top of the Middle Devonian Onondaga Limestone in eastern Coshocton and western Tuscarawas counties, Ohio.

Baranowski, 1993). Partially as a result of this seismic line interpretation, the #3-A Reiss well (permit number 6379) was drilled 500 feet to the southeast of an anomaly on this line. There were no commercial quantities of hydrocarbons present in the Knox/Gatesburg interval.

During logging of this well, Schlumberger Well Services also ran a VSP to evaluate the seismic response of the Trenton through Copper Ridge/Ore Hill interval. The well is approximately 500 feet southeast of the seismic line. This might cause correlation difficulties with the seismic data because some of the potentially productive remnants might not be very extensive laterally. Three vibrator sources were placed at distances of 675 feet and 4,501 feet northwest of the borehole to achieve zero-offset and offset vertical seismic profiles (ZVSP and OVSP, respectively). The source consisted of eight sweeps from 15 to 120 Hertz for each profile. The ZVSP provided the well-log tie to the surface-acquired reflection seismic data. The company used standard processing flow as described in Appendix I, with the exception of F/K filtering to remove the effects of tube waves in the ZVSP. The processing resulted in a vertical seismic profile, or corridor stack. We correlated the logged intervals and depths of the Wells Creek/

Shadow Lake through Copper Ridge/Ore Hill units with the ZVSP and displayed it as a Seisview log (Figure 94). The Seisview log displays lithology, compressional- and shear-wave slowness, bulk density, acoustic impedance, reflection coefficients, synthetic seismogram, ZVSP corridor stack and dipmeter computation results. Using the convention that a peak represents a positive reflection coefficient, we interpret the seismic signature of the "Gull River"/Loysburg-to-Copper Ridge/Ore Hill interval in the #3-A Reiss well as a saddle peak, followed by a large trough, followed by an equally large magnitude peak, followed by a trough with 0.8 magnitude of the last trough and a peak 0.5 magnitude of the large peak.

Noise from converted shear waves and monochromatic noise at 30 Hertz compromised the OVSP. It offers good vertical and horizontal resolving power because raypaths to the horizons are shorter; therefore, frequency losses due to propagation are less. Migration velocities for the OVSP were verified by

ray tracing prior to migration of the offset profile. The model was thus adjusted to tie with the synthetic seismogram within two milliseconds. The OVSP signal was rotated to zero-phase and presented as a stacked section (Figure 95A). Horizon interpretation provided a listing of depths to each horizon from which we calculated formation isopachs. These isopachs demonstrate rapidly varying thicknesses in the Wells Creek/Shadow Lake-through-Copper Ridge/Ore Hill interval. Trace attribute analysis on the OVSP helped to pick horizons and note amplitude changes. Instantaneous phase analysis allowed correlation of horizons across the seismic section. The OVSP showed a large amplitude anomaly at approximately 750 feet from the well (Figure 95B). The value of the amplitude anomaly decreased by 50 percent from 750 to 1,800 feet away from the well. The vertical breadth of the amplitude envelope changes at the same distance that the decrease in amplitude occurs. This suggests that the Rose Run is either depleted in hydrocarbons or is less porous farther than 750 feet from the well.

Ten different scenarios were modeled using the seismic reflection information data gathered by the vertical

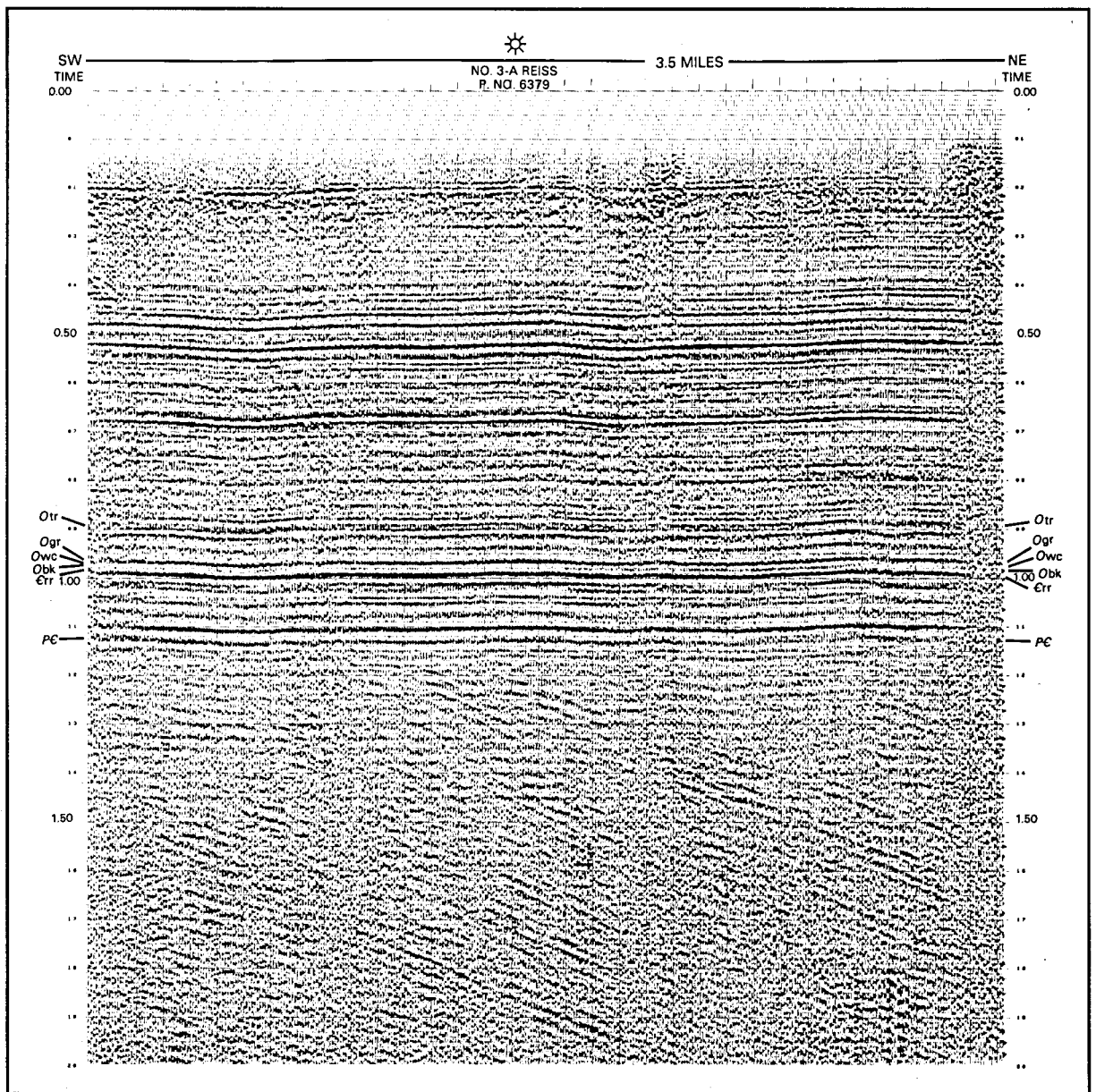


Figure 93. Interpreted seismic section display, Coshocton County, Ohio: 1984 processing without refraction statics, 2.0 seconds travel time, vibrators, 30-fold, unmigrated. See Figure 24 for legend.

seismic profiling (see Appendix VII for information). A seismic pseudosection was prepared by interpolating between values for the model acoustic impedance logs, impedances, convolving the reflectivity series with an assumed wavelet, and plotting the synthetic seismic traces across a two-dimensional model. The resultant seismic pseudosection was analyzed for amplitude anomalies (Figure 96). Modeling of these scenarios showed that a four percent decrease in Rose Run interval velocity, caused by the presence of gas, increases the magnitude of the Rose Run reflection by ten percent. This would have a dramatic impact on the calculation of reflection coefficients and amplitude attribute processing. In the

seismic pseudosection, only models 1, 2, 7, and 9 included a Copper Ridge/Ore Hill sandstone (Figure 96). In these models the Copper Ridge/Ore Hill sandstone is indicated by a well-developed, high amplitude trough that is separated from the overlying Rose Run trough by a peak. The presence of the Copper Ridge/Ore Hill sandstone appears to dampen the amplitude of the Rose Run, so the interpreter must use caution when trying to detect gas in the Rose Run interval.

The thickness of the Beekmantown/Mines is very difficult to predict by VSP pseudoprofile analysis. Thicknesses less than 35 feet and greater than 65 feet can be predicted in a

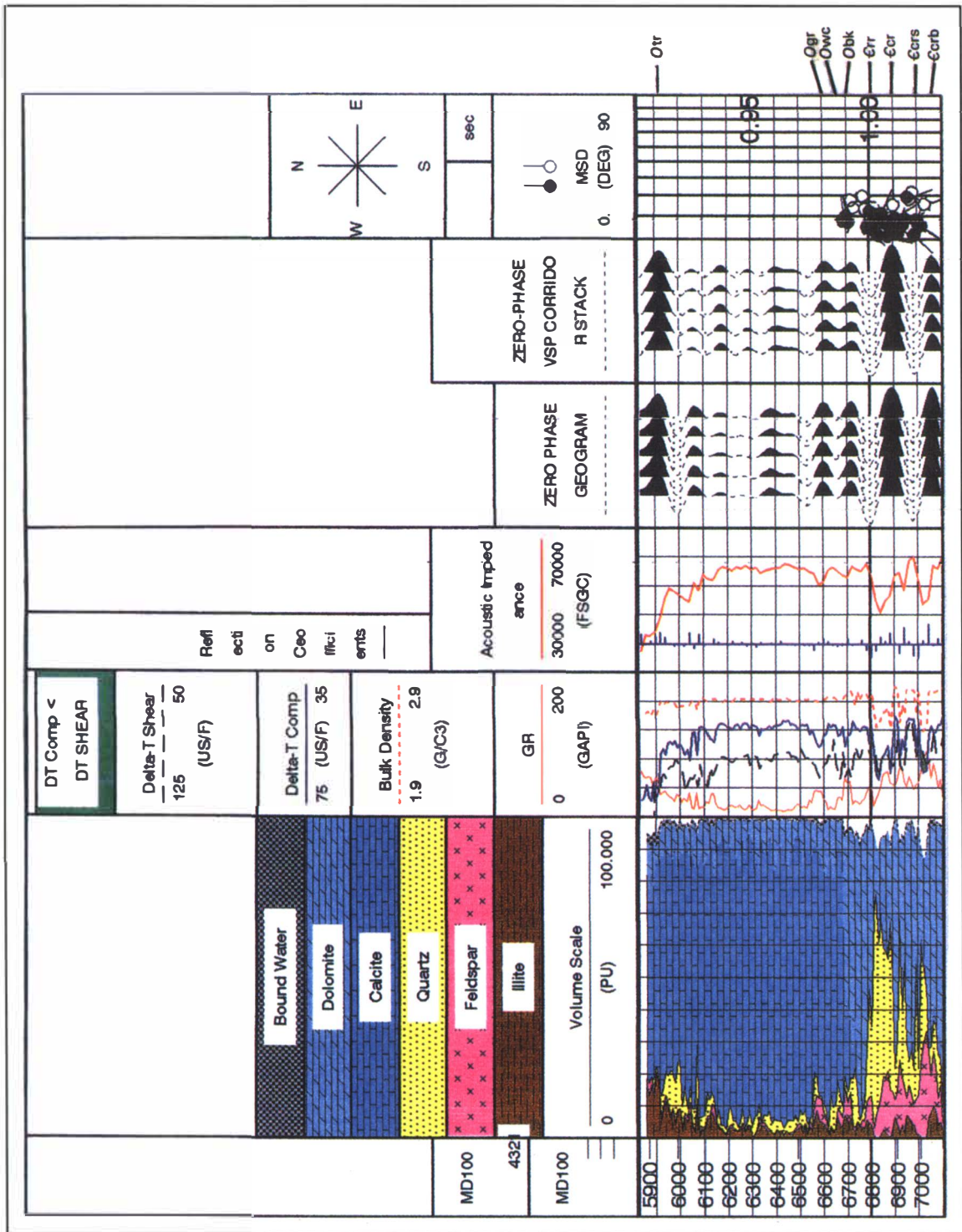


Figure 94. Plot of ELAN lithology, delta-T compressional, delta-T shear, bulk density, gamma ray, acoustic impedance, reflection coefficients, zero phase synthetic seismogram stack, zero phase vertical seismic profile corridor stack, and dipmeter at 15 inches/second scale. From the #3-A Reiss well in Coshocton County, Ohio.

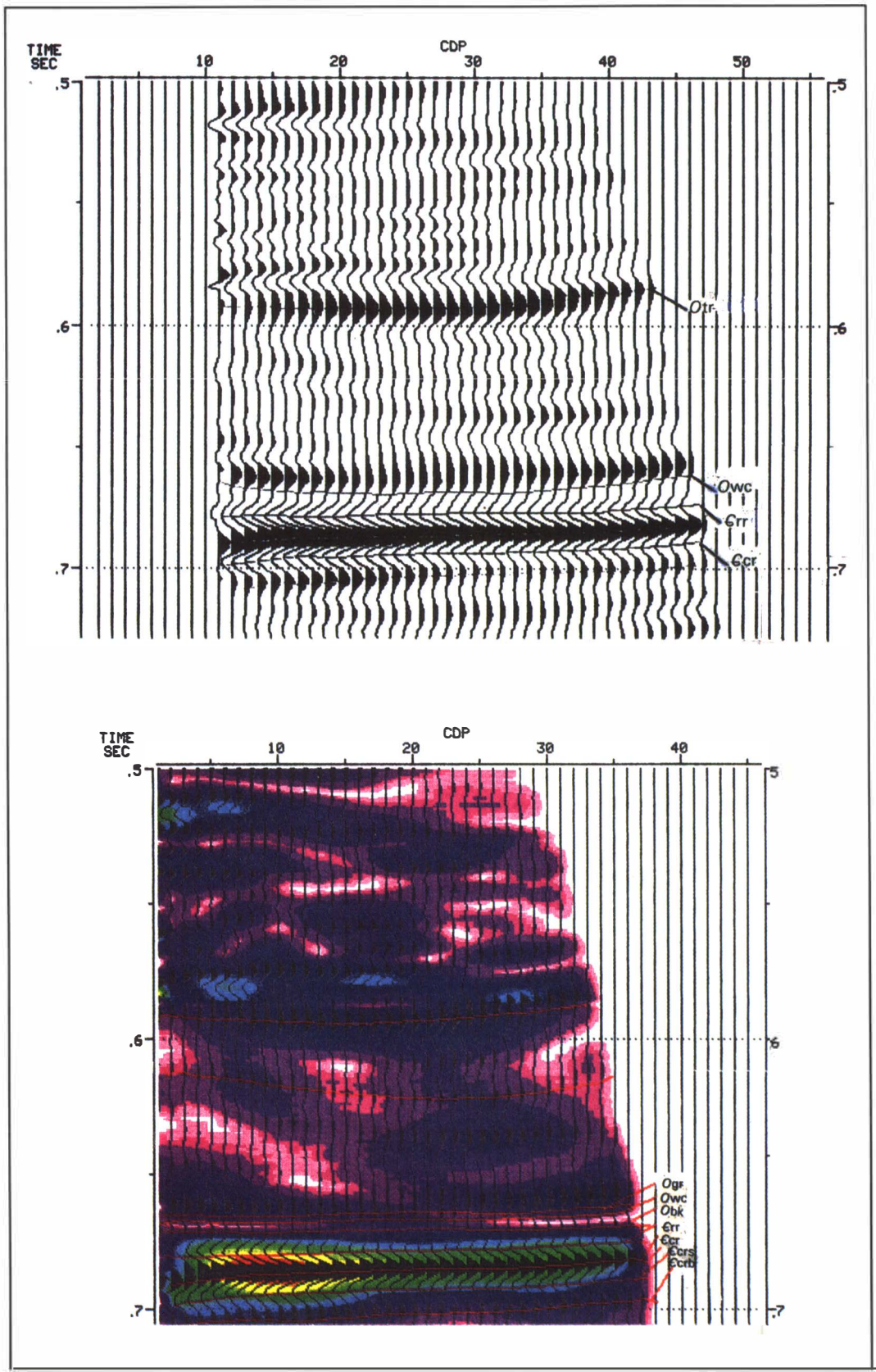


Figure 95. A—Plot of interpreted offset vertical seismic profile with correlation from the #3-A Reiss well in Coshocton County, Ohio. B—Plot of interpreted offset VSP amplitude envelope with depth migration from the #3-A Reiss well. Red and yellow are highest amplitude, white and pink are lowest amplitude.

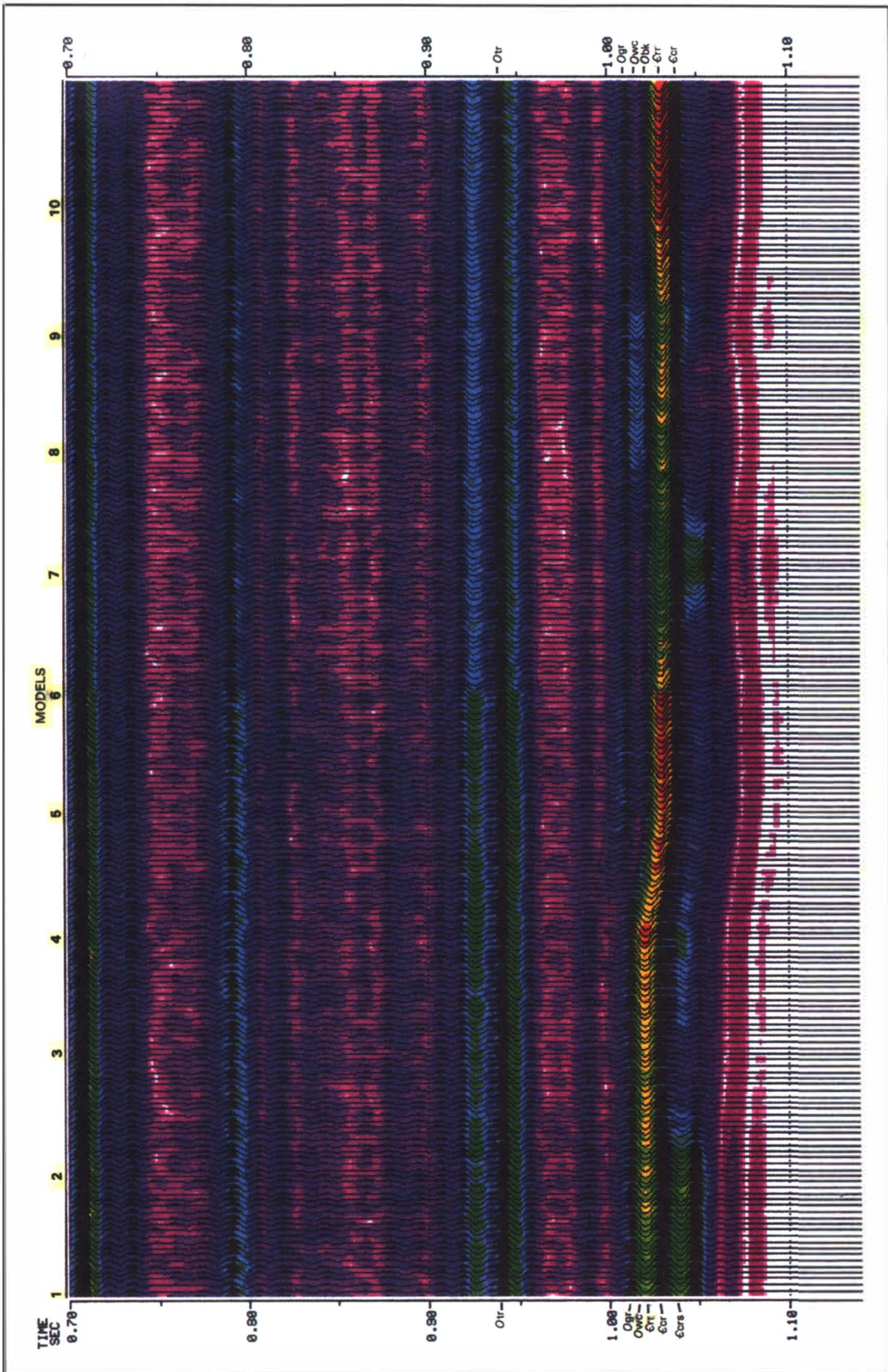


Figure 96. Plot of amplitude envelope of synthetic profile incorporating models 1 to 10 at zero phase. See Figure 24 for legend.

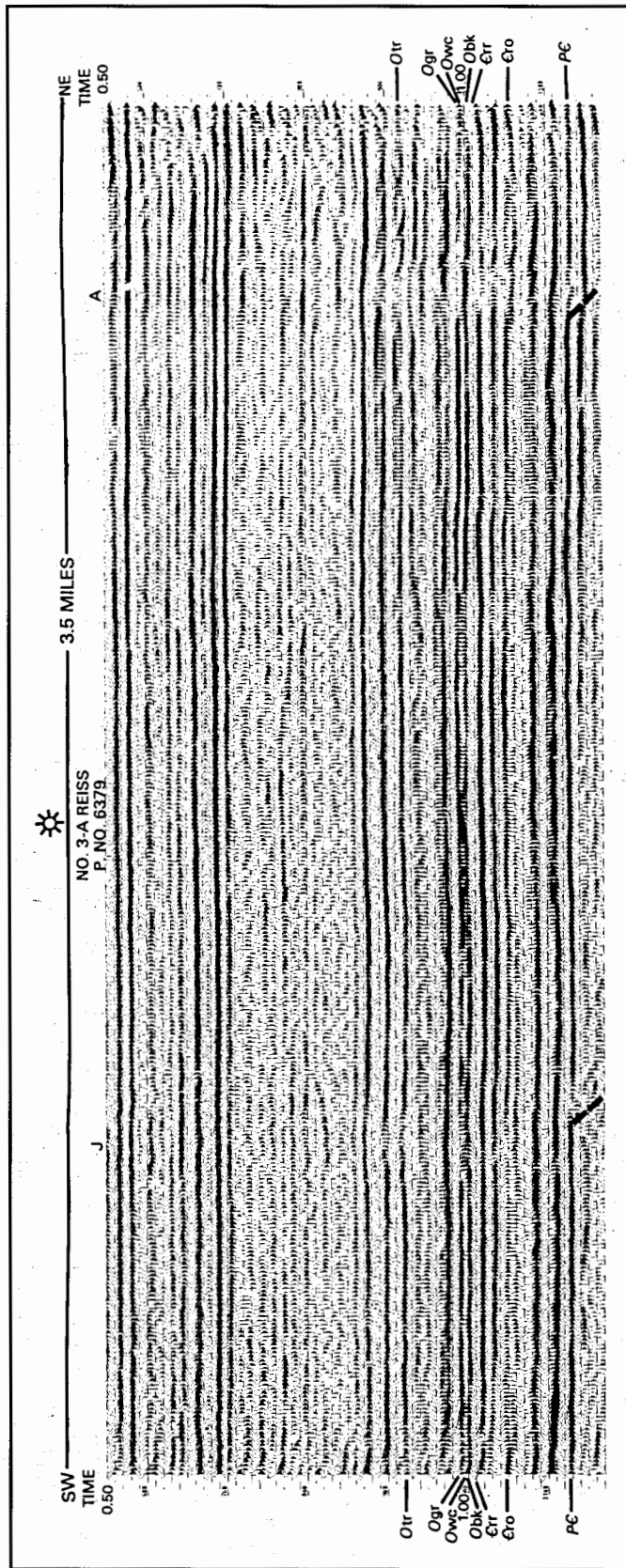


Figure 97. Seismic section display, Coshocton County, Ohio: 1992 processing 1.1 seconds travel time, vibrators, 30-fold, final migration, 45° phase rotation, normal polarity. See Figure 24 for legend.

general sense. A Beekmantown/Mines thickness greater than 65 feet will occur as a seismic peak doublet. For thicknesses less than 35 feet, a single peak is present at the level of the Wells Creek/Shadow Lake interval. A knowledge of the local stratigraphy is imperative to make these interpretations because similar wavelet packages can be created by other scenarios. Modeling also indicated that vuggy porosity in the Beekmantown/Mines can be predicted. Models 8 and 9 (Figure 96) were the only scenarios that incorporated 5 feet of 15 per-cent vuggy porosity in the Beekmantown/Mines. The presence of this zone caused a dramatic increase in the Beekmantown doublet amplitude.

As a result of the VSP survey, the seismic line was reprocessed (Figure 97). The data were corrected for refraction statics and spectrally enhanced between 30 and 120 Hertz. The results of the VSP corridor stack were tied to the seismic line (Figure 97). The well is actually 500 feet southeast of that shotpoint on the line. The "Gull River"/Loysburg-through-Beekmantown/Mines signal (Ogr-Obk) from the VSP correlates well with normal polarity, migrated, enhanced data. This signal is a doublet peak separated by a trough about half the wavelength of the peaks. The doublet might result from either a thick Wells Creek/Shadow Lake section in the area or vuggy porosity in the Beekmantown/Mines. The #2 Huff well (permit number 5890) lies approximately 0.25 miles northwest of the line and produced oil and gas from the Beekmantown/Mines. Signals generated by the Wells Creek/Shadow Lake interval and by vuggy porosity in the Beekmantown/Mines are not dissimilar (Puckett, 1992). In general, caution should be employed in extrapolating results from wells greater than 500 feet from seismic lines. In addition, the direction of the seismic line parallels regional strike; as such, it may not accurately reflect true structure.

The seismic line was sent out for additional reprocessing and attribute analyses (Figures 98 and 99). Reprocessing included migration, spectral whitening, and 45 degree phase rotation of the data to match the synthetic generated by the VSP survey of the #3-A Reiss well (Figures 98 and 99). Examination of the reprocessed line indicates the Ogr-Obk signal appears as a doublet across most of the seismic section. At six locations, however,

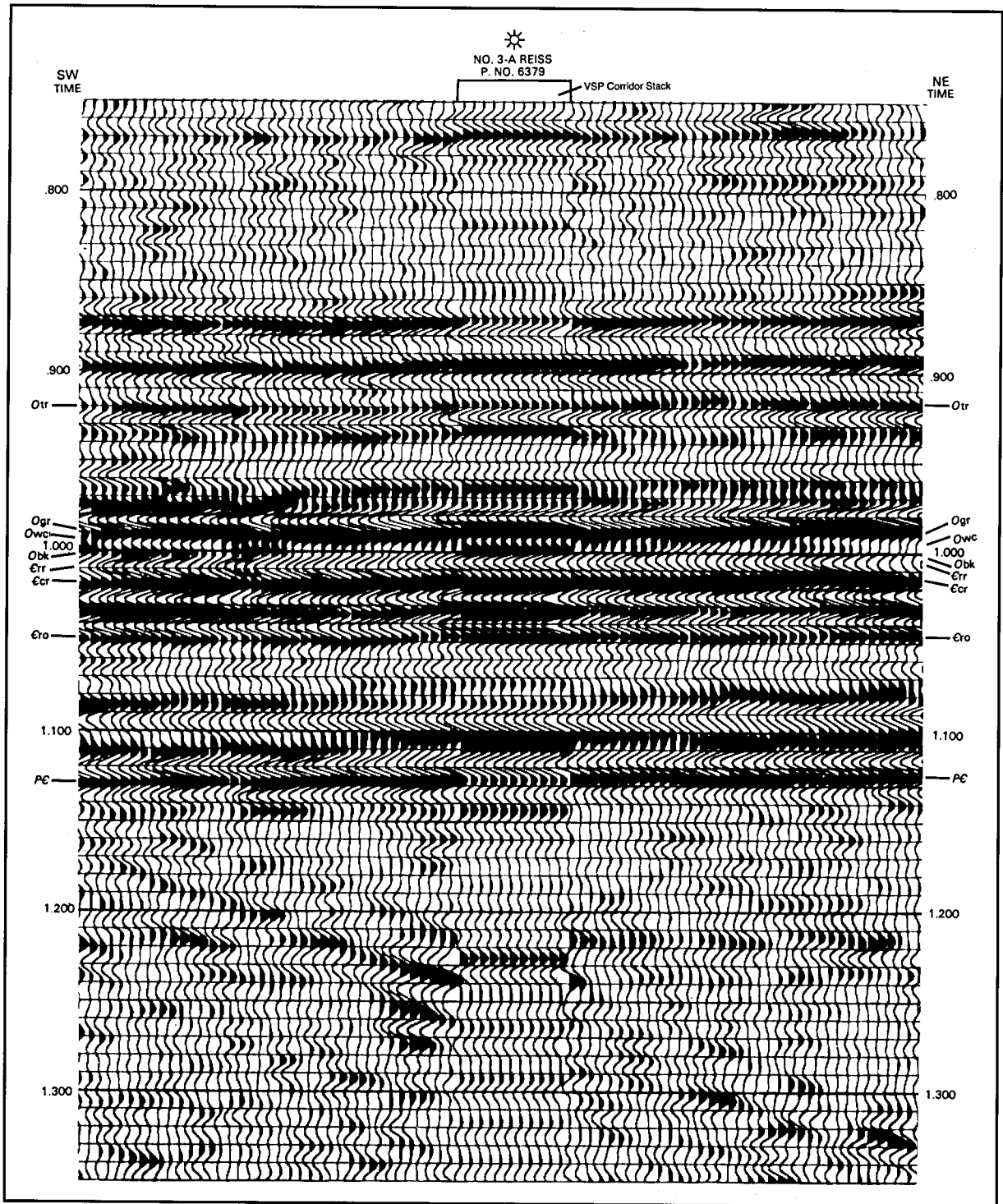
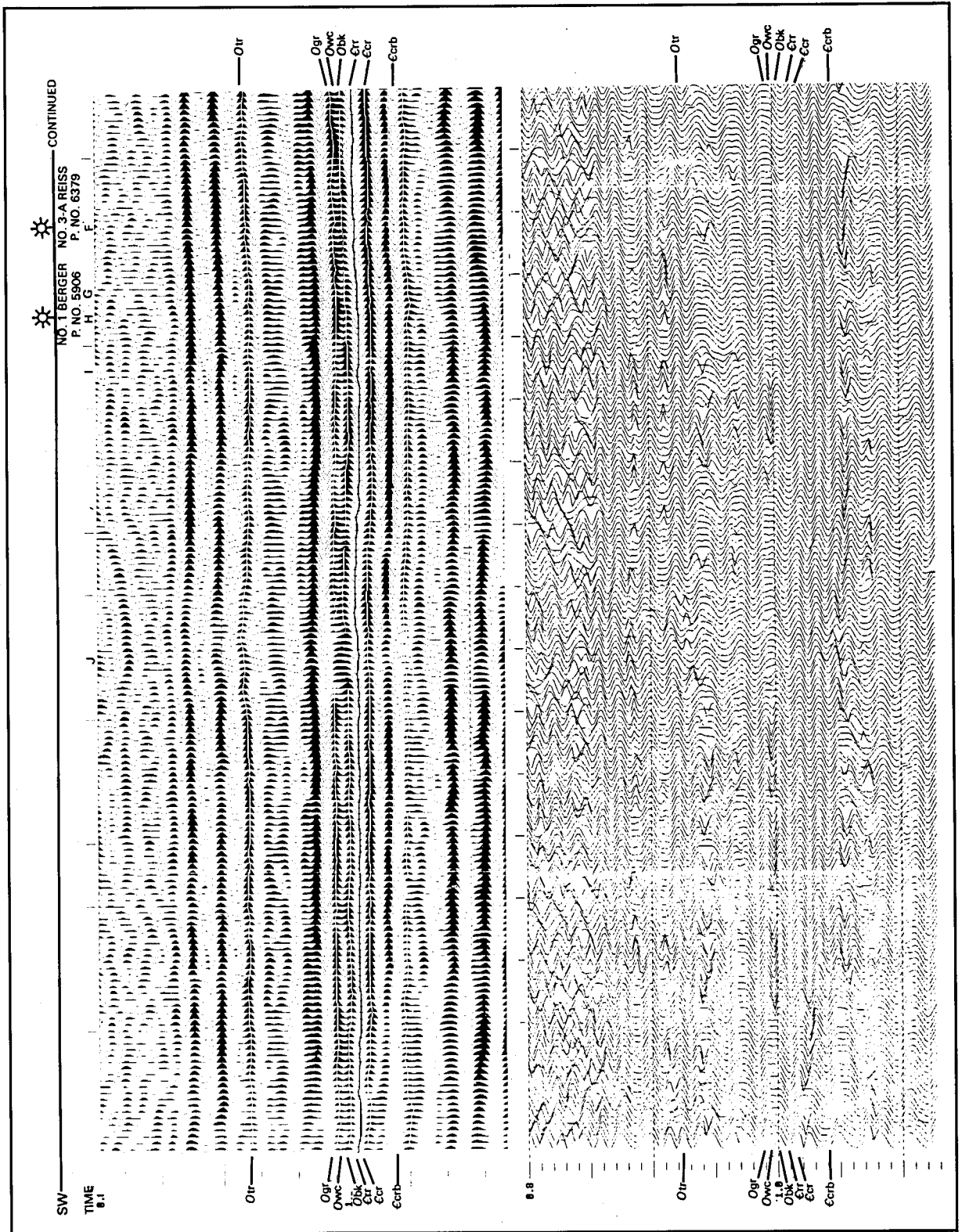


Figure 98. Seismic section display, Coshocton County, Ohio: 1992 reprocessing, 0.8 to 1.3 seconds travel time, vibrators, 30-fold, final migration, normal polarity, with corridor stack seismogram inserted from the #3-A Reiss well. See Figure 24 for legend.

the Ogr-Obk signal changes, becoming either “dimmed out” or a single flat-topped peak with lower frequency. Three producing oil and gas wells situated adjacent to the seismic line are very close to the surface shot-point locations of the seismic section anomalies represented in the Ogr-Obk signal.

At location A near the northeast end of the line, a shouldered peak that gives the appearance of a “dim-out” of the Ogr peak replaces the Beekmantown/Mines doublet. The #1 Huff well, located approximately 600 feet south-east of the line near location A, had a show of gas in the Knox but was plugged back to the Clinton/Medina.



The #2 Huff well (permit number 5890), located approximately 1,500 feet southeast of location A, produces from a Beekmantown/Mines paleoremnant. A “dim-out” of the Beekmantown/Mines peak occurs at location C, but the Ogr-Obk signal remains essentially intact. The #1 Pilabaum well (permit number 5809), located very near the east side of the line at this location, produces gas from vuggy Beekmantown/Mines. At location D, the Ogr-Obk doublet changes to a single flat-topped peak of lower frequency. The #1 Robinson well (permit number 5849), located slightly east of this location, produces oil and gas from a Beekmantown/Mines paleoremnant. At location E, the Ogr-Obk reflector series appears to be high with some “dim-out” of the Beekmantown/Mines signal. The #1 Singleton well (permit number 5796), located approximately 900 feet west of this location, was completed in the Beekmantown/Mines as a gas well. The #3-A Reiss well, which is located approximately 400 feet southeast of the line at location F, had a show of gas in the Knox/Gatesburg interval. No anomalous reflector signals occur at this location. The Beekmantown/Mines might be slightly high structurally at location F, but the well is offset from the line far enough to make extrapolation to the well difficult. At locations G to I the Ogr-Obk signal progresses from a doublet having a lower amplitude upper peak to the Ogr-Obk doublet characteristic of Beekmantown/Mines having a porous upper zone and no overlying Wells Creek/Shadow Lake section. The #1 Berger well (permit number 5906), located approximately 200 feet west of location H, produces gas from the Clinton/Medina. At location J the Ogr-Obk signal is a flat-topped peak that appears to be constructive interference between high, thick Beekmantown/Mines and overlying “Gull River”/Loysburg. This type of seismic reflection signal is known to be associated with Beekmantown/Mines production; however, there are no wells adjacent to this feature on this particular line.

Roth (1992) performed 1-D and 2-D modeling for Beekmantown/Mines paleoremnants (Figures 100A to D). The 1-D model does not explicitly describe porous zones in the top of the Beekmantown/Mines, but does account for a missing Wells Creek/Shadow Lake section. For at least two different model thicknesses of Beekmantown/Mines, the doublet signature is best imaged only when high frequencies are preserved in the synthetic seismogram. Two dimensional modeling of a Beekmantown/Mines remnant (Figures 100A to D) yields a seismic signature very similar to that seen at the northeast end of the reprocessed seismic line at location A and at the southwest end of the line at location J. An anomaly

appears only where high frequencies are preserved at the processing stage (Figure 100D).

Attribute analyses of the seismic line were performed to determine whether or not these processing schemes would be diagnostic of reservoir heterogeneity, and/or to detect the presence of hydrocarbons (Figures 101 and 102). An automatic event picking program was used to follow horizons of interest. At several locations, especially at the northeast end of the line at locations A to B, the program could not follow the “Gull River”/Loysburg wavelet over a deeper anomaly. The color attribute processing of the phase demonstrates that there are phase anomalies associated with nearly all of the wavelet anomalies (Figure 102). Neither phase anomaly nor apparent wavelet anomaly occurs at the location of the #3-A Reiss well (location F). Near the northeast end of the line, at location A, the “Gull River”/Loysburg horizon appears to “dim-out”. Automatic event picking on the plot of the phase cannot follow phase characteristics above the Beekmantown/Mines time horizon through this anomaly. There are smaller, but similar phase anomalies associated with each of the described well locations and at location J. Frequency attribute processing demonstrates low frequency anomalies (Figure 102) at the above described phase anomalies. The amplitude attribute processing shows a dramatic low-amplitude anomaly on the northeast end of the line through all horizons of interest (Figure 102). Additionally, there are amplitude anomalies associated with nearly all of the wavelet, phase, and frequency anomalies (Figure 102).

The results of the investigation of Knox reservoir heterogeneity in Coshocton County, Ohio, illustrate the importance of attribute analyses and VSP data. Similar to seismic anomalies observed in Holmes County, attribute analyses are excellent diagnostic tools in addition to conventional processing techniques in the detection and prediction of hydrocarbons trapped in remnants, faults, and stratigraphic changes in the Copper Ridge/Ore Hill. Instantaneous phase and frequency and amplitude processing revealed anomalies at wells located on the seismic line (Figures 101 and 102). These changes have been interpreted to be the result of the presence of oil and gas. However, changes in frequency and amplitude causing these unique seismic signatures may have been compromised by the possible occurrence of the Copper Ridge/Ore Hill sandstone below the location of the producing wells. The significant velocity contrast between sandstone and dolomite within the Copper Ridge/Ore Hill may have caused the anomalies. The anomalies observed

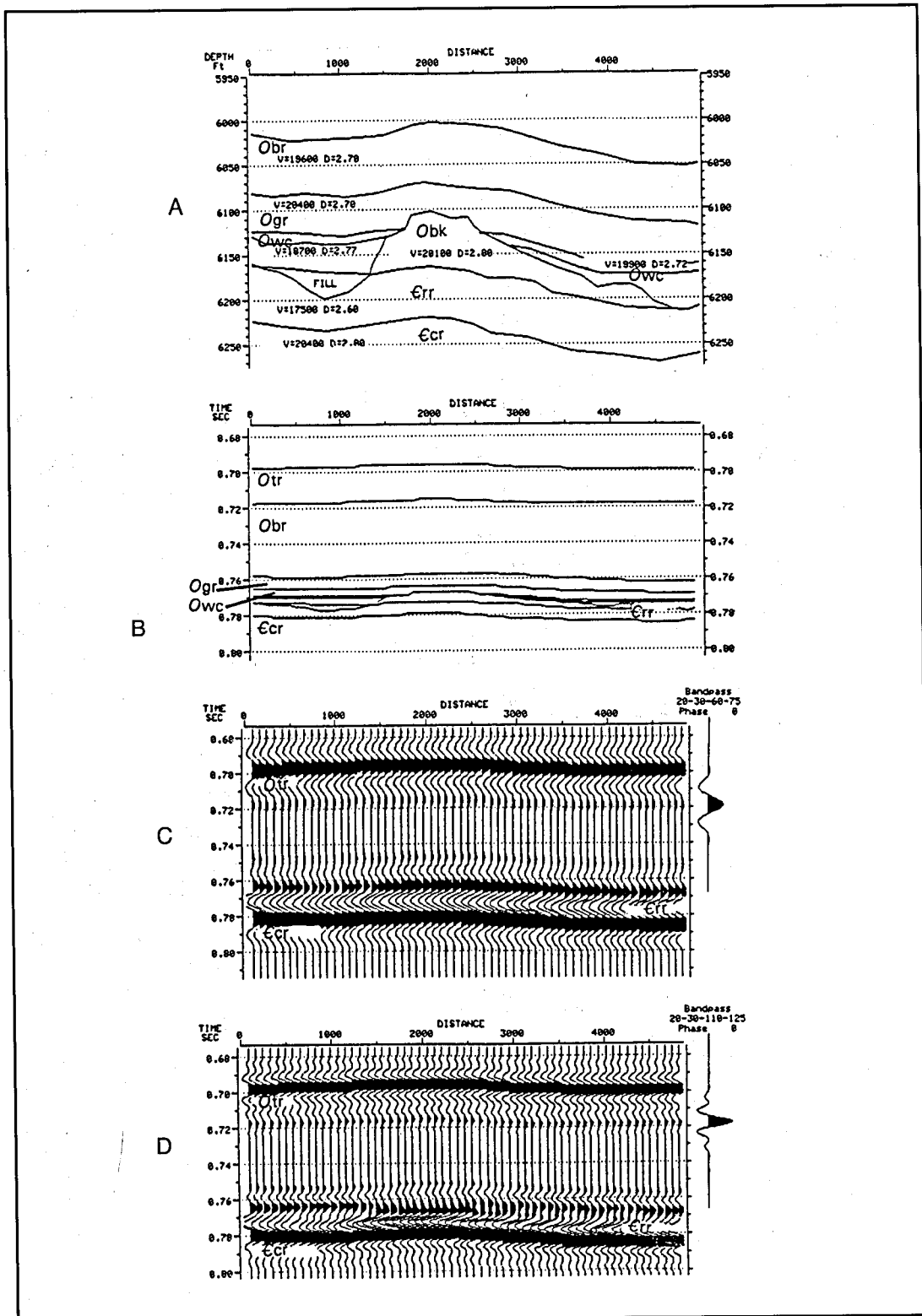


Figure 100. A—Geologic model of a Beekmantown/Mines remnant adjacent to a channel-fill sandstone in the Rose Run. B—Time section of the Beekmantown/Mines remnant model adjacent to the channel-fill sandstone in the Rose Run. C—Low-frequency 2-D model of the Beekmantown/Mines remnant adjacent to the channel-fill sandstone in the Rose Run. D—High-frequency 2-D model of the Beekmantown/Mines remnant adjacent to the channel-fill sandstone in the Rose Run. All figures from Roth (1992).

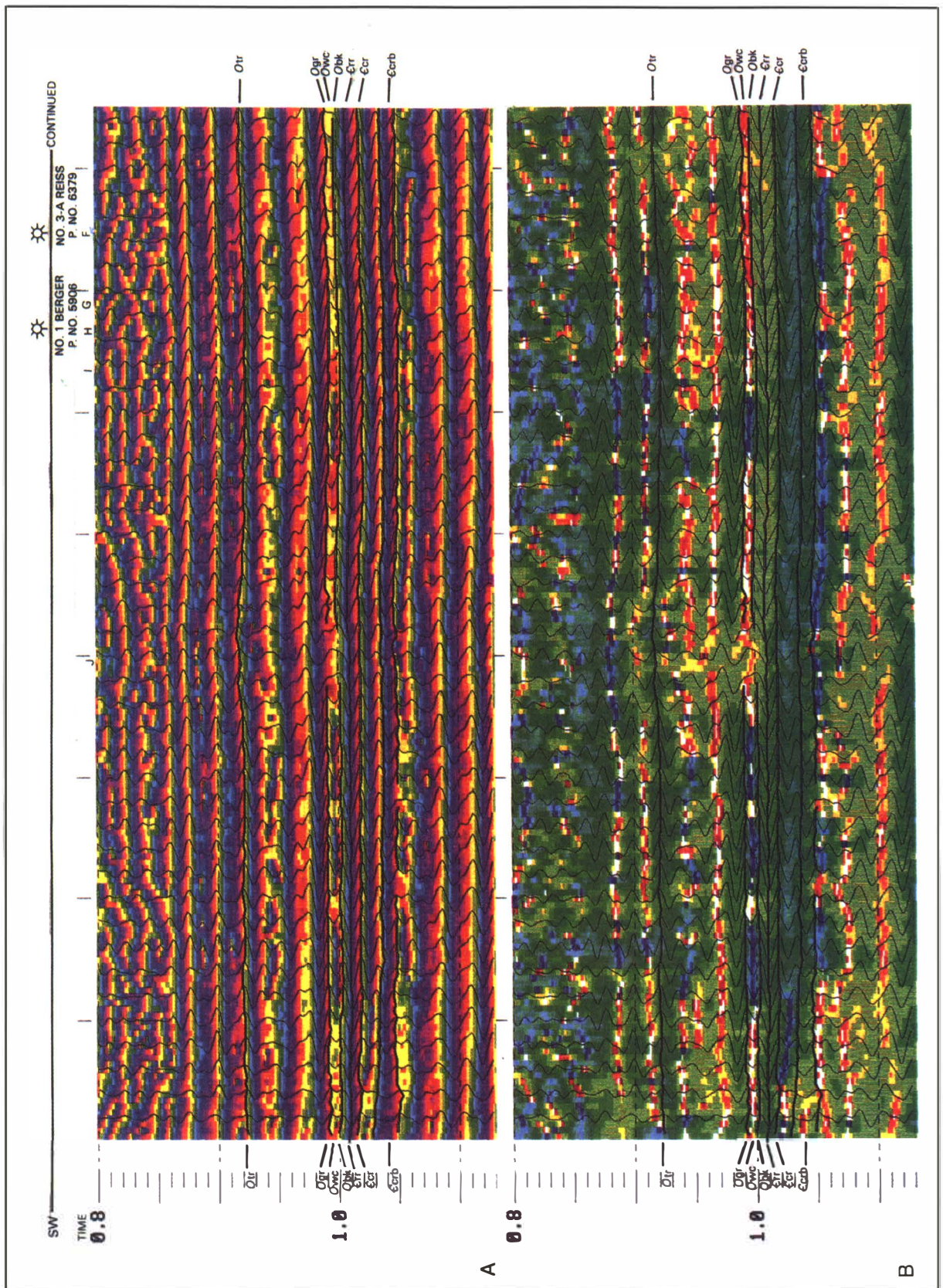


Figure 101. Interpreted seismic section attribute displays, Coshocton County, Ohio: 1992 reprocessing, vibrators, 0.8 to 1.1 seconds travel time, 30-fold, migration 45° phase rotation. A—instantaneous phase, B—instantaneous frequency. See Figure 24 for legend.

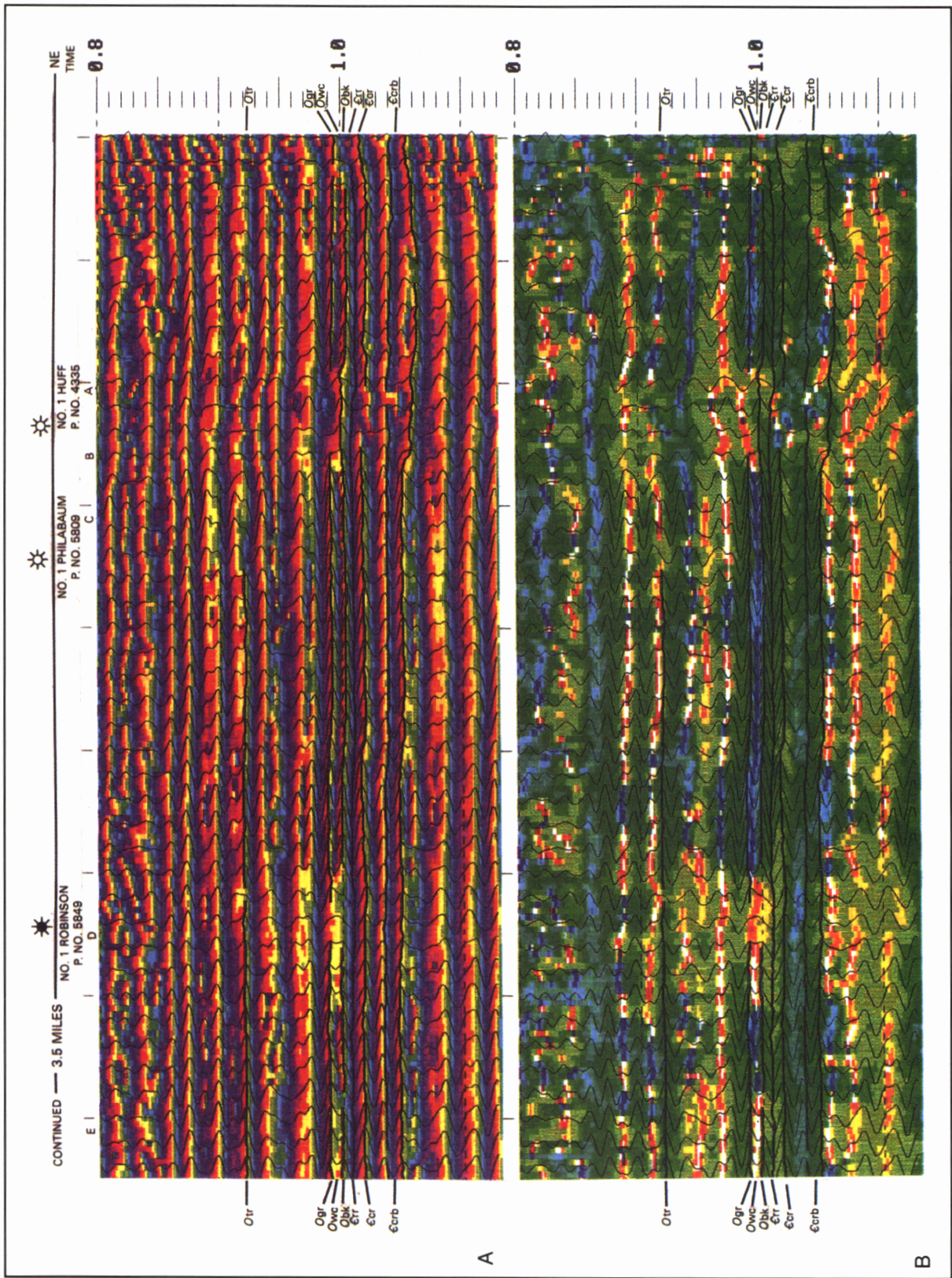


Figure 101 continued.

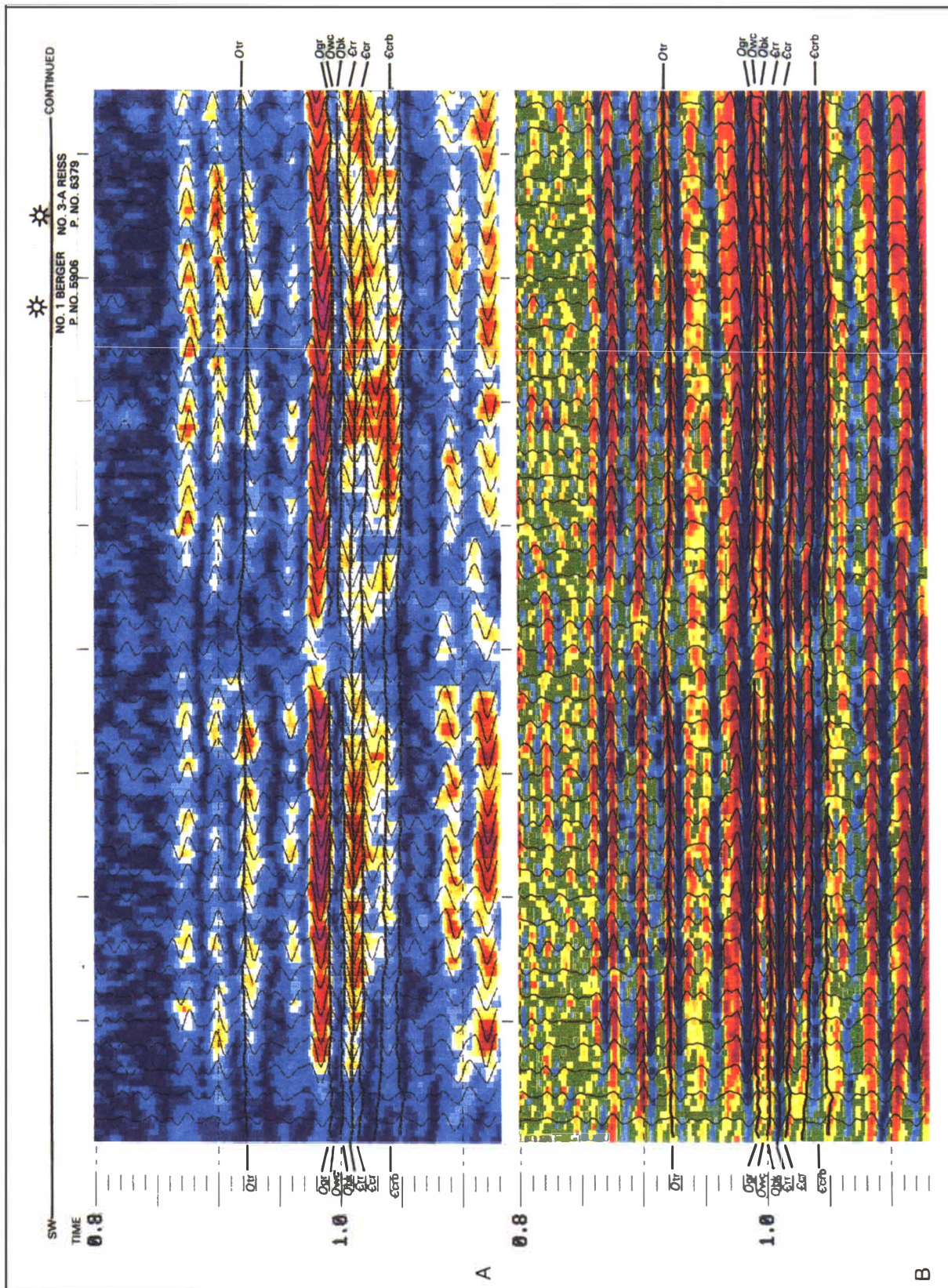


Figure 102. Interpreted seismic section attribute displays, Coshocton County, Ohio: 1992 reprocessing, vibrators, 0.8 to 1.1 seconds travel time, 30-fold, migration 45° phase rotation. A—amplitude envelope, B—trace amplitude. See Figure 24 for legend.

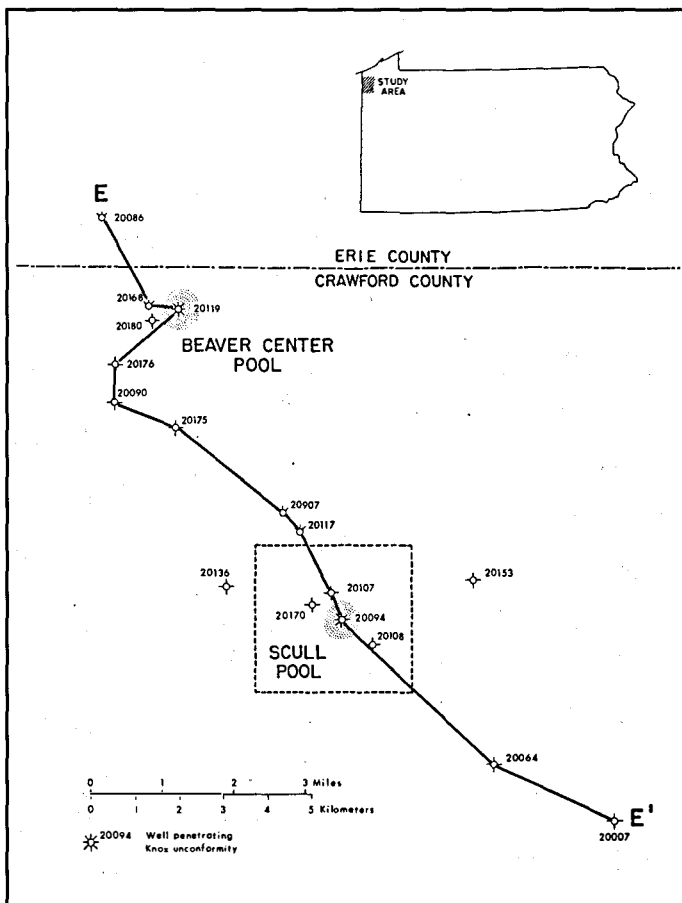


Figure 103. Map showing the location of Rose Run producing area in western Crawford and Erie counties, Pennsylvania.

in the Copper Ridge/Ore Hill also may be the result of constructive interference due to the presence of hydrocarbons in the Rose Run. Although there appears to be no conclusive evidence for faulting and fracturing on the seismic reflection data, the amplitude, frequency, and phase anomalies illustrated in this seismic record section may be attributed to the presence of hydrocarbons in fractured formations, possibly from the Clinton/Medina through the Beekmantown/Mines.

Northwestern Crawford County, Pennsylvania

Western Crawford County has been the primary site of Rose Run exploration in Pennsylvania (Figure 103). However, because of the discouraging early drilling history of the area, the difficulty in establishing potential drilling locations, and the more readily productive target of the Lower Silurian Medina/Clinton at shallower depths, only one well has been drilled in the area since the initial phase from 1963 to 1965. Only two wells, the Transamerican Petroleum #1 Scull (permit number 20094) and the Transamerican Petroleum #1 Voorhees (permit number 20119) (Figure 103), have ever produced from the Rose

Run. Both wells had significant natural gas and gas condensate production before water invasion of the reservoir caused them to be plugged and abandoned.

All seismic data from this portion of Pennsylvania are proprietary, and only one map interpreted from seismic data has been made available. Therefore, the following discussion centers around standard mapping techniques.

Geophysical logs available include gamma ray, neutron, density, and laterolog in most wells. An examination of these logs from the wells in the area indicates that the subtle stratigraphic changes found in producing fields in Ohio may not be the most important types of reservoir heterogeneity in the Rose Run sandstone in this area. Log-derived porosity values in the producing zones are fairly consistent between the Scull and Voorhees wells at 10.8 and 9.5 percent, respectively. Water saturations were calculated at 24.6 percent for the Scull well and 27.9 percent for the Voorhees well. Although productive zones might be slightly compartmentalized by local lateral changes in porosity, the primary control of reservoir heterogeneity appears to result from a combination of the juxtaposition of reservoir sandstones to the unconformity and small offsets in the strata due to tilting and faulting. However, with so few data available, this may be a premature conclusion.

Geologic and seismic mapping of this area indicates a faulted zone trending north northwest-south southeast through the study area (Figure 104) that offsets strata at least between the Copper Ridge/Ore Hill and Trenton Limestone intervals. The lateral extent of this zone and the number of faults that might be involved have not been fully determined. Without seismic survey data the question of whether this zone is related to basement tectonics or the result of deformation during plate-margin convergence in the Early Ordovician cannot be answered satisfactorily. The structure map on the Knox unconformity (Figure 104) shows dip of the erosional surface southeastward, offset by at least two faults that form a horst. The #1 Scull well is situated on the eastern edge of the horst block, whereas the #1 Voorhees is situated on the downthrown side of the easternmost fault. The isopach map of the Wells Creek/Shadow Lake interval (Figure 105) indicates that paleo-remnants occur in the same trend as the fault zone. Curves and recesses in the Wells Creek/Shadow Lake contours

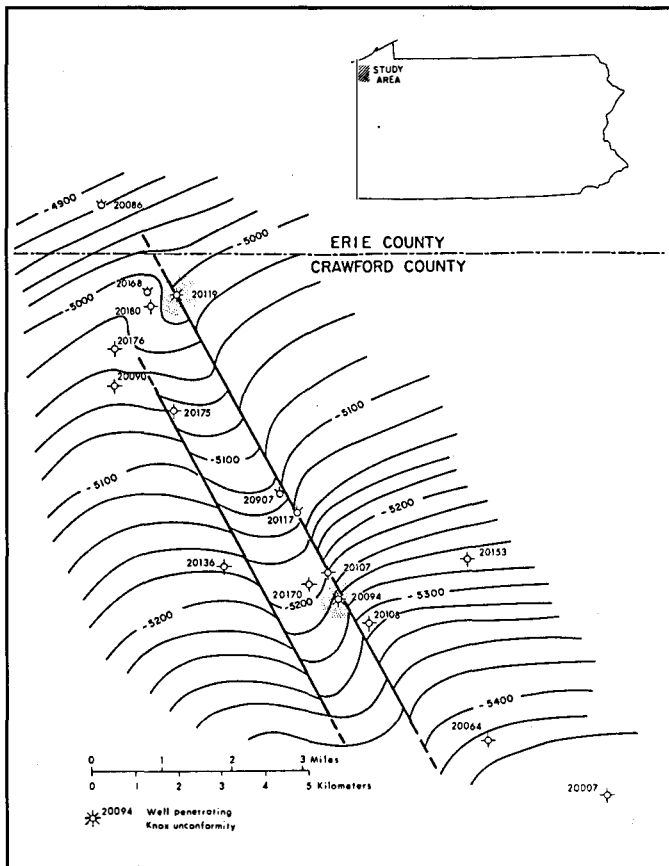


Figure 104. Structure contour map on top of the Knox unconformity in western Crawford and Erie counties, Pennsylvania.

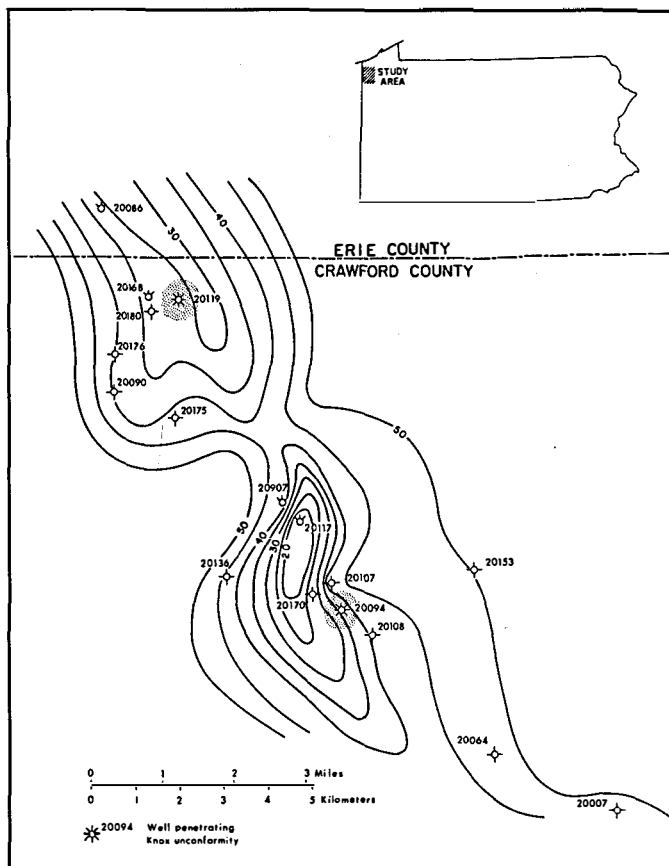


Figure 105. Isopach map of the Middle Ordovician Wells Creek/Shadow Lake interval in western Crawford and Erie counties, Pennsylvania.

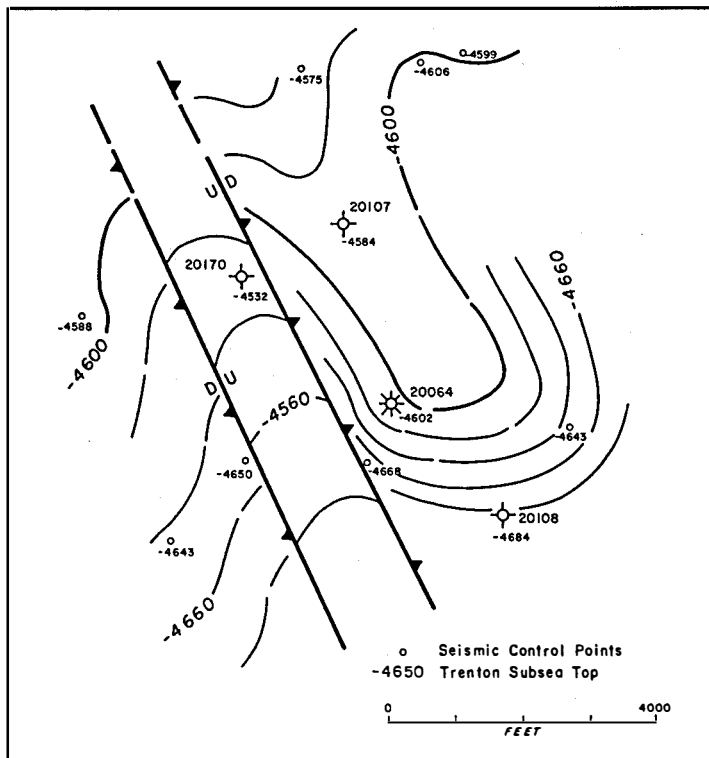


Figure 106. Structure contour map on top of the Upper Ordovician Trenton Limestone, generated from seismic data, in the vicinity of the #1 Scull well, western Crawford County, Pennsylvania. Modified from Harper and others (in press). See Figure 104 for location.

might even be representative of paleoremnants offset across at least one fault. The structure map on the Trenton Limestone in the vicinity of the #1 Scull well (Figure 106) was generated in the 1960's from seismic data collected at that time. It shows the #1 Scull well situated on the flank of a southward plunging anticline, and to the east of the horst block. The anticline is not evident in maps generated from well data, but that probably is due to a lack of well control. The horst block is considerably narrower in the Trenton than it is at the level of the Knox unconformity (Figure 104), suggesting that the fault planes dip at very high angles.

Based on well control, this area had an interesting history during the Late Cambrian through Middle Ordovician. Following deposition of the Rose Run and Beekmantown/Mines, the Lower Ordovician Beekmantown carbonates were deposited. Tectonic deformation of the shallow continental shelf during plate-margin convergence resulted in tilting and fracturing of the section. Subsequent erosion during development of the Knox unconformity beveled an irregular surface, complete with low relief monadnocks, down to the Rose Run and Beekmantown/Mines level in this area (Figure 107). The Ordovician Beekmantown carbonates were removed completely; they do not appear

for 50 miles to the southeast of the #1 Scull well. Given a total thickness of 285 feet for the Beekmantown/Mines interval in the Manufacturers Light and Heat #1 Hock-enberry well in Butler County, Pennsylvania, tilting of the rocks beneath the Knox unconformity was 5.7 feet/mile to the southeast. During the Middle Ordovician, sea level rose, and/or the Laurentian continental margin subsided, allowing deposition of transgressive shelf sandstones, shales, and carbonates on the erosion surface. Examination of Figure 105 reveals the presence of the aforementioned monadnocks (paleoremnants in the form of areas beneath thin Wells Creek/Shadow Lake). Distortions in formation boundaries and correlatable key beds in Figure 107 also indicates that these paleoremnants affected later deposition, particularly in the "Gull River"/Loysburg interval. At some later time (during Alleghanian deformation/) the faults that developed probably during Early Ordovician plate-margin convergence were reactivated and affected higher formations (Figure 106).

These faults might reach the current surface in northwestern Pennsylvania in the form of fracture traces, as suggested by patterns of stream channels and buried glacial valleys (Harper, 1992).

Reservoir heterogeneity cannot be predicted with a high degree of reliability in this area at this time because of the lack of well control, the lack of modern geophysical logs, and the lack of non-proprietary seismic data. Further drilling should help to substantiate or modify many of the concepts presented here. In addition, the acquisition of modern seismic data, processed with the methods currently available, will give operators a much clearer picture of the geology of northwestern Pennsylvania.

Microscopic (Thin Section-Scale) Heterogeneity

Introduction

On a microscopic scale, heterogeneity in the Cambrian rocks of Ohio and Pennsylvania is reflected primarily by diagenetic changes and by variability in microstructures and textural features. Combined with paleotopographic, stratigraphic, and structural factors, microstructures (sedimentary structures at the scale of thin-sections),

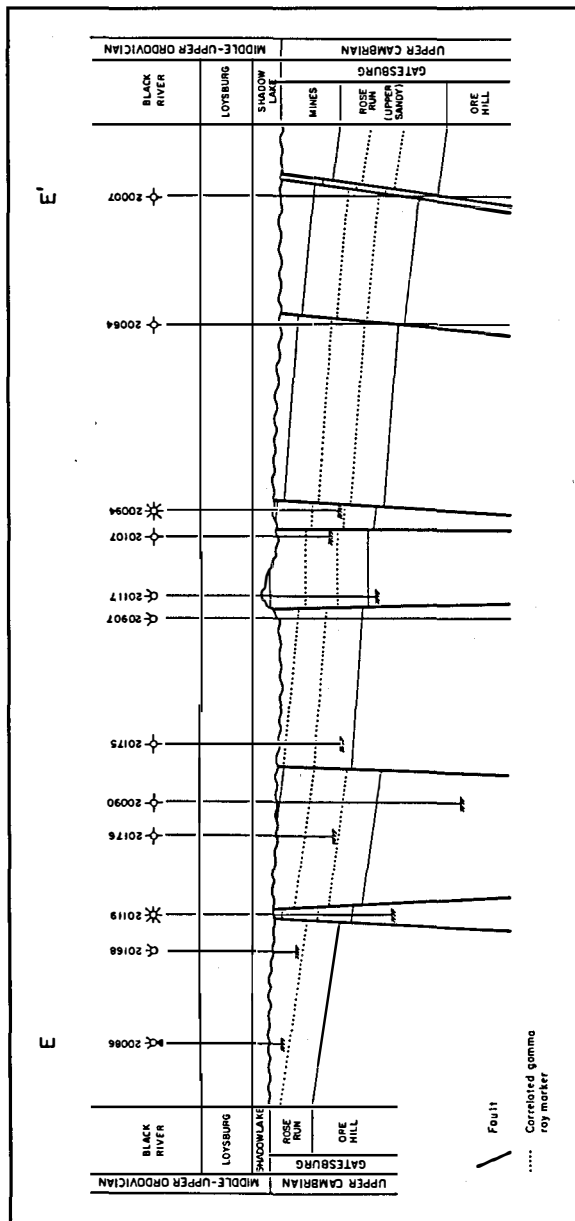


Figure 107. Paleostructural cross section E-E' in western Crawford and Erie counties, Pennsylvania. Datum is the top of the Middle Ordovician Wells Creek/Shadow Lake interval.

diagenetic modifications, and textural variability directly affect the oil and gas producing potential of the Rose Run sandstone and the Beekmantown/Mines dolomite. The ability to understand, measure, and predict these factors should help the explorationist to decipher the hydrocarbon potential of the Rose Run sandstone and associated strata.

Petrographic data from previous studies were available on Rose Run cores from several counties in Ohio. Enterline (1991) provided data on two cores from Ashtabula County wells (permit numbers 2038 and 2071). Heald and Baker (1977) and Baker (1974) reported on the petrography of

Rose Run sandstone in the U.S. Steel well in Scioto County, Ohio (permit number 212, core 2958). Petrographic data were modified from Baker's unpublished master's thesis (1974) and used in this report.

Ohio Geological Survey personnel examined seven partial cores of the Rose Run interval. Four of these cores are from wells in Coshocton County. Core 2963 is from Tuscarawas County and core 2898 is from Jackson County. The seventh core examined, core 2598, is the same that Baker (1974) and Heald and Baker (1977) examined from the U.S. Steel well. Supplementary data were obtained from reports by NuCorp Energy Company (1977), and Reservoirs, Inc. (1992), for the Jackson County core and the #3-A Reiss well core, respectively.

Personnel from the Pennsylvania Geological Survey examined three cores from the Hammermill Paper Co. #2 Fee well in Erie County, Pennsylvania. These cores contain both sandstones and dolostones. A fourth core, from the Shell Oil Co. #1 Shade Mountain Unit well in Juniata County, central Pennsylvania, contains carbonates and evaporites. In addition, samples from outcrops in central Pennsylvania provided the opportunity to compare petrographic characteristics of rocks from outcrops with subsurface equivalents throughout the region.

The primary purpose of this portion of the study is to obtain a better understanding of the microscopic heterogeneity of the Rose Run sandstone and adjacent reservoir rocks by investigating their textural, mineralogical, and diagenetic history. However, the ultimate goal is to be able to measure and predict Rose Run heterogeneity using a combination of modern petrographic, geophysical and mapping techniques.

Petrography, Petrology, and Petrophysics

The sandstone rock nomenclature used here follows the classification recommended by Pettijohn and others (1973). Sandstone porosity classification is based on the criteria and terminology discussed by Schmidt and McDonald (1979). A dolomite textural classification using the terminology of Sibley and Gregg (1987) was used to define eight dolomite types, based on dolomite morphology, size, and occurrence.

Beekmantown/Mines and Copper Ridge/Ore Hill Dolostones

The Beekmantown/Mines dolomite, which overlies the Rose Run sandstone in eastern Ohio and throughout

western and central Pennsylvania, has been described from well cuttings by Wagner (1966) and Janssens (1973). In Ohio, the Beekmantown/Mines generally is a microcrystalline to medium-crystalline dolostone, in part peloidal and oolitic. Locally the rock is glauconitic and silty. Two thin sections of Beekmantown/Mines interval from within 15 feet of the Knox unconformity were examined in sidewall cores from the #3-A Reiss well in Coshocton County, Ohio. These rocks are relatively pure dolostones with a mottled appearance and one to two percent intercrystalline porosity. The original depositional texture has been completely obliterated and many of the rhombs show dissolution along their edges (Reservoirs, Inc., 1992). A small amount of authigenic clay occurs in the carbonates, either lining or filling pore spaces, and SEM analysis of the sample from 6,715 feet indicates the clay is mixed-layer illite-smectite (Reservoirs, Inc., 1992). However this clay identification has not been confirmed by X-ray analysis for this sample.

The dolostones contain types 6 and 8 dolomite (Appendix VIII). Two Beekmantown/Mines dolostone samples from Coshocton County, Ohio had 1.5 percent average porosity, and 14 Copper Ridge/Ore Hill dolostone samples from Ashtabula and Tuscarawas counties, Ohio had 2.6 percent porosity. Fourteen Copper Ridge/Ore Hill sandstones from Tuscarawas and Ashtabula counties, Ohio have slightly higher porosities averaging about 4.3 percent. The lack of interconnection between the intercrystalline and vuggy pores, and the presence of pore-lining clays, accounts for the low permeability of these carbonates (Reservoirs, Inc., 1992). Oil and gas production from vuggy porosity in the Beekmantown/Mines occurs near the subcrop edge in Coshocton and Tuscarawas counties, Ohio.

The clay minerals of a Beekmantown/Mines shale bed in one core were identified by X-ray diffraction. This sample contained poorly crystallized illite as the dominant clay, with a trace of mixed-layer clay. Shales from the Copper Ridge/Ore Hill dolomites also contain poorly crystallized illite as the dominant clay. Shale samples contained minor amounts of detrital chlorite, in addition to the illite.

The Beekmantown/Mines dolomite overlies the Rose Run sandstone throughout most of western Pennsylvania, except for some areas in Erie and Crawford counties where it has been removed by erosion at the Knox unconformity. The basal Beekmantown/Mines and the unconformity itself were cut and recovered in core 1 from the #2 Hammermill well in Erie County (Figure 39).

The Beekmantown/Mines in the #2 Hammermill well core is mottled, light- to medium-gray and light olive-gray

dolostone. The depositional texture of these rocks is obscure except for minor bioturbation. The rock consists of decimicron- to centimicron-sized polymodal planar-s dolomite with nonmimically replaced ooids and peloids. Previously developed vuggy pores are now filled with polymodal planar-s to planar-e dolomite. The intercrystalline pores of this latter fabric are further filled with bladed to equant megaquartz (drusy quartz) and very fine- to medium-sized, irregularly shaped crystals of a mineral that has the characteristics of gypsum (see Fleischer and others, 1984). The texture of the gypsum crystals resembles that of the gypsum replacing anhydrite (due to uplift) in Permian evaporites from England (Adams and others, 1984). No anhydrite inclusions were found in the thin sections, however, so that such comparisons are very speculative. Porosity is low in the Beekmantown/Mines dolomite core samples from western Pennsylvania, on the order of three percent or less. The pores are mostly intercrystalline to slightly and irregularly vuggy.

Rose Run Sandstone

Composition and Texture—The mineralogical composition of detrital grains in sandstone has a direct bearing on reservoir quality. The rate of porosity loss with increasing burial depth, due to compaction, recrystallization, cementation, and replacement processes, is related in large part to the original sand composition (Hayes, 1979). Because quartz is chemically and mechanically stable, porosity is often preserved in quartzose rocks. Feldspars are mechanically stable and chemically unstable; feldspar alterations may reduce porosity whereas feldspar dissolution might enhance it. Lithic fragments are mechanically and chemically unstable and, thus, very prone to porosity-reducing and porosity-enhancing processes. Lithic sandstones are especially susceptible to mechanical compaction. Dickinson and Suczek (1979) demonstrated the close relationship of sandstone composition, plate tectonics, and ultimate reservoir quality.

The primary rock types found in the Rose Run sandstone are quartz arenites, subarkoses, arkoses, and dolostones (Appendix IX). The sandstones contain subrounded to rounded, very fine- to medium-grained, poorly to moderately sorted constituents. Atha (1981) and Enterline (1991) reported bimodal size distributions in Rose Run sandstones from Ohio. Although no grain measurements were taken, many of the sandstones studied in this report appear to be bimodal as well. In Ashtabula and Scioto counties, Ohio, Enterline (1991) and Baker (1974) found framework grain compositions and textures very similar to those examined in this study (compare Enterline, 1991 and

Baker, 1974 with Appendix X). Baker (1974) reported well sorted sandstone rather than poorly to moderately sorted sandstone in the U.S. Steel well (core 2598) in Scioto County.

Mean grain size and sorting of the Rose Run sandstones in the cores from the #2 Hammermill well in Erie County, Pennsylvania are displayed in Figure 108 and Table 1 (pg.123). Most samples are either fine or medium grained and moderately well or well sorted; three samples are only moderately sorted and one is very well sorted. The sandstones display a range of fabric types. Most grain contacts are concavo-convex to long. Some floating grains occur in the more dolomitic sandstones. Conversely, a few samples exhibit many sutured grain contacts and a high packing density. These fabric variations occur over the space of a meter or less.

Monocrystalline quartz and potassium feldspar are the major sandstone framework constituents in the Rose Run sandstone of Ohio and Pennsylvania. (Appendix X and Table 1, pg. 123). In the #2 Hammermill well cores from Erie County, Pennsylvania, quartz ranges from 87 to 100 percent of the framework grains, with a mean of 94.4 percent (Table 1, pg. 123). In Ohio, quartz grains range from 59 to 99 percent of framework grains, with a mean of 88.3 percent (Appendix X). Feldspar (mostly microcline) ranges in abundance from 0 to 13 percent of the framework grains, with a mean of 5.3 percent, in Pennsylvania whereas in Ohio feldspar ranges from 1 to 35 percent of framework grains, with a mean of 11.6 percent. Untwinned orthoclase and potassium feldspar grains with perthitic intergrowths occur in subordinate amounts. Feldspar amounts determined in many of the samples might be underestimated because of feldspar dissolution and the formation of moldic porosity. There is no statistically significant correlation between observed feldspar percentages and mean grain size (correlation coefficient=0.1). Polycrystalline quartz and chert, generally comprising less than one percent of the sandstone, appear in the more feldspathic samples. Lithic fragments, including chert, shale clasts, and altered igneous lithics range from zero to one percent of the framework grains observed. Small amounts of muscovite and the accessories zircon, tourmaline, garnet, and pyrite occur locally in the cores. Allochems are locally abundant in the sandstone and include dolostone clasts, glauconite, colophonite and peloid and ooid dolomitized ghosts visible when the thin sections are examined under diffused plane-polarized light.

Rose Run sandstones rarely contain detrital quartz and feldspars less than 20 or 30 micrometers in diameter (e.g. matrix). Clay minerals are present in some sandstones but

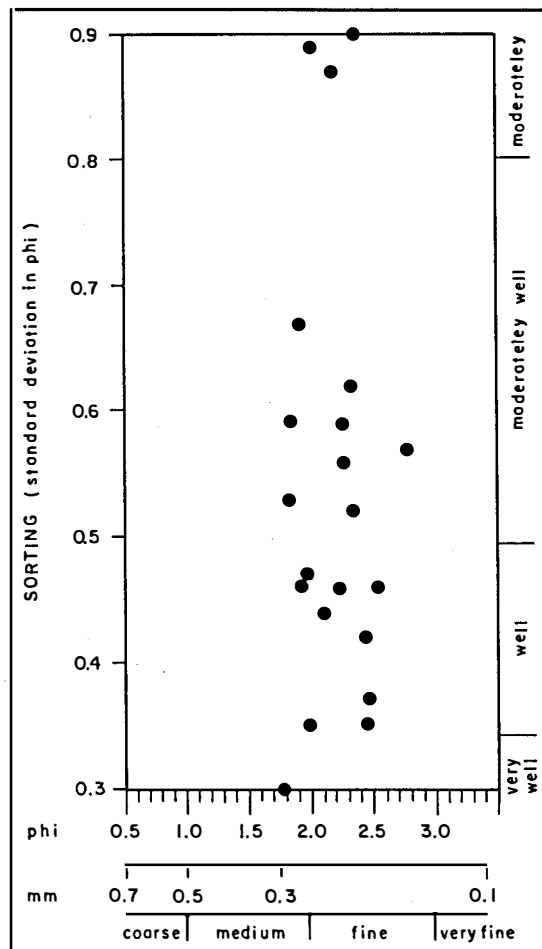


Figure 108. Mean grain size versus sorting in Rose Run sandstones from cores 1 and 2 from the #2 Hammermill well in Erie County, Pennsylvania.

in most cases the origin (detrital versus authigenic) of these clays is difficult to determine, except where clay or shale stringers and laminae exist. Some of the interstitial clays may have originated as infiltration clays, or were deposited along with the coarser detrital particles and have since been regenerated. Sandstones with excessive detrital clays are rare in modern day sediments, and where they are found they should be suspected of being authigenic (Wilson and Pittman, 1977). Therefore, significant amounts of the interstitial clay in the Rose Run sandstone probably represent a neomorphic origin.

Cement—Four major cementing agents found in the Rose Run sandstone include: 1) dolomite, averaging 11 percent; 2) clays, four percent in Ohio and one percent in Pennsylvania; 3) quartz overgrowths, four to five percent; and 4) feldspar overgrowths, one percent. These averages are based on 70 thin section analyses of Rose Run sandstone in cores from wells in Ohio, in Ashtabula County (Enterline, 1991), Coshocton County (this study), Jackson

County (this study), Scioto County (Baker, 1974), and one well in Erie County, Pennsylvania (this study). Table 2, on page 124, lists the average cement percentages by county in Ohio; similar averages occur in Pennsylvania (Table 1, pg. 123).

The dominant cementing agent in the Rose Run sandstone is dolomite. This cement is found throughout the region, but is somewhat less in Jackson and Scioto counties, Ohio than in other areas (Table 2, pg. 124). No calcite was observed in stained thin sections or detected by X-ray diffraction. In 24 samples the mole percent magnesium in dolomite, as determined by X-ray diffraction using the method described by Scholle (1978), varied only slightly, from 49.3 +/-0.5 to 51.0 +/-0.5. This suggests that either pore water composition was similar during the different dolomitization phases or that the last dolomitization event overprinted earlier phases. A third possibility is that X-ray of whole rock samples is not sensitive enough to detect compositional differences in the different dolomites. Dolomite zoning detectable by plane light microscopy is very rare in the samples studied. Also, the lack of any significant shift of the 104 carbonate peak at 2.886 Å indicates that very little cation substitution for magnesium has occurred in these samples.

The sandstones exhibit three principal dolomite cement textures. Most of the dolomite is nonplanar; the cement consists of tightly packed anhedral crystals. The nonplanar textures vary from unimodal to polymodal. Some dolomite cement has a planar-s texture, i.e. it is subhedral. These cements also vary between unimodal and polymodal, although the latter is more common. A few samples have planar-e dolomite cement. We identified eight dolomite types in the Rose Run interval, based on dolomite morphology, size, and occurrence (Sibley and Gregg, 1987) (Appendix VIII). Dolomite types are discussed under the heading Porosity/Microstructure Relationships.

Syntaxial quartz overgrowths and feldspar overgrowths occur in all cores studied (Tables 1 and 2, pgs. 123, 124). Feldspar overgrowths are more abundant than quartz overgrowths only in Scioto County, Ohio (Table 2, pg. 124). Quartz plus feldspar overgrowths average six percent or less of the rock in all regions, but can exceed ten percent in individual beds (Appendix X). Most quartz overgrowths are recognizable because distinctive crystal faces and clay coats or "dust rims" on detrital grains are clearly visible. In some samples with advanced stages of silica cementation, however, the boundaries between quartz grain nuclei and overgrowth cement are vague. Feldspar cements occur in the Rose Run sandstones as euhedral overgrowths on detrital feldspar grains and as pore-filling, euhedral feldspar crystals.

Clay minerals generally make up less than five percent of the total rock (Tables 1 and 2, pg. 123, 124). Clay minerals identified by X-ray diffraction and microscopy include illite, randomly interstratified illite-smectite, chlorite, and glauconite. Even small quantities of clay minerals can have a profound effect on reservoir quality, particularly permeability and water saturation. They are responsible for creating problems during drilling, stimulation, and production of hydrocarbons as a result of their ability to block pores by expansion or migration (Wilson and Pittman, 1977). In the Rose Run sandstone, clays have been partially leached from many of the more porous sandstone zones. In these areas, permeabilities remain high and the clay does not seem to create barriers for lateral fluid flow because of the large interconnecting pores. Migration of these clays might eventually cause problems during production of hydrocarbons.

Two dolostones from within the Rose Run sandstone from Coshocton County, Ohio (cores 2853 and 2989) contained moderate to well crystallized illite and a trace of chlorite. Both dolostones are sandy, and one was apparently glauconitic, based on megascopic inspection of the cores. Microscopic examination of the glauconitic samples reveals a bright green clay, typically associated with 10- to 20-micrometer size pyrite grains. It occurs as irregular, equant grains to elongate grains 90 micrometers to one millimeter long. Shrinkage cracks are common, and some portion of the clay commonly has been replaced by dolomite rhombs. Also, the green clay occurs as pore fillings in intercrystalline and vuggy areas. X-ray diffraction analysis of the less than two-micrometer size fraction of this rock indicates a well crystallized 10 Å mineral (glauconite?) and a trace of chlorite.

The second sandy dolostone contains a moderately to poorly crystallized 10 Å mineral. In thin section this mineral was usually green, but brownish coloration was also common. As in the first dolostone, this mineral occurs in intercrystalline and vuggy pores, as tiny (90-micrometer diameter) grains, and as larger pellets. In both dolostones most pore fillings are partially leached. In some cases extensive dolomite replacement of the glauconite(?) pellet makes it difficult to distinguish pellets from pore fillings, although the localized, spherical nature of the mineral suggests that it is a pellet partially replaced by dolomite in those examples. In both dolomites, the 10 Å d-spacing, the morphology, and the mode of occurrence strongly suggest glauconite, but further analyses would have to be performed in order to confirm this identification (Bentor and Kastner, 1965).

Seven samples of Rose Run sandstone were analyzed for their clay minerals by X-ray diffraction from Coshocton County, Ohio. Clay minerals identified include illite, mixed-layer illite-smectite, and chlorite. Illite and illite-smectite are sometimes difficult to distinguish in thin section. Both appear to occur as pore fillings, matrix (usually in silty, very fine-grained sandstone laminae), in thin, wispy, clay stringers, and as infiltration clay. True grain coatings of illite on detrital quartz as reported by Heald and Baker (1977) were not identified in the Coshocton County core.

Illite and mixed-layer illite-smectite were identified in four samples from the Jackson County, Ohio core. These samples contained significantly more mixed-layer clay than samples from Coshocton County, Ohio. The non-glycolated illite and illite-smectite peaks at about 8.6 degrees two theta were moderately well crystallized in three samples and poorly crystallized in one sample. The clays occur in silty, very fine-grained sandstone laminae where the dominant clay appears to be illite. This clay probably originated as clay stringers and matrix that has been regenerated (Wilson and Pittman, 1977). Pore filling clay also occurs in the sandstone, generally as low birefringent, mixed-layer illite-smectite, probably intimately intergrown with illite. Leaching has destroyed much of the clay and dolomite in many of the Jackson County core samples.

Clay minerals were identified by X-ray diffraction in one Rose Run sandstone sample from Scioto County, Ohio. This sample is very similar to those examined in Jackson County. Four- to five-millimeter thick silty, very fine-grained sandstone laminae contain abundant, moderately to well crystallized illite and illite-smectite. In the non-silty sandstone laminae (generally medium grained), clay occurs as pore fillings and as regenerated matrix or infiltration clays, but is less abundant than in the silty laminae. Heald and Baker (1977) report illite grain coatings in this core, which inhibit quartz overgrowths from forming.

In the Hammermill well in Erie County, Pennsylvania, illite, identified by X-ray diffraction, occurs in the Rose Run as a minor grain coating, and in rare instances, as pore-bridging or pore-filling cement. It formed as a product of feldspar alteration and as a partial coating on detrital quartz grains.

Intergranular Volume-Cement Diagrams—

Houseknecht (1987) introduced a useful diagram (Figure 109) for evaluating the relative importance of

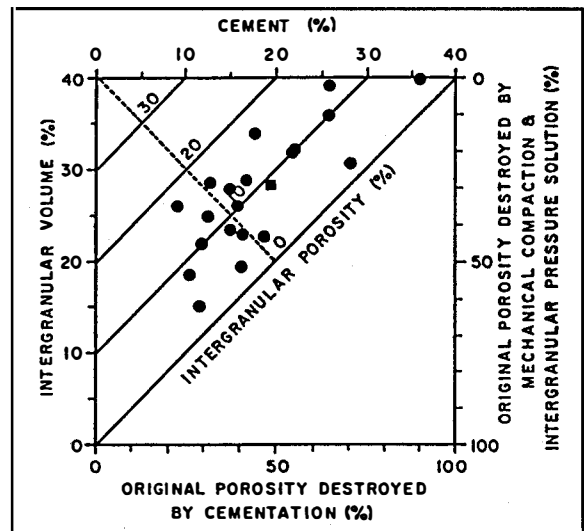


Figure 109. Intergranular volume-cement diagram with all Rose Run samples from the #2 Hammermill well in Erie County, Pennsylvania plotted. Data are listed in Table 1. The square denotes the mean of all data.

compactional and cementational processes to porosity modification in sandstones. The vertical axis in Figure 109 delineates a quantity called intergranular volume. Intergranular volume is, “minus cement porosity,” i.e. the sum of intergranular porosity and the amount of cement present in a sandstone (Houseknecht, 1987, p. 633). The original intergranular volume of well-sorted sands is estimated to be about 40 percent, and this volume is reduced during burial by compactional processes. Mechanical compaction commonly can reduce the intergranular volume to about 30 percent; further reductions occur through pressure solution, chemical compaction, and/or stylolitization.

The horizontal axis of Figure 109 delineates the amount of cement in the sandstone. It can be utilized to determine the percentage of original porosity occluded by cementation. The straight diagonal lines on Figure 109 are plots of equal intergranular porosity. The dashed diagonal line separates samples in which either cementation or compaction has been more important in modifying porosity.

Intergranular volume-cement diagrams are useful for assessing the relative importance of compaction and cementation in controlling the final reservoir quality of a sandstone. The diagrams also can be used to illustrate diagenetic pathways by plotting cement percentages and intergranular volumes for specific diagenetic phases based on cement stratigraphy (Houseknecht, 1987). The diagrams provide a powerful tool for measuring reservoir heterogeneity in the Rose Run sandstones.

Figure 109 shows an intergranular volume-cement diagram with plots of all the Rose Run sandstone samples from cores 1 and 2 from the Hammermill well in Erie County, Pennsylvania. The data used to build the plot are shown in Table 3 on page 124. Solid circles are individual sandstone samples; the solid square is the mean value of all the data. Sixty-two percent of the sandstone samples plot in the upper right portion of the diagram, implying² that a greater percentage of their original porosity has been reduced by cementation than by compaction processes. Thirty-eight percent of the samples plot in the lower left portion of the diagram; mechanical and chemical compaction reduced much of the original porosity in these samples. The mean values for all Rose Run sandstone data on the diagram are 28.3 percent intergranular volume and 19.4 percent cements (which include all cements).

A third (33.3 percent) of the sandstone samples do not contain any, or have just traces of, dolomite cement. The dolomite cements in the sandstones clearly postdate all the other cements; therefore, examination of these dolomite-free samples provides a first approximation of the diagenetic pathway in these rocks (Figure 110). Porosities in the sandstones that lack dolomite cement were reduced by mechanical compaction, illite clay coatings and fillings, quartz and feldspar overgrowths, and pressure solution. In the quartz arenites, this diagenetic pathway went to completion, i.e. porosity was reduced to minimal values (<3 percent). The same processes reduced the pore volumes in the feldspathic sandstones too, but the dissolution of feldspar grains yielded some moldic porosity. These subarkoses have between 8 and 14 percent porosity. One interesting exception to this pattern is the sample from 5,164 feet in core 1 of the Hammermill well in Erie County, Pennsylvania. This is a subarkose with only 3 percent porosity. Most of the porosity in this sample is reduced intergranular, grain-to-grain contacts are numerous, packing density is very high, the cements present are quartz overgrowths and clay, and porosity is low. Most feldspars are intact and well preserved; little moldic porosity developed and that which did develop is largely plugged by clay. The clay that fills moldic pores is a feldspar alteration product. These clays are not compacted, indicating feldspar alteration and dissolution occurred after chemical compaction.

² In Houseknecht's diagram, compactional porosity loss is calculated as the simple difference between an assumed initial porosity and the modern-day porosity of the sample. This method does not take into account the bulk volume reduction that occurs during compaction and can result in underestimating compactional porosity loss (Lundegard, 1992). Grain dissolution will also cause an underestimation of compaction.

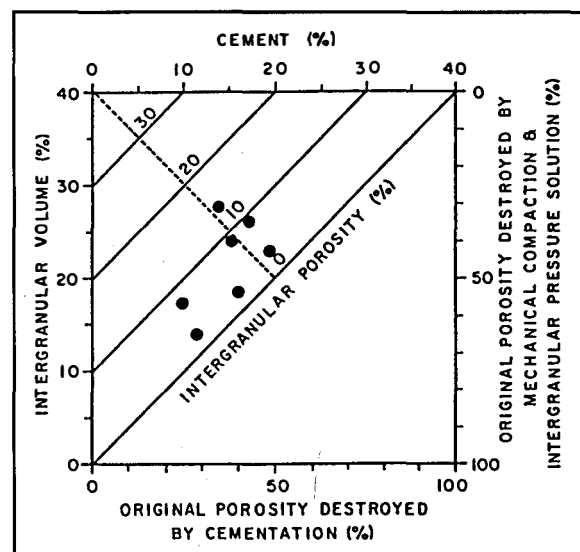


Figure 110. Intergranular volume-cement diagram with only Rose Run samples that lack dolomite cement plotted.

All of the remaining sandstone samples contain relatively significant amounts of dolomite cement. Most of these plot in the upper right area of the diagram in Figure 109, reflecting the importance of cementation in reducing porosity in the rocks. A few samples plot along the dashed diagonal line, indicating that both compaction and cementation were important in reducing porosity.

In Figure 111, each of the samples that contain important amounts of dolomite cement is plotted as two separate points (indicated by triangles). Open triangles include clay, feldspar, and silica cements only and solid triangles include the sum of these earlier cements plus dolomite. Dolomite cement clearly postdates the clay, feldspar, and quartz cements in all thin sections, so the two points representing each sample in Figure 111 illustrate two distinct steps in the diagenetic history of the samples. A very few of these samples apparently were cemented by carbonate very early in their burial history. Three open triangles plot in the uppermost left corner of the diagram and their corresponding solid triangles plot to the far upper right in the diagram. These three samples did not undergo any significant compaction. Most of the samples, however, did experience significant compaction prior to dolomite cementation. Dolomite replaces much of the earlier framework and binder in the sandstones. The sandstones appear to have experienced compaction, both mechanical and chemical, associated cementation by silicates, and later dolomite cementation and replacement.

Generalized diagenetic pathways can be discerned by combining all the information from the diagrams in Figures 109 through 111 into a single diagram

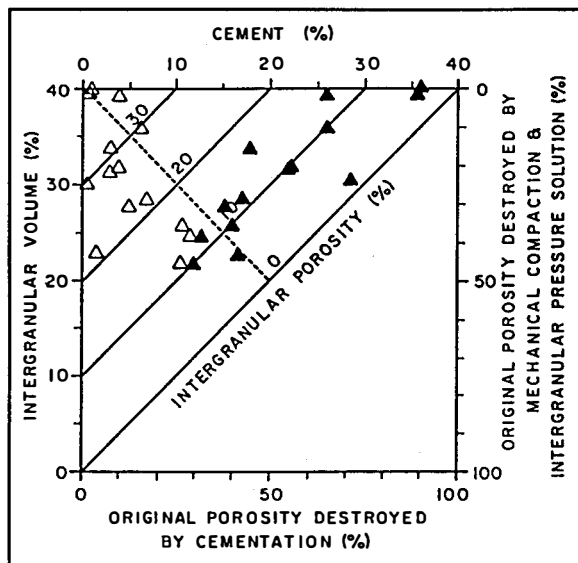


Figure 111. Intergranular volume-cement diagram with only dolomite-cemented samples plotted (solid triangles). The open triangles are the same samples plotted after subtracting the percentage of dolomite cement present.

(Figure 112). Except for the few sandstones cemented by carbonates prior to deeper burial (path 1 in Figure 112), intergranular volumes in the sandstones were reduced to about 30 percent (mean intergranular volume=28.3 percent) during an early phase of diagenesis. The sandstones that now lack dolomite cement (circles in Figure 110) followed a rather straight diagenetic pathway towards almost complete porosity destruction (path 2 in Figure 112). Primary intergranular porosity was almost completely destroyed; moldic porosity due to feldspar dissolution developed in the subarkoses and was largely preserved, except where clay plugged the secondary voids.

Sandstones that contain significant amounts of dolomite cement followed a path similar to those described above, except dolomite cementation and replacement of framework materials interrupted the progression to porosity occlusion (path 3 in Figure 112). Compaction appears to have been more important than cementation prior to extreme dolomite cementation (note the open triangles and arrows for path 3 in Figure 112).

As mentioned in the footnote on page 108, these diagrams fail to account for compactional bulk volume reduction, thus underestimating compactional porosity loss. Lundegard (1992) also points out that grain dissolution may enhance porosity or lead to local precipitation of authigenic cement; both processes induce error in compactional porosity loss estimates.

Figure 113 is a plot of the amount of compactional porosity loss versus cementational porosity loss in all of

the sandstones, taking bulk volume reduction into account. The values plotted in Figure 113 were derived from the data on porosity, intergranular volume, and amount of cement present in Table 3 on page 124 using calculations devised by Lundegard (1992). The diagram illustrates that most of the Rose Run sandstones in the Hammermill well lost porosity through compaction rather than cementation. The few samples having high values of cementational porosity loss were affected by dolomite cementation before deeper burial. Compaction indices for each of the samples are mostly greater than 0.5 (Table 3, pg. 124), also indicating that the sandstones lost more porosity through compaction than through cementation. The significance of compactional porosity loss is most likely still underestimated for carbonate-cemented samples in Figure 113.

Porosity— Five pore textures, as defined by Schmidt and McDonald (1979, p. 211), occur within the Rose Run sandstone samples examined in this report, including: 1) intergranular pores; 2) oversized pores; 3) moldic pores; 4) intraconstituent pores; and 5) fractures. A sixth pore texture, intercrystalline (a carbonate pore texture discussed by Choquette and Pray, 1970), occurs in a few of the sandstones. Intergranular pores form between framework grains, and may be lined with cement. Three types of secondary pore textures have been identified by Schmidt and McDonald (1979). These are regular, reduced, and enlarged intergranular. Oversized pores are defined as those that exceed the diameter of adjacent grains by a factor of at least 1.2. Oversized pores are created from

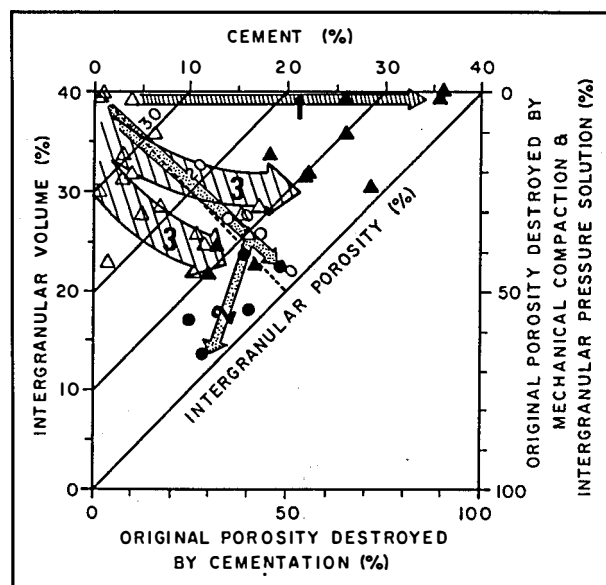


Figure 112. Intergranular volume-cement diagram with all data shown in Figures 110–112 combined. Numbered arrows illustrate directions of compactional and diagenetic modifications in altering porosity.

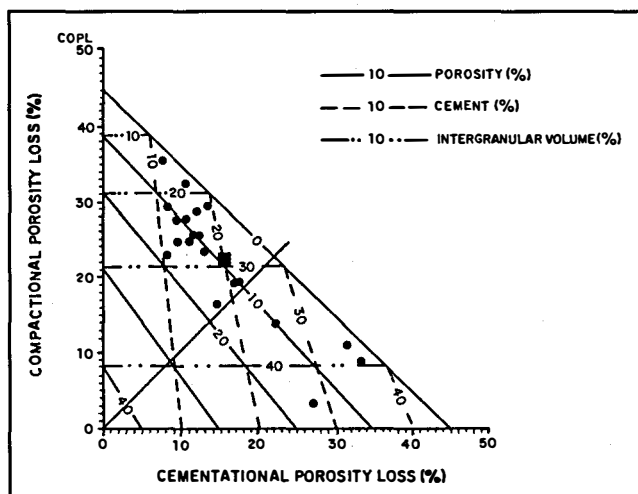


Figure 113. Diagram showing compactional porosity loss plotted against cementational porosity loss in the Rose Run sandstone samples from the #2 Hammermill well in Erie County, Pennsylvania. The solid square is the mean of all values. This diagram assumes an initial porosity of 45 percent (Lundegard, 1992). The illustration shows lines of equal porosity, volume percent cement, and intergranular volume. The solid line labeled 1:1 divides the field in which compaction is more important (upper right) from the field in which cementation is more important (lower right).

three classes of oversized fabric-selective pore textures, i.e. a combination of voids formed through: 1) dissolution of grains; 2) dissolution of cement; and 3) dissolution of replacement dolomite. Moldic pores in the Rose Run sandstone are the result of dissolution of feldspar and lithic grains, and can be identified by characteristic shape and size of the mold. Intraconstituent pores are created by dissolution of grain interiors. In the Rose Run sandstone feldspar grains commonly show this type of porosity. Fracture porosity is created by partings and separations of rock or minerals. This type of porosity is rare in the Rose Run sandstone except along fault zones such as the Akron-Suffield and Highlandtown faults. Hybrid pores are pores of complex origin, either resulting from several classes of secondary porosity or being part primary and part secondary (Schmidt and McDonald, 1979).

The average Rose Run sandstone porosity determined by point count methods on 70 samples is 7.5 percent. Porosities are listed in Table 2 (pg. 124) by county for the Rose Run sandstone samples from Ohio. The relative percent of moldic, oversized/hybrid, intergranular, intraconstituent, fracture and intercrystalline porosity was determined for 29 Rose Run sandstones from cores in Ohio (Appendix XI). Intergranular porosity makes up 48 percent of the total porosity followed by 19 percent moldic, 12 percent oversized/hybrid, 11 percent intercrystalline, 9 percent intraconstituent, and 2 percent fracture. In these same

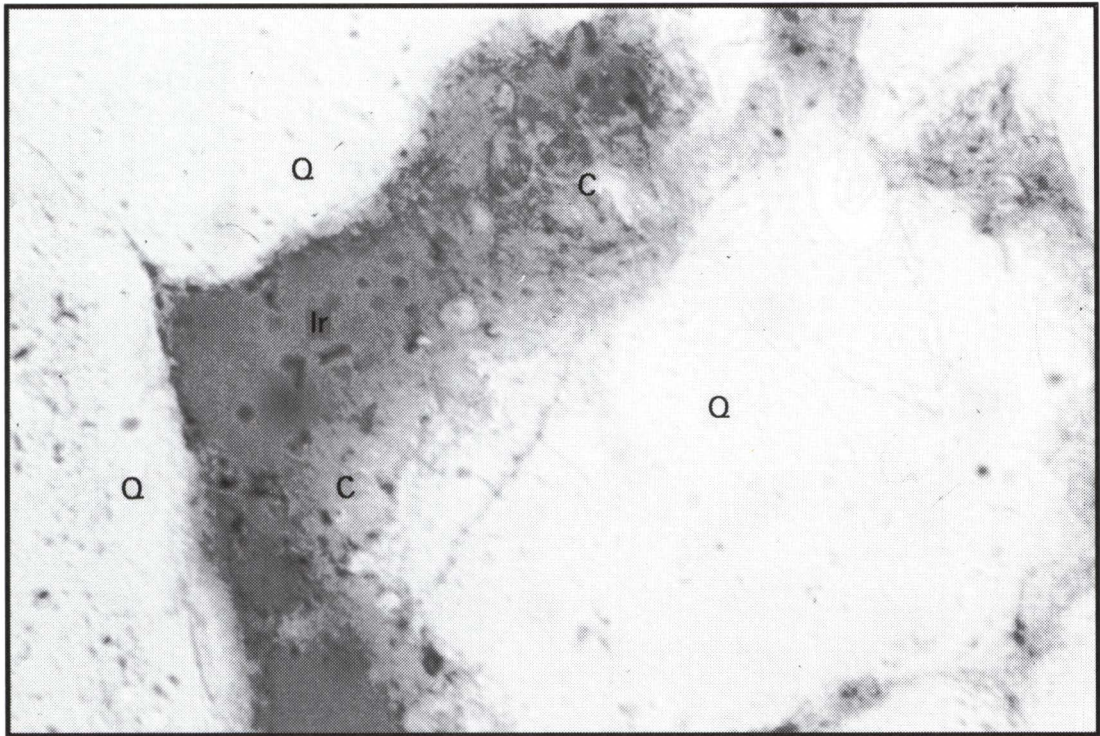
29 samples of Rose Run sandstone total porosity averages 7 percent and ranges from 0 to 25 percent. According to Enterline (1991) the most abundant type of porosity in two cores from Ashtabula County, Ohio is moldic. In core 2958 from Scioto County, Ohio, from which five thin sections were made, porosity types and relative percentages appear to be similar to those seen in cores from Coshocton and Jackson Counties, Ohio.

Nearly all of the intergranular porosity observed in thin sections made for this study is considered secondary. Triangular-shaped voids suggestive of primary porosity occur in some cases, but these pores invariably have corroded boundaries that strongly suggest carbonates or some other cement has been leached from the pore. In addition to corroded framework grain margins (Figure 114A and 114B), corroded remnants of dolomite and silica cement, and elongated intergranular voids all indicate a post-depositional origin for the intergranular porosity. Enlarged intergranular voids vary in size from 0.15 mm, where dissolution has widened triangular pores between grains, to lengths of 0.42 mm along elongate voids. Larger secondary voids are classified as oversized pores. Secondary intergranular porosity is the most abundant porosity type found in the Rose Run sandstone. According to Pittman (1979), the best sandstone reservoirs have this type of porosity.

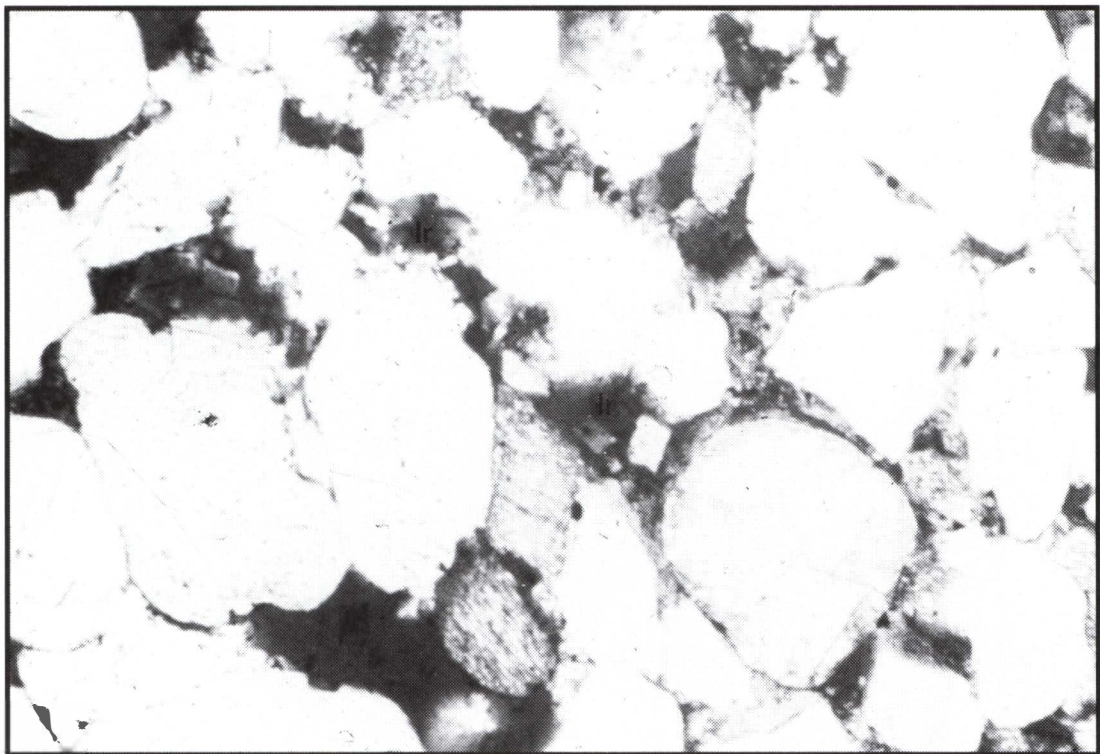
Oversized hybrid pores in the Rose Run sandstones are created primarily by dissolution of dolomite and feldspar grains. Oversized hybrid pore diameters as long as 0.19 mm occur in the sandstones.

Moldic pores (Figure 115A) occur in the sandstones, especially in the more feldspathic samples. Moldic and intraconstituent porosities are interrelated because most of the moldic porosity is the result of complete feldspar grain dissolution, whereas intraconstituent porosity is found within partially dissolved feldspars (Figure 115B). Moldic void diameters approximate the mean grain size of the specific mineral. Moldic porosity alone generally is not conducive to the formation of good reservoirs (Wescott, 1982). Where moldic and enlarged intergranular pores merge, however, oversized and hybrid pores are formed in the Rose Run sandstone, and permeabilities should be high.

Intraconstituent pores are voids formed within specific components of the rocks. They occur as minute pores within framework grains, within cements, and within dolomite replacement material. These pores are very

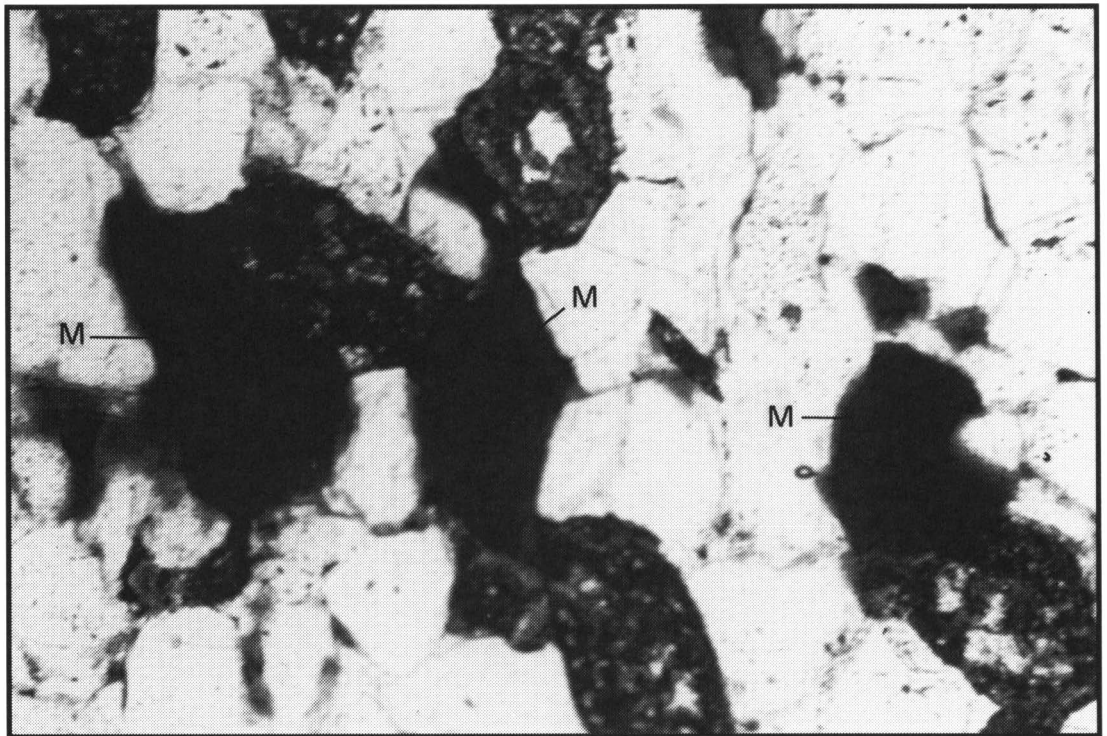


A



B

Figure 114. Photomicrographs of enlarged intergranular porosity (Ir) in Rose Run sandstone samples from Ohio. A—Note the extreme corrosion of the quartz grains (Q) and later filling of the pore with clay (C). Width of photo 0.41 mm, plane polarized light. B—Note the interconnecting pores. Width of photo 1.1 mm, plane-polarized light.



A



B

Figure 115. Photomicrographs of porosity developed in Rose Run sandstone samples from Ohio. A—moldic porosity (m) created by dissolution of feldspar. Width of photo 1.1 mm, plane-polarized light. B—intraconstituent porosity (la) forming in potassium feldspar. Width of photo 1.1 mm, cross-polarized light.

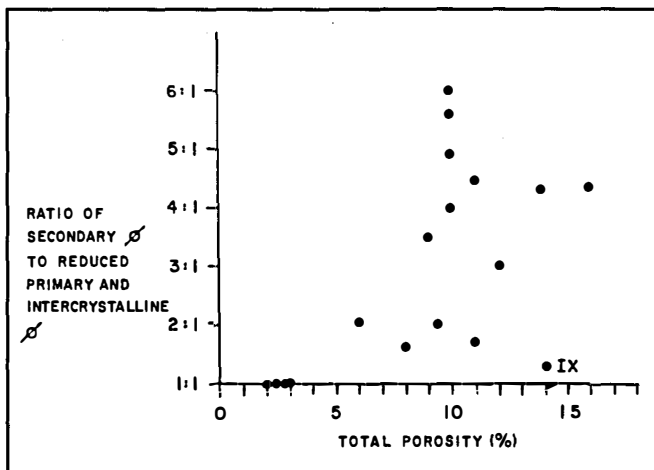


Figure 116. Plot of the ratio of secondary porosity to reduced primary and intercrystalline porosity versus total porosity for Rose Run sandstones from the #2 Hammermill well in Erie County, Pennsylvania.

small, usually a fraction of a micron to a few microns wide, and are essentially insignificant. They are most easily observed in feldspar grains in the Rose Run arkoses and subarkoses.

Very little fracture porosity was observed in the Rose Run sandstone. Where they were found, the parting planes of the open rock fractures extend over several grains and along intergranular void spaces. They are of local importance only. The scarcity of this porosity requires that other methods must be hypothesized for providing fluids capable of diagenetic changes in the Rose Run sandstone. Irreducible lamellar porosity may have provided the access for these fluids (Schmidt and McDonald, 1979), assuming that the Rose Run sandstone had low porosity at the time of major diagenetic mineral formation.

In this study intercrystalline porosity denotes porosity between individual dolomite crystals that most commonly have a unimodal, planar-e texture type. This is considered to be a form of secondary porosity (Choquette and Pray, 1970). In these rocks, the primary intergranular void space was filled with dolomite and the available porosity occurs between crystals of cement. Intercrystalline porosity is most abundant in the dolostones of the Rose Run interval, but it is also present in the dolomitic Rose Run sandstones (Appendix XI).

Figure 116 is a plot of total porosity versus the ratio of secondary pore textures to the sum of reduced primary intergranular and intercrystalline porosities in the sandstones from the Hammermill well in Erie County, Pennsylvania. In general, the higher porosity sandstones

contain secondary pore textures and those rocks with only reduced intergranular voids have very low ineffective porosity. One interesting exception is a sample (marked IX) with high intercrystalline porosity. This sample contains 22 percent dolomite cement with unimodal, planar-e texture, i.e. a porous, sucrose texture.

Porosity and permeability in the sandstone samples from the Hammermill well are highly variable. Porosities, determined from thin section data, range from 2 to 16 percent, with a mean of 8.38 percent (Table 4, pg. 125). The standard deviation of these porosity values (4.18) indicates considerable heterogeneity in this reservoir parameter. The porosity distribution in the sandstones also appears bimodal, as illustrated in the frequency polygon in

Figure 117. Core analyses of selected samples from the low porosity population yield measured porosity values of 2.6 to 2.7 percent and permeabilities less than 0.1 millidarcies (md). Core analyses of selected samples from the high porosity population yield measured porosity values of 9.4 to 13.9 percent and horizontal permeabilities of 1.33 to 192 md; vertical permeabilities range from 0.19 to 53.2 md (Appendix IV).

Porosity/Microstructure Relationships—In the Rose Run interval six categories of microstructures can be identified in 55 thin sections from Ohio (Appendix IX). These include: 1) interbedded or interlaminated sandstone and dolostone or dolomitic sandstone and sandstone; 2) mottled or bioturbated sandstone; 3) massive sandstone; 4) stromatolitic laminae; 5) interlaminated clay stringers or clayey and silty sandstone and sandstone; and 6) laminated or bedded sandstone. Each type of microstructure is assigned to one of four lithofacies already defined.

Rose Run sandstone characterized by interlaminated sandstone and dolostone or dolomitic sandstones (Appendix IX, type 1 microstructure) averages seven percent

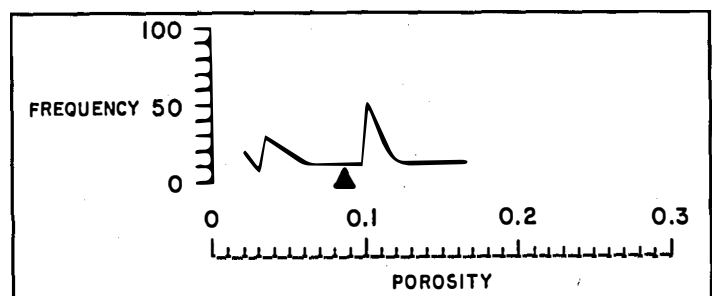


Figure 117. Frequency polygon for porosity in the Rose Run sandstones from the #2 Hammermill well in Erie County, Pennsylvania.

porosity. Intergranular porosity comprises 50 percent of the total porosity and moldic and oversize pores 16 and 14 percent, respectively. Intraconstituent, intercrystalline and fracture porosity make up seven, nine, and four percent respectively (Appendix XI). These units may be thin laminae or beds of dolostone alternating with laminae or beds of sandstone as in core 2853 at a depth of 5981.5 feet or thin units of sandstone alternating with dolomitic sandstone. In the latter case, dolomite appears to have been leached from non-dolomitic zones. Evidence of this leaching is found along quartz boundaries that are highly corroded in the non-dolomitic zones. In the carbonate-rich areas dolomite cement replaces the quartz grains. No readily apparent differences exist in framework mineralogy, but quartz overgrowths and clay in the form of partially leached pore fillings, and as widely scattered interstitial matrix, appear to be more common in the non-dolomitic zones.

Type 4 dolomite (Figure 118A) is the most common dolomite type found in the interlaminated sandstone and dolostones or dolomitic sandstones, followed by types 2 and 3 (see Appendix VIII for a detailed discussion of dolomite types). Type 4 dolomite is medium to very coarse-crystalline, non-planar dolomite. This type of dolomite may be partially dissolved and fractured and its occurrence and morphology suggests type 4 dolomites may have replaced sparry calcite. Type 2 dolomite is very fine to fine crystalline, bimodal(?), planar-s and planar-e dolomite (Figure 118B and Appendix IX). This dolomite is a void filler and may occupy moldic or enlarged intergranular pores as well as other secondary pore spaces. Type 2 dolomite formed very late in the diagenetic history of the Rose Run sandstone.

Dissolution of dolomite, observed in the interlaminated sandstone and dolomitic sandstone, generally follows bedding planes, both in horizontal and cross-bedding. Leaching of the dolomite which occurred late in the post-depositional history of the rock followed the most permeable paths along bedding planes. No single reason appears to explain why some zones would be more permeable to the corrosive fluids than others. In the thin sections examined, differences in grain sorting of the sandstones, variations in clay content and quartz overgrowths, and differences in mechanical compaction in adjacent laminae all may have influenced permeabilities prior to the leaching of the dolomite. Where dolostone and dolomitic sandstone beds and laminae are present, vertical permeabilities are expected to be very low, although the rock as a whole may show good porosities (Table 5, core no. 3260, pg. 125). High horizontal permeabilities should

be present when dissolution of dolomite along sandstone laminae has occurred.

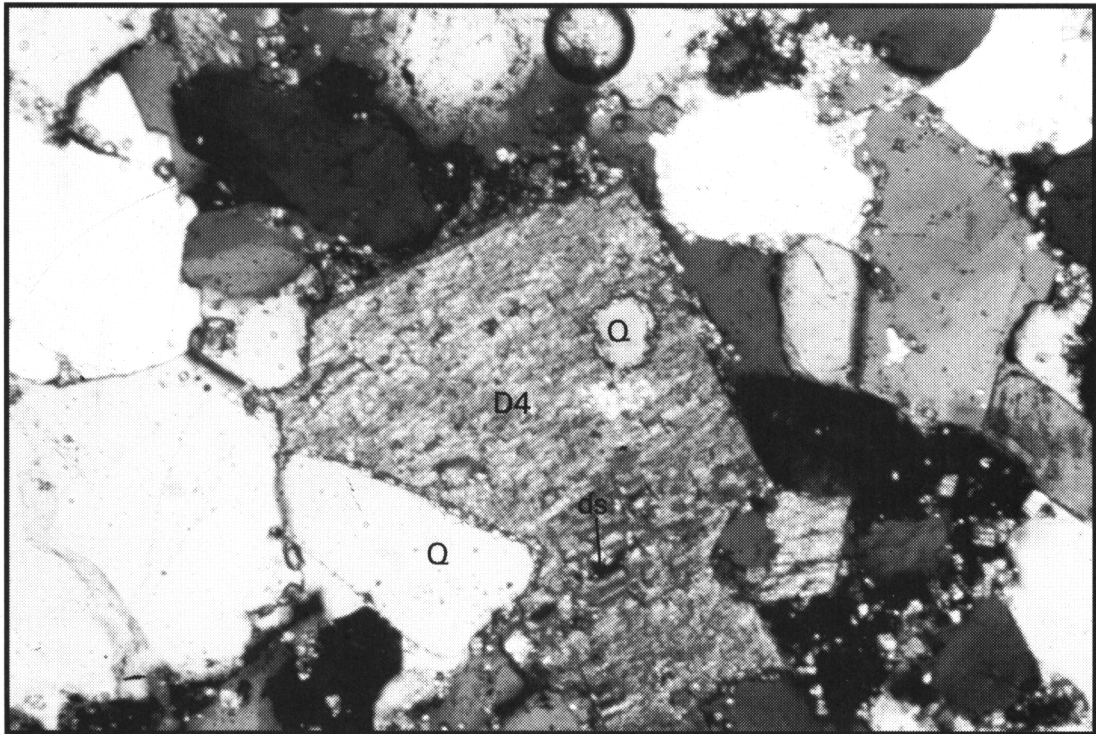
Coshocton County, Ohio core samples with interlaminated dolostone and sandstone microstructures were placed in the interbedded sandstone and dolostone lithofacies. Jackson County, Ohio core samples (core 2898) with interlaminated dolostone and sandstone microstructures were placed in the cross-bedded and flaser-bedded sandstone lithofacies (Appendix IX). In the Jackson County samples, sandstone in which dolomite has been leached, alternated with dolomitic sandstones. In Coshocton County, true interlaminated sandstone and dolostones occur, as well as the type found in Jackson County.

Four thin sections were examined which appear to have a mottled texture (Appendix IX, microstructure type 2). The average porosity of these four samples was seven percent. Mottling appears to be the result of variations or irregularities in dolomite cementation. The mottled samples, in this case, belong to either the interbedded dolostone and sandstone type 1 microstructure, or to the clayey, silty sandstone interlaminated with sandstone (type 5 microstructure), and are diagenetically mottled rather than bioturbated. Type 4 dolomite is found almost to the exclusion of other dolomite cements in these four samples. Type 1 dolomite, although rare in the Rose Run interval, is found in two samples with type 2 microstructures (Figure 119A).

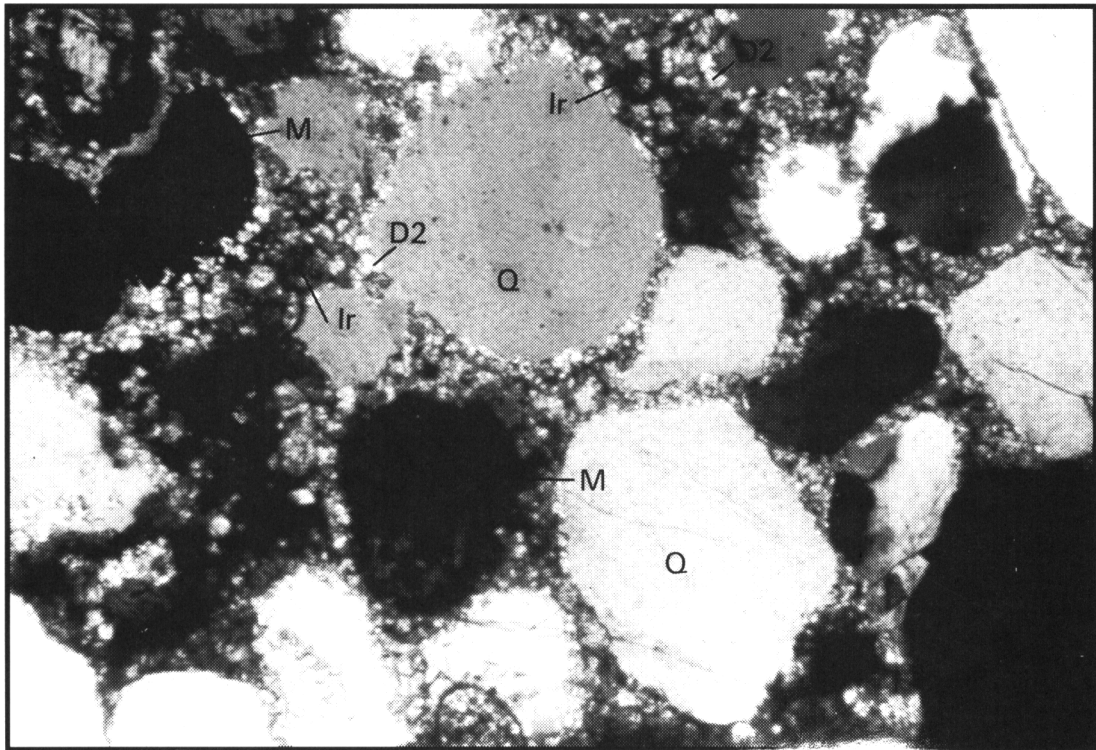
The two most abundant dolomite types found in interbedded dolostones in the Rose Run sandstone are types 7 and 5 (Appendix VIII). Type 7 occurs as very fine- to medium-crystalline, non-planar, replacement dolomite with allochem ghosts of ooids and peloids (Figure 119B). Dark inclusions give the dolostone a dirty appearance. Small authigenic grains of pyrite are commonly associated with this dolomite. Type 5 dolomite is fine- to medium-crystalline, non-planar, replacement(?) dolomite, but it has no distinct allochem ghosts. Dusty inclusions and pyrite are randomly scattered throughout the dolomite.

Microstructure in the Rose Run sandstone with a massive appearance (Appendix IX, type 3) are probably related to a larger macrostructure. In this case two-thirds of the sandstones with massive microstructure are found in the cross-bedded and flaser-bedded sandstone lithofacies, and about one-third occur in the interbedded sandstone and dolostone lithofacies.

Porosities range from zero to 11 percent and average 5.9 percent. Intergranular and moldic porosities are the two most common porosity types (Appendix XI). Porosities are lowest when quartz overgrowths and

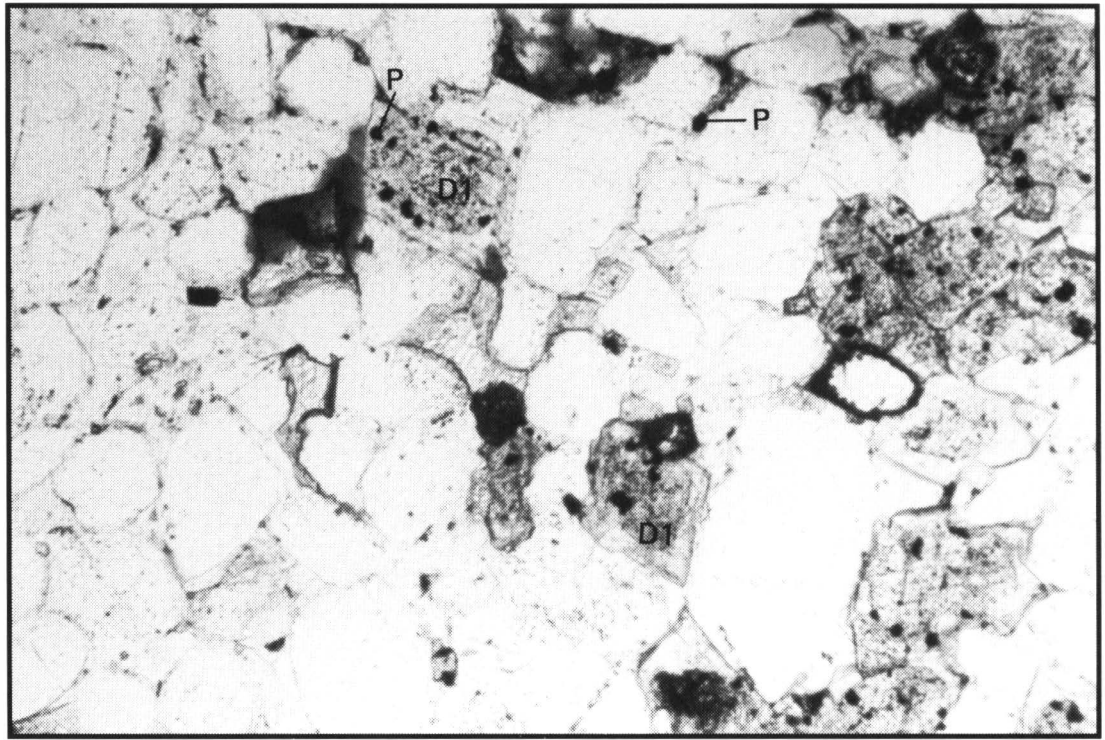


A

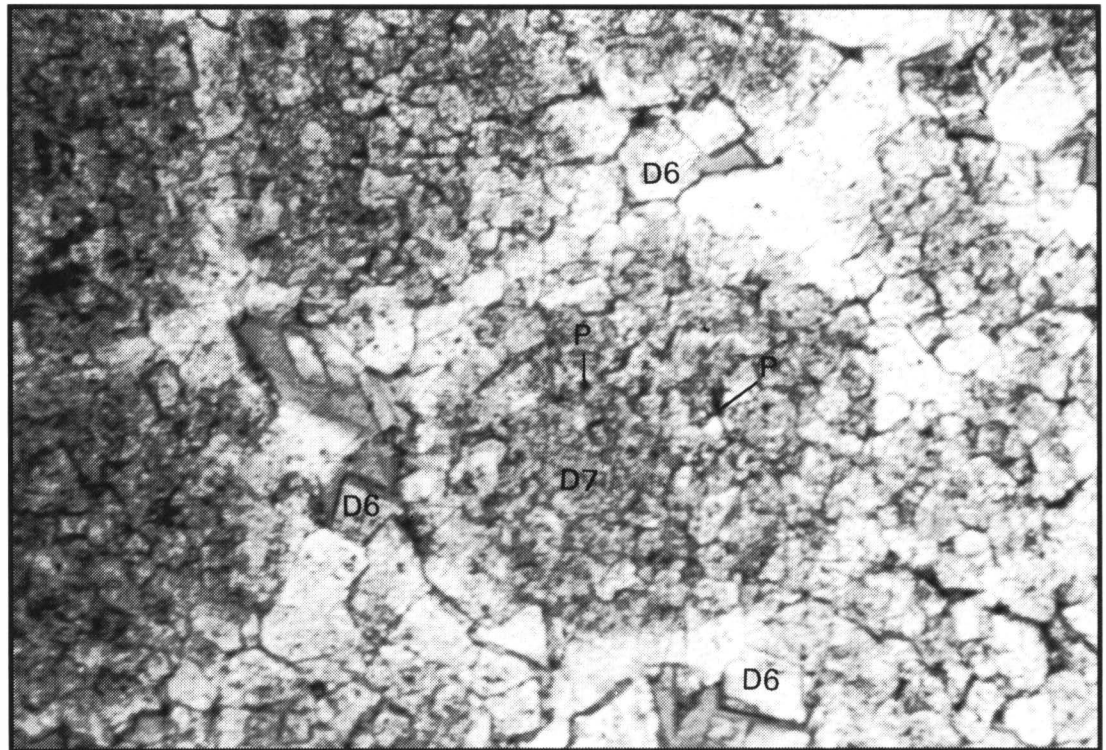


B

Figure 118. Photomicrographs of dolomites from Ohio. A—type 4 dolomite (D4) attacks detrital quartz grains (Q) and typically has evidence of dissolution (ds). Width of photo 1.1 mm, crossed-polarized light. B—type 2 dolomite (D2). Very fine- to fine-crystalline void-filling dolomite attacks quartz (Q) and occupies enlarged pores (Ir), but not moldic pores (m) in this example. Width of photo 1.1 mm, crossed-polarized light.



A



B

Figure 119. Photomicrographs of dolomites from Ohio. A—type 1 dolomite (D1), a replacement dolomite with clear rims and non-mimic replacement of feldspars or allochems, typically associated with pyrite (P), rare in Rose Run sandstones. Width of photo 1.1 mm, plane-polarized light. B—type 7 dolomite (D7), a nonplanar dolomite shown replacing peloids. Multiple dolomite crystals replace a single allochem. Pyrite (P) is common. Also type 6 dolomite (D6) is shown along the outer margins of peloid ghosts. Width of photo 1.1 mm, plane-polarized light.

dolomite are abundant, and highest when extreme leaching of dolomite and clays has occurred. We classify the three most abundant dolomites found in rocks with massive (type 3) microstructure as dolomite types 6, 2, and 4 (Appendix VIII).

Type 4 microstructures (stromatolitic laminae) are found in slightly to highly sandy Rose Run dolostone lithofacies. These rocks have low porosities and contain types 3, 5, and 6 dolomites.

Of the 55 Rose Run sandstone thin sections examined from Ohio, 17 exhibit microstructure that classify them as interlaminated clay stringers or clayey, silty sandstone interlaminated with sandstone (Appendix IX, microstructure type 5). Sandstones with type 5 microstructures average 7.3 percent porosity. Intergranular porosity comprises 54 percent of the total porosity followed by moldic (25 percent) and oversize (12 percent). Intraconstituent and intercrystalline porosity each make up about five percent of the total porosity (Appendix XI). These units consist of very thin, wispy stringers of clay or clayey, silty sandstone interlaminated with cleaner, sometimes better sorted (but still poorly sorted) sandstone. Where clay and silt laminae are abundant, as in core 2989 at a depth of 6,629.9 feet (Appendix XI), porosity (and permeabilities?) are low. Where clay stringers are thin and scarce, as in core 2898 at a depth of 4,505 feet (Appendix XI), the rock remains relatively porous (seven percent), but vertical permeability is probably low because of the interlaminated clay-rich zones which have low porosities.

Rose Run sandstone with clay stringers or clayey, silty sandstone interlaminated with sandstone (type 5 microstructure) contains type 2, 3, 4, and 5 dolomite (Appendix VIII). However, dolomite is generally rare in rocks with type 5 microstructure. These sandstones are found predominantly in the cross-bedded and flaser-bedded sandstone lithofacies, but a few occur in the interbedded sandstone and dolostone lithofacies.

Laminated or bedded sandstone (type 6 microstructure—Appendix IX) have high porosities and permeabilities, and are found in the interbedded sandstone and dolostone lithofacies except for one sample that was classified in the cross-bedded and flaser-bedded sandstone lithofacies. Laminae are formed mainly by sorting and grain size differences. Mineralogical differences, especially in feldspar content, often accompany the textural differences. Relative percentages of pore types were determined for only one thin section (Table 5, pg. 125), but examination of the

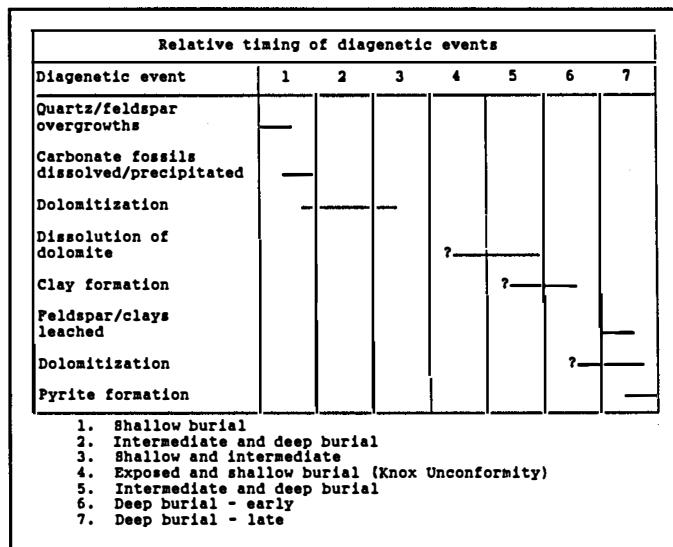


Figure 120. Relative timing of major diagenetic events for the Rose Run sandstone.

remaining thin sections indicates that oversize, moldic, and intraconstituent pores are dominant in these rocks. Type 4 dolomite occurs in two of five samples, but dolomite in general is rare and has apparently been leached from these sandstones.

Paragenesis—The ordering of diagenetic events with respect to time is one of the most important aspects to the complete understanding of how the composition and texture of a sandstone is affected by its geological and geochemical history (Pettijohn and others, 1973). The Rose Run sandstone contains authigenic dolomite, quartz, feldspar, illite, illite-smectite, pyrite, and rare anhydrite, chert, and chlorite(?). Figure 120 presents a summary of the paragenesis of the Rose Run sandstones for dolomite, quartz, feldspar, pyrite, and clays (except for chlorite). Hardie (1987) provided a similar summary of diagenetic events for Upper Cambrian carbonates of the central Appalachians, including western Pennsylvania. Growth position of chert, anhydrite, and chlorite with major authigenic minerals was not observed and consequently the relative timing of their formation could not be determined.

Petrographic evidence indicates that quartz and feldspar overgrowths formed prior to dolomite. Dolomitization was pervasive and may have occurred as several events separated by significant time intervals. Detrital clay regeneration probably occurred over a long interval of time, but most of the identifiable neofomed clay formed prior to and during(?) type 2 dolomite formation (Figure 120).

Post-Depositional History— The model for the post-depositional history of the Rose Run sandstone in the

study area is based upon facts gleaned from examination of 91 thin sections from Ohio well cores, and information derived from the literature. The model is presented as a starting point, to be supported or disproved, by the addition of future information.

Siliciclastic sediments of the Rose Run sandstone and interbedded dolostones were gradually buried beneath a thick sequence of Beekmantown sediments and subjected to mechanical and chemical diagenesis. The original carbonate components were dolomitized leaving oolitic and peloidal ghosts, glauconite pellets, and occasional stromatolitic laminae as evidence of the original peritidal deposition environment.

Silica cementation is generally thought to occur because of pressure solution at point contacts between quartz grains, or from silica supersaturated pore water in areas where groundwater recharge is great (Pettijohn and others, 1973). Long, concavo-convex and sutured grain contacts in the Rose Run sandstone indicate the occurrence of pressure solution. However, silica precipitation from supersaturated groundwater might have occurred also. Conditions were favorable for precipitation of feldspar overgrowths at about this same time, although the exact time relationship between feldspar and quartz overgrowths is not known. Calcite may have dissolved at this time, because calcite is more susceptible to pressure solution than quartz (Pettijohn and others, 1973). However, conditions within the Rose Run sandstone were apparently not conducive to calcite precipitation until later. Compaction may have forced carbonate rich pore waters upward where it was precipitated as calcite cement in the Beekmantown sediments and as burial progressed, in the Rose Run sandstone.

Dolomitization began at some point after quartz and feldspar overgrowth development ceased. Massive dolomitization on a scale found in the Knox/Gatesburg most likely occurred where stable gravity-driven or thermally-driven regional groundwater systems were long lived, large enough, and deeply circulated enough to provide replacement dolomitization that cuts across facies boundaries (Hardie, 1986).

As the Rose Run sandstone was buried for the first time (pre-Knox unconformity), it may have been subjected to a gravity-driven regional groundwater system which, given sufficient time, could dolomitize limestones by passing normal seawater through the rock (Hardie, 1987). Also, after significant burial by the Beekmantown dolomite (both the Upper Cambrian Mines equivalent and the true Lower and Middle Ordovician Beekmantown), warm

upflowing basinal brines may have contributed to the dolomitization process (Hardie, 1987, p. 179).

Corrosion of dolomite rhombs indicates that a period of dolomite dissolution occurred during the diagenetic history of the Rose Run sandstone. This dissolution probably took place after the formation of the Knox erosional surface. Although evidence exists for karst development by meteoric waters on the Knox unconformity surface in other regions (Amthor and Friedman, 1992; Desrochers and James, 1988; Anderson, 1991, and Mussman and others, 1988), no definitive evidence exists for karst development in the Beekmantown/Mines dolomite in most of Ohio and western Pennsylvania. However, dissolution of the dolomite in the Rose Run sandstone, and resultant high porosity, occur in this sandstone where it has been buried 200 to 300 feet below the Knox unconformity (in Scioto and Jackson Counties, Ohio). In deeper parts of the basin even greater thicknesses of carbonates lie between the Knox unconformity surface and the Rose Run sandstone, at depths generally not affected by meteoric groundwater. Yet, evidence from geophysical logs indicates the Rose Run continues to have high porosities in these areas. Hence, dissolution of dolomite in the Rose Run interval probably occurred after intermediate to deep burial by basinal brines undersaturated in carbonate rather than by meteoric groundwater.

Authigenic mixed-layer illite-smectite and illite are two of the last authigenic cements formed in the Rose Run sandstone. They occur as pore fillings, or are associated with shale clasts (pseudomatrix) and clay laminae, and are generally intimately intermixed. These clays probably formed after the creation of the Knox unconformity, in deeply buried areas where potassium- and magnesium-rich pore fluids were available. These pore fluids may have been derived from earlier erosion of dolomite and other minerals on the Knox unconformity surface and by dissolution of dolomite preceding the formation of clay after burial.

In deeply buried rocks, illite crystallinity (sharpness of the 10Å peak) increases with increasing depth of burial (Segonzac, 1970). Mixed-layer illite-smectite clays generally form during degradation by weathering or during aggradation by deep diagenesis (Segonzac, 1970). Powers (1959) noted that illite-smectite was relatively common in many boreholes he surveyed at depths between 6,500 and 13,000 feet. At greater depths these mixed-layer clays were transformed into illite. Hence, the illite-smectite in the Rose Run sandstone may be the result of burial between 6,500 and 13,000 feet.

At a later period of time, when the Rose Run sandstone was still deeply buried, corrosive basinal brines apparently attacked the silicate minerals, especially feldspars and clays. This may have occurred during some late tectonic event that mobilized deep, warm, basinal brines that then moved through the Rose Run sandstone in the basin (Anderson, 1991, p. 22). The leaching of feldspars and clays in combination with pores formed from the dissolution of dolomite (and calcite?) cement earlier resulted in oversized and hybrid pores that are now observed in the Rose Run sandstone. A minor dolomitization event occurred about the time silicates were being leached and pyrite was being formed. Evidence of this secondary dolomitization is found in the type 2 dolomite (Appendix VIII) that rims large hybrid and oversized pores, and is also found replacing larger dolomite crystals. The last identifiable diagenetic event was the formation of pyrite as small micrometer size grains and masses that appear to replace dolomite.

Porosity and Permeability Heterogeneities—The Rose Run sandstone possesses, on a microscopic scale, a number of interrelated features that display considerable variability, and that affect the hydrocarbon potential of the rock. These features are related to diagenesis and include permeability and porosity variability, clay and dolomite variability, and microfacies variability.

Porosities and permeabilities from Rose Run sandstones in Ohio vary as shown in Table 5 (pg. 125). Sandstones having fair to good porosities and low permeabilities tend to have significant amounts of dolomite. They may be interbedded with sandstone deficient in dolomite or occur in massive dolomitic sandstones. Grain contacts are generally floating to long. Quartz overgrowths may be present. Porosity is generally intergranular where some walls of the pores are dolomite, or intercrystalline and vuggy. These pores are generally relatively equant and have poor connectivity with other pores. Clays are generally rare to absent.

Rose Run sandstones having good porosities and high permeabilities tend to have quartz grains with long and concavo-convex contacts. Dolomite is rare to absent but clays are not uncommon, reaching six percent in one sample (Appendix X). Quartz overgrowths are common. Pores tend to be elongate, and classified as reduced and enlarged intergranular with good connectivity to other pores (Schmidt and McDonald, 1979). Boundaries of quartz grains generally show extensive corrosion.

Rose Run sandstones that have low porosities and permeabilities tend to be poorly sorted, dolomite-rich, interlaminated or interbedded medium- to coarse-grained

sandstone with very fine-grain, silty sandstone. In the silty layers, regenerated matrix clay may be present, but in at least one case dolomite replaced most of the clay. Intercrystalline and intergranular pores are the most common, but are widely scattered and have poor connectivity.

One-quarter of the permeability tests run on sandstone samples from the #2 Hammermill well in Erie County, Pennsylvania yielded reversed flow values greater than the initial flow values, suggesting the possibility of minor amounts of mobile fine clays blocking pore throats in the rock. The standard deviation of all porosity values from these samples is 4.18 (Table 4, pg. 125). Porosity variations generally are as great within different sandstone facies as they are for all collective samples; that is, porosity variations are not related to facies variations, with the remotely possible exception of the interpreted eolian Facies *S* sandstones. The “eolian” Facies *S* sandstones are uniformly tight (average porosity is 2.85 percent, with a standard deviation of 0.15). The highest porosities occur in the thicker bedded mixed sandstone-dolostone facies (*Me*) and in the interpreted fluvial sandstone facies (*S*). Mean porosity values in these facies are 13 percent and 9.83 percent respectively. Standard deviations are 3 in Facies *Ms* and 2.9 in “fluvial” Facies *S*. Intermediate porosity values characterize the thinner bedded mixed sandstone-dolostone facies. Mean porosity in Facies *Me* is 7.75 percent, with a standard deviation of 4.02, whereas mean porosity in Facies *Md* is 6 percent, with a standard deviation of 4.

Figure 121 illustrates the relative amounts of principal pore types in the core samples from the #2 Hammermill well in Erie County, Pennsylvania. Intergranular and intercrystalline voids, oversized, moldic, and intracon-stituent voids, and fracture voids have been grouped into three end members or general porosity classes. These three classes were selected because they define specific pore geometries that influence the path of electrical current flow in reservoirs (induced by geophysical logging tools) (Asquith, 1985). Rocks with moldic and oversized voids are the most porous ones in the samples and have excellent reservoir storage capacity. Rocks with roughly equal amounts of secondary oversized and moldic porosity and intergranular/intercrystalline porosity have pore volumes of only six to eight percent. Rocks with only intergranular/intercrystalline void textures are very tight and have no reservoir capacity.

The only good carbonate pore texture noted in these cores was limited vuggy void space in the interval between 5,123 and 5,124 feet in core 1 (Figures 39 and 122).

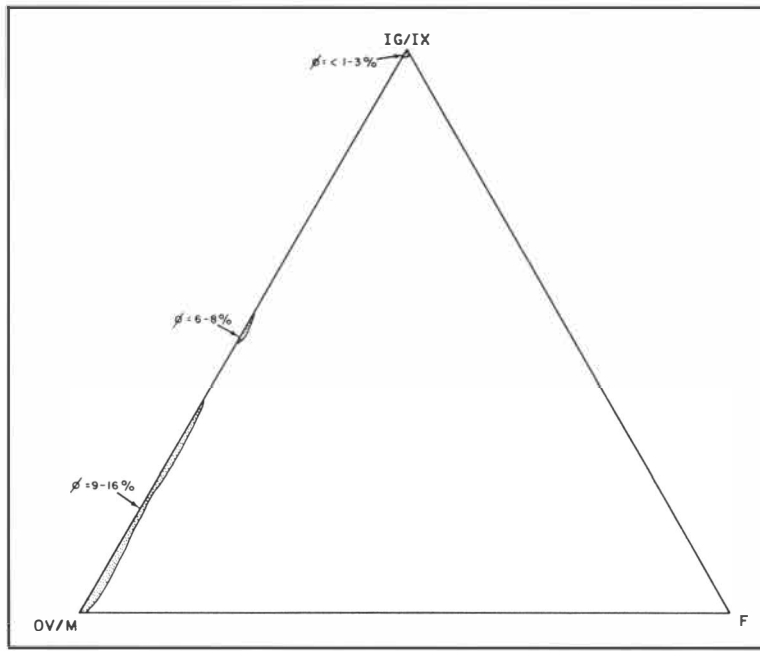


Figure 121. Triangular plot of porosity types in the Rose Run sandstones from the #2 Hammermill well in Erie County, Pennsylvania. IG—intergranular, IX—intercrystalline, OV—oversized, M—moldic F—fracture, ϕ —porosity.

Appendix IV contains selected porosity and permeability measurements for core samples of the Rose Run sandstone from the #2 Hammermill well. There is very little correlation between porosity and either vertical or horizontal permeability (correlation coefficients=0.25 and 0.4, respectively). This very low correlation indicates that compaction and diagenesis influenced permeability in a significantly different way from porosity. Morgan and Gordon (1970) and Dunn and Surdam (1989) note that the distribution of a diagenetic phase within pore systems is more important than its volumetric amount in affecting permeability.

Permeabilities are quite variable within sandstones that have good porosity. For example, Figure 123 shows the capillary pressure curves derived from three samples of porous Rose Run sandstone from the Hammermill core. Porosities and horizontal permeabilities of these samples include: 1) sample A, 4.3 percent and 192 md; 2) sample B, 12.2 percent and 5.14 md; and 3) sample C, 9.4 percent and 0.43 md. Sample A, an example of Facies S from 5,154.5 feet, is a moderately well

sorted (standard deviation is 5.7), fine-grained subarkose cemented by silica, feldspar, and authigenic illite. The latter two cements occur in minor amounts (Table 1, pg. 123). Silica cement occurs as syntaxial quartz overgrowths. Contacts are mostly long and concavo-convex, with some sutured grains. The compaction index is 0.72 (Table 1, pg. 123). Among the diagenetic phases, quartz overgrowths reduced the porosity by about 11 percent; they also reduced permeability somewhat, but compaction was more important in this respect. Compaction reduced porosity by approximately 14 percent and further reduced permeability. Permeability is anisotropic; horizontal permeability is 192 md, but vertical permeability is only 11.1 md. The capillary pressure curve for sample A in Figure 123 shows an exceedingly rectilinear curve that we interpret as the result of desaturation of

a very fine fracture. The initial threshold of the curve is characterized by immediate injection followed by a sharp break to a final desaturation of 23 percent at 500 pounds per square inch (psi), indicating the channeling of high permeability.

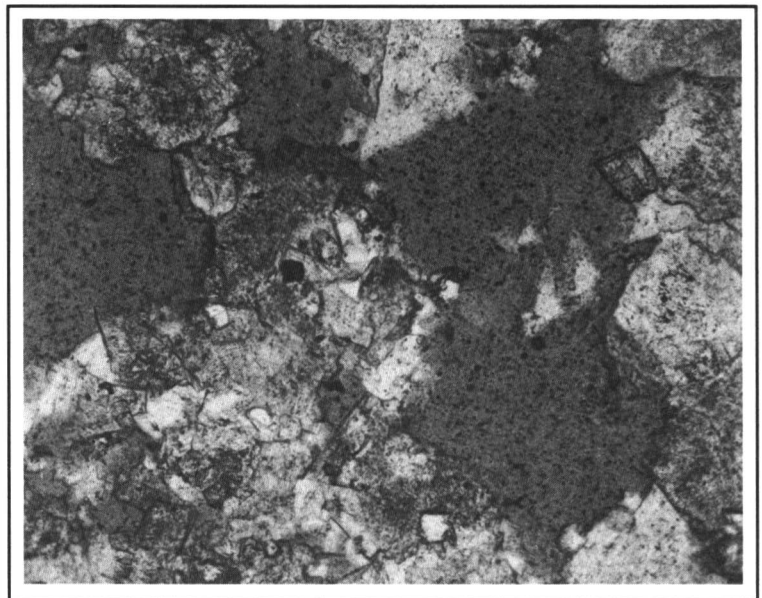


Figure 122. Photomicrograph of vuggy porosity in a Beekmantown/Mines dolomite from the #2 Hammermill well in Erie County, Pennsylvania.

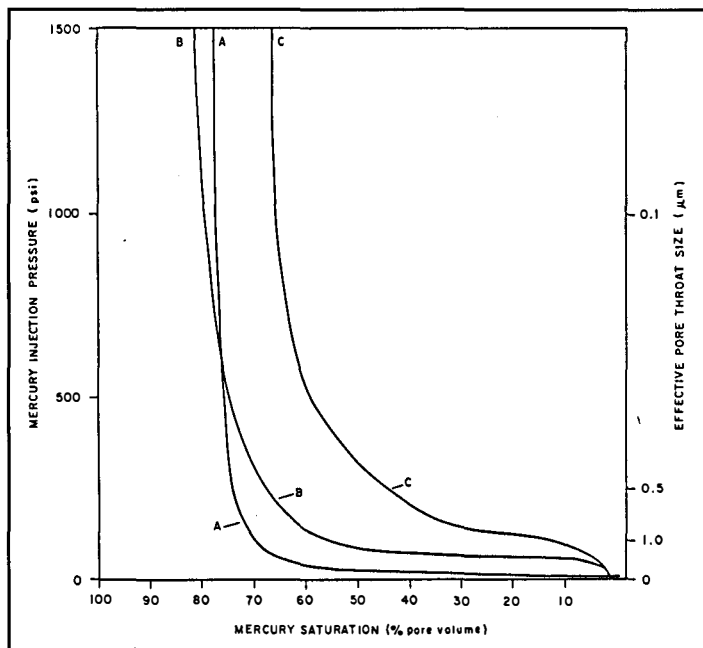


Figure 123. Capillary pressure curves of three Rose Run samples from the #2 Hammernill well in Erie County, Pennsylvania. A—5,154 feet, B—5,155 feet, C—5,163 feet.

Sample B in Figure 123 is a fine-grained, moderately sorted subarkose from Facies S at 5,155 feet in the Hammernill core. Permeability is similar in both horizontal and vertical directions; horizontal permeability is 5.14 md and vertical permeability is 6.34 md. Fracturing did not alter the petrophysical fabric of the rock. Porosity and permeability were reduced mostly by silica and some dolomite cementation as well as by compaction. Porosity is mostly moldic to enlarged intergranular.

Sample C in Figure 123 is a well sorted, medium-grained subarkose from 5,163 feet that contains significant dolomite cement exhibiting polymodal, planar-s fabric. The capillary pressure curve for this sample is somewhat irregular, but it does exhibit recognizable threshold and desaturation segments (Figure 123). The curve exhibits relatively immediate injection from a slight initial threshold. Horizontal permeability is 0.43 md and vertical permeability is 0.19 md. Reduced permeability is a function of the subhedral dolomite crystal fabric, i.e. planar-s dolomite.

Pore Geometry and Fluid Distribution—Pore structures in the Rose Run sandstone samples from northwestern Pennsylvania were modified by the superposition of different diagenetic and compactional processes. Diagenetic and compactional attributes acquired by the sandstones during burial dictates the distribution of fluids and the amount of recoverable hydrocarbons in the rocks. The amount of irreducible water saturation (S_{wi}) in the

sandstones recovered from the Hammernill well range from 20 to 25 percent in rocks with little or no dolomite cement and from 33 to 36 percent in rocks with moderate (approximately 10 percent) to large amounts of dolomite cement (Laughrey, in press). Higher values of S_{wi} are related to the micropores associated with dolomite crystal fabrics. Interestingly enough, pore throats in both permeable (Figure 123, sample A) and low permeability (Figure 123, samples B and C) sandstones are well sorted. Pore throat sorting (Jennings, 1987) in samples A, B, and C is 1.6, 1.5, and 1.6, respectively. Although the pore throats of these samples are well sorted (i.e. of relatively uniform size in each sample), the effective pore aperture size decreases from A (fracture-enhanced permeability) to B (compaction- and cementation-reduced permeability) to C (extensive dolomite cementation-reduced permeability). The good sorting of pore throats in all three samples means that

once a threshold buoyancy pressure is reached in these rocks, oil would quickly saturate the available porosity up to the reservoir's maximum capacity (Jennings, 1987, p. 1,199). Low S_{wi} values in the relatively dolomite-free sandstone, however, limit the acceptable S_w values in these rocks. Such sandstones would produce water rather quickly, if it is present. Higher S_{wi} values in sandstones with significant dolomite cement, permit somewhat higher values of S_w in completion decisions. Given the heterogeneity of pore throat size in these rocks, it is recommended that bulk volume water (BVI) be routinely evaluated in Rose Run reservoirs (Asquith, 1985, Chapter III).

Kerbel/Lower Sandy

Core 3 in the #2 Hammernill well contains rocks of the Kerbel/Lower Sandy interval (Figure 3). Core 3 contains 18 feet of mostly sandstone, with minor limestone, siltstone, and shale (Figure 124). The sandstones are very light gray, well sorted, fine-grained to medium-grained arkosic arenites. The quartz grains are mostly monocrystalline, of high sphericity, and subrounded to rounded. Feldspars are composed of orthoclase, microcline, and some perthite. Untwinned orthoclase grains are partially altered to sericite and display considerable vacuolization. Microcline and perthite show similar alteration. Accessories include zircon, tourmaline, and apatite. The sandstones are cemented by dolomite, feldspar and quartz overgrowths, and some clay. Sedimentary structures

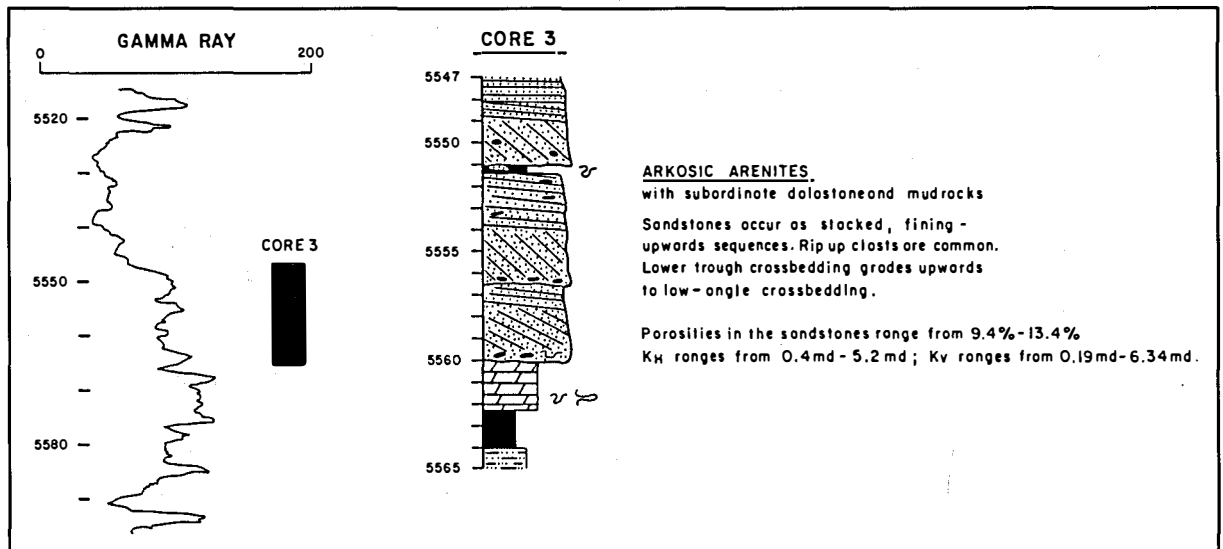


Figure 124. Graphical description of core 3 from the #2 Hammernill well in Erie County, Pennsylvania (from Laughrey, in press). See Figure 39 for explanation.

include low-angle and high-angle cross-lamination and bedding. Shale rip-up clasts are common, particularly near the bases of fining-upwards sequences. Figure 125 illustrates the X-ray diffraction scan of the Lower Sandy Member in Core 3. Porosities are between 9.4 and 13.4 percent. Pore throat sorting is good, although the pore throats are quite small. The smallest pore throats yield higher irreducible water saturations. Horizontal permeability ranges from 0.4 to 5.2 md; vertical permeability ranges from 0.19 to 6.34 md.

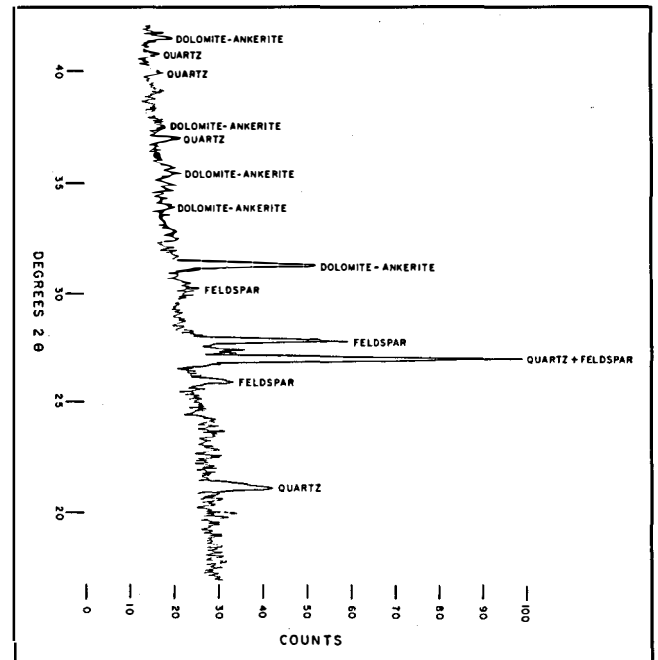


Figure 125. X-ray diffraction scan of a Kerbel/Lower Sandy arkosic arenite from core 3 in the #2 Hammernill well, Erie County, Pennsylvania from a depth of 5,559 feet.

Table 1. Petrographic data for sandstones from the #2 Hammermill well, Erie County, Pennsylvania.

Depth (ft.)	Framework Gains %		Matrix %	Cement %					Porosity %	Intergranular Volume (%)	\bar{x} (phi)	ϕ (phi)	FACIES	
	Total	Q, F, L		Total	Dolomite	SiO ₂	Feldspar	Clay						Other
Core #1														
5104	68	98,2,0	0	22	18.5	1	1.5	1	0	10	32	2.48	0.35	Md
5105	66	100,0,0	0	18	15	2	0	1	0	16	34	1.85	0.53	Ms
5106	68	98.5,1.5,0	0	22	18	3.2	0	0.8	0	10	32	2.26	0.56	Ms
5108	77	100,0,0	1	19	0	15	0	4	0	3	22	2.45	0.42	S
5110	81.3	97,2,1	0	16	trace	10	1	5	0	2.7	18.7	2.47	0.37	S
5112	62	98,2,0	0	36	35	0.5	0.5	trace	0	2	38	2.53	0.46	Mem
5112-5113	73	96,4,0	0	15	10	3	1	1	0	12	27	2.15	0.44	Met
5113	72	97,3,tr	0	17	10	5	1	1	0	11	28	2.24	0.46	Met
5113-5116	77	96,4,0	0	17	15	0.5	0.5	1	0	6	23	1.78	0.30	Met
5119	60	98,2,0	0	37	36	1	0	0	0	3	40	1.91	0.67	Met
5130	70	100,0,0	0	28	27	1	0	0	0	2	30	2.01	0.35	Md
Core #2														
5154	73.5	92,7,1	0	17.1	0	15.6	0.5	1	0	9.4	26.5	2.32	0.62	S
5154.5	73.1	87,12,1	0	13	0	11.2	0.8	1	0	13.9	26.9	2.78	0.57	S
5155	74	87,13,0	0	16	5	5	1	2	3	10	26	2.2	0.87	S
5156	76	98,8,1	0	15	0	6	2	4	3	9	24	2.32	0.52	S
5160	78	92,7,1	0	12	1	7	1	2	1	10	22	1.83	0.59	S
5161	76	93,7,0	0	13	1	10	1	1	trace	11	24	1.92	0.46	S
6162	60	87,13,0	0	26	22	3	1	0	0	14	40	2.28	0.59	S
5163	64	88,12,0	0	26	20	3.8	0.2	0	2	10	36	1.99	0.47	S
5164	85	94,6,0	0	12	0	6	0.36	5.64	0	3	15	2.37	0.90	S
5165	81.3	93,7,0	0	10.7	0	7.3	0.4	3	0	8	28.7	2.06	0.89	S

Table 2. Average percent dolomite, clay, quartz overgrowths (OG), feldspar overgrowths, and porosity for each county studied.

County	Average Dolomite	Average Clay	Average Quartz OG	Average Feldspar OG	Average Porosity
Ashtabula	15.3	4.5	3.7	0.1	6.1
Coshocton	17.8	2.1	4.7	0.3	8.2
Jackson	5.3	3.3	3.9	1.1	7.2
Scioto	2.5	5.3	1.4	3.7	8.3

Table 3. Summary of sandstone data sets for plot shown in Figure 110. Data are for the #2 Hammermill well in Erie County, Pennsylvania.

Depth (ft.)	Cement (%)	Intergranular Volume (%)	COPL(5)	CEPL (%)	CI
Core #1					
5104	22	32	19.2	17.7	0.52
5105	18	34	16.7	14.9	0.53
5106	22	32	19.2	17.7	0.52
5108	19	22	29.5	13.4	0.69
5110	16	18.7	32.3	10.8	0.75
5112	36	38	11.3	32.0	0.26
5112-5113	15	27	24.7	11.2	0.69
5113	17	28	23.6	13.0	0.64
5113-5116	17	23	28.6	12.1	0.7
5119	37	40	8.4	33.6	0.2
5130	28	30	21.4	21.9	0.49
Core #2					
5154	17.1	26.5	25.2	12.6	0.66
5154.5	13	26.9	24.8	9.7	0.72
5155	16	26	25.7	11.9	0.68
5156	15	24	27.7	10.7	0.72
5160	12	22	29.5	8.4	0.78
5161	13	24	27.7	9.3	0.75
5162	26	40	3.4	27.0	0.1
5163	26	36	14.1	22.2	0.39
5164	12	15	35.3	7.7	0.82
5165	10.7	28.7	22.9	8.2	0.74

COPL—compactional porosity loss

CEPL—cementational porosity loss

CI—compaction index=COPL/ (COPL+CEPL)

Table 4. Variations in Porosity for Sandstone Facies in the #2 Hammermill Well, Erie County, Pennsylvania.

Facies (environment)	Mean Porosity (%)	Standard Deviation (σ)
S	8.6	3.74
s (eolian)	2.85	0.15
s (fluvial)	9.83	2.9
M	8	4.7
Ms	13	3
Me	7.75	4.02
Md	6	4
All sandstones	8.38	4.18

Table 5. Examples of Rose Run sandstones that display the various combinations of porosity and permeability.

Core No.	Depth (ft.)	Porosity (%)	Permeability (md)
3260	6905.0	7.4–8.5	<.3
2989	6622.0	7.0–9.0	<.7
2898	4502.0	10.0–12.0	26-33
2898	4528.0	12.0–13.0	109-180
3260	6819.5	12.0–13.0	43.0
2989	6628.5	2.0	low
2852	5992.5	2.3	low
2898	4515.0	0.3	low

Table 6. Typical Seismic Reflection Processing Parameters

1. Demultiplex/Correlate Traces—True amplitude output	10. Normal moveout correction
2. Pre-processing—Trace editing	11. Pre-stick noise attenuation
Spread Geometry	12. Common depth point trim statics
Datum Statics @ approximately 9000'	13. Mute first breaks
3. Surface consistent Deconvolution—source and receiver	14. CDP stack
4. Spherical divergence gain	15. Migration (F/K, Kirchoff, or finite difference)
5. Spectral banding	16. Time-variant filter
6. Common depth point sort	17. Automatic Gain Control
7. Velocity analyses	18. Display normal and reverse polarities of stacked and migrated data
8. Surface consistent statistics	
9. Iterate steps 7 and 8	

Summary of Research Results

This study represents the results of two years of cooperative research on the Upper Cambrian Rose Run sandstone and adjacent units in eastern Ohio and western Pennsylvania by the Ohio Division of Geological Survey and the Pennsylvania Bureau of Topographic and Geologic Survey. These results include:

1. Three scales of heterogeneity occur within the Rose Run: megascopic, or global- to regional-scale; mesoscopic, or field- to well-scale; and microscopic, or thin-section scale.
2. Recurrent movement along basement-involved structures appears to have affected Cambrian deposition throughout the region. The more prominent structures include the Rome trough, Waverly arch, Grenville thrust sheets, the Akron-Suffield-Smith-Highlandtown-Pittsburgh-Washington fault system, the Cambridge cross-strike structural discontinuity, and the Tyrone-Mt. Union lineament. Many of these features appear to have occurred along pre-existing zones of weakness in the basement defined by Grenville thrust sheets.
3. Dolomitization of the overlying Black River Limestone in Ohio is often associated with faulting, and may have hydrocarbon potential associated with the porous and permeable dolomitized zones.
4. Geophysical log correlations, core descriptions, and seismic data indicate the major control of reservoir heterogeneity and hydrocarbon production in the Rose Run sandstone and Beekmantown/Mines dolomite is related to erosional truncation and paleotopography on the Knox unconformity.
5. Eight types of reservoir heterogeneity, as modified from Weber (1986), affected hydrocarbon production in the Rose Run sandstone and Beekmantown/Mines dolomite in varying proportions of importance. These types include sealing faults, boundaries between genetic units, permeability zonation within genetic units, baffles within genetic units, lamination and cross-bedding, microscopic heterogeneities, fracturing, and erosional truncation and paleotopography.
6. A number of lithofacies is present in the Rose Run. In Ohio, four lithofacies have been defined, including: 1) cross-bedded and flaser-bedded sandstone; 2) interbedded sandstone; 3) bioturbated dolostone; and 4) laminated dolostone. In Pennsylvania, these lithofacies could not be recognized. Instead, a set of generalized sandstone and dolostone lithofacies have been described. The cross-bedded and flaser-bedded sandstone lithofacies of Ohio has the best reservoir quality.
7. We have identified four types of traps in productive Rose Run sandstone Beekmantown/Mines dolomite reservoirs through subsurface mapping and seismic interpretation. These include: 1) erosional remnants sealed beneath impermeable strata; 2) fault-related traps; 3) combination fault-related and erosional remnants; and 4) erosional truncation (the Knox unconformity).
8. Erosional remnants, typically 80 acres or less, are the dominant reservoirs. Development and infill drilling of Rose Run pools are difficult because of the small areal extent of these remnant-related fields.
9. Exploration for these remnants has been met with some success through mapping leads on shallow horizons such as the "Packer Shell" (Silurian). This is evident along the entire subcrop trend. Thinning of Wells Creek/Shadow Lake interval and the Wells Creek/Shadow Lake-through-Trenton interval also is evident over these Knox/Gatesburg remnants.
10. In case studies, comparison of structure maps on the Knox unconformity, top of the Trenton, base of the "Packer Shell," and top of the Berea suggests reactivation of basement faults in the Holmes and Portage Counties area of Ohio.
11. Based on subsurface mapping in Ohio, the Rose Run and Copper Ridge/Ore Hill sandstones display two types of geometry, narrow channels and reworked widespread sheets. Historically, hydrocarbon production has been found only in the sheet sandstones, but recently there has been significant hydrocarbon production in the channel sandstones in Holmes County, Ohio.
12. Zones of solution-enlarged vuggy porosity in the Beekmantown/Mines dolomite, associated with paleotopographic highs, have yielded the best hydrocarbon production to date from the Rose Run subcrop play. This is shown by the Bakersville field in Coshocton County, Ohio, which has produced over 5.5 bcf of gas and 17,420 bbl of oil.

13. Based on examination of cores, secondary mineralization of dolomite affected lateral variations in these zones of solution-enlarged vuggy porosity.
14. Reprocessing of seismic data during this investigation indicates that additional steps of refraction statics and spectral whitening of migrated data made a dramatic improvement in the quality and interpretation of the data. In the Holmes County, Ohio seismic line, a phase rotation of 120° of migrated spectrally enhanced data yielded the best results.
15. Phase rotation of seismic data for attribute analyses resulted in a higher degree of correlation to synthetic seismograms generated from well data.
16. Based on attribute analyses of seismic data, color area plots of instantaneous phase, frequency, amplitude-envelope, and trace amplitude are good diagnostic tools for location of stratigraphic anomalies, fracturing, and hydrocarbon presence.
17. Modeling of VSP data by Schlumberger for this project (Puckett, 1992) indicates that zones of vuggy porosity can be recognized on seismic data as an increase in amplitude of the Beekmantown/Mines reflector. However, caution should be made in interpreting vuggy porosity from the seismic wavelet character. Stratigraphic changes in the thickness of Knox/Gatesburg units may also create similar seismic wavelet character.
18. Modeling of the VSP shows that the presence of gas in the Rose Run causes a four percent decrease in Rose Run velocity that results in a ten percent reduction of acoustic impedance. This amplitude variation of the Rose Run reflector is a diagnostic tool in predicting hydrocarbons in the reservoir.
19. Modeling of the VSP shows that the narrow channel sandstone in the Copper Ridge/Ore Hill interval can be recognized on seismic data. It is interpreted by a well-developed trough that occurs beneath the trough of the Rose Run sandstone interval.
20. Attribute analyses of a seismic line in Coshocton County, Ohio show that color display of instantaneous phase, instantaneous frequency, amplitude envelope, and trace amplitude are useful in diagnosing stratigraphic changes, fracturing, and hydrocarbon presence in the Knox/Gatesburg and adjacent units.
21. The most abundant cement in Rose Run sandstones is dolomite, which formed during two or more periods of dolomitization and plays an important role in permeability and porosity variability. Other cements present in the Rose Run include clay minerals, quartz overgrowths, and feldspar overgrowths.
22. Dolomitization was pervasive, and has obliterated nearly all of the original carbonate textures and textural features.
23. Local dissolution of dolomite and, to a lesser extent, feldspars and clays, created good to excellent porosity in many of the Rose Run sandstone beds and laminae. However, thin dolostones, dolomitic sandstones, argillaceous sandstones, and, less commonly, shales created barriers between the highly porous zones, thereby inhibiting vertical porosity.
24. Porous zones appear to be the result of dissolution along bedding planes. No single reason appears to explain why some zones were more permeable to the corrosive fluids than others, but grain size and sorting differences, the presence of clays and quartz overgrowths, and differences in mechanical compaction in adjacent laminae all may have influenced permeabilities prior to the leaching of the dolomite. Capillary pressure data from Pennsylvania demonstrate that microfractures can influence permeability.
25. Although hydrocarbon production has been limited primarily to the Rose Run subcrop, porosity and permeability data indicate good potential exists at least 30 to 40 miles downdip from the subcrop in southeastern Ohio. Hydrocarbon exploration for Rose Run reservoirs should be good in the deeper parts of the basin in Ohio in areas with favorable structure.
26. The Rose Run sandstone underwent a long and complicated burial and diagenetic history. The burial and diagenetic sequence is interpreted as follows:
 - 1) burial of siliciclastic and interbedded carbonates;
 - 2) silica and feldspar overgrowths with dissolution of calcite;
 - 3) dolomitization prior to the formation of the Knox unconformity;
 - 4) dissolution of dolomite by meteoric water and/or basinal brines during the creation of the Knox unconformity;
 - 5) formation of clays;
 - 6) reflective chemical compaction and pressure solution;
 - 7) dolomitization after deep burial with creation of type 2 and type 6 dolomite, and some replacement of clays by dolomite;
 - 8) leaching of feldspars and clays; and
 - 9) formation of pyrite.

References

- Adams, A.E., MacKenzie, U.S., and Guilford, C., 1984, Atlas of Sedimentary Rocks Under the Microscope. Halstead Press, New York, 104 p.
- Aitken, J.D., 1966, Middle Cambrian to Middle Ordovician cyclic sedimentation, southern Rock Mountains of Alberta. Canadian Petroleum Geology bulletin, v. 14, p. 405–441.
- Amthor, J.E., and Friedman, G.M., 1992, Early- to late-diagenetic dolomitization of platform carbonates: Lower Ordovician Ellenburger Group, Permian Basin, West Texas. Journal of Sedimentary Petrology, v. 62, p. 131–144.
- Anderson, W.H., 1991, Mineralization and hydrocarbon emplacement in the Cambrian-Ordovician Mascot Dolomite of the Knox Group in south-central Kentucky. Kentucky Geological Survey Report of Investigation no. 4, 31 p.
- Asquith, G.B., 1985, Handbook of log evaluation techniques for carbonate reservoirs. American Association of Petroleum Geologists Methods in Exploration Series no. 5, 47 p.
- A.T. Kearney, Inc., 1991, Unpublished Rose Run/Copper Ridge report, prepared for Aristech Chemical Corporation, vol. II, Appendices A–K, 137 p.
- Atha, T. M., 1981, A subsurface study of the Cambro-Ordovician Rose Run sandstone in eastern Ohio. Unpublished M.S. thesis, Ohio University, 81 p.
- Baker, G. F., 1974, Petrology and diagenesis of the Mt. Simon and Rose Run sandstones in West Virginia and southeastern Ohio. Unpublished M.S. thesis, West Virginia University, 64 p.
- Ball, M.M., 1967, Carbonate sand bodies of Florida and the Bahamas. Journal of Sedimentary Petrology, v. 43, p. 812–821.
- Baranoski, M.T., 1989, Another opinion about the origin of the Cambridge Arch of southeastern Ohio (abs.). Ohio Geological Society, November, 1989 Geogram.
- Baranoski, M.T., 1993, Regional tectonic features affecting the Knox Group including the Rose run sandstone in eastern Ohio and adjacent areas (abs.), in Innovative concepts in reservoir characterization. 24th Annual Appalachian Petroleum Geology Symposium, Morgantown, WV, I.C. White Memorial Fund Publication 5, p. 2.
- Baranoski, M.T., and Riley, R.A., 1988, Analysis of stratigraphic and production relationships of Devonian-shale gas reservoirs in Lawrence County, Ohio. Ohio Division of Geological Survey Open-file Report 88–2, 30 p.
- Baranoski, M.T., and Riley, R.A., in press, Analysis of stratigraphic, structural and production relationships of Devonian-shale gas reservoirs in Monroe, Noble, and Washington Counties, Ohio. Ohio Division of Geological Survey Report of Investigations.
- Bathurst, R.G., 1975, Carbonate Sediments and Their Diagenesis, 2nd ed. Elsevier Scientific Publishing Co., Amsterdam, Developments in Sedimentology 12, 658 p.
- Beadsley, R.W., 1992, Overview of the evolution of the Appalachian basin (oral presentation). Appalachian Energy Group Conference, Columbus, OH, June 15, 1992.
- Beadsley, R.W., and Cable, M.S., 1983, Overview of the evolution of the Appalachian basin. Northeastern Geology, v. 5, p. 137–145.
- Bentor, Y.K., and Kastner, M., 1965, Notes on the mineralogy and origin of glauconite. Journal of Sedimentary Petrology, v. 35, p. 155–166.
- Borer, J.M., and Harris, P.M., 1991, Depositional facies and model for mixed siliciclastics and carbonates of the Yates Formation, Permian Basin, in Lomando, A.J., and Harris, P.M., eds, Mixed carbonate-siliciclastic sequences. SEPM Core Workshop 15, Dallas, TX, April 7, 1991, p. 1–134.
- Bracewell, R., 1965, The Fourier Transform and its applications. McGraw-Hill Book Company, New York, 444 p.
- Butts, C., 1918, Geologic section of Blair and Huntington Counties, central counties, central Pennsylvania. American Journal of Science, 4th ser., v. 46, p. 523–537.
- Butts, C., 1945, Hollidaysburg-Huntington, Pennsylvania. U.S. Geological Survey Folio 227, 20 p.
- Butts, C., and Moore, E.S., 1936, Geology and mineral resources of the Bellefonte quadrangle, Pennsylvania. U.S. Geological Survey Bulletin 855, 111 p.
- Calvert, W.L., 1962, Sub-Trenton rocks from Lee County, Virginia, to Fayette County, Ohio: Ohio Geological Survey Report of Investigations 45, 57 p.
- Canich, M.R., and Gold, D.P., 1977, A study of the Tyrone-Mt. Union lineament by remote sensing techniques and field methods. Office of Remote Sensing and Earth Resources (ORSER) Technical Report 12–77, Pennsylvania State University, State College, PA, 59 p.
- Canich, M.R., and Gold, D.P., 1985, Structural features in the Tyrone-Mt. Union lineament, across the Nittany Anticlinorium in central Pennsylvania, in Gold, D.P., and others, Central Pennsylvania Revisited. Guidebook, 50th Annual Field Conference of Pennsylvania Geologists, State College, PA, p. 120–137.
- Chaffin, D.L., 1981, Implications of regional gravity and magnetic data for structure beneath western Pennsylvania. Unpublished MS thesis, Pennsylvania State University, 72 p.
- Chavetz, H. S., 1969, Carbonates of the Lower and Middle Ordovician in central Pennsylvania. Pennsylvania Geological Survey, 4th ser., General Geology Report 58, 39 p.

- Choquette, P.W., and Pray, L.C., 1970, Geologic nomenclature and classification of porosity in sedimentary carbonates. *American Association of Petroleum Geologists Bulletin*, v. 54, p. 207–250.
- Clark, V., 1992, The effect of oil under in-situ conditions on the seismic properties of rocks. *Geophysics*, v. 57, p. 894–901.
- Clarke, J. M., and Schuchert, C., 1899, The nomenclature of the New York series of geological formations. *Science, new ser.*, v. 10, p. 874–878.
- Colton, G.W., 1970, The Appalachian basin—its depositional sequences and their geologic relationships, *in* Fisher, G. W., and others, eds., *Studies of Appalachian Geology: Central and Southern*. Interscience Publishers, New York, p. 5–47.
- Culotta, R.C., Pratt, T., Oliver, J., and Kaufman, S., 1990, A tale of two sutures: COCORP deep seismic surveys of the Grenville province in the eastern U.S. midcontinent: *Geology*, v. 18, p. 646–649.
- Davies, G.R., 1970, Carbonate bank sedimentation, eastern Shark Bay, Western Australia, *in* Logan, B.W., and others, *Carbonate sedimentation and environments, Shark Bay, western Australia*. American Association of Petroleum Geologists Memoir 13, p. 85–168.
- Davis, W.F., 1980, Two methods of automatic depth determination applied to a study of the magnetic basement of western Pennsylvania. Unpublished M.S. thesis, Pennsylvania State University, 72 p.
- Demico, R.V., 1985, Patterns of platform and off-platform carbonates of the Upper Cambrian of western Maryland. *Sedimentology*, v. 32, p. 1–22.
- Desrochers, A., and James, N.P., 1988, Early Paleozoic surface and subsurface paleokarst; Middle Ordovician carbonates, Mingan Islands, Quebec, *in* James, N.P., and Choquette, P.W., eds., *Paleokarst*. Springer-Verlag, New York, p. 183–210.
- Dewey, J. F., and Bird, J. M., 1970, Mountain belts and the new global tectonics. *Journal of Geophysical Research*, v. 75, p. 2625–2647.
- Dickinson, W.R., Beard, L.S., Brackenkridge, G. R., and others, 1983, Provenance of North American Phanerozoic sandstones in relation to tectonic setting. *Geological Society of America Bulletin*, v. 94, p. 222–235.
- Dickinson, W.R., and Suczek, C.A., 1979, Plate tectonics and sandstone compositions. *American Association of Petroleum Geologists Bulletin*, v. 63, p. 2164–2182.
- Dietz, R.S., 1972, Geosynclines, mountains, and continent building. *Scientific American*, v. 226, no. 3, p. 30–38.
- Dolly, E.D., and Busch, D.A., 1972, Stratigraphic, structural, and geomorphologic factors controlling oil accumulation in Upper Cambrian strata of central Ohio. *American Association of Petroleum Geologists Bulletin*, v. 56, p. 2335–2368.
- Dott, R. H., and Batten, R. L., 1976, *Evolution of the Earth*, 2d ed. McGraw-Hill Book Co., New York, 504 p.
- Drahovzal, J.A., Harris, D.C., Wickstrom, L.H., Walker, D., Baranoski, M.T., Keith, B., and Furer, L.C., 1992, The East Continent rift basin: A new discovery. Ohio Division of Geological Survey Information Circular 57, 25 p.
- Dunn, T.L., and Surdam, R.C., 1989, Recognizing the influence of burial history and diagenesis on reservoir heterogeneity. *Proceedings of the Fifth Annual Enhanced Oil Recovery Symposium*, p. 47–59.
- Enterline, D.S., 1991, Depositional environments of the Cambro-Ordovician Rose Run formation in N.E. Ohio and equivalent, Gatesburg Formation in N.W. Pennsylvania. Unpublished M.S. thesis, University of Akron, 163 p.
- Fettke, C.R., 1948, Subsurface Trenton and sub-Trenton rocks in Ohio, New York, Pennsylvania and West Virginia. *American Association of Petroleum Geologists Bulletin*, v. 32, p. 1457–1492.
- Flagler, C.W., 1966, Subsurface Cambrian and Ordovician stratigraphy of the Trenton Group-Precambrian interval in New York State. New York State Museum and Science Service, Map and Chart Series 8.
- Fleischer, M., Wilcox, R.E., and Matzko, J.J., 1984, Microscopic determination of the nonopaque minerals. *U.S. Geological Survey Bulletin* 1627, 453 p.
- Folk, R.L., and Pittman, J.S., 1971, Length-slow chalcedony: A new testament for vanished evaporites. *Journal of Sedimentary Petrology*, v. 41, p. 1045–1058.
- Freeman, L.B., 1949, Regional aspects of Cambrian and Ordovician subsurface stratigraphy in Kentucky. *American Association of Petroleum Geologists Bulletin*, v. 22, p. 1655–1681.
- Ginsburg, R.N., 1982, Actualistic depositional models for the Great American Bank (Cambro-Ordovician) (abs.). *International Association of Sedimentologists, 11th International Congress on Sedimentology, Abstracts*, Hamilton, Ontario, p. 114.
- Goldring, R. and Bridges, P., 1973, Sublittoral sheet sandstones. *Journal of Sedimentary Petrology*, v. 43, p. 736–747.
- Gray, J.D., Struble, R.A., Carlton, R.W., and others, 1982, An integrated study of the Devonian-age black shales in eastern Ohio. U.S. Department of Energy, DOE/ET/12131–1399, p. 1.1–8.5.
- Green, D.A., 1957, Trenton structure in Ohio, Indiana, and northern Illinois. *American Association of Petroleum Geologists Bulletin*, v. 41, p. 672–642.
- Handford, C.R., and Francka, B.J., 1991, Mississippian carbonate-siliciclastic eolianites in southwestern Kansas, *in* Lomando, A.J., and Harris, P.M., eds., *Mixed carbonate-siliciclastic sequences*. SEPM Core Workshop 15, Dallas, TX, April 7, 1991, p. 205–243.
- Hardie, L.A., 1986, Ancient carbonate tidal-flat deposits, *in* Hardie, L.A., and Shinn, E.A., *Carbonate Depositional Environments, Modern and Ancient, Part 3: Tidal Flats*. *Colorado School of Mines Quarterly*, v. 81, no. 1, p. 37–57.

- Hardie, L.A., 1987, Dolomitization: A critical view of some current views. *Journal of Sedimentary Petrology*, v. 57, p. 166–183.
- Harding, T.P., and Lowell, J.D., 1979, Structural styles in petroleum provinces. *American Association of Petroleum Geologists Bulletin*, v. 63, p. 1016–1058.
- Harper, J.A., 1989, Effects of recurrent tectonic patterns on the occurrence and development of oil and gas resources in western Pennsylvania. *Northeastern Geology*, v. 11, p. 225–245.
- Harper, J.A., 1991, Preliminary assessment of the stratigraphy and structure of the Cambro-Ordovician carbonate sequence in western Pennsylvania, in *Exploration strategies in the Appalachian basin*. 22nd Annual Appalachian Petroleum Geology Symposium, Morgantown, WV, I.C. White Memorial Fund Pub. 3, p. 30–32.
- Harper, J.A., 1992, Possible basement influence on glaciation in NW Pennsylvania and adjacent areas (abs.). *Geological Society of America, Abstracts with Programs*, v. 24, no. 3, p. 27.
- Harper, J.A., Kelley, D.R., and Linn, E.H., in press, Deep oil and natural gas, in Shultz, C.H., ed., *The Geology of Pennsylvania*. Pennsylvania Geological Survey, 4th ser., Special Publication 1, Chapter 38B.
- Harper, J.A., and Laughrey, C.D., 1987, Geology of the oil and gas fields of southwestern Pennsylvania. Pennsylvania Geological Survey, 4th ser., Mineral Resource Report 87, 166 p.
- Harris, A.G., and Repetski, J.E., 1982, Conodonts revise the Lower-Middle Ordovician boundary and timing of miogeoclinal events in the east-central Appalachian basin (abs.). *Geological Society of America, Abstracts with Programs*, v. 14, no. 5, p. 261.
- Harris, L.D., 1978, The eastern interior aulacogen and its relation to Devonian shale gas production. Preprints, Second Eastern Gas Shales Symposium, METC/SP-78/6, v. II, p. 55–72.
- Hayes, J.B., 1979, Sandstone diagenesis—the hole truth, in Scholle, P.A., and Schluger, P.R., eds., *Aspects of diagenesis*. Society of Economic Paleontologists and Mineralogists Special Publication 26, p. 127–139.
- Heald, M. T., and G. F. Baker, 1977, Diagenesis of the Mt. Simon and Rose Run sandstones in western West Virginia and southern Ohio. *Journal of Sedimentary Petrology*, v. 47, p. 66–77.
- Heinrich, E.W., 1965, *Microscopic Identification of Minerals*. McGraw-Hill Book Co., New York, 414 p.
- Hine, A.C., 1977, Lily Bank, Bahamas: History of an active oolite sand shoal. *Journal of Sedimentary Petrology*, v. 47, p. 1554–1582.
- Hoffman, P., Dewey, J.F., and Burke, K., 1974, Aulacogens and their genetic relationship to geosynclines, with a proterozoic example from Great Slave Lake, Canada, in Dott, R.H., and Shaver, R.H., eds., *Modern and ancient geosynclinal sedimentation*, Society of Economic Paleontologists and Mineralogists Special Publication 19, p. 38–55.
- Houseknecht, D.W., 1987, Assessing the relative importance of compaction processes and cementation to reduction of porosity in sandstones. *American Association of Petroleum Geologists Bulletin*, v. 71, p. 633–642.
- Jacobi, R.D., 1981, Peripheral bulge—A causal mechanism for the Lower/Middle Ordovician unconformity along the western margin of the northern Appalachians. *Earth and Planetary Science Letters*, v. 56, p. 245–251.
- Janssens, A., 1973, Stratigraphy of the Cambrian and Lower Ordovician rocks in Ohio. *Ohio Division of Geological Survey Bulletin* 64, 197 p.
- Janssens, A., 1992, Oil and gas from Rose Run sandstone and Beekmantown dolomite in Ohio (oral presentation). 1992 Ohio Oil and Gas Association Winter Meeting, Columbus, Ohio, March 11, 1992, 13 p.
- Jennings, J.B., 1987, Capillary pressure techniques: Application to exploration and development geology. *American Association of Petroleum Geologist Bulletin*, v. 71, p. 1196–1209.
- Johnson, H.D., 1978, Shallow siliciclastic seas, in Reading, H.G., ed., *Sedimentary Environments and Facies*. Elsevier, New York, p. 207–258.
- Kay, G.M., 1944, Middle Ordovician of central Pennsylvania: *Journal of Geology*, v. 52, p. 1–23, 97–116.
- Kendall, A.C., 1984, Evaporites, in Walker, R. G., ed., *Facies Models*, 2d ed. Geoscience Canada, Reprint Series 1, p. 259–296.
- Klein, G. de V., 1977, *Clastic Tidal Facies*. Continuing Education Publishing Company, Inc., Champaign, IL, 149 p.
- Knowles, R.R., 1966, Geology of a portion of the Everett 15-minute quadrangle, Bedford County, Pennsylvania: Pennsylvania Geological Survey, 4th ser., Progress Report 170, 90 p.
- Krynine, P.D., 1946, From the Cambrian to the Silurian near State College and Tyrone. 12th Annual Field Conference of Pennsylvania Geologists, State College, PA, 32 p.
- Kulander, B.R., and Dean, S.L., 1978, Gravity, magnetics, and structure of the Allegheny Plateau-western Valley and Ridge in West Virginia and adjacent states. *West Virginia Geological and Economic Survey, Report of Investigations* 27, 91 p.
- Lavin, P.M., Chaffin, D.L., and Davis, W.F., 1982, Major lineaments and the Lake Erie-Maryland crustal block. *Tectonics*, v. 1, p. 431–440.
- Laughrey, C.D., in press, Oil and gas reservoir rocks of Pennsylvania. Pennsylvania Geological Survey, 4th ser., Mineral Resource Report.
- Laughrey, C.D., and Harper, J. A., 1986, Comparisons of Upper Devonian and Lower Silurian tight formations in Pennsylvania—geological and engineering characteristics, in Spencer, C.W., and Mast, R.F., eds., *Geology of tight gas reservoirs*. American Association of Petroleum Geologists Studies in Geology 24, p. 9–43.
- Lees, J.A., 1967, Stratigraphy of the Lower Ordovician Axemann Limestone in central Pennsylvania. Pennsylvania Geological Survey, 4th ser., General Geology Report 52, 79 p.

- Lidiak, E.G., and Ceci, V.M., 1991, Authigenic K-feldspar in the Precambrian basement of Ohio and its effect on tectonic discrimination of the granitic rocks. *Canadian Journal of Earth Sciences*, v. 28, p. 1624–1634.
- Logan, B.W., Rezak, R., and Ginsburg, R.N., 1964, Classification and significance of algal stromatolites. *Journal Geology*, v. 72, p. 1–83.
- Lomando, A.J., and Harris, P.M., 1991, Preface, in Lomando, A.J., and Harris, P.M., eds, Mixed carbonate-siliciclastic sequences. SEPM Core Workshop 15, Dallas, TX, April 7, 1991, 569 p.
- Longman, M.W., 1980, Carbonate diagenetic textures from near-surface diagenetic environments. *American Association of Petroleum Geologists Bulletin*, v. 64, p. 461–487.
- Lundegard, P.D., 1992, Sandstone porosity loss—a “big picture” view of the importance of compaction. *Journal of Sedimentary Petrology*, v. 62, p. 250–260.
- Lytle, W.S., Heyman, L., Kelley, D.R., and Wagner, W.R., 1971, Future Petroleum potential of western and central Pennsylvania, in Cram, I.H., ed., Future petroleum provinces of the United States—their geology and potential. *American Association of Petroleum Geologists Memoir* 15, v. 2, p. 1232–1242.
- Markello, J.R., and Read, J.F., 1981, Carbonate ramp-to-deeper shale shelf transitions of an Upper Cambrian intrashelf basin, Nolichucky Formation, southwest Virginia Appalachians. *Sedimentology*, v. 28, p. 573–597.
- Markello, J.R., and Read, J.F., 1982, Upper Cambrian intra-shelf basin, Nolichucky Formation, southwest Virginia Appalachians. *American Association of Petroleum Geologists Bulletin*, v. 66, p. 860–878.
- Mazzullo, S.J., and Harris, P.M., 1992, Mesogenetic dissolution: Its role in porosity development in carbonate reservoirs. *American Association of Petroleum Geologists Bulletin*, v. 76, p. 607–620.
- McCormac, M.P., 1992, 1991 Ohio Oil and Gas Developments “The Debrosse Report,” presented at the winter meeting of the Ohio Oil and Gas Association, March 11, 1992, Columbus, Ohio, 34 p.
- McGuire, W.H., and Howell, P., 1963, Oil and gas possibilities of the Cambrian and Lower Ordovician in Kentucky. Lexington, KY, Spindletop Research Center, 216 p.
- Miall, A.D., 1984, *Principals of Sedimentary Basin Analysis*. Springer-Verlag, New York, 490 p.
- Morgan, J.T., and Gordon, D.T., 1970, Influence of pore geometry on water-oil relative permeability. *Journal of Petroleum Technology*, v. 22, p. 1199–1200.
- Mussman, W.J., and Read, J.F., 1986, Sedimentology and development of a passive- to convergent-margin unconformity: Middle Ordovician Knox unconformity, Virginia Appalachians. *Geological Society of America Bulletin*, v. 97, p. 282–295.
- Mussman, W.J., Montanez, I.P., and Read, J.F., 1988, Ordovician Knox paleokarst unconformity, Appalachians, in James, N.P. and Choquette, P.W., eds., *Paleokarst*. Springer-Verlag, New York, p. 211–229.
- Neidell, and Poggiagliolmi, 1977, Stratigraphic modelling and interpretation—Geophysical principles and Techniques, in Payton, C.E., ed., *Seismic Stratigraphy—Applications to hydrocarbon exploration*. *American Association of Petroleum Geologists Memoir* 26, p. 389–416.
- NuCorp Energy Company, 1977, NuCorp Energy Company’s Cambro-Ordovician Prospect well, #1 Trepanier report, compiled by Thomas P. Sanders and Wayne Bears, prepared for OEROA, contract no. 76-3, 27 p.
- Orton, E., 1890, First annual report of the Geological Survey of Ohio (Third Organization). Columbus, OH, 323 p.
- Osleger, D., and Read, J.F., 1991, Relation of eustasy to stacking patterns of meter-scale carbonate cycles, Late Cambrian, U.S.A. *Journal of Sedimentary Petrology*, v. 61, p. 1225–1252.
- Palmer, A. R., 1983, The Decade of North American Geology 1983 geologic time scale. *Geology*, v. 11, p. 503–504.
- Parrish, J.B., and Lavin, P.M., 1982, Tectonic model for kimberlite emplacement in the Appalachian Plateau of Pennsylvania. *Geology*, v. 10, p. 344–347.
- Pelto, C.R., 1942, *Petrology of the Gatesburg Formation of central Pennsylvania*. Unpublished M.S. thesis, Pennsylvania State University, 60 p.
- Pettijohn, F.J., Potter, P.E., and Siever, R., 1973, *Sand and Sandstone*. Springer-Verlag, New York, 618 p.
- Pfeil, R.W., and Read, J.F., 1980, Cambrian carbonate platform margin facies, Shady Dolomite, southwestern Virginia, U.S.A. *Journal of Sedimentary Petrology*, v. 50, p. 91–116.
- Pittman, E.D., 1979, Porosity, diagenesis and productive capability of sandstone reservoirs, in Scholle, P.A., and Schluter, P.R., eds., *Aspects of Diagenesis*. Society of Economic Paleontologists and Mineralogists Special Publication 26, p. 159–173.
- Powers, M.C., 1959, Adjustment of clays to chemical change and the concept of equivalence level, in Swineford, A., ed., *Clays and clay minerals*. International Series of Monographs on Earth Sciences, v. 2, p. 309–326.
- Puckett, Mark, 1992, Borehole Seismic report for Reiss #3-A well in Coshocton County, Ohio. Schlumberger Technical Report prepared for the Ohio Division of Geological Survey, 10 p.
- Rankin, D.W., 1976, Appalachian salients and recesses: Late Precambrian continental breakup and the opening of the Iapetus Ocean. *Journal of Geophysical Research*, v. 81, p. 5605–5619.
- Read, J.F., 1980, Carbonate ramp-to-basin transitions and foreland basin evolution, Middle Ordovician, Virginia Appalachians. *American Association of Petroleum Geologists Bulletin*, v. 64, p. 1575–1612.

- Read, J.F., 1989, Controls on evolution of Cambrian—Ordovician passive margin, U.S. Appalachians, in Crevello, P.D., and others, eds., Controls on carbonate platform and basin development. Society of Economic Paleontologists and Mineralogists Special Publication 44, p. 147–165.
- Reading, H.G., ed., 1978, Sedimentary Environments and Facies. Blackwell Scientific Publications, Oxford, 557 p.
- Reeckmann, A., and Friedman, G.M., 1982, Exploration for Carbonate Petroleum Reservoirs. Wiley-Interscience Publications, New York, 213 p.
- Reineck, H.E., and Wunderlich, F., 1968, Classification and origin of flaser and lenticular bedding. *Sedimentology*, v. 11, p. 99–104.
- Reservoirs, Inc., 1992, Geological evaluation of rotary sidewall cores from the Beekmantown/Rose Run/Copper Ridge Formations, NGO–D,CRA,ODNR Reiss no. 3-A Coshocton County, Ohio. Unpublished report prepared for the Ohio Department of Natural Resources, 9 p.
- Rickard, L.V., 1973, Stratigraphy and structure of the subsurface Cambrian and Ordovician carbonates of New York. New York State Museum and Science Service, Map and Chart Series 18, 26 p.
- Riley, R.A., and Baranoski, M.T., 1991, Regional stratigraphy of the Rose Run sandstone in Ohio (abs.), in Exploration strategies in the Appalachian basin. 22nd Annual Appalachian Petroleum Geology Symposium, Morgantown, WV, I.C. White Memorial Fund Pub. 3, p. 82.
- Rodgers, M.R., and Anderson, T.H., 1984, Tyrone-Mt. Union cross-strike lineament of Pennsylvania: A major Paleozoic basement fracture and uplift boundary. *American Association of Petroleum Geologists Bulletin*, v. 68, p. 92–105.
- Root, S.I., 1964, Cyclicity of the Conococheague Formation. *Pennsylvania Academy of Science Proceedings*, v. 38, p. 157–160.
- Root, S.I., 1986, The Suffield fault, Stark County, Ohio. *Ohio Journal of Science*, v. 86, no. 4, p. 161–163.
- Roth, B., 1992, Seismic Modeling of Ordovician Rose Run/Beekmantown dolomite oil and gas traps in east-central Ohio. Unpublished M.S. thesis, Wright State University, 84 p.
- Ryder, R.T., 1989, Stratigraphic framework of Cambrian and Ordovician rocks in the central Appalachian basin of West Virginia and adjoining states (abs.), in Horizontal and inclined drilling in the Appalachian Basin. 20th Annual Appalachian Petroleum Geology Symposium, Program and Abstracts, West Virginia Geological and Economic Survey Circular 44, p. 69–73.
- Ryder, R.T., 1992, Stratigraphic framework of Cambrian and Ordovician rocks in the central Appalachian basin from Morrow County, Ohio, to Pendleton County, West Virginia. *U.S. Geological Survey Bulletin* 1839–G, 25 p.
- Ryder, R.T., in press, The Knox unconformity and adjoining strata, western Morrow County, Ohio, in Shafer, W.E., ed., Morrow County, Ohio. Ohio Geological Society.
- Ryder, R.T., Harris, A.G., and Repetski, J.E., 1992, Stratigraphic framework of Cambrian and Ordovician rocks in central Appalachian basin from Medina County, Ohio—through southwestern and south-central Pennsylvania—to Hampshire County, West Virginia. *U.S. Geological Survey Bulletin* 1839–K, 32 p.
- Safford, J. M., 1869, *Geology of Tennessee*, Nashville, TN, 550 p.
- Sanders, T.P. and Bears, W., 1977, Cambro-Ordovician prospect well, #1 Trepanier. Unpublished report prepared by NUCORP Energy, OERDA Grant 76–3, 27 p.
- Schmidt, V., and McDonald, D.A., 1979, Texture and recognition of secondary porosity in sandstone, in Scholle, P.A., and Schluger, P.R., eds., Aspects of Diagenesis. Society of Economic Paleontologists and Mineralogists Special Publication 26, p. 209–225.
- Scholle, P.A., 1978, Carbonate rock constituents, textures, cements, and porosities. *American Association of Petroleum Geologists Memoir* 27, 228 p.
- Scotese, C.R., and McKerrow, W.S., 1991, Ordovician plate tectonic reconstructions, in Barnes, C.R., and Williams, S.H., eds., Advances in Ordovician Geology. Geological Survey of Canada, Paper 90–9, p. 271–282.
- Segonzac, G.D., 1970, The transformation of clay minerals during diagenesis and low-grade metamorphism: A review. *Sedimentology*, vol. 15, p. 281–346.
- Shearrow, G.G., 1987, Maps and cross sections of the Cambrian and Lower Ordovician in Ohio. Ohio Geological Society, 31 p.
- Sheriff, R.E., 1977, Limitations on resolution of seismic reflections and geologic detail derivable from them, in Payton, C.E., ed., Seismic stratigraphy—applications to hydrocarbon exploration. *American Association of Petroleum Geologists Memoir* 26, p. 3–14.
- Sheriff, R.E., 1982, *Encyclopedic Dictionary of Exploration Geophysics*. Society of Exploration Geophysicists. 266 p.
- Shinn, E.A., 1980, (talk summary by Horowitz, D.H., 1981), in Byers, C.W., and Dott, R.H., SEPM Research Conference on modern shelf and ancient cratonic sedimentation—the orthoquartzite-carbonate suite revisited. *Journal of Sedimentary Petrology*, v. 51, p. 329–397.
- Shinn, E.A., 1983, Tidal flat environment, in Scholle, P.A., and others, eds., Carbonate depositional environments. *American Association of Petroleum Geologists Memoir* 33, p. 171–211.
- Sibley, D.F., and Gregg, J.M., 1987, Classification of dolomite rock textures. *Journal of Sedimentary Petrology*, v. 57, p. 967–975.
- Smith, R.E., 1969, Petrography-porosity relations in carbonate-quartz system, Gatesburg Formation (Late Cambrian), Pennsylvania. *American Association of Petroleum Geologists Bulletin*, v. 57, p. 261–278.
- Starkey, H.C., Blackmon, P.O., and Hauff, P.L., 1985, The routine mineralogical analysis of clay-bearing samples. *U.S. Geological Survey Bulletin* 1563, 31 p.

- Swanson, R.G., 1981, Sample Examination Manual. American Association of Petroleum Geologists, Methods in Exploration Series.
- Taner, M.T., and Sheriff, R.E., 1977, Application of amplitude, frequency, and other attributes to stratigraphic and hydrocarbon determination, *in* Payton, C.E., ed., Seismic stratigraphy—applications to hydrocarbon exploration. American Association of Petroleum Geologists Memoir 26, p. 301–328.
- Thomas, W.A., 1977, Evolution of the Appalachian-Ouachita salients and recesses from reentrants and promontories in the continental margin. *American Journal of Science*, v. 277, p. 1233–1278.
- Tucker, M.E., 1981, Sedimentary Petrology: An Introduction. Halsted Press, New York, 252 p.
- Tucker, K.E., and Chalcraft, R.G., 1991, Cyclicity in the Permian Queen Formation-U.S.M. Queen field, Pecos County, Texas, *in* Lomando, A.J., and Harris, P.M., eds, Mixed carbonate-siliciclastic sequences. SEPM Core Workshop 15, Dallas, TX, April 7, 1991, p. 385–428.
- Wagner, W.R., 1961, Subsurface Cambro-Ordovician stratigraphy of northwestern Pennsylvania and bordering states. Pennsylvania Geological Survey, 4th ser., Progress Report 156, 22 p.
- Wagner, W.R., 1966a, Exploration for hydrocarbons in the Cambrian rocks of northwestern Pennsylvania. *in* Petroleum geology of the Appalachian Basin. 25th Technical Conference on Petroleum Production, Proceedings, University Park, PA, October 19–21, 1966, p. 75–95.
- Wagner, W.R., 1966b, Pennsylvanians must delve into rocks of ancient age. *Oil and Gas Journal*, v. 64, no. 50, p. 152–158.
- Wagner, W.R., 1966c, Stratigraphy of the Cambrian to Middle Ordovician rocks of central and western Pennsylvania. Pennsylvania Geological Survey, 4th ser., General Geology Report 49, 156 p.
- Wagner, W.R., 1976, Growth faults in Cambrian and Lower Ordovician rocks of western Pennsylvania. *American Association of Petroleum Geologists Bulletin*, v. 60, p. 414–427.
- Walker, R.G., 1979, Facies models. Geological Association of Canada Publications, 211 p.
- Weber, K.J., 1986, How heterogeneity affects oil recovery, *in* Lake, L.W. and Carroll, Jr., H.B., ed., Reservoir characterization. Academic Press, Inc., Florida, p. 487–545.
- Wescott, W.A., 1982, Nature of porosity in Tuscarora sandstone (Lower Silurian) in the Appalachian Basin. *Oil and Gas Journal*, v. 80, no. 34, p. 159–173.
- Wheeler, R.L., 1980, Cross-strike structural discontinuities: Possible exploration tool for natural gas in Appalachian overthrust belt. *American Association of Petroleum Geologists Bulletin*, v. 64, p. 2166–2178.
- Wickstrom, L.H. and Gray, J.D., 1988, Geology of the Trenton Limestone in northwestern Ohio, *in* Keith, B.D., ed., The Trenton Group (Upper Ordovician Series) of eastern North America—deposition, diagenesis, and petroleum. American Association of Petroleum Geologists Studies in Geology 29, p. 159–172.
- Wilde, P., 1991, Oceanography in the Ordovician, *in* Barnes, C. R., and Williams, S. H., eds., Advances in Ordovician Geology. Geological Survey of Canada, Paper 90–9, p. 283–298.
- Wilson, J.L., 1952, Upper Cambrian stratigraphy in the central Appalachians. *Geological Society of America Bulletin*, v. 63, p. 275–322.
- Wilson, J.L., 1975, Carbonate Facies in Geologic History. Springer-Verlag, New York, 471 p.
- Wilson, J.L., 1983, Middle shelf environment, *in* Scholle, P.A., and others, eds., Carbonate depositional environments. American Association of Petroleum Geologists Memoir 33, p. 297–345.
- Wilson, M.D., and Pittman, E., 1977, Authigenic clays in sandstone: Recognition and influence on reservoir properties. *Journal of Sedimentary Petrology*, v. 47, p. 3–31.
- Woodward, H.P., 1961, Preliminary subsurface study of southeastern Appalachian Interior Plateau. *American Association of Petroleum Geologist Bulletin*, v. 45, p. 1634–1655.
- Zietz, I., Gilbert, F.P., and Kirby, J.R., 1980, Aeromagnetic map of Delaware, Maryland, Pennsylvania, West Virginia, and parts of New Jersey and New York. U.S. Geological Survey Geophysical Investigations Map GP-927.

Appendices

Appendix I:
Summary of Current Methodology

General

Various rock units from the top of the Precambrian (Grenvillian) to the Berea Sandstone (Upper Devonian or Lower Mississippian) were correlated for geologic mapping purposes in selected fields, with emphasis placed on the Rose Run and adjacent units such as the "B" zone in the Copper Ridge/Ore Hill dolomite of Ohio (Figure 4). These correlations are very important for mapping structure on the Knox because the "B" zone is the only marker within the Knox Group below the Rose Run that can be correlated over long distances in the subsurface using geophysical logs. Study of Appalachian basin architecture during Cambrian and Ordovician time requires mapping of units deeper than the Rose Run. Drill cuttings from southern Ohio, and drill-cutting descriptions throughout western Pennsylvania, supplemented geophysical logs as an aid in documenting stratigraphic variations within the Knox/Gatesburg interval. Detailed mapping in five field-scale areas, tied in with production data (Appendix VI), helped understand the influence of heterogeneity on production.

The Ohio Division of Geological Survey, in cooperation with NGO Development Corp. and Consolidated Resources of America, participated in a cooperative reservoir evaluation program of a Rose Run/Beekmantown/Mines well in Adams Township, Coshocton County, Ohio (the #3-A Reiss well, Ohio permit no. 6379). Schlumberger Well Services performed sidewall coring, geophysical logging, and faroffset vertical seismic profiling (VSP) of this borehole to aid in the evaluation of reservoir heterogeneity for both the Rose Run and Beekmantown/Mines. This area was chosen for the following reasons: 1) historical production from both the Rose Run and Beekmantown/Mines; 2) the highest density of well control to enable the most accurate location selection for stratigraphic testing; 3) occurrence of a complete section of Rose Run and a portion of Beekmantown/Mines; 4) availability of seismic data for seismic modeling of the reservoir; and 5) availability of nearby whole-diameter cores for studies of well- and field-scale reservoir heterogeneity.

Geophysical logs run by Schlumberger Well Services included a compensated neutron/litho-density log, dual laterolog, micro-spherically focused log, natural gamma ray spectrometry log, digital sonic tool, electro-magnetic propagation tool, and a Formation Microscanner (FMS). Schlumberger also extracted 50 sidewall cores in the well to evaluate reservoir properties, and to relate lithology to geophysical log responses. The FMS tool was run between

the Copper Ridge/Ore Hill dolomite and the Wells Creek/Shadow Lake interval (Figures 3 and 4), from a depth of 6,680 feet to 7,020 feet; it also was run through the Silurian Clinton/Medina and Lockport ("Newburg") intervals from 3,975 feet to 4,400 feet. Detailed electrical images produced from the FMS tool provided valuable information regarding sedimentary structures, textural changes, thin bed identification, and fracture analysis of the Knox/Gatesburg and overlying Wells Creek/Shadow Lake interval. Sidewall-core locations were easily identified on the FMS images, and could be oriented and matched to depth. Core descriptions extrapolated to the FMS gave better detail of lithologic changes and heterogeneity of the Rose Run sandstone.

Examination of whole-diameter cores from 14 wells in Ohio and Pennsylvania (Figure 5), and 50 sidewall cores taken from one well in Ohio form the basis of petrologic studies for this investigation. The underlying rock units of the Copper Ridge/Ore Hill dolomite and the overlying Beekmantown/Mines dolomite and Wells Creek/Shadow Lake interval in Ohio also were examined in order to better understand the depositional environment of the Rose Run sandstone. Similarly, in Pennsylvania, the underlying Kerbel/Lower Sandy interval, and Knox/Gatesburg carbonates also were examined. Studies of several outcrops of the Knox/Gatesburg Formation in central Pennsylvania were related to the cores to develop a better understanding of lithologic and depositional heterogeneities at the regional and local scales.

Petrographic work included slabbing of all cores and sampling of outcrops for mesoscopic examinations, and descriptions of lithology, including color, grain size, roundness, sorting, sedimentary structures, porosity types and distribution, and oil staining of this material. Appendix XII contains a list of all of the cores used in this study, and Appendix V contains graphical descriptions of these cores. Geophysical logs from the cored Ohio wells, particularly gamma-ray and density logs where available, were digitized and correlated to the cores. Neutron or resistivity curves were substituted where ever density logs were unavailable. Appendix III shows the stratigraphic positions of all cores as related to the associated geophysical logs. Core photographs helped illustrate various depositional or post-depositional features.

Basic rock property data from core analyses of whole-diameter cores from five Ohio wells and one Pennsylvania well, as well as analyses of 50 sidewall cores taken from the #3-A Reiss well in Ohio (Appendix IV), aided in understanding mesoscopic reservoir heterogeneity and

hydrocarbon potential. These core data include measurements of porosity, horizontal and vertical permeability, oil and water saturation, and grain density. Porosity and permeability data from these analyses were correlated to geophysical log responses and to petrographic characteristics to better understand reservoir heterogeneity.

A total of 91 thin sections of seven cores from Coshocton, Jackson, Perry, Scioto, and Tuscarawas counties, Ohio were examined. One-half of each thin section was stained for potassium feldspar and the remaining one-half was stained for calcite. All thin sections were impregnated with a blue-dyed epoxy cement. Each analysis included approximately 300 point counts covering nearly the entire thin section. Theses by Baker (1974) and Enterline (1991) supplied 57 additional thin section analyses. In all cases, raw point count data were recalculated so that framework plus matrix plus cement totaled 100 percent. Microscopy equipment included petrographic microscopes with plane and cross-polarized light at magnifications of 125 and 500 power, and a binocular microscope with variable power from 10 to 30X.

In Pennsylvania, point counts of 108 thin sections from four cores in Erie and Juniata counties, Pennsylvania, and three outcrops in Bedford and Blair counties, Pennsylvania, comprise the bulk of petrographic analyses. All thin sections were impregnated with a blue-dye epoxy cement. These thin sections were not stained for potassium feldspar. Feldspars were distinguished from quartz and identified by relief, cleavage, inclusions, dissolution, and chemical dissolution or weathering patterns, as well as by optic sign where possible (quartz is uniaxial and optically positive; feldspars are biaxial and optically negative). Each sandstone thin section was analyzed using 300 point counts. Carbonates were examined according to the format presented by Wilson (1975, p. 60–63). Special analyses included UV fluorescence and cathodoluminescence microscopy of selected Rose Run samples.

Studies of whole rock samples and clays included mineralogical identification by X-ray diffraction, using CuK alpha radiation at 35 Kv and 20 Ma, and scanning electron microscopy (SEM) of five sidewall core samples from the #3-A Reiss well. Clays less than one and less than two micrometers were separated using standard procedures similar to those described by Starkey and others (1985) prior to diffraction analysis. SEM studies of the five sidewall cores provided a detailed examination of authigenic and allogenic components, with emphasis on porosity type and distribution. Four scanning electron photomicrographs were taken of each sample.

Seismic Methodology

The acquisition, processing, and interpretation of seismic reflection data in conjunction with geophysical logs constitute the most precise method for locating paleotopographic remnants, structures, and faults that might define potential Rose Run sandstone reservoirs. Approximately thirty companies were contacted regarding the use of seismic data for the study. Their response indicates the availability of 268 miles of modern common depth point (CDP) dynamite and vibrator data in Ohio from both industry and the public domain (Figure 6). The amount and detail of seismic information in Pennsylvania is unknown; other than a few public domain sonic velocity logs, all seismic data are strictly proprietary. Appendix XIII shows the results of a survey of 34 companies active in the Rose Run play in Ohio who were asked to provide current information regarding the use of seismic data to explore and develop this play.

The seismic reflection data used for interpretation purposes in the Rose Run reservoir heterogeneity study were acquired by industry over a period of approximately ten years, during a time when great advances were being made with respect to seismic acquisition and processing techniques. The availability of faster and more modern computer hardware and software permitted this advance. A brief review of the technologies used, and what was considered to be industry standard at the time of acquisition and processing follows. A glossary of terms used in the discussion of seismic reflection data acquisition and processing methods is included in Appendix XIV.

Seismic Reflection Data Acquisition

The seismic reflection data acquisition parameters used in the study of heterogeneity characteristics of the Rose Run sandstone of Ohio were consistent with state of the art industry standard techniques. Various data vintages demonstrate the results of changes in industry standard seismic reflection acquisition.

The choice of parameters for recording seismic reflection data in the state of Ohio is governed by a number of factors and local conditions. Much of Ohio is covered by a veneer of glacial till in which seismic waves generate a low velocity associated ground roll, which must be taken in to consideration when planning and executing a seismic reflection survey. Typical velocities of seismic waves propagating in this low velocity layer are approximately 7,000 feet/second, with an associated range of frequencies in the 14–22 Hz. bandwidth. First arrival velocities must

also be accurately estimated, as they vary from 9,000 feet/second in heavily weathered zones to approximately 14,000 feet/second in zones less weathered. Power lines and underground utilities and conduits generate strong 60 Hz. and 120 Hz. noise, which should be filtered out at the time of data recording if it causes data to have a low signal-to-noise ratio. The depths to the target of interest help to determine the energy source to be used and the length of the recording spread. For deep targets such as the Rose Run, the longest workable offset recording spread will yield the best data. The thickness of certain horizons of interest, for example, the Wells Creek/Shadow Lake interval, can help to determine the frequency range necessary for recording the highest resolution data. Thinner beds require that higher frequencies be acquired at the recording stage. Another set of factors affecting seismic data acquisition parameters in Ohio is that of terrain and culturally imposed limitations to actual acquisition. This may range from access denial to a property, to terrain with swampy conditions or extreme topographic effects. Any of these cultural or terrain conditions may force shots to be missed, hence skipping cycles in the data acquired and lessening the fold, and therefore, confidence level of the data.

Typical energy sources used in seismic reflection data acquisition for the Rose Run in Ohio include both dynamite and vibrator sources. Energy sources such as Mini-Sosie and air gun sources are generally too weak to effectively image the Beekmantown/Mines and Rose Run, but work well in central and western Ohio where the Knox/Gatesburg and Trenton are less than 4,000 feet. Dynamite as a source was arranged either as a single shot of 1/4# dynamite or in patterns of 3 to 5 shotholes, each shothole containing 1/4# dynamite, at 110 feet or 220 feet shot intervals. Vibrator data were acquired using three sources with eight sweeps from 20–120 Hz. Vibrator source point intervals were at 110 feet or 220 feet, depending upon the fold of data desired.

A split-spread recording configuration was used. The typical offset from the source to first receiver was 275 feet, with a spread length of each split spread at 6,765 feet for a total spread length of 13,530 feet. The receivers used in most of the acquisition were 28 Hz. geophones. Lower peak response geophones (10, 14, and 18 Hz.) may also be used if ground roll is weak or will be suppressed in data processing. The receiver array was an in-line array of 12 to 24 geophones evenly spaced over the 110 foot receiver interval. A weighted, in line array of geophones is also acceptable to attenuate noise and ground roll. Shorter

receiver group lengths can encounter strong ground roll interference.

Representative recording devices included Texas Instruments DFS-V recording instruments. Over the study areas, the number of channels recorded varied from 48–120. Two seconds of data were recorded in the 18–128 Hz. bandwidth, with the 60 Hz. notch in when the data were recorded. A two millisecond sampling interval was standard.

Seismic Data Processing

Proprietary seismic reflection data over three areas of known production in the Knox/Gatesburg was donated to this reservoir heterogeneity study. Most of the data were acquired and processed prior to the inception of the study. The data in its initial processing state suffered from poorer resolution and imaging characteristics than present day acquired and processed data. This is because certain techniques which are now industry standard were not routinely used at the time that the data were originally acquired and processed. For this reason, all data donated to the study were sent out to data processing contractors for a variety of reprocessing formats.

The original data processing streams followed industry state of the art formats for the time period during which they were processed. A flow chart of typical data processing procedures used for data in this study is presented in Table 6 on page 125. Variations to this processing flow were added when the donated data were reprocessed. These variations included single and multiple spectral whitening and enhancement passes of the data. Optional processing steps used to enhance the data also included F/K (frequency/wavenumber) migration and statistical noise filtering. While F/K migration and statistical noise filtering are fairly common industry standard practices, multiple spectral whitening or enhancement passes of the data are not commonly performed. Ultimately, the best resolution and structural information was obtained by spectrally enhancing migrated data. Interpretation was performed on paper prints of migrated, spectrally whitened and enhanced, normal and reverse polarity data.

One- and Two-Dimensional Modeling of Seismic Data

Forward modeling of seismic data first involves the creation of a geologic model that contains velocity, density, and depth information for the formations of interest. From

this geologic model, a reflectivity model is generated using acoustic impedances (formation velocity x density) to generate a series of reflection coefficients at horizons of interest. An assumed wavelet is convolved with the reflectivity model to yield either a one- or two-dimensional model of the response of the earth to the passage of seismic waves through it. In many cases, however, the models do not account for full elastic wave behavior, dispersion, source generated noise, and non-normal wave incidence.

One-Dimensional Modeling—Synthetic Seismograms

A synthetic seismogram is a mathematical simulation of a single, zero-offset seismic trace recorded at the surface of the earth. Synthetic seismograms can be used to demonstrate seismic response of various formations, the frequency bandwidth necessary to resolve discrete features, to correlate and define events, and to determine the wavelet characteristics of stratigraphic sections. Velocity, density and depth information are obtained from geophysical borehole logs. The acoustic impedance of horizons of interest is derived as the products of density and velocity. The reflectivity series derived from acoustic impedances is convolved with an assumed wavelet to yield the synthetic seismogram. Discrepancies between synthetic seismograms and actual data may be the result of small systematic errors which eventually accumulate over the length of the seismogram, filter delays in recording and/or processing, different reference datums, and different filtering systems on the synthetic seismogram and the seismic record section (Sheriff, 1977). Synthetic seismograms have often been generated for wells of interest in the state of Ohio. Interest in prolific but risky oil and gas production from deep horizons has prompted recent interest in synthetic seismographic models of various geologic scenarios that could help correlate well data to processed seismic reflection data.

Two-Dimensional Modeling—Synthetic Seismic Sections

A synthetic seismic record section is a mathematical simulation of the response of a two dimensional hypothetical geologic sequence or sequences to the passage of seismic waves through them. Seismic modeling accepts a description of a subsurface condition in terms of geometry and acoustic parameters, including compressional wave velocity, density, and an attenuation factor (Neidell, and Poggiagliolmi, 1977). It is assumed that lateral continuity and homogeneity exist out of the plane of the seismic

model. Any complex geometry may be treated and seismic parameters may be allowed to vary both horizontally and vertically to represent lithologic transitions and similar subtle stratigraphic effects (Neidell and Poggiagliolmi, 1977). A geologic cross section is first generated. A time thickness section is generated based on the geologic cross section. From this time thickness section, the seismic response of various reflectors is observed, and can be compared with actual field acquired data. Alternatively, a synthetic well log model can be generated from synthetic acoustic impedance logs based on hypothetical seismic stratigraphic scenarios. The acoustic impedance of the models can be interpolated from well to well across a synthetic profile. The reflectivity series of the synthetic logs can be generated and convolved with an assumed wavelet. The result is a seismic pseudosection.

Vertical Seismic Profile (VSP)

The vertical seismic profile (VSP) is generated using near and far offset energy sources such as dynamite or a vibrator and recording the passage of seismic waves at equally spaced intervals in a borehole. Downgoing energy on the seismic section represents the first breaks and upgoing energy represents single or multiple reflected waves. VSPs represent an excellent way to tie well data to actual field acquired seismic profile data, to calibrate surface seismic data, and to delineate the seismic stratigraphy. With offset VSPs, it is also a way to "see beyond the well" (Puckett, 1992).

The results of vertical seismic profiling are presented as zero-offset seismic profiles (ZVSP) and offset seismic profiles (OVSP). The ZVSP in this study was the result of a source offset 675 feet from the borehole, recorded at fifty foot levels in the borehole, from total depth (TD) of 7,167 feet to 4,000 feet in the borehole. The source was offset from the borehole this distance to lessen the effects of tube waves in the borehole. The OVSP was the result of a source which was offset from the borehole 4,500 feet to the northwest, recorded at fifty foot levels in the borehole from TD to 2,600 feet depth in the borehole.

The processing scheme for the ZVSP and OVSP were standard. The processing consisted of interactive time break picking, F/K filter to reduce the effects of the tube wave in the ZVSP, spherical divergence correction, amplitude normalization, and median velocity filter. The data were rotated to zero phase and filtered with a 12–90 Hz. spectral enhancement operator of 450 milliseconds length. The operator length prevented the tube wave from influencing the deconvolution of the data in the ZVSP.

Following deconvolution, the upgoing wavefield for the ZVSP was summed into a corridor stack, which represents the measured seismic response at the well. The upgoing wavefield for the OVSP was summed into a horizontal seismic profile. Attribute processing for instantaneous amplitude and phase was also accomplished for the OVSP.

Attribute Processing

Seismic waves which are detected by seismic recording devices are analytic signals with both real and imaginary parts, of which only the real part is detected and displayed. The signal may also be expressed as a time-dependent phasor (Bracewell, 1965), expressed by the equation:

$$g(t) = R(t)\cos(\phi(t))$$

where $g(t)$ = the observed seismic trace, $R(t)$ = reflection strength envelope of the seismic trace, and $\phi(t)$ = the instantaneous phase.

A complex seismic trace is generated by a vector whose length varies with time, rotating as a function of time. The actual seismic trace ($g(t)$) is the projection of this vector onto the real plane, and the quadrature trace ($h(t)$) is the projection onto the imaginary plane. The quadrature trace can be generated from the real trace by Hilbert transform techniques so that both real and imaginary components of the seismic trace are available for analysis. From the real

and imaginary trace, both reflection strength (amplitude) and instantaneous phase can be calculated for every point, rather than being averaged over a number of samples (Taner and Sheriff, 1977).

Reflection strength (amplitude) may have its maximum at phase points other than peaks and troughs, especially when the reflection observed is a composite signal of several reflections. This fact is useful when attempting to distinguish single interface reflections from composite reflections, as single interface reflections tend to remain more constant over larger areas. Changes in reflection strength can be indicative of interference due to horizon pinchout, changes in porosity or accumulations of hydrocarbons (Puckett, 1992; Clark, 1992). Instantaneous phase is completely independent of reflection strength. Instantaneous phase indicates the continuity of events, hence it is especially useful to define the coherency of reflectors. Phase attribute processing can also be used to define areas of pinchout, angularities, and the interference of events with different dip attitudes (Taner and Sheriff, 1977).

The use of reflection strength and phase attribute processing was done in this study of reservoir heterogeneity in the subsurface of Ohio with vertical seismic profiling data and with seismic record section data, to look for amplitude and phase anomalies. These could indicate pinchouts, unconformities, and/or oil and gas accumulations.



Appendix II:
Availability of Products

Products Currently Available

Ohio Division of Geological Survey

Digital Chart and Map Series (DCMS)—Open File Maps

1. DCMS-1 Knox and Deeper Wells in Southeast Ohio; Scale 1:250,000.
 2. DCMS-2 Knox and Deeper Wells in Northeast Ohio; Scale 1:250,000.
 3. DCMS-3 Knox and Deeper Wells in Portions of Coshocton, Holmes, and Tuscarawas Counties; Scale 1:62,500.
 4. DCMS-5 Cambrian and Lower Ordovician Stratigraphic Cross Section—Greenup County, Ky. to Crawford County, Pa.
 5. DCMS-6 Cambrian and Lower Ordovician Stratigraphic Cross Section—Morrow County, Ohio to Wood County, W.Va.
 6. DCMS-7 Map of basement structures in Ohio Scale 1:500,000. With accompanying list of references.
 7. DCMS-8 Structure map on the Knox unconformity in southeastern Ohio. Scale 1:250,000, contour interval 100 feet.
 8. DCMS-9 Structure map on the Knox unconformity in northeastern Ohio. Scale 1:250,000, contour interval 100 feet.
 9. DCMS-11 Structure map on the top of the Rome Formation in eastern Ohio. Scale 1:500,000, contour interval 100 feet.
 10. DCMS-12 Structure map on the Precambrian unconformity in eastern Ohio. Scale 1:500,000, contour interval 100 feet.
- Digital data file 2 (DDF2) completion card and logtop database for all Knox penetrations in study area.

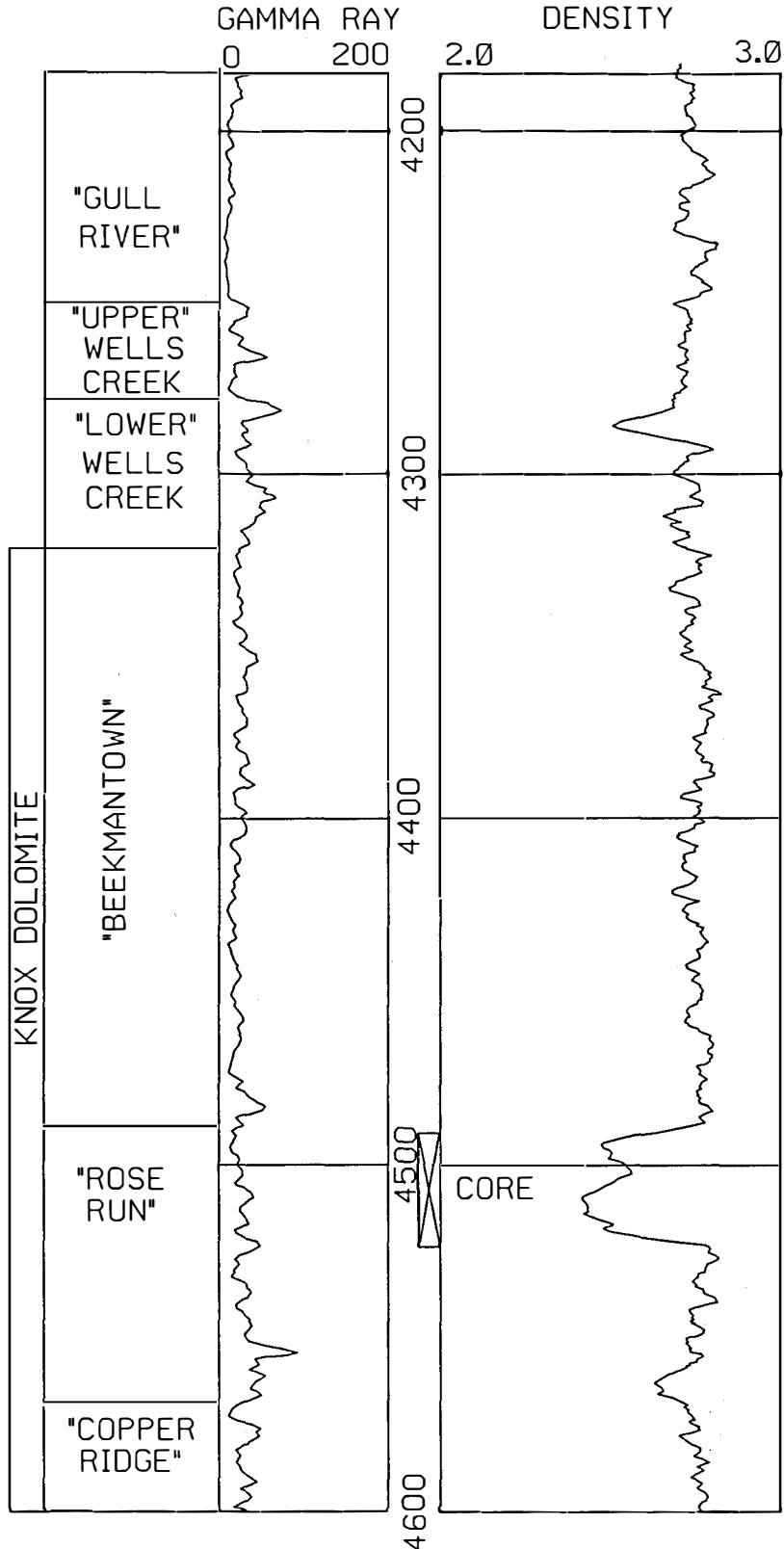
Pennsylvania Bureau of Topographic and Geologic Survey

Formation top database for all wells penetrating top of Middle Ordovician carbonates or deeper.

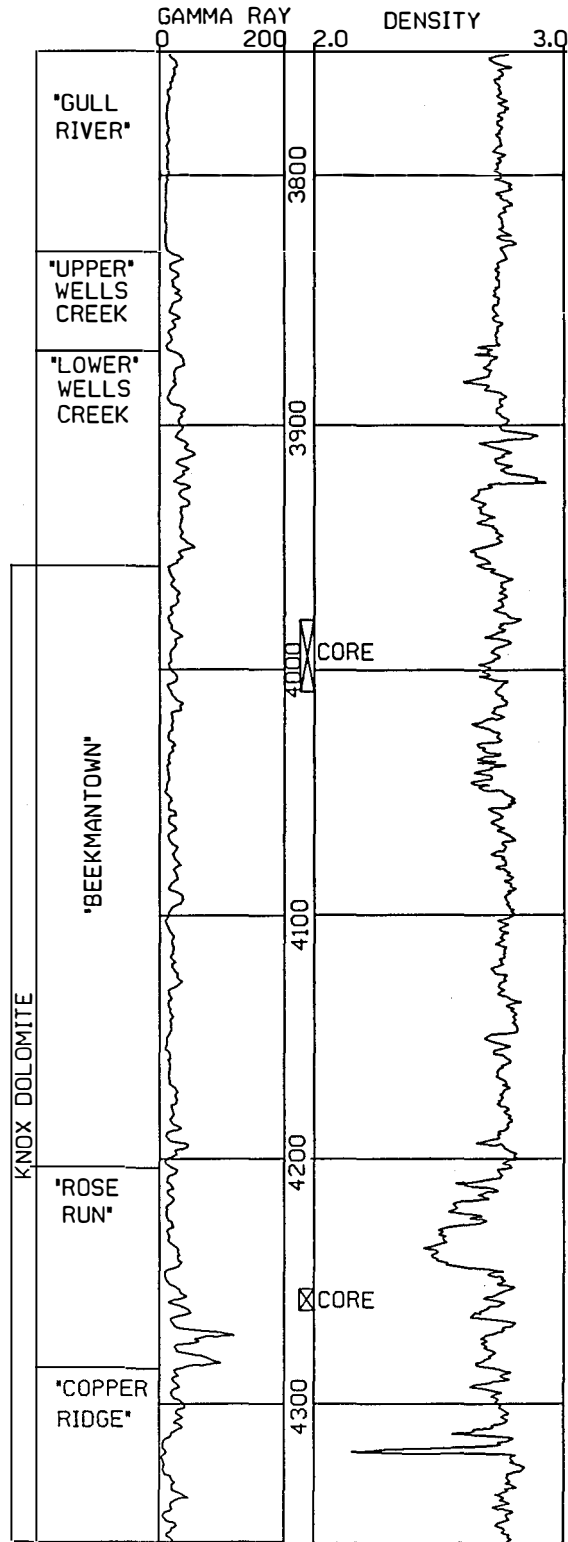
Open-filed Middle Ordovician to Precambrian cross sections of wells and outcrops in Pennsylvania and adjacent states.

Appendix III:
Stratigraphic Relationship of Ohio Cores
to Geophysical Logs

PERMIT NUMBER 102 (CORE NUMBER 2898)

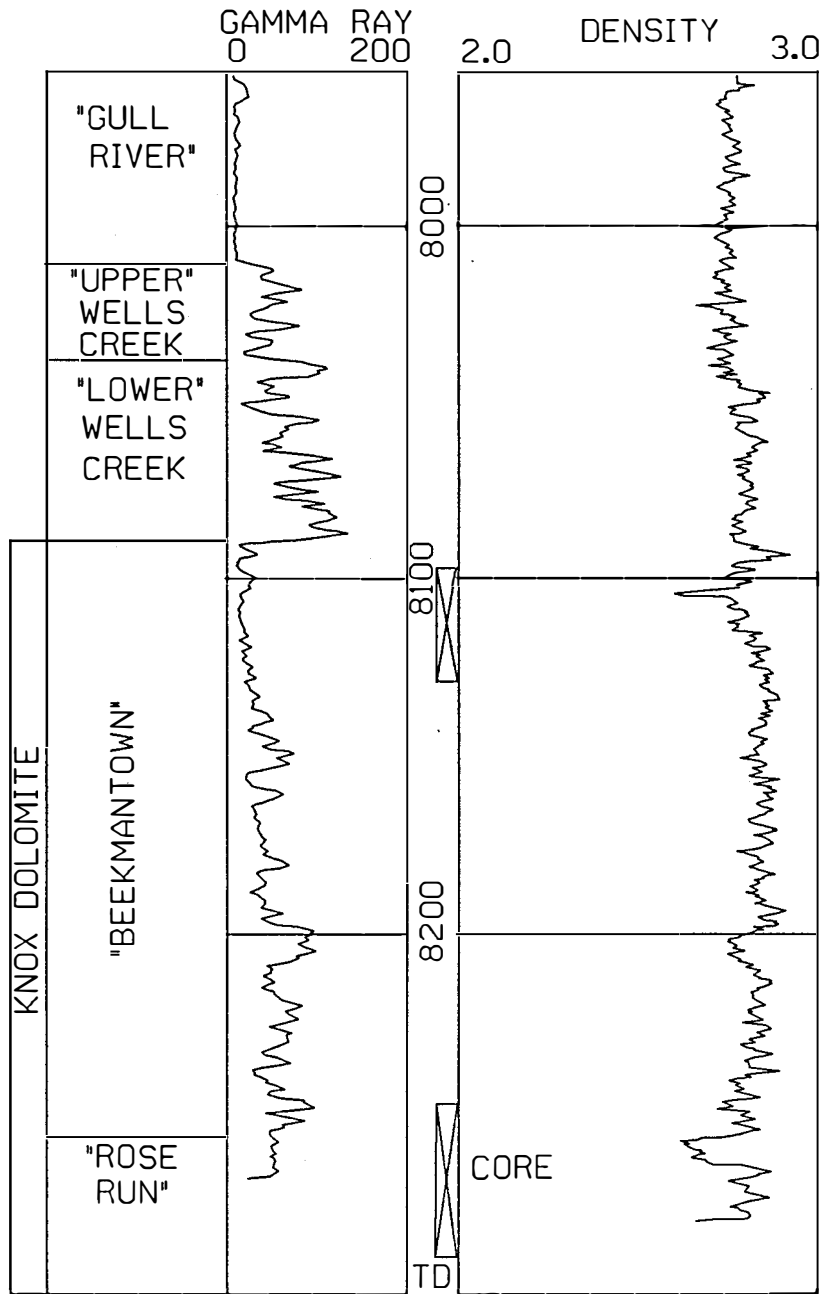


TD 6043

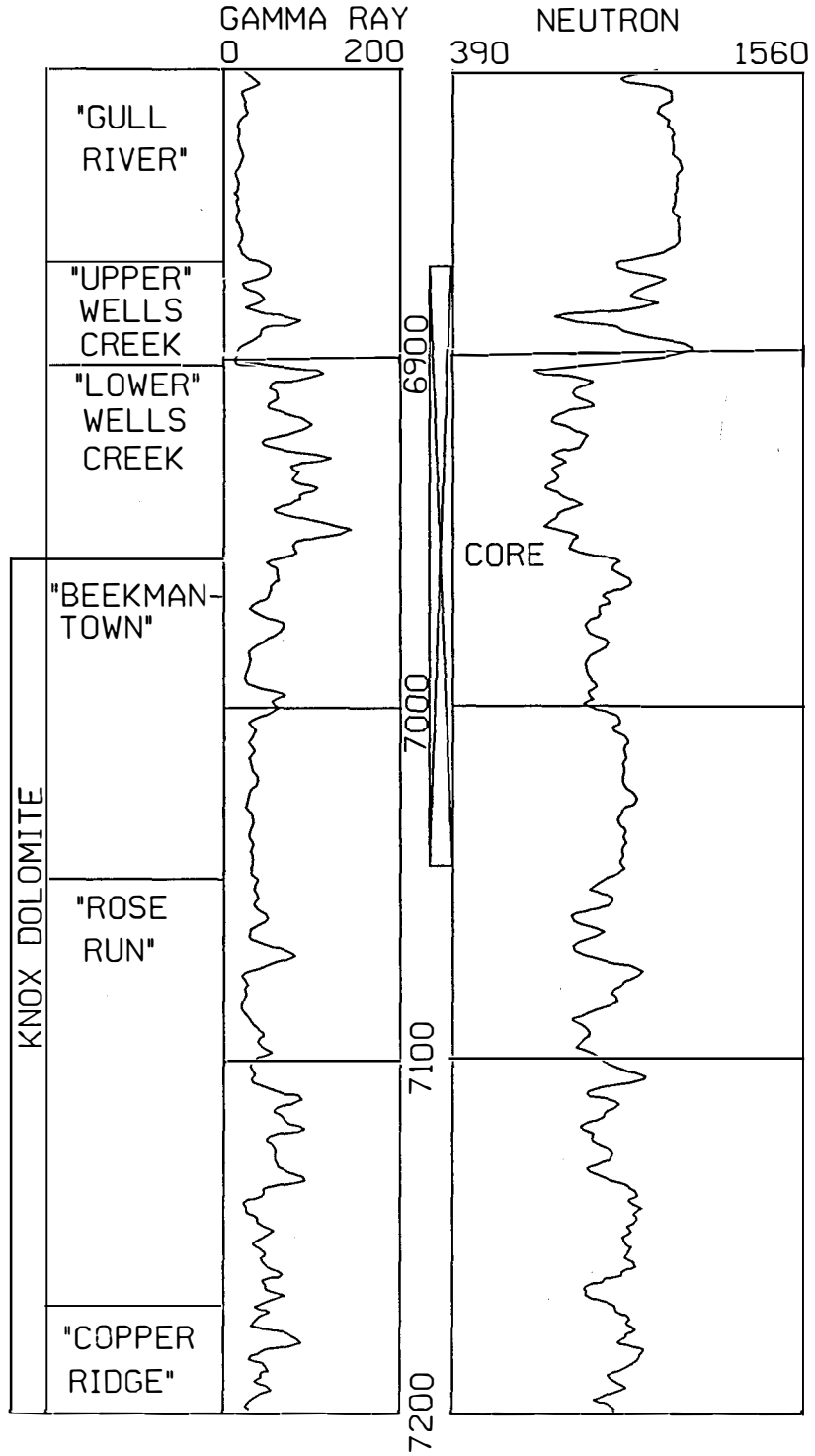


TD 5617

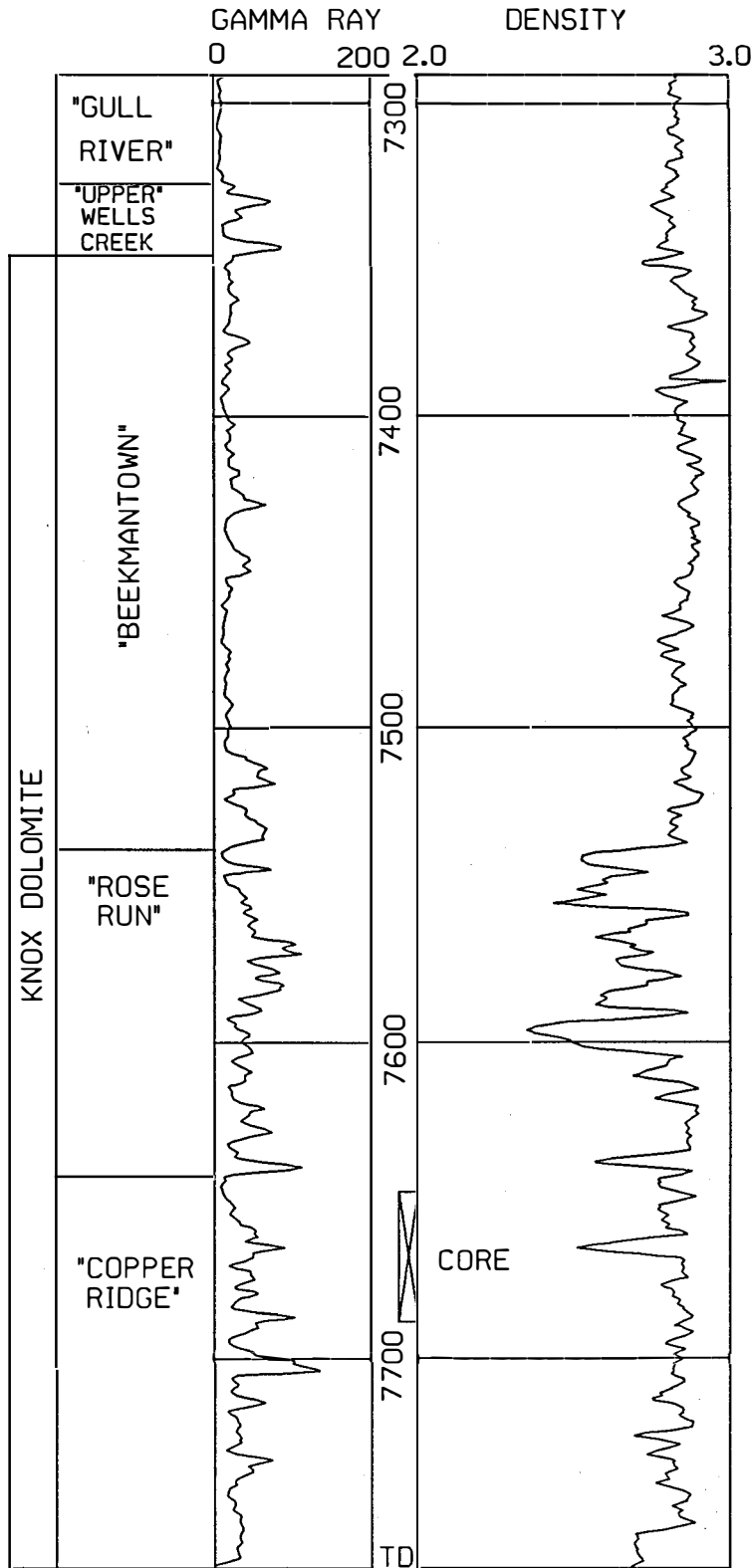
PERMIT NUMBER 592 (CORE NUMBER 2850)



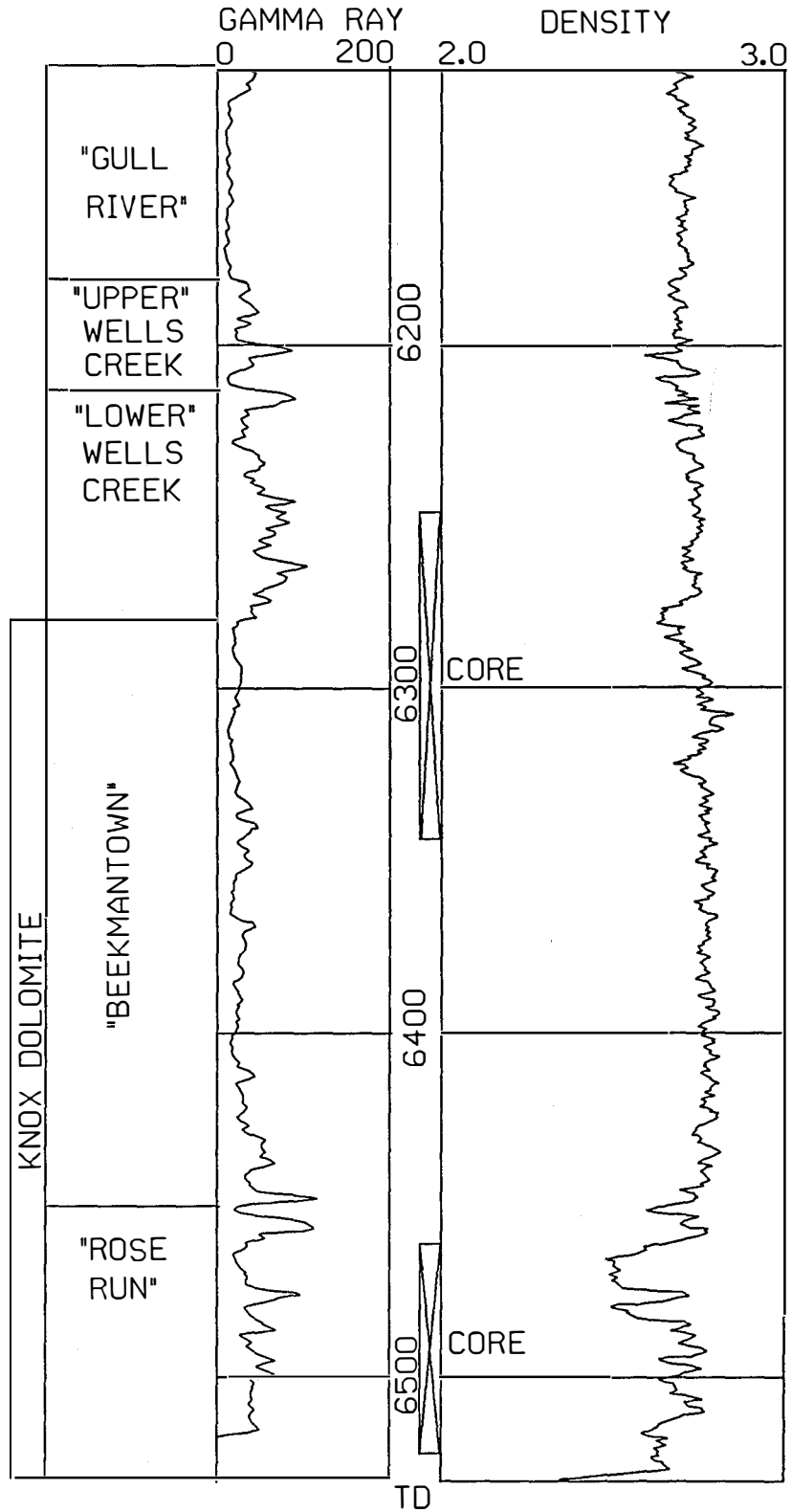
PERMIT NUMBER 782 (CORE NUMBER 867)



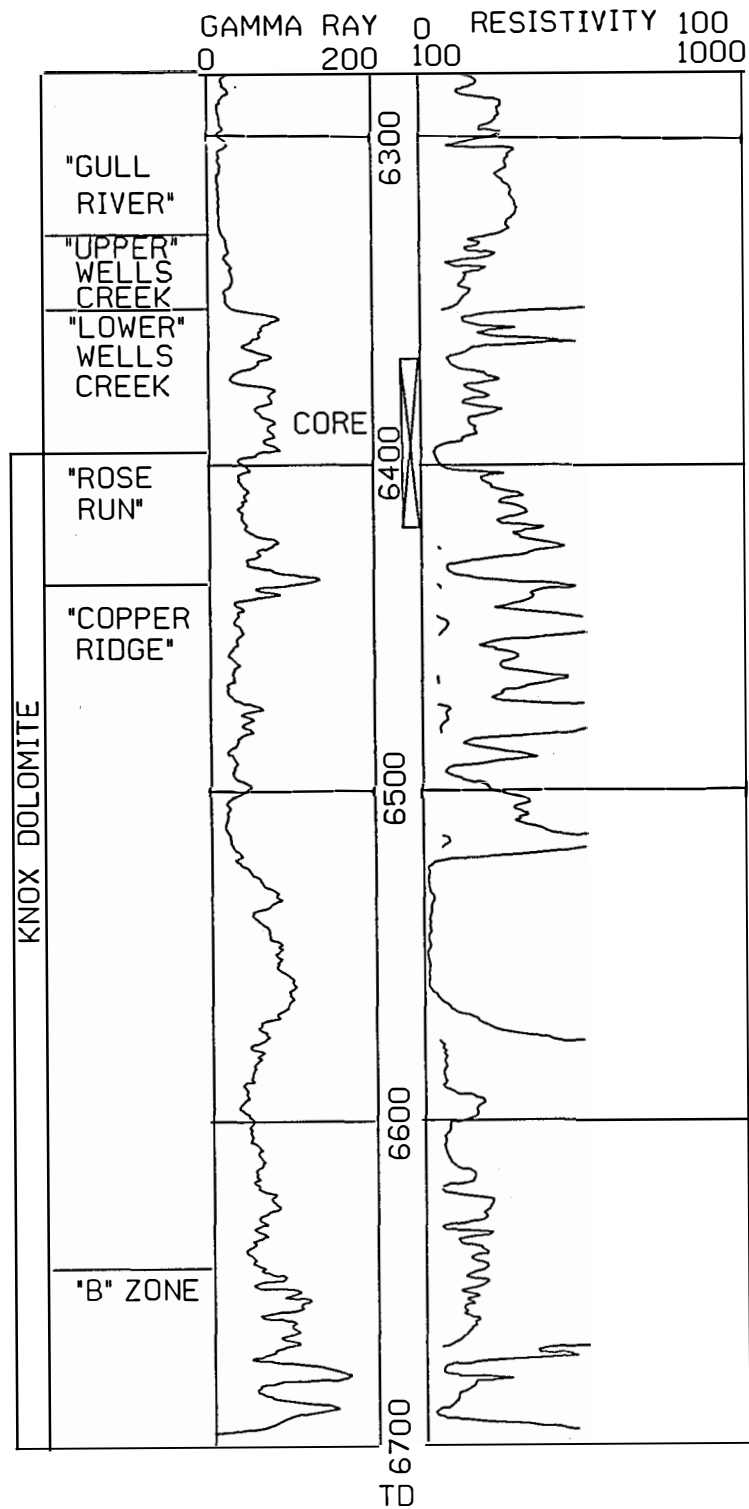
PERMIT NUMBER 955 (CORE NUMBER 2963)



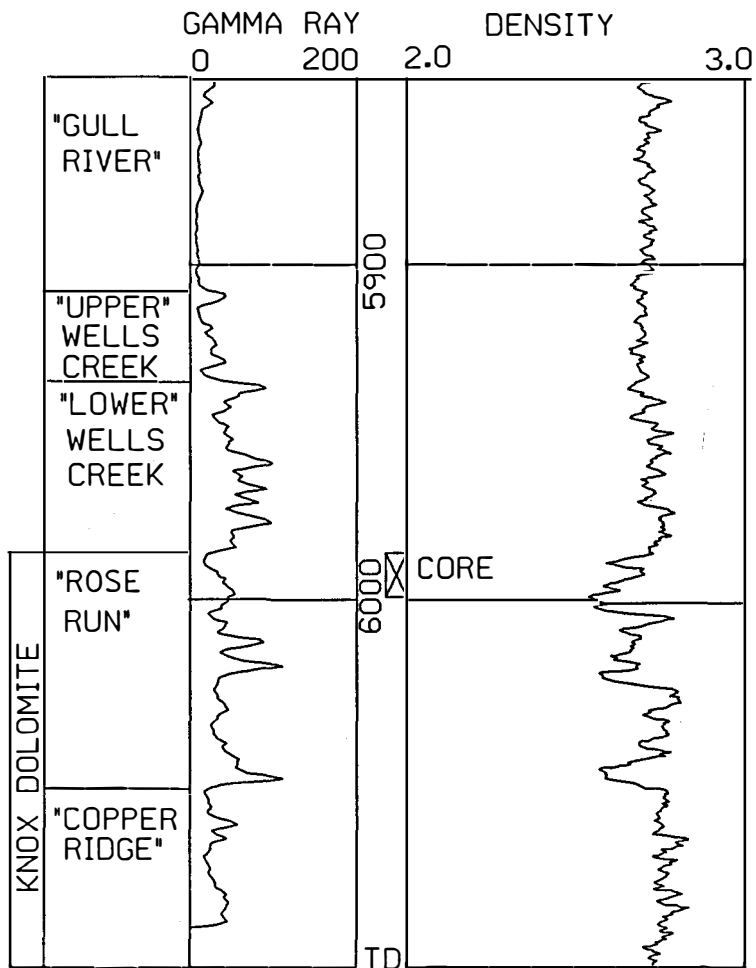
PERMIT NUMBER 1249 (CORE NUMBER 2923)



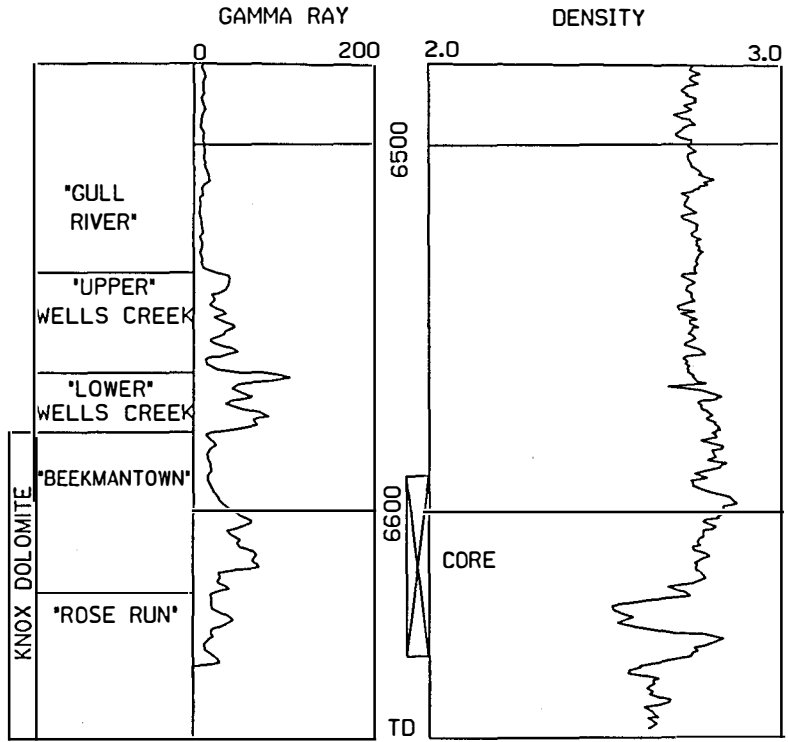
PERMIT NUMBER 1279 (CORE NUMBER 2892)



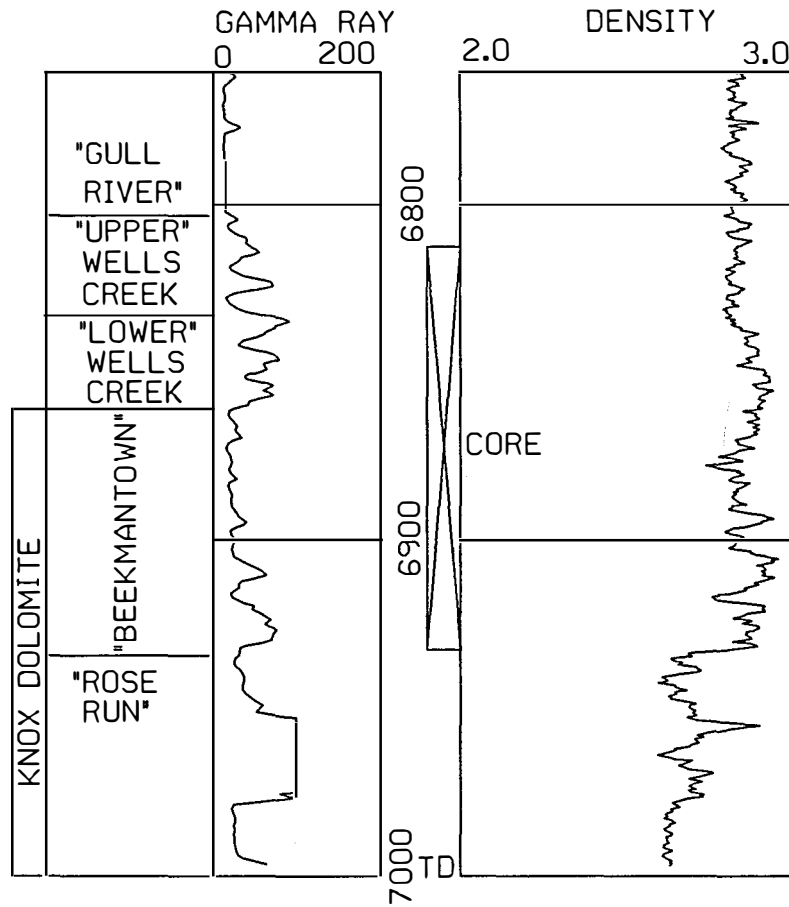
PERMIT NUMBER 2183 (CORE NUMBER 2852)



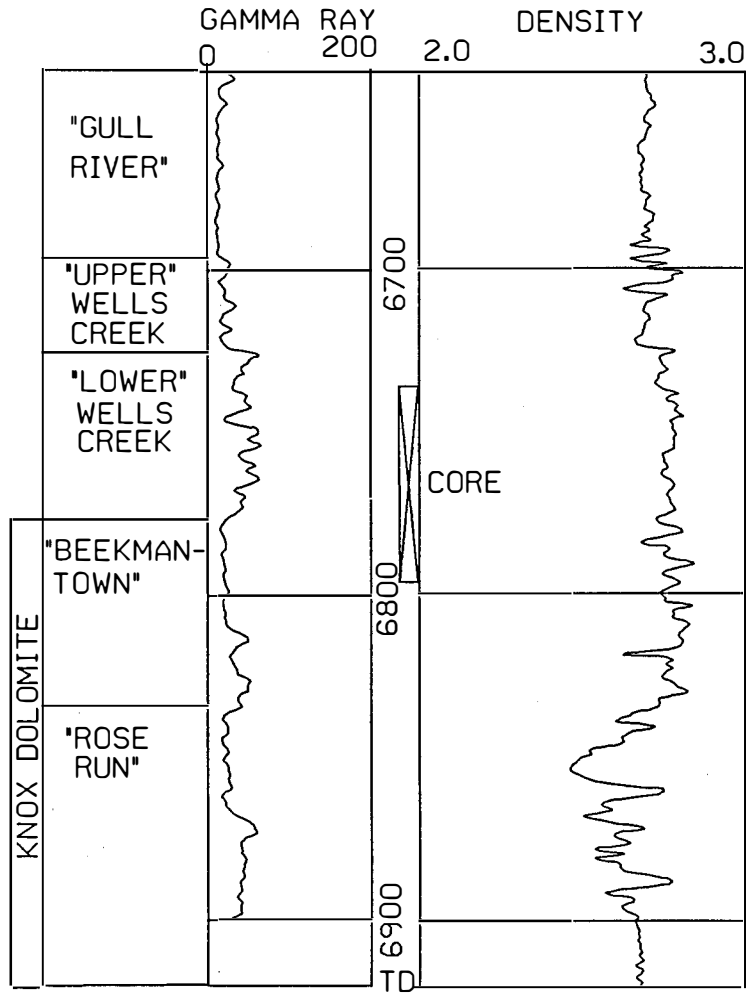
PERMIT NUMBER 2653 (CORE NUMBER 2989)



PERMIT NUMBER 4092 (CORE NUMBER 2713)



PERMIT NUMBER 5962 (CORE NUMBER 3006)



**Appendix IV:
Porosity and Permeability Data**

Coshocton County, Ohio
Adams Township, Section 2
Permit Number 4092 (Core Number 2713)
Pomstone
Oaklief #1-A

Depth	Perm to Air Md.		Vertical	Porosity	Fluid Sats.	
	Maximum	90°			Oil	Wtr.
6815.0-16.0	<0.1	<0.1	<0.1	0.5	22.9	54.3
6816.0-17.0	<0.1	<0.1	<0.1	0.2	16.7	43.3
6817.0-18.0	<0.1	<0.1	<0.1	0.3	0.0	66.7
6818.0-19.0	0.1	<0.1	<0.1	0.3	0.0	66.7
6819.0-20.0	<0.1	<0.1	<0.1	0.2	0.0	50.0
6820.0-21.0	<0.1	<0.1	<0.1	1.0	0.0	88.9
6821.0-22.0	<0.1	<0.1	<0.1	1.2	0.0	94.4
6822.0-23.0	<0.1	<0.1	<0.1	0.4	0.0	83.3
6823.0-24.0	<0.1	<0.1	<0.1	1.1	0.0	90.9
6824.0-25.0	<0.1	<0.1	<0.1	2.2	0.0	94.7
6825.0-26.0	<0.1	<0.1	<0.1	0.8	0.0	85.7
6826.0-27.0	<0.1	<0.1	<0.1	0.8	0.0	87.5
6827.0-28.0	<0.1	<0.1	<0.1	1.2	0.0	85.7
6828.0-29.0	<0.1	<0.1	<0.1	0.5	0.0	80.0
6829.0-30.0	<0.1	<0.1	<0.1	0.4	0.0	66.7
6830.0-31.0	<0.1	<0.1	<0.1	0.3	0.0	50.0
6831.0-32.0	<0.1	<0.1	<0.1	0.2	0.0	50.0
6835.0-36.0	<0.1	<0.1	<0.1	1.2	0.0	87.5
6836.0-37.0	<0.1	<0.1	<0.1	0.1	0.0	50.0
6837.0-38.0	<0.1	<0.1	<0.1	0.5	0.0	50.0
6838.0-39.0	<0.1	<0.1	<0.1	0.3	0.0	50.0
6839.0-40.0	<0.1	<0.1	<0.1	0.2	0.0	50.0
6840.0-41.0	<0.1	<0.1	<0.1	0.2	0.0	50.0
6841.0-42.0	<0.1	<0.1	<0.1	0.4	0.0	75.0
6842.0-43.0	<0.1	<0.1	<0.1	0.8	0.0	87.5
6843.0-44.0	<0.1	<0.1	<0.1	1.7	0.0	83.3
6844.0-45.0	*	<0.1	<0.1	2.3	0.0	90.0
6845.0-46.0	<0.1	<0.1	<0.1	2.8	0.0	95.8
6846.0-47.0	*	<0.1	<0.1	3.5	0.0	96.2
6847.0-48.0	<0.1	<0.1	<0.1	4.3	0.0	98.1
6848.0-49.0	<0.1	<0.1	<0.1	3.6	0.0	94.7
6849.0-50.0	*	<0.1	<0.1	2.6	0.0	93.6
6850.0-51.0	<0.1	<0.1	<0.1	1.6	0.0	95.0
6851.0-52.0	<0.1	<0.1	<0.1	0.4	0.0	66.7
6852.0-53.0	<0.1	<0.1	<0.1	0.2	0.0	50.0
6853.0-53.5	<0.1	<0.1	<0.1	0.9	0.0	87.5
6856.0-57.0	<0.1	<0.1	<0.1	2.7	0.0	95.5
6857.0-58.0	<0.1	<0.1	<0.1	1.6	0.0	97.5
6858.0-59.0	<0.1	<0.1	<0.1	4.3	0.0	97.4
6859.0-60.0	<0.1	<0.1	<0.1	2.2	0.0	94.1
6860.0-61.0	<0.1	<0.1	<0.1	0.5	0.0	80.0

(cont.)

Depth	Perm to Air Md.		Vertical	Porosity	Fluid Sats.	
	Maximum	90°			Oil	Wtr.
6861.0-62.0	*	<0.1	<0.1	0.9	0.0	95.1
6862.0-63.0	*	<0.1	<0.1	1.1	0.0	87.6
6863.0-64.0	*	<0.1	<0.1	0.8	0.0	91.3
6864.0-65.0	*	<0.1	<0.1	1.2	0.0	84.2
6865.0-66.0	*	<0.1	<0.1	1.5	0.0	97.2
6866.0-67.0	<0.1	<0.1	<0.1	1.8	0.0	96.3
6867.0-68.0	<0.1	<0.1	<0.1	1.0	0.0	83.3
6868.0-69.0	*	<0.1	<0.1	1.9	0.0	88.2
6869.0-70.0	<0.1	<0.1	<0.1	2.6	0.0	87.5
6870.0-71.0	<0.1	<0.1	<0.1	2.4	0.0	55.3
6871.0-72.0	<0.1	<0.1	<0.1	4.8	0.0	29.1
6872.0-73.0	0.2	0.2	<0.1	6.4	1.9	14.3
6873.0-74.0	<0.1	<0.1	<0.1	2.2	4.0	30.5
6874.0-75.0	<0.1	<0.1	<0.1	2.5	1.8	55.9
6875.0-76.0	<0.1	<0.1	<0.1	3.7	1.7	62.1
6876.0-77.0	0.1	<0.1	<0.1	5.5	1.2	44.1
6877.0-78.0	<0.1	<0.1	<0.1	0.9	0.0	90.0
6878.0-79.0	<0.1	<0.1	<0.1	0.7	0.0	75.0
6879.0-80.0	0.2	0.1	<0.1	3.9	0.0	34.8
6880.0-81.0	1.1	0.2	<0.1	5.9	2.5	35.1
6881.0-82.0	1.0	<0.1	<0.1	4.0	2.3	30.6
6882.0-83.0	<0.1	<0.1	<0.1	3.2	2.3	36.4
6883.0-84.0	0.3	0.1	<0.1	5.0	2.2	32.4
6884.0-85.0	0.2	0.1	<0.1	6.4	2.6	38.6
6885.0-85.7	0.8	0.6	<0.1	5.1	0.6	29.8
6887.5-88.0	0.2	0.2	0.1	6.7	1.1	47.5
6888.0-89.0	0.2	0.1	<0.1	7.1	0.8	36.9
6889.0-90.0	<0.1	<0.1	<0.1	6.5	1.8	37.1
6890.0-91.0	<0.1	<0.1	<0.1	4.9	2.1	47.3
6891.0-92.0	240.0	<0.1	60.0	8.4	1.6	58.4
6892.0-93.0	0.2	0.1	<0.1	6.5	0.8	29.5
6893.0-94.0	0.2	0.1	<0.1	7.0	0.9	31.0
6894.0-95.0	<0.1	<0.1	<0.1	6.1	2.1	37.1
6895.0-96.0	<0.1	<0.1	<0.1	7.5	1.9	34.5
6896.0-97.0	0.1	<0.1	<0.1	6.3	2.8	40.7
6897.0-98.0	0.1	<0.1	<0.1	6.9	2.7	39.1
6898.0-99.0	<0.1	<0.1	<0.1	2.9	1.0	34.6
6899.0-00.0	<0.1	<0.1	<0.1	7.4	1.0	38.9
6900.0-01.0	<0.1	<0.1	<0.1	6.9	1.0	40.6
6901.0-02.0	<0.1	<0.1	<0.1	6.2	3.4	15.8
6902.0-03.0	<0.1	<0.1	<0.1	5.0	3.3	14.9
6903.0-04.0	<0.1	<0.1	<0.1	3.2	0.0	86.4
6904.0-05.0	<0.1	<0.1	<0.1	2.3	0.0	92.3
6905.0-06.0	<0.1	<0.1	<0.1	3.2	0.0	93.8
6906.0-07.0	0.1	<0.1	<0.1	3.4	1.4	53.9

(cont.)

Depth	Perm to Air Md.		Vertical	Porosity	Fluid Sats.	
	Maximum	90°			Oil	Wtr.
6907.0-08.0	0.2	0.2	<0.1	4.4	1.4	56.9
6908.0-09.0	0.2	0.2	<0.1	8.5	1.1	45.6
6909.0-10.0	<0.1	<0.1	<0.1	6.4	2.2	42.6
6910.0-11.0	<0.1	<0.1	<0.1	5.7	2.7	51.9
6911.0-12.0	<0.1	<0.1	<0.1	7.1	1.2	36.5
6912.0-13.0	<0.1	<0.1	<0.1	3.3	1.7	45.6
6913.0-14.0	0.2	0.1	<0.1	7.5	1.1	32.8
6915.0-16.0	<0.1	<0.1	<0.1	5.8	0.7	68.6
6916.0-17.0	<0.1	<0.1	<0.1	4.0	0.7	64.9
6917.0-18.0	<0.1	<0.1	<0.1	2.1	0.0	96.7
6918.0-19.0	<0.1	<0.1	<0.1	1.9	0.0	95.8
6919.0-20.0	<0.1	<0.1	<0.1	1.8	0.0	94.4
6920.0-21.0	<0.1	<0.1	<0.1	1.8	0.0	93.8
6921.0-22.0	<0.1	<0.1	<0.1	1.6	0.0	95.7
6922.0-23.0	<0.1	<0.1	<0.1	1.1	0.0	92.3
6923.0-24.0	<0.1	<0.1	<0.1	1.2	0.0	88.9
6924.0-25.0	<0.1	<0.1	<0.1	1.8	0.0	91.7
6926.0-27.0	<0.1	<0.1	<0.1	4.3	4.5	41.8
6927.0-28.0	<0.1	<0.1	<0.1	4.0	5.4	49.6
6928.0-29.0	0.1	<0.1	<0.1	5.4	2.0	37.2
6929.0-29.5	<0.1	<0.1	<0.1	2.4	3.3	58.3

Coshocton County, Ohio
White Eyes Township, Section 17
Permit Number 2653 (Core Number 2989)
Redstone
Barth #1

Depth	Perm to Air Md.		Vertical	Porosity Gex.Fld.	Fluid Sats.	
	Maximum	90°			Oil	Wtr.
6610.5-12.1	2.10	<0.10	0.51	3.1	0.0	90.8
6613.6-15.0	1.10	0.70	0.66	4.2	0.0	39.9
6615.0-16.4	0.70	0.70	0.58	7.5	7.8	41.8
6616.4-18.4	0.96	0.82	1.10	8.9	17.3	36.4
6618.4-19.6	<0.10	<0.10	0.54	4.9	7.7	59.8
6619.6-21.0	0.33	0.17	0.54	9.2	6.4	82.0
6621.0-22.4	0.70	0.70	0.68	8.8	10.1	72.3
6622.4-23.2	0.42	0.42	0.80	7.3	8.9	85.0
6631.0-32.5	<0.10	<0.10	<0.10	4.9	6.9	82.5
6632.5-33.9	7.50	<0.10	0.47	6.7	7.1	83.6
6633.9-34.9	2.10	0.70	0.64	8.0	3.7	74.9
6634.9-35.9	0.47	0.34	0.54	4.6	0.0	96.0
6635.9-36.8	<0.10	<0.10	<0.10	4.3	0.0	83.0
6636.8-37.8	<0.10	<0.10	<0.10	3.1	0.0	93.1
6637.8-38.9	<0.10	<0.10	<0.10	4.2	0.0	90.8

Coshocton County, Ohio
 Adams Township, Section 12
 Permit Number 5962 (Core Number 3006)
 Stone
 Lower #1-A

Sample Depth	Perm. (md)	Porosity %	Grain Density	H-C Sat. %	Wat. Sat. %
6736.1	.02510	0.7	2.750	++	++
6736.8	+++	0.7	2.758	0.0	0.0
6738.0	.003084	0.8	2.756	0.0	0.0
6738.6	.004411	2.0	2.770	0.0	0.0
6740.2	.003939	2.7	2.788	23.4	49.2
6741.5	.003321	0.1	2.797	0.0	0.0
6742.5	4.8262	3.7	2.832	0.0	0.0
6743.7	54.047	2.3	2.839	0.0	0.0
6745.0	10.021	0.9	2.829	++	++
6746.5	.003596	0.4	2.776	0.0	0.0
6747.5	.003366	0.4	2.775	0.0	0.0
6748.5	.003588	0.2	2.753	0.0	0.0
6750.0	.003753	0.1	2.804	++	++
6751.5	.003471	0.1	2.757	0.0	0.0
6753.0	.003471	0.1	2.794	0.0	0.0
6754.0	.003450	0.1	2.768	0.0	0.0
6755.0	.006022	0.1	2.756	++	++
6756.4	.003942	0.1	2.742	0.0	0.0
6758.3	+++	1.4	2.771	0.0	0.0
6760.0	.003840	0.1	2.799	++	++
6761.5	.005330	1.5	2.774	0.0	0.0
6763.5	.004153	1.0	2.787	0.0	0.0
6765.0	.005423	0.9	2.811	++	++
6766.5	.003644	0.7	2.772	0.0	0.0
6768.5	.003617	0.3	2.762	0.0	0.0
6769.4	.003864	0.2	2.759	0.0	0.0
6770.0	.004508	0.8	2.789	++	++
6771.0	.08212	1.0	2.810	0.0	0.0
6771.9	.004119	0.9	2.784	0.0	0.0
6772.5	.003538	0.8	2.801	0.0	0.0
6773.0	.005862	1.4	2.810	++	++
6773.5	.43637	1.6	2.833	0.0	0.0
6774.1	.12469	4.6	2.825	0.0	0.0
6775.0	.32249	8.2	2.834	1.5	22.9
6775.3	.52174	10.3	2.826	0.0	0.0
6775.6	.11342	5.6	2.836	0.0	0.0
6776.0	.04479	4.7	2.836	0.0	0.0
6776.4	.07451	2.9	2.831	0.0	0.0
6776.9	.20483	7.9	2.838	0.0	0.0
6777.4	.005938	2.2	2.847	0.0	0.0
6778.0	.004084	0.9	2.837	++	++

(cont.)

Depth	Perm. (md)	Porosity %	Grain Density	H-C Sat. %	Wat. Sat. %
6779.1	0.619850	2.2	2.835	0.0	0.0
6780.1	0.045380	1.8	2.831	0.0	0.0
6780.5	17.281000	2.2	2.824	0.0	0.0
6781.0	3.275500	3.0	2.832	27.6	29.6
6781.5	0.296890	2.0	2.838	0.0	0.0
6782.5	1.894100	1.4	2.830	0.0	0.0
6783.5	0.653470	8.4	2.822	0.0	0.0
6785.3	0.158310	2.2	2.834	++	++
6785.8	1.196300	2.0	2.836	0.0	0.0
6786.9	7.923800	1.8	2.835	0.0	0.0
6788.3	0.029420	2.3	2.836	0.0	0.0
6789.2	0.004676	0.8	2.833	0.0	0.0
6790.1	0.004871	0.5	2.811	++	++
6791.9	0.154660	5.2	2.824	0.0	0.0
6793.5	2.340500	4.1	2.825	0.0	0.0
6794.2	0.003493	0.5	2.834	0.0	0.0
6794.3	2.450700	3.9	2.833	0.0	0.0
6795.9	0.005032	1.8	2.821	++	++

++Inadequate pore volume for accurate fluid determination.
+++Sample unsuitable for permeability measurement.

Coshocton County, Ohio
 Adams Township, Section 12
 Permit Number 6379 (Core Number 3260)
 NGO Development/Ohio Department of Natural Resources
 Reiss #3-A

Sample	Depth (ft.)	Permeability to Gas (md)	Porosity (% BV)	Grain Density (G/CC)
R 482	3980.0	2.890	6.0	2.84
R 483	3995.0	0.007	1.9	2.84
R 484	6680.0	**	0.3	2.70
R 485	6691.0	0.004	3.0	2.81
R 486	6706.0	0.031	1.3	2.81
R 487	6714.0	0.001	2.1	2.83
R 488	6715.0	0.010	1.8	2.82
R 489	6719.0	0.046	2.5	2.82
R 490	6720.0	0.008	2.2	2.83
R 491	6721.0	0.008	1.3	2.84
R 492	6722.0	0.027	5.1	2.82
R 493	6723.0	—	—	—
R 494	6759.0	0.009	3.5	2.83
R 495	6775.0	0.006	1.7	2.80
R 496	6777.0	0.016	5.4	2.73
R 497	6779.0	0.149	4.1	2.76
R 498	6784.0	0.005	1.2	2.80
R 499	6796.0	0.006	1.8	2.72
R 500	6799.5	0.790	4.8	2.69
R 501	6800.5	0.010	3.8	2.72
R 502	6803.0	0.010	2.5	2.72
R 503	6805.0	0.045	4.0	2.62
R 504	6807.5	0.026	4.4	2.63
R 505	6809.0	2.260	7.5	2.63
R 506	6811.5	4.780	9.0	2.63
R 507	6813.0	0.313	7.7	2.61
R 508	6816.0	0.237	6.2	2.62
R 509	6819.5	42.800	12.7	2.64
R 510	6825.0	**	5.3	2.65
R 511	6826.0	0.911	7.0	2.62
R 512	6828.0	4.650	7.9	2.61
R 513	6836.5	2.450	7.6	2.64
R 514	6838.0	0.074	4.8	2.72
R 515	6875.0	0.018	1.8	2.69
R 516	6861.0	2.380	5.9	2.61
R 517	6865.0	29.700	10.2	2.60
R 518	6897.0	0.014	1.2	2.73
R 519	6901.0	**	6.0	2.67
R 520	6905.0	0.237	7.4	2.68
R 521	6907.0	0.675	8.1	2.67
R 522	6917.0	0.130	6.9	2.67
R 523	6920.0	0.049	6.1	2.63
R 524	6966.0	0.026	3.4	2.81
R 525	6969.0	0.051	4.5	2.66
R 526	6973.0	0.147	6.0	2.67
R 527	6990.0	1.860	10.2	2.61
R 528	6993.0	3.430	8.9	2.63
R 529	7000.0	6.430	10.2	2.67
R 530	7006.0	0.128	6.7	2.67
R 531*	7130.0	—	—	—

*Rubble—no sample

**Irregular shaped sample

Jackson County, Ohio
Franklin Township, Section 8
Permit Number 102 (Core Number 2898)
Nucorp
Trepanier #1

Depth	Perm to Air Md.		Vertical	Porosity Gex.Fld.	Fluid Sats.		Gr. Den.
	Maximum	90°			Oil	Wtr.	
4498.0-99.0	<0.1	<0.1	<0.1	1.5	0.0	94.7	2.77
4499.0-00.0	3.0	2.5	0.2	3.1	0.0	56.5	2.68
4500.0-01.0	17.0	17.0	0.9	7.8	0.0	24.8	2.67
4501.0-02.0	33.0	32.0	1.9	9.6	0.0	62.3	2.64
4502.0-03.0	26.0	26.0	14.0	11.5	0.0	89.5	2.65
4503.0-04.0	156.0	152.0	11.0	12.8	0.0	94.0	2.63
4504.0-05.0	60.0	17.0	1.2	10.4	0.0	82.8	2.62
4505.0-06.0	17.0	15.0	0.6	8.6	0.0	71.6	2.64
4506.0-07.0	6.3	5.8	0.5	8.4	0.0	71.4	2.64
4507.0-08.0	6.7	6.6	1.0	9.1	0.0	72.9	2.66
4508.0-09.0	3.5	3.4	0.6	7.7	0.0	73.4	2.64
4509.0-10.0	0.3	0.2	<1.0	5.2	0.0	85.4	2.63
4510.0-11.0	<0.1	<0.1	<0.1	2.9	0.0	85.3	2.70
4511.0-12.0	<0.1	<0.1	0.5	5.3	0.0	77.3	2.68
4512.0-13.0	0.2	0.1	0.3	5.6	0.0	75.0	2.68
4513.0-14.0	8.6	7.0	2.0	8.0	0.0	75.8	2.67
4514.0-15.0	8.1	7.3	0.4	7.3	0.0	76.9	2.66
4515.0-16.0	3.5	3.4	0.5	9.5	0.0	79.5	2.68
4516.0-17.0	0.9	0.8	<0.1	9.0	0.0	86.0	2.65
4517.0-18.0	20.0	16.0	0.2	11.6	0.0	79.1	2.64
4518.0-19.0	18.0	16.0	1.7	12.5	0.0	80.7	2.68
4519.0-20.0	159.0	144.0	35.0	14.9	0.0	73.1	2.68
4520.0-21.0	28.0	26.0	46.0	10.8	0.0		
4521.0-22.0	63.0	59.0	41.0	13.2	0.0		
4522.0-23.0	71.0	70.0	27.0	13.6	0.0		
4523.0-24.0	198.0	194.0	98.0	14.8	0.0	89.3	2.68
4524.0-25.0	20.0	19.0	<0.1	9.9	0.0	72.0	2.68
4525.0-26.0	184.0	152.0	22.0	13.2	0.0	95.3	2.67
4526.0-27.0	178.0	159.0	51.0	13.0	0.0	98.8	2.68
4527.0-28.0	180.0	162.0	76.0	13.1	0.0	98.1	2.68
4528.0-29.0	109.0	103.0	41.0	12.1	0.0	97.8	2.68
4529.0-30.0	11.0	3.4	0.7	7.0	0.0	69.6	2.67
4530.0-31.0	<0.1	<0.1	0.1	4.3	0.0	75.6	2.68
4531.0-32.0	0.2	0.1	0.1	2.0	0.0	75.0	2.67

Scioto County, Ohio
Green Township
No Permit or Core Number Assigned
Test/Monitor Well
Aristech

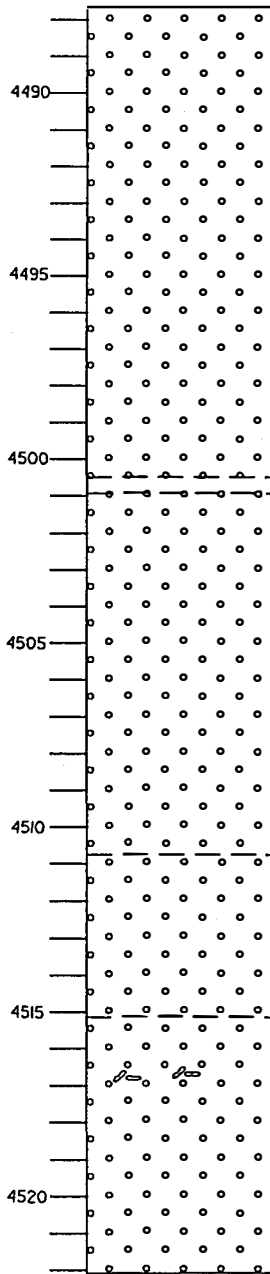
Depth	Kmax (md)>	Permeability K-90 (m ^d)	Vertical (md)	Porosity	Grain Density (gm.cc)
4021.0-22.0	231.00	0.02	0.02	2.2	2.79
4193.0-94.0	6.00	3.30	0.07	9.1	2.65
4202.0-03.0	86.00	70.00	1.40	12.7	2.64
4592.5-93.1	0.10	0.06	<.01	2.7	2.73
5196.5-97.0	1.80	0.04	1.70	3.6	2.84

**Erie County, Pennsylvania
City of Erie
Permit Number 20109
Hammermill Paper Company
Fee #2**

Depth	Vertical Permeability to Gas (in md)	Horizontal Permeability to Gas (in md)	Porosity (%)
5,110	<0.10	<0.10	2.7
5,154A	11.10	192.00	13.9
5,154B	53.20	76.00	11.2
5,159	<0.10	<0.10	2.6
5,552	6.34	5.14	13.4
5,556	2.05	1.33	12.6
5,559A	0.19	0.43	9.4
5,559B	1.84	1.92	12.9

Appendix V:
Graphical Descriptions of Ohio Cores

PERMIT NUMBER 102 (CORE NUMBER 2898)



Sandstone, white-medium brown, fine-medium grained, subrounded, thin lenses that are glauconitic, good intergranular porosity.
Rose Run

Sandstone, white-light brown, fine grained, well sorted, subrounded, good intergranular porosity, low-angle cross bedding.

Sandstone, as above.

Sandstone, white-light brown, fine grained, subrounded, moderately sorted, good intergranular porosity, trace of glauconite.

Sandstone, as above, green shale rip-up clasts up to 1 inch diameter. Asymmetric ripples with 1/2 inch wavelength on end of core. Locally green shale laminae lined with pyrite. Trace of glauconite. Green shale rip-up clasts.

Sandstone, white-light brown, fine grained, well sorted, subrounded, dolomite cement, good intergranular porosity, good cross bedding.

Sandstone, as above, green shale laminae

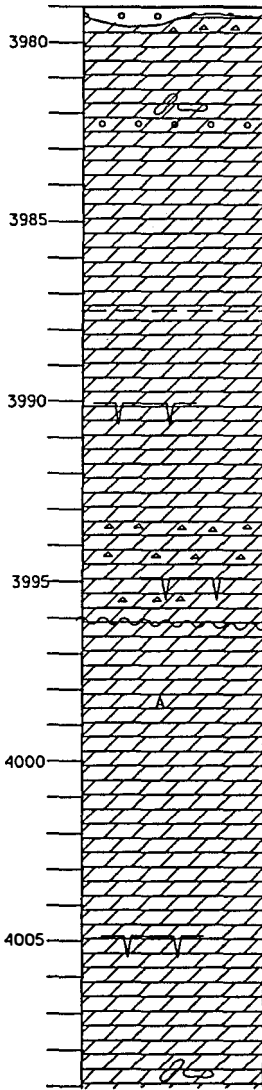
Sandstone, white-light brown, fine grained, good intergranular porosity, good low-angle cross bedding.

Thin lens of green shale.

Dolostone rip-up clasts.

Sandstone, white-light brown, fine grained, well sorted, sub-well rounded, good intergranular porosity.

Sandstone, as above, trace of glauconite



Local scour surface filled with sandstone. Sandstone, white, fine grained, very glauconitic, thin black shale partings.
Dolostone, light grey-brown, microcrystalline, stylolitic, trace of glauconite, chert clasts. Beekmantown

Dolostone, light grey-brown, microcrystalline, highly mottled, dense, no visible porosity, stylolitic. Rip-up clasts of dolostone up to 1 inch diameter. Scattered quartz grains in dolomite matrix, glauconite.

Dolostone, light grey-light brown, microcrystalline, thin wispy shale partings.

Thin bed of greenish-grey shale, 3/4 inch thick.
Dolostone, grey-brown, microcrystalline, thin hairline subvertical fractures lined with pyrite.

Dessication cracks on end of core.

Dolostone, light grey, microcrystalline, argillaceous, hairline fractures lined with pyrite.

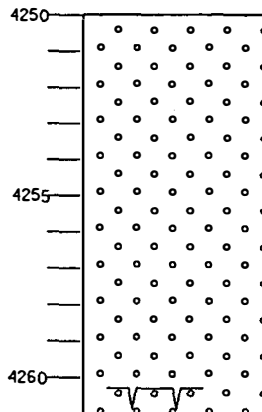
Dolostone, light grey medium crystalline, white chert nodules up to 1 inch diameter. Small vug (1/2 inch diameter) lined with quartz. Hairline vertical fractures lined with pyrite, some cutting across chert nodules.
Dessication feature.
Vertical hairline fractures lined with quartz.
Sharp contact with quartz and high concentration of glauconite.

Dolostone, light grey-light brown, microcrystalline, mottled.
Nodule of anhydrite in dolomite matrix, .2 inches in diameter.

Dolostone, light grey-light brown, microcrystalline, mottled, locally stylolitic, dense, no visible porosity. Hairline subvertical fractures healed with pyrite.

Dolostone, light grey-light brown, microcrystalline, mottled, dessication feature.
Subvertical hairline fractures healed with pyrite. Trace of glauconite.

Dolostone, light grey-light green, coarsely crystalline.
Wavy laminations (algal?). Rip-up clasts of dolostone up to 1/4 inch across.

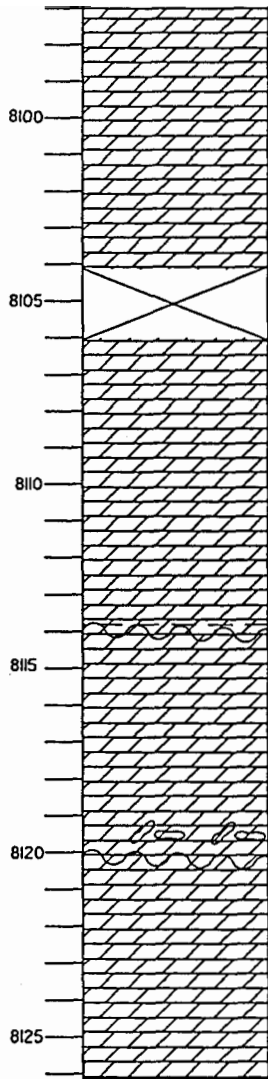


Sandstone, white-light brown, fine-very fine grained, subrounded, dolomite cement fair-good intercrystalline porosity. Rose Run

Sandstone, as above, good intergranular porosity.

Sandstone, white, fine-medium grained, scattered lenses of coarse grained, trace of glauconite, trace of pyrite.

Sandstone, white, fine-medium grained, subrounded, fair-good intergranular porosity, dolomite cement, trace of glauconite. Sand-filled mudcracks.



Dolostone, grey-medium to dark brown, microcrystalline, mottled, good vuggy porosity, vugs up to 1 inch, often filled with white dolomite. Trace of pyrite. Beekmantown

Dolostone, as above, rip-up clasts of dolostone.

Dolostone, grey-medium brown, microcrystalline, mottled, good vuggy porosity, vugs up to 1 inch, some filled with white dolomite.

Dolostone, grey-medium brown, microcrystalline, mottled, locally stylolitic no visible porosity.

Dolostone, as above, argillaceous dark grey shale partings.

Dolostone, grey-brown, microcrystalline, mottled, numerous vugs up to 2 inches filled with white dolomite, not interconnected, also pinpoint vuggy porosity. Soft sediment deformation.

Erosional contact. Lens of dark green shale, 1/4 inch thick.

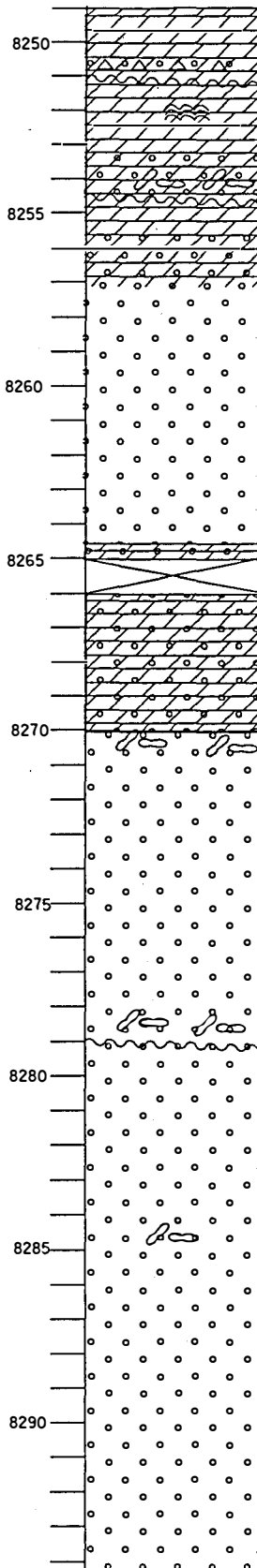
Dolostone, grey-brown, microcrystalline, mottled, locally stylolitic, pinpoint vuggy porosity.

Dolostone, as above, hairline fractures lined with pyrite. Thin fractures filled with white dolomite.

Dolostone rip-up clasts up to 1/2 inch across.

Dolostone, grey-light to medium brown, microcrystalline, highly mottled, poor to no visible porosity.

PERMIT NUMBER 592 (CORE NUMBER 2850)



Dolostone, medum brown, microcrystalline, thin argillaceous laminae lined with pyrite. Oolitic chert intraclasts. Intraclasts are up to 3 inches and are angular. Interbedded dolostone, sandstone, and sandy dolostone. Quartz is fine-coarse grained, subrounded, poorly sorted. Beekmantown
Thin lens of green shale at base of brecciated zone.
Digitate algalstromatolite in dolostone matrix

Sharp contact at 8254 feet with microcrystalline dolostone overlain by sandy dolostone. Chert and dolostone rip-up clasts up to 3 inches diameter above contact.

Alternating beds of microcrystalline, brown dolostone and white sandstone.

Sandstone, white, fine-very fine grained, well rounded, moderately sorted, well-developed low-angle cross bedding, good intergranular porosity. Several dolostone rip-up clasts less than 1/2 inch in diameter. Numerous shale laminae. Rose Run

Sandstone, white, fine-very fine grained, subrounded, moderately sorted, siliceous cement, good intergranular porosity.

Interbedded dolostone, sandstone, and sandy dolostone.

Dolostone, grey-medium brown, microcrystalline, sandy in part. Several vugs filled with white dolomite. Sandstone, white, very fine-medium grained, poorly sorted, subrounded, glauconitic. Numerous argillaceous shale partings.

Sandstone, white-light grey, very fine-medium grained, good intergranular porosity. Rip-up clasts up to 2 inches diameter composed of sandy dolomite. Numerous argillaceous shale partings.

Good low-angle cross bedding at 8274 feet.

Sandstone, white-light brown, very fine-medium grained, good intergranular porosity. Numerous shale laminae with pyrite.

Erosional contact. Thin lens of green shale 1/4 inch across. Numerous rip-up clasts of dolostone up to 2 inches diameter. Open vug 2 inches diameter lined with quartz and dolomite.

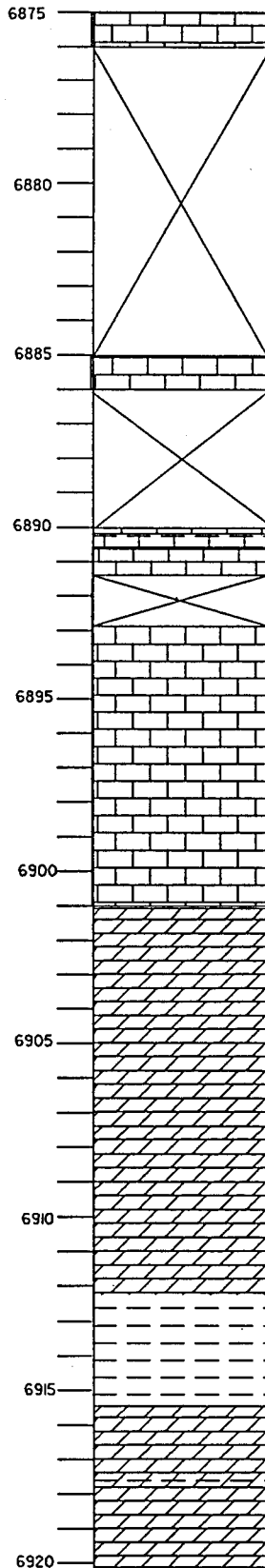
Sandstone, white, very fine-medium grained, good intergranular porosity, trace of glauconite.

Sandstone, as above. Rip-up clasts of dolostone near base of thin shale laminae.

Sandstone, as above, numerous argillaceous shale partings.

Sandstone, white, fine grained, good intergranular porosity, good low-angle cross bedding. Contorted bedding at 8292 feet.

PERMIT NUMBER 782 (CORE NUMBER 867)



Limestone, medium-dark grey, microcrystalline, highly mottled, argillaceous, fossiliferous-ostracods, brachiopods, trace of pyrite. no visible porosity.

Limestone, light grey-light brown, microcrystalline, thin argillaceous shale partings, trace of pyrite.

Limestone, as above.

Limestone, medium-dark brown, microcrystalline, slightly mottled, trace of pyrite. No visible porosity.

Limestone, dark grey-dark brown, microcrystalline, thin parallel laminations, stylonitic, no visible porosity.

Limestone, dark grey-dark brown, microcrystalline, mottled.

Dark green-black shale.

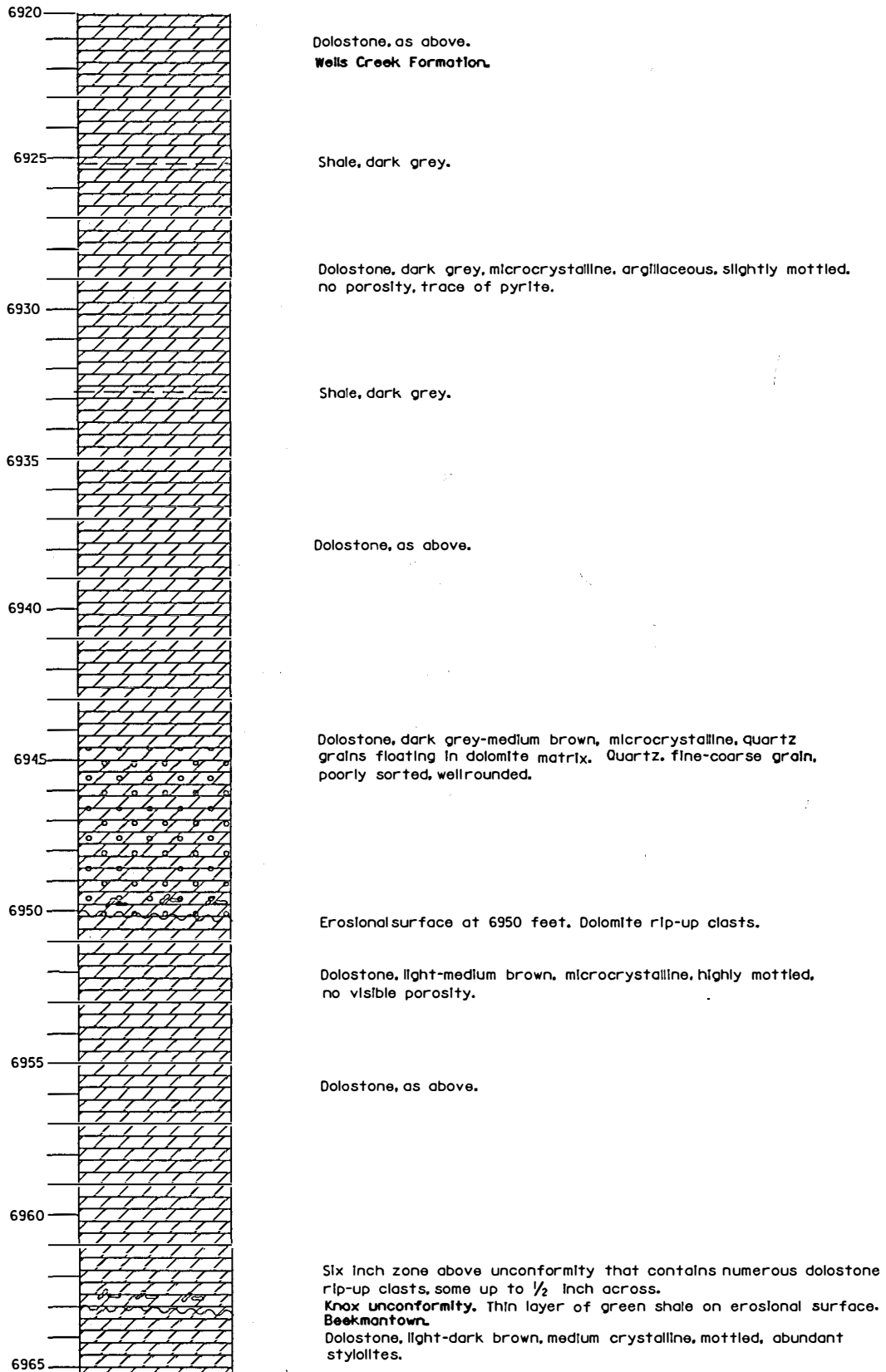
Dolostone, grey-brown, microcrystalline, slightly mottled, no visible porosity.

Dolostone, as above.

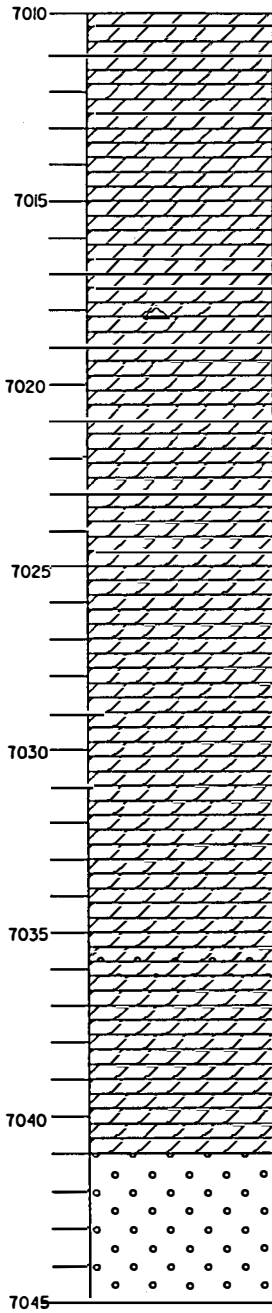
Shale, dark grey, calcareous.

Dolostone, dark grey-dark brown, microcrystalline, argillaceous shale partings.

PERMIT NUMBER 782 (CORE NUMBER 867)



PERMIT NUMBER 782 (CORE NUMBER 867)



Dolostone, grey-medium brown, fine-medium crystalline, nodular, glauconitic, at 7011 feet.

Dolostone, light-medium brown, fine-medium crystalline, highly mottled, very glauconitic at 7013 feet, thin argillaceous shale partings.

Dolostone, medium brown, medium crystalline, argillaceous, mottled in part, pyrite concentrated along stylolite surface.

Dolostone, as above, chert nodule up to 1/2 inch across at 7118 feet. Mottled in part

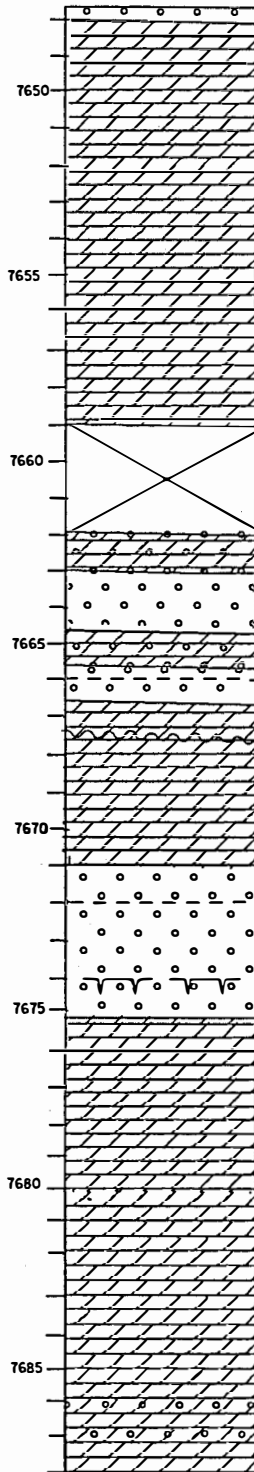
Dolostone, light-medium brown, medium crystalline, mottled.

Dolostone, medium brown, sandy in part. Quartz, very fine grain, very glauconitic.

Dolostone, medium brown, medium crystalline, mottled, vug up to 1 inch across filled with white dolomite.

Dolostone, medium brown, fine crystalline, poor porosity.

Sandstone, white-light green, very fine grain, glauconitic, good cross bedding, good intergranular porosity. **Rose Run** Subvertical fracture at 7041 feet lined with pyrite.



Sandstone, white-light grey, fine grained, glauconitic
Copper Ridge.

Dolostone, light grey-brown, microcrystalline, good pinpoint vuggy porosity, dolomite rhombs filling in vugs, mottled in part, stylolitic.

Dolostone, medium-dark brown, coarser grained than above.

Dolostone, light-medium brown, microcrystalline, highly mottled, poor porosity, stylolitic, trace of glauconite.

Dolostone, light-medium brown, microcrystalline, very sandy.

Sandstone, light grey-brown, fine-coarse grained, poorly sorted, trace of glauconite. Good intergranular porosity.

Sharp depositional contact. Concentration of pyrite and glauconite
Dolostone rip-up clasts above surface.

Dolostone, light-medium brown microcrystalline, sandy in part, soft sediment deformation, trace of pyrite and glauconite.

Sandstone, white-light grey, fine-medium grained, subrounded, brown staining, yellow fluorescence. Shale bed 2 inches thick, grey-green.

Sandstone, white-light grey, fine-coarse grained, poorly sorted, subrounded, thin argillaceous partings with pyrite concentrated along surface, low-angle cross-bedding. Good intergranular porosity. Mudcracks filled with sandstone.

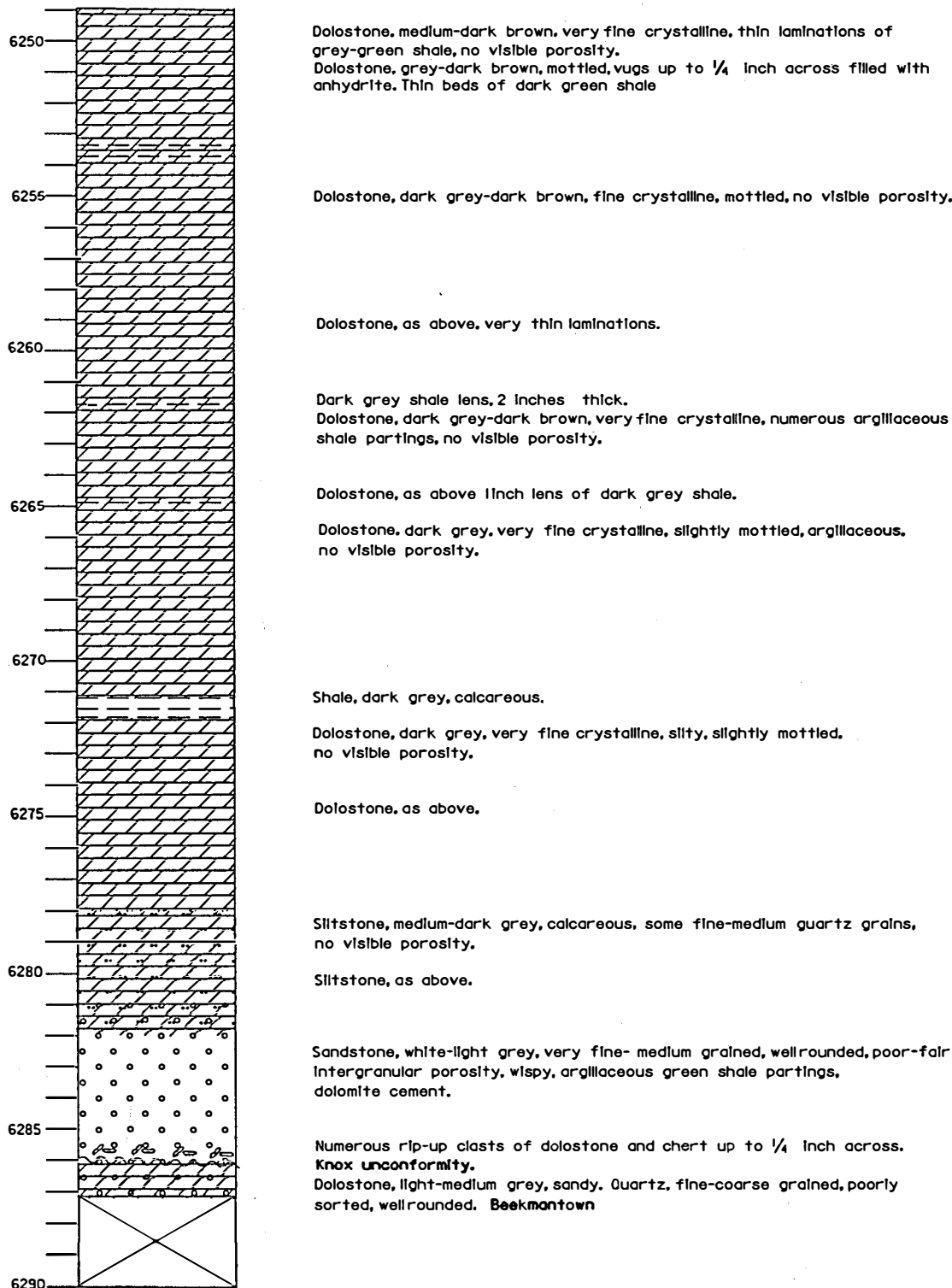
Dolostone, microcrystalline, grey-brown, local green-grey shale laminae, stylolitic.

Oncolites up to 1 inch in diameter. Some have rip-up clasts as nucleus.

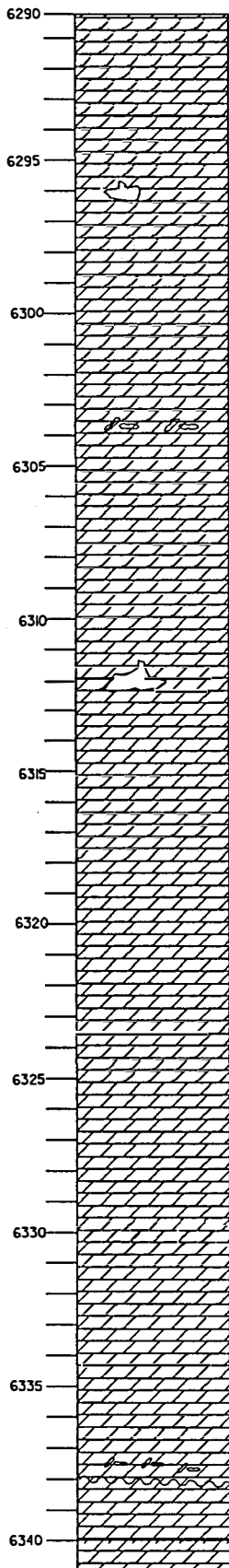
Dolostone, microcrystalline, light brown-grey, mottled, local thin shale laminae

Sandstone, fine-medium grained, thin shale laminae. Dolostone rip-up clasts.
Dolostone, microcrystalline, brown-grey, vuggy, 1/4 inch vug filled with white dolomite. Dolostone rip-up clasts.

PERMIT NUMBER 1249 (CORE NUMBER 2923)



PERMIT NUMBER 1249 (CORE NUMBER 2923)



Dolostone, light brown-medium grey, microcrystalline, highly mottled.

Subvertical fracture 4 inches long filled with sandstone.

Dolostone, as above.

Brecciated zone at 6296 feet. Angular clasts of dolostone, green shale. Vugs up to 1 inch filled with white dolomite, fractures filled with green shale, stylolitic.

Dolostone, grey-medium brown, microcrystalline, vugs up to 1 inch filled with white dolomite.

Dolostone, grey-medium brown, microcrystalline, highly mottled, healed fractures filled white dolomite. Vugs up to 1 inch filled with white dolomite.

Fractured zone at 6304 feet, 6 inches thick. Fractures healed with white dolomite. Numerous dolostone clasts up to 2 inches across.

Dolostone, light-medium brown, microcrystalline, thin green shale partings. 4 inches interval of alternating thin beds of brown and grey dolostone.

Dolostone, grey-medium brown, microcrystalline, highly mottled, stylolitic locally, occasional green-black shale partings.

Dolostone, as above, vugs up to 1 inch filled with white dolomite.

Highly fractured and brecciated zone. Fractures are healed with white dolomite. Associated vugs are filled with white dolomite. No visible secondary porosity.

Dolostone, grey-brown, microcrystalline, mottled.

Dolostone, grey-medium brown, microcrystalline, mottled locally. Hairline fractures healed with white dolomite. Vugs up to 1 inch filled with white dolomite.

Dolostone, as above, mottled.

Fractured zone at 6319 feet. Brecciated dolostone, fractures healed with white dolomite.

Dolostone, as above, vugs up to 3 inches associated with fractures. Vugs lined with 1/4 inch yellow dolomite rhombs.

Dolostone, grey-brown, microcrystalline, hairline vertical fractures filled with dolomite, some open vugs and pinpoint vuggy porosity.

Dolostone, grey-brown, microcrystalline, mottled, locally stylolitic, hairline fractures healed with white dolomite.

Dolostone, grey-brown, microcrystalline, mottled, vugs up to 1 inch filled with white dolomite.

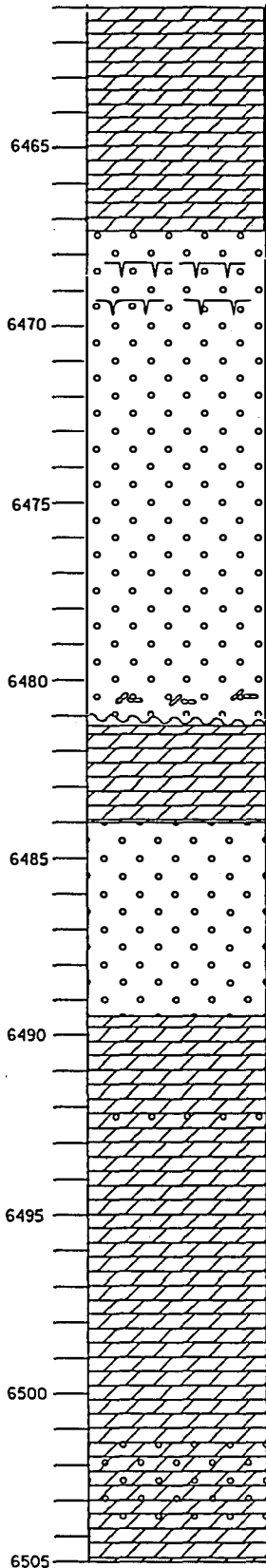
Dolostone, grey-brown, microcrystalline, mottled, occasional thin green shale partings, locally vugs up to 1/2 inch filled with white dolomite.

Dolostone, grey-brown, microcrystalline, mottled, green-grey shale partings, locally, trace of vugular porosity.

Numerous dolomite rip-up clasts. Sharp erosional contact at 6338 feet. 1 inch of greenish grey shale,

Dolostone, grey-brown, microcrystalline, mottled in part.

PERMIT NUMBER 1249 (CORE NUMBER 2923)



Dolostone, light-dark brown, microcrystalline, thin parallel bedding no visible porosity. Occasional green argillaceous shale partings.
Rose Run

Dolostone, as above, no visible porosity.

Vertical fracture healed with dolomite
Vugs up to 2 inches across filled with chert.

Sandstone, white, fine-medium grained, subrounded, moderately sorted, good intergranular porosity. Excellent polygonal mudcracks on end of core.

Sandstone, white, fine-medium grained, good intergranular porosity, wispy shale laminae, several upward fining sequences bound by sharp contact.

Sandstone, as above, low-angle cross bedding.

Sandstone, white, fine-medium grained, subrounded, good intergranular porosity, wispy argillaceous shale partings.

Sharp contact at 6481.4 feet. 4 inch lens of grey-green shale. Numerous rip-up clasts of dolomite, glauconitic.
Dolostone, medium-dark brown, microcrystalline, no porosity, contains thin green shale lenses. Subvertical stylolite at 6483 feet.

Sandstone, white, fine-very fine grained, well sorted, subrounded, good intergranular porosity, trace of glauconite, cross bedding.

Dolostone, grey-medium brown, microcrystalline, silty, thin grey-green shale partings, no visible porosity. Large vug at 6491 feet filled with white chert. Numerous hairline fractures below vug lined with pyrite.

4 inch zone of fine-coarse sandstone, dolostone and chert clasts at 6493 feet.

Dolostone, brown, microcrystalline, good pinpoint vuggy porosity.
Pisolithic dolostone, at 6494.5 feet. 6 inch zone with numerous pisoliths, some replaced by glauconite, stylolitic.

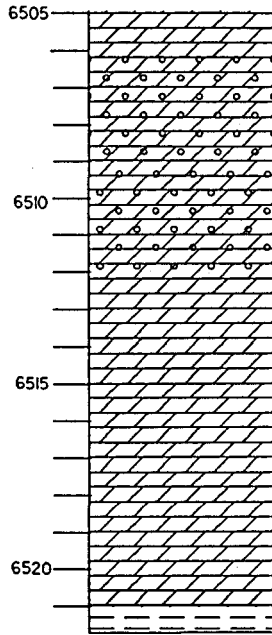
Dolostone, grey-light brown, microcrystalline, highly mottled.

3 inch vug at 6497.5 feet filled with white chert.

Alternating beds of sandstone and dolostone. Sandstone, white, fine-medium grained, fining upward sequences. Dolostone, grey-brown, microcrystalline, dolostone is brecciated and fractures are filled with sandstone.

Dolostone, grey-brown, microcrystalline, mottled, glauconitic, hairline fractures lined with pyrite.

PERMIT NUMBER 1249 (CORE NUMBER 2923)



3 Inch vug at 6505 feet filled with white chert.
Glaucinitic sandstone with dolomite rip-up clasts.

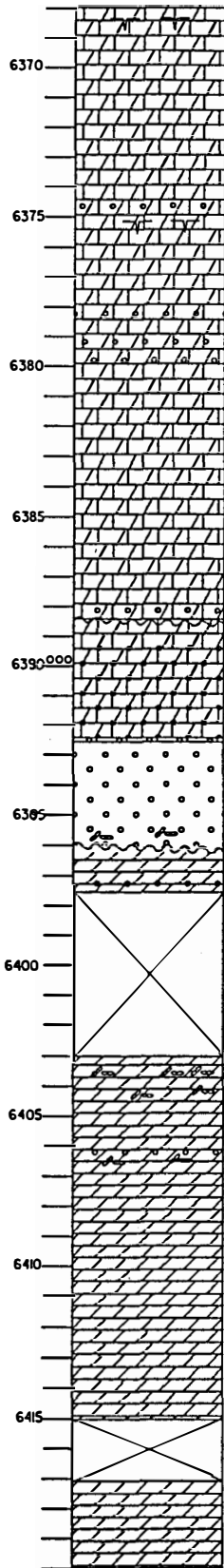
Interbedded sandstone, sandy dolostone, and dolostone.

Dolostone, brown, microcrystalline, 1/2 Inch vugs filled with white dolomite.
Laminated dolostone.

Sandy dolostone. 2 Inch dolostone rip-up clast.

Dolostone, grey-brown, microcrystalline, mottled.

Shale, grey-green.



Limestone, grey-medium brown, microcrystalline, mottled, dolomitic, no visible porosity, numerous dolostone rip-up clasts. Desiccation crack at 6368 feet. WELLS CREEK FORMATION

Limestone, dark brown-dark grey, microcrystalline, mottled, dolomitic, no visible porosity.

6375 Floating grains of quartz, fine-coarse grained, poorly sorted, Desiccation cracks.

Limestone, dark grey, argillaceous, dolomitic, no visible porosity.

6380 Limestone, brown, microcrystalline, Quartz, predominantly fine fine grained, some coarse grained.

Limestone, medium-dark grey, very fine crystalline, argillaceous, dolomitic, Quartz, very fine-coarse grained, subrounded.

Limestone, as above.

6385

Sharp erosional contact at 6388 feet. Lens of sandstone above contact, Quartz, fine-coarse grained, poorly sorted, sub-well rounded, good intergranular porosity, friable, glauconitic.

6390

Limestone, medium grey, microcrystalline, dolomitic, sandy in part.

Sandstone, white-light green, well rounded, fine-coarse grained, very friable, good intergranular porosity, poorly consolidated.

6395

Rip-up clasts of green shale, KNOX unconformity

Dolomite, light grey-light brown, microcrystalline, mottled, vugs up to 1/2 inch across filled with white dolomite. 2 inch lens of sandstone, white, very fine grained, well sorted. ROSE RUN

6400

Dolostone, light grey-light brown, microcrystalline, COPPER RIDGE
1 inch dark grey-green shale lens at 6403 feet. Numerous dolostone rip-up up to 1 inch across below shale lens.

6405

Dolostone, as above, mottled, numerous stylolites.
Thin lens (1/8 inch) of sandstone, white, very fine grained, well sorted, glauconitic. Rip-up clasts of dolostone up to 1/4 inch across.

6410

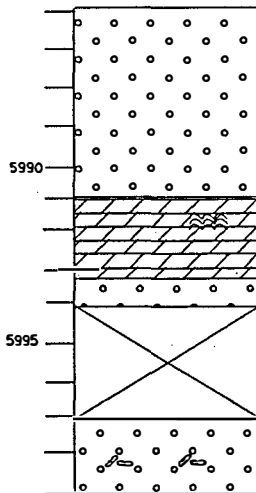
Dolostone, light grey-light brown, microcrystalline, highly mottled, no visible porosity.

Dolostone, as above, vug filled with white dolomite, up to 1 inch across.

6415

Dolostone, light-medium brown, microcrystalline, subvertical fractures filled with green, argillaceous shale, Hairline vertical fracture lined with pyrite.

PERMIT NUMBER 2183 (CORE NUMBER 2852)



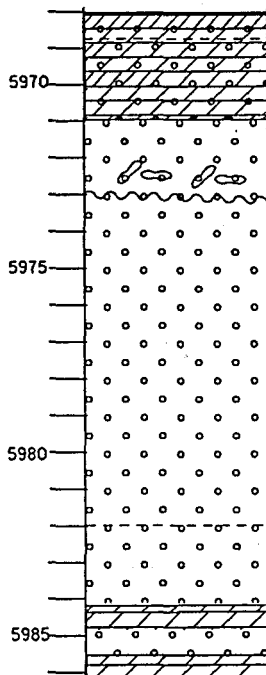
Sandstone, grey, fine-very fine grained, massive bedded, good porosity, silty in part, trace of glauconite, trace of pyrite. **Rose Run.**

Dolostone, microcrystalline, poor porosity, stromatolitic, dolomite rip-up clasts up to 1 inch in diameter.

Sandstone, grey, fine-medium grained, thin beds of dolomite, and shale partings.

Sandstone, grey, fine-very fine grained, good porosity, glauconitic numerous rip-up clasts of dolomite and oolitic chert.

PERMIT NUMBER 2268 (CORE NUMBER 2853)



Dolostone, grey-brown, microcrystalline, quartz grains in dolomite matrix. Thin green shale bed. **Wells Creek Formation.**

Dolomite, as above, sandy, increase in quartz from above.

Sandstone, grey, fine grained, fair intergranular porosity.

Knox unconformity. Wispy green shale bed on erosional surface with pyrite. Dolomite rip-up clasts near erosional surface. Trace of glauconite. **Rose Run**

Sandstone, light grey, fine grained, abundant glauconite, friable, good intergranular porosity, dolomite cement. Low-angle cross bedding.

Interbedded glauconitic sandstone and dolamitic sandstone.

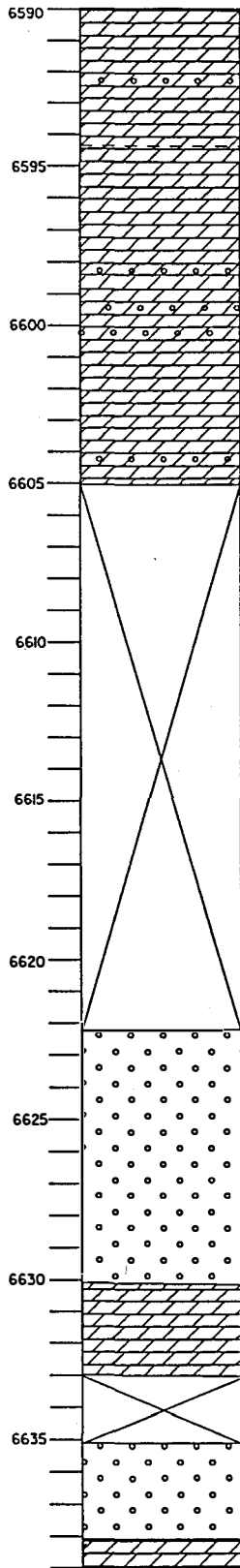
Thin green shale bed $\frac{1}{4}$ inch thick.

Sandstone, fine grained, glauconitic.

Dolostone, grey-brown, microcrystalline, no visible porosity.

Sandstone, fine grained, glauconitic, good intergranular porosity.

Dolostone, grey-brown, microcrystalline, no visible porosity.



Dolostone, grey-light brown, microcrystalline, dense, no visible porosity, sandy in part, trace of pyrite. Vertical fracture 6590-92 feet, and 6592-93 feet. Sandstone, fine grained, glauconitic, interbedded with thin beds of dolomite, trace of pyrite. **Beekmantown**

Thin 1 inch bed of greenish grey shale, pyritic.
Dolostone, grey-light brown, microcrystalline, dense no visible porosity.

Dolostone, as above, vuggy porosity, vugs lined with dolomite.

Dolostone, as above, sandy in part.

Dolostone, sandy dolostone, and interbedded sandstone. Sandstone is glauconitic.

Dolostone, grey-brown, microcrystalline, dense, no visible porosity.

Dolostone, as above, sandy in part. Vertical fracture lined with pyrite.

Sandstone, white-light brown, fine-medium grained, sub-well rounded, moderately sorted, good intergranular porosity. **Rose Run**

Sandstone, as above, good low-angle cross bedding.

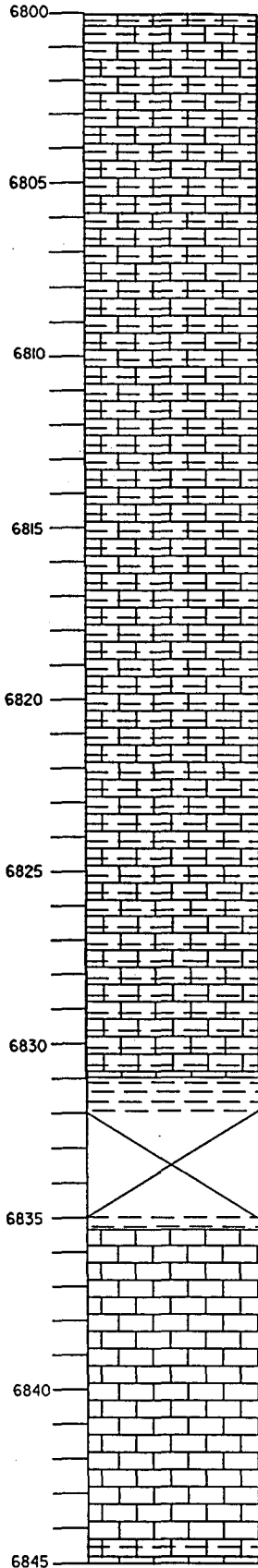
Sandstone, as above, good low-angle cross-bedding.

Dolostone, grey-light to medium brown, microcrystalline, highly mottled, dense, no visible porosity.

Sandstone, white-light brown-grey, fine-medium grained, subrounded, shale laminations, good intergranular porosity.

Dolostone, grey-light brown, sandy in part, glauconitic.

PERMIT NUMBER 4092 (CORE NUMBER 2713)



Limestone, dark brown-grey, very fine crystalline, numerous wispy, dark grey-black shale lenses separating nodular limestone, no visible porosity. Small trace of anhydrite, less than 1 percent. Trace of pyrite.
Wells Creek Formation.

Limestone, as above, fossiliferous, ostracod fragments.

Limestone, dark grey-dark brown, very fine crystalline, very nodular, nodules separated by dark grey-black organic lenses. Fossiliferous, ostracods, brachiopods, bryozoan fragments. No visible porosity.

Limestone, as above. Fossiliferous, ostracods and bryozoan fragments.

Shale, dark grey-black, calcareous.

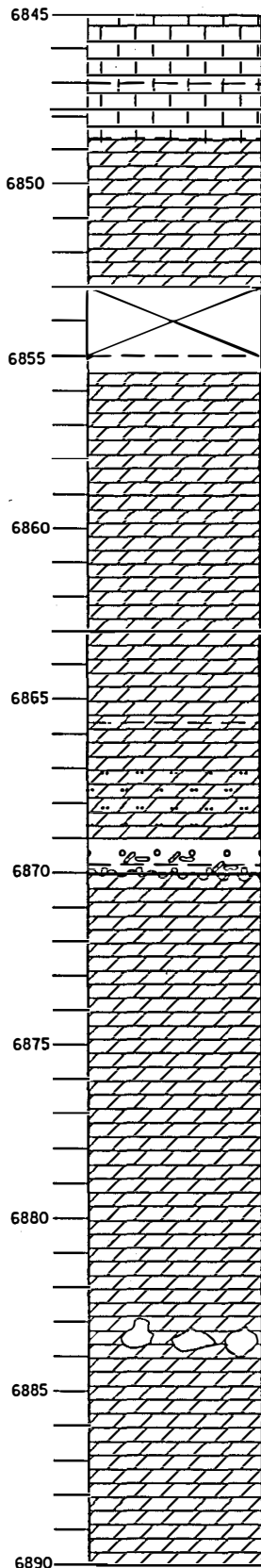
Shale, dark grey-black, calcareous.

Limestone, grey-dark brown, very fine crystalline, numerous wispy organic laminae, no visible porosity.

Limestone, dark grey, very fine crystalline, massive bedding, no visible porosity. Trace of pyrite.

Shale, dark grey-black 2 inches thick.

PERMIT NUMBER 4092 (CORE NUMBER 2713)



Limestone, dark grey-dark brown, fine crystalline, dolomitic.

Dolostone, grey-dark brown, fine crystalline, mottled, locally argillaceous, no visible porosity, trace of pyrite.

Shale, dark green-grey, 6 inch bed.

Dolostone, grey-medium brown, fine crystalline, mottled, argillaceous, no visible porosity.

Shale, dark grey-green, 2 inches thick.

Dolostone, grey-medium brown, fine crystalline, mottled, locally argillaceous.

Shale, dark grey.

Dolostone, grey-brown, fine crystalline, mottled, locally argillaceous.

Dolostone, as above, and siltstone, glauconitic.

Angular rip-up clasts of dolostone up to 3 inches in diameter above unconformity. Knox unconformity. Thin veneer of green shale on unconformity. Numerous fine-medium quartz grains floating in dolomite matrix. Trace of pyrite. Beekmantown.

Dolostone, grey-medium brown, medium crystalline, slightly mottled, fair pinpoint vuggy porosity. Open vug at 6873 feet lined with 1/4 inch white dolomite rhombs, green-grey argillaceous shale partings locally.

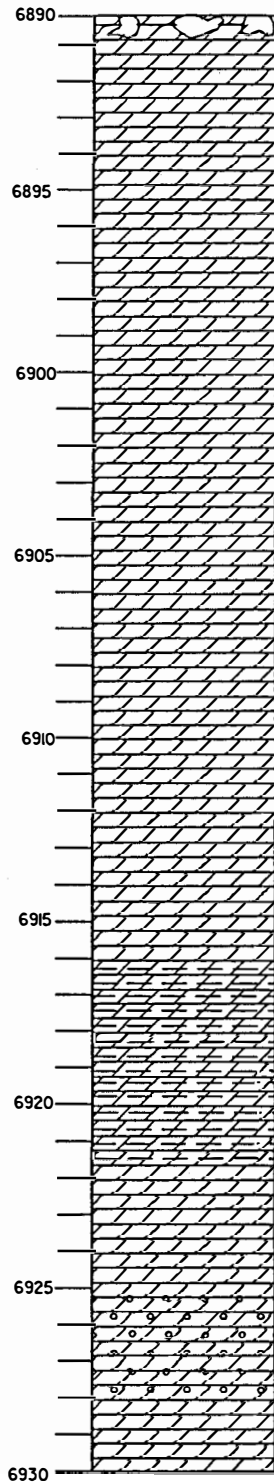
Dolostone, grey-medium brown, fine crystalline, slightly mottled, locally argillaceous shale partings. Locally small vugs, many filled with white dolomite. Vertical fracture at 6877 feet lined with pyrite.

Dolostone, as above.

Brecciated zone at 6884 feet, 6 inches thick, composed of dolostone clasts and green shale. Trace of fine-medium quartz grains.

Dolostone, grey-medium brown, fine crystalline, slightly mottled, locally stylolitic, locally trace of vuggy porosity.

PERMIT NUMBER 4092 (CORE NUMBER 2713)



Brecciated zone at 6891 feet, 6 inches thick, composed of dolostone clasts and green shale.

Dolostone, grey-medium brown, medium crystalline, good intergranular porosity, locally mottled, locally stylolitic.

Dolostone, as above.

Dolostone, grey-medium brown, medium crystalline, very thin argillaceous laminations, glauconitic.

Fractured zone at 6905.5 feet. Numerous fractures with dolostone clasts up to 2 inches across, vertical healed fractures filled with light brown dolomite rhombs, some fractures contain pyrite. 6 inch zone below fractured interval with well-developed vugular porosity. Vugs are up to 1 inch across and often filled with white dolomite rhombs.

Dolostone, grey-brown, medium crystalline, locally mottled, locally argillaceous shale partings.

Fractured zone with dolostone clasts up to 1 inch across at 6913 feet. Large vug, 2 inches across lined with 1/4 inch dolomite rhombs.

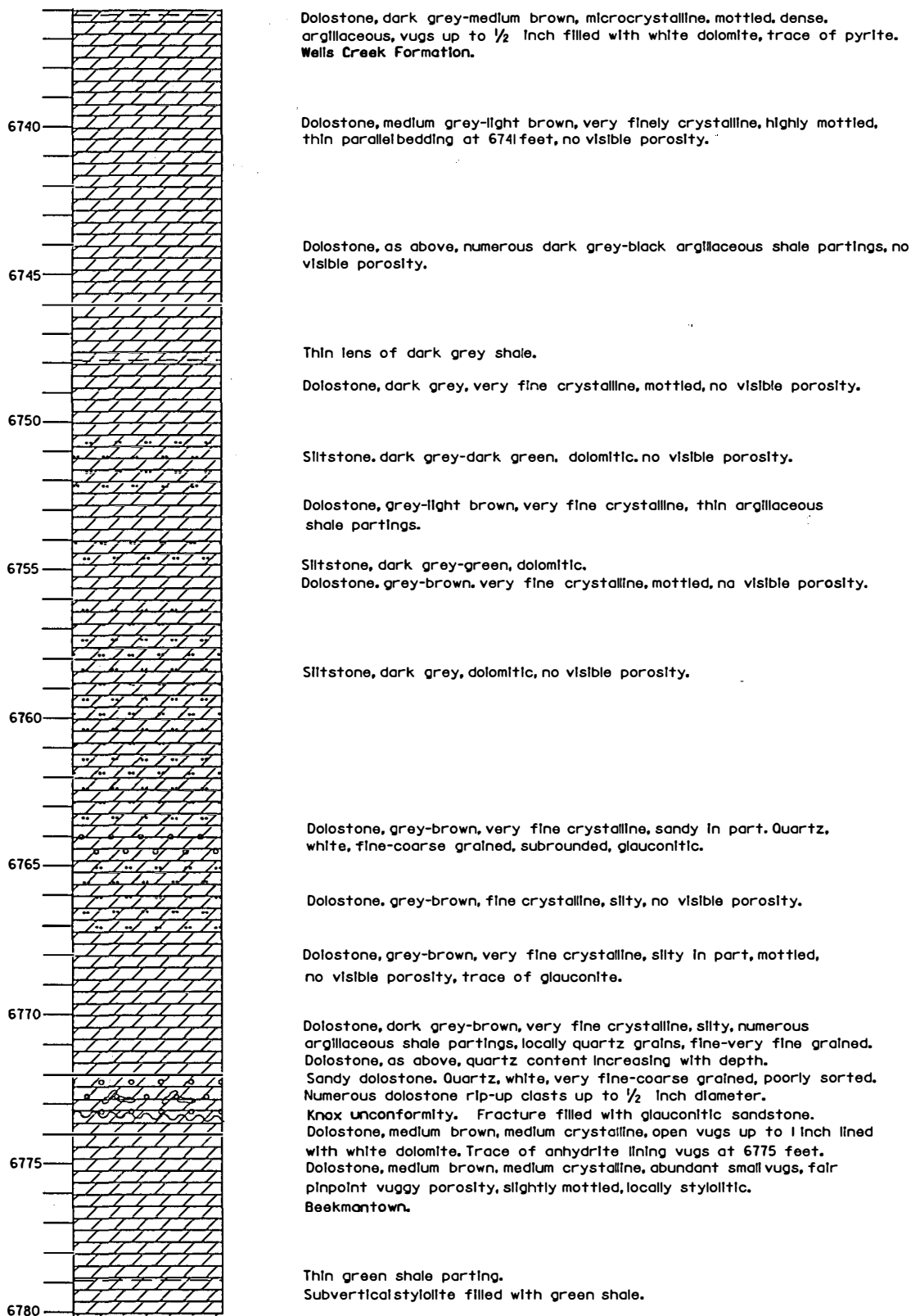
Dolostone, grey-brown, medium crystalline, mottled.

Dolostone, and interbedded light green shale.

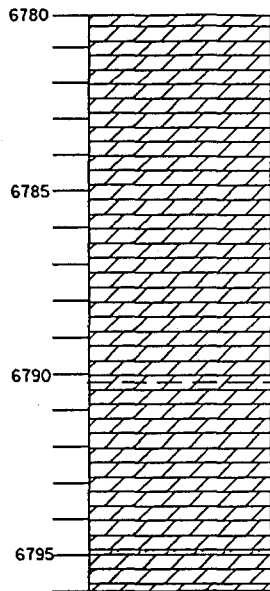
Dolostone, grey-medium brown, medium crystalline, mottled.

Dolostone, as above, locally green, argillaceous shale partings.

Interbedded sandstone and sandy dolostone. Sandstone, white, very fine-grained, moderately sorted, subrounded, good intercrystalline porosity, locally glauconitic, low-angle cross bedding.



PERMIT NUMBER 5962 (CORE NUMBER 3006)



Dolostone, medium brown, medium crystalline, poor pinpoint vuggy porosity. Small vugs less than 1/4 inch diameter filled with white dolomite.

Dolostone, textural change from above, light-medium brown, medium crystalline, enhanced intergranular porosity, mottled, locally stylolitic.

Dolostone, as above, 3 inch fractured vug at 6785.9 feet filled with white dolomite mottled, locally stylolitic.

Dolostone, medium brown, medium crystalline, locally stylolitic, no visible porosity.

Thin green shale parting.

Dolostone, light-medium brown, fine crystalline, highly mottled, locally stylolitic, no visible porosity, trace of glauconite at 6793 feet.

**Appendix VI:
Production Data From Ohio Wells**

PRODUCTION DATA OF ROSE RUN AND BEEKMANTOWN WELLS IN OHIO AS OF 1/92
 (From Janssens, 1992)

COUNTY	Township	BO	KCF	'91	'90	'89	'88	'87	'86	'85	'84	'83	'82	'81	'80	'79	'78	'77	'76	'75
	PERMY TD PH	CUMUL	CURGAS																	
ASHTABULA Her Lyle																				
	1847	04/82	RR	1313	2101	3793	3413	4876	8916	20702	52828	165264	512068							
	3907	03/90	RR	NA	44660															
	3970	11/90	RR	NA	NA	NA														
ASHTABULA Rose																				
	3842	02/89	RR	NA	5777	81491														
	3859	06/89	RR	NA	5777	81491														
	1521	06/90	DK	99	30642	6643	23999													
COLUMBIANA Knox																				
	3443	10/78	RR	0	0	PB 4/79														
	3478	03/79	RR	2547	912530	16330	18680	23100	26240	27040	31420	33020	47570	68150	105660	165980	185520	163720		
	3486	04/79	RR	0	5360	PB 10/85														
	3494	06/80	RR	0	14080	PB 5/84						200	1420	11790	670					
	3529	05/79	RR	2557	904570	PB 8/90	30	28490	27610	21880	15510	61590	61360	51420	174480	269160	193010			
	3573	07/79	RR	0	9800	PB 3/84														
	3622	12/79	DK	0	3230	PB 12/83														
	3692	05/80	RR	0	220	PB 2/82														
	3893	05/80	DK	8538	2662210	146600	158720	171830	179750	188780	205950	222180	269920	305660	338720	370850	103230			
	3895	05/80	RR	750	80	PB 2/82														
	4092	12/80	DK	0	47910	3682	3565	2453	2800	3400	3990	4980	5970	7230	7490					
	4093	11/80	RR	0	0	PB 7/84														
	4094	10/80	RR	143	53450	PB 2/86														
	4738	04/82	DK	2971	1140490	67050	75970	78060	72010	86330	102100	124880	151520	202560	180030					
	5787	03/85	DK	1155	419770	38830	47720	65380	82470	103490	81610									
	5803	12/86	RR	277	69560	4390	9250	11320	14110	30490										
	5809	04/86	DK	0	67270	10460	7460	9200	10520	16440	13190									
	5849	12/86	RR	0	1698															
	5852	10/86	RR	NS	NS															

CORNELL CUEGALS		'91	'90	'89	'88	'87	'86	'85	'84	'83	'82	'81	'80	'79	'78	'77	'76	'75	
COSHOCTON Adams cont'd																			
5885 12/86 BK	274	101510	PB	770	19720	73610	7410												
5887 10/87 BK	418	200870		53540	68820	11470													
5890 12/86 BK	20755	726650	27620	41420	53540	68820	11470												
			68060	85460	114450	171890	280390	6400											
			3636	3780	3951	4850	4557												
5908 01/87 BK	60651	62350	8230	8530	16240	17550	11800												
			7588	8951	12019	12866	19227												
5926 01/87 BK	0	0	PB 7/87																
5929 01/87 BK	0	700	PB 9/87																
5933 11/87 BK	1631	405070	59070	77130	82420	96440	90010												
5935 03/88 BK	533	203620	31610	37140	58150	74720													
5940 12/87 BK	786	222220	26940	33280	51280	97750	12970												
5940 11/87 BK	MS	MS																	
5989 08/87 BK	MS	MS																	
5993 11/87 BK	0	96120	3980	5870	14140	54500	17630												
6024 01/89 BK	22647	106060	14250	16580	75730														
			6762	7093	8790														
6109 06/82 BK	17411	32950	5240	7040	13940	6730													
			3619	4109	5342	4341													
6156 04/89 BK	11583	23090	7190	10990	4910														
			3894	4109	3580														
6187 07/89 BK	790	284750	89410	173780	21560														
6230 08/90 BK	1900	393160	296350	96810															
COSHOCTON Clark																			
6339 03/91 BK	194	28993	28993																
COSHOCTON Crawford																			
2883 11/76 BK	0	14463	NA	NA	4037	3641	6785	NA	NA	NA	NA	NA	NA	NA	NA	NA	NA	NA	NA
3081 07/78 BK	92	23435	NA	NA	5550	5781	11104	NA	NA	NA	NA	NA	NA	NA	NA	NA	NA	NA	NA
6064 01/88 BK	266	20122	4833	5166	7336	2787													
6074 12/87 BK	110	18740	4557	3832	5429	4922													
6253 04/90 BK	746	94944	51657	43287															
6309 11/90 BK	843	0	NA	0															
COSHOCTON Keene																			
3493 07/79 BK	4933	217730	PB 8/84						1710	18850	27840	61680	80510	27140					
3825 03/80 BK	31	1870	PB 11/83																
5659 06/85 BK	245	23500	PB 7/86																
6296 09/90 BK	412	0	NA	0															
COSHOCTON Lafayette																			
2888 12/78 BK	212	9643	NA	NA	NA	1658	1751	2195	2636	1403	NA	NA	NA	NA	NA	NA	NA	NA	NA
3261 12/78 BK	MS	MS																	
3347 11/78 BK	MS	MS																	
3668 11/79 BK	MS	MS																	
3967 10/80 BK	5052	297998	13300	14480	10310	10720	13430	19750	19000	20450	25689	45252	87980	17637					

	'91	'90	'89	'88	'87	'86	'85	'84	'83	'82	'81	'80	'79	'78	'77	'76	'75	
CUBOIL CURGAS																		
COSROCTOR White Eyes cont'd																		
2828 10/76 RR	454	68720	2210	2200	2410	2450	2960	3240	3100	3360	3320	2860	1560	3060	5150	10340	21200	300
2837 05/78 RR	550	533040	610	540	8130	23700	25140	25310	24590	33040	35620	44110	57020	63790	79680	111760		
2838 09/76 RR	678	224615	PB 9/83							1400	2700	4030	7050	30160	80360	83395	15520	
2895 11/76 RR	1773	512885	12390	12080	12470	13840	15380	17590	19240	23210	28790	32080	38650	40410	63890	92010	90855	
2919 02/77 RR	0	0	PB 5/77															
2970 05/77 RR	0	0	PR 7/82								460	1440	1410	14810	770			
3091 10/77 RR	2131	18890	PB 3/82															
3138 04/78 RR	0	4890	PB 8/79															
3169 04/78 RR	346	191929	PB 10/83															
3213 04/78 RR	557	72310	PB 4/84															
3241 11/88 RR	61	34920	7240	9850	16580	1250												
3244 07/78 RR	359	188580	PB 5/83															
3632 10/79 RR	477	107628	NA	NA	8213	16038	17695	NA	32557	33125	NA	NA	NA	NA	NA	NA	NA	
3753 03/80 RR	BS	BS																
3820 03/80 GR	243	63212	NA	NA	6103	9207	10280	11432	11794	14396	NA	NA	NA	NA	NA	NA	NA	
4282 05/81 RR	0	5900	PB 10/82															
4590 01/87 RR	0	280	PB 5/87															
5536 10/85 RR	0	14360	NA	NA	976	2331	2379	8285	389									
5653 06/85 RR	2401	225290	13970	14310	18770	24490	34320	67620	51810									
5955 11/87 GR	0	54810	5300	7900	12530	26220	2860											
6009 01/85 GR	294	42140	9180	10510	11770	10680												
6032 11/87 RR	494	48101	NA	10099	7236	30766												
6135 09/88 RR	198	17335	NA	10099	7236													
6152 11/88 RR	0	42400	NA	19291	23109													
6186 07/89 RR	884	67490	32040	26690	8760													
6245 01/90 RR	0	5560	PB 3/91															
6261 04/90 RR	166	8785	NA	8785														
PAIPIRED Hocting																		
1085 07/91 RR	0	0	Awaiting pipeline															
PAIPIRED Richard																		
1076 11/90 RR	NA	NA	NA	NA	NA	NA	NA	NA	NA	NA	NA	NA	NA	NA	NA	NA	NA	NA
GRANGA Barton																		
1109 01/85 RR	3911	138626	3525	4515	5376	9977	21225	21293	72715									
GRANGA Troy																		
1456 10/87 RR	85	73768	108	3736	5752	64172												
1567 10/88 RR	0	27231	3458	9825	13948													
BOHEBS Berlin																		
4783 08/88 RR	1821	138181	29100	46437	54766	7878												
4895 04/90 RR	75501	141956	125875	16481	48386	27115												
4902 04/90 RR	5293	65523	59150	6373	4284	1009												

			'91	'90	'89	'88	'87	'86
CORGILL COXGAS								
BOULE Noble								
1576 12/72 RR	80	232467						
PERRY COUNTY Reading								
3358 11/73 RR	NA	NA						
PORTAGE Randolph								
3778 05/90 RR	1700	87965	56748	31217				
3810 11/90 RR	132	15681	15681					
3841 06/91 RR	1000	54499	54499					
STARK Sugar Creek								
4637 05/90 RR	1379	73414	47607	25807				
4666 10/90 RR	2754	153952	148394	5558				
			2547	207				
4672 08/90 RR	825	74282	27483	46799				
4700 04/91 RR	206	9680	9680					
TUSCARAWAS Bucks								
3635 09/81 KH	72	2440						
4462 12/86 RR	74317	53169	11054	11053	11351	9120	9969	622
			6668	11492	13463	18768	21034	2892
4595 11/87 RR	0	370	NA	NA	NA	370		
4705 07/89 RR	0	1065	NA	1065	NA			
TUSCARAWAS Oxford								
4497 01/87 BK	2631	297872	55214	69619	61632	62414	48993	
4574 01/88 BK	249	81931	11984	16579	20295	33073		
4658 04/88 BK	167	37459	1684	5911	18446	11418		
4732 11/89 RR	NA	NA	NA	NA				
4778 10/90 BK	588	37833	37833					
TUSCARAWAS Wayne								
4815 7/91 BK	266	7148						
WAYNE Paint								
4798 10/90 RR	1177	117995	117995	NA				
4860 06/91 RR	16923	12911	12911					

Produced this from '73 to '81; inactive since

Produced 52 MCF intermittently since 10/78; prior production NA

NS= No significant production (and gaps in data)

NA= Not available

????= Operator, production, and status unknown

Significant annual-oil-production data shown below annual gas figures

RR= Rose Run sandstone

BK= Beethantown dolomite

KH= Knox Dolomite

GR= Gull River limestone

WELL IDENTIFICATION

ASHTABULA COUNTY

PERMIT SUBDIV OWNER LEASE

New Lyme Township

1847 L-8 ATWOOD EN RHOA 3
 3907 L-14 EQUITY O & G REEVE R-1
 3970 L-26 FREMONT EN WILKINS 1

Rome

3842 L-49 HALL IVAN BOGDAN U 5
 3859 L-48 HALL IVAN BOGDAN U 6

COLUMBIANA COUNTY

Knox Township

1521 SEC 28 BILL BLAIR BLICKENSDEPER 5

COSHOCTON COUNTY

Adams Township

3343 3Q NGO DEV ROEMER 2
 3478 L-1 2Q NGO DEV WILSON WM E 1-A
 3486 L-15 2Q NGO DEV PEPPER 1
 3494 SEC 1 NGO DEV WILSON 1-B
 3529 L-12 2Q NGO DEV ROEMER MARG. 1-A
 3573 L-10 2Q REDMAN OIL SKELTON 1
 3622 L-14 2Q NGO DEV PEPPER 2
 3892 L-6 2Q NGO DEV GARBER 2
 3893 SEC 2 NGO DEV NIZER STANLEY 1
 3895 L-1 2Q NGO DEV WILSON 1C
 4092 SEC 2 NGO DEV OAKLIEF WALDO 1
 4093 L-5 2Q NGO DEV WEAVER/PATTERSON 1
 4094 SEC 9 NGO DEV HAWK 1
 4738 SEC 2 NGO DEV NIZER STANLEY 3
 5787 SEC 10 NGO DEV STAHL KENNETH 5
 5803 L-13 2Q NGO DEV ROEMER 3-A
 5809 SEC 9 NGO DEV PHILABAUM M 1
 5849 SEC 12 ATWOOD EN ROBINSON 1
 5852 SEC 20 RED HILL DEV MILLER JOHN C 2
 5885 SEC 2 NGO DEV HAWK ELEANOR 2
 5887 SEC 10 NGO DEV STAHL KENNETH 4
 5890 SEC 10 NGO DEV HUFF GLENN 2
 5908 SEC 20 NGO DEV HACKENBRACHT MABEL 1
 5926 SEC 19 NGO DEV POGLE 1
 5929 SEC 9 NGO DEV DAVIS 1
 5933 SEC 1 NGO DEV AULT RUSSELL 1
 5935 SEC 1 NGO DEV AULT 2
 5940 SEC 19 NGO DEV REISS 1-A
 5980 SEC 6 RED HILL DEV ROBINSON E 1
 5989 SEC 11 RED HILL DEV MILLER JOHN 1
 5993 SEC 11 NGO DEV MOORE W D 1
 6024 SEC 11 NGO DEV CUNNINGHAM L 1
 6109 SEC 11 NGO DEV HUFF GLENN 5
 6156 SEC 20 NGO DEV HACKENBRACHT OSCAR
 6187 L-1 2Q CONSOL RES AM WILSON UNIT 5
 6290 SEC 1 NGO DEV NIZER STANLEY 7

Clark Township

6339 SEC 20 JEFFERSON O&G CROSS 1

Crawford Township

2883 L-15 1Q ENERGY DEV WILSON 1
 3081 SEC 12 ENERGY DEV THOMAS 1
 6064 SEC 12 LAKE REGION OIL TROYER D J 1
 6074 SEC 19 LAKE REGION OIL RABER L 1
 6253 SEC 6 JERRY MOORE SCHEETZ M U 1

COSHOCTON COUNTY Crawford Township cont'd

6309 SEC 6 JERRY MOORE WELLINGTON LARRY U 1
 Keene Township

3493 SEC 1 NGO DEV DREHER 1
 3825 SEC 1 NGO DEV NATHIAS 1-A

COSHOCTON COUNTY Keene Township cont'd

5659 SEC 10 NGO DEV WELLING 1
 6296 L-9 2Q JERRY MOORE ENDSLEY LARRY A U 1
 Lafayette Township

2888 2Q ROSCOE O&G NOBLE HAROLD U 1
 3261 L-11 3Q REDMAN OIL ROEMER 1
 3347 2Q REDMAN OIL NOBLE 1
 3668 L-9 3Q REDMAN OIL DILLON 3
 3967 L-3 3Q REDMAN OIL DILLON 4
 6081 L-4 3Q ATWOOD EN RABER C L 1
 6092 L-8 3Q ATWOOD EN GRACE U 1
 6271 L-9 4Q RED HILL DEV BLUCK-HICKORY FLATS 2
 6278 L-1 4Q NGO DEV EVANS RICHARD 1

Mill Creek Township

6313 SEC 2 COL NAT RES 22248 NISLEY D&E
 6352 SEC 21 JERRY MOORE GILMORE U 1

Oxford Township

6014 1Q RED HILL DEV WENTZ JEAN 1
 6029 1Q RED HILL DEV DALE E 3
 6113 2Q RED HILL DEV HOFFMAN K U 3
 6116 3Q RED HILL DEV HACKENBRACHT R 4
 6122 1Q RED HILL DEV DORSEY R 1
 6273 3Q RED HILL DEV DIEGIDIO MARY 1

Tuscarawas Township

2617 L-11 4Q ??? EATON CORA 1
 2686 L-8 3Q REDMAN OIL PRETTY PRODUCTS 1
 2733 L-16 1Q REDMAN OIL SEWELL RIVER 1
 2758 L-9 1Q MID-OHIO EN PETERS-WEAVER R 1
 2775 L-16 1Q MID-OHIO EN COUNTY COMM. 1
 2917 L-1 1Q MANITOU EXPL BECK D O 1
 3658 L-19 4Q CYCLOPS PORTEUS J & L 2
 3671 L-1 1Q ROSCOE O&G PEW C & O 2-A
 3981 L-7 4Q ??? HUNT LARRY 1
 4610 L-9 4Q REDMAN OIL JOHNSON H 1
 4824 L-7 1Q REDMAN OIL WILKINS 1
 5298 L-1 1Q REDMAN OIL MARLATT 1
 5299 L-1 1Q REDMAN OIL MARLATT 2
 5810 L-8 1Q REDMAN OIL BECK 2
 5998 L-1 1Q ATWOOD EN PEW CHESTER 7
 6007 L-9 3Q ATWOOD EN PORTEUS 3

Virginia Township

6140 L-25 4Q OXFORD OIL VICKERS-WRIGHT U J-1
 6335 L-16 4Q OXFORD OIL VICKERS CLYDE J-1

White Eyes Township

2653 SEC 17 NGO DEV BARTH 1
 2688 SEC 16 NGO DEV ADAMS1
 2724 SEC 17 NGO DEV BARTH FRED 8
 2725 SEC 17 NGO DEV ADAMS W T 2
 2735 SEC 17 NGO DEV BICKLE/FRANK 1
 2736 SEC 16 NGO DEV ADAMS W T 3
 2768 SEC 24 ??? ROEMER M 1
 2828 SEC 16 NGO DEV ADAMS W T 4
 2837 SEC 24 NGO DEV BARTH FRED 2
 2838 SEC 24 NGO DEV BARTH 3
 2919 SEC 6 NGO DEV MASON 1
 2895 SEC 17 NGO DEV BARTH FRED 6
 2970 SEC 4 NGO DEV ZINKON 1

COSHOCTON COUNTY White Eyes Township cont'd

3091 SEC 24 NGO DEV BARTH 5
3138 L-8 4Q NGO DEV THOMAS W
3169 SEC 14 NGO DEV MOORE S 1
3213 SEC 7 NGO DEV SEWELL RIVER 1
3241 SEC 24 NGO DEV PARKER-ROEMER 1
3244 SEC 17 NGO DEV BARTH 7
3632 L-17 1Q ENERGY DEV SCARR 1
3753 SEC 5 ??? NORMAN 3
3820 L-16 1Q RED HILL DEV STEIN & CUTSHALL 1
4282 SEC 18 NGO DEV NEWTON 3
4590 SEC 24 NGO DEV DOOLITTLE 1
5536 SEC 25 HOPCO MCALISTER 1
5653 SEC 7 NGO DEV SEWELL RIVER 2
5955 SEC 6 NGO DEV EBERWINE RBT 1
6009 SEC 15 NGO DEV BOALS 1
6032 L-19 1Q WOOD CHAS MILLER 1
6135 L-12 1Q WOOD CHAS MILLER WM 3
6152 L-20 1Q WOOD CHAS OINGER BRUCE 1
6186 SEC 14 CONSOL RES AM BOALS U 2
6245 L-1 4Q NGO DEV GAUMER 1
6261 L-21 1Q WOOD CHAS FRANK-LAYMAN 1

FAIRFIELD COUNTY
Hocking Township
1085 SEC 7 BELDEN & BLAKE TOOILL 1

Richland Township
1076 SEC 27 HOPEWELL O & G SHADY MAPLE FARMS 1

GEAUGA COUNTY
Burton Township
1109 L-43 LONAK PETR HESS-WHITING U 1

Troy Township
1456 SEC 11 LONAK PETR DOBRA J U 1
1567 SEC 11 LONAK PETR ZALE C 1

HOLMES COUNTY
Berlin Township
4783 SEC 14 BELDEN BRICK BURKHOLDER E&A 1-A
4895 L-25 4Q KENOIL TROYER-RABER 2
4902 SEC 23 KENOIL SCHLABACH-TROYER U 1
4931 L-23 4Q MASON DLG YODER ET AL U 1
4987 SEC 23 KENOIL SCHLABACH MANELIUS 3
4996 SEC 23 TATUM PETR KELLY 1
5005 SEC 23 TATUM PETR CHRISTEN 1

Clark Township
1328 SEC 23 BUCKEYE OIL ERB R 1
4615 SEC 24E H & S OP SMITH ET AL 6
4759 SEC 11 JEFFERSON O&G HERSHBERGER RUDY 1
4760 SEC 25E JEFFERSON O&G RABER MOSE 2
4770 SEC 17 JERRY MOORE YODER NOAH N 2-17
4793 SEC 12 ATWOOD EN YODER 8
4800 SEC 21 JEFFERSON O&G YODER ROY 2
4801 SEC 17 TATUM PETR RABER E&F 2
4807 SEC 23 JEFFERSON O&G YODER ROMAN 2
4808 SEC 22 JEFFERSON O&G LIMBACHER DORIS 1
4815 SEC 24W JEFFERSON O&G MILLER NOAH 1
4820 SEC 19 LAKE REGION OIL YODER NOAH& AMANDA 3
4821 SEC 23 TATUM PETR WISE & SHUTT 2
4843 SEC 13 JERRY MOORE RABER ELI A U 6253
4853 SEC 16 LAKE REGION OIL BARKMAN MENNO 1
4854 SEC 22 LAKE REGION OIL RABER MOSE E 2
4860 SEC 23 TATUM PETR WISE & SHUTT 3

HOLMES COUNTY Clark Township cont'd
4883 SEC 14 BAKERWELL SCHROCK M 1

4913 SEC 25 SENECA EN SHUTT ROLAND E 1
4919 SEC 23 TATUM PETR WISE & SHUTT 4
4930 SEC 14 JERRY MOORE RABER ELI A 1
4932 SEC 6 BAKERWELL YODER M & F 1

HOLMES COUNTY Hardy Township
4916 SEC 14 TATUM PETR MILLER-RABER U 1
5002 SEC 17 MASON DLG GLICK ALLEN 1
5008 SEC 14 MASON DLG TROYER ALVIN 1

Mechanic Township
4818 L-21 2Q MASON DLG ERB-MILLER 9
4845 SEC 8 BI JOE BAGLE B-1
4859 SEC 3 MASON DLG RABER-MILLER U 1
4873 L-7 3Q JEFFERSON O&G YODER JOHN J 1
4878 SEC 2 STOCKER&SITLER HERSHBERGER E U. 1
4888 SEC 12 MASON DLG HERSHBERGER-ERB U 1
4889 SEC 3 MASON DLG RABER JOHN A 1
4890 L-6 2Q H & S OP WAYNE COUNTY 5
4912 SEC 13 MASON DLG YODER-MILLER U 1
4915 SEC 13 MASON DLG LOGSDON HELEN 2
4922 L-3 3Q COL NAT RES 22184 HERSHBERGER
4943 L-20 3Q COL NAT RES TROYER DJ&M 22249
4947 SEC 19E MASON DLG STUTZMAN F & E
4946 L-26 3Q TATUM PETR ERB U 1
4949 L-20 2Q MASON DLG MILLER E & L U 1
4950 L-25 2Q TATUM PETR STALLMAN U 1
4952 SEC 18, EQUITY O & G YODER-SCHLABACH U 1
4960 SEC 20W BI JOE DEV WAGERS TIM 1-B
4972 L-15 3Q BAKERWELL RABER-MILLER U 1
4991 SEC 19W MASON DLG STRAITS-AMY U 1
4999 L-16 3Q BAKERWELL YODER MATTIE 2
5003 L-6 3Q JEFFERSON O&G YODER JOHN J U 2
5014 L-11 3Q BAKERWELL KEIM R 2
5024 SEC 10 MASON DLG HICKORY LAKE IMC 1

Walnut Creek Township
4954 SEC 20 SHERMAN DUTCH CORP 1

LICKING COUNTY
Lima Township
5314 L-3 1Q CLINTON OIL YEARLING 2

MORGAN COUNTY
Bristol Township
3341 SEC 21 REDMAN OIL PALMER JOHN L 3

MUSKINGUM COUNTY
Cass Township
7679 L-11 1Q CLINTON OIL MCBRIDE U 3-1554

Muskingum Township
7629 L-15 1Q OXFORD OIL MILLER-GOODRICH U J1
7680 SEC 4 CAMERON BROS JORDON C R-1

Perry Township
7624 3Q CAMERON BROS JOHNSTON K&R 1-R
7635 SEC 15W HOPEWELL O & G HAYES 3

Washington Township
7576 3Q T1R7 CAMERON BROS CAMERON ET AL 1-R

NOBLE COUNTY
Noble Township
1576 SEC 3 HAYS & CO DANFORD ET AL 1

PERRY COUNTY

Reading Township

3358 SEC 26W HOPEWELL O&G BIGHAM-STRAIT 1

PORTAGE COUNTY

Randolph Township

3778 L-57 BELDEN & BLAKE CONNOR C COMM. 1

3810 L-50 EXCALIBUR EXPL SCHAEFER 1

3841 L-56 BELDEN & BLAKE SCRUGGS A&S COMM. 1

STARK COUNTY

Sugar Creek Township

4637 SEC 26 BELDEN & BLAKE WOOD J ET AL COMM. 1

4666 SEC 34 BELDEN & BLAKE HARROLD E & M 2

4672 SEC 26 BELDEN & BLAKE WEISGARBER R & D 1

4700 SEC 26 BELDEN & BLAKE HARROLD 1-A

TUSCARAWAS COUNTY

Bucks Township

3645 SEC 24 NGO DEV REGULA 1

4462 SEC 18 ATWOOD EM TROENDLY E 3

4595 SEC 7 RED HILL DEV REGULA M U 1

4705 SEC 5 RED HILL DEV BAAB-HERSHBERGER U 2

Oxford Township

4497 SEC 19 ATWOOD EM ARMSTRONG L 2

4574 2Q ATWOOD EM NEWCOMERST. LNDPL 1

4658 SEC 27 ATWOOD EM BRODE ET AL 2

4732 L-28 RED HILL DEV WENTZ GREG 4

4778 SEC 19 TIPKA AW O&G NEWCOMERSTOWN TRP CLB 1

Wayne Township

4815 L-23 1Q BELDEN BRICK HALL RUSSELL 2

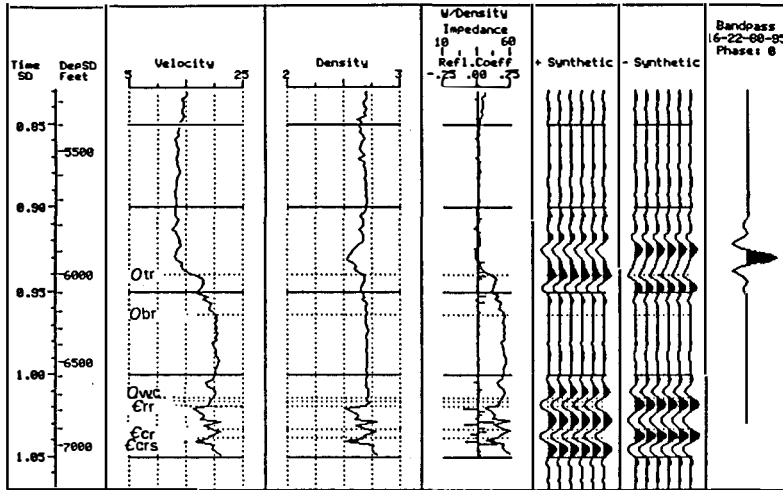
WAYNE COUNTY

Paint Township

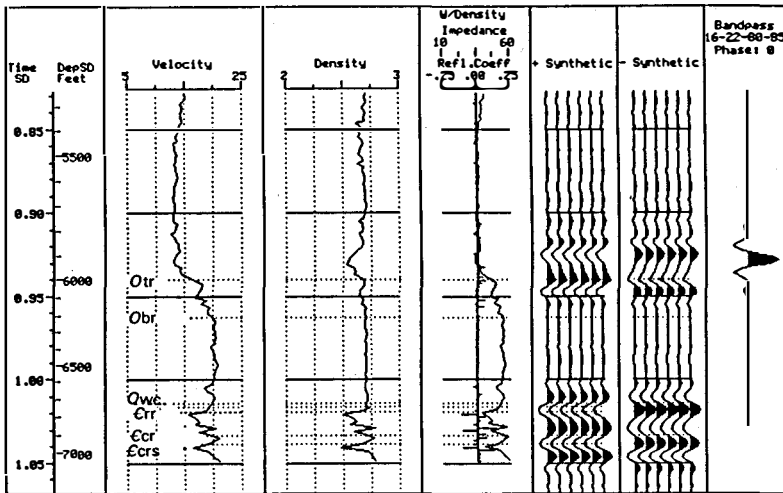
4978 SEC 23 MILLER O & G SCHLABACH U 2

4860 SEC 11 MILLER O & G VALLEY SPRINGS FARM 1

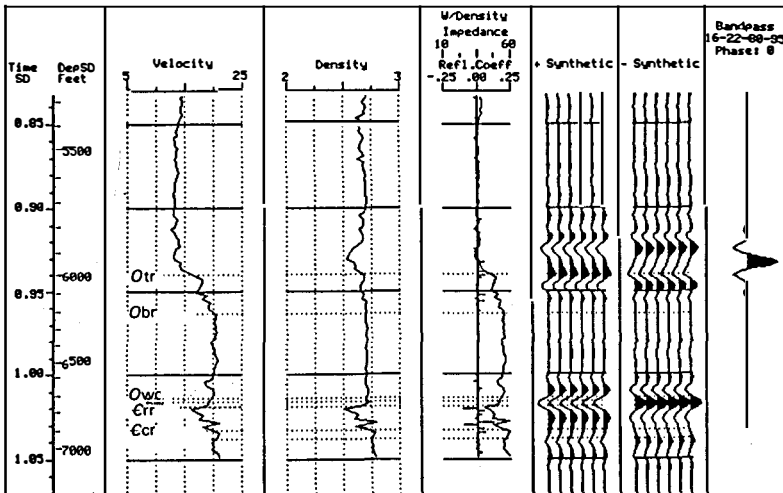
Appendix VII:
One-Dimensional Seismic Models



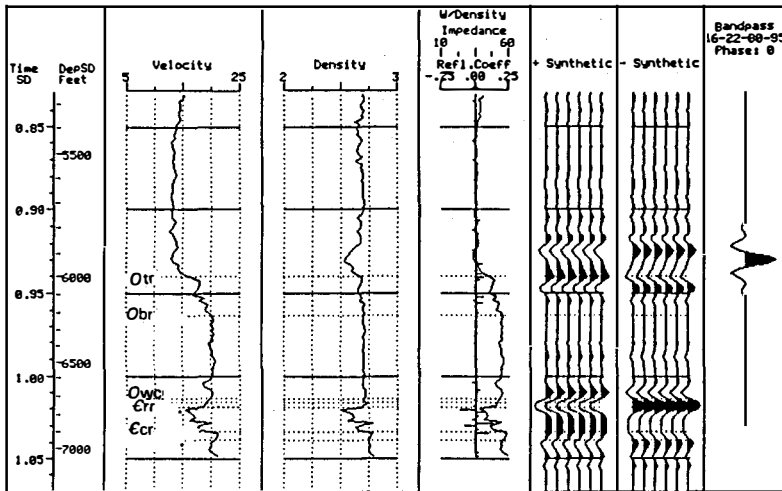
Model 1:
 765' Trenton-Wells Creek
 80' Wells Creek
 0' Beekmantown
 110' Rose Run
 20' Copper Ridge Ss.



Model 2:
 765' Trenton-Wells Creek
 80' Wells Creek
 0' Beekmantown
 110' Rose Run (w/ gas)
 20' Copper Ridge Ss.

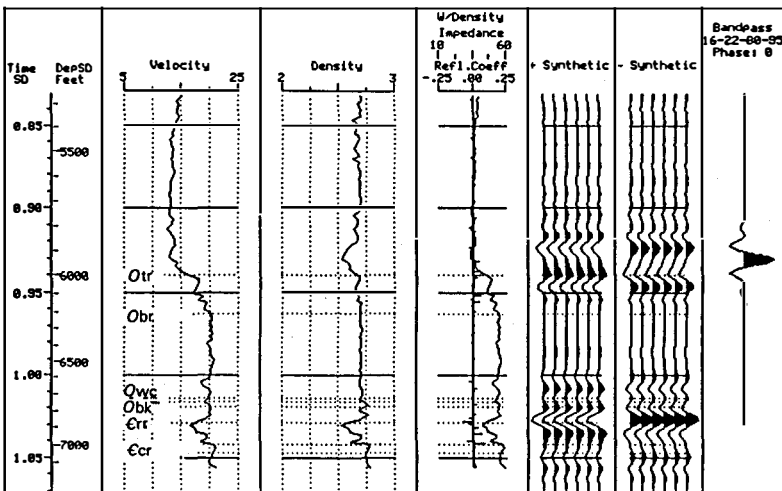


Model 3:
 765' Trenton-Wells Creek
 80' Wells Creek
 0' Beekmantown
 110' Rose Run
 0' Copper Ridge Ss.



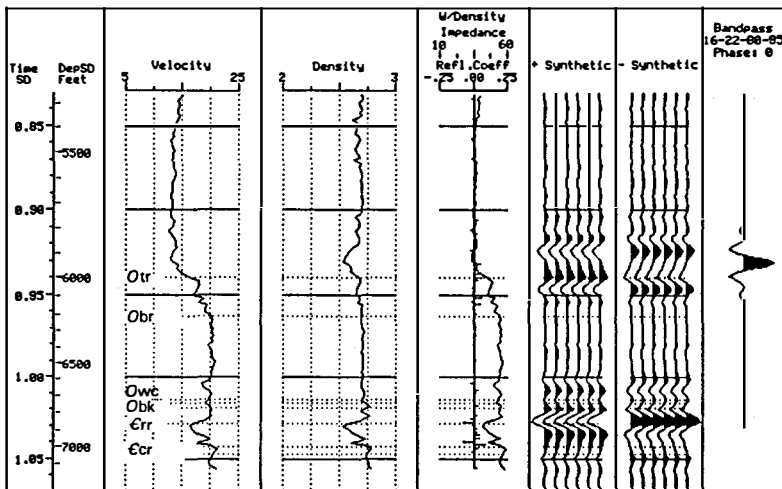
Model 4:

765' Trenton-Wells Creek
80' Wells Creek
0' Beekmantown
110' Rose Run (w/ gas)
0' Copper Ridge Ss.



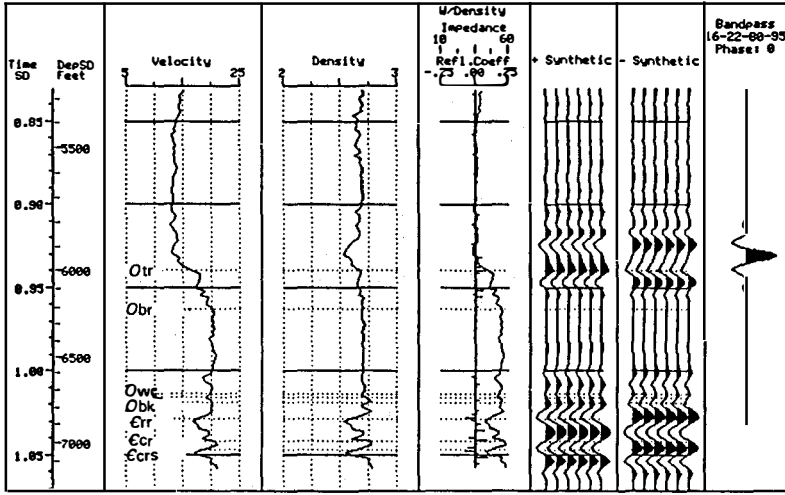
Model 5:

750' Trenton-Wells Creek
50' Wells Creek
80' Beekmantown
110' Rose Run
0' Copper Ridge Ss.

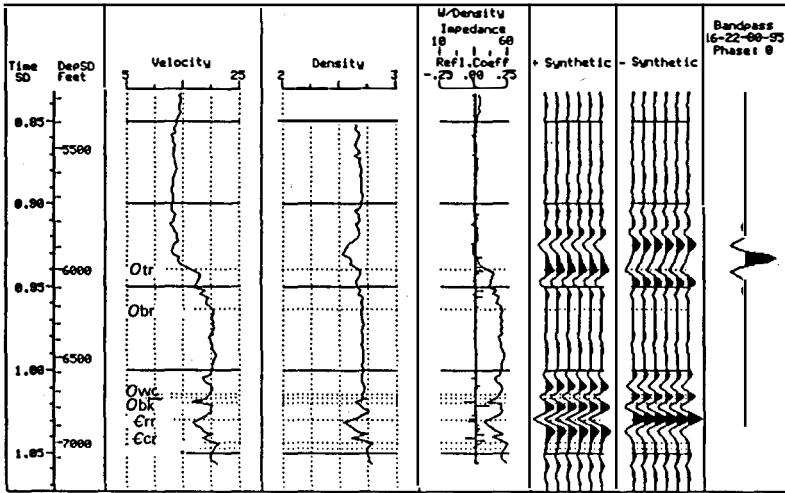


Model 6:

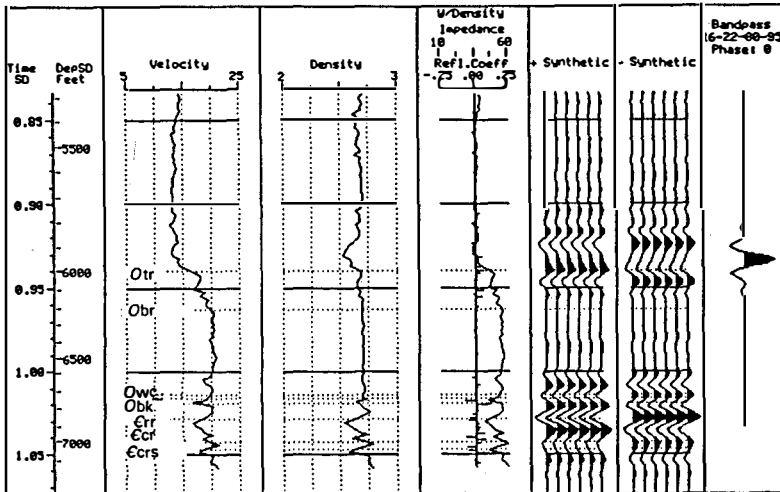
750' Trenton-Wells Creek
50' Wells Creek
80' Beekmantown
110' Rose Run (w/ gas)
0' Copper Ridge Ss.



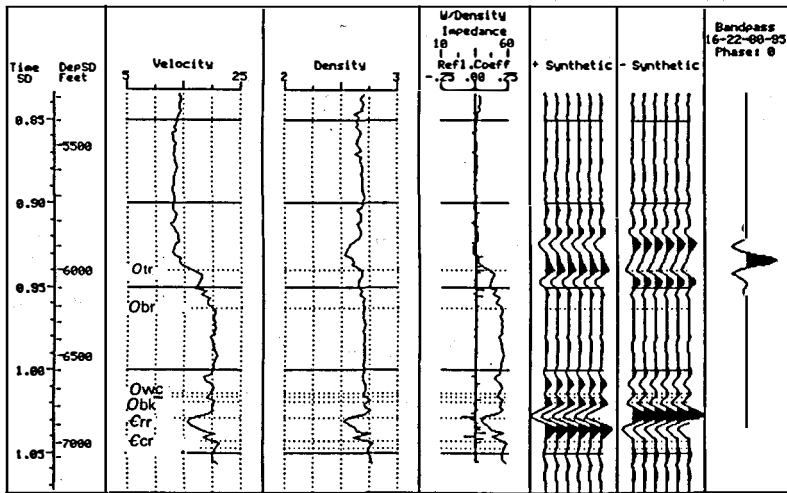
Model 7:
 750' Trenton-Wells Creek
 50' Wells Creek
 80' Beekmantown
 110' Rose Run
 20' Copper Ridge Ss.



Model 8:
 750' Trenton-Wells Creek
 50' Wells Creek
 80' Beekmantown
 (Five feet of high porosity w/gas)
 110' Rose Run
 0' Copper Ridge Ss.



Model 9:
 750' Trenton-Wells Creek
 50' Wells Creek
 80' Beekmantown
 (Five feet of high porosity w/gas)
 110' Rose Run
 20' Copper Ridge Ss.



Model 10:
 750' Trenton-Wells Creek
 50' Wells Creek
 80' Beekmantown
 110' Rose Run
 (Upper 60 feet w/gas, lower 50 feet w/oil
 0' Copper Ridge Ss

**Appendix VIII:
Dolomite Types Found in Thin Sections
of Cores From Ohio**

Eight dolomite types, described below, are found in the Rose Run sandstone interval using light microscope techniques. Types 1, 3, 4, 5, and 7 are probably the result of relatively early dolomitization. They are all replacement dolomites of either allochems, detrital grains, calcite cement, or stromatolites. Type 2 and type 6 dolomites are probably the same dolomite (polymodal), simply occurring under different diagenetic conditions or replacing a different rock texture. Type 2 and 6 dolomite types are believed to have occurred very late in the diagenesis of the Rose Run sandstone. Type 2 and 6 occur as pore fillings and linings, and occasionally they are found sparsely scattered in clay laminae, replacing the clay, or attacking earlier dolomites. Type 8 dolomite, a medium to coarse planar-s dolomite, appears to be a replacement of earlier carbonates.

The different textural and morphological characteristics of types 1, 3, 4, 5, 7, and 8 might, at least in part, be the result of having formed in different lithofacies. Types 1 and 7 appear to be dolomite replacement of allochems or feldspar that were deposited in an intertidal or subtidal environment. Type 3 is associated with stromatolitic laminae and in interbedded muddy laminae in sandy dolomite and sandstone. Type 5 is similar but coarser grained. Type 4 occurs in sandstone and is probably a replacement of sparry calcite cement. Type 8 dolomite apparently replaced earlier pure or nearly pure carbonates.

Type 1. Medium to coarse crystalline, unimodal, non-planar to planar-s, clear-rim, vague nonmimic replacement of feldspars or allochems. Usually associated with pyrite. Single crystals of dolomite replace the feldspar or allochem. Rare in sandstones.

Type 2. Very fine to fine crystalline, bimodal(?), planar-s and planar-e, relatively clear, and generally does not occupy moldic. Void filler found in sandstones where grain contacts are long or concavo-convex. May replace shale laminae. Generally sparsely scattered.

Type 3. Very fine to fine crystalline, non-planar, replacement dolomite. Occurs as dolomite laminae, sandy dolomite and in sandstones. Found where grain contacts are floating and in stromatolitic laminae. May have indistinct dusty inclusions and pyrite associated with it.

Type 4. Medium to very coarse crystalline, non-planar, and has mottled appearance upon extinction which may be caused by clay inclusions. Attacks detrital quartz grains and usually has evidence of dissolution. Some crystals appear fractured. Occurs in sandstones as a replacement of calcite cement(?)

Type 5. Fine to medium crystalline, non-planar, replacement(?) dolomite. No distinct ghosts, but dusty inclusions and quartz grains in sandy dolomites.

Type 6. Mostly medium crystalline, bimodal(?), planar-s and planar-e dolomite with minor inclusions. Void filler rarely associated with pyrite. May grade in type 2. Found where grain contacts float and around outer margins of ooid ghosts lining voids. Also may replace shale laminae.

Type 7. Very fine to medium crystalline, non-planar dolomite. Replaces allochems (ooids and peloids). Multiple dolomite grains replace a single allochem. Pyrite common. Ghosts are the result of dust size inclusions giving the dolomite a dirty appearance.

Type 8. Medium to coarse, planar-s dolomite. Minor inclusions. Found in relatively pure dolomites. Associated with pyrite. Replacement(?)

County	Core Number	Depth (in ft.)	Relative Abundances of Dolomite Types		
			Abundant ¹	Common ²	Rare ³
Coshocton	C2852	5986.0	1	4	5
Coshocton	C2852	5988.0	1	4	5
Coshocton	C2852	5989.5	1	0 ⁴	4
Coshocton	C2852	5991.0	6	7	4
Coshocton	C2852	5991.5	3	6	9
Coshocton	C2852	5992.0	5	6	1
Coshocton	C2852	5992.5	2	4	7
Coshocton	C2852	5994.0	0	0	0
Coshocton	C2852	5997.0	3	2	6
Coshocton	C2852	5998.0	3	2	4
Coshocton	C2853	5967.0	5	4	2
Coshocton	C2853	5968.0	1	5	9
Coshocton	C2853	5969.0	5	2	1
Coshocton	C2853	5970.0	3	1	5
Coshocton	C2853	5971.0	1	2	6
Coshocton	C2853	5972.0	2	6	1
Coshocton	C2853	5973.0	2	6	3
Coshocton	C2853	5974.0	2	4	6
Coshocton	C2853	5975.0	2	3	4
Coshocton	C2853	5976.0	3	2	6
Coshocton	C2853	5977.0	4	0	0
Coshocton	C2853	5979.0	5	1	6
Coshocton	C2853	5981.5	3	2	0
Coshocton	C2853	5982.5	1	2	6
Coshocton	C2853	5983.0	5	6	1
Coshocton	C2853	5983.5	7	3	6
Coshocton	C2853	5984.0	3	2	7
Coshocton	C2853	5985.0	4	0	0
Coshocton	C2853	5986.0	3	0	0
Coshocton	C2989	6622.0	6	4	2
Coshocton	C2989	6624.0	3	4	2
Coshocton	C2989	6627.0	4	6	2
Coshocton	C2989	6628.5	5	3	6
Coshocton	C2989	6629.9	5	3	99 ⁵
Coshocton	C2989	6633.0	5	6	99
Coshocton	C2989	6635.0	7	6	1
Coshocton	C3260	6715.0	8	6	0
Coshocton	C3260	6722.0	8	0	0
Coshocton	C3260	6811.5	0	0	0
Coshocton	C3260	6819.5	0	0	0
Coshocton	C3260	6828.0	0	0	0
Coshocton	C3260	6865.0	0	0	0
Coshocton	C3260	6905.0	4	5	2
Coshocton	C3260	7000.0	2	6	4

cont.

County	Core Number	Depth (in ft.)	Relative Abundances of Dolomite Types		
			Abundant ¹	Common ²	Rare ³
Jackson	C2898	4499.0	4	0	0
Jackson	C2898	4501.0	0	0	0
Jackson	C2898	4502.0	0	0	0
Jackson	C2898	4504.0	4	0	0
Jackson	C2898	4505.0	0	0	0
Jackson	C2898	4506.0	0	0	0
Jackson	C2898	4507.0	4	0	0
Jackson	C2898	4508.0	4	0	0
Jackson	C2898	4509.0	4	0	0
Jackson	C2898	4512.0	3	2	4
Jackson	C2898	4513.0	2	6	4
Jackson	C2898	4514.0	4	0	0
Jackson	C2898	4515.0	0	0	0
Jackson	C2898	4516.0	0	0	0
Jackson	C2898	4517.0	4	0	0
Jackson	C2898	4518.0	0	0	0
Jackson	C2898	4520.0	0	0	0
Jackson	C2898	4521.0	0	0	0
Jackson	C2898	4522.0	0	0	0
Jackson	C2898	4523.0	0	0	0
Jackson	C2898	4525.0	0	0	0
Jackson	C2898	4527.0	4	0	0
Jackson	C2898	4528.0	4	0	0
Jackson	C2898	4529.0	2	6	4
Jackson	C2898	4530.0	4	4	3
Scioto	C2958	4255.5	0	0	0
Scioto	C2958	4256.0	0	0	0
Scioto	C2958	4258.0	0	0	0
Scioto	C2958	4259.0	4	0	0
Scioto	C2958	4260.0	0	0	0
Tuscarawas	C2963	7646.0	4	2	6
Tuscarawas	C2963	7653.0	7	6	99
Tuscarawas	C2963	7653.5	7	6	5
Tuscarawas	C2963	7655.0	5	6	7
Tuscarawas	C2963	7659.0	7	9	6
Tuscarawas	C2963	7664.0	7	1	2
Tuscarawas	C2963	7668.0	5	6	9
Tuscarawas	C2963	7668.5	5	6	9
Tuscarawas	C2963	7670.0	5	3	2
Tuscarawas	C2963	7672.0	3	2	7
Tuscarawas	C2963	7673.0	2	4	99
Tuscarawas	C2963	7675.0	2	6	4
Tuscarawas	C2963	7677.0	7	6	9
Tuscarawas	C2963	7681.0	5	3	6
Tuscarawas	C2963	7683.0	3	5	6
Tuscarawas	C2963	7686.0	7	6	3

¹Abundant: Makes up >50 percent of the total dolomite in the sample.

²Common: Makes up 10 to 50 percent of the total dolomite in the sample.

³Rare: Makes up <10 percent of the total dolomite in the sample.

⁴0: No dolomite in sample.

⁵99: Dolomite type not determined.

**Appendix IX:
Petrographic Data for the
Rose Run Sandstone of Ohio**

County	Core (C) or Permit (P)	Depth (in ft.)	Depth Below Knox Unconformity (in ft.)	Formation	Rock Type	Lithology Modifier	Microstructure ¹	Grain Contacts ²	Sand Unit ³
Ashtabula	P2038	6170.2	-10.2	Rose Run	Subarkose	dolomitic	99 ⁴	99	98 ⁵
Ashtabula	P2038	6173.9	-13.9	Rose Run	Subarkose	dolomitic	99	99	98
Ashtabula	P2038	6174.4	-14.4	Rose Run	Subarkose	dolomitic, clayey	99	99	98
Ashtabula	P2038	6177.2	-17.2	Rose Run	Subarkose	none	99	99	98
Ashtabula	P2038	6177.7	-17.7	Rose Run	Quartz arenite	dolomitic	99	99	98
Ashtabula	P2038	6178.8	-18.8	Rose Run	Subarkose	dolomitic, clayey	99	99	98
Ashtabula	P2038	6180.8	-20.8	Rose Run	Dolostone	sandy	99	99	98
Ashtabula	P2038	6187.0	-27.0	Rose Run	Dolostone	sandy	99	99	98
Ashtabula	P2038	6192.4	-32.4	Rose Run	Dolostone	sandy	99	99	98
Ashtabula	P2038	6194.5	-34.5	Rose Run	Subarkose	dolomitic	99	99	98
Ashtabula	P2038	6198.5	-38.5	Rose Run	Subarkose	none	99	99	98
Ashtabula	P2038	6202.0	-42.0	Rose Run	Subarkose	dolomitic	99	99	98
Ashtabula	P2038	6202.8	-42.8	Rose Run	Dolostone	sandy	99	99	98
Ashtabula	P2038	6208.3	-48.3	Rose Run	Dolostone	sandy	99	99	98
Ashtabula	P2038	6214.9	-54.9	Rose Run	Dolostone	none	99	99	98
Ashtabula	P2038	6219.7	-59.7	Rose Run	Arkose	none	99	99	98
Ashtabula	P2038	6222.5	-62.5	Copper Ridge	Subarkose	dolomitic, clayey	99	99	98
Ashtabula	P2038	6231.8	-71.8	Copper Ridge	Dolostone	sandy	99	99	98
Ashtabula	P2038	6232.8	-72.8	Copper Ridge	Subarkose	dolomitic	99	99	98
Ashtabula	P2038	6232.9	-72.9	Copper Ridge	Subarkose	dolomitic	99	99	98
Ashtabula	P2038	6234.8	-74.8	Copper Ridge	Dolostone	none	99	99	98
Ashtabula	P2038	6235.7	-75.7	Copper Ridge	Dolostone	sandy	99	99	98
Ashtabula	P2038	6238.8	-78.8	Copper Ridge	Dolostone	sandy	99	99	98
Ashtabula	P2038	6238.9	-78.9	Copper Ridge	Subarkose	dolomitic, clayey	99	99	98
Ashtabula	P2038	6242.8	-82.8	Copper Ridge	Dolostone	sandy	99	99	98
Ashtabula	P2038	6243.4	-83.4	Copper Ridge	Dolostone	none	99	99	98
Ashtabula	P2038	6245.0	-85.0	Copper Ridge	Dolostone	sandy	99	99	98
Ashtabula	P2038	6250.0	-90.0	Copper Ridge	Dolostone	sandy	99	99	98
Ashtabula	P2038	6284.2	-124.2	Copper Ridge	Subarkose	dolomitic	99	99	98
Ashtabula	P2038	6285.1	-125.1	Copper Ridge	Dolostone	clayey	99	99	98
Ashtabula	P2071	6255.5	0.5	Rose Run	Quartz arenite	dolomitic	99	99	98
Ashtabula	P2071	6258.2	-2.2	Rose Run	Subarkose	dolomitic	99	99	98
Ashtabula	P2071	6260.7	-4.7	Rose Run	Subarkose	none	99	99	98
Ashtabula	P2071	6263.5	-7.5	Rose Run	Subarkose	dolomitic	99	99	98
Ashtabula	P2071	6264.1	-8.1	Rose Run	Subarkose	clayey	99	99	98
Ashtabula	P2071	6266.9	-10.9	Rose Run	Subarkose	clayey	99	99	98

County	Core (C) or Permit (P)	Depth (in ft.)	Depth Below Knox		Formation	Rock Type	Lithology Modifier	Microstructure ¹	Grain Contacts ²	Sand Unit ³
			Unconformity (in ft.)	Unconformity (in ft.)						
Ashtabula	P2071	6270.3	-14.3		Rose Run	Subarkose	none	99	99	98
Ashtabula	P2071	6274.2	-18.2		Rose Run	Dolostone	sandy	99	99	98
Ashtabula	P2071	6274.9	-18.9		Rose Run	Dolostone	sandy	99	99	98
Ashtabula	P2071	6275.3	-19.3		Rose Run	Subarkose	clayey	99	99	98
Ashtabula	P2071	6276.7	-20.7		Rose Run	Subarkose	clayey	99	99	98
Coshocton	C2852	5986.0	-1.0		Rose Run	Subarkose	dolomitic	2	2	2
Coshocton	C2852	5988.0	-3.0		Rose Run	Subarkose	dolomitic	1	4	2
Coshocton	C2852	5989.5	-4.5		Rose Run	Subarkose	dolomitic	3	3	2
Coshocton	C2852	5991.0	-6.0		Rose Run	Quartz arenite	dolomitic, intraclasts	3	2	2
Coshocton	C2852	5991.5	-6.5		Rose Run	Dolostone	none	4	1	2
Coshocton	C2852	5992.0	-7.0		Rose Run	Dolostone	sandy	1	1	2
Coshocton	C2852	5992.5	-7.5		Rose Run	Subarkose	dolomitic, clayey	1	4	2
Coshocton	C2852	5994.0	-9.0		Rose Run	Subarkose	clayey	5	2	2
Coshocton	C2852	5997.0	-12.0		Rose Run	Not determined	99	3	99	2
Coshocton	C2852	5998.0	-13.0		Rose Run	Not determined	99	1	99	2
Coshocton	C2853	5967.0	-7.0		Wells Creek	Dolostone	sandy	2	1	99
Coshocton	C2853	5968.0	-8.0		Wells Creek	Dolostone	sandy	2	1	99
Coshocton	C2853	5969.0	-9.0		Wells Creek	Dolostone	sandy	5	1	99
Coshocton	C2853	5970.0	-10.0		Wells Creek	Dolostone	sandy	2	1	99
Coshocton	C2853	5971.0	-11.0		Wells Creek	Dolostone	sandy	2	1	99
Coshocton	C2853	5972.0	-12.0		Wells Creek	Subarkose	dolomitic	1	2	99
Coshocton	C2853	5973.0	-13.0		Wells Creek	Not determined	99	3	3	99
Coshocton	C2853	5974.0	-14.0		Rose Run	Sandstone	dolomitic	3	3	99
Coshocton	C2853	5975.0	-15.0		Rose Run	Subarkose	dolomitic	1	2	99
Coshocton	C2853	5976.0	-16.0		Rose Run	Arkose	dolomitic	5	1	99
Coshocton	C2853	5977.0	-17.0		Rose Run	Sandstone	none	6	2	99
Coshocton	C2853	5979.0	-19.0		Rose Run	Sandstone	dolomitic	1	1	99
Coshocton	C2853	5981.5	-21.5		Rose Run	Arkose	dolomitic	1	2	99
Coshocton	C2853	5982.5	-22.5		Rose Run	Not determined	99	2	1	99
Coshocton	C2853	5983.0	-23.0		Rose Run	Dolostone	clayey, sandy	2	1	99
Coshocton	C2853	5983.5	-23.5		Rose Run	Dolostone	glaucconitic, sandy	3	1	99
Coshocton	C2853	5984.0	-24.0		Rose Run	Not determined	99	5	2	99
Coshocton	C2853	5985.0	-25.0		Rose Run	Sandstone	dolomitic	1	3	99
Coshocton	C2853	5986.0	-26.0		Copper Ridge	Sandstone	sandy	1	99	99 (cont.)

County	Core (C) or Permit (P)	Depth (in ft.)	Depth Below Knox		Formation	Rock Type	Lithology Modifier	Microstructure ¹	Grain Contacts ²	Sand Unit ³
			Unconformity (in ft.)	Knox						
Coshocton	C2989	6622.0	-44.0		Rose Run	Sandstone	dolomitic	3	1	2
Coshocton	C2989	6624.0	-46.0		Rose Run	Sandstone	dolomitic	1	1	2
Coshocton	C2989	6627.0	-49.0		Rose Run	Sandstone	dolomitic	1	3	2
Coshocton	C2989	6628.5	-50.5		Rose Run	Sandstone	dolomitic	1	1	2
Coshocton	C2989	6629.9	-51.9		Rose Run	Wacke	none	5	3	2
Coshocton	C2989	6633.0	-55.0		Rose Run	Dolostone	none	2	99	99
Coshocton	C2989	6635.0	-57.0		Rose Run	Dolostone	sandy	2	1	99
Coshocton	C3260	6715.0	-8.0		Beekmantown	Dolostone	none	2	99	99
Coshocton	C3260	6722.0	-15.0		Beekmantown	Dolostone	none	2	99	99
Coshocton	C3260	6811.5	-104.5		Rose Run	Quartz arenite	none	6	3	2
Coshocton	C3260	6819.5	-112.5		Rose Run	Quartz arenite	clayey	5	3	2
Coshocton	C3260	6828.0	-121.0		Rose Run	Subarkose	none	6	3	3
Coshocton	C3260	6865.0	-158.0		Rose Run	Subarkose	none	6	3	4
Coshocton	C3260	6905.0	-198.0		Rose Run	Subarkose	dolomitic	1	1	5
Coshocton	C3260	7000.0	-293.0		Copper Ridge	Subarkose	dolomitic	1	2	6
Jackson	C2898	4499.0	-178.0		Rose Run	Quartz arenite	dolomitic	2	3	98
Jackson	C2898	4501.0	-180.0		Rose Run	Not determined	99	5	3	98
Jackson	C2898	4502.0	-181.0		Rose Run	Quartz arenite	none	3	3	98
Jackson	C2898	4504.0	-183.0		Rose Run	Not determined	99	1	2	98
Jackson	C2898	4505.0	-184.0		Rose Run	Quartz arenite	clayey	5	4	98
Jackson	C2898	4506.0	-185.0		Rose Run	Not determined	99	5	4	98
Jackson	C2898	4507.0	-186.0		Rose Run	Subarkose	none	2	3	98
Jackson	C2898	4508.0	-187.0		Rose Run	Not determined	99	5	4	98
Jackson	C2898	4509.0	-188.0		Rose Run	Subarkose	dolomitic	1	5	98
Jackson	C2898	4512.0	-191.0		Rose Run	Not determined	99	1	5	98
Jackson	C2898	4513.0	-192.0		Rose Run	Quartz arenite	dolomitic	3	2	98
Jackson	C2898	4514.0	-193.0		Rose Run	Not determined	99	1	2	98
Jackson	C2898	4515.0	-194.0		Rose Run	Subarkose	clayey	5	3	98
Jackson	C2898	4516.0	-195.0		Rose Run	Not determined	99	5	2	98
Jackson	C2898	4517.0	-196.0		Rose Run	Subarkose	clayey	2	3	98
Jackson	C2898	4518.0	-197.0		Rose Run	Not determined	99	3	3	98
Jackson	C2898	4520.0	-199.0		Rose Run	Not determined	99	3	3	98
Jackson	C2898	4521.0	-200.0		Rose Run	Not determined	99	5	4	98
Jackson	C2898	4522.0	-201.0		Rose Run	Subarkose	none	5	3	98
Jackson	C2898	4523.0	-202.0		Rose Run	Not determined	99	5	4	98
Jackson	C2898	4525.0	-204.0		Rose Run	Not determined	99	3	3	98

(cont.)

County	Core (C) or Permit (P)	Depth (in ft.)	Depth Below Knox Unconformity (in ft.)	Formation	Rock Type	Lithology Modifier	Microstructure ¹	Grain Contacts ²	Sand Unit ³
Jackson	C2898	4527.0	-206.0	Rose Run	Quartz arenite	none	1	3	98
Jackson	C2898	4528.0	-207.0	Rose Run	Not determined	99	6	3	98
Jackson	C2898	4529.0	-208.0	Rose Run	Not determined	99	1	2	98
Jackson	C2898	4530.0	-209.0	Rose Run	Subarkose	dolomitic	1	1	98
Scioto	C2958	4255.5	-295.5	Rose Run	Subarkose	clayey	5	4	98
Scioto	C2958	4256.0	-296.0	Rose Run	Not determined	99	5	4	98
Scioto	C2958	4258.0	-298.0	Rose Run	Not determined	99	3	4	98
Scioto	C2958	4259.0	-299.0	Rose Run	Not determined	99	5	2	98
Scioto	C2958	4260.0	-300.0	Rose Run	Not determined	99	3	3	98
Scioto	P0212	4254.0	-294.0	Rose Run	Subarkose	none	99	99	99
Scioto	P0212	4255.0	-295.0	Rose Run	Subarkose	clayey	99	99	99
Scioto	P0212	4255.8	-295.8	Rose Run	Subarkose	clayey	99	99	99
Scioto	P0212	4256.0	-296.0	Rose Run	Subarkose	clayey	99	99	99
Scioto	P0212	4256.5	-296.5	Rose Run	Subarkose	0	99	99	99
Scioto	P0212	4258.5	-298.5	Rose Run	Subarkose	clayey	99	99	99
Scioto	P0212	4258.8	-298.8	Rose Run	Subarkose	clayey	99	99	99
Scioto	P0212	4258.9	-298.9	Rose Run	Subarkose	none	99	99	99
Scioto	P0212	4259.0	-299.0	Rose Run	Subarkose	clayey	99	99	99
Scioto	P0212	4259.2	-299.2	Rose Run	Subarkose	dolomitic, clayey	99	99	99
Scioto	P0212	4259.6	-299.6	Rose Run	Subarkose	clayey	99	99	99
Scioto	P0212	4259.8	-299.8	Rose Run	Subarkose	clayey	99	99	99
Scioto	P0212	4260.0	-300.0	Rose Run	Subarkose	none	99	99	99
Scioto	P0212	4260.2	-300.2	Rose Run	Subarkose	none	99	99	99
Scioto	P0212	4260.5	-300.5	Rose Run	Subarkose	none	99	99	99
Scioto	P0212	4261.0	-301.0	Rose Run	Subarkose	dolomitic	99	99	99
Tuscarawas	C2963	7646.0	-297.0	Copper Ridge	Sandstone	dolomitic, clayey	5	4	5
Tuscarawas	C2963	7653.0	-304.0	Copper Ridge	Dolostone	none	3	1	99
Tuscarawas	C2963	7653.5	-304.5	Copper Ridge	Subarkose	99	2	1	99
Tuscarawas	C2963	7655.0	-306.0	Copper Ridge	Dolostone	none	1	1	99
Tuscarawas	C2963	7659.0	-310.0	Copper Ridge	Dolostone	none	2	1	99
Tuscarawas	C2963	7664.0	-315.0	Copper Ridge	Sandstone	dolomitic	1	2	5
Tuscarawas	C2963	7668.0	-319.0	Copper Ridge	Dolostone	sandy	2	1	99
Tuscarawas	C2963	7668.5	-319.5	Copper Ridge	Not determined	99	4	1	99
Tuscarawas	C2963	7670.0	-321.0	Copper Ridge	Sandstone	none	1	3	99
Tuscarawas	C2963	7672.0	-323.0	Copper Ridge	Sandstone	dolomitic	5	2	6

(cont.)

County	Core (C) or Permit (P)	Depth (in ft.)	Depth Below Knox Unconformity (in ft.)	Formation	Rock Type	Lithology Modifier	Microstructure ¹	Grain Contacts ²	Sand Unit ³
Tuscarawas	C2963	7673.0	-324.0	Copper Ridge	Sandstone	dolomitic	1	3	6
Tuscarawas	C2963	7675.0	-326.0	Copper Ridge	Sandstone	dolomitic	1	3	6
Tuscarawas	C2963	7677.0	-328.0	Copper Ridge	Not determined	99	2	1	99
Tuscarawas	C2963	7681.0	-332.0	Copper Ridge	Dolostone	sandy	4	1	99
Tuscarawas	C2963	7683.0	-334.0	Copper Ridge	Not determined	99	1	1	99
Tuscarawas	C2963	7686.0	-337.0	Copper Ridge	Dolostone	sandy	1	1	99

¹Microstructures

1. Interlaminated (bedded) sandstone/dolomite
2. Mottled
3. Massive
4. Stromatolitic laminae
5. Interlaminated clay stringers and sandstone, or clayey, silty sandstone and sandstone
6. Laminated or bedded sandstone

²Grain contacts

1. Floating and point
2. Point and long
3. Long and concavo/convex
4. Concavo/convex and sutured
5. All types common

³Sandstone units: 1 through 5 are Rose Run sandstone units.

Number 1 is uppermost, number 5 lowermost.

Number 6 is considered Copper Ridge Dolomite.

⁴99: Not determined or non-dolomite

⁵98: Sandstone unit undifferentiated

Appendix X: Modal Analyses of Cores

Cement/Diagenetic Minerals (%)

County	Formation	Core (C) or Permit (P)	Depth (ft.)	Total Framework			Total Cement			Cement/Diagenetic Minerals (%)							Total Porosity (%)
				Framework (%)	Matrix (%)	Total (%)	Framework Grains (%)	Other (%)	Dolomite	Clay	Quartz		Feldspar		Other		
											Quartz	Feldspar	OG	OG			
Ashtabula	Rose Run	P2038	P6170.2	61.3	0.0	38.8	54.8	5.4	1.1	36.6	0.0	2.2	0.0	0.0	5.0		
Ashtabula	Rose Run	P2038	P6173.9	62.1	0.0	37.9	57.9	4.2	0.0	34.7	2.1	1.1	0.0	0.0	4.0		
Ashtabula	Rose Run	P2038	P6174.4	56.0	0.0	44.0	47.0	9.0	0.0	34.0	7.0	2.0	0.0	1.0	0.0		
Ashtabula	Rose Run	P2038	P6177.2	83.6	0.0	16.4	79.3	4.3	0.0	3.3	2.2	9.8	0.0	1.1	9.0		
Ashtabula	Rose Run	P2038	P6177.7	68.3	0.0	31.6	66.3	2.0	0.0	25.5	1.0	4.1	0.0	1.0	3.0		
Ashtabula	Rose Run	P2038	P6178.8	62.2	0.0	37.8	52.0	10.2	0.0	18.4	18.4	0.0	0.0	1.0	2.0		
Ashtabula	Rose Run	P2038	P6180.8	5.0	0.0	94.9	2.0	3.0	0.0	93.9	0.0	0.0	0.0	1.0	1.0		
Ashtabula	Rose Run	P2038	P6187.0	13.3	0.0	86.7	10.2	3.1	0.0	85.7	0.0	0.0	0.0	1.0	3.0		
Ashtabula	Rose Run	P2038	P6192.4	7.0	0.0	93.1	4.0	1.0	2.0	92.1	1.0	0.0	0.0	0.0	1.0		
Ashtabula	Rose Run	P2038	P6194.5	64.2	0.0	35.9	54.7	7.4	2.1	29.5	1.1	4.2	1.1	0.0	7.0		
Ashtabula	Rose Run	P2038	P6198.5	86.9	0.0	13.1	76.8	10.1	0.0	0.0	1.0	12.1	0.0	0.0	2.0		
Ashtabula	Rose Run	P2038	P6202.0	66.3	0.0	33.6	59.2	7.1	0.0	30.6	1.0	2.0	0.0	0.0	2.0		
Ashtabula	Rose Run	P2038	P6202.8	8.0	0.0	92.0	6.0	2.0	0.0	88.0	1.0	1.0	1.0	1.0	0.0		
Ashtabula	Rose Run	P2038	P6208.3	28.2	0.0	71.7	24.2	4.0	0.0	70.7	0.0	1.0	0.0	0.0	0.0		
Ashtabula	Rose Run	P2038	P6214.9	2.0	0.0	98.0	2.0	0.0	0.0	97.0	1.0	0.0	0.0	0.0	0.0		
Ashtabula	Rose Run	P2038	P6219.7	87.3	0.0	12.6	51.7	35.6	0.0	0.0	2.3	9.2	1.1	0.0	15.0		
Ashtabula	Copper Ridge	P2038	P6222.5	75.0	0.0	25.0	62.0	13.0	0.0	8.0	10.0	6.0	0.0	1.0	2.0		
Ashtabula	Copper Ridge	P2038	P6231.8	48.9	0.0	51.0	41.8	7.1	0.0	51.0	0.0	0.0	0.0	0.0	2.0		
Ashtabula	Copper Ridge	P2038	P6232.8	64.3	0.0	35.8	53.7	9.5	1.1	32.6	1.1	2.1	0.0	0.0	6.0		
Ashtabula	Copper Ridge	P2038	P6232.9	78.3	0.0	21.7	68.0	10.3	0.0	16.5	0.0	5.2	0.0	0.0	2.0		
Ashtabula	Copper Ridge	P2038	P6234.8	1.0	0.0	99.0	1.0	0.0	0.0	99.0	0.0	0.0	0.0	0.0	2.0		
Ashtabula	Copper Ridge	P2038	P6235.7	19.8	0.0	80.2	17.7	2.1	0.0	80.2	0.0	0.0	0.0	0.0	3.0		
Ashtabula	Copper Ridge	P2038	P6238.8	5.2	0.0	94.8	4.2	1.0	0.0	94.8	0.0	0.0	0.0	0.0	4.0		
Ashtabula	Copper Ridge	P2038	P6238.9	69.7	0.0	30.4	60.6	9.1	0.0	17.2	7.1	6.1	0.0	0.0	2.0		
Ashtabula	Copper Ridge	P2038	P6242.8	5.4	0.0	94.7	4.3	1.1	0.0	94.7	0.0	0.0	0.0	0.0	3.0		
Ashtabula	Copper Ridge	P2038	P6243.4	2.0	0.0	98.0	1.0	1.0	0.0	98.0	0.0	0.0	0.0	0.0	0.0		
Ashtabula	Copper Ridge	P2038	P6245.0	12.0	0.0	88.0	9.0	3.0	0.0	88.0	0.0	0.0	0.0	0.0	1.0		
Ashtabula	Copper Ridge	P2038	P6250.0	7.1	0.0	92.9	6.1	1.0	0.0	91.9	0.0	0.0	0.0	0.0	1.0		
Ashtabula	Copper Ridge	P2038	P6284.2	56.9	0.0	43.2	47.4	9.5	0.0	42.1	1.1	0.0	0.0	0.0	5.0		
Ashtabula	Copper Ridge	P2038	P6285.1	2.0	0.0	97.9	2.0	0.0	0.0	86.7	11.2	0.0	0.0	0.0	1.0		

OG—Overgrowths
Data modified from Enterline (1991)

County	Formation	Core (C) or Permit (P)	Depth (ft.)	Total Framework (%)	Total Matrix (%)	Total Cement (%)	Cement/Diagenetic Minerals (%)										Total Porosity (%)				
							Framework Grains (%)			Dolomite			Clay		Quartz			Feldspar		Other	
							Quartz	Feldspar	Other	Dolomite	Clay	OG	OG	OG	OG	OG		OG			
Ashtabula	Rose Run	P2071	B6255.5	79.6	0.0	20.3	75.5	3.1	1.0	17.3	1.0	1.0	0.0	0.0	1.0	2.0					
Ashtabula	Rose Run	P2071	B6258.2	52.0	0.0	48.0	46.0	5.0	1.0	48.0	0.0	0.0	0.0	0.0	0.0	0.0					
Ashtabula	Rose Run	P2071	B6260.7	89.8	0.0	10.2	81.8	8.0	0.0	0.0	1.1	8.0	0.0	1.1	11.0	8.0					
Ashtabula	Rose Run	P2071	B6263.5	88.2	0.0	11.9	76.3	9.7	2.2	7.5	2.2	0.0	0.0	2.2	8.0	8.0					
Ashtabula	Rose Run	P2071	B6264.1	83.3	0.0	16.7	74.4	8.9	0.0	0.0	15.6	0.0	0.0	1.1	11.0	11.0					
Ashtabula	Rose Run	P2071	B6266.9	93.5	0.0	6.5	87.0	6.5	0.0	0.0	5.4	1.1	0.0	0.0	8.0	8.0					
Ashtabula	Rose Run	P2071	B6270.3	89.9	0.0	10.1	80.9	9.0	0.0	0.0	1.1	9.0	0.0	0.0	11.0	11.0					
Ashtabula	Rose Run	P2071	B6274.2	29.7	0.0	70.3	20.8	5.9	3.0	65.3	4.0	0.0	0.0	1.0	0.0	0.0					
Ashtabula	Rose Run	P2071	B6274.9	9.1	0.0	90.9	7.1	2.0	0.0	89.9	0.0	0.0	0.0	1.0	1.0	1.0					
Ashtabula	Rose Run	P2071	B6275.3	83.7	0.0	16.4	71.7	12.0	0.0	1.1	12.0	2.2	0.0	1.1	7.0	7.0					
Ashtabula	Rose Run	P2071	B6276.7	83.3	0.0	16.6	71.7	12.2	0.0	3.3	11.1	2.2	0.0	0.0	9.0	9.0					

OG—Overgrowths
Data modified from Enterline (1991)

County	Formation	Core (C) or Permit (P)	Depth (ft.)	Total Framework (%)	Total Matrix (%)	Total Cement (%)	Framework Grains (%)						Cement/Diagenetic Minerals (%)						Total Porosity (%)
							Framework Grains (%)			Cement/Diagenetic Minerals (%)			Framework Grains (%)			Cement/Diagenetic Minerals (%)			
							Quartz	Feldspar	Other	Dolomite	Clay	Quartz OG	Feldspar OG	Other	Dolomite	Clay	Quartz OG	Feldspar OG	
Coshocton	Rose Run	C2852	5986.0	51.7	0.0	48.4	49.3	2.4	0.0	40.9	0.0	6.8	0.0	0.7	3.3				
Coshocton	Rose Run	C2852	5988.0	65.8	0.0	34.2	60.6	4.9	0.3	26.4	0.0	7.5	0.0	0.3	7.3				
Coshocton	Rose Run	C2852	5989.5	59.4	0.0	40.5	55.6	3.5	0.3	28.0	0.0	12.2	0.3	0.0	1.0				
Coshocton	Rose Run	C2852	5991.0	67.4	0.0	32.5	54.1	0.6	12.7	27.4	0.3	4.5	0.0	0.3	3.1				
Coshocton	Rose Run	C2852	5991.5	0.0	0.0	100.0	0.0	0.0	0.0	100.0	0.0	0.0	0.0	0.0	0.0				
Coshocton	Rose Run	C2852	5992.0	*	*	*	*	*	*	*	*	*	*	*	1.0				
Coshocton	Rose Run	C2852	5992.5	74.8	0.0	25.1	70.1	4.4	0.3	15.1	4.0	5.7	0.0	0.3	2.3				
Coshocton	Rose Run	C2852	5994.0	87.1	0.0	13.0	69.3	16.7	1.1	0.0	11.1	1.5	0.4	0.0	12.6				
Coshocton	Rose Run	C2852	5997.0	*	*	*	*	*	*	*	*	*	*	*	0.4				
Coshocton	Rose Run	C2852	5998.0	*	*	*	*	*	*	*	*	*	*	*	1.0				

OG—Overgrowths

*—Examined but not point counted.

County	Formation	Core (C) or Permit (P)	Depth (ft.)	Total			Cement/Diagenetic Minerals (%)						Total Porosity (%)			
				Framework (%)	Matrix (%)	Cement (%)	Framework Grains (%)			Cement/Diagenetic Minerals (%)						
							Quartz	Feldspar	Other	Dolomite	Clay	Quartz		Feldspar	Other	
Coshocton	Wells Creek	C2853	5967.0	24.3	0.0	75.7	20.3	4.0	0.0	0.0	75.7	0.0	0.0	0.0	0.0	
Coshocton	Wells Creek	C2853	5968.0	24.3	0.0	75.8	20.1	3.2	1.0	0.0	72.9	0.0	0.0	0.0	2.9	0.3
Coshocton	Wells Creek	C2853	5969.0	47.2	0.0	52.8	44.0	2.8	0.4	0.0	50.0	0.0	0.0	0.0	2.8	2.5
Coshocton	Wells Creek	C2853	5970.0	30.5	0.0	69.6	25.6	4.9	0.0	0.0	69.3	0.0	0.0	0.0	0.3	1.0
Coshocton	Wells Creek	C2853	5971.0	43.9	0.0	56.1	*	*	*	*	*	*	*	*	*	1.3
Coshocton	Wells Creek	C2853	5972.0	74.4	0.0	25.5	69.9	4.2	0.3	0.0	20.3	0.0	4.9	0.3	0.0	9.5
Coshocton	Wells Creek	C2853	5973.0	*	*	*	*	*	*	*	*	*	*	*	*	10.0
Coshocton	Rose Run	C2853	5974.0	83.1	0.0	16.9	*	*	*	*	8.2	0.0	7.5	0.7	0.4	11.0
Coshocton	Rose Run	C2853	5975.0	73.4	0.0	26.7	59.3	14.1	0.0	0.0	24.1	0.0	2.2	0.4	0.0	15.4
Coshocton	Rose Run	C2853	5976.0	61.8	0.0	38.1	44.3	17.5	0.0	0.0	36.8	0.3	0.0	0.7	0.3	4.6
Coshocton	Rose Run	C2853	5977.0	96.9	0.0	3.0	*	*	*	*	0.4	0.0	1.3	1.3	0.0	25.4
Coshocton	Rose Run	C2853	5979.0	74.2	0.0	25.8	*	*	*	*	19.0	0.8	4.8	0.8	0.4	16.0
Coshocton	Rose Run	C2853	5981.5	69.4	0.0	30.6	41.8	19.2	8.4	0.0	30.0	0.0	0.3	0.3	0.0	3.3
Coshocton	Rose Run	C2853	5982.5	*	*	*	*	*	*	*	*	*	*	*	*	*
Coshocton	Rose Run	C2853	5983.0	39.9	0.0	60.0	33.1	6.8	0.0	0.0	56.5	2.3	0.6	0.0	0.6	1.3
Coshocton	Rose Run	C2853	5983.5	28.1	0.0	71.8	19.9	1.6	6.6	0.0	70.9	0.0	0.0	0.0	0.9	0.3
Coshocton	Rose Run	C2853	5984.0	*	*	*	*	*	*	*	*	*	*	*	*	*
Coshocton	Rose Run	C2853	5985.0	89.8	0.0	10.2	74.0	15.9	0.0	0.0	4.1	0.3	4.1	1.3	0.3	8.7
Coshocton	Rose Run	C2853	5986.0	*	*	*	*	*	*	*	*	*	*	*	*	*

OG—Overgrowths

*—Examined but not point counted.

County	Formation	Core (C) or Permit (P)	Depth (ft.)	Total Framework (%)	Total Matrix (%)	Total Cement (%)	Cement/Diagenetic Minerals (%)										Total Porosity (%)								
							Framework Grains (%)			Dolomite			Clay			Quartz			Feldspar			Other			
							Quartz	Feldspar	Other	Dolomite	Clay	Quartz	OG	Other	Quartz	OG		Other	Quartz	OG	Other	Quartz	OG	Other	
Coshocton	Rose Run	C2989	6622.0	69.1	0.0	30.9	*	*	*	27.6	0.0	0.0	2.9	0.4	0.0	0.0	8.6								
Coshocton	Rose Run	C2989	6624.0	65.5	0.0	34.5	*	*	*	28.3	0.0	0.0	5.9	0.3	0.0	0.0	3.3								
Coshocton	Rose Run	C2989	6627.0	80.2	0.0	19.8	*	*	*	12.8	0.4	0.0	6.6	0.0	0.0	0.0	9.0								
Coshocton	Rose Run	C2989	6628.5	50.7	0.0	49.3	*	*	*	48.6	0.7	0.0	0.0	0.0	0.0	0.0	2.0								
Coshocton	Rose Run	C2989	6629.9	76.5	0.0	23.5	*	*	*	0.3	20.1	0.0	2.4	0.0	0.0	0.7	2.3								
Coshocton	Rose Run	C2989	6633.0	0.0	0.0	100.0	0.0	0.0	0.0	100.0	0.0	0.0	0.0	0.0	0.0	0.0	0.0								
Coshocton	Rose Run	C2989	6635.0	30.5	0.0	69.6	*	*	*	62.5	2.1	0.0	4.6	0.0	0.4	0.0	5.0								

OG—Overgrowths

*—Examined but not point counted.

County	Formation	Core (C) or Permit (P)	Depth (ft.)	Total Framework (%)	Total Matrix (%)	Total Cement (%)	Framework Grains (%)						Cement/Diagenetic Minerals (%)						Total Porosity (%)
							Framework Grains (%)			Cement/Diagenetic Minerals (%)									
							Quartz	Feldspar	Other	Dolomite	Clay	Quartz OG	Feldspar OG	Other					
Coshocton	Beekmantown	C3260	6715.0	0.0	0.0	100.0	0.0	0.0	0.0	100.0	TR	0.0	0.0	0.0	0.0	0.0	1.1		
Coshocton	Beekmantown	C3260	6722.0	0.0	0.0	100.0	0.0	0.0	0.0	95.9	4.1	0.0	0.0	0.0	0.0	0.0	2.4		
Coshocton	Rose Run	C3260	6811.5	90.0	0.0	10.0	89.0	1.0	0.0	0.0	3.0	7.0	0.0	0.0	0.0	0.0	9.1		
Coshocton	Rose Run	C3260	6819.5	92.0	0.0	7.0	90.0	2.0	0.0	0.0	6.0	1.0	0.0	0.0	0.0	0.0	11.7		
Coshocton	Rose Run	C3260	6828.0	87.0	0.0	14.0	77.0	10.0	0.0	0.0	1.0	13.0	0.0	0.0	0.0	0.0	10.1		
Coshocton	Rose Run	C3260	6865.0	92.0	0.0	7.0	80.0	12.0	0.0	0.0	0.0	7.0	0.0	0.0	0.0	0.0	10.1		
Coshocton	Rose Run	C3260	6905.0	64.0	0.0	36.0	55.0	9.0	0.0	32.0	0.0	4.0	0.0	0.0	0.0	0.0	8.5		
Coshocton	Copper Ridge	C3260	7000.0	89.0	0.0	11.0	71.0	18.0	0.0	8.0	1.0	2.0	0.0	0.0	0.0	0.0	14.2		

OG—Overgrowths

TR—Trace

Data modified from Reservoirs, Inc. (1992)

County	Formation	Core (C) or Permit (P)	Depth (ft.)	Total Framework Matrix (%)	Total Cement (%)	Cement/Diagenetic Minerals (%)										Total Porosity (%)																				
						Framework Grains (%)					Dobomite						Clay					Quartz					Feldspar					Other				
						Quartz	Feldspar	Other	Dobomite	Clay	Quartz	Feldspar	Other	Dobomite	Clay		Quartz	Feldspar	Other	Dobomite	Clay	Quartz	Feldspar	Other	Dobomite	Clay	Quartz	Feldspar	Other							
Jackson	Rose Run	C2898	4499.0	84.5	0.0	15.2	83.1	1.7	0.0	0.0	8.6	0.7	5.2	0.7	0.0	0.0	0.0	0.0	0.0	0.0	0.0	0.0	0.0	0.0	6.8											
Jackson	Rose Run	C2898	4501.0	*	*	*	*	*	*	*	*	*	*	*	*	*	*	*	*	*	*	*	*	*	*	*										
Jackson	Rose Run	C2898	4502.0	83.1	0.0	16.9	82.1	1.0	0.0	0.0	0.0	3.4	12.8	0.0	0.7	0.0	0.0	0.0	0.0	0.0	0.0	0.0	0.0	0.0	11.3											
Jackson	Rose Run	C2898	4504.0	*	*	*	*	*	*	*	*	*	*	*	*	*	*	*	*	*	*	*	*	*	*	*										
Jackson	Rose Run	C2898	4505.0	92.6	0.0	7.5	88.5	4.1	0.0	0.0	0.0	5.8	1.0	0.7	0.0	0.0	0.0	0.0	0.0	0.0	0.0	0.0	0.0	0.0	6.9											
Jackson	Rose Run	C2898	4506.0	*	*	*	*	*	*	*	*	*	*	*	*	*	*	*	*	*	*	*	*	*	*	*										
Jackson	Rose Run	C2898	4507.0	91.4	0.0	8.7	87.1	4.3	0.0	0.0	2.2	2.2	2.9	1.4	0.0	0.0	0.0	0.0	0.0	0.0	0.0	0.0	0.0	0.0	7.3											
Jackson	Rose Run	C2898	4508.0	*	*	*	*	*	*	*	*	*	*	*	*	*	*	*	*	*	*	*	*	*	*	*										
Jackson	Rose Run	C2898	4509.0	87.0	0.0	13.1	80.3	6.7	0.0	0.0	5.7	3.0	1.7	2.7	0.0	0.0	0.0	0.0	0.0	0.0	0.0	0.0	0.0	0.0	3.2											
Jackson	Rose Run	C2898	4512.0	*	*	*	*	*	*	*	*	*	*	*	*	*	*	*	*	*	*	*	*	*	*	*										
Jackson	Rose Run	C2898	4513.0	77.3	0.0	22.6	74.2	3.1	0.0	0.0	17.1	0.0	5.2	0.0	0.3	0.0	0.0	0.0	0.0	0.0	0.0	0.0	0.0	0.0	5.9											
Jackson	Rose Run	C2898	4514.0	*	*	*	*	*	*	*	*	*	*	*	*	*	*	*	*	*	*	*	*	*	*	*										
Jackson	Rose Run	C2898	4515.0	85.9	0.0	14.1	77.6	8.3	0.0	0.0	0.0	11.9	2.2	0.0	0.3	0.0	0.0	0.0	0.0	0.0	0.0	0.0	0.0	0.0	0.3											
Jackson	Rose Run	C2898	4516.0	*	*	*	*	*	*	*	*	*	*	*	*	*	*	*	*	*	*	*	*	*	*	*										
Jackson	Rose Run	C2898	4517.0	88.8	0.0	11.2	83.5	5.3	0.0	0.0	1.4	7.0	0.7	2.1	0.0	0.0	0.0	0.0	0.0	0.0	0.0	0.0	0.0	0.0	10.7											
Jackson	Rose Run	C2898	4518.0	*	*	*	*	*	*	*	*	*	*	*	*	*	*	*	*	*	*	*	*	*	*	*										
Jackson	Rose Run	C2898	4520.0	*	*	*	*	*	*	*	*	*	*	*	*	*	*	*	*	*	*	*	*	*	*	*										
Jackson	Rose Run	C2898	4521.0	*	*	*	*	*	*	*	*	*	*	*	*	*	*	*	*	*	*	*	*	*	*	*										
Jackson	Rose Run	C2898	4522.0	91.8	0.0	8.1	87.0	4.8	0.0	0.0	0.0	0.7	5.9	1.5	0.0	0.0	0.0	0.0	0.0	0.0	0.0	0.0	0.0	0.0	12.9											
Jackson	Rose Run	C2898	4523.0	*	*	*	*	*	*	*	*	*	*	*	*	*	*	*	*	*	*	*	*	*	*	*										
Jackson	Rose Run	C2898	4525.0	*	*	*	*	*	*	*	*	*	*	*	*	*	*	*	*	*	*	*	*	*	*	*										
Jackson	Rose Run	C2898	4527.0	90.5	0.0	9.5	87.9	2.6	0.0	0.0	2.9	1.1	4.4	1.1	0.0	0.0	0.0	0.0	0.0	0.0	0.0	0.0	0.0	0.0	10.2											
Jackson	Rose Run	C2898	4528.0	*	*	*	*	*	*	*	*	*	*	*	*	*	*	*	*	*	*	*	*	*	*	*										
Jackson	Rose Run	C2898	4529.0	*	*	*	*	*	*	*	*	*	*	*	*	*	*	*	*	*	*	*	*	*	*	*										
Jackson	Rose Run	C2898	4530.0	76.2	0.0	23.7	68.7	7.5	0.0	0.0	20.4	0.0	1.0	2.0	0.3	0.0	0.0	0.0	0.0	0.0	0.0	0.0	0.0	0.0	3.3											

OG—Overgrowths

*—Examined but not point counted.

County	Formation	Core (C) or Permit (P)	Depth (ft.)	Total Framework (%)	Total Matrix (%)	Total Cement (%)	Cement/Diagenetic Minerals (%)										Total Porosity (%)									
							Framework Grains (%)			Cement			Dolomite					Clay			Quartz		Feldspar		Other	
							Quartz	Feldspar	Other	Quartz	Feldspar	Other	Dolomite	Clay	Other	OG		OG	OG	OG	OG	OG	OG	OG		
Scioto	Rose Run	C2598	4254.0	85.4	0.0	14.5	81.3	4.1	0.0	0.0	0.0	1.8	8.2	4.3	0.2	12.4										
Scioto	Rose Run	C2598	4255.0	83.1	0.0	16.9	74.6	7.8	0.7	0.0	11.4	0.0	5.2	0.3	1.3											
Scioto	Rose Run	C2598	4255.8	90.9	0.0	9.2	78.0	12.9	0.0	0.0	5.2	0.2	3.2	0.6	11.2											
Scioto	Rose Run	C2598	4256.0	86.6	0.0	13.3	70.8	15.8	0.0	0.0	6.7	0.4	5.1	1.1	10.2											
Scioto	Rose Run	C2598	4256.5	85.0	0.0	15.0	66.5	18.5	0.0	0.0	0.0	0.0	4.7	10.3	7.0											
Scioto	Rose Run	C2598	4258.5	90.2	0.0	9.7	78.5	11.5	0.2	0.0	5.8	0.0	3.5	0.4	9.6											
Scioto	Rose Run	C2598	4258.8	86.8	0.0	13.1	74.4	12.2	0.2	0.0	7.0	0.0	4.9	1.2	10.2											
Scioto	Rose Run	C2598	4258.9	89.1	0.0	10.8	78.5	10.6	0.0	0.0	4.4	1.1	5.1	0.2	8.7											
Scioto	Rose Run	C2598	4259.0	86.4	0.0	13.6	75.1	11.3	0.0	0.4	9.2	0.0	3.8	0.2	9.6											
Scioto	Rose Run	C2598	4259.2	81.1	0.0	18.9	69.5	11.6	0.0	6.8	6.4	0.4	4.4	0.9	8.6											
Scioto	Rose Run	C2598	4259.6	86.8	0.0	13.3	75.3	11.5	0.0	0.0	5.1	0.9	6.4	0.9	6.0											
Scioto	Rose Run	C2598	4259.8	86.6	0.0	13.3	71.5	15.1	0.0	0.0	10.2	0.0	2.0	1.1	10.2											
Scioto	Rose Run	C2598	4260.0	92.7	0.0	7.3	80.3	12.4	0.0	0.0	3.9	0.0	2.5	0.9	12.6											
Scioto	Rose Run	C2598	4260.2	85.4	0.0	14.6	74.1	11.3	0.0	0.0	0.0	3.9	3.5	7.2	8.2											
Scioto	Rose Run	C2598	4260.5	85.8	0.0	14.2	75.7	10.1	0.0	0.0	3.6	7.5	2.6	0.5	8.8											
Scioto	Rose Run	C2598	4261.0	62.0	0.0	38.0	56.1	5.9	0.0	36.1	1.1	0.0	0.4	0.4	1.0											

OG—Overgrowths

Data modified from Baker (1974)

County	Formation	Core (C) or Permit (P)	Depth (ft.)	Total Framework Matrix (%)	Total Cement (%)	Framework Grains (%)						Cement/Diagenetic Minerals (%)						Total Porosity (%)
						Framework Grains (%)		Framework Grains (%)		Dolomite	Clay	Quartz		Feldspar		Other		
						Quartz	Feldspar	Quartz	Feldspar			OG	OG					
Scioto	Rose Run	C2958	4255.5	89.0	11.0	84.7	4.3	0.0	0.0	8.5	0.0	2.1	0.0	0.0	6.3			
Scioto	Rose Run	C2958	4256.0	*	*	*	*	*	*	*	*	*	*	*	*			
Scioto	Rose Run	C2958	4258.0	*	*	*	*	*	*	*	*	*	*	*	*			
Scioto	Rose Run	C2958	4259.0	*	*	*	*	*	*	*	*	*	*	*	*			
Scioto	Rose Run	C2958	4260.0	*	*	*	*	*	*	*	*	*	*	*	*			

OG—Overgrowths

*—Examined but not point counted.

This is the same core that Baker (1974) point counted. Then sections for this study were incorrectly inscribed C2958. Correct core number is C 2598.

County	Formation	Core (C) or Permit (P)	Depth (ft.)	Total Framework (%)	Total Matrix (%)	Total Cement (%)	Cement/Diagenetic Minerals (%)										Total Porosity (%)
							Framework Grains (%)					Cement/Diagenetic Minerals (%)					
							Quartz	Feldspar	Other	Dolomite	Clay	Quartz OG	Feldspar OG	Other			
Tuscarawas	Copper Ridge	C2963	7646.00	65.1	0.0	35.0	*	*	*	19.5	9.6	3.1	2.1	0.1	0.0		
Tuscarawas	Copper Ridge	C2963	7653.00	0.7	0.0	99.3	*	*	*	99.3	0.0	0.0	0.0	0.0	7.0		
Tuscarawas	Copper Ridge	C2963	7653.50	*	*	*	*	*	*	*	*	*	*	*	*		
Tuscarawas	Copper Ridge	C2963	7655.00	27.7	*	*	*	*	70.2	0.3	1	0.7	0	0	2.7		
Tuscarawas	Copper Ridge	C2963	7659.00	0.3	0	99.7	*	*	*	99.7	0	0	0	0	4.7		
Tuscarawas	Copper Ridge	C2963	7664.00	55.7	0	44.2	*	*	*	37.3	2.1	3.1	1.4	0.3	4.3		
Tuscarawas	Copper Ridge	C2963	7668.00	17.1	0	82.8	*	*	*	78.9	2.3	1.3	0	0.3	0.3		
Tuscarawas	Copper Ridge	C2963	7668.50	*	*	*	*	*	*	*	*	*	*	*	*		
Tuscarawas	Copper Ridge	C2963	7670.00	85.1	0	14.9	*	*	*	1.8	3.6	9	0.5	0	9.4		
Tuscarawas	Copper Ridge	C2963	7672.00	59.7	0	40.4	*	*	*	34.7	0	5	0.7	0	0		
Tuscarawas	Copper Ridge	C2963	7673.00	79.2	0	20.7	*	*	*	10	0	8.3	2.4	0	3.7		
Tuscarawas	Copper Ridge	C2963	7675.00	74.7	0	25.3	*	*	*	12.1	1.7	8.7	2.8	0	3.7		
Tuscarawas	Copper Ridge	C2963	7677.00	*	*	*	*	*	*	*	*	*	*	*	*		
Tuscarawas	Copper Ridge	C2963	7681.00	4	0	95.9	*	*	*	95.6	0	0.3	0	0	0.7		
Tuscarawas	Copper Ridge	C2963	7683.00	*	*	*	*	*	*	*	*	*	*	*	*		
Tuscarawas	Copper Ridge	C2963	7686.00	4.2	0	95.8	*	*	*	95.8	0	0	0	0	5		

OG—Overgrowths

*—Examined but not point counted.

**Appendix XI:
Relative Percent Porosity Types
Found in Thin Sections**

County	Core (C) or Permit (P)	Depth (ft.)	Pore Type										Total % Pores
			Moldic	Over-Size	Inter-Granular	Intra-Constituent	Fracture	Inter-Crystalline	Pore Size ¹				
Coshocton	C2852	5986.0	1	29	0	0	0	0	0	70	2	3	
Coshocton	C2852	5988.0	40	0	58	0	0	0	0	2	4	7	
Coshocton	C2852	5989.5	30	0	70	0	0	0	0	0	2	1	
Coshocton	C2852	5991.0	6	0	4	0	0	0	0	90	3	3	
Coshocton	C2852	5991.5	0	0	0	0	0	0	0	0	2	0	
Coshocton	C2852	5992.0	1	0	0	0	0	0	0	99	2	1	
Coshocton	C2852	5992.5	35	35	30	0	0	0	0	0	5	2	
Coshocton	C2852	5994.0	50	49	0	1	0	0	0	0	4	13	
Coshocton	C2852	5997.0	999 ²	999	999	999	999	999	999	999	2	0	
Coshocton	C2852	5998.0	999	999	999	999	999	999	999	999	3	1	
Coshocton	C2853	5967.0	50	0	0	0	0	0	0	50	99	0	
Coshocton	C2853	5968.0	50	0	0	0	0	0	0	50	5	0	
Coshocton	C2853	5969.0	100	0	0	0	0	0	0	0	2	3	
Coshocton	C2853	5970.0	9	0	0	0	0	1	90	2	2	1	
Coshocton	C2853	5971.0	0	0	0	0	0	0	100	3	1	1	
Coshocton	C2853	5972.0	29	31	23	6	6	0	11	4	4	10	
Coshocton	C2853	5973.0	29	31	23	6	6	0	11	4	4	10	
Coshocton	C2853	5974.0	67	6	21	3	3	0	3	4	4	11	
Coshocton	C2853	5975.0	23	21	21	9	9	0	26	4	4	15	
Coshocton	C2853	5976.0	9	9	36	18	18	0	27	3	3	5	
Coshocton	C2853	5977.0	26	43	1	29	29	0	0	4	4	25	
Coshocton	C2853	5979.0	6	52	15	15	15	8	4	4	4	16	
Coshocton	C2853	5981.5	17	30	9	9	9	35	0	3	3	3	
Coshocton	C2853	5982.5	999	999	999	999	999	999	999	999	999	999	
Coshocton	C2853	5983.0	40	20	40	0	0	0	0	0	3	1	
Coshocton	C2853	5983.5	0	0	0	0	0	0	0	0	4	0	
Coshocton	C2853	5984.0	999	999	999	999	999	999	999	999	999	999	
Coshocton	C2853	5985.0	23	20	23	30	30	0	3	4	4	9	
Coshocton	C2853	5986.0	0	0	0	0	0	100	0	2	2	0	

(cont.)

Pore Type

County	Core (C) or Permit (P)	Depth (ft.)	Moldic	Over- Size	Inter- Granular	Intra- Constituent	Fracture	Inter- Crystalline	Pore Size ¹	Total % Pores
Coshocton	C2989	6622.0	4	0	81	4	0	12	4	9
Coshocton	C2989	6624.0	0	0	70	10	0	20	3	3
Coshocton	C2989	6627.0	0	22	67	7	0	4	5	9
Coshocton	C2989	6628.5	33	0	17	0	0	50	2	2
Coshocton	C2989	6629.9	0	0	86	14	0	0	3	2
Coshocton	C2989	6633.0	0	0	0	0	0	99	2	0
Coshocton	C2989	6635.0	7	7	13	7	0	67	3	5
Jackson	C2898	4499.0	5	0	0	95	0	0	4	7
Jackson	C2898	4501.0	999	999	999	999	999	999	999	999
Jackson	C2898	4502.0	27	8	65	0	0	0	5	11
Jackson	C2898	4504.0	999	999	999	999	999	999	999	999
Jackson	C2898	4505.0	64	5	32	0	0	0	4	7
Jackson	C2898	4506.0	999	999	999	999	999	999	999	999
Jackson	C2898	4507.0	9	0	91	0	0	0	3	7
Jackson	C2898	4508.0	999	999	999	999	999	999	999	999
Jackson	C2898	4509.0	0	0	100	0	0	0	3	3
Jackson	C2898	4512.0	999	999	999	999	999	999	999	999
Jackson	C2898	4513.0	17	6	78	0	0	0	4	6
Jackson	C2898	4514.0	999	999	999	999	999	999	999	999
Jackson	C2898	4515.0	0	0	100	0	0	0	3	0
Jackson	C2898	4516.0	999	999	999	999	999	999	4	99
Jackson	C2898	4517.0	24	9	62	6	0	0	5	11
Jackson	C2898	4518.0	999	999	999	999	999	999	999	999
Jackson	C2898	4520.0	999	999	999	999	999	999	999	999
Jackson	C2898	4521.0	999	999	999	999	999	999	999	999
Jackson	C2898	4522.0	25	8	68	0	0	0	5	13
Jackson	C2898	4523.0	999	0	999	999	999	999	999	999
Jackson	C2898	4525.0	999	0	999	999	999	999	999	999
Jackson	C2898	4527.0	10	3	87	0	0	0	5	10
Jackson	C2898	4528.0	999	0	999	999	999	999	999	999
Jackson	C2898	4529.0	999	0	999	999	999	999	999	999
Jackson	C2898	4530.0	0	0	100	0	0	0	3	3
Tuscarawas	C2963	7646.0	0	0	0	0	0	0	0	0
Tuscarawas	C2963	7653.0	0	0	0	0	0	100	5	7
Tuscarawas	C2963	7653.5	0	0	0	0	0	100	4	99
Tuscarawas	C2963	7655.0	0	0	0	12	0	88	4	3

(cont.)

County	Core (C) or Permit (P)	Depth (ft.)	Pore Type							Total % Pores	
			Moldic	Over-Size	Inter-Granular	Intra-Constituent	Fracture	Inter-Crystalline	Pore Size ¹		
Tuscarawas	C2963	7659.0	0	0	0	0	0	0	100	4	5
Tuscarawas	C2963	7664.0	0	0	54	15	0	0	30	3	4
Tuscarawas	C2963	7668.0	0	0	0	0	0	0	100	3	0
Tuscarawas	C2963	7668.5	0	0	0	0	0	0	100	4	99
Tuscarawas	C2963	7670.0	0	22	74	4	0	0	0	4	9
Tuscarawas	C2963	7672.0	0	0	0	0	0	0	0	5	0
Tuscarawas	C2963	7673.0	9	0	82	0	0	0	9	4	4
Tuscarawas	C2963	7675.0	18	9	55	18	0	0	0	4	4
Tuscarawas	C2963	7677.0	0	0	0	0	0	0	100	4	99
Tuscarawas	C2963	7681.0	0	0	0	0	0	0	100	3	1
Tuscarawas	C2963	7683.0	0	0	0	0	0	0	100	4	99
Tuscarawas	C2963	7686.0	0	0	0	0	0	0	100	4	5

¹Pore size (micrometers)

1. <4
2. 4-63
3. 63-125
4. 125-250
5. 250-500
6. 500-1000
7. >1000

²999=Not determined

**Appendix XII:
Catalogue of Upper Cambrian
and Lower Ordovician Cores**

1. *County and State:* Coshocton Co., Ohio
Township and Location: White Eyes Twp., Sec. 17
Core Number and Permit: Core #2989, Permit #2653
Well Name: Stone Resource #1 Barth
Cored Interval: 6,590–6,639 ft.
Stratigraphic Interval: Wells Creek to “Rose Run”
Condition: Slabbed
2. *County and State:* Coshocton Co., Ohio
Township and Location: Virginia Twp., Lot 21, 4th Quarter
Core Number and Permit: Core #2852, Permit #2183
Well Name: Gallegher #1 McLeod Heirs
Cored Interval: 5,986–5,999 ft.
Stratigraphic Interval: Wells Creek to “Rose Run”
Condition: Slabbed
3. *County and State:* Coshocton Co., Ohio
Township and Location: Virginia Twp., Lot 24, 4th Quarter
Core Number and Permit: Core #2853, Permit #2268
Well Name: Gallegher #1 Vickers
Cored Interval: 5,967–5,986 ft.
Stratigraphic Interval: Wells Creek to “Rose Run”
Condition: Slabbed
4. *County and State:* Coshocton Co., Ohio
Township and Location: Adams Twp., Section 2
Core Number and Permit: Core #2713, Permit #4092
Well Name: Pomstone #1 Oaklief
Cored Interval: 6,800–6,930 ft.
Stratigraphic Interval: Beekmantown
Condition: Partially Slabbed
5. *County and State:* Coshocton Co., Ohio
Township and Location: Adams Twp., Sec. 12
Core Number and Permit: Core #3006, Permit #5962
Well Name: Stone #1-A Lower
Cored Interval: 6,736–6,796 ft.
Stratigraphic Interval: Wells Creek to “Rose Run”
Condition: Slabbed
6. *County and State:* Columbiana Co., Ohio
Township and Location: Knox Twp., Sec. 12
Core Number and Permit: Core #2850, Permit #592
Well Name: East Ohio Gas #1–2468 Denny
Cored Interval: 8,097–8,126 and 8,249–8,295 ft.
Stratigraphic Interval: Beekmantown and “Rose Run”
Condition: Slabbed
7. *County and State:* Guernsey Co., Ohio
Township and Location: Adams Twp., Sec. 15
Core Number and Permit: Core # 867, Permit # 782
Well Name: Lakeshore #1 Marshall
Cored Interval: 6,875–7,045 ft.
Stratigraphic Interval: Wells Creek, Beekmantown, and “Rose Run”
Condition: Slabbed
8. *County and State:* Holmes Co., Ohio
Township and Location: Berlin Twp., Lot 12
Core Number and Permit: Core #2892, Permit #1279
Well Name: Amerada #1 Geib
Cored Interval: 6,368–6,419 ft.
Stratigraphic Interval: Wells Creek to Knox
Condition: Unslabbed
9. *County and State:* Jackson Co., Ohio
Township and Location: Franklin Twp., Sec. 8
Core Number and Permit: Core #2898, Permit #102
Well Name: Nucorp #1 Trepanier
Cored Interval: 4,488–4,522 ft.
Stratigraphic Interval: “Rose Run”
Condition: Slabbed
10. *County and State:* Morgan Co., Ohio
Township and Location: Homer Twp., Frac. 32
Core Number and Permit: Core #2923, Permit #1249
Well Name: Columbia Gas #11125 Kittle
Cored Interval: 6,249–6,343 and 6,401–6,521 ft.
Stratigraphic Interval: Wells Creek to Beekmantown, and “Rose Run”
Condition: Slabbed
11. *County and State:* Scioto Co., Ohio
Township and Location: Green Twp
Core Number and Permit: Core #2598, Permit #212
Well Name: Earlougher #1 USS Chemical Div.
Cored Interval: 3,979–4,009 and 4,254–4,262 ft.
Stratigraphic Interval: Beekmantown and “Rose Run”
Condition: Slabbed
12. *County and State:* Tuscarawas Co., Ohio
Township and Location: Clay Twp., Lot 14 N
Core Number and Permit: Core #2963, Permit #955
Well Name: Stocker and Sitler #1 Mizer
Cored Interval: 7,647–7,688 ft.
Stratigraphic Interval: “Rose Run”
Condition: Slabbed

13. *County and State:* Scioto Co., Ohio¹
Township and Location: Green Twp.
Core Number and Permit: No numbers assigned
Well Name: Aristech test/monitor well
Cored Interval: 10-5,443 ft.
Stratigraphic Interval: Logan to Rome
Condition:
14. *County and State:* Erie Co., Pennsylvania
Township and Location: City of Erie
Core Number and Permit: Permit # 20109
Well Name: Hammernil Paper Co. #2 Fee
Cored Interval: 5,102-5,131, 5,154-5,166,
and 5,547-5,565 ft.
Stratigraphic Interval: Shadow Lake and Gatesburg
Condition: Slabbed and unslabbed

15. *County and State:* Juniata Co., Pennsylvania
Township and Location: Fayette Twp.
Core Number and Permit: Permit # 20001
Well Name: Shell Oil Co. #1 Shade
Mountain Unit
Cored Interval: 10,010-10,035 ft.
Stratigraphic Interval: Gatesburg
Condition: Slabbed

¹To be donated to Ohio Division of Geologic Survey.

**Appendix XIII:
Survey of Industry's Use of Seismic Data
for the Location of Exploration and
Development Wells Drilled in Ohio**

Prepared by the Ohio Division of Geological Survey

Numbers in the three columns are average numbers from the responses submitted. The number in parentheses refers to the number of responses for each question. The results are divided into three columns based on the number of employees per company. Column A represents less than or equal to five employees. Column B represents more than five but less than 25 employees. Column C represents greater than or equal to 25 employees.

	A	B	C
1. Number of companies responding to survey.	3	13	7
2. Approximately how many miles of new data will your company acquire for 1992?	10 (3)	61 (12)	
3. Approximate percentage of exploration budget used for new data acquisition and processing.	18 (3)	47 (10)	
4. Does your company purchase brokerage data?	yes no 1 2	yes no 5 8	yes no 6 1
5. Percentage of exploration budget used to purchase brokerage data.	5 (3)	4 (13)	9 (4)
6. Does your company reprocess purchased brokerage data?	yes no 1 2	yes no 5 -	yes no 5 -
7. Does your company utilize advanced seismic processing (e.g. attribute analyses, VSP, inversion, color plots, etc.)?	yes no 1 2	yes no 6 7	yes no 3 -
8. Number of years drilling for Rose Run production.	4 (3)	7 (13)	8 (7)
9. Estimated success percentage for drilling and locating a Rose Run geologic anomaly <i>with seismic data</i> .	75 (3)	45 (12)	70 (6)
10. Estimated success percentage of economic objectives for drilling to find Rose Run production <i>with seismic data</i> .	- (0)	38 (10)	55 (5)
11. Estimated success percentage of drilling and locating a Rose Run geologic anomaly <i>without seismic data</i> .	25 (1)	24 (12)	26 (4)
12. Estimated success percentage of drilling and producing Rose Run <i>without seismic data</i> .	25 (1)	31 (11)	17 (4)
13. Would your company drill for Rose Run production without seismic data?	yes no - 3	yes no 6 7	yes no 2 -

Appendix XIV:
Glossary of Geophysical Terms Used
in this Study (from Sheriff, 1982)

- Amplitude:** the maximum departure of a wave from the average value
- Common depth point (CDP):** the situation for which the same portion of the subsurface is involved in producing reflections at different offset distances, on the same profile
- Convolution:** change in waveshape as a result of passing through a linear filter
- Damp:** to slow or oppose oscillation
- Deconvolution:** process of undoing the effect of another filter
- First breaks:** the first recorded signal attributable to seismic-wave travel from a known source
- Fold:** common depth point multiplicity, e.g., where the same CDP point is sampled at 30 different offset distances, the resultant data is referred to as "30-fold"
- Frequency:** repetition rate of a periodic waveform, measured in per second, or Hertz (Hz.); the reciprocal of period
- Ground roll:** the vertical component of dispersive surface waves, often responsible for near surface noise
- Migration:** plotting of dipping reflectors in true spatial position, rather than as a CDP location
- Normal move out:** the difference between the value for two-way time at a certain offset and the value for two-way time at zero-offset
- Notch filter:** a filter designed to remove a single narrow band of frequencies
- Phase:** the displacement of a sine wave with respect to a reference, i.e., how far into the period of rotation; commonly expressed in angular measure.
- Polarity:** the condition of a reflector signal (reflectivity convolved with acoustic impedance) being represented as a peak or a trough (positive or negative); SEG convention polarity is that a large amplitude is represented as a trough, log-normal polarity is that a large amplitude is represented as a peak.
- Reflection coefficient:** the ratio of the amplitude of the displacement of a reflected wave to that of an incident wave.
- Refraction statics:** a method of statics corrections based on absolute first break arrive time; used to estimate long period statics components
- Resolution:** separations of two features which are very close together
- Signal-to-noise ratio:** energy of desired events divided by all remaining energy (S/N)
- Spherical divergence:** decrease in wave strength (energy/amount of area of a wavefront) with distance, as a result of geometric spreading
- Spiking deconvolution:** the process by which a seismic wavelet is compressed into a zero lag spike
- Spread geometry:** layout of geophone groups from which data from a single shot are recorded simultaneously
- Stacking:** composite record made by mixing traces from different records. CDP stack: combines data which have a common midpoint between source and receiver locations, after correcting for normal moveout
- Statics:** corrections applied to seismic data to eliminate the effects of variation in elevation
- Wavelet:** a seismic pulse usually containing 1 1/2 to 2 cycles
- White noise:** containing all frequencies in equal proportion
- Whitening:** adjustment of the amplitudes of all frequencies in a certain bandpass range to the same level.
- Zero-phase:** a filter which results in a phase shift of zero for all frequencies

